Mingtian Fan, Zuping Zhang and Chengmin Wang

Mathematical Models and Algorithms for Power System Optimization

Modeling Technology for Practical Engineering Problems

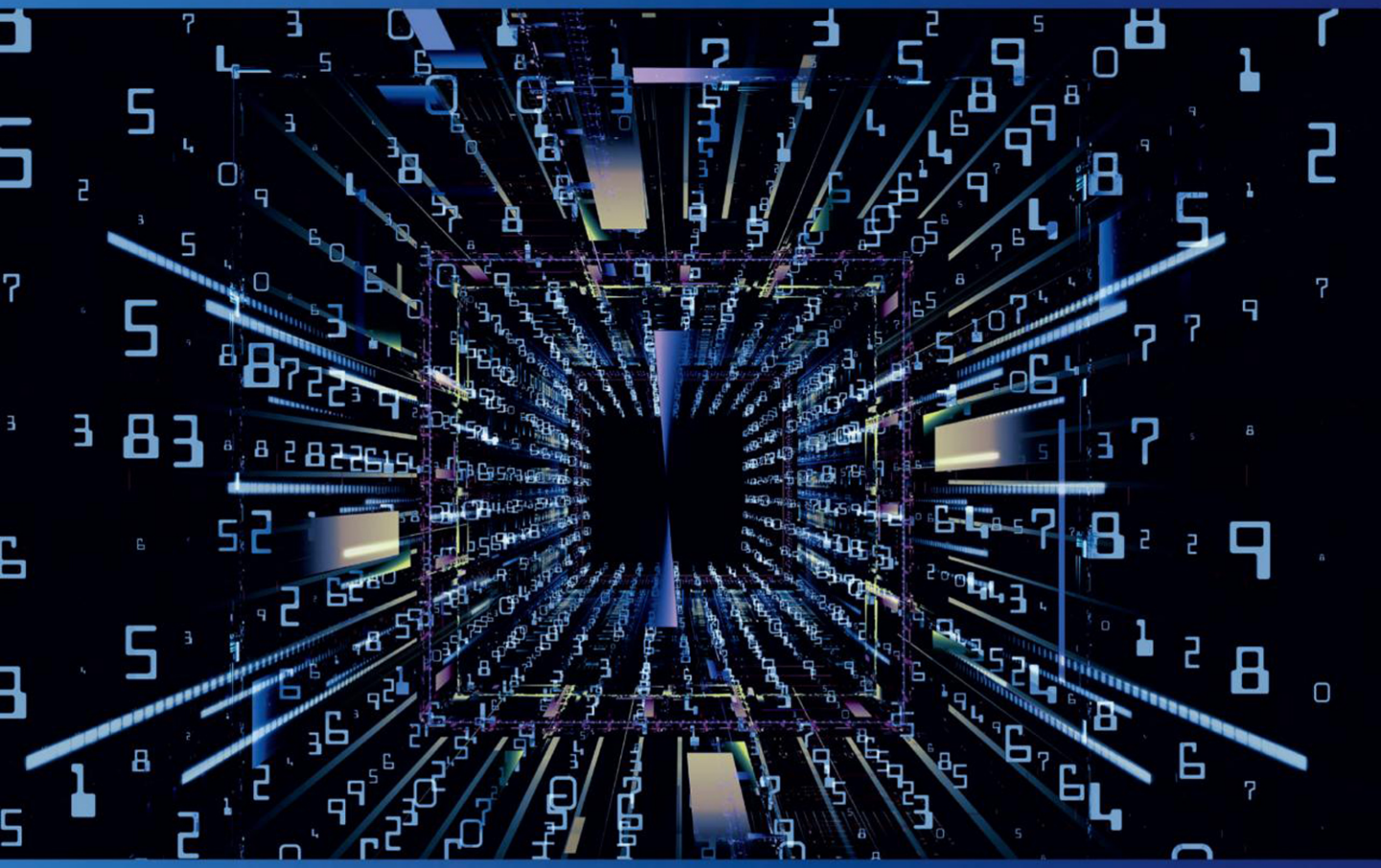

中国电力出版社
CHINA ELECTRIC POWER PRESS

Mathematical Models and Algorithms for Power System Optimization

Mathematical Models and Algorithms for Power System Optimization

Modeling Technology for Practical Engineering Problems

Mingtian Fan
Zuping Zhang
Chengmin Wang

ACADEMIC PRESS
An imprint of Elsevier

Academic Press is an imprint of Elsevier
125 London Wall, London EC2Y 5AS, United Kingdom
525 B Street, Suite 1650, San Diego, CA 92101, United States
50 Hampshire Street, 5th Floor, Cambridge, MA 02139, United States
The Boulevard, Langford Lane, Kidlington, Oxford OX5 1GB, United Kingdom

Notices
Knowledge and best practice in this field are constantly changing. As new research and experience broaden our understanding, changes in research methods, professional practices, or medical treatment may become necessary.

Practitioners and researchers must always rely on their own experience and knowledge in evaluating and using any information, methods, compounds, or experiments described herein. In using such information or methods they should be mindful of their own safety and the safety of others, including parties for whom they have a professional responsibility.

To the fullest extent of the law, neither the Publisher nor the authors, contributors, or editors, assume any liability for any injury and/or damage to persons or property as a matter of products liability, negligence or otherwise, or from any use or operation of any methods, products, instructions, or ideas contained in the material herein.

Library of Congress Cataloging-in-Publication Data
A catalog record for this book is available from the Library of Congress

British Library Cataloguing-in-Publication Data
A catalogue record for this book is available from the British Library

ISBN 978-0-12-813231-9

中国电力出版社

中国电力出版社
CHINA ELECTRIC POWER PRESS

Publisher: Glyn Jones
Acquisition Editor: Glyn Jones
Editorial Project Manager: Naomi Robertson
Production Project Manager: Prem Kumar Kaliamoorthi
Cover Designer: Victoria Pearson

Typeset by SPi Global, India

Abstract

A number of mathematical models and algorithms are presented in this book for solving the practical problems in planning, operation, control, and marketing decisions for power systems. It focuses on economic dispatching, generator maintenance scheduling, load flow, optimal load flow, load optimization, reactive optimization, load frequency control, transient stability, and electricity marketing where mathematical models are transformed into relatively standard optimization models to make optimization applications possible. The optimization models discussed include linear (0–1, integer, mixed-integer), nonlinear, mixed integer, and nonlinear mixed integer models. Both numerical and non-numerical optimization algorithms are used in this book, the former (mathematical programming approachs) includes linear programming, nonlinear programming, mixed integer programming and dynamic programming, the latter (rules based approaches) includes Genetic Algorithm (GA), Simulated Annealing (SA), and Expert System (ES). Based on the authors' extensive research experience in developing models and algorithms for power system optimization, this book also provides an in-depth analysis of some practical modeling techniques which are seldom explained comprehensively in the existing textbooks, both from theoretical and practical standpoints, for example, validity testing of data, type setting of variables, special setting of limit values of variables, special setting of constraints, and preprocessing of parameter and data. These techniques can be effectively applied to the modeling of power system optimization problems. Therefore, the readers of *Mathematical Models and Algorithms for Power System Optimization* will gain important insights into: how to transform the practical problems into mathematical models, how to develop the standard optimal mathematical models and utilize commercially available and reliable programming software, how to deal with various issues that affect the performance of a model, and how to evaluate the effectiveness of the models.

The authors hope that the ideas and practices of the modeling techniques presented in this book will be informative and helpful for the future modeling research on power systems. This book will be a useful reference for those in universities and research institutes who are actively engaged in power system optimization.

Preface

The practical models for power system planning, operation, control, and electricity markets are provided in this book based on the authors' research achievements in the development of mathematical models and algorithms. The models include optimization models (linear, nonlinear, mixed integer, nonlinear mixed integers), differential equations, difference equations, and time series models. This book not only uses numerical algorithms (mathematical programming methods), such as linear programming, nonlinear programming, mixed integer programming and dynamic programming, but also uses some non-numerical algorithms such as Genetic Algorithm (GA), Simulated Annealing (SA), and Expert System (ES). The mathematical models and calculation methods provided in this book have been proven by typical calculation examples or applied in engineering practices. Therefore, this book follows a highly original and very practical approach.

The current research results on modeling technology for power systems can be found in research papers and textbooks. However, research papers mainly focus on related theoretical aspects, whereas textbooks emphasize general knowledge, but neither describes the modeling process in detail. Considering both theoretical and practical aspects, this book not only introduces the methods and processes for the development of optimization models but also provides some practical techniques, such as mutual transformation of variables and functions, transformation of equation types, and transformation of constraints. It also provides some special techniques such as setting of variable types and preprocessing of data and parameters. The practical techniques mentioned above allow us to solve the modeling problems encountered in new generation power systems more effectively.

The power system is a typical large-scale man-made system, though all the conventional components have a complete model, any new component needs to have a new model so as to be connected to the power system. To properly handle the new coming problems in power system planning, operation, and control, the development of corresponding optimization mathematical models and investigation of feasible algorithms should take many relationships into consideration, such as the relationships between old and new components, between old and new models, between the power system and the external environment, to name a few.

In recent years, there has been an evident tendency for a large number of distributed resources, such as distributed generation, energy storage devices, and interactive loads, to be connected to the power grid. In addition, information and communication technologies have been widely applied in many fields of power systems. To adapt to this new progress, many new relationships need to be dealt with and many new models need to be developed, and traditional mathematical models of power systems need to be further improved.

The modeling of power systems is extremely challenging due to the complexity of practical problems, which requires fairly good mathematical knowledge and deep understanding of the physical system. Although the reasonable reproducibility of mathematical models allows us to simulate practical problems more effectively, the selecting of an optimization model nearly always involves compromise among conflicting goals, such as discrete versus continuous, accurate versus approximate, simple use versus comprehensive analysis, etc. The modeling techniques for power system optimization deserve to be discussed in depth in this book.

Four types of basic variables are considered in the steady-state analysis and calculation of the power system in this book: active power, reactive power, voltage, and phase angle (namely P, Q, U, and θ). Among them, active power and reactive power can be divided into active power generation output and reactive power generation output (P_G, Q_G), and active load and reactive power load (P_L, Q_L), respectively. Occasionally, the "P" and "Q" on the node are considered as the corresponding impedances rather than the variables. Besides the basic variables described previously, two more variables are considered in the transient calculation of the power system: the power angle δ and the angular frequency or rotational speed of the generator $\omega = 2\pi f$ (where f is the system frequency).

Chapter 1 introduces the fundamental issues of modeling techniques deduced from practical engineering problems, including some general and special modeling techniques. It provides some ideas for the setting of variables and functions, the selection of model types, and the selection of algorithms, all of which provide main aspects for power system model constructions and solutions.

The rest of the book is divided into four parts: operation, planning, control, and marketing for power systems. All four parts describe the mathematical models and the calculation methods to optimize the variables P, Q, U, and θ, from different points of view. The first part comprising Chapters 2 and 3 focuses on the power generation operation plan, which optimizes the generated output of the generator hourly, daily, and yearly. The second part of the book, Chapters 4, 5 and 6, focuses on the investment and operation planning of the power network, which optimizes the variables active power P (including P_G and P_L), reactive power Q_G, voltage U, phase angle θ, transformer ratio T, capacitor bank C, and reactor bank R in hourly and yearly cycles. The third part of this book, Chapters 7 and 8, describes the power system control on small or large disturbances in a second and millisecond time cycle, which mainly optimizes variables such as the generator output P_G, the power angle δ of the generator, and the

system frequency f. The last part, Chapter 9, integrates the principles of microeconomics into the practical operation of the power system and establishes an optimal decision model for all the market participants based on the Nash equilibrium and the Walrasian general equilibrium.

Chapter 2 studies the optimization model of daily economic dispatch of a pump storage plant in a practical multiregional system in a province in China. This chapter describes how to optimize the arrangement for the generator output P_G within a daily cycle based on hourly intervals, of which the power output of each generating unit is treated as a continuous variable and pump storage output as a discrete variable. It proposes a mixed-integer programming (MIP)-based optimization model with both linear objective function and the constraints and two categories of variables (continuous and discrete). The MIP method is then used to solve the problem. The proposed model effectively optimizes the operation of the pump storage plant and meets all constraints, thus achieving the goal of shifting the peak load and filling the valley of the load curve. Therefore, it has a high relevance for the current smart operation of the power grid.

Chapter 3 focuses on the optimization model of the annual generator maintenance scheduling (GMS). This chapter describes how to optimize the arrangement for the generator output PG within an annual cycle based on hourly intervals. The GMS model based on fuzzy logic dynamic programming is proposed. Because GMS constraints (such as maintenance window interval, spare capacity, maintenance manpower, regional maintenance capability, and generator maintenance time) cannot be overlapped, the concept of a fuzzy set, which handles the boundary of the objective function and constraints of GMS, is used to obtain a more feasible solution for GMS. The objective function and constraint function in the GMS model are both linear functions whose variables are continuous variables. Knowledge based on expert systems is also used in the solution process. The method has been effectively applied to GMS problems in an actual provincial power system.

Chapter 4 deals with two types of new power flow models, ill-conditioned power flow and discrete optimal power flows, by way of construction of objective function and constraints. This chapter first describe how to develop a new power flow model based on the combination of the simulated annealing (SA) method and the Newton-Raphson power flow method. Then, it describes how to develop a discrete optimal power flow (discrete OPF) model by constructing a linear objective function with P_G, Q_G, U, and θ as constraints. The discrete OPF model is solved by the successive linear programming (SLP) based algorithm and the approximate mixed-integer linear programming algorithms, in which a method to change the increment of variables in the iterative calculation of the linear programming is applied. Both models have been successfully applied to practical power systems.

Chapter 5 addresses the models for minimizing load curtailment and maximizing load supply capability based on the DC power flow algorithm to optimize the load P_L, where U and θ are treated as constants. This chapter first describe how to develop the node load minimization

model of the node load curtailment in the event of faults, where node load curtailment (P_C) is a variable (node load P_L is a limit), and the objective function is to minimize the sum of node load curtailment P_C. Then, this chapter presents the maximizing load supply capability model of the node under the normal condition that the node load P_C is a variable, where the objective function is to maximize the sum of the node power supply and load P_L. Both models are applicable to the actual situation of urban power grids.

Chapter 6 studies the discrete optimal reactive power (VAR) planning (a mixed-integer nonlinear programming problem) models for some actual power systems. This chapter describes how to develop a discrete VAR planning optimization model based on successive linear programming (SLP), where the number "*C*" of the capacitor bank, "*R*" of the reactor bank, and "*T*" of the transformer tap ratio are treated as discrete variables, and the other variables (P, Q, U, and θ) are treated as continuous variables. First, a single state discrete optimal VAR planning model is given. Then, a multistate model with a shape of a block diagonal matrix is proposed, in which the corresponding decomposition coordination algorithm is also presented by decomposing, coordinating, and solving all states to minimize the total investment in reactive power equipment. This chapter also combines expert rules, fuzzy mathematical concepts, and GA algorithms with traditional optimization methods to improve the possibility of obtaining discrete solutions. The results of practical test systems show that the proposed algorithm can effectively solve the discrete optimization VAR problems of power systems.

Chapter 7 addresses the model of load frequency control under small disturbances. Based on the *Z*-transform load frequency feedforward control method, this chapter describes how to develop a model and algorithm for controlling the power angular acceleration of the generator in the given interval level of seconds to maintain the frequency of the generator. First, the power system load disturbance model is established by the identification method. Then, the system state estimators are constructed according to the hierarchical decomposition principle. Finally, the load frequency control rules are derived according to the invariance principle. Furthermore, this chapter also proposes three practical mathematical model transformation methods, such as the eigenvalue method, the logarithmic matrix expansion method and the successive approximation method, to make the transformation of difference equations into differential equations, and the mutual transformation of differential transfer functions. The results of simulation showed that the control method proposed can effectively control different types of disturbances in power systems.

Chapter 8 studies the local stability control problem of power systems under large disturbances. Based on the decoupling control method, this chapter introduces a new state space that can stably monitor the operation of the system based on local measurements without losing synchronization in the case of large disturbances, and provides rules to control the stability of the entire system in two stages with only locally applied stability control measurements.

In addition, this chapter has mathematically proven that the newly constructed state space is observable, decoupled, and topologically equivalent to the original state space of the system. Based on the two stage control criteria given in the chapter, new mathematical models for stage control and integrated computing processes have been developed. Finally, the chapter explores the realistic feasibility of the defined criteria and methodologies via the case study of the offline calculation.

Chapter 9 focuses on the decision-making model in the power market. This chapter studies the single commodity market with transactions of only active power and the multicommodity market with transactions of both active and reactive power, using the power pool mode. This chapter establishes an optimal decision model, and illustrates that this model and the competition equilibrium model are consistent in form. It indicates that the result of decision optimization has reached a competitive equilibrium. Based on the characteristics of the power systems, the accounting pricing method is used to distribute the loss of a power transmission network and the cost of transmission congestion reasonably among market participants. This eliminates market surpluses and avoids unfair posttrade distribution issues.

There are three appendices in this book. Appendix A describes the approximate algorithm for MIP (which has been applied in Chapters 4 and 6). Appendix B presents the derivation of the difference expressions for transformer T and shunt capacitor C in the optimization model proposed in Chapter 6. Appendix C introduces the derivation of the decoupling benchmark δ_{ei} proposed in Chapter 8 by using the DC power flow calculation method.

Finally, the authors gratefully appreciate the edification and inspiration of several respected mentors, the contributions of collaborators, as well as the participation of several graduate students, especially the assistance of Dr. Su Aoxue, who made the book more concise and more reflective of the authors' most innovative work. The authors are also particularly grateful to Dr. Liu Yunren, a retired engineer from the California Independent System Operator (CAISO) in the United States, who carefully read the manuscripts of the book and made valuable comments. The authors also thank to Dr. QianXin, who provided support on the English proof reading and promoted the publishing of the book.

The authors hope to help improve the professional skills of power engineers as well as senior undergraduates and graduates from the relevant universities in their work on the modeling technology of power system optimization.

Fan Mingtian
Zhang Zuping
Wang Chengmin
August 2017

CHAPTER 1

Introduction

Chapter Outline

1.1 General Ideas about Modeling

Many practical power system problems can be represented as mathematical models and sets of rules that connect the model's elements. Because of the mathematical model's good reproducibility, the inherent law of practical problems can be found via numerical algorithms. Therefore, it is necessary to study the model and algorithms of power systems in depth.

An appropriate approximation is reasonable for guiding practical theory. It is generally believed that, as long as human observation of practical problems reaches 10-6 orders of magnitude, it can meet actual needs of measurement. Beyond this limit, only theorists are interested. As the famous mathematician Klein has said, approximation mathematics is the very part of mathematics applied to practical applications, whereas precision mathematics is the solid framework on which approximation mathematics is built. Approximate mathematics is not "approximate mathematics" but "precision mathematics about approximate relationships." Therefore, the priority of modeling is to determine how to approximately solve a problem by taking advantage of the existing solvable conditions of the problem.

In modeling research of power system optimization, it is necessary to dialectically deal with the different types of variables, such as discreteness and continuous variables; the different types of models, such as linear and nonlinear; and the different types of algorithms, such as

Mathematical Models and Algorithms for Power System Optimization. https://doi.org/10.1016/B978-0-12-813231-9.00001-7

numerical or non-numerical procedures. To integrate more new elements and meet new development trends, new models should be developed using existing and newly developed methods based on the current computer technology to satisfy the actual requirements of the power system, which require a solid mathematical foundation and engineering background knowledge. The development of the power system optimization model is full of dialectic wisdom. The authors' main ideas are as follows:

(1) The optimization modeling is to transfer a practical problem into a mathematical problem and obtain a feasible solution for the practical problem considering the existing conditions. It has to fully consider the compromise among conflicting goals, such as the simple model versus the complex calculation procedure, and vice verse, nonlinear model versus linearized solution, and large-scale discrete optimization model versus the current computing condition.
(2) Whether the developed model is solvable must consider many problems from the theoretical perspective. For example, the problem with local solutions for any optimization algorithm, which can be avoided by the method of the multi-point search in the solution space. As for the nonconvex problem, there is a possibility of converting the model from nonconvex to convex by some recent researches. In addition, for some problems that cannot be solved by mathematical formulation, some non-numerical procedures could be successfully applied.
(3) What the top issue of numerical calculation is that an approximate solution with engineering precision can be obtained, by which the difficulty of the optimization model could be tested under the conditions without need of an analytical solution, and the consistency between the theoretical model and actual problem could be verified. However, because any numerical calculation method has its own limitation, the complex relationship between a theoretical model and a practical problem may be expressed by computer vision technology in the near future.
(4) The mutual transformation of mathematical models is very helpful for solving difficult problems, because mathematical models can be transformed into each other under such certain conditions, such as discrete and continuous, accurate and approximate, differential and difference, solvable and nonsolvable, convex and nonconvex, optimal and suboptimal, etc.

Solvability discussions about mathematical models are also explained in this book, such as search scope, initial point, the limit of the variables, and the range of the equations. Some special modeling techniques for practical engineering problems are also provided in this book. Some ideas are briefly given in the following, including ideas about how to set variables and functions, ideas about how to determine model types and algorithms. These modeling techniques have been implemented in the practical problems of this book and can be effectively applied to help solve power system optimization problems.

1.2 Ideas about the Setting of the Variable and Function

(1) Ideas about the variable in conventional power system analysis:
Two kinds of the basic components, single-ended and double-ended (which could also be briefly represented as node and branch), are included in power system analysis, in which the former can represent loads, generators, capacitors, reactors, and other grounded components, whereas the latter can represent lines, switches, transformers, and other branch components. The conventional calculation model of AC power flow for each node i is as follows:

$$P_{Gi} - P_{Li} - U_i \sum_{j \in i} U_j \left(G_{ij} \cos\theta_{ij} + B_{ij} \sin\theta_{ij} \right) = 0$$
$$Q_{Gi} - Q_{Li} - U_i \sum_{j \in i} U_j \left(G_{ij} \sin\theta_{ij} - B_{ij} \cos\theta_{ij} \right) = 0$$

where $\theta_{ij}=\theta_i-\theta_j$, which is the angle difference between node i and j. The assigned values include the load (P_L, Q_L), some generations (P_G, Q_G), and some voltages and phase angles (U and θ). That is, there are only two variables and two equations for each node.
The basic variables in the analysis and calculation for the steady-state of a power system can be classified into four types: active power, reactive power, voltage, and phase angle (namely: P, Q, U, and θ). Among them, active power and reactive power can be divided into active power generation and reactive power generation (P_G, Q_G), and active load and reactive power load (P_L, Q_L), respectively. Sometimes, the "P" and "Q" on the node can be considered as the corresponding impedance rather than the variable. In the transient calculation of a power system, besides the basic variables previously described, the power angle δ and the angular frequency or rotational speed of the generator $\omega = 2\pi f$ are also included (where f is the system frequency).
When all of P, Q, U, and θ are treated as variables, with their upper and lower limits added, the conventional optimization method can be applied to search for an optimal solution. In addition, all these variables can be subscripted to indicate changes over time (such as seconds, minutes, hours, months, or years). For example, the power generation output of unit (i) in a different time period (t) can be expressed as $P_{Gi}(t)$.

(2) The parameter and variable can be transformed from one to another:
If the parameters of components are taken as variables with upper and lower limits, then they can be adjusted in the optimization calculation. For example, if the expression of the transformers and capacitors, are expanded as variables with limits for the capacitor bank number C and the transformer tap ratio T, then they can be optimized by way of an optimization method.
The idea to optimize the parameters of the components is to taken component parameters as variables is to optimize the parameters of the components. However, in optimization

calculation models, the device parameters are usually given as constants or transformed into impedances, but they are rarely directly handled as variables. The general way to convert device parameters to variables is to transform $F(x_1, \ldots, x_n)=0$ to $F(x_1, \ldots, x_{n-1}, x_n(y))=0$, where $y=T$ or C.

(3) The variable and function can be switched from one to another.
There is one way to process variables as functions. For example, the traditional AC power flow equation previously given can be written as $F(x_1, \ldots, x_n)=g$, which can then be transformed to $F(x_1, \ldots, x_n)-g=0$, $F(x_1, \ldots, x_n, g)=0$, so the right hand side (the node injection power g) can be considered as a variable.

1.3 Ideas about the Selection of the Model Type

Under certain conditions, some model types can be mutually transformed into each other, such as discrete and continuous, differential and difference, linear and nonlinear, complex and simple, etc. Whatever deciding the model type, it is not only to pursue an accurate theoretical description but able to solve the practical problem. Mathematically, the model types depend on the relationship among the number of variables and constraints. The different models used in the static analysis of the power system, such as power flow, state estimation, and optimal power flow (OPF), depends upon the different relations among the number of equations and the number of variables.

(1) When the number of equations is equal to the number of variables
The traditional power flow model can be applied when the numbers of rows and columns in the coefficient matrix are equal. Many textbooks do not indicate the reason why the node type must be set up in the load flow calculation. In fact, there are only two equations (P balance and Q balance), however there are four variables (P, Q, U, and θ) for each node. Therefore, two of four variables must be fixed to satisfy the solvable conditions for which the number of equations and the number of variables must be equal. This method is called load flow (LF), in which some variables are specified and then the remaining variables can be solved. It generally can only be used to obtain feasible solutions, rather than optimal solutions.

(2) When the number of equations is less than the number of variables
The OPF model can be applied when the number of rows is less than the number of columns in the coefficient matrix. Therefore, the global optimal solution of the variable can be obtained by OPF in one solution procedure without needing to use the power flow program to approximate the optimal solution by point-by-point trial calculation. The correctness of the developed optimal calculation model (OPF model) can be verified by setting the upper and lower limits of some variables as the same value, that is, setting as the fixed value (the same as the specified value in LF calculation). Under such a condition, the same solution can be obtained by two methods to verify the correctness of the OPF model. This is discussed further in Chapter 4.

(3) The way to reduce solution difficulty
One way to simplify the model is to set up the auxiliary variables in different ways, which makes it easier for the optimization calculation to obtain the expected results. For example, to reduce the solution's difficulty, basic variables may be represented as constraints by decreasing the number of variables (in this case, the model would be more complicated). Another way to eliminate the need to develop different models for different operating conditions is to use virtual cost coefficients. For example, in Chapter 2, the virtual cost coefficient enables the pump storage unit to pump more water at the valley of the load curve, generating more power at the peak of the load curve.

(4) The way to select a model type for a large-scale problem
The control objects of a large-scale power system are widely distributed, but there is a closed coupling relationship among them. Centralized control makes it difficult to collect information from an entire system, whereas full decentralized control (using only local information) makes it difficult to achieve a global optimal solution. In addition, it is obviously uneconomical and unreasonable to achieve large-scale information exchange among the objects to be controlled in the power system. The problem could be solved by establishing a decomposition coordination model or a decoupling control observation model, that is, using hierarchical estimation or decoupling control methods. Under conditions where the search space is clear and small, stochastic optimization methods can also be applied.

1.4 Ideas about the Selection of the Algorithm

Available algorithms are prerequisites for optimization modeling. If the developed model is a standard one, then it can be solved the existing or standard algorithm, otherwise it is necessary to develop a new calculation method. In the procedure of formulating the model, we should especially consider to formulate whether simple or complex model. The simple model has to deal with complex results, whereas the complex model only needs to handle simple results. Some ideas about the selections of the algorithm, including models versus results, use of the standard solution tools, local solutions and future expectations, are explained as follows:

(1) Considerations of compromises for models versus results
If an approximated continuous algorithm is adopted, then there are many existing algorithms, by which the calculation complexity could be reduced. However, the complexity of the solution in a practical application is increased because the variables are continuous rather than discrete. Thus, the solution in this way can not satisfy the practical needs. This example explains the relationship between a simple model and complex results. If a discrete model is to be considered when formulating the model, then there is no ready-made algorithm, which will significantly increase the calculation complexity. However, the complex algorithm could derive a straightforward integer solution, and the calculation result would not require further processing, which is the relationship between a complex model and simple results.

(2) Considerations for the use of the existing solution tools
A linear programming-based algorithm can be applied because many excellent software packages are available. To solve large-scale optimization problems, it is better to take advantage of the existing calculation conditions, because the computing time is related to the dimension of the models. From a mathematical perspective, a linear programming method is normally suited for the problems of large-scale power systems.
A large-scale discrete optimization algorithm is difficult to solve even with today's rapid advancement of computer performance. From a point of pure mathematics, the states of all of the equipment in a power system—with its hundreds to tens of thousands of nodes—needs to be represented with integer variables, which makes the calculation time to be difficult to bear. Therefore, it becomes necessary to develop approximation integer programming algorithms based on the existing software packages, so that discrete optimization calculations for a large-scale power system becomes possible.
A nonlinear optimization method also requires a practical approximation algorithm. Some nonlinear models of power system optimization are derived by a linearization method, of which some variable coefficients are derived from the first and second derivative of the transcendental functions of the power flow equation. The precondition for a derivative-based optimization algorithm is that these transcendental functions are continuously differentiable, which is a very hard condition even if difference function is proved to be able to approximately represent differential function. In practice, it's been proven that some approximation processing methods based on the existing software packages can also satisfy the requirements of engineering precision.

(3) Considerations for the local solution
Any optimization algorithm has a problem of the local solution. Optimization algorithms can be divided into two categories, namely, numerical and non-numerical method. However, both methods have a problem with local solutions, that is, the optimal point can only be obtained around the current starting point. For example, the method for calculating the discrete reactive power optimization model is based on a successive linearization method. However, considering the discrete variable, the model cannot guarantee convexity. As for nonconvex optimization, different initial values may give different solutions.
An expert system approach could help screen and filter some obviously unreasonable optimization search directions. Some actual problems cannot be solved by analytical mathematics but may be solved with an expert system approach. For instance, in discrete reactive power optimization, the expert system approach could help determine the direction of continuous variable truncation, so as to derive the integer feasible solution more quickly. A combination of the stochastic searching method, expert system approach, and traditional analytical algorithm could significantly reduce calculation time and obtain a reasonable discrete solution, efficiently processing the integer variables for some practical optimization problems.

The stochastic optimization algorithms could avoid optimization around the local points, by which further improvement of the objective function of the optimization model could randomly restart from many directions. The genetic algorithm and simulated annealing method are the typical stochastic optimization algorithms that attempt to consider optimization from a biological or physical point of view rather than from an engineering point of view. The process of biological evolution is a process of survival of the fittest, whereas the process of metal sintering annealing is a process of changing the lattice structure and raising the metal strength. Both algorithms can avoid optimizing around the local points but with multipoint searching in the solution space, so as to obtain the global optimal point. Furthermore, these algorithms do not require such conditions: the objective function and constraint function should be continuous.

(4) Considerations for the future expectations
The complex relationship between the variables and models for the actual problems is expected to be expressed by some new technologies in the near future. With the invention and development of artificial intelligent and computer vision technology, it is possible to understand the relationship that is not intuitive and convert the original nonvisual problem into a visual image, which provides us with vivid and intuitive perceptual materials, allows us to understand the complex process, and inspires researchers to form scientific conjectures and viewpoints, to make theoretical creations. Therefore, the use of simple computer simulations to obtain the complex relationship between theoretical models and actual problems is expected.

1.5 Ideas about the Applications of Artificial Intelligence Technology

Although most optimization algorithms involve complicated mathematics and logic, nearly every optimization method involves a smart imaginative step to find the best solution by comprehensively analyzing the solvability, such as search scope, initial point, the type of the variables, and the range of the equations.

Generally speaking, optimization mathematics is complicated, but the application of the concept is very simple. There are many modeling methods to obtain optimal solutions in nature, such as human evolution, insect behavior, and steel cooling processes, which can be mathematically used to form new algorithms.

AI (Artificial Intelligence) and big data technologies have become very important tools in recent years. In terms of applications in the field of optimization, they are actually composed of several different non-numerical methods that can be used to build a set of rules and not just rely on smart imagination and experience. This book has many examples of initiatives in the field of AI based on human experience and manual approaches or natural methods that help to solve the problems in a reasonable way by computers (heuristics method).

As for data processing and mining, the logic and rationality of the original input data need to be considered, because if there is no logical relationship among the data, then the data is meaningless like sand, even for huge amounts of data. This is a prerequisite to obtain a feasible solution for the optimization calculation. For the original information processing, this book proposes a method to confirm a solution space for linear programming to avoid no solution (Chapter 2), proposes a mathematical conversion model between different interval measurements to reduce the measurement data (Chapter 7), and demonstrates the equivalence between local information and global control to ensure the effectiveness of local control (Chapter 8).

As for the applications of AI technology in this book, the stochastic search algorithm is applied as a nonnumeric and integer method, which is used to relax the hard boundaries of variables and equations and form a better starting point. Since Simulated Annealing (SA) method can be used to represent nonlinear, mixed integer problems, this book combines it with the Newton-Raphson method to create new algorithms to solve nonlinear power flow problems (Chapter 4). Since Genetic Algorithm (GA) is a random search algorithm with the ability to obtain a global optimal solution, it is a nonnumeric and integer method, and can be used to search for better integer solutions. This book combines the expert rules, fuzzy mathematical concepts, and GA algorithms with traditional optimization methods to improve the possibility of obtaining discrete solutions (Chapter 6). Since the expert rules can be used to create a knowledge base, this book uses it to accumulate the experience of operational personnel to improve the efficiency of a generator maintenance scheduling (GMS) solution (Chapter 3).

CHAPTER 2

Daily Economic Dispatch Optimization With Pumped Storage Plant for a Multiarea System

Chapter Outline

Mathematical Models and Algorithms for Power System Optimization. https://doi.org/10.1016/B978-0-12-813231-9.00002-9

2.1 Introduction

2.1.1 Outline of the Problem

The daily economic dispatch problem in this chapter focuses on an actual multiarea system with many hydrothermal plants and a pumped storage plant. It may be simplified as daily economic dispatch optimization with pump storage plant. The pumped storage plant normally operates as a pump on the duration of off-peak load and as a generator on the duration of peak load.

The studied system consists of six areas, including east, west, south, north, and central areas, along with the power outsourcing purchase area (defined as the purchase area) in a purchase agreement. The power grids in each area within the province are connected with tie lines, presenting the problem of joint economic operation and dispatch among multiareas. The provincial power grid is characterized by a large pumped storage plant in the country, so its regulation capacity plays an important role in daily economic dispatch.

The generated output plan for the plants in each area needs to be considered, avoiding the overload on tie lines among the six areas. There are 27 power plants in the provincial system, among which there are 14 thermal plants, 7 hydroplants, and 1 pumped storage plant. This system consists of 82 units, of which there are 50 thermal units, 23 hydro units, 2 purchase units, and 4 pumped storage units. The total installed generation capacity is 13,179 MW (refer to Table 2.1). The property rights vary from different types of power plants. There are Power Purchase Agreements between the provincial power grid and five purchase power plants, that is, Tianshengqiao Power Plant, Guangxi Power Purchase, Guizhou Power Purchase, Yunnan Power Purchase, and Zhongdian Power Purchase. For these power plants to complete their plan of generated output and energy, the power grid needs to consider the existing agreements with these power plants.

The basic interconnection relationship of the provincial power grid is shown in Fig. 2.1. Briefly, there are N areas and M tie lines in the provincial power system, including M_1 hydropower plants (each plant has N_{1i} units), M_2 thermal power plants (each plant has N_{2j} units), and M_3 pumped storage plants (each plant has N_{3k} units).

The power generation characteristics of thermal and hydropower plants should be considered in the daily economic dispatch schedule of pumped storage, for example, during 24 h in a day, the hydropower plant may start or stop at any time, the run-of-river hydropower plant could generate power only in a given period, and the thermal power plant must satisfy the limitations on interval between startup and shutdown time. The characteristics of the pumped storage plant should be also fully considered, that is, during 24 h in a day, it generates power during the peak periods and pumps water during the valley periods. There is a large difference between peak and valley loads in the province (around 4000 MW), as shown in Fig. 2.2. If the pumped storage plant (a total installed capacity of 1200 MW) can be fully utilized in peak load shifting, the

Table 2.1 Basic composition of generating units in a provincial power grid

Area	*T* Plant	*H* Plant	*P* Plant	Total Plant	*T* Unit	*H* Unit	*P* Unit	Total Unit	*T* Install (MW)	*H* Install (MW)	*P* Install (MW)	Total Install (MW)
Purchase	Equivalent plant			**5**	Equivalent unit			**5**	Purchase power			**740**
East	2	4		6	5	14		19	825	669		1494
South	1			1	4			4	1200			1200
West	2			2	6			6	800	60		860
North	2	3		5	12	9		21	800	195		995
Middle	7		1	8	23		4	27	6690		1200	7890
Total	14	7	1	27	50	23	4	82	10,315	924	1200	13,179

Note: *T*: thermal; *H*: hydro; *P*: pump.

power supply reliability of the whole power grid can be improved. The economic performance of the daily dispatching plan will be fully exploited.

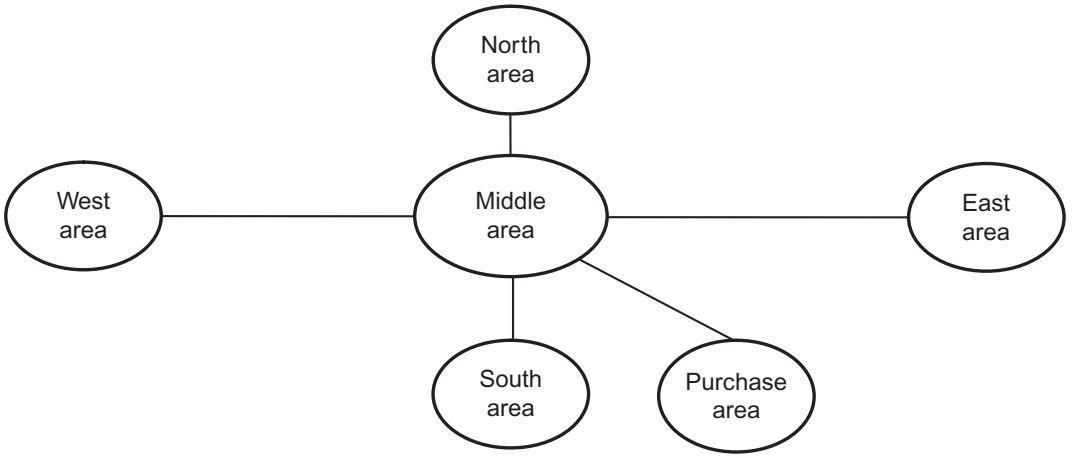

Fig. 2.1
Basic interconnection relationship of a provincial power grid.

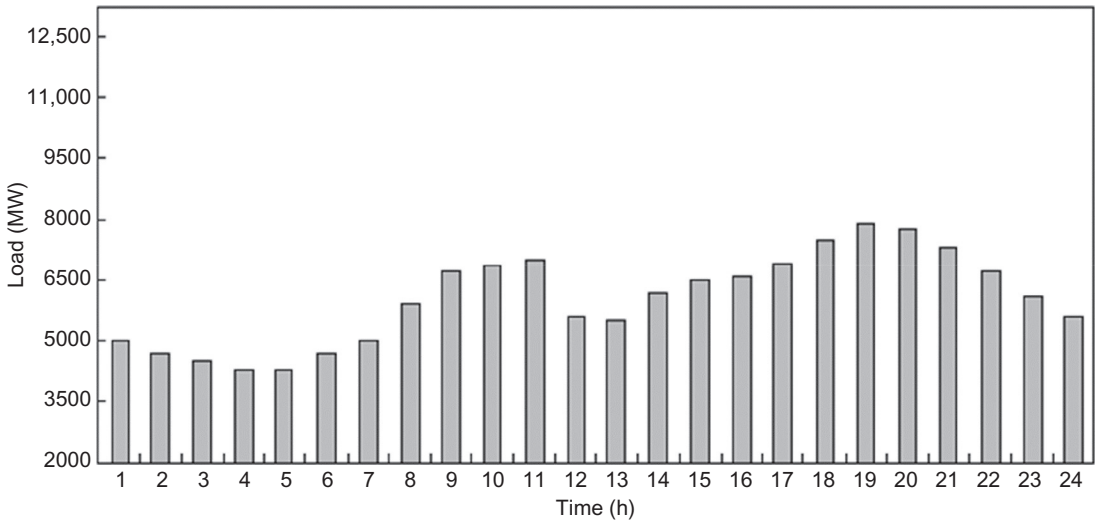

Fig. 2.2
The typical daily load curve in the province.

2.1.2 Basic Requirements of Pumped Storage Plant Operation

There is a big difference between the peak and the valley loads during day and night in the provincial power grid. Take the actual load curve of a certain day as an example; the peak load is 7000 MW and the valley load is 4350 MW, therefore, the leading peak-valley

difference is 2650 MW and the average load is 5244 MW. To ensure the security and overall economic efficiency of the power system operation, some units have to be started up or shut down. However, even a 20 MW conventional coal-fired thermal power unit requires about 10 h to recover from shutdown to full loading operation. Therefore, if this thermal power unit is used to regulate peak load, the system capability of tracking the load variations would be very poor.

To adapt to the large load variations from 2000 to 4000 MW within the normal upper and lower output limits of all generation units, some more units shall be started up during the peak load period yet some units will have to be shut down during valley load period. However, the economic efficiency of units is often poor because of the startup and shutdown operations. Moreover, there may be many startup and shutdown combinations with units in different time periods, making it impossible to guarantee the overall economic efficiency of the units' operation. Therefore, the peak regulating capacity of the pumped storage plant must be fully utilized to shift the peak load and reduce the number of startups and shutdowns of thermal power plants, so as to improve the overall economic efficiency, security, and rationality of the power system operation.

The load variations of the power system can be represented by the minimum load rate $P_{\min}/P_{\max}$ (where $P_{\min}$ represents the minimum load and $P_{\max}$ the maximum load) and average load rate $P_{\text{ave}}/P_{\max}$ (where P_{ave} represents the average load). Generally, the minimum load rate is expected to be larger than 0.7–0.75, and the average load rate larger than 0.85–0.9. If the peak load is only regulated by the thermal units, the installed capacity should be more than the difference between $P_{\max}$ and $P_{\min}$. If the peak load is regulated by the pumped storage plant, the installed capacity just has to meet the difference between P_{avep} and $P_{\max}$ (where P_{avep} represents the average load after putting pumped storage plant into operation), of which P_{avep} may be slightly larger than P_{ave}. Generally, the installed capacity of the pumped storage plant is required to be 3%–6% of the total installed capacity in the system, or about one-third of the peak-valley load difference, then the remaining load variation is easily regulated by thermal units.

Therefore, when analyzing the economic efficiency of a pumped storage plant, the combination of the thermal power plants used for base load and the pumped storage plant used for regulation should be considered, rather than simply using the same peak load regulating capacity to compare the economic efficiency of the pumped storage plant and thermal power plant. Generally, the comparison can be made based on the equivalent peak load regulating capacity by the two methods outlined as follows:

(1) Comparing the generating costs of the equivalent peak load: according to the calculation of the unit cost of power generation from the pumped storage units and thermal power peak load regulating units with peak load of 1500 h per year in China, the ratio (ratio = cost of pumped storage/cost of thermal generation) is 63% and 70%, respectively, in Guangdong.

(2) Comparing the pumped storage plant and the peak load regulating unit of thermal power plant: the economical nature of pumped storage plants is that they have higher efficiency than that of the replaced thermal unit for peak load regulating. When compared to the economic efficiency of the pumped storage plant, it is also necessary to consider how much it can be matched with the base-load capacity.

Taking the province's daily peak-valley load difference as 4000 MW as an example, if the peak load is regulated by the pumped storage plant, the plant needs to have 1200 MW installed capacity, which is about one-third of the peak-valley difference. Thus, it can basically meet the demand of peak load shifting and give full play to the economic benefits of the daily dispatch schedule of the power grid. As for the capacity allocation of storage devices in the distributed power generation system, the difference of peak-valley daily load and the variations of generator outputs must be fully considered.

Generally, it just takes 100–200 s for pumped storage units to generate power from a stopped state to full load. The units have the characteristics of fast startup speed and power generation. Normally, the electricity price in the peak period is several times higher than that in the valley period. The valley price is charged for power consumption of a pumped storage plant while pumping water, whereas the peak price is paid for the power generation of the pumped storage plant. Thus, besides the technical factors, peak load regulating with the pumped storage units in the power grid will bring more efficient economic benefits.

Although the pumped storage units have a significant peak load regulating capacity, in actual operation the pumped storage power plant must also meet a series of constraints, such as the initial and end reservoir storage, the maximum and minimum operating storage per hour, etc. Similar to the constraint of a storage battery's charge-discharge period, the pumping status variable of a pumped storage plant must be an integer. Therefore, considering the regional operation characteristics of the province's power grid, coupled with the limitations of various operational constraints, the mathematical model obtained is a large-scale mixed-integer programming model. It is necessary to select a reasonable and feasible algorithm to solve these large-scale pumped storage daily economic dispatch optimization problems.

2.1.3 Overview of This Chapter

This chapter studies the optimization model and algorithm for daily multiarea economic dispatch with a pumped storage plant based on the mixed-integer programming. The objective of the study is to improve the optimization theoretical knowledge and computer technology application in daily economic dispatch.

This chapter not only introduces the proposed mathematical model and algorithm but also presents the basic ideas of the modeling process, which is to transform the practical problems of complicated multihydro and multithermal power plants and multiarea operations into a

standard mixed-integer programming mathematical model. In the model, both objective function and constraint function are linear, and there are two kinds of variables: continuous variables (output of hydropower and thermal power units) and integer variables (output of pumped storage units), each with a large calculation scale. The model in this chapter can effectively optimize the operation of the pumped storage unit, achieve the purpose of peak load shifting, and provide great reference to the intelligent operation of a power grid with energy storage devices.

Section 2.2 specifically presents the basic ideas of optimization modeling for reference. Section 2.3 proposes the optimization mathematical model for daily economic dispatch of a pumped storage plant. Section 2.4 introduces the preprocessing work required before the optimization calculation. Section 2.5 introduces the optimization algorithm and processes. Section 2.6 first uses a small-scale example to verify the proposed optimization model and algorithm, then presents and analyzes the detailed results of a large-scale practical system.

2.2 Basic Ideas of Developing an Optimization Model

A daily multiarea economic dispatch making use of the capacity of a pumped storage plant should satisfy all related constraint conditions so as to ensure that the total power generated in each hour by different power plants in the multiarea system can satisfy the total load of the system (in each hour), and make the best use of the pumped storage plant's capacity. The practical problem should be firstly described in a familiar mathematical language before it is transformed into a mathematical problem.

The daily multiarea economic dispatch with a pumped storage plant is expressed in mathematical language as follows: to satisfy the daily load demand (24 h) of the whole system, the objective is to minimize the total generating cost of all generating units, while subjecting to satisfy all kinds of constraints, such as hourly load balancing, hourly output schedule of each area, hourly output of power plant and daily power energy schedule, hourly output limit of each unit, and hourly limits of generated output and water quantity for the pumped storage plant, as well as limits of initial water quantity and final water quantity for the pumped storage plant.

In general, based on practical operation conditions, the seemingly complicated practical problem shall be transformed into a standard mixed-integer programming mathematical model, in which both objective function and constraint function are linear ones. The objective function is unit piecewise linear cost function. There are two kinds of variables: continuous ones and integer ones. All variables of generating unit outputs are continuous ones.

The concrete ideas and processing methods about how to develop a mathematical model by converting the physical problem into brief mathematical expressions (objective function and constraints) are given as follows, as well as the method how to transform the pumping variables of the pumped storage plant into integer variables.

2.2.1 Way of Processing Objective Function

As previously mentioned, the problem of the daily multiarea economic dispatch with pumped storage plant is to minimize total fuel costs under the condition of satisfying all security operations, using the specific peak regulation capacity of the pumped storage plant as rationally as possible. Minimizing total fuel costs means that, on the premise of assuring system security, as few generating units as possible of the thermal power plant shall be put into operation, whereas as many generating units as possible of the hydropower plants and pumped storage plant shall be put into operation. Because the problem will be formulated as a minimization problem of a linear programming, where the total cost is equal to the sum of $c_i{}^*x_i$, the basic idea of setting a cost coefficient is to make the decision variables x_i contribute to the total cost as minimally as possible within the feasible solutions; the details are explained as follows:

(1) Setting of cost coefficient for units of thermal power plant: the practical startup and shutdown cost coefficients of thermal units in the different periods are directly used (i.e., c_i is set as the positive value), by which the decision variables x_i of thermal units will make the total cost as minimally as possible within the feasible solutions (the output of thermal units will certainly be as small as possible).

(2) Setting of cost coefficient for units of hydropower plant: the startup and shutdown cost coefficients of hydro units in different time periods are basically ignored (i.e., c_i is set as zero for the generating costs of hydro units), by which the decision variable x_i of the hydro units will not have any impact on the total cost within the feasible solutions (the output of hydro units will certainly be as large as possible).

(3) Setting of cost coefficient of units of pumped storage plant: with the objective to make the pumped storage plant pump more water at the valley load and to generate more electricity at the peak load, so as to smooth the equivalent load curve after the optimization calculation, the concept of virtual pumped storage cost coefficient is introduced, which is calculated through the following steps:

    1. Calculate the average load of the given load curve.
    2. Calculate the difference sequence between the given load curve and the average load.
    3. Take the negative value of the difference sequence as the cost coefficient of the pumped storage plant under pumping conditions.
    4. Take the minus of the positive value of the difference sequence as the cost coefficient (c_i is a negative value for pumped storage plant under the specific generating conditions).

       Because the virtual cost coefficient of the pumped storage plant is a negative value (less than zero), which could automatically reduce the value of the objective function when solving the linear programming, the larger peak-valley load difference, the less the objective function value. Therefore, within the feasible solutions, the pumped

storage plant will operate at peak and valley periods as long as possible, so as to better shift peak load, thus improving the economic efficiency, operation security, and stability of the overall power system.

2.2.2 Way of Processing Variables and Constraints

The basic steps to develop a mathematical model are to introduce the number of key variables as few as possible, so as to reduce the complexity of the solution algorithm, by which to form an expression of constraints that can reflect the physical meaning. The basic idea of developing a mathematical model is to avoid introducing excessive variables, so as to reduce the complexity of the solution algorithm; based upon the variables, constraints have to be analyzed from physical meanings to mathematical expressions. However, the number of variables and constraints shall be matched, because linear programming basically requires the number of variables to be larger than that of its constraints.

Generation output of units is determined as the most crucial variable of the mathematical model, which must satisfy the upper and lower limits in various time periods through an analysis of the problem of daily multiarea economic dispatch with a pumped storage plant. By contrast, although other outputs of power plants and areas, and power plant generating capacity also have to satisfy their respective upper and lower limits, all of them can be indirectly derived by summing up the generation output of all units in various time periods.

The constraints for practical operation through the analysis of the problem are defined as follows:

(1) Constraints of all plants: hourly load balancing in a day, hourly output of all areas in a day, hourly output of all plants, total generated energy of all plants in a day.
(2) Constraints of the pumped storage plant: hourly reservoir capacity, reservoir water balancing, generation output, and pumping output. As previously mentioned, the most crucial variable is generation output of units. As long as the identification of areas and plants where generation units belong are given, the total output of generating units in different areas or in various time periods can be summed up, respectively.

On the basis of taking the generation output of respective units as the key decision variable, other constraints are processed as follows:

(1) Constraints for hourly load balancing in a day: basic expression is that hourly generation is equal to hourly load. That is, sum up the generation output of all units in each hour, then make the summation equal to the forecasted value of the daily load in each hour.
(2) Constraints for output of all plants in each hour: basic expression is that the sum of unit generation daily is within the given limits. That is, sum up the total generation output of all units of each plant in each hour, then make the summation satisfy the upper and lower limits of the power plant.

(3) Constraints for total generated energy of all plants in a day: basic expression is that daily total generated energy of plants is within the given limits. That is, sum up the total generation output of all units in all power plants within the total time period (one day), then make the sum satisfy the upper and lower limits of the power plant generating capacity.
(4) Constraints for output of all areas in each hour: basic expression is that area generation is within the given limits. That is, sum up the total generation output of all units in all power plants of all areas in each time period, then make the sum satisfy the upper and lower output limits of the area.
(5) Constraints for reservoir capacity of pumped storage plant in each hour: basic expression is that hourly reservoir capacity is within the given limits. To satisfy the starting and ending capacity of each day, the pumped storage plant must satisfy the reservoir capacity constraint in each hour in operation. On the basis of transforming water balancing into power balancing for the pumped storage plant, first, obtain the former by summing up the generation output of all units of the pumped storage plant in each time period, then obtain the later by adding up the pumping output of all units of the pumped storage plant in each time period. Finally, obtain the difference between the former and the latter, which have to satisfy the upper and lower limits of the reservoir capacity of the pumped storage plant in the time period. Based on operational requirements, the output of a pumped storage plant in each hour must be one of 0, 165, 330, 495, 660, 825, 990, 1155, and 1320 MW.
(6) Constraints for daily reservoir water balancing of the pumped storage plant: basic expression is that hourly reservoir water is within the given limits. With reference to the method of processing reservoir capacity, first, obtain the total generation output of all units of the pumped storage plant in the total time period (one day), then obtain the total pumping output of all units of the pumped storage plant in the total time period (one day), and finally calculate the difference between total generation output and total pumping output, which have to satisfy the daily reservoir water quantity difference of the pumped storage plant in one day.

Based on the actual situation in the provincial power grid, in terms of calculation scale, the number of areas is 6, the number of power plants is 30, the number of units is 100, and the number of time periods is $24D$ ($D = 1, 2, 4$, i.e., $D = 1$ for one point in 1 h, $D = 2$ for one point in 0.5 h, or $D = 3$ for one point in 20 min, to describe load). Correspondingly, the number of constraints shall be less than 3000, and the number of continuous variables shall be 2400–7200. The pumping condition of pumped storage units is transformed into an integer variable. The corresponding number of discrete variables shall be 24–72.

Due to the large calculation scale with many discrete variables, it is difficult to choose a calculation method for the studied problem. After the following special processing, the number of integer variables may be greatly reduced from 24–72 to 9–27. The detailed processing method is introduced as follows:

2.2.3 Way of Processing Integer Variables for Pumped Storage Plant

Setting the power consumption under the pumping condition P_{pp} is a discrete integer variable: the power consumption for pump water P_{pp} should be an integer variable based on practical needs, which should be selected within nine options such as 0, 165, 330, 495, 660, 825, 990, 1155, or 1320 (MW). If such nine options are taken as 0–1 variables, then there should be nine 0–1 variables in each time period. That is, $24D$ time periods require $9 \times 24D$ variables, $9 \times 24D$ ($D = 1, 2, 3$), which means if P_{pp} should be represented by 0–1 variable, the number is up to 216–648. Such a huge number of integer variables, together with thousands of continuous variables, makes optimization a very complex mixed-integer problem. There should be some other ways to deal with the integer variables as follows:

$$P_{pp}(t) = 0, 165, 330, 495, 660, 825, 990, 1155, 1320 \text{MW}.$$

(1) Let Y_p represent an integer variable with the range of 0–9 and with the unit step of 1. When $Y_p = 1$, then P_{pp} is 165, and when $Y_p = 2$, then P_{pp} is 330. Therefore, the number 165 can be used as the coefficient of variable $Y_p(t)$, and the following equation can be used to represent $P_{pp}(t)$:

$$P_{pp}(t) = 165 Y_p(t), Y_p(t) = 0 - 9.$$

(2) Setting the operating period of pumped storage plant: as the pumping power and generation power may be alternatively changed in a very short time, this model does not consider its continuous operation time limit in the calculation process. Based on the changing tendency of the load curve, the operating period of a pumped storage plant can be divided into three periods in advance based on the limits for $Y_p(t)$ and $P_{pg}(t)$: storage period [the upper limit of $Y_p(t)$ is not 0], generation period [neither the upper nor lower limit of $P_{pg}(t)$ is 0], and stop period [the upper limit of $Y_p(t)$ is 0, and the upper and lower limits of $P_{pg}(t)$ is 0].

2.3 Formulation of the Problem

Based on the considerations for the optimization modeling previously mentioned, as well as the processing methods for objective function, constraint conditions, continuous variables, and integer variables, and by setting up notations for various variables, the mathematical model of daily multiarea economic dispatch with a pumped storage could be easily formulated. To illustrate the correctness and feasibility of a developed mathematical model, it is necessary to form the basic structure of a constraint matrix based on the mathematical model and provide an example of the small-scale mathematical model on which verification calculation can be performed. In the following sections, the details of notations, mathematical models, and basic structure of constraint matrixes are given.

2.3.1 Notations

See Table 2.2.

Table 2.2 Mathematical notations

Notation Name	Description	Notation Name	Description
i	Unit number	NP	Set of power plant j
j	Power plant number	N_{PLANT}	Total number of power plants
t	Time period	N_{AREA}	T number of areas
N	Total number of units	N_k	Set of area k
T	Total number of time periods	$P_{pg}(t)$	Generated output of pumped storage plants in time t MW, continuous variable
$C_i(t)$	Cost of unit i in time period t	$P_{PP}(t)$	Pumping output of pumped storage plant in time t MW, discrete variable
F_i	Fixed cost of unit i	$Y_p(t)$	Pumping step of pumped storage plant in time t Discrete variable
$X_i(t)$	Power output of unit i in time t, continuous variable	$P_{i\max}$, $P_{i\min}$	Output limits of unit i
$Y_i(t)$	Fixed power output of unit i, 0, 1 variable	$P_{pg_{max}}$, $P_{pg_{min}}$	Generated output limits of pumped storage plant
$PL(t)$	Load in each time t, MW	$P_{PP_{max}}$	Upper limit of pumping output for pumped storage plant
W_0	Initial water quantity of pump storage plant, 10,000 m^3	$P_{PP_{unt}}$	Unit capacity of pumping output for pumped storage plant
W_{24}	Ending water quantity of pumped storage plant, 10,000 m^3	SA_j, SI_j	Generated output limits of power plant j
W_{min}	Minimum water storage quantity of pumped storage plant, 10,000 m^3	SAT_j, SIT_j	Planned energy limits of power plant j
W_{max}	Maximum water storage quantity of pumped storage plant, 10,000 m^3	AA_k, AI_k	Generated output limits of area k

2.3.2 Basic Expression of the Optimization Model

A practical optimization problem after reorganization can be formed as the following standard mathematical programming model.

Problem P:

$$\min f(X, Y) \tag{2.1}$$

$$\text{s.t. } g(X, Y) = 0 \tag{2.2}$$

$$h(X, Y) \leq 0 \tag{2.3}$$

$$X_{\min} \le X \le Y_{\max} \tag{2.4}$$

$$Y_{\min} \le Y \le Y_{\max} \tag{2.5}$$

where Eq. (2.1) is a linear objective function, Eq. (2.2) is an equality constraint, Eq. (2.3) is an inequality constraint, Eq. (2.4) is a continuous variable constraint, and Eq. (2.5) is a constraint with integer variables. Problem P is a standard mixed-integer programming model, which can be solved with a standard mixed-integer programming method. If integer constraint Eq. (2.5) is relaxed, then the model can also be solved with a standard linear programming method, so that an approximate optimal solution can be efficiently obtained.

Daily multiarea economic dispatch optimization with a pumped storage plant is designed to minimize total fuel cost of a system under certain constraints, so as to make full use of the peak regulating ability of the pumped storage plant. The calculation cycle of the daily dispatch schedule with a pumped storage plant is $24D$ ($D=1$, 2, 4, when $D=1$, time interval $=60$ min, $D=2$, time interval $=30$ min, $D=4$, time interval $=15$ min) periods, where both objective function and constraint functions are linear functions, and the variables are divided into continuous and integer ones, so the following programming model can be formed:

Problem PZ:

Linear objective function

$$\min \sum_{i=1}^{N} \left[\sum_{t=1}^{T} C_i(t) X_i(t) + F_i Y_i \right] \tag{2.6}$$

Constraint equations:

(1) Load balance constraint in each time period (equality constraint with the total number of $24D$, $D=1$, 2, 4)

$$\sum_{i=1}^{N} X_i(t) + P_{\text{pg}}(t) - 165 Y_{\text{pp}}(t) = PL(t), \quad t = 1, \ldots, 24D \tag{2.7}$$

(2) Generated output constraint of each plant in each time period (inequality constraints with the total number of $N_{\text{PLANT}} \times 24D$)

$$SI_j \le \sum_{i \in NP} X_i(t) \le SA_j, \quad j = 1, \ldots, N_{\text{PLANT}}; \quad t = 1, \ldots, 24D \tag{2.8}$$

(3) Generated energy constraint of the power plant in each time period (inequality constraints with the total number of N_{PLANT})

$$SIT_j \le \sum_{i \in NP} \sum_{t=1}^{24D} X_i(t) \le SAT_j, \quad j = 1, \ldots, N_{\text{PLANT}} \tag{2.9}$$

(4) Generated output constraint of areas in each time period (inequality constraints with the total number of N_{AREA})

$$AI_k \le \sum_{i \in Nk} X_i(t) \le AA_k, \quad k = 1, \ldots, N_{\mathrm{AREA}}; \quad t = 1, \ldots, 24D \tag{2.10}$$

(5) Reservoir capacity constraint of the pumped storage plant in each time period (inequality constraints with the total number of $24D$)

1. Original expression of reservoir capacity constraint

$$\begin{aligned} W_{\min} - W_0 \sum_{t=1}^{T} \le P_{\mathrm{pp}}(t) \cdot PPC - \sum_{t=1}^{T} P_{\mathrm{pg}}(t) \cdot PGC \le W_{\max} - W_0, \\ t = 1, \ldots, 24D; \quad n_t = 1, \ldots, 24D \\ W_0 - W_{\min} \ge \sum_{t=1}^{24D} P_{\mathrm{pg}}(t) \times 870 - \sum_{t=1}^{24D} P_{\mathrm{pp}}(t) \times 640 \ge W_0 - W_{\max} \end{aligned}$$

where PPC and PGC are transformation coefficients for water reserve/generated energy during water pumping and power generation.

$$\begin{aligned} PPC &\approx 0.64 \text{ m}^3/\text{kWh} = 0.64 \times 10^3 \text{ m}^3/\text{MWh} = 640 \text{ m}^3/\text{MWh} \\ PGC &\approx 0.87 \text{ m}^3/\text{kWh} = 0.87 \times 10^3 \text{ m}^3/\text{MWh} = 870 \text{ m}^3/\text{MWh} \end{aligned}$$

2. Final expression of the reservoir capacity constraint of the pumped storage plant

$$(W_0 - W_{\max})/640 \le \sum_{t=1}^{24D} P_{\mathrm{pg}}(t) \times 1.36 - \sum_{t=1}^{24D} 165 Y_{\mathrm{p}}(t) \le (W_0 - W_{\min})/640 \tag{2.11}$$

(6) Water quantity balancing constraint of the pumped storage plant in each time period (equality constraints with the total number of $24D$)

1. Original equation of water balancing constraint

$$\sum_{t=1}^{24D} P_{\mathrm{pp}}(t) \cdot PPC - \sum_{t=1}^{24D} P_{\mathrm{pg}}(t) \cdot PGC = W_{24} - W_0$$

2. Final water quantity balancing expression of the pumped storage plant (transfer water quantity balance into pump generation balance)

$$\begin{aligned} \sum_{t=1}^{24D} P_{\mathrm{pg}}(t) \times 870 - \sum_{t=1}^{24D} P_{\mathrm{pg}}(t) \times 640 = W_0 - W_{24} \\ \sum_{t=1}^{24D} P_{\mathrm{pg}}(t) \times 870/640 - \sum_{t=1}^{24D} Y_{\mathrm{p}}(t) \times 165 = (W_0 - W_{24})/640 \end{aligned} \tag{2.12}$$

(7) Generated output constraint of each unit in each time period (continuous variable constraints with the total number of $N \times 24D$)

$$P_{i\min} \le X_i(t) \le P_{i\max} \tag{2.13}$$

(8) Generated output constraint of the pumped storage plant in each time period (continuous variable constraints with the total number of $24D$)

$$P_{\mathrm{pg}_{\min}} \le P_{\mathrm{pg}}(t) \le P_{\mathrm{pg}_{\max}} \tag{2.14}$$

(9) Pumping output of the pumped storage plant in each time period (integer variable constraints with the total number of $24D$)

1. Initial expression

$$0 \le P_{\mathrm{pp}}(t) \le P_{\mathrm{pp}_{\max}}$$

2. Final expression

$$\begin{aligned} 0 \le Y_{\mathrm{p}}(t) \le Y_{\mathrm{p}_{\max}} \\ Y_{\mathrm{p}_{\max}} = P_{\mathrm{pp}_{\max}} / P_{\mathrm{pp}_{\mathrm{unt}}} \end{aligned} \tag{2.15}$$

where $Y_{\mathrm{p}}(t)$ is an integer variable.

2.3.3 Basic Structure of the Constraint Matrix

To have a certain understanding of the structure of the mathematical model and better comprehend its complexity, the structure of the constraint matrix in this mathematical model is specified and shown in Table 2.3.

2.4 Preprocessing of the Optimization Calculation

The daily economic operation planning problem can be solved by two solution procedures: one is a standard mixed-integer mathematical programming method, and the other is a linear mathematical programming method in which integer variables are relaxed first then rounded. The relaxed problem can be solved repeatedly by the standard linear mathematical programming method to obtain an integer solution or by random optimization method. Many technical treatments are used before a standard linear mathematical programming method is employed.

After having finished the conversion of practical problems into mathematical models, it does not mean that the correct results can be obtained by simply applying the existing solution methods or by developing new algorithms. It is necessary to preprocess the data before carrying out a series of calculations and to consider whether some special computational demands can be satisfied by setting data without needs to modify the mathematical model. Because the pumped storage plant cannot operate by both pumping and generating at the same time, the pumping variable (integer variable) and generating variable (continuous variable) are set in

Table 2.3 Structure of constraint matrix

Left Hand Side Constraint	Relation	Constraint Matrix	Relation	Right Hand Side Constraint
		Summation of power outputs for each unit in each of 24*D* time periods, including units in thermal, hydro and pumped storage plants	=	Load in each time period
Lower limit of generated output for each power plant in each time period	≤	Generated output of each power plant in each of 24*D* time periods	≤	Upper limit of generated output for each power plant in each time period
Lower limit of generated energy for each power plant within one day	≤	Generated energy of each power plant (summation of output for each unit in 24*D*)	≤	Upper limit of generated energy for each power plant within one day
Lower limit of generated output for each area in each time period	≤	Summation of generated output of each area in each of 24*D* time periods	≤	Upper limit of generated output for each area in each time period
Lower limit of reservoir capacity in each time period	≤	Reservoir capacity of pumped storage plant in each of 24*D* time periods	≤	Upper limit of reservoir capacity in each time period
		Water quantity balancing of pumped storage plant in 24*D*	=	The given balancing value of water quantity within one day

the mathematical model. If the cost coefficient of pumping and generating are adjusted, the required optimal solution can be automatically obtained by the optimization algorithm.

Specific preprocessing works before optimization calculation include: (1) verifying the reasonableness of input data to ensure a feasible solution from the optimization calculation; (2) modifying input data to meet the requirement of data reasonableness; (3) forming the virtual cost coefficients of the pumped storage plant to ensure the basic operational mode (pumping water at valleys and generating power at peaks); (4) forming the virtual cost coefficients of each power plant to differentiate power plants with base load, middle load, peak load, and valley load; and (5) establishing constraints for each unit in various time intervals to determine whether the sum of unit output and pumped storage unit output meets the maximum and minimum value of the load curve.

2.4.1 Validity Test of the Input Data

Reasonability of original input data is a precondition for obtaining a feasible solution for the optimization calculation. To meet the optimization calculation requirements, computational personnel sets a series of limits according to the operation schedule, such as unit operating conditions (shutdown, maintenance, and startup), and also defines the upper and lower limits of the area output, power plant output and energy generated by power plants, and water balancing constraint, as well as reservoir capacity constraint, all of which shall be checked to ensure all are within a reasonable range. Thus, it is quite necessary to verify the reasonableness of the input data. The main contents of validity testing of data include:

(1) Solve the allowable output range of each area under the given operating conditions, and compare the range with the manual setting for upper and lower output limits of each area; if the given upper and lower output limits of the area do not satisfy the allowable range, then the name of the area and corresponding over limit value will be output, allowing calculation personnel to make necessary modifications.
(2) Solve the allowable output range of each power plant under the given operating conditions, and compare the range with the manual setting for upper and lower output limits of each power plant; if the given upper and lower output limits of power plant do not satisfy the allowable range, then the name of the power plant and corresponding over limit value will be output, allowing calculation personnel to make necessary modifications.
(3) Solve the allowable generated energy range of each power plant under the given operating conditions, and compare the range with the manual setting for upper and lower generated energy limit of each power plant; if the given upper and lower generated energy limit does not satisfy the allowable generated energy range, then the name of the power plant and corresponding over limit value will be output, allowing calculation personnel to make necessary modifications.
(4) Sum all upper limits and lower limits of all unit outputs. First check whether the sum complies with the varying range of the load curve (especially the sum of upper limits); if not, check whether the sum can comply with the varying range of load curve with the operation of the pumped storage units. Otherwise, calculation personnel will be notified to make necessary modifications.

2.4.2 Validity for the Rationality of the Constraints

As previously mentioned, when manually setting generated output and energy constraints for power plants and generated output constraints for areas, the constraints should be within a reasonable range, otherwise feasible solutions in the optimization calculation cannot be obtained. Therefore, the reasonability of the specified constraints should be confirmed by the necessary modifications as follows:

(1) The generated output constraint specified for the power plant shall be compatible with the sum of generated output of all units of the plant, namely, only if there is an intersection with the sum of generated output of all units of the plant in any time, then the specified constraints are reasonable.

For instance, the specified range of total generated output for a certain power plant is assumed to be [200 MW, 550 MW], for which the reasonability only happens in the first three situations, except the last one as follows:

1. If the sums of upper and lower limits of the generated output for all plant units in various time periods are both within the specified range of the generated output for the power plant, such as [250 MW, 500 MW], then the specified range is reasonable, shown in Fig. 2.3.

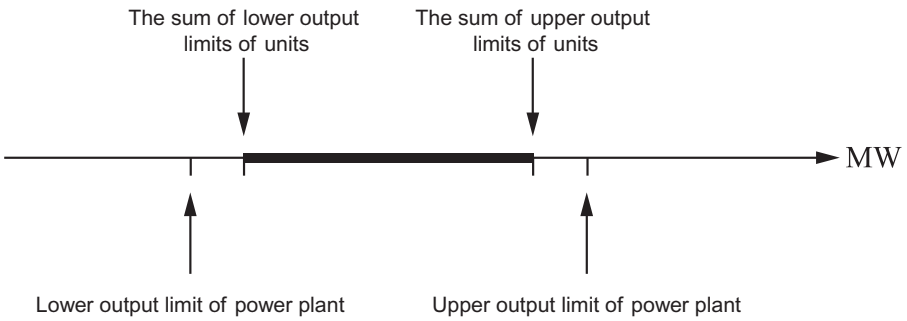

Fig. 2.3
Reasonable range 1 of power plant output.

2. If the sums of upper limits of generated output for all units of the plant in various time periods is within the specified range for the power plant, yet the sum of lower output limits of all units of the plant in various time periods is smaller than the lower limit of the specified range, such as [100 MW, 300 MW], the specified range is also reasonable, as shown in Fig. 2.4.

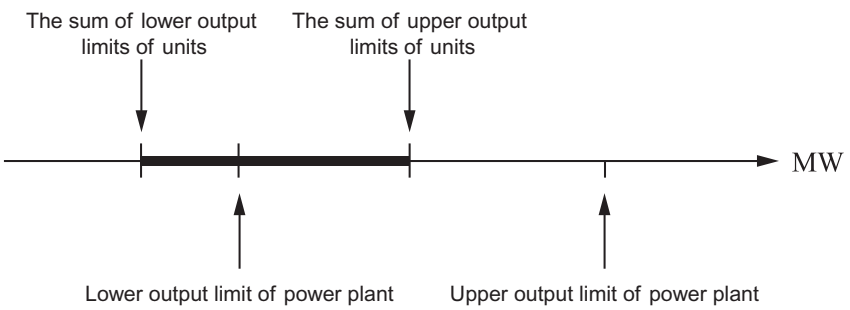

Fig. 2.4
Reasonable range 2 of power plant output.

3. If the sum of lower limits of generated output for all units of the plant in various time periods is within the specified range of the power plant, yet the sum of upper limits of generated output for all units of the plant in various time periods is larger than the upper limit of the specified range, such as [450 MW, 600 MW], the specified range is reasonable, as shown in Fig. 2.5.

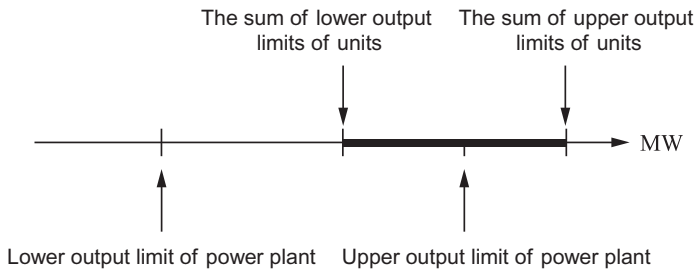

Fig. 2.5
Reasonable range 3 of power plant output.

4. If the sum of upper and lower limits of generated output for all units of the plant in various time periods is beyond a specified range, such as [550 MW, 700 MW] or [50 MW, 200 MW], the specified is unreasonable. As shown in Fig. 2.6, for the situation in Fig. 2.6A, the specified upper limit should be enlarged, or some units of

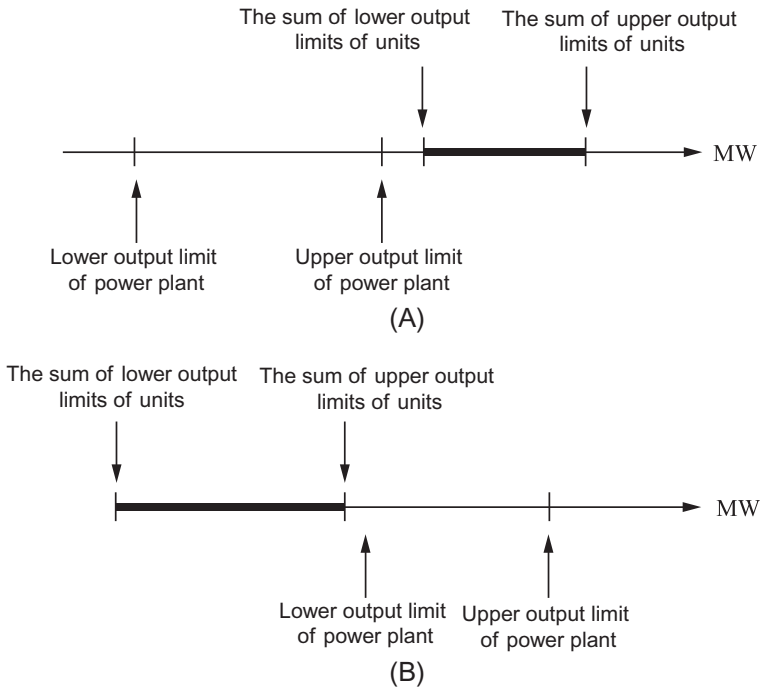

Fig. 2.6
Unreasonable range of power plant output. (A) Beyond the upper limit; (B) Below the lower limit.

the power plant should be shut down; for the situation in Fig. 2.6B, the lower limit of the specified range should be reduced, or some standby units of the power plant should be put into operation.

(2) The generated energy constraint specified for all power plants shall also be compatible with the sum of generated output of all units of the plant, namely, it should have an intersection with the sum of output of all units of the plant in all periods so that the specified range is reasonable. An unreasonable range may be modified according to the modification method for power plant output constraint previously mentioned.

(3) The generated output constraint specified for all areas shall also be compatible with the sum of the output of all units of the plant in the area, namely, it should have an intersection with the sum of the output of all units in the area in any period so that the specified ranges are reasonable. An unreasonable range may be modified according to the modification method for power plant output constraint previously mentioned.

2.4.3 Forming the Virtual Cost Function for a Pumped Storage Plant

During optimization, the cost coefficient of a pumped storage plant is normally assumed as zero to gain the peak shift ability of the pumped storage plant. The virtual cost coefficient introduced can make the pumped storage plant pump as much water as possible during valley load duration and to generate power as much as possible during peak load duration.

All virtual cost coefficients for a pumped storage plant are negative and proportional to the fluctuations of the load curve, by which a pumped storage plant can reduce the difference between load curve and average load during the optimization procedure, so that the economy and safety of the whole power system can be improved. The details are given as follows:

(1) Calculate average load P_{avg}:

$$P_{\text{avg}} = \frac{1}{24D}\sum_{i=1}^{24D} PL(t)$$

(2) Calculate differences ΔP_{L}, between load and average load P_{avg}:

$$\Delta P_{\text{L}}(t) = P_{\text{L}}(t) - P_{\text{avg}}$$

(3) Calculate deviation $[P_{a\min}, P_{a\max}]$:

$$\left[P_{a}\min, P_{a}\max\right] = \left[P_{\text{avg}} - \Delta P_{\text{L}}, P_{\text{avg}} + \Delta P_{\text{L}}\right]$$

(4) Set the duration when load $< P_{a\min}$ as the duration of pumping for the pumped storage plant, set the duration when load $> P_{a\min}$ as the duration of generation, and set the duration of $[P_{a\min}, P_{a\max}]$ as the duration of stop. If $\Delta P_{\text{L}} = 0$, the pumped storage plant never stops.

(5) Calculate virtual cost coefficient $C_{\text{pr}}(t)$ as follows; take the cost coefficient for pump state:

$$C_{\text{pr}}(t) = PL_{\text{t}} - P_{\text{avg}}(\leq 0), \quad t = 1 - 24D$$

Take the cost coefficient for generating state:

$$C_{\mathrm{pr}}(t) = P_{\mathrm{avg}} - PL_{\mathrm{t}}(\leq 0), \quad t = 1 - 24D$$

(6) Form the right hand side and left hand side of each constraint.
(7) Form the matrix of mixed-integer programming model.
(8) Solve the mixed-integer programming problem by standard method or by approximation method.

2.4.4 Forming the Cost Function for an Individual Power Plant

(1) Based on the cost coefficient of units of the plant in various time periods, the cost weight coefficient curve of each unit in all time is formed to distinguish the power plants responsible for base load, middle load, peak load, and valley load.
(2) As is known, the fixed cost of each unit does not change with time, which would be happen once the unit is put into operation. Therefore, the variable for the fixed cost could be ignored in the optimization model, and the fixed cost is only necessary to add up to the cost of each operating unit in various time periods.

2.4.5 Forming the Constraints at Different Periods for Each Unit

(1) Form upper and lower limits of generation output for all units in the network in various time periods.
(2) Perform validity testing of data: (1) check if the possible output of units satisfies the generated energy and output constraint of the power plant, as well as the area output constraint; (2) check if the possible sum of outputs for units of the plant and sum of outputs for the pumped storage meets the maximum value and minimum value of the load curve.

2.4.6 Forming the Coefficient Matrix

(1) Form the right hand side terms and left hand side terms for each constraint.
(2) Form coefficients for mixed-integer programming model, including cost coefficient.

2.5 Computation Procedure for Optimization

The daily economical operation planning problem stated in Section 2.3 can be solved by two solution procedures: one is a standard mixed-integer mathematical programming method, and the other is a linear mathematical programming method in which integer variables are first relaxed then are rounded. The relaxed problem can be solved repeatedly by the standard linear mathematical programming method to obtain an integer solution or by a random optimization

method. Many technical treatments mentioned in Section 2.4 are used before the standard linear mathematical programming method is employed.

2.5.1 Main Calculation Procedure

The optimization calculation procedure consists of five steps:

Step 1: Input data, to which operators may as well add some special calculation requirements. The input data include load curve and unit parameters, such as startup and shutdown cost, operation cost, generated output and generated energy constraints of power plants, and output constraint of areas.
Step 2: Perform validity testing of the input data, during which operators may modify constraint conditions to meet special calculation requirements or add some special calculation requirements to input data.
Step 3: Form objective function, constraint function matrix, left and right hand side constraints, upper and lower limits of variables, etc.
Step 4: Solve the problem with the standard mixed-integer programming mathematical software, directly obtaining the mixed-integer solution.
Step 5: Output optimization calculation results.
The basic calculation flow is shown in Fig. 2.7.

The calculation of standard mixed-integer programming adopted in Step 4 is as follows:

(1) Form cost coefficient, coefficient matrix of continuous variables, coefficient matrix of integer variables, range constraints, and variable constraints.
(2) The mixed-integer solution is directly obtained with standard MIP mathematical software. However, this method can only be used to solve small-scale problems.

If the self-developed mixed-integer programming is adopted in Step 4 to solve the mixed-integer programming model, calculation shall be:

(1) Relax the integer constraint.
(2) Solve with standard LP software.
(3) Round off the obtained relaxation solution and fix it at the integer value.
(4) Use standard linear programming mathematical software to obtain the mixed-integer solution based on the fixed discrete variables.
(5) If a feasible mixed-integer solution can be obtained, then stop, otherwise return to Step 2.

2.5.2 Description of the Input Data

The input data consist of the following categories:

(1) Calculation time period card (CA), including CA identification, calculation date, calculation day number, calculation starting time (hour), calculation ending time (hour), print selection, and load average value deviation range (MW).

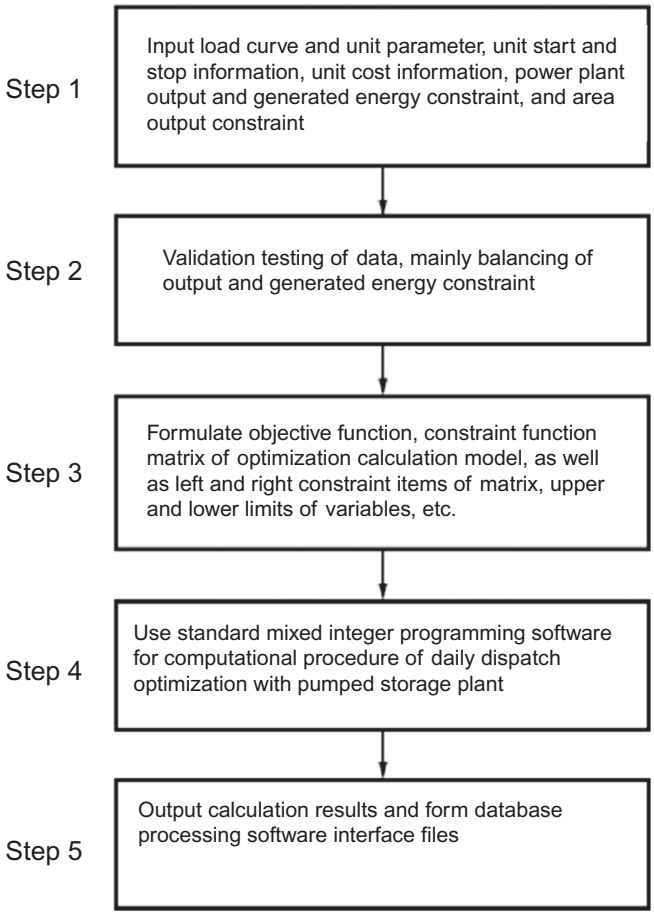

Fig. 2.7
Basic calculation flowchart.

(2) Load data card (LO) consists of LO identification, load time period (hour), and load data (MW).
(3) Area output control card (AC), including AC identification, area name, and upper and lower limits of area output (MW).
(4) Power plant daily generated energy control card (GC), including GC identification, area name, power plant name, power plant type (1 for thermal power or nuclear power, 2 for hydropower, 3 for purchased power), upper and lower limits of daily generated energy of power plant (MWh), and upper and lower limits of generated output power plant (MW).
(5) Pumped water quantity control card (PU), including PU identification, initial and final water storage (10,000 m^3), upper and lower limits of water storage (10,000 m^3), upper limit of generated output of pumped storage plant for pumping (MW), and generated output of pumping units (MW, which shall be divided exactly by the upper limit of generated output for pumping).

(6) Unit start and stop control card (GS), including GS identification, area name, power plant name, unit name, unit type (1 for thermal power or nuclear power, 2 for hydropower, 3 for purchased power), and including upper and lower limits of unit output (MW), unit starting and stopping time (hour), and unit start and stop state (0 for stop, 1 for start, −1 for maintenance) in five time periods within one day, respectively.
(7) Unit start and stop cost parameter card (GY), including GY identification, area name, power plant name, unit name, unit starting time (hour), unit stopping time (hour) in five time periods, respectively, unit cost (yuan/MWh), and unit fixed cost (yuan/MWh).
(8) Comment card (**), excluding data involved in optimization calculation; comments can be added after ** to make data files readable, including ** identification and note information.

2.5.3 Special Settings to Meet the Calculation Requirements

Whenever the formulation of a mathematical model has been developed, it is just for some purposes. However data is changeable, and some expected results can be reached by settings of input data without the need to develop some special or new model. The details are shown as follows:

(1) If some power plants are needed to operate with a base load or at a given output in certain time periods, the lower and upper limits of the generated output for power plants, whether hydropower plants or thermal power plant, will be set to be equal or almost equal to each other at a certain time period; then the optimization model can automatically make the plant undertake the base load in different time periods. Thus, the constraints of generated output and generated energy can also be dealt with for all power plants in this way, so power plants with different property rights can fulfill the amount of generated energy specified in the agreement.
(2) If some units are needed to satisfy some special operation conditions, for example, for peak load regulating in a specific time period, different cost coefficients can be set for each unit in different time periods, that is, with different prices for peak and valley load. Then, each unit can automatically either generate power or purchase power by setting different cost coefficients in different time periods.
(3) If a pumped storage plant is needed to meet the changing requirement of a reservoir water level, the water quantity constraints can be set to automatically control the operation condition of the pumped storage plant.
(4) If a pumped storage plant is needed to avoid operating both in generating and pumping states at the same time, the load difference can be used as indexes of operation states. The time period when load is larger than an average load is set as a generating state, and the time period when load is smaller than an average load is set as a pumping state, so that

approximately half the number of integer variables can be reduced, which can also greatly reduce the calculation burdens.

(5) If the pumped storage power station must run at the peak load time when the peak-valley difference is large, it is possible to reasonably arrange the pumping and generating conditions of the pumped storage power station by setting the virtual cost coefficients in advance.

(6) If the pumped storage plant must run to satisfy water storage balancing constraints when the peak-valley difference is small (despite the fact that only the thermal power unit can achieve peak regulation), a virtual cost coefficient is set in advance to realize the optimized operation of pumped storage plant at all times, taking into account the capacity of the pumped storage power station shared with Hong Kong.

(7) If the regional tie line is needed to satisfy a certain amount of transmission power, then the generated output constraint for each area can be set so that the transmission power of the regional tie line can be automatically controlled to satisfy the requirement of stable operation of the power system.

2.5.4 Description of the Output Results

Output results include the following:

(1) Optimization calculation results concerning pumping and generating for the pumped storage plant in each time period.
(2) Optimization calculation results concerning water balancing and reservoir capacity constraint for the pumped storage plant.
(3) Optimization results of generated output of each unit in each time period.
(4) Optimization results of generated output of each power plant in each time period.
(5) Optimization calculation results of daily generated energy of each power plant.
(6) Optimization results of generated output of each area in various time periods.
(7) Load curves upon optimized operation of the pumped storage plant.

2.6 Implementation

2.6.1 Concrete Expression of Objective and Constraint Functions for a Small Scale System

Before optimization calculation on full-scale systems, it is better to verify the proposed model and calculation method using a small-scale one, to confirm whether the cost coefficient setting, variables, and constraint conditions are right or not.

First, a simplified mathematical testing model is derived for the small-scale system to give a clear view about the proposed model. The testing system consists of one area, one thermal

power plant (two units), and one pumped storage plant (one unit), where two calculation time periods (i, j) are considered. According to the proposed mathematical model, the variables of the two thermal units in two time periods are X_{i1}, X_{i2}, X_{j1}, X_{j2}; the generating and pumping variables of the pumped storage unit are x_{g1}, x_{g2} and y_{p1}, y_{p2}.

The number of constraints $\leq$ the number of time period (load) + the number of power plants $\times$ the number of time periods (power plant generated output) + the number of power plants (power plant generated energy) + the number of areas $\times$ the number of time periods (area generated output) + the number of time periods (pumping output) + 1 (water balancing) = 2 + 1 $\times$ 2 + 1 + 1 $\times$ 2 + 2 + 1 = 10.

The number of continuous variables = the number of units $\times$ the number of time periods = 3 $\times$ 2 = 6, the number of integer variables = the number of time periods = 2, and total number of variables = 8.

Thus, it can be seen that the number of constraints in the model is irrelevant to the number of units, and there should be at least five units to make the model solvable (because the number of variables has to be greater than that of constraints in the LP calculation). Generally, an actual system can meet this requirement. Due to space limitations, the objective and constraint function expressions for a small-scale test system with only two units are shown as follows.

Coefficient expression of objective function:

$$f = C_{i1}X_{i1} + C_{i2}X_{i2} + C_{j1}X_{j1} + C_{j2}X_{j2} + c_{g1}x_{g1} + c_{g2}x_{g2} + c_{p1}y_{p1} + c_{p2}y_{p2}$$

Where variables are:

$$X_{i1}, \quad X_{i2}, \quad X_{j1}, \quad X_{j2}, \quad x_{g1}, \quad x_{g2}, \quad y_{p1}, \quad y_{p2}$$

Formation of constraint equation:

$$\begin{bmatrix} S_I \\ S_I \\ H_I \\ A_I \\ A_I \\ W_I \\ W_I \end{bmatrix} \begin{matrix} \leq \\ \leq \\ \leq \\ \leq \\ \leq \\ \leq \\ \leq \end{matrix} \begin{bmatrix} I & I & 1 & & -165 & & \\ & I & I & & 1 & & -165 \\ I & I & & & & & \\ & I & I & & & & \\ I & I & I & I & & & \\ I & & I & 1.36 & & -165 & \\ & I & & I & 1.36 & & -165 \\ & & & 1.36 & & -165 & \\ & & & 1.36 & 1.36 & -165 & -165 \\ & & & 1.36 & 1.36 & -165 & -165 \end{bmatrix} \begin{bmatrix} X_{i1} \\ X_{i2} \\ X_{j1} \\ X_{j2} \\ x_{g1} \\ x_{g2} \\ y_{p1} \\ y_{p2} \\ t_2 \\ t_2 \end{bmatrix} \begin{matrix} = \\ = \\ \leq \\ \leq \\ \leq \\ \leq \\ \leq \\ \leq \\ \leq \\ = \end{matrix} \begin{bmatrix} L_1 \\ L_2 \\ S_A \\ S_A \\ H_A \\ A_A \\ A_A \\ W_A \\ W_A \\ W_0 - W_{24} \end{bmatrix}$$

where C is cost coefficient, of which the cost of each unit in each time period is input data, whereas the cost of pumped storage unit is the virtual cost coefficient; L_1—load in time

period 1; L_2—load in time period 2; S_I, S_A—output limits of the power plant in time period 1, 2; H_I, H_A—generated energy limits of the power plant in total time periods; A_I, A_A—generated output limits of area in time period 1, 2; W_I, $\mathrm{W_A}$—limits of water quantity of the pumped storage plant in time period 1, 2; W_0–W_{24}—balancing value of water quantity of the pumped storage plant in total time period; X_{it}—generated output of unit i, continuous variable, the number of variables = the number of units × the number of time periods, $t = 1, 2$; X_{jt}—generated output of unit j, continuous variable, the number of variables = the number of units × the number of time periods, $t = 1, 2$; $X_{\mathrm{g}t}$—generated output of the pumped storage plant, continuous variable, the number of variables = the number of pumped storage plants × the number of time periods, $t = 1, 2$; $Y_{\mathrm{p}t}$—pumping output of the pumped storage plant, integer variable, the number of variables = the number of units for pumped storage plant × the number of time periods, $t = 1, 2$; t_2—virtual variable.

(1) Constraint for load balancing in time period 1; $X_{i1} + X_{j1} - 165y_{\mathrm{p}1} = L_1$
(2) Constraint for load balancing in time period 2; $X_{i2} + X_{j2} - 165y_{\mathrm{p}2} = L_2$
(3) Constraint for power plant output in time period 1; $S_\mathrm{I} \le X_{i1} + X_{j1} \le S_\mathrm{A}$
(4) Constraint for power plant output in time period 2; $S_\mathrm{I} \le X_{i2} + X_{j2} \le S_\mathrm{A}$
(5) Constraint for area output in time period 1; $A_\mathrm{I} \le X_{i1} + X_{j1} \le A_\mathrm{A}$
(6) Constraint for area output constraint in time period 2; $A_\mathrm{I} \le X_{i2} + X_{j2} \le A_\mathrm{A}$
(7) Constraint for generated energy of the power plant in total time periods; $H_\mathrm{I} \le X_{i1} + X_{j1} + X_{i2} + X_{j2} \le H_\mathrm{A}$
(8) Constraint for reservoir capacity in time period 1; $W_\mathrm{I} \le 1.36X_{\mathrm{g}1} - 165y_{\mathrm{p}1} \le W_\mathrm{A}$
(9) Constraint for reservoir capacity in time period 2; $W_\mathrm{I} \le 1.36X_{\mathrm{g}1} + 1.36X_{\mathrm{g}2} - 165y_{\mathrm{p}1} - 165y_{\mathrm{p}2} \le W_\mathrm{A}$
(10) Constraint for water storage of the pumped storage plant in total time periods; $1.36X_{\mathrm{g}1} + 1.36X_{\mathrm{g}2} - 165y_{\mathrm{p}1} - 165y_{\mathrm{p}2} = W_0 - W_{24}$

The small-scale system shows that the proposed setting of cost coefficient, variables, and constraint conditions are correct.

2.6.2 Scale of the Practical System

The practical scale system is comprised of 6 areas, 1 pumped storage plant with 4 pumped storage units, and 27 other power plants, which is a total of 70 hydro and thermal (nuclear) plants, and purchased units, with a daily load curve divided into 24 time periods. According to the optimization model, the scale of the mathematical model consists of 743 constraints, 1680 continuous variables, 24 integer variables, and 7368 nonzero elements, with nonzero element proportion in the constraint matrix of 0.58%. Therefore, the proposed model is a highly sparse one. The scale of variables of the practical scale system is shown in Table 2.4.

Table 2.4 Scale of variables of the practical scale system

The number of constraints < the number of time periods (load balancing) + the number of power plants × the number of time periods (power plant generated output) + the number of power plants (power plant generated energy) + the number of areas × the number of time periods (area output) + the number of time periods (pumping reservoir capacity) + 1 (pumping water balance)	$\approx(1+30+6+1)\times 24D+30\le 930D$ $D=1, 2, 4$
The number of continuous variables = (total number of units) × the number of time periods	$\approx 100\times 24D=2400D$
The number of integer variables < the number of time periods	$\approx 1\times 24D=24D$

2.6.3 Analysis of Peak-Valley Difference in the Load Curve

Fig. 2.8 shows the peak-valley value of load curve, also known as the difference between load and average load, in which there are two valleys ([hour 1–7] and [hour 12–13]), two peaks ([hour 9–11] and [hour 15–22]), and three periods (hour 8, 14, and 23) close to the average load in load curve, including period 24 in the valley. The maximum load is 7000 MW, and the minimum is 4350 MW, leading the maximum peak-valley difference to 2650 MW, average load is 5244 MW, average load variation rate is 0.62 (4350/7000), and average load rate is 0.75 (5244/7000). Both load variation rate and average load rate are lower than the lower limit of the predicted range of 0.7–0.75 and 0.85–0.9. Thus, the shifting capacity of the pumped storage plant is rather important. Detailed information of daily load curve is shown in Table 2.5.

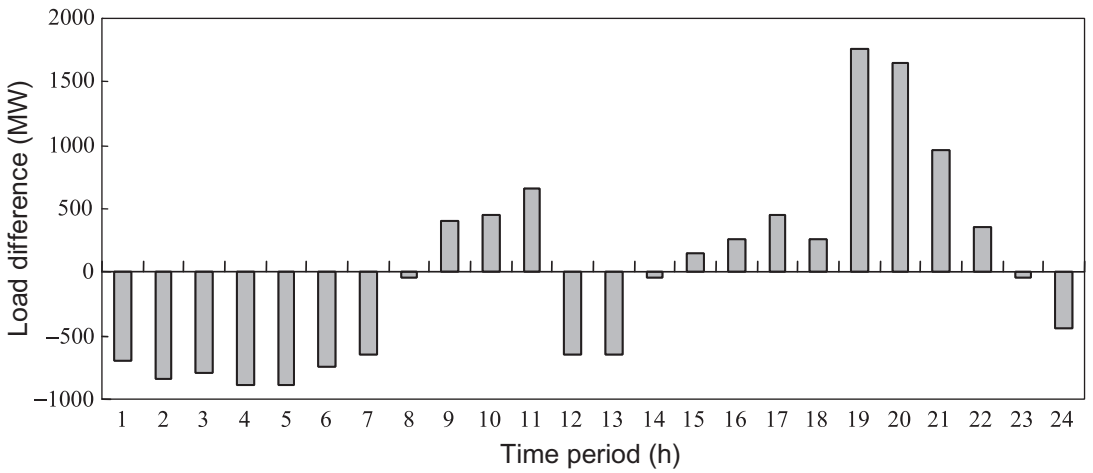

Fig. 2.8
Difference between load and average load.

Table 2.5 Daily load curve data before optimization (MW)

Time period	1	2	3	4	5	6	7	8	9	10	11	12
Load curve	4550	4400	4450	4350	4350	4500	4600	5200	5650	5700	5900	4600
Average load	5244	5244	5244	5244	5244	5244	5244	5244	5244	5244	5244	5244
Difference	−694	−844	−794	−894	−894	−744	−644	−44	406	456	656	−644

Time period	13	14	15	16	17	18	19	20	21	22	23	24
Load curve	4600	5200	5400	5500	5700	5500	7000	6900	6200	5600	5200	4800
Average load	5244	5244	5244	5244	5244	5244	5244	5244	5244	5244	5244	5244
Difference	−644	−44	156	256	456	256	1756	1656	956	356	−44	−444

2.6.4 Constraints of Pumped Storage Plant and Related Conversion Calculation

(1) Initial conditions are given as follows:

Initial water storage quantity $W_0 = 310.0 \times 10^4 (\mathrm{m}^3)$
Final water storage quantity $W_{24} = 350.0 \times 10^4 (\mathrm{m}^3)$
Maximum water storage quantity $W_{\max} = 850.0 \times 10^4 (\mathrm{m}^3)$
Minimum water storage quantity $W_{\min} = 0.0 \times 10^4 (\mathrm{m}^3)$

(2) Energy balance of pumped storage plant:

$$W_{\mathrm{H}} = (W_0 - W_{24})/640 = -40/640 \times 104 = -625 \ (\mathrm{MWh})$$

If the energy is a negative value, it means that the energy consumed by pumping is larger than that by generating.

(3) Lower limit of generated energy for pumped storage plant:

$$W_1 = (W_0 - W_{\max})/640 = -540/640 \times 104 = -8437.5 \, (\mathrm{MWh})$$

(4) Upper limit of generated energy for pumped storage plant:

$$W_{\mathrm{A}} = (W_0 - W_{\min})/640 = 310/640 \times 104 = 4843.8 \ (\mathrm{MWh})$$

(5) Constraint of pumped storage units for generating: the calculation condition is that four pumped storage units are put into operation, with the output constraint of each unit as [180 MW, 300 MW]. Thus, the total output constraint of four pumped storage units shall be [180 MW, 1200 MW].

(6) Constraint of pumped storage units for pumping: the calculation condition is that output constraint in water pumping is 0, 165, 330, 495, and 825 MW, with integer constraint as [0, 5] and unit step size of 165 MW.

(7) In the optimization calculation of reservoir capacity constraint, average water balancing constraint of the pumped storage plant is converted into an energy balancing constraint. However, when output it is still converted back to water quantity unit, the upper limit of generated energy by pumped storage plant is 8500 MWh, the lower limit 5000 MWh, and the energy by reservoir capacity is 3500 MWh (8500–5000).

The correctness and reasonableness of the proposed mathematical model is verified by daily economic optimization dispatch of pumped storage plant calculation using practical system data of the province. The calculation results show that the mathematical model proposed in this chapter can fully use the peak load regulating capacity of a pumped storage plant and effectively adjust the load curve by peak load shifting while meeting all operational constraints. The detailed results are shown in the following section.

2.6.5 Optimization Calculation Results

(1) Optimization calculation results of pumped storage and generated output of a pumped storage plant in various time periods: the operating status of the pumped storage plant in various time periods is shown in Fig. 2.9, in which time periods [hours 1–7] and [hours 12–13] are in pumping operation, where generated output in each time period is 825 MW and the total energy for pumping is 7425 MWh. In periods 8, 14, 23, and 24, the units are stopped, and in periods [hours 8–10] and [hours 15–22], all units are generating power, with the energy for generating as 5002.3 MWh. The result is related to the fact that the given initial water storage is less than the final one. In the other one for generating, the calculation results in Fig. 2.9 show that the proposed mathematical model meets the practical calculation requirements. Table 2.6 shows operating results of the pumped storage plant in various time periods.

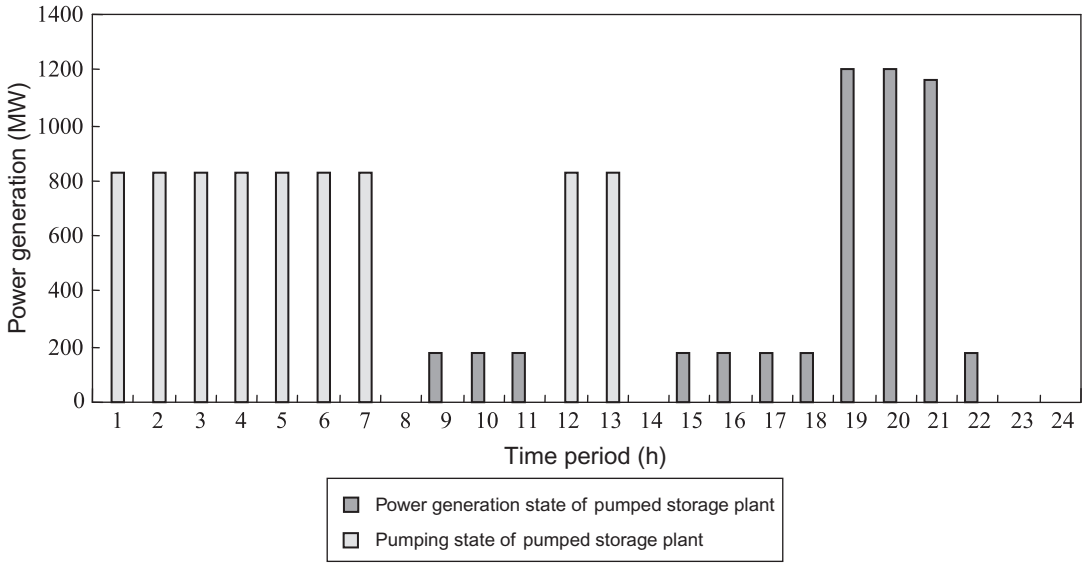

Fig. 2.9
Daily arrangements of water pumping and power generation for pumped storage plant.

Table 2.6 Daily arrangements of pumping and generating for pumped storage plant (MW)

Time period	1	2	3	4	5	6	7	8	9	10	11	12
Generating	0	0	0	0	0	0	0	0	180	180	180	0
Pumping	825	825	825	825	825	825	825	0	0	0	0	825

Time period	13	14	15	16	17	18	19	20	21	22	23	24
Generating	0	0	180	180	180	180	1200	1200	1162	180	0	0
Pumping	825	0	0	0	0	0	0	0	0	0	0	0

(2) Optimization calculation results of water balancing and reservoir capacity constraint of a pumped storage plant: in a daily economic dispatch optimization calculation, the pumped storage plant shall meet not only the generation output constraint but also the water balancing constraint and reservoir capacity constraint in various time periods. Fig. 2.10 shows water storage optimization calculation results of the pumped storage plant. It can be seen from Fig. 2.10 that the reservoir water variation of the pumped storage plant is also within the range of constraint. Table 2.7 shows the reservoir water variation of the pumped storage plant.

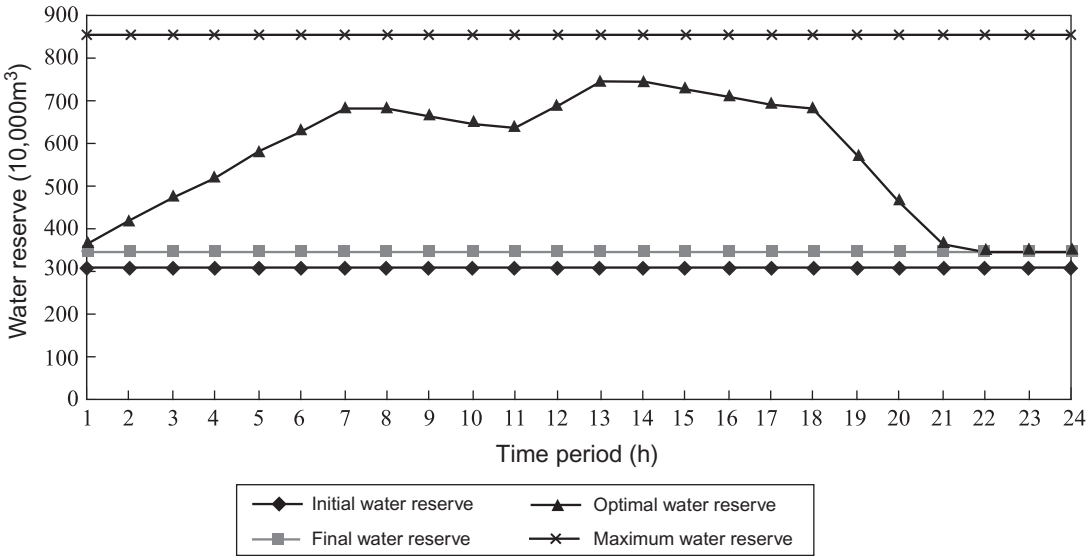

Fig. 2.10
Water storage optimization calculation results of pumped storage plant.

Table 2.7 Reservoir water variation of pumped storage plant (10,000 m^3)

Time period	1	2	3	4	5	6	7	8	9	10	11	12
Initial water storage	310	310	310	310	310	310	310	310	310	310	310	310
Final water storage	350	350	350	350	350	350	350	350	350	350	350	350
Optimized water storage	362.8	415.6	468.4	521.2	574	626.8	679.6	679.6	663.9	648.3	632.6	685.4
Maximum water storage	850	850	850	850	850	850	850	850	850	850	850	850

Continued

Table 2.7 Reservoir water variation of pumped storage plant (10,000 m^3)—Cont'd

Time period	13	14	15	16	17	18	19	20	21	22	23	24
Initial water storage	310	310	310	310	310	310	310	310	310	310	310	310
Final water storage	350	350	350	350	350	350	350	350	350	350	350	350
Optimized water storage	738.2	738.2	722.6	706.9	691.2	675.6	571.2	466.8	365.7	350	350	350
Maximum water storage	850	850	850	850	850	850	850	850	850	850	850	850

(3) Optimization results of generated output of each unit in various time periods: optimization results of output of each unit in various time periods include area name, power plant name, unit name, upper and lower limits of each unit output, and generated output of unit in various time periods (24 h). Due to space limitations, detailed results given here are the outputs only for the north area, as shown in Fig. 2.11.

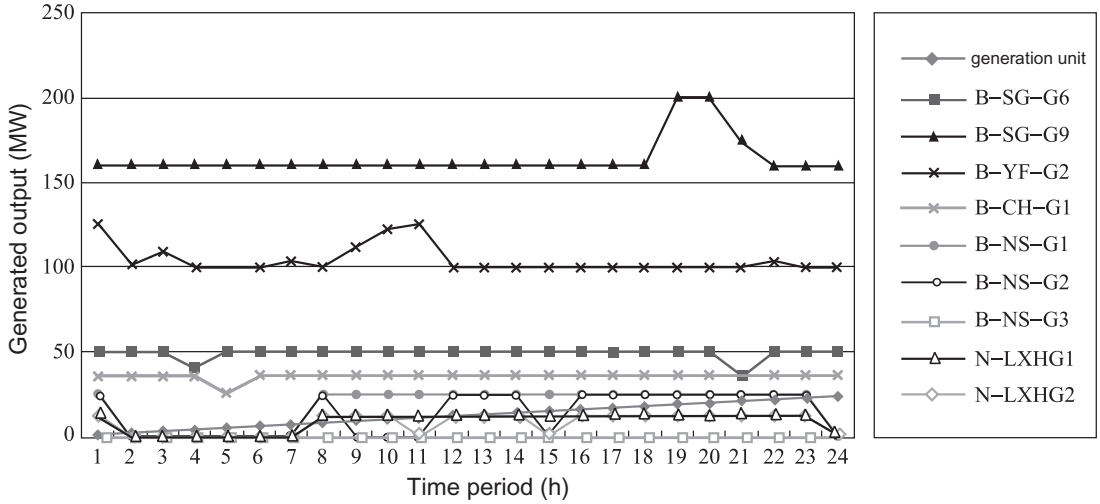

Fig. 2.11
Generated output of each unit of north area in various time periods.

(4) Optimization results of generated output of each power plant in various time periods: optimization results of generated output of each power plant in various time periods include area name, power plant name, upper and lower output limit of power plant, and generated output of power plant in various time periods (24 h). Due to space limitations, detailed results given here are only the power outputs for north area, as shown in Fig. 2.12.

(5) Optimization calculation results of generated energy by each power plant are shown in Table 2.8.

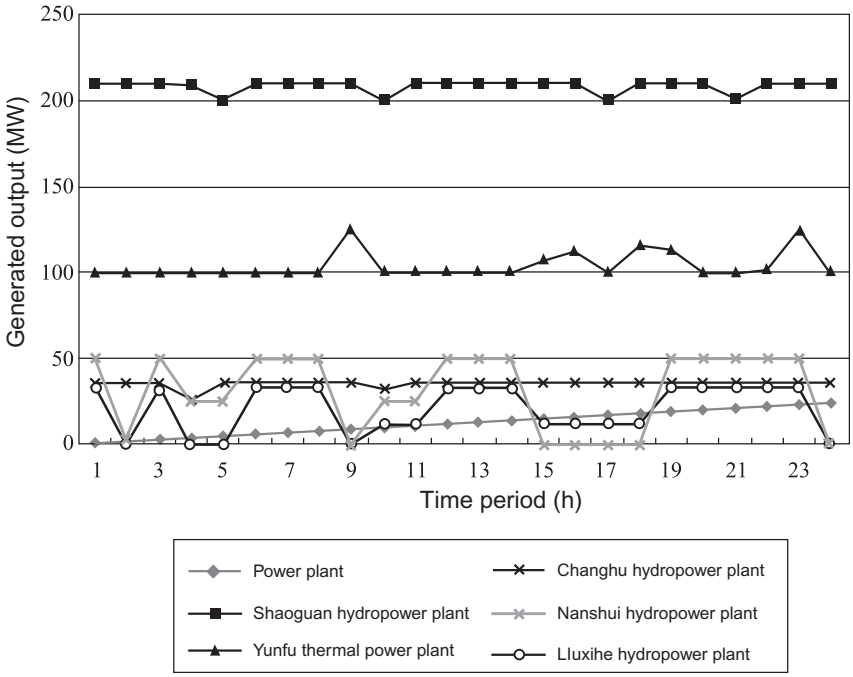

Fig. 2.12
Output of north area power plants in various time periods.

Table 2.8 Optimization calculation results of each power plant (MWh) with generated energy constraints

Area	Power Plant Name	Upper Limit	Lower Limit	Optimized Energy
Purchase area	Tianshengqiao Purchased Power	1920.0	1920.0	1920.0
East area	Meixian Thermal Power Plant	4000.0	3000.0	4000.0
	Shantou Thermal Power Plant	5500.0	4500.0	5500.0
	Xinfengjiang Hydropower Plant	3000.0	2800.0	3000.0
	Fengshuba Hydropower Plant	1400.0	1200.0	1400.0
	Changtan Hydropower Plant	850.0	600.0	660.0
	Qingxi Hydropower Plant	1200.0	1000.0	1200.0
South area	Mawan Thermal Power Plant	16000.0	4500.0	9209.0

Continued

Table 2.8 Optimization calculation results of each power plant (MWh) with generated energy constraints—Cont'd

Area	Power Plant Name	Upper Limit	Lower Limit	Optimized Energy
West area	Maoming Thermal Power Plant	3000.0	2000.0	3000.0
	Zhanjiang Thermal Power Plant	6500.0	4500.0	6366.0
North area	Shaoguan Thermal Power Plant	8000.0	5000.0	5108.7
	Yunfu Thermal Power Plant	2500.0	1800.0	2500.0
	Changhu Hydropower Plant	900.0	850.0	853.0
	Nanshui Hydropower Plant	1000.0	750.0	750.0
	Liuxihe Hydropower Plant	600.0	500.0	501.0
Middle area	Huangpu Thermal Power Plant	12000.0	10000.0	10779.0
	Sha A Thermal Power Plant	15000.0	12000.0	13580.0
	Sha C Thermal Power Plant	36500.0	30000.0	31066.0
	Sha B Thermal Power Plant	80000.0	5200.0	5280.0
	Dayawan Nuclear Power Plant	12500.0	9840.0	9840.0
	Zhujiang Thermal Power Plant	20500.0	8500.0	8640.0
	Xintian Thermal Power Plant	3500.0	2000.0	3120.0

(6) Optimization results of generated output of each area in various time periods: optimization results of generated output of each area in various time periods are shown in Fig. 2.13. Numerical values of area generated output are given Table 2.9. Fig. 2.13 shows that the generated output curves are almost flat in 24 h for some areas, such as purchase area, north area, south area, and west area. As for east area, because there are more hydropower plants with stronger peak regulating ability, its generated output curve changes along time with load curve. And for the middle area, the variation tendency of output curve is opposite to that of load curve, because the pumped storage plant is located in this area, which pumps water in the valley period and generates power in the peak period, functioning as peak load shifting.

(7) Results of load curve after optimized operation of the pumped storage plant: the test system is large in scale, in which the installed capacity of thermal power is 10,315 MW, hydropower 924 MW, and pumping power 1200 MW. Table 2.10 shows total load and average load of the pumped storage plant before and after output optimization. According to the table, the maximum system load before optimization is 7000 MW, minimum load is

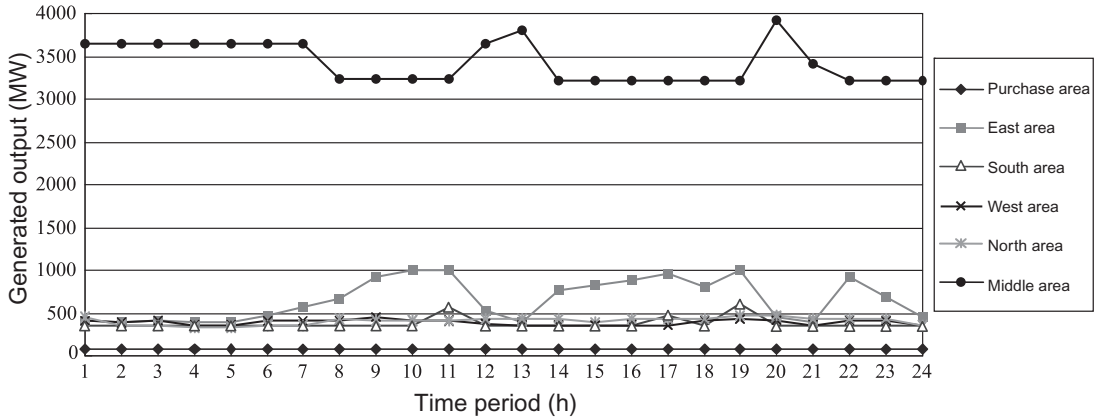

Fig. 2.13
Optimization results of generated outputs for each area.

Table 2.9 Optimization results of generated output of each area (MW)

Time period	1	2	3	4	5	6	7	8	9	10	11	12
Purchase area	80	80	80	80	80	80	80	80	80	80	80	80
East area	421	400	420	400	400	479	576	676	928	998	998	536
South area	360	360	360	360	360	360	360	360	360	360	569	360
West area	410	388	410	350	350	410	410	410	450	420	420	370
North area	454	347	355	336	335	346	349	429	407	417	408	429
Middle area	3650	3650	3650	3649	3650	3650	3650	3245	3245	3245	3245	3650

Time period	13	14	15	16	17	18	19	20	21	22	23	24
Purchase area	80	80	80	80	80	80	80	80	80	80	80	80
East area	400	761	817	881	961	811	991	453	400	918	691	444
South area	360	360	360	360	480	360	600	360	360	360	360	360
West area	350	350	360	350	350	420	440	418	350	410	420	350
North area	429	429	383	429	429	429	469	469	427.7	432	429	346
Middle area	3806	3220	3220	3220	3220	3220	3220	3920	3420	3220	3220	3220

4350 MW, and maximum peak-valley difference reaches 2650 MW. After optimization, except for the pumped storage plant, the maximum output of other units is reduced 5375 MW, and the minimum output is increased to 4800 MW. Thus, maximum peak-valley difference is reduced to 575 MW, and no more than one-fifth of the original. Fig. 2.14 shows overall load curve and average load curve before and after generated output optimization of the pumped storage plant. According to Fig. 2.14, the pumped storage plant plays the role of peak load shifting, which makes the overall output curve of other units except pumped storage plant smoother. Hence, optimized operation of the

Table 2.10 Daily load curve data after optimization (MW)

Time period	1	2	3	4	5	6	7	8	9	10	11	12
Before optimization	4550	4400	4450	4350	4350	4500	4600	5200	5650	5700	5900	4600
Original average load	5244	5244	5244	5244	5244	5244	5244	5244	5244	5244	5244	5244
After optimization	5375	5225	5275	5175	5175	5325	5220	5470	5470	5520	5720	5425

Time period	13	14	15	16	17	18	19	20	21	22	23	24
Before optimization	4600	5200	5400	5500	5700	5500	7000	6900	6200	5600	5200	4800
Original average load	5244	5244	5244	5244	5244	5244	5244	5244	5244	5244	5244	5244
After optimization	5425	5200	5200	5320	5520	5320	5800	5700	5038	5420	5200	4800

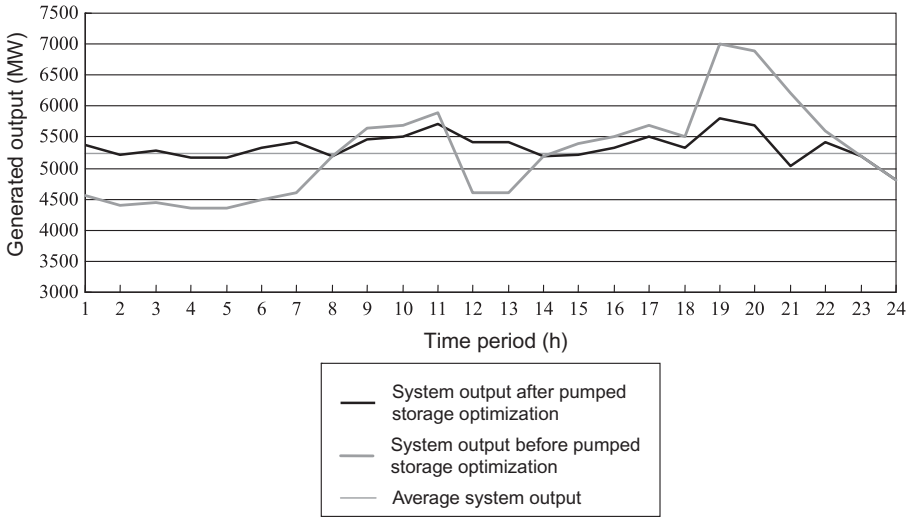

Fig. 2.14
Optimization calculation results of system output upon daily economic dispatch.

pumped storage plant not only reduces the number of startups and shutdowns of the thermal power units but also reduces the startup pressure during peak load, improving the technical economic efficiency of thermal power units. Thus, from both the perspectives of reducing the startup and shutdown cost of thermal power units and creating economic benefits from the difference between peak-valley electricity tariffs, the optimization calculation results can contribute to considerable overall technical and economic benefits.

(8) Analysis of benefits from optimized operation of the pumped storage plant: according to electricity tariff benefit and peak load shaving benefit, economic benefits from optimized operation of the pumped storage plant are briefly summarized as follows:

1. Electricity tariff benefit: Based on peak price of 0.6 yuan/kWh and valley price of 0.3 yuan/kWh, power generated by the test system in the peak period was 5000 MWh and in the valley period 7500 MWh on the day.

$$\text{Total electricity tariff benefit} = (5000 \times 0.6 - 7500 \times 0.3) \times 1000 = 900{,}000\,\text{yuan}$$

Based on the maximum load hours of 4800 h (i.e., 200 days per year), the benefits per year shall be 180 million yuan ($200 \times 900{,}000$ yuan). Even if including operating cost, the investment can still be recovered within several years.

2. Peak shaving benefit: the original peak load was 7000 MW and the present peak load is 5244 MW, peak shaving by approximately 1756 MW. If load shaving of such scale was realized by standby thermal power units, 2000 MW thermal power units could be installed. In other words, peak load shifting helps defer investment. Based on the

assumption that pumped storage and thermal power investment is 3500 yuan/kW, the total investment for the pumped storage plant of 1200 MW is 4.2 billion yuan, which means the investment for a thermal power plant of 2000 MW installed capacity can be deferred.

3. Reliability benefit: assuming that system outage loss is 10,000 yuan/MWh, the power failure ratio of pumped storage units is less than that of thermal power units. If the forced interruption ratio of pumped storage units is 0.1%, and that of thermal power units is 0.39%, energy generated by pumped storage units during peak load period is 5000 MWh, so that the reliability benefit per day shall be

$$\text{Reliability benefit} = (0.39\% - 0.1\%) \times 5000 \times 10{,}000 = 145{,}000 \text{ yuan}$$

Accordingly, the reliability benefit per year (operating for 200 days per year) shall be 29 million yuan ($145{,}000 \times 200$).

2.7 Conclusion

A new approach based on mixed-integer programming is proposed for the daily economic operation planning problem for a multiarea system with hydrothermal plants and a pumped storage plant. The special treatments for integer variables and virtual cost are effective for practical problems. The optimization problem can be solved by a standard mixed-integer programming method or by an approximation method.

The testing system is a large-scale system, where the installed capacity of thermal power units is 10,315 MW, hydropower units 924 MW, and pumped storage units 1200 MW. In the practical test system, the maximum peak-valley difference was 2650 MW before optimization, reduced to 575 MW after optimization. Thus, the proposed optimization model can effectively reduce the peak-valley difference.

The calculation results show that the approach proposed can be successfully shift the peak of the load curve through a pumped storage plant, so that the operation condition of the whole power system can be greatly improved. Whether it is from the reduction of startups and shutdowns costs of thermal power units or the benefits created by the difference in peak-to-valley electricity prices, the economic benefits are very substantial.

The main characteristics of the proposed approach are summarized as follows:

(1) The proposed mixed-integer programming model can be directly solved by the mixed-integer programming method, or approximately solved by the linear programming method.
(2) It can create validity testing among the basic operating constraints, so as to ensure a feasible solution in the optimization calculation.

(3) It can indirectly limit the power transmission on tie lines among areas by processing the generated output constraints of a multiarea.
(4) It can make power plants operate automatically on the periods of base load or peak load by adjusting the generated output and generated energy constraints (making them as equal or unequal constraints).
(5) It can reduce the numbers of integer variables in the optimization calculation. In such a way, the operating time periods of load curve are divided into three categories: peak, valley, and outage, upon which the steps of pumped storage are changed, so that optimization calculation speed is improved.

CHAPTER 3

Optimization of Annual Generator Maintenance Scheduling

Chapter Outline

Mathematical Models and Algorithms for Power System Optimization. https://doi.org/10.1016/B978-0-12-813231-9.00003-0

3.1 Introduction

3.1.1 Description of the Problem

Generator maintenance scheduling (GMS) is one of the most important measures in the economic operation of power systems. It can improve the system operating reliability, reduce the generation cost, extend the generator lifetime, and relax the new installation pressure. Due to the rapid increase of demand, the expansion of power system scale has made the GMS problem more difficult and complex. The normal maintenance schedule is the basis of increasing the security of generation equipment and avoiding imminent faults. A scheduled maintenance outage has less impact on the power system than a forced outage.

Solution techniques for GMS have been investigated for several decades. Examples of these techniques are integer programming and dynamic programming. An expert system (ES), fuzzy dynamic programming (FDP), has been applied. However, these techniques are effective only for some systems under certain conditions. A GMS problem is a large-scale integer-programming problem. The objective function is to maximize the reserve margins or to minimize the production costs. The constraints consist of a reserve margin, maintenance windows (i.e., between the admissive earliest and latest start time of maintenance), simultaneous maintenance, continuous maintenance, the maximum area maintenance capacity, manpower, etc.

The number of integer variables of a GMS problem is very large, even for a middle-scale system, at about 103–104 (equal to the number of units multiplied by time intervals), so the existing integer-programming methods cannot be used to solve such a large-scale integer problem. However, a GMS problem can be formulated into a multistage decision-making problem with a noncontinuous objective function and constraints with nonanalytical equations, which can be solved by dynamic programming. Recently, a prototype ES with FDP has been shown to be effective for a special system. However, because of the complexity of the power system, a prototype ES cannot satisfy the diversification of a GMS problem of different power systems.

The ES with generalized construction is discussed in this chapter, which can be applied to different power systems or different operation conditions of the same system. The ES can be assembled from different rules that can be used to decide the maintenance priorities of the generators and to treat the constraints of a GMS problem. The inherence of GMS is that a feasible solution is very hard to find, but it must be obtained for practical purposes. If no feasible solution exists, then the constraints must be modified, or the forecasting load in certain time intervals should be curtailed by an amount that's as small as possible. With the aid of the ES and the "fuzzification" of constraints, the solution time and memory of GMS will be greatly reduced, and a reasonable strategy will be more easily obtained.

An approach based on the generalized ES and fuzzy constraints is proposed in this chapter. In this approach, users can define the rules of the ES with generalized construction. The constraints of a GMS problem are represented by fuzzy membership functions. A new GMS program based on this approach has been developed that fully considers the special requirements of different systems.

The generator capacity scale of a provincial power system used in this study is shown in Table 3.1, totaling 4 areas, 9 power plants, and 55 generating units, with a total installed capacity of 4083 MW, and the unit capacity of the 55 generating units ranging from 12 to 350 MW; the relation of annual load curve and total installed capacity is shown in Fig. 3.1. The maximum difference between the annual load curve (only step points are given) and total

Table 3.1 Capacity scale of generator

Unit Capacity (MW)	Number of Units	Total Capacity (MW)
12	14	168
12.5	2	25
25	14	350
40	1	40
50	10	500
100	2	200
200	9	1800
300	1	300
350	2	700
Total	55	4083

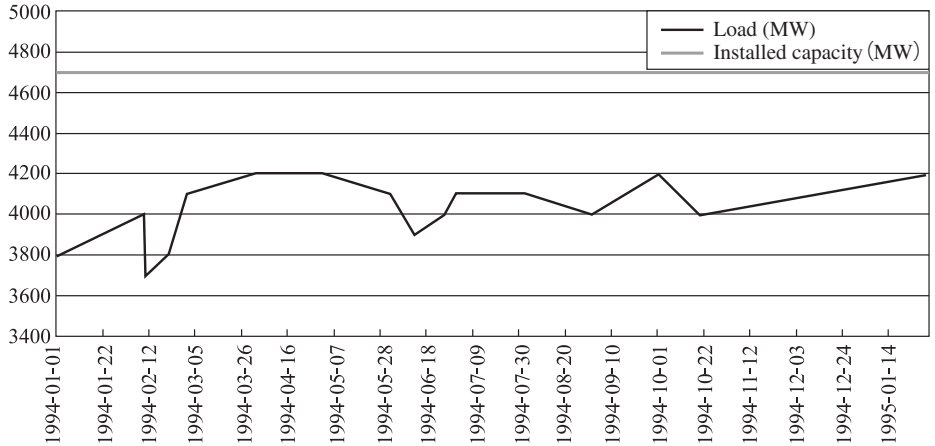

Fig. 3.1
Relation between annual load curve and total installed capacity.

installed capacity is 1000 MW, and the minimum is 500 MW, which means the two largest generating units cannot be maintained simultaneously because it will exceed the maximum allowable maintenance capacity.

3.1.2 Basic Requirements for Annual Generator Maintenance Scheduling

GMS is a medium- and long-term planning problem. GMS is used to arrange the generator maintenance sequence and schedule. The units should be considered as being in an outage state from the start to completion of maintenance. Therefore, the basic requirements of GMS are, on the one hand, not only to determine the capacity of the maintainable units in the maintenance period, that is, deducting the capacity (disabled capacity) of the units unable to reach their full capacity from the generating capacity of the whole system, but also to meet the load demand and minimum reserve capacity during the maintenance period. On the other hand, GMS also takes into overall consideration the maintenance durations of all units, makes feasible combinations of unit maintenance under the previously mentioned conditions, and further confirms each unit and its capacity are available to be maintained in the maintenance period.

3.1.3 Overview of This Chapter

This chapter studies the optimization method of the annual GMS based on the dynamic fuzzy logic method and takes the GMS problem in a province as an example. This chapter uses the expertise of professionals to form the ES knowledge base, simulates the inference method of the power grid dispatcher to form GMS solution rules and the basis for logic judgment, and replaces the conventional rigid constraints with flexible ones based on FDP. It provides a rapid, effective, and convenient tool for the comparison of several GMS solutions as well as a scenario in which the maintenance schedules of the generating plant need to be updated as soon as possible after system failure or when load conditions have a great change.

This chapter presents the basic idea of optimizing modeling, specifically in Section 3.2 as reference. Section 3.3 presents the optimization mathematical model of GMS. Section 3.4 introduces the fuzzification of a GMS mathematical model. Section 3.5 introduces the ES for solving GMS. Section 3.6 introduces the optimization calculation algorithm and process of GMS dynamic programming. Section 3.7 presents detailed results of actual calculation examples and analysis.

3.2 Basic Ideas of Developing an GMS Model

GMS is a medium-term planning problem, whose scheduling interval is quite long (about 1 year). When considering all necessary operating conditions and constraints, the GMS problem is very complicated.

A GMS problem should have the following characteristics: the maintenance time for full or partial maintenance can be different. Each unit's maintenance can be performed multiple times within a given interval. When developing a GMS, the proposed ES can determine the priority.

The objective function should consider both the maximizing reserve margin and minimizing production cost. The constraints should consider the maximum area maintenance capability, the reserve margin of generators, the maintenance window cycle, continuous maintenance conditions, and available manpower.

The GMS problem mentioned earlier requires a lengthy solution time and large computing memory. The existing programming techniques cannot be directly applied. However, a dispatch engineer with GMS experience may potentially be able to solve the GMS problem. Using their experience, an ES can be constructed. But the prototype ES can only be used to solve the GMS problem of a particular system. The generalized ES proposed in this chapter can be applied to GMS problems of different power systems.

In view of the large differences in the number of generators and the capacity of each power plant in each region, maintenance periods vary in length; some are shorter (more than 7 days), whereas some are much longer (more than 35 days). Some generators must be maintained within a given time, whereas others can be handled in a flexible way. There are many necessary conditions and constraints to be considered in the GMS problem. The following briefly introduces the modeling ideas of GMS.

3.2.1 Way of Handling Unit Maintenance Intervals

A GMS problem can divide the units in need of maintenance into two categories based on maintenance time: fixed maintenance and flexible maintenance.

(1) Fixed maintenance refers to the unit being maintained or the unit that needs to be maintained at the specified time. Its maintenance capacity must be reserved in the GMS. For those units that have shut down due to a fault, the maintenance should obviously be classified as a fixed maintenance. Therefore, the fixed maintenance arrangement can also be used to simplify the GMS in some cases.
(2) Flexible maintenance refers to the units that are not included in the fixed maintenance, that is, the units whose maintenance start time can be flexibly arranged and optimized to some extent. In the case of the current general lack of electricity in the power grid, the objective function of GMS in the flexible maintenance can be set to maximize the reserve margin of the system for the general system, and to minimize the production and maintenance costs of the system with adequate reserve margin.

3.2.2 Principles to Set Priority for Unit Maintenance

Determining the priority sequence of unit maintenance is the key to shorten the GMS calculation time. Without a priority sequence, the arrangement order of GMS with N generator units will have too many possible options (up to $N!$). For example, for a system with only a dozen units, the number of options would be 12! It is a large astronomical number. It is impossible to evaluate each option individually to choose the best scheme within an acceptable computation time. Fortunately, for a practical system, most of the options (close to $N!$) are unreasonable and unnecessary to be evaluated. Thus, before the GMS calculation, it is feasible and very necessary to preset a priority sequence for the unit maintenance in accordance with the system's reliability, economy, and rationality.

The general principles for setting the priority of unit maintenance are:

(1) Principle of handling production expenses. Units of high production expenses should have higher priorities of maintenance for the sake of economy.
(2) Principle of handling unit capacity. Units of larger capacity exert a greater impact on the system's reliability, so from the perspective of system reliability, a unit with a large capacity should have a higher priority for maintenance, especially for units with the same production expenses.
(3) Principle of handling the last maintenance completion time. Normally, the maintenance sequence of units in the same power plant should not be easily rearranged from a rationality point of view. Thus, in the same power plant, units whose last maintenance completion time was earlier should have higher maintenance priorities than those whose last maintenance completion time was later.

The maintenance priority of the unit can be determined based on the previously mentioned comprehensive principles or manually specified by the grid dispatcher in reference to these principles in terms of the difficulty of the unit's maintenance schedule, that is, those with a long maintenance time, large unit capacity, and difficult arrangements can be given priority. In addition, under abnormal conditions, the unit maintenance priority should also be able to change. For example, in the case of a serious fault, the broken-down units need higher priorities for maintenance in the GMS.

3.2.3 Way of Processing the Objective Function

There are two processing methods for GMS to select an objective function:

(1) For systems with high load level and small system reserve, GMS can select the maximum reserve margin of maintenance as the objective function.
(2) For systems with low load level and large system reserve, GMS can select the minimum production and maintenance expenses as the objective function.

3.2.4 Way of Processing the Variable Settings and Constraints

After analyzing the GMS, the maintenance period of each unit is identified as the core variable, because the sum of power generation output of each unit in each period needs to maximize the reserve margin. Once the unit enters the maintenance period, the output of the unit is zero.

Based on the analysis on GMS, all constraints are determined, which should be satisfied in the actual operation, specifically the balance constraints among the maintenance reserve, plus system output and the forecasting load in each period for an annual load of 360 h, the earliest and latest maintenance start time constraints of units, the capacity constraint of the maintained units simultaneously in the area, as well as the human maintenance constraints of the power plant.

As previously mentioned, the most important variable is the maintenance period of each unit. As long as the definition of each unit involves the identification of its own affiliated area and power plant, the output of the generator units in different regions under different time periods can be separately summed. On the basis of setting the maintenance period of all units as the kernel variable, and to make the system's power generation capacity meet the load demand with a certain reserve margin, the GMS should satisfy the following constraints related to system operation characteristics, geographical distribution, and some practical situations:

(1) General constraints.
    1. Maintenance window interval constraint, which specifies the earliest and latest start times of the generating equipment for maintenance. The specific maintenance interval of generating equipment should be in accordance with relevant regulations.
    2. Reserve capacity constraint, which will ensure a secure reserve capacity in the unit maintenance phase. If there is any conflict between the unit maintenance and minimum reserve, the schedule should be rearranged or a load adjustment measure taken. Otherwise the system cannot operate in a secure and reliable way.
    3. Maintenance manpower constraint, which limits the number of units maintainable at the same time. This constraint is not significant for an old power plant staffed with full-time maintenance personnel, but it is meaningful for new power plants that do not have full-time maintenance personnel. The full-time maintenance team not only guarantees maintenance quality but also saves maintenance costs. It is better to have a unified, full-time maintenance team for all power plants.

(2) Special constraints.
    1. Area maintenance capacity, which reflects a requirement to balance the generating capacity and load demand in the area as much as possible. If the area in which the unit is scheduled to be maintained requires a distant generator to compensate the regional power demand, the system transmission loss will be increased, even if such an arrangement can satisfy the reserve constraint of the whole system. More importantly,

such an arrangement will also sometimes affect the reliability of the power transmission. The area maintenance capacity constraint regulates the maximum capacity or the maximum number of units for simultaneous maintenance in the area.

2. Maintenance time nonoverlapping constraint, which is an important constraint related to the actual operation of GMS. Due to limitations such as site, tool, equipment, available manpower, etc., it is generally not feasible to have two or more units maintained in the same power plant. Therefore, the maintenance time of all units should not be overlapped. In other words, in each power plant, only one unit can be maintained at a time generally.

3.3 Formulation of the GMS Problem

3.3.1 Notations

Notations are shown in Table 3.2.

Table 3.2 Notations

Notation	Description
N	Total number of units involved in the GMS
T	Total number of time intervals in the GMS period (one time interval = one time unit)
i	Count variable of units
t	Count variable of time intervals
$P_{sc}(t)$	The total generation capacity in interval t, in MW
P_{Gi}	The rated capacity of unit i, in MW
$P_{L}(t)$	The system forecast load in interval t, in MW
$P_{EL}(t)$	The system equivalent load in interval t, in MW
$P_{HY}(t)$	Dependable system capacity of hydropower plant not involved in the GMS in interval t, in MW
$P_{SG}(t)$	Dependable system capacity of small thermal power plant not involved in the GMS in interval t, in MW
$P_{EP}(t)$	Exchange power with external system in interval t $P_{EP}(t)>0$: with input power; $P_{EP}(t)<0$: without output power; $P_{EP}(t)=0$: no exchange power
$P_{SZ}(t)$	Sum of disabled capacities where the units fail to reach full capacity in interval t or the minimum reserve capacity of the system, in MW
$P_{RM}(i,t)$	Maintenance reserve margin in interval t, in MW
Y_{it}	Maintenance state variable, $Y_{it}=1$ or 0, meaning that unit i is either under or not under maintenance in interval t
$Z_i(t)$	Maintenance start variable, $Z_i(t)=1,0$ means that t-th interval is either the maintenance start time or not of unit i, I
C_{Pi}	Unit production expenses (or coal consumption) of unit i
C_{Mi}	Maintenance expenses of unit i
R_t	Lower limit of the ratio (maintenance reserve power/forecast load)
Period(i)	Number of time intervals in maintenance cycle of unit i
Shift(i)	Number of shiftable time intervals within maintenance cycle of unit i

Based upon the modeling approaches in Section 3.2 and these notation definitions, the following objective functions and constraints of GMS can be formed.

3.3.2 Objective Function

(1) The GMS may select the reserve margin of maintenance as the objective function for systems of high load level and small system reserve:

$$\max\{\min\{P_{\mathrm{RM}}(i,t)\}\} \quad i\in\{i,\ldots,N\}, \quad t\in\{1,\ldots,T\} \tag{3.1}$$

The meaning of the objective function is that, for each unit i to be maintained, first find the minimum values of maintenance reserve $\mathrm{P_{RM}}(i,t)$ in every possible "maintenance period," then find the maximum among these minimum values. The "maintenance period" corresponding to the maximum is considered the optimal maintenance arrangement time of unit i.

(2) The GMS may select the production and maintenance expenses as the objective function for systems of low load level and large system reserve:

$$\min\left\{\sum_{i=1}^{N}\sum_{t=1}^{T}C_{\mathrm{P}i}P_{\mathrm{G}i}(1-Y_{it})+\sum_{t=1}^{N}C_{\mathrm{M}i}Z_i(t)\right\} \tag{3.2}$$

3.3.3 Constraints

(1) Maintenance reserve constraint. In the GMS problem, relations between the maintenance reserve and system output and forecast load of the system in interval t are shown here:

$$P_{\mathrm{SC}}(t)=\sum_{i=1}^{N}P_{\mathrm{G}i}+P_{\mathrm{HY}}(t)+P_{\mathrm{SC}}(t)+P_{\mathrm{EP}}(t)-P_{\mathrm{SS}}(t) \tag{3.3}$$

$$P_{\mathrm{RM}}(t)=P_{\mathrm{SC}}(t)-P_{\mathrm{D}}(t)-\left(\sum_{i=1}^{N}Y_{it}P_{\mathrm{G}i}\right) \tag{3.4}$$

Based on Eq. (3.4), the maintenance reserve constraint of the system is given:

$$P_{\mathrm{RM}}(t)/P_{\mathrm{L}}(t)\geq R_t \tag{3.5}$$

In a practical system, R_t is generally 10%–15% or P_{RM} is equal to or greater than the capacity of one or two units with the maximum capacity in the system.

(2) Maintenance window constraint, which means the earliest and latest maintenance start time constraint of the unit. For unit i, it is expressed as:

$$Z_i(t)=\begin{cases}0, & t>E_i \text{ or } t>L_i\\ 1, & E_i\leq t\leq L_i \text{ and } t=\text{maintenance start time}\end{cases} \tag{3.6}$$

$$\begin{aligned} Y_{it}(t) &= \begin{cases} 0, & t > E_i \text{ or } > L_i \\ 1, & E_i \le t \le L_i + \mathrm{MD}_i \end{cases} \\ E_i &= \mathrm{Period}(i) - \mathrm{Shift}(i) \\ L_i &= \mathrm{Period}(i) + \mathrm{Shift}(i) \end{aligned} \tag{3.7}$$

where E_i—the feasible earliest maintenance start time of unit i, L_i—the feasible latest maintenance start time of unit i, MD_i—maintenance duration of unit i.

(3) Maintenance time nonoverlapping constraint, which reflects the technical requirements of two or more units generally unable to be maintained simultaneously in the same power plant, is expressed as:

$$\sum_{i \in F} Y_{it} = 1 \tag{3.8}$$

where F—power plant F in the system.

(4) Area maintenance capacity constraint, which limits the total capacity of units maintained simultaneously in the area, is expressed as:

$$\sum_{i \in J} P_{\mathrm{G}i} Y_{it} \le M_{\mathrm{g}}(J)_{\max} \tag{3.9}$$

where J—area J in the system, $M_{\mathrm{g}}(J)\mathrm{max}$—maximum capacity of units maintained simultaneously in the area J.

(5) Maintenance manpower constraint, which limits the number of units to be maintained at the same time for those power plants not staffed with full-time maintenance personnel, is expressed as:

$$\sum_{i=1}^{N} M_{\mathrm{P}i} Y_{it} \le M_{\mathrm{Pmax}} \tag{3.10}$$

where $M_{\mathrm{P}i}$—maintenance manpower required for unit i, M_{Pmax}—maximum human resources available for maintenance of the system.

Because GMS is a problem of medium- and long-term planning, its optimization objective and constraint boundary are often uncertain and even fuzzy. Such uncertainty and fuzzy factors make it sometimes difficult to carry out accurate numerical evaluation for optimization results, often with larger trends based on experiential knowledge. For instance, different maintenance scheduling in a specific time window will produce different expense indexes or reserve margin indexes. However, the uncertainty in load, unit output, and other factors in the time window make it unable to determine which index is the optimal one. At present, the empirical subjective evaluation with "satisfaction degree" is more appropriate for the actual situation. Thus, proper fuzzification of the GMS objective function and constraints will make the GMS solution procedure more flexible.

3.4 Fuzzification of GMS Model

3.4.1 Selection of Fuzzy Membership Function

Fuzzy membership function is a proper mathematical description for the "subject" to make subjective evaluation of the "object." However, different "subjects" may have different evaluations of the "object," and hence it is required to employ different fuzzy membership functions to describe them.

Among numerous forms of fuzzy membership functions, three are commonly used: linear, parabolic, or reversed parabolic, as shown in Fig. 3.2.

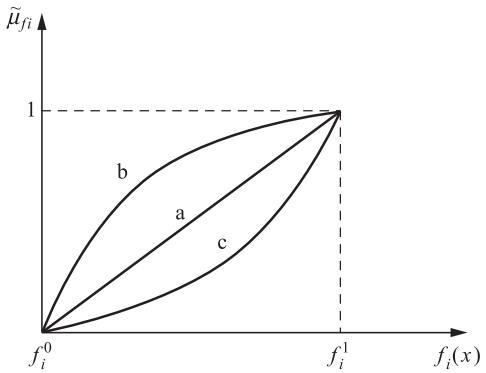

Fig. 3.2
Fuzzy membership functions of different forms.

In Fig. 3.2, curve a is the linear fuzzy membership function, representing the moderate decision maker. Curve b is the reversed parabolic function for the conservative decision maker, and curve c is the parabolic function for the adventurous decision maker. Different experienced experts may, according to the features of their evaluation of actual problems, use different fuzzy membership functions to fit and select the most suitable one.

When solving GMS problems, the linear fuzzy membership function shaped like curve a is adopted, mainly to simplify the mathematical description. Although the forms of fuzzy membership functions are different, the basic ideas are consistent. The linear membership function is generally expressed as:

$$\overline{\mu}_{fi}(x) = \frac{f_i(x) - f_i^0}{f_i^1 - f_i^0} \tag{3.11}$$

and

$$\overline{\mu}_{fi}(x) = 0, \quad f_i(x) \le f_i^0$$
$$\overline{\mu}_{fi}(x) = 1, \quad f_i(x) \ge f_i^1$$

In Eq. (3.11), f_i^0 is at an unacceptable level, whereas f_i^1 is at a fully desirable level; the fuzzy membership function $\overline{\mu}_{fi}(x)$ reflects the membership degree of function $f(x)$ between f_i^0 and f_i^1.

3.4.2 Formation of Fuzzy Objective Index of GMS

The fuzzy performance index corresponds to the fuzzy goal. Depending on the OPindex (0,1) interval of system operation index, the GMS may consider two fuzzy performance indexes, that is, reserve margin and production expenses. When the system is at a high load level, fuzzy performance index with reserve margin may be selected as objective index. When the system is at a low load level, either the fuzzy performance index with reserve margin or with production expenses may be selected as objective index.

(1) Fuzzy membership function with reserve margin as objective index is expressed as:

$$\overline{\mu}_{\mathrm{gl}}(i,t) = \begin{cases} 0, & P_{\mathrm{RM}}(i,t) < R_{\mathrm{mn}} \\ 1 - W_{\mathrm{rm}} \dfrac{\overline{R}_{\mathrm{m}}(i) - R_{\mathrm{RM}}(i,t)}{\overline{R}_{\mathrm{m}}(i) - \underline{R}_{\mathrm{m}}(i)}, & P_{\mathrm{RM}}(i,t) \ge R_{\mathrm{ma}} \\ 1, & P_{\mathrm{RM}}(i,t) \ge R_{\mathrm{ms}} \end{cases} \tag{3.12}$$

where $P_{\mathrm{RM}}(i,t)$—minimum surplus capacity when reaching to the state (i,t), W_{rm}—weight coefficient of reserve margin, R_{ma}—acceptable minimum reserve capacity, R_{ms}—reserve capacity to the reliability requirements, $\overline{R}_{\mathrm{m}}(i)$ — $\max\limits_{T}\{P_{\mathrm{RM}}(i,t)\}$; $\underline{R}_{\mathrm{m}}(i)$ — $\min\limits_{T}\{P_{\mathrm{RM}}(i,t)\}$.

(2) Fuzzy membership function with production expenses as objective index is expressed as:

$$\overline{\mu}_{\mathrm{g2}}(i,t) = 1 - W_{\mathrm{cp}} \frac{C_{\mathrm{P}}(i,t) - \underline{C}_{\mathrm{P}}(i)}{\overline{C}_{\mathrm{P}}(i) - \underline{C}_{\mathrm{P}}(i)} \tag{3.13}$$

where $C_{\mathrm{P}}(i,t)$—minimum production expenses when reaching to the state (i,t), W_{cp}—weight coefficient of production expenses, $\overline{C}_{\mathrm{P}}(i)$ — $\max\limits_{T}\{C_{\mathrm{P}}(i,t)\}$; $\underline{C}_{\mathrm{P}}(i)$ — $\min\limits_{T}\{C_{\mathrm{P}}(i,t)\}$.

The fuzzy membership function curve of production expenses is shown in Fig. 3.3.

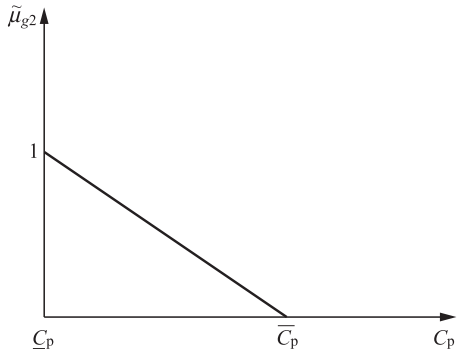

Fig. 3.3
Fuzzy membership function curve of production expenses.

3.4.3 Formation of Fuzzy Constraints for GMS Problem

The constraint boundary of GMS may be described by the fuzzy membership function $\overline{\mu}_c(x)$.

(1) Fuzzy maintenance window constraint. Two edges of the maintenance window are the earliest and latest maintenance start times of the unit. The fuzzy membership function is expressed as:

$$\overline{\mu}_{c1}(i,t) = \begin{cases} 1 - W_{sle}\ \dfrac{M_{slb}(i) - M_{st}(i,t)}{M_{stb}(i) - M_{sle}(i)}, & M_{sle} \le M_{st}(i,t) < M_{stb} \\ 1 - W_{sll}\ \dfrac{M_{st}(i,t) - M_{st}(i)}{M_{sll}(i) - M_{slb}(i)}, & M_{sle} \le M_{st}(i,t) < M_{sll} \end{cases} \tag{3.14}$$

where $M_{st}(i,t)$—maintenance start time in state (i,t), $M_{sle}(i)$—the earliest acceptable maintenance start time for unit i, $M_{sll}(i)$—the latest acceptable maintenance start time for unit i, $M_{slb}(i)$—the optimal maintenance start time for unit i, W_{sle}—weight coefficient that advances maintenance time, W_{sll}—weight coefficient that delays maintenance time. The fuzzy membership function curve of maintenance window is shown in Fig. 3.4.

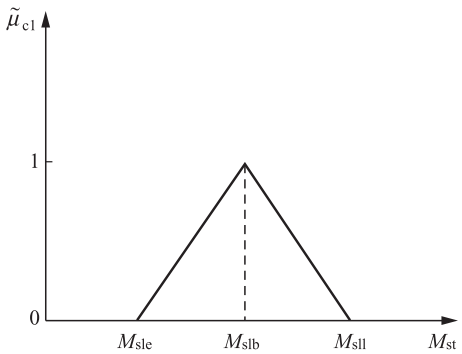

Fig. 3.4
Fuzzy membership function curve of maintenance window.

(2) Fuzzy maintenance time nonoverlapping constraint, which reflects whether the units meet the technical conditions for maintenance. The fuzzy membership function is expressed as:

$$\widetilde{\mu}_{c2} = \begin{cases} 0, & D_e(i,t) < D_{1\min} \\ 1 - W_1 \dfrac{\overline{D}_1(i) - D_1(i,t)}{\overline{D}_1(i) - \underline{D}_1(i)}, & d_1(i,t) \geq D_{1\min} \\ 1, & D_1(i,t) \geq D_{1s} \end{cases} \tag{3.15}$$

where $D_1(i,t)$—minimum maintenance interval time when reaching to state (i,t), W_1—weight of maintenance time nonoverlapping, $D_{1\min}$—minimum acceptable maintenance interval time, D_{1s}—maintenance interval time meeting the normal requirement, $\overline{D}_1(i)$ — $\max_T \{D_1(i,t)\}$; $\underline{D}_1(i)$ — $\min_T \{D_1(i,t)\}$.

The fuzzy membership function curve of maintenance time constraint is shown in Fig. 3.5.

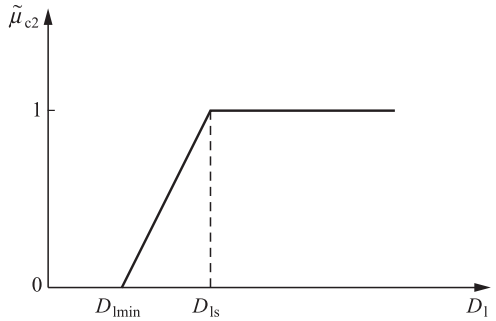

Fig. 3.5
Fuzzy membership function curve under maintenance time constraint.

(3) Fuzzy area constraint. The area constraint divides the system into several areas by geographical location, limits the concurrent maintenance capacity in each area, and decreases the power exchange between areas so as to reduce the transmission loss and maintain the reliability of power supply. The fuzzy membership function of constrained boundary is expressed as:

$$\widetilde{\mu}_{c3} = \begin{cases} 0, & M_g(i,t) > M_g(j)_{\max} \\ 1 - W_g \dfrac{\overline{M}_g(i) - M_g(i,t)}{\overline{M}_g(i) - \underline{M}_g(i)}, & M_g(i,t) \leq M_g(j)_{\max} \\ 1, & M_g(i,t) \leq M_g(j) \end{cases} \tag{3.16}$$

where $M_g(i,t)$—minimum maintenance capacity when reaching to state (i,t), $M_g(j)$—acceptable maintenance capacity in area j (the unit i is in the area), $M_g(j)_{\max}$—maximum

maintenance capacity in area j, W_g—weight coefficient of area maintenance capacity constraint, $\overline{M}_g(i) = \max_T \{M_g(i,t)\}$; $\underline{M}_g(i) = \min_T \{M_g(i,t)\}$.

The fuzzy membership function curve of area maintenance capacity constraint is shown in Fig. 3.6.

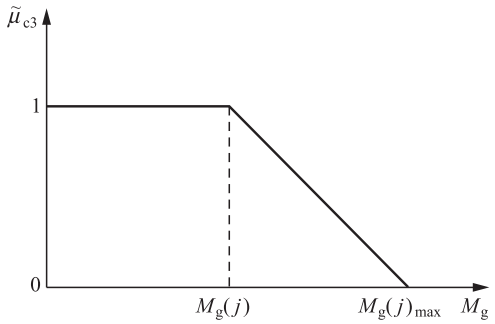

Fig. 3.6
Fuzzy membership function curve of area maintenance capacity constraint.

(4) Fuzzy manpower constraint. For those power plants staffed with full-time maintenance personnel, the effect of manpower constraints may not be considered, but it must be considered for those without such personnel. In other words, the power plants not staffed with full-time maintenance personnel may be subject to manpower constraints given that too much maintenance is conducted at the same time. The fuzzy membership function of manpower constraint is expressed as:

$$\widetilde{\mu}_{c4}(i,t) = \begin{cases} 0, & M_p(i,t) > M_{pmax} \\ 1 - W_p \dfrac{\overline{M}_p(i) - M_p(i,t)}{\overline{M}_p(i) - \underline{M}_p(i)}, & M_p(i,t) \le M_{pmax} \\ 1, & M_p(i,t) \le M_{pav} \end{cases} \tag{3.17}$$

where $M_p(i,t)$—minimum manpower required to reach state (i,t), W_p—weight coefficient of manpower constraint, M_{pmax}—maximum manpower available, M_{pav}—Normal average manpower available,
$\overline{M}_p(i) = \max_T \{M_p(i,t)\}$; $\underline{M}_p(i) = \min_T \{M_p(i,t)\}$.

The fuzzy membership function curve of manpower constraint is shown in Fig. 3.7.

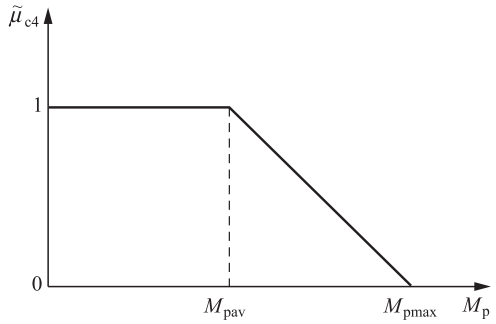

Fig. 3.7
Fuzzy membership function curve of manpower constraint.

3.5 Expert System Developed for GMS

The expert rules are well defined so that the linguistic rules can be expressed as a mathematical set or logical expression, and can be input by the user into the GMS program. Based on the system requirements for GMS and the experience of the dispatch engineers, the generalized ES, which is abstracted from reasoning rules, can be constructed.

The GMS ES knowledge base could be constructed based on the actual requirements of the system and the GMS scheduling experience of the power grid dispatchers. The GMS ES consists of several abstract reasoning rules and can be used to optimize, accelerate, and standardize the GMS solution procedure.

Some special factors considered in this GMS are explained in detail as follows.

3.5.1 Selecting of Time Units

Prior to the GMS, a proper time unit shall be selected. A shorter time unit will increase the computation time but make the maintenance combination more flexible; a longer time unit will make the GMS inflexible but decrease the computation time. Hence, various factors should be comprehensively considered for selecting the time unit.

At present, the GMS of all power grid dispatching departments may be roughly divided into annually, quarterly, and monthly plans. The system will often suffer from unexpected changes in conditions, which inevitably prevents the annually and quarterly plans from precise execution. Thus, such plans may be somewhat rough, and their time units may be measured in weeks. However, the monthly GMS is generally a real one that must be executed, so the time unit of that one should be accurately set as a day.

To make the GMS procedure work for all the annual, quarterly, and monthly plans, a day should be selected as the time unit of GMS calculation, which not only keeps the annually and quarterly plans more flexible but also ensures the operability of monthly plans.

3.5.2 Introducing of Operation Index

The GMS's ability should be evaluated before GMS calculation. The GMS ability is defined as the difference between the installed system capacity and the equivalent load. The larger the difference or reserve margin, the stronger the GMS ability. Thus, the concept of operation index may be introduced to represent GMS ability of power systems.

The operation index is defined as follows:

$$OP_{\text{index}} = \frac{\sum_{i=1}^{N_M} P_{\text{G}i} M_{\text{D}i}}{T\sum_{i=1}^{N} P_{\text{G}i} - \sum_{i=1}^{T} P_{\text{EL}}(t)} \tag{3.18}$$

$$P_{\text{EL}}(t) = P_{\text{L}}(t) - P_{\text{HY}}(t) - P_{\text{SG}(t)} - P_{\text{EP}}(t) + P_{\text{SZ}}(t) \tag{3.19}$$

where N_M—total number of units involved in maintenance in the total study time interval, $M_{\text{D}i}$—number of maintenance duration of unit i, T—total time intervals to be studied, $P_{\text{G}i}$—capacity (MW) of unit i, $P_{\text{EL}}(t)$—system equivalent load (MW) in the time interval t.

The operation index, whose significance is shown in Fig. 3.8, can be used to represent the GMS's ability so that a GMS strategy can be selected under the following conditions.

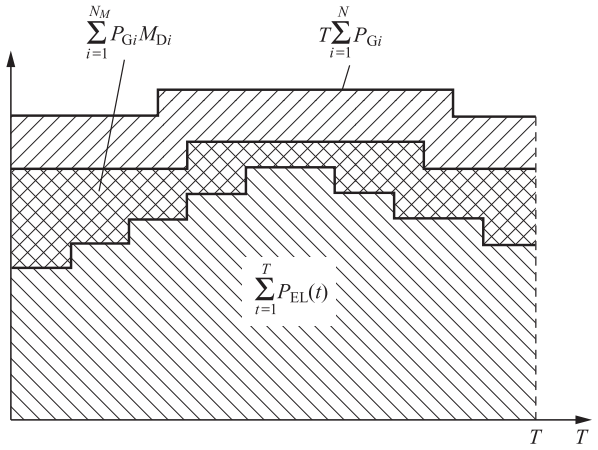

Fig. 3.8
Significance of operation index.

In Fig. 3.8, $T\sum_{i=1}^{N}P_{Gi}$ and $\sum_{i=1}^{N}P_{EL}(t)$ are two fixed curves in the whole period T. The area enclosed by the two curves has constituted the total maintenance reserve area of the system, which is a constant. If a GMS is feasible, then the maintenance area of a scheduled unit must be less than this area. Otherwise, the system may not meet the load demand, and such a GMS is hazardous to the system, that is, the system has no ability to fulfill the GMS. The introduction of an operation index can quantify the system's GMS ability, so that different GMS control strategies can be selected in a targeted manner.

(1) Operation index OPindex > 1.0. This indicates that the capacity of units scheduled for maintenance is greater than allowable in the studied time interval. Under such a condition, not all units scheduled for maintenance can be arranged in the studied time interval. Possible control process would be:
Step 1: Where possible (judged by the experts), move some to-be-maintained units out of the studied period, then recalculate the operation index.
Step 2: If the feasible movement in Step 1 still fails to make the operation index less than 1.0, then there is only one way to achieve this, which is to decrease the partial forecast loads of the system.
When OPindex > 1.0, obviously, the generation output cannot meet the load demand, thus, it is necessary to delay maintenance (if possible) or curtail the loads.

(2) Operation index OPindex < 1.0. This indicates that the system allowable maintenance margin is greater than the scheduled one. This is the essential prerequisite condition to make the GMS calculation. Under such a condition, the GMS is feasible if other system constraints can be met at the same time period. There are many constraints for the system to complete GMS. Based upon the expert's experience, the main constraints are:
   1. Maintenance window constraint of units.
   2. Maintenance time nonoverlapping constraint of units.

   The two constraints play a significant role in completing the GMS, which raises requests for the system to make the GMS respectively from two aspects:
   1. Maintenance window constraint reflects the running state whether generating units shall be maintained, thus, this constraint can be satisfied as long as there is adequate maintenance reserve capacity in the system.
   2. Maintenance time nonoverlapping constraint reflects whether generating units are technically qualified for maintenance (such as site, manpower, equipment etc.), therefore, this constraint may not be satisfied even if there is adequate maintenance reserve capacity. The following are two unsatisfied situations:
      a. For all generating units that participated in the inspection of concurrent maintenance time nonoverlapping constraints, if the sums of their maintenance time and minimum intervals between maintenance times is greater than the total

GMS study period, then the system cannot schedule maintenance for such units in the studied period. The only feasible way is to postpone the maintenance cycles of some units from the GMS study period.

b. For all generating units that participated in the inspection of concurrent maintenance time nonoverlapping constraints, if the sums of their maintenance time and minimum intervals between maintenance times is less than the total GMS study period, then the system has the prerequisite for maintenance scheduling. However, some units may not be tightly scheduled for maintenance (such as pursuing maximum reserve capacity of the system), which causes an inability of other unit maintenance to be inserted in the studied period. For this situation, in case of failure to delay the maintenance scheduling of other units from the GMS study period, it is required to give up the pursuit of maximum system reserve capacity; instead, the maintenance start time for these units depends on their sequence of last maintenance completion time and refers to their earliest and latest start time of next maintenance of each unit. In addition, if the reserve margin in some periods is unable to meet the system's load demand due to such a schedule, the load level in such a period must be curtailed to comply with the GMS requirements.

3.5.3 Related Rules of the Expert System

3.5.3.1 Rules of determining priorities for unit maintenance

Rule 1: The maintenance priority manually assigned by the system dispatch engineer is the highest one over others determined by other methods.

Rule 2: The unit with highest production cost has highest maintenance priority.

Rule 3: If two units have the same production cost, then the one with larger capacity has highest maintenance priority.

Rule 4: If two units have the same production cost and capacity, then the one with early completion time of the last maintenance has highest priority.

3.5.3.2 Rules of verifying GMS capability

Rule 5: If the system's GMS operation index OPindex > 1.0, then try to extend the interval between the maintenance period of some units.

Rule 6: If an interval between the maintenance period of some units cannot be extended or if the operation index is still OPindex > 1.0 after extension, then forecast loads in some time intervals should be curtailed to make the operation index less than 1.0.

3.5.3.3 Rules of verifying area constraint

Rule 7: In the given time intervals, if the scheduled maintenance capacity or the number of maintenance units in a certain area is over the constraint, then the maintenance schedule of some units with lower maintenance priority should be shifted.

3.5.3.4 Rules of verifying power plant constraint

Rule 8: In the given time intervals, the maintenance duration of the units within two plants should not be overlapped. Namely, units in one power plant and those in another shall be staggered in terms of maintenance scheduling.

Rule 9: If the two units within the same plant have the overlapping maintenance duration, then the maintenance duration of the unit with lower priority should be shifted away.

3.5.3.5 Rules of verifying manpower constraint

Rule 10: If the maintenance manpower of a unit is not enough, then the maintenance duration of the unit should be shifted.

The constraints and objectives of the GMS problem can be described by fuzzy membership functions, such as fuzzy maintenance window constraint, fuzzy constraint of area maintenance capacity, fuzzy simultaneous maintenance constraint, and fuzzy manpower constraint, as well as fuzzy objectives of reserve margin and production costs, etc.

3.6 Calculation Procedure of GMS Optimization

3.6.1 Search Paths and Recursive Formulas of Fuzzy Dynamic Programming

The optimized decision of GMS depends on the intersection of objective function and fuzzy membership function of constraint boundary $\widetilde{\mu}_{g1}$,$\widetilde{\mu}_{g2}$ and $\widetilde{\mu}_{c1}$, $\widetilde{\mu}_{c2}$,$\widetilde{\mu}_{c3}$,$\widetilde{\mu}_{c4}$, $\widetilde{\mu}_{D}(i,t)$ is used to express the highest fuzzy membership function value of all maintenance schedule states from the previous unit to the current unit in the recursive process of FDP, and the optimal decision $\widetilde{\mu}_{D}(opt)$ of FDP depends on such $\widetilde{\mu}_{D}(i,t)$.

The search strategy of the FDP is shown in Fig. 3.9.

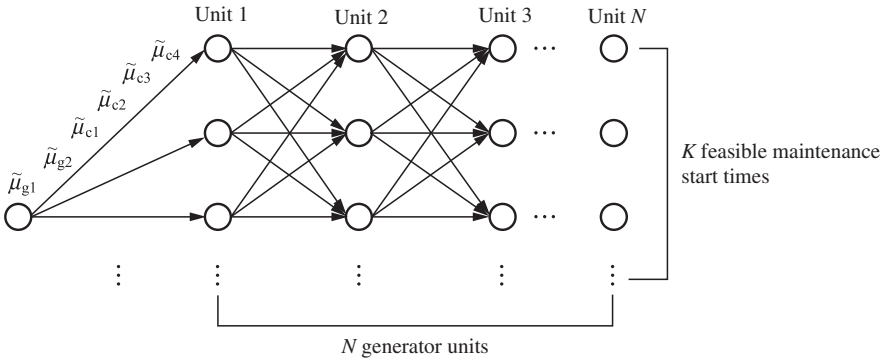

Fig. 3.9
Search strategy of the fuzzy dynamic programming.

The recursive algorithm of the FDP is:

$$\widetilde{\mu}_{\mathrm{D}}(i,t) = \max_{J}\left\{\min_{T}\left\{\widetilde{\mu}_{\mathrm{g1}}(i,t), \widetilde{\mu}_{\mathrm{g2}}(i,t), \widetilde{\mu}_{\mathrm{c1}}(i,t), \widetilde{\mu}_{\mathrm{c2}}(i,t), \widetilde{\mu}_{\mathrm{c3}}(i,t), \widetilde{\mu}_{\mathrm{c4}}(i,t), \widetilde{\mu}_{\mathrm{D}}(i-1,t)\right\}\right\} \tag{3.20}$$

The optimal decision is:

$$\widetilde{\mu}_{\mathrm{D}}(opt) = \max_{K}\left\{\widetilde{\mu}_{\mathrm{D}}(l,k)\right\} \tag{3.21}$$

where $\widetilde{\mu}_{\mathrm{D}}(i,t)$—highest fuzzy membership function value when reaching state (i,t), J—$j \in J$, the set of maintenance start time acceptable for unit i, T—$t \in T$, the set of maintenance start time for unit i, K—$k \in K$, the set of maintenance start time acceptable for the last unit i, l—last unit l scheduled for maintenance.

3.6.2 Main Calculation Procedure

The solution procedure based on the proposed approach is shown in Fig. 3.10. At Step 1, the GMS data file is read in. At Step 2, the general information, such as the study interval and time intervals of each date, etc. are formed. At Step 3, the priority is determined by the ES or dispatcher in the input data. At Step 4, the equivalent load curve is formed. At Step 5, the reserve margin is constructed. At Step 6, based on the ES, dynamic programming is applied to

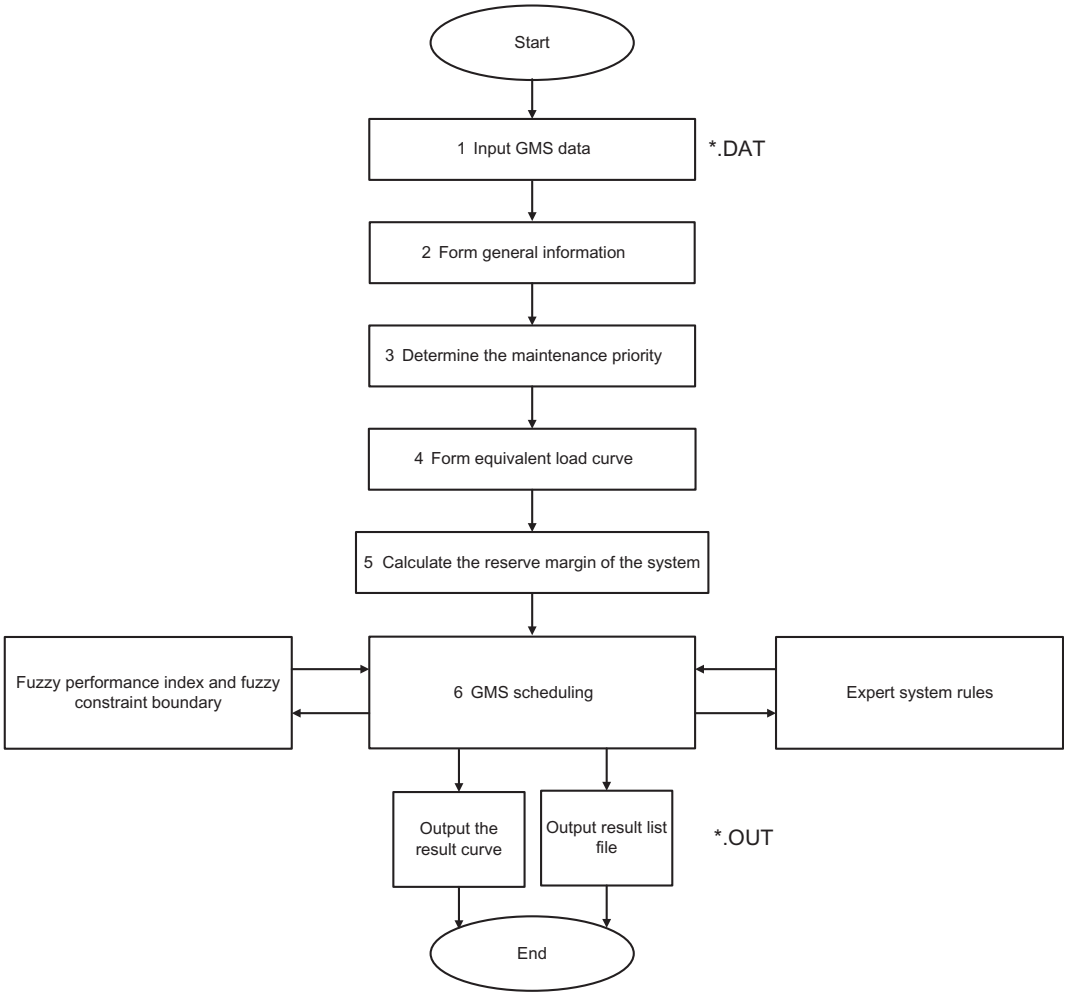

Fig. 3.10
Optimization calculation procedure of generator maintenance scheduling.
Note: * may be any character string given by the user (up to 20 bytes).

the GMS under the condition of satisfying the fuzzy constraints. Lastly, the GMS results are output.

The calculation procedure of generator maintenance scheduling is shown in Fig. 3.10. The file types of generator maintenance scheduling are as follows:

(1) GMS input data file type: *.DAT.

(2) GMS output list file type: *.OUT.

3.6.3 Description of the Input Data

The input data of generator maintenance scheduling mainly consists of the following eight parts: GMS calculation begin card (BEGIN card), generator maintenance information card (GE card), area maintenance capacity restraint card (RA card), maintenance time nonoverlapping card (RP card, for power plants), maintenance time nonoverlapping card (RG card, for generator groups), equivalent load curve card (CC card), GMS data file end card (END card), and information comment card (** card).

Among them, BEGIN, GE, CC, and END cards are necessary in the input data files; otherwise the procedure cannot be executed. Although the RA, RP, and RG cards can be combined by the procedure, users can at-will construct the ES knowledge base for the system based on the characteristics of their own system. Therefore, the GMS solution process can be intervened to obtain the generator maintenance scheduling in compliance with the system requirements. The details of the eight data cards are described as follows:

(1) GMS calculation begin card (BEGIN card), which includes scheduling start time, end time, as well as the case name and print options (see Table 3.3).

Table 3.3 Contents of BEGIN card

Identifier	Contents
BEGIN	BEGIN, denoting the begin card
START	Schedule start time (YY-MM-DD), for example, 94-12-31
CASENAME	Case name (optional)
P	Print options, $P=0$: output the calculation results only $P=1$: output the reduced input data and calculation results

(2) The generator maintenance information card (GE card), which includes all information required for maintenance scheduling of generating units (see Table 3.4).

Table 3.4 Contents of GE card

Identifier	Contents
GE	GE, denoting the generator maintenance information card
AERA	Name of area where the generating unit is located
PLANT	Name of power plant where the generator is located
GEN	Name of generating unit
BUREAU	Fill in B, which means the generator belongs to the Bureau, otherwise left blank
CAP	Rated capacity of the generator (MW, if CAP = 0 or left blank, it means this line is header boiler)

Continued

Table 3.4 Contents of GE card—Cont'd

Identifier	Contents
RULE	Fill in Y, which means the generator maintenance scheduling shall satisfy the ES rules; if fill in 0 or left blank, it means the generator maintenance scheduling does not have to be tested by ES rules
PERIORTY	Manually given maintenance priority, optional
RERIOD	Generator maintenance period (days)
SHIFT	Margin before and after the maintenance period (days)
PRETIME	Last maintenance start time (YY-MM-DD)
FINISH	Last maintenance finish time (YY-MM-DD)
DUR1	Time (days) required for the first maintenance after the last maintenance
DUR2	Time (days) required for the second maintenance after the last maintenance, optional
DUR3	Time (days) required for the third maintenance after the last maintenance, optional
DUR4	Time (days) required for the fourth maintenance after the last maintenance, optional
COST	Production expenses or coal consumption, optional
MAN	Manpower required for maintenance, optional

(3) Area maintenance capacity restraint card (RA card), which gives the name of the area to limit the maintenance capacity, maintenance restraint capacity, and time range where the card works (see Table 3.5).

Table 3.5 Contents of RA card

Identifier	Contents
RA	RA, denoting the area maintenance capacity restraint card
AERA	Name of area
ACAP	Upper limit of area maintenance capacity (MW)
A-START	Start date (YY-MM-DD) of area maintenance capacity restraint, optional
A-END	End date (YY-MM-DD) of area maintenance capacity restraint, optional

Note: If A-START and A-END are left blank, it indicates the area maintenance capacity restraint card works in the whole GMS study period. If dated YY-MM-DD, the area maintenance capacity shall be restrained in the given time range.

(4) Maintenance time nonoverlapping (for power plants) card (RP), which can restrain all unit maintenance time from overlapping in the given power plant, with card contents shown in Table 3.6.

Table 3.6 Contents of RP card

Identifier	Contents
RP	RP, denoting the maintenance time nonoverlapping (power plant) card
PLANT1	Name of power plant 1
PLANT2	Name of power plant 2 (may be the same as power plant 1)
DT	Time interval (days) between maintenance time, optional
PCAP	Lower limit of unit capacity that this card works, if left blank, no such limit
P-START	Start date (YY-MM-DD) of maintenance time nonoverlapping restraint, optional
P-END	End date (YY-MM-DD) of maintenance time nonoverlapping restraint, optional

Notes: (1) If PLANT1 = PLANT2, it means the maintenance time of generating unit in the same power plant cannot be overlapped; if PLANT1 ≠ PLANT2, it means the maintenance time of units in the two power plants cannot be overlapped. (2) If P-START and P-END are left blank, it means that the maintenance time nonoverlapping (for power plants) card will work in the entire GMS study period.

(5) Maintenance time nonoverlapping (generator) card (RG) can restrain two given units from overlapping in their maintenance time, with card contents shown in Table 3.7.

Table 3.7 Contents of RG card

Identifier	Contents
RG	RG, denoting the maintenance time nonoverlapping (generator) card in this line
GEN1	Name of generator 1
GEN2	Name of generator 2
DT	Time interval (days) between maintenance time, optional
G-START	Start date (YY-MM-DD) of maintenance time nonoverlapping restraint, optional
G-END	End date (YY-MM-DD) of maintenance time nonoverlapping restraint, optional

Note: If G-START and G-END are left blank, it means that the maintenance time nonoverlapping (generator) card will work in the entire GMS study period.

(6) Equivalent load curve card (CC). The equivalent load of the system in each period is composed of actual forecast load minus the output of hydro plants and small unit and the power provided by the external system in the stress reduction period, plus the disabled capacity (capacity of units not reaching their full capacity) of the system during such period.

The contents of equivalent load curve card are shown in Table 3.8.

Table 3.8 Contents of CC card

Identifier	Contents
CC	CC, denoting equivalent load curve card
DATE	Period corresponding to equivalent load curve (YY-MM-DD)
PL	Load forecasting value in corresponding period (MW)
HY	Sum of hydro power outputs in corresponding period (MW), optional
SG	Sum of other small power plant outputs in corresponding period (MW), optional
PA	Power imports from the external system in corresponding period (MW, PA = 0, no power exchange; PA > 0, import power; PA < 0, export power)
SZ	Sum (MW) of capacities of units in the system not reaching their full capacity in the corresponding period or minimum reserve capacity (MW) of the system

Notes: (1) To minimize the repeated input of data, in case of no changes in the equivalent load curve data in adjacent periods, only fill in the period when the data appear for the first time, and never fill in the curve data in new periods until the curve data have changes. That is, only fill in the data of curve inflection points in the equivalent load curve card, without any evenly spaces filled out. (2) The period filled in the equivalent load curve card shall cover the entire GMS time range, otherwise the GMS cannot proceed.

(7) GMS data file end card (END). The last line of the data file shall be filled as END, as shown in Table 3.9.

Table 3.9 Contents of END card

Identifier	Contents
END	End, denoting the end line of input data (required)

(8) Comment card (**), which allows users to add some comments not involved in calculation when inputting the data, to make the input data more readable, and keep data revision more convenient. The format of the comment card is shown in Table 3.10.

Table 3.10 Contents of ** card

Identifier	Contents
**	* *, denotes the message comment line Any string of characters

Note: The comment line may inserted anywhere in the data files, without limit of lines.

3.6.4 Description of the Output Results

The main outputs of generating an equipment maintenance scheduling program are the scheduled maintenance start and end times of each generating unit, in which all the units in the system can be sorted in a uniform order. Thus, the GMS personnel can have a comprehensive understanding of the generator maintenance schedule of the whole system. Furthermore, the maintenance schedule of generating units can be organized based on the sequence of power plants. Generating units for each power plant can be listed in the order of maintenance start time in a small separate table, so that the GMS personnel can clearly understand the generator maintenance schedule in the power plant.

3.7 Implementation

This study, which is based on the real usage of a GMS in a domestic power system, fully considers the special requirements of the different areas and derives the ES rules of considerable adaptation. Therefore, the program is suitable for domestic conditions and is easier to be executed and expanded. It provides a tool with simple operation condition, quick computation, and reasonable results for power system dispatch engineers.

The solution procedure proposed in the chapter is tested by a real system with the conditions shown in Tables 3.11 and 3.12 (study period is from 94-01-01 to 95-01-31). Where Equivalent load = Forecast Load – Hydro – Exchange + Res. Cap., Res. Cap. (reserved capacity) is equal to that of the total rated capacity minus the total real output capacity, which means some generators may not be operated up to their rated capacity.

The examples of rules for the real case are given in Tables 3.13–3.15, where START to END means the active period of rules; if START to END is defaulted, then the active period is all over the study period. Table 3.13 shows the area maximum maintenance capacity constraints. Table 3.14 provides simultaneous maintenance constraints in both one and two different plants. In the table, PLANT 1 and PLANT 2 are the plant names. If the two names are the same, then units in one plant cannot be simultaneously in maintenance outage. If the two names are different, then units in the two plants cannot be simultaneously in outage for maintenance. DT (default = 0) represents the interval time of maintenance between two units. RPC represents the rule is active when unit capacity is larger than RPC (default = 0). Table 3.15 suggests which two units cannot occur simultaneously. DT has the same meaning as that in Table 3.14.

3.7.1 Input Data of a Real Scale System

Basic calculation conditions are listed in Table 3.11.

Table 3.11 Basic calculation conditions

Item		Number
Number of areas		4
Number of power plants		9
Number of units		55
Unit capacity (MW) and number of units	12 12.5 25 40 50 100 200 300 350	14 2 14 1 10 2 9 1 2
Total capacity: 4083 MW		

Some points of forecast loads are shown in Table 3.12.

Table 3.12 Some forecast load with step points (MW)

Date	Load	Hydropower Output	Power Exchange	Reserve Capacity
1994-01-01	3800	450	120	40
1994-01-24	3800	450	120	40
1994-02-01	3800	450	120	40
1994-02-09	4000	450	120	40
1994-02-10	3700	450	120	40
1994-02-20	3800	450	120	40
1994-03-01	4100	450	120	40
1994-04-01	4200	450	120	90
1994-05-01	4200	450	120	90
1994-06-01	4100	450	120	90
1994-06-12	3900	450	120	90
1994-06-26	4000	450	120	90
1994-07-01	4100	450	120	120
1994-08-01	4100	450	120	120
1994-09-01	4000	450	120	120

Expert rules for area constraints are shown in Table 3.13.

Table 3.13 Expert rules for area constraints

ID	Area Name	Max. Maintenance Capacity (MW)	Start Time	End Time
RA	HD	250.0	1994-05-01	1994-12-31

Some expert rules for power plant constraints are shown in Table 3.14.

Table 3.14 Some expert rules for power plant constraints

ID	Name of Plant *i*	Name of Plant *j*	Maintenance Interval	RPC	Start Time	Start Time
RP	MATOU1	MATOU1	5			
RP	MATOU2	MATOU2	5			
RP	SHEXIAN	SHEXIAN				
RP	MATOU2	XING2			1994-03-15	1994-05-31

Some expert rules for unit constraints are shown in Table 3.15.

Table 3.15 Some expert rules for unit constraints

ID	Name of Unit *i*	Name of Unit *i*	Maintenance Interval	Start Time	Start Time
RG	SA1	SA2	20	1994-01-01	1994-12-31

3.7.2 Part of Output Results

Due to limited space, this section only provides a partial example of the outputs, including maintenance start/end time and durations for some units, as shown in Fig. 3.11 and Table 3.16. Table 3.16 gives the GMS results of this real system, in which only the part concerning generators is given in detail.

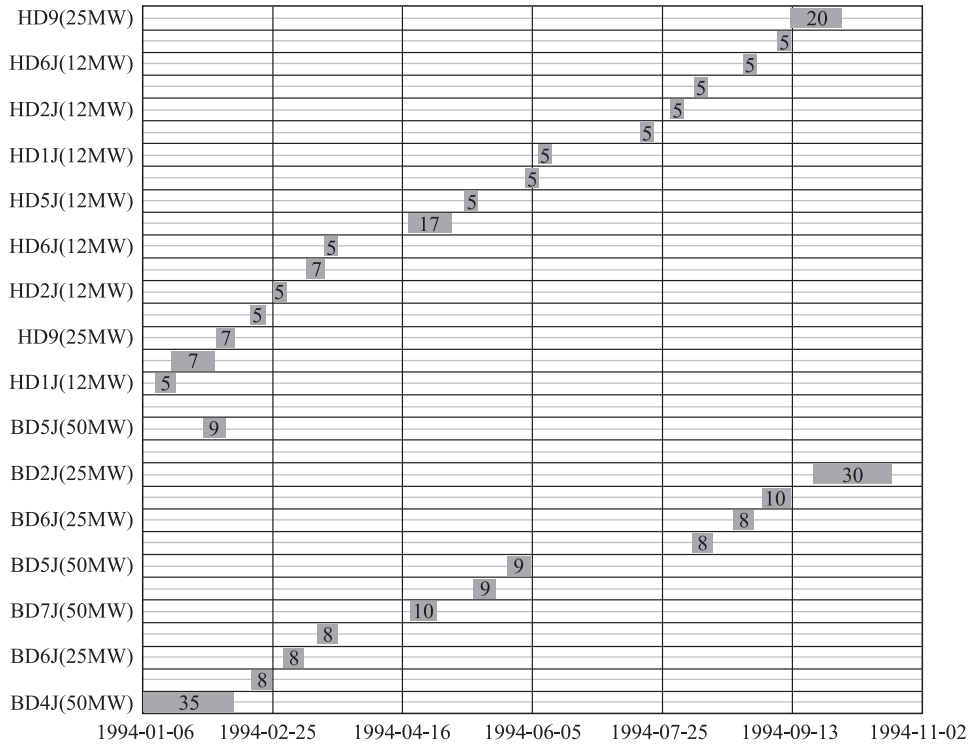

Fig. 3.11

Outputs of maintenance start and end time and durations of some units. Maintainable capacity = Total capacity − total load in each interval.

Table 3.16 Some detailed results of generator maintenance schedule

Plant	Generator	Capacity (MW)	Maintenance Start Time	Maintenance End Time	Duration
BAOJ	BD4J	50.0	1994-01-06	1994-02-09	35
BAOJ	BD2J	25.0	1994-02-17	1994-02-24	8
BAOJ	BD6J	25.0	1994-03-01	1994-03-08	8
BAOJ	BD1J	25.0	1994-03-14	1994-03-21	8
BAOJ	BD7J	50.0	1994-04-19	1994-04-28	10
BAOJ	BD3J	50.0	1994-05-13	1994-05-21	9
BAOJ	BD5J	50.0	1994-05-26	1994-06-03	9
BAOJ	BD1J	25.0	1994-08-05	1994-08-12	8
BAOJ	BD6J	25.0	1994-08-21	1994-08-28	8
BAOJ	BD4J	50.0	1994-09-02	1994-09-11	10
HANJ	HD1J	12	1994-01-12	1994-01-16	5

Table 3.16 Some detailed results of generator maintenance schedule—Cont'd

Plant	Generator	Capacity (MW)	Maintenance Start Time	Maintenance End Time	Duration
HANJ	HD7J	12	1994-01-17	1994-02-02	17
HANJ	HD9	25	1994-02-03	1994-02-09	7
HANJ	HD4J	12	1994-02-17	1994-02-21	5
HANJ	HD2J	12	1994-02-25	1994-03-01	5
HANJ	HD10	25	1994-03-10	1994-03-16	7
HANJ	HD6J	12	1994-03-17	1994-03-21	5
HANJ	HD8J	12	1994-04-18	1994-05-04	17
HANJ	HD5J	12	1994-05-10	1994-05-14	5
HANJ	HD3J	12	1994-06-02	1994-06-06	5
HANJ	HD1J	12	1994-06-07	1994-06-11	5
HANJ	HD4J	12	1994-07-16	1994-07-20	5
HANJ	HD2J	12	1994-07-28	1994-08-01	5
HANJ	HD7J	12	1994-08-06	1994-08-10	5
HANJ	HD6J	12	1994-08-25	1994-08-29	5
HANJ	HD8J	12	1994-09-07	1994-09-11	5
HANJ	HD9	25	1994-09-12	1994-10-01	20
HANJ	HD10	25	1994-11-08	1994-11-14	7
HANJ	HD5J	12	1995-01-04	1995-01-08	5
HANJ	HD3J	12	1995-01-10	1995-01-14	5

3.8 Conclusion

Based on the present maintenance situation of the generating equipment in the power system, the model has taken full consideration of the special requirements of different areas. The abstracted ES rules are adaptable and have good scalability and operability. The main characteristics are:

(1) The maintenance unit can be directly specified, and the current maintenance states of the units can be changed at any time while considering the long-term impact on the operation of the units.
(2) The model can handle the priority of the unit maintenance, indirectly transforming the huge factorial number of maintenance schemes into a finite number and greatly shortening the optimization calculation time.
(3) The model can employ the expert rules in the GMS optimization calculation and flexibly handle the power output constraints of units in different power plants, etc.
(4) The basic operation constraints can be "fuzzified" so that the GMS optimization calculation process can obtain a feasible solution.

(5) The resulting GMS optimization decision depends on the intersection of the objective function and the fuzzy membership function of constraints, which can be solved by the dynamic programming method.
(6) The unit maintenance period and duration given by the study case show that the optimization model can effectively guarantee the maximum possible capacity margin.

Therefore, this study has provided power grid dispatchers with a GMS tool of easy operation, fast calculation, and reasonable results.

CHAPTER 4

New Algorithms Related to Power Flow

Chapter Outline

Mathematical Models and Algorithms for Power System Optimization. https://doi.org/10.1016/B978-0-12-813231-9.00004-2

4.1 Introduction

Power flow calculation is used to calculate the steady-state characteristics of a power system under a given condition, which is widely applied in power system operation and planning calculations. There are many excellent power flow algorithms; Newton-Raphson (N-R) and PQ decomposition methods are the ones most widely used in current engineering practices. Both methods are very effective in conventional power flow calculations in terms of calculation speed and convergence characteristics. However, in some special circumstances, such as power flow calculation in ill conditions and at a high R/X ratio, the problem of nonconvergence may still occur. The improvement of convergence characteristics remains a common concern that deserves further study.

The nonlinearity of power and voltage expressions makes power flow calculation a nonlinear problem, which is usually solved by the iterative method. In general, the existing power flow algorithms are nonlinear ones with nonobjective and unconstrained. It is necessary to set a specified value at the beginning of the calculation. For example, P and V need to be assigned for PV bus, P and Q need to be assigned for PQ bus, and V and θ need to be assigned for $V\theta$ bus. In addition, transformer tap "T" and number of capacitor banks "C" need to be specified. To obtain a feasible solution, these settings need to be repeatedly adjusted during iterations until solutions for V and θ are within appropriate limits. This is almost an impossible task for those without prior calculation experience.

For those problems that are difficult to solve by conventional power flow, this chapter reformulates the power flow model. Based on the introduction of objective function, the simulated annealing (SA) algorithm is used to provide a new solution to the problem of ill-conditioned power flow with difficult convergence in engineering practice. Based on the introduction of constraint function, mixed-integer programming (MIP) is used to solve the discrete optimal power flow (OPF) problem.

This section first summarizes the traditional power flow problem-solving approach from the perspective of equation solving and provides a basic reference system for two power flow algorithms (unconstrained power flow algorithm with objective and constrained power flow algorithm with objective) in this chapter.

4.1.1 Way of Processing Variables in Traditional Power Flow Equation

The formulation of traditional AC power flow is as follows:

$$P_{\mathrm{G}i} - P_{\mathrm{L}i} - U_i \sum_{j \in i} U_j \left(G_{ij} \cos\theta_{ij} + B_{ij} \sin\theta_{ij} \right) = 0$$

$$Q_{\mathrm{G}i} - Q_{\mathrm{L}i} - U_i \sum_{j \in i} U_j \left(G_{ij} \sin\theta_{ij} - B_{ij} \cos\theta_{ij} \right) = 0$$

For a network with N buses, each bus has four operation variables (V = voltage magnitude, θ = voltage phase angle, P = active power, and Q = reactive power). In power flow calculation,

there are generally three types of buses: PQ, PV, and $V\theta$. For each bus, there are only two equations (P balance and Q balance), but there are four variables. Therefore, for each bus, two of its variables are handled as known conditions, whereas the other two are to be solved. In the N bus system, there is a balance bus ($V\theta$), M PV buses with $2M$ equations, and $(N-M-1)$ PQ buses with $2(N-M-1)$ equations. Thus, there is a total of $2(N-1)$ equations and $2(N-1)$ variables. In this way, the number of variables equals the number of equations, of which a Jacobian matrix is a nonsingular square matrix.

In N-R method of power flow calculation, the polar coordinate matrix of the linearization of AC power flow calculation model is as follows:

$$\begin{bmatrix} \Delta P \\ \Delta Q \end{bmatrix} = -\begin{bmatrix} H & N \\ M & L \end{bmatrix} \begin{bmatrix} \Delta\theta \\ \Delta V/V \end{bmatrix}$$

4.1.2 Way of Processing Variables in New Power Flow Equation

In traditional power flow calculation, V and θ are independent variables, and P and Q are derived variables. If P and Q are added to the variables of a traditional power deviation expression, and let X represent includes variables V, θ, P, and Q, then the calculation model of traditional AC power flow can be expressed as:

$$F_1(X) = 0$$
$$F_2(X) = 0$$

Where $F_1(X)$ and $F_2(X)$ are the active and reactive power deviations, respectively. This is a completely different solutions (4n unknows for 2n equations), from traditional power flow (2n unknows for 2n equations), which is a new way to solve the power flow problem. This chapter provides two new methods to solve the power flow problem. One is to use the SA method by developing a suitable expression of the objective function. The other is to use the OPF method by developing a suitable expression of the objective function and constraints.

4.1.3 Overview of Unconstrained Power Flow with Objective Function (based on SA Method)

The power flow calculation of power systems is used to mathematically solve a set of multivariate nonlinear equations. The basic principles upon which the existing algorithms applied are inseparable from the iterative process. In these algorithms, the modified step length of each iteration process is derived from the previous step. The iterative process approaching to the final solution is generally monotonous, that is, when the iterative process is a downhill form of monotonous drop, the solution converges; when the iterative process is an uphill form of monotonous rise or zigzag, it is difficult to obtain a convergent solution.

Some references suggest power flow calculations should be formulated as nonlinear programming (NLP) problems. The direction and step size in the power flow calculation are determined by minimizing the objective function. However, under ill conditions, this may still result in a local solution, rather than a final convergent one due to the nonlinearity of the power flow problem.

This chapter explores the application of the SA technique in solving the ill-conditioned power flow of a power system and proposes a combined algorithm based on both N-R and SA methods. The SA technique is used to probabilistically determine the corrected step size of variables in the N-R method. The possible direction of a true solution is sought through random searching to improve the convergence in ill-conditioned power flow calculations. The numerical case study for the actual system shows that the algorithm proposed in this chapter is an alternative algorithm for power flow calculation, which can indeed effectively improve the convergence characteristics of large-scale ill-conditioned power flow.

4.1.4 Overview of Constrained Power Flow with Objective Function (based on OPF Method)

With the growing complexity of the power system operation, the OPF problem becomes increasingly important. For the OPF, the objective function generally is to minimize the operating cost of the generator, and the constraint function generally is to satisfy the operating condition of the power system. In numerous papers published in recent years, OPF is usually treated as a nonlinear problem in which the transformer tap ratio, number of capacitor banks, and number of reactor banks are all treated as continuous variables.

However, as some references point out, the transformer tap ratio, number of the capacitor banks, and number of the reactor banks in OPF should be all treated as discrete variables. Otherwise, the solution obtained by using these algorithms may not be the optimal or even feasible after truncation. The OPF problem in this chapter is the same as the conventional one. It is treated as a mixed-integer nonlinear problem in which the transformation ratio, number of capacitor banks, and number of reactor banks are all treated as discrete variables. Therefore, the OPF in this chapter can also be named as a discrete OPF.

The existing generalized benders decomposition (GBD) method can be used to solve the mixed-integer nonlinear problem. However, the GBD method needs a large amount of computational time to solve the large-scale discrete OPF problem, which is not practically applied. Some mathematical programming methods also have certain difficulties in accurately solving a discrete-sized OPF problem of actual scale.

To solve the discrete power flow problem of actual scale, this chapter uses the method and concept of successive linear programming (SLP) to solve the mixed-integer LP problem in each iteration process. As the discrete OPF is nonconvex, the optimal solution obtained using the SLP technique is relative to the initial value.

4.1.5 Overview of This Chapter

(1) The power flow calculation method based on SA is studied. In this chapter, the traditional power flow model is first constructed as an unconstrained nonlinear quadratic programming model, then the SA method is combined with the N-R method to construct a new combinatorial algorithm. The new algorithm uses SA technology to determine the appropriate step size of the solution variable in the N-R method so that it does not fall into the local solution, thereby improving the problem of difficult convergence in power flow calculation, and minimizing the divergence situation. For the calculation of power flow in normal systems, the new algorithm has the same convergence as the N-R algorithm, yet for the ill-conditioned systems where the N-R method is difficult to converge, as long as the solution exists, the new algorithm may obtain a convergent solution.

(2) A discrete OPF algorithm is studied. This algorithm requires an initial integer solution that can be obtained by truncating the solution from traditional continuous OPF or a general power flow solution. On this basis, the near-optimal solution can be obtained. Therefore, even if the initial integer solution is infeasible, the algorithm proposed can still be applied to search for a feasible integer solution. Two algorithms are proposed: the first algorithm uses a continuous OPF to calculate an initial value, then rounds off the corresponding integer variables and finally searches for the discrete optimal solution; the second algorithm uses the power flow method to calculate the initial value, then uses the LP method to calculate the continuous optimal solution, in which corresponding integer variables are rounded off, and finally searches for a discrete optimal solution based on SLP approach.

Section 4.2 in this chapter gives the basic ideas of formulating the unconstrained power flow model; Section 4.3 provides the unconstrained power flow model in the form of a nonlinear quadratic function; Section 4.4 shows the calculation process of solving unconstrained power flow; Section 4.5 gives the detailed results from actual case studies and their analyses; Section 4.6 introduces the discrete OPF model; Section 4.7 describes the discrete OPF algorithm; Section 4.8 gives the concrete formulation of 5-Bus system and then the results of 135-Bus real scale system by using traditional OPF and LF as initial values respectively; and Section 4.9 is a summary of the chapter.

4.2 Ideas of Modeling for Unconstrained Power Flow with Objective Function

4.2.1 Description of Ill-Conditioned Power Flow Problem

As previously mentioned, the N-R method and the fast *PQ* decoupled load flow method are most widely used. Both methods are efficient, however, in some special situations, nonconvergence may be encountered. Whether a power flow calculation will converge or not depend on many factors, such as operating conditions, reactive power distributions, and solution algorithms.

Sometimes, the practical system will still operate (i.e., a power flow solution exists), but the existing power flow algorithm is likely unable to lead to a convergent solution, which is called an ill-conditioned power flow.

A power system with such features may be described by a set of ill-conditioned nonlinear algebraic equations. In other words, a small change in parameters will produce a large change in the solution. When power systems are ill conditions, the existing algorithms can hardly ensure convergence of the power flow calculation. Ill-conditioned power problems have been investigated in many publications. However, most of these methods were either designed for a specific ill condition or required substantial modifications from the standard load flow method.

A new load flow method for solving ill-conditioned systems is proposed. The goal of this proposed method is two-fold: (1) this method should be easily incorporated into the existing load flow method, and (2) this method should be able to address different types of ill conditions. To achieve this goal, the proposed load flow technique is a hybrid model between the N-R and SA methods. The SA technique is employed to determine proper correction steps of N-R solution variables, such that these variables will not be trapped into a local solution.

One of the important advantages of the SA method is that it can selectively accept "uphill movement", that is, the objective function moves in an increasing direction to avoid falling into a local solution. On this basis, this chapter combines the SA and N-R methods to formulate a new combined algorithm to solve ill-conditioned power flow problems. The new algorithm determines the appropriate step size of variables in the N-R method using the SA technique to prevent them from falling into a local solution, so as to improve the convergence problem of the ill-conditioned power flow calculation and minimize divergence occurrence. For the power flow calculation of a normal system, the algorithm proposed in this section has the same convergence characteristics as the N-R algorithm. For ill-conditioned systems where the N-R method is difficult to achieve convergence, the new algorithm may lead to a convergent solution as long as the solution exists.

As commonly known, any probabilistic method for solving stochastic processes is effective for samples of a certain scale, the effect of which is not obvious for small samples. The algorithm proposed in this chapter is no exception. In processing small cases with an infinitely large single unit or just a few buses, this algorithm and the N-R method have the same critical convergence point with increasingly heavy operation conditions of the system. Therefore, in terms of the effect of theoretical and actual calculation, the algorithm proposed in this chapter is effective for systems of a certain scale in processing ill-conditioned power flow problems. Because typical real systems in a certain scale are sufficient to meet the requirement of this algorithm, these systems are solvable with this algorithm.

4.2.2 Outline of Simulated Annealing Method

The SA method is a general purpose technique for solving combinatorial optimization problems, which is a simulation of the annealing process in the heat treatment of a physical system. At high temperature, atoms in metal move violently, even in a melted state. Metal gradually cools to crystal during annealing. The random atom crystal structure may be optimized by controlling the cooling speed to obtain the desired physical properties of the metal. The objective function in the SA method corresponds to the energy of a physical system in the process of annealing, whereas the final crystal structure of a metal corresponds to an optimal solution of the SA method. As the atom arrangement is completely random during annealing, the SA method simulating this process is also a stochastic algorithm.

There are four important elements in the SA process: (A) configuration space, (B) perturbation mechanism, (C) a cost function, and (D) a cooling scheme. The details are explained as follows:

(A) Configuration space is a set of allowed system configurations over which the optimal solution variables are searched for. Design of configuration space is critical to the efficiency of the SA-based solution algorithm and the quality of final solutions.

(B) The perturbation mechanism is a set of feasible moves by which variables are to be solved. These moves allow the system to alter from one state of configuration to another. Moves are chosen randomly.

(C) Moves that reduce the value of the system cost function (i.e., improve the configuration) are called "downhill" moves, and moves that increase the system cost are called "uphill" moves. All downhill moves are accepted; uphill moves are accepted with a probability of exp $(-\Delta C/T)$, where ΔC is the increase in cost and T is a temperature derived from the cooling scheme. All uphill moves that do not satisfy the probability condition will be rejected. One of the attractive features of the SA technique is that it can probabilistically accept uphill moves, based on certain criteria, without being trapped into a local solution.

(D) The cooling scheme shall determine the initial temperature and temperature drop rule at the beginning of the annealing process. These two can be determined through experiments. In principle, the initial temperature is usually set such that a majority of the moves can be accepted. The temperature drop rule is a control strategy of the SA technique. The ideal temperature drop rule is that the temperature will be lowered after the heat balance is established at each stage. A sufficient number of moves should be performed so the heat balance corresponds to each stage. That is, only after a certain number of moves are performed, the temperature is lowered, and the annealing process moves to the next stage. The temperature drop rule is as follows:

$$T_{k+1} = b(T_k)T_k$$

where T_k—temperature at stage k during annealing; $b(T_k)$—cooling rate.

In SA, the temperature of the system is slowly lowered to 0°C; if the temperature falls slowly enough, the system should end up within the minimum energy states of sufficiently low energy. Hence SA algorithm can be viewed as minimizing the cost function (energy) over a finite set of the system state. By simulating such an annealing process, global minimum cost solutions can be found for very large optimization problems.

4.2.3 Way of Modifying Iteration Step Size by SA Method

Mathematically, this is a problem of solving a set of multivariate nonlinear equations. The basic principles of the previously discussed algorithms all depend on iterative processes. In these algorithms, the modified size of each iterative step is calculated from the iterative process in the previous step. The iterative process approaching to final solution is generally monotonous. In other words, when the iterative process is in a form of monotonous descending downhill, the solution is convergent. When it is in a form of monotonous ascending uphill or zigzags, a convergent solution is difficult to obtain.

4.2.4 Way of Constructing a Nonlinear Quadratic Objective Function

To apply the SA technique to solve the power flow problem in power systems, the modified bus power equation in the power flow calculation may be used to construct a quadratic function that is analogous to the nonlinear objective function. The specific mathematical model is as follows:

$$\min\left\{F(X)=\sum\Delta P_i^2+\sum\Delta Q_i^2\right\}$$

4.3 Formulation of Unconstrained Power Flow Model with Nonlinear Quadratic Objective Function

4.3.1 Notation

The mathematical notations are listed in Table 4.1.

Table 4.1 Mathematical notations

Notation	Description	Notation	Description
N	Set of all buses	P_{iL}, Q_{iL}	Active and reactive load at bus i
X=(U,θ)	Vector of voltage magnitude value and phase angle	P_{iLO}, Q_{iLO}	Initial active and reactive load at bus i
P_i, Q_i	Active and reactive power injected at bus i	a_P, b_P, c_P	Characterization factor of static voltage under active load
P_{ij}, Q_{ij}	Active and reactive power flow from bus i to bus j	a_Q, b_Q, c_Q	Characterization factor of static voltage under reactive load
P_{iG}, Q_{iG}	Active and reactive generated power at bus i		

4.3.2 Formulation of Power Flow with Quadratic Function

Bus power equations for the power flow calculation in form of polar coordinates are as follows:

$$\begin{cases} P_i = U_i \sum_{j \in i} U_i \left(G_{ij} \cos\theta_{ij} + B_{ij} \sin\theta_{ij} \right) \\ Q_i = U_i \sum_{j \in i} U_i \left(G_{ij} \sin\theta_{ij} - B_{ij} \cos\theta_{ij} \right) \end{cases}$$

Modified into nonlinear equation sets:

$$\begin{cases} \Delta P_i = P_{is} - U_i \sum_{j \in i} U_i \left(G_{ij} \cos\theta_{ij} + B_{ij} \sin\theta_{ij} \right) = 0 \\ \Delta Q_i = Q_{is} - U_i \sum_{j \in i} U_i \left(G_{ij} \sin\theta_{ij} - B_{ij} \cos\theta_{ij} \right) = 0 \end{cases}$$

To apply the SA technique to solve power flow problems of power systems, the modified bus power equations of power flow calculation are used to construct a quadratic function that is similar to the nonlinear objective function. The detailed mathematical model with quadratic objective function is as follows:

$$\min \left\{ F(X) = \sum \Delta P_i^2(X) + \sum \Delta Q_i^2(X) \right\} \tag{4.1}$$

$$\Delta P_i(X) = P_i(X) - P_{is}, \quad i \in N \tag{4.2}$$

$$\Delta Q_i(X) = Q_i(X) - Q_{is}, \quad i \in N \tag{4.3}$$

$$P_i(X) = \sum P_{ij}(X) \tag{4.4}$$

$$Q_i(X) = \sum Q_{ij}(X) \tag{4.5}$$

$$\begin{aligned} P_{is} &= P_{i\mathrm{G}} - P_{i\mathrm{L}} \\ Q_{is} &= Q_{i\mathrm{G}} - Q_{i\mathrm{L}} \\ P_{i\mathrm{L}} &= P_{i\mathrm{Lo}} \left(a_P U^2 + b_P U + c_P \right) \end{aligned} \tag{4.6}$$

$$Q_{i\mathrm{L}} = Q_{i\mathrm{Lo}} \left(a_Q U^2 + b_Q U + c_Q \right) \tag{4.7}$$

$$\begin{aligned} a_P + b_P + c_P &= 1.0 \\ a_Q + b_Q + c_Q &= 1.0 \end{aligned}$$

4.4 Calculation Procedure of SA based N-R Method

Based on the original calculation procedure of the N-R method, it is easy to implement the new program for the new combined algorithm. The following steps outline the detailed solution procedures:

Step 1: Input the power system data required by the conventional power flow calculation and the SA parameters, such as the initial temperature T_0, a random seed (a nonzero integer used to generate a random number), the cooling ratio b, the maximum number of moves at each temperature N_{max}, and the final temperature T_{min}. Initially, set $N_{accept}=0$, and $N_{reject}=0$; where N_{accept} is the number of the accepted moves in each temperature T_k, and N_{reject} is the number of the rejected moves in each T_k. Set iteration count $k=0$.
Step 2: Set $k=1$, then calculate initial point X_k. Linearize modified power Eqs. (4.2) and (4.3) to form Jacobian matrix J_k. Calculate mismatch power M_k and objective function $F(X_k)$.
Step 3: Use $X_k=J_k^{-1}M_k$ to calculate the original modified step size ΔX_k for the N-R method.
Step 4: Select a uniformly distributed random number $r=\text{random}[0,1]$. Perturb $X_{k+1}=X_k+r\Delta X_k$ and calculate $\Delta F=F(X_{k+1})-F(X_k)$.
Step 5: If $\Delta F<0$ or $\exp(-\Delta F/T_k)>\text{random}[0,1]$, then accept X and go to the next step. Otherwise reject X, let $N_{reject}=N_{reject}+1$, and go back to Step 4.
Step 6: Update the Jacobian matrix J_k and let $N_{accept}=N_{accept}+1$.
Step 7: ① Evaluate whether the stop criterion is met in the temperature range of T_k; if it is not met, execute ②; ② if $N_{accept}+N_{reject}<N_{max}$, then turn to Step 3; otherwise go to next step.
Step 8: Let $T_{k+1}=bT_k$ and check the stop criterion again. If $T_{k+1}<T_{min}$, $\Delta F(X_k)<\varepsilon$, or $M(X_k)<\varepsilon'$, then the calculation is completed. Otherwise go back to Step 3.
The proposed algorithm imposes very minimal changes on the existing N-R method. This method does not change the structure of the Jacobian matrix. Therefore, it does not change the sparsity of the matrix. In the proposed algorithm, the modifications to the existing N-R method can be implemented in a separate subfunction or subroutine. If this subfunction or subroutine is not used, then the proposed method is identical to the standard N-R method.

As previously mentioned, the design of any SA-based algorithm is required to include four key components, that is, system structure space, a disturbance mechanism, objective function, and a cooling scheme. Here is our design of the four components for the SA technique combining the N-R method for power flow calculation.

(1) Structure space: The structure space of the power flow problem in the power system is the variable set $X=X(U,\theta)$ that meet Eqs. (4.2) and (4.3).
(2) Disturbance mechanism: In the power flow calculation, the system transfers from current structure status to a new one by modifying current iterative variables, as detailed here:
(3) Objective function:
Step 1: Calculate ΔX_k:

$$\Delta X_k=J^{-1}M(X_k)$$

where J is the same Jacobian matrix as in the N-R method and $M(X_k)$ is an unbalanced power vector.

Step 2: Select a random number r:

$$r = \text{random}[0, 1]$$

Step 3: Generate a new ΔX:

$$\Delta X = r\Delta X_k$$

Step 4: Move the current system structure status to a new one:

$$X_{k+1} = X_k + \Delta \text{X}$$

Step 5: Judge objective function values $F(X_k+1)$ and $F(X_k)$. If $\Delta F = F(X_{k+1}) - F(X_k) < 0$ or $\exp(-\Delta F/T) > \text{random}[0, 1]$, then accept new X_{k+1}; otherwise reject this X_{k+1}, return to Step 2 to select a new random number r, then recalculate X_{k+1}.

$$\min\left\{F(X) = \sum \Delta P_i^2 + \sum \Delta Q_j^2\right\}$$

(4) Cooling scheme:

1. Set the initial temperature. To determine initial temperature T_0, first calculate the balanced increment ΔF^+ of the objective function after a set of random movements, then obtain T_0 by solving the equation:

$$a_0 = \exp\left(-\Delta \text{F} + /T_0\right) \tag{4.8}$$

where a_0 is an acceptable value equivalent to the ratio of feasible status transfer number to proposed movement number in each temperature range. At the beginning of iteration, typically take $a_0 = 0.75$–0.85; in other words, at this point, at least 75%–85% of transfers must be accepted. From Eq. (4.1), T_0 can be derived from:

$$T_0 = \Delta F^+ / \ln\left(a_0{}^{-1}\right) \tag{4.9}$$

2. Set the cooling rate. Typically, cooling rate $b(T_k)$ is as follows:

$$b(T_k) = 0.85 - 0.95$$

$$T_{k+1} = b(T_k)T_k$$

3. Final stopping criterion:

$$T_k < T_{\min} \text{ or } F(X_{k+1}) - F(X_k) < \varepsilon \text{ or } M(X_k) < \varepsilon'$$

4. Maximum number of movements in each temperature range: Typically, the maximum number of movements $N_{\max}$ can be determined according to actual problems. For an ill-conditioned system, $N_{\max}$ is a very loose number. When the sum of the numbers of

accepted movements and the number of rejected movements exceeds N_{max}, the temperature drops. At this point, the numbers of accepted and rejected movement are reset to 0, and N_{max} only affects the rate of temperature drop. For a normal situation, the typical iteration counter in the power flow calculation is several to a few dozen. To avoid affecting the calculation speed, N_{max} is generally above the upper limit of the iteration number. Therefore, $N_{max} = 10–100$ is recommended.

4.5 Implementation of SA based N-R Method

4.5.1 Initial Conditions of 197-Bus System

The actual operation mode of a 1990 winter peak load in a Chinese provincial network has been selected in this section as a numerical example of an ill-conditioned power flow calculation. For this operation mode, the N-R algorithm, *PQ* decoupled algorithm, and optimal multiplier algorithm all failed to find a convergent solution. Therefore, it can be deemed as an ill-conditioned system. This system consists of 197 buses, 28 equivalent generating units, 87 loads, 91 AC branches, and 136 transformer branches (including three-winding transformers). The static voltage characteristic coefficients of the load buses are shown in Table 4.2. To test the robustness of the proposed methods, the following ill-conditions were studied:

- *R/X* ratio ill-conditions
  The power system data were manipulated to generate a system of high *R/X* ratios. The ratio varied from 50 to 2000. The data were tested for single line as well as multiple lines. The high *R/X* ratio was simulated at different lines taken individually, as well as five or six lines at a time. The ratio was increased gradually when the test for multiple lines was performed, and the results from the proposed method proved much better than that from the N-R method.
- Heavy loading conditions
  In this case study, the loads at a group of buses were treated as voltage dependent loads. The data were once again manipulated to create a heavy loading condition. The heavy load was imposed on the system at various points considering a single bus system as well as a multiple bus system. A very high degree of load severity could be imposed on the system for all buses. Based on the static voltage characteristic coefficients, six different levels of load severity could be created. The results indicated that the proposed method surpassed the performance of the N-R method and gave a convergent solution. However, it was also noticed that the proposed method could not always guarantee a convergent solution.
- Long-to-short line reactances
  One of the other conditions that could create an ill-conditioned system is a high ratio of long-to-short line reactance terminating at the same bus. The situation was simulated by choosing buses where long-to-short lines terminate. Here, it was found that both N-R and SA performed well and, as mentioned earlier, the computational time was quite long for SA.

- Location of reference or slack bus
  The data were tested by changing the location of the slack bus. However, both the methods converged for this kind of ill-conditioned system.

Table 4.2 Static voltage characteristic coefficients at load buses

Type	a_p	b_p	c_p	a_q	b_q	c_q
1	0.0	0.0	1.00	0.0	0.0	1.00
2	1.00	−1.40	1.40	3.33	−4.66	2.33
3	1.00	−1.40	1.40	4.17	−5.83	2.66

In this table, Type 1 refers to the constant power load, and Type 2 and 3 refer to different load voltage static characteristics, respectively.

4.5.2 Conditions and Results of Four Cases

To examine the effectiveness of the combined model algorithm, this chapter carried out calculations for four case studies. All case studies used a flat starting method.

Case study 1 uses the original system data provided by the provincial dispatching center and the new algorithm to obtain a convergent solution. As this system is an ill-conditioned system, the convergence curve is zigzag, reflecting the random search optimization process of the algorithm proposed in this chapter.

Case study 2 modifies the load voltage static characteristics of the original system data and still results in a convergent solution. To simulate more severe conditions, case study 3 increases the power output of all generators and loads in case study 2 by 10% and still results in a convergent solution. This shows that the convergence characteristics of the algorithm proposed in this chapter are stable.

The iteration number in case studies 1, 2, and 3; the CPU time used by a VAX-11/780 computer; and load static voltage characterization coefficients are shown in Table 4.3.

Case study 4 includes the power flow calculation with a set of high R/X ratio of 1.0–10.0; the number of branches with a high R/X ratio accounts for about 10% of the total number of AC branches in the original system, and the load voltage static characteristics are the same as in case study 2. All calculations in case study 4 result in convergence. This shows the combined

Table 4.3 Iteration number and CPU time of the first three cases

Case Study	1	2	3
Iteration number	35	15	15
CPU(s)	140.35	81.23	81.70

model algorithm proposed in this chapter retains good convergence characteristics of the N-R method for high *R*/*X* ratio systems. Table 4.4 gives the iteration number and CPU times for the calculation results of case study 4.

Table 4.4 Calculation results of case 4 (iteration number and CPU time)

R/*X* Ratio	2.0	3.0	4.0	5.0	10.0
Iteration number	16	16	16	16	16
CPU(s)	83.95	83.88	84.45	84.00	84.41

The N-R method, *PQ* decoupled method, and optimal multiplier method are also applied in case study 1 and 2. The calculation results are shown in Tables 4.5 and 4.6, respectively. Figs. 4.1 and 4.2 give the comparison of iteration curves between the algorithm proposed in this

Table 4.5 Iteration results of different algorithms for case study 1

Iteration Number	SA Method	N-R Method	*PQ* Decoupled Method	Optimal Multiplier Method
0	110.919563	110.919563	207.888217	110.919563
1	170.788623	292.803494	96.951614	98.525243
2	98.461830	10825.667767	23.051102	61.660412
3	14.046558	514897.234766	171723.786316	39.123108
4	34.560182	1055424.734328	510465.097463	34.989980
5	11.420726		1103428.603472	28.075667
6	26.424113			25.065202
7	9.852771			26.857728
8	17.705175			27.339888
9	10.316829			27.470294
10	9.852771			27.506939
11	8.625845			27.517712
12	2.375822			27.521011
13	11.218251			27.521053
14	2.355714			27.522389
15	4.741337			27.522498
16	5.765086			27.522537
17	9.816529			27.522549
18	5.592344			27.522553
19	4.660007			27.522556
20	2.435602			30.346724
21	2.517654			30.327643
22	4.115390			30.335300
23	1.342672			30.342986
24	2.261429			30.347456
25	0.716623			30.349673
26	0.731194			30.350696
27	0.714000			30.351151
28	0.064956			30.351348

Table 4.5 Iteration results of different algorithms for case study 1—Cont'd

Iteration Number	SA Method	N-R Method	*PQ* Decoupled Method	Optimal Multiplier Method
29	0.136827			30.351433
30	0.052871			30.351470
31	0.088922			30.351486
32	0.010957			30.351494
33	0.001423			30.351501
34	0.000133			30.352492
35	0.000014			30.352514
36				30.352523
37				30.352527
38				30.355403
39				30.355468
40				30.355516
41				30.355526
42				30.355912
43				30.355917
44				30.356041
45				30.356043
46				30.702784
47				30.716376
48				30.721623
49				30.723709
50				30.724557

Table 4.6 Iteration results of different algorithms for case study 2

Iteration Number	SA Method	N-R Method	*PQ* Decoupled Method	Optimal Multiplier Method
0	110.919563	110.919563	207.888217	110.919563
1	170.788623	292.803494	96.608760	98.525243
2	98.461830	4749.794926	27.658470	66.843264
3	18.127275	567950.613160	36912.256932	43.116666
4	58.728716	1074296.454478	378625.194275	32.347055
5	26.195611		1202473.473347	12.905974
6	27.731655			1.350618
7	8.833099			9.156640
8	1.882653			8.595202
9	1.373997			0.814346
10	0.116296			9.035141
11	0.214595			10.186459
12	0.031148			1.230680
13	0.003738			12.416705
14	0.000266			15.912906
15	0.000023			9.789914

Continued

Table 4.6 Iteration results of different algorithms for case study 2—Cont'd

Iteration Number	SA Method	N-R Method	*PQ* Decoupled Method	Optimal Multiplier Method
16				17.413954
17				16.060220
18				1.664940
19				13.844970
20				9.113379
21				8.183083
22				0.744811
23				5.511558
24				2.482840
25				1.347360
26				0.123009
27				0.164268
28				0.015497
29				0.003715
30				0.000395
31				0.000046

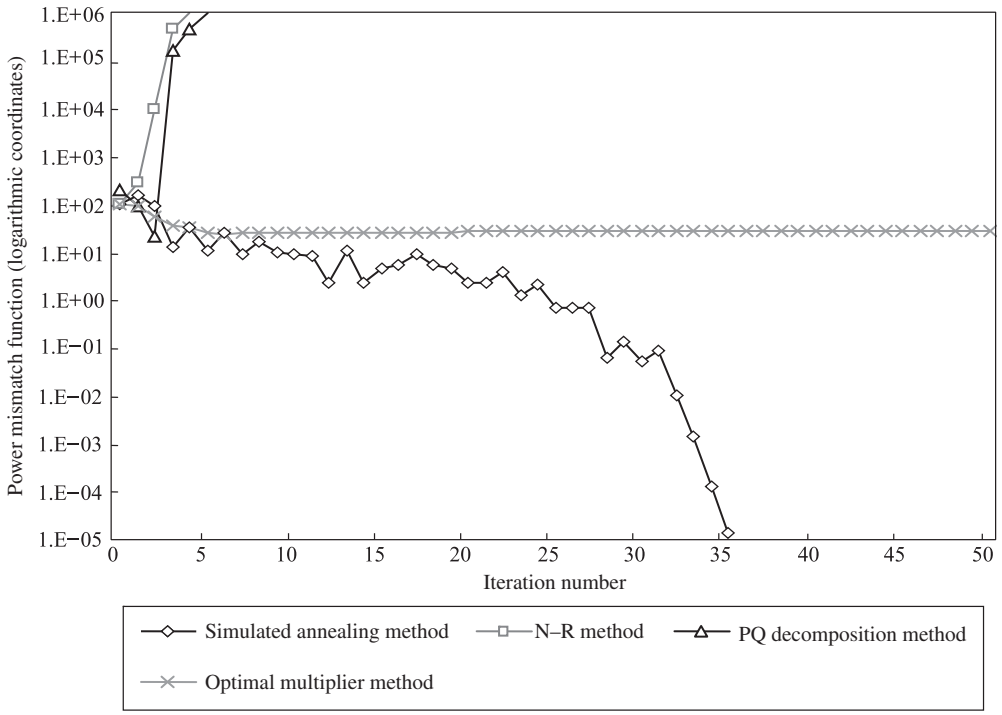

Fig. 4.1
Iteration curves of different algorithms for case study 1.

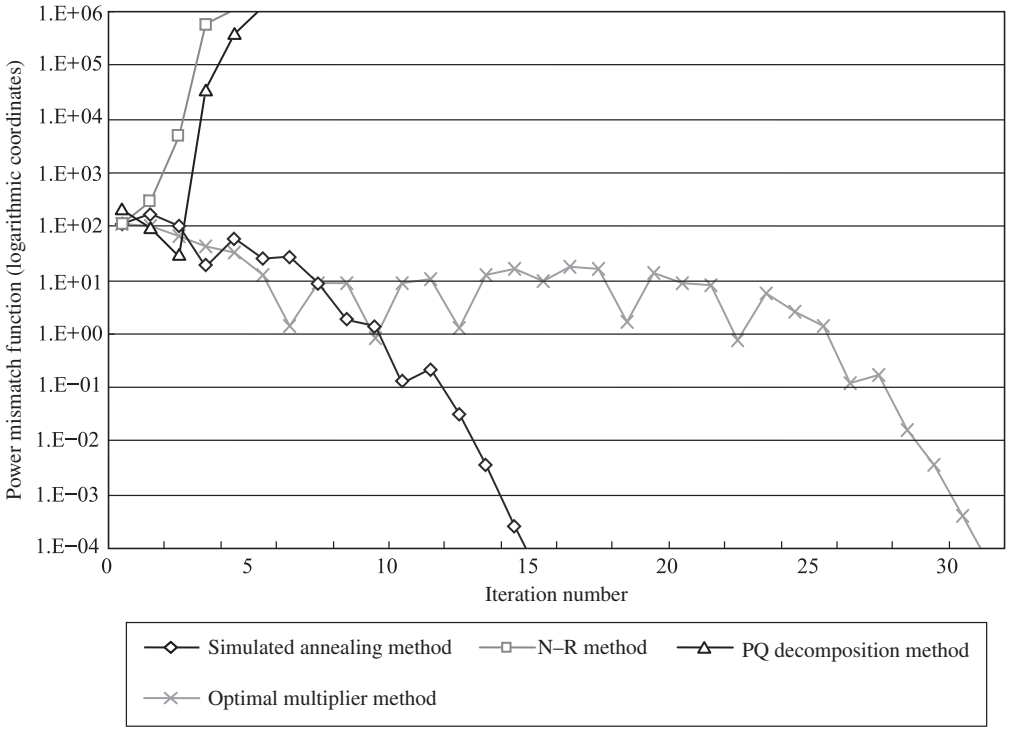

Fig. 4.2
Iteration curves of different algorithms for case study 2.

chapter and the other three algorithms. According to the tables and figures, the combined model algorithm using the SA technique results in better convergence characteristics than the other three methods in the case studies given in this chapter.

The probability search in solution space performed by the algorithm proposed in this chapter requires a random number generator. Obviously, different seeds will generate different random number sequences, which lead to different starting points and search processes. To illustrate the effect of different seeds, seed1 = 541214 and seed2 = 765432 are used in case study 2 calculation. The two seeds are randomly selected. Starting from these two different seeds, convergent solutions resulted for case study 2. Table 4.7 shows the calculation results for case study 2 with different seeds; Fig. 4.3 shows the convergence curves obtained from different seeds.

Table 4.7 Calculation results for case study 2 with different seeds

Iteration Number	seed1 = 541214	seed2 = 765432
0	110.919563	110.919563
1	170.788623	100.227714
2	98.461830	45.328022
3	18.127275	28.919270
4	58.728716	14.830517
5	26.195611	2.799354
6	27.731655	0.122168
7	8.833099	0.168261
8	1.882653	0.089857
9	1.373997	0.007552
10	0.116296	0.000989
11	0.214595	0.000149
12	0.031148	0.000018
13	0.003738	
14	0.000266	
15	0.000023	

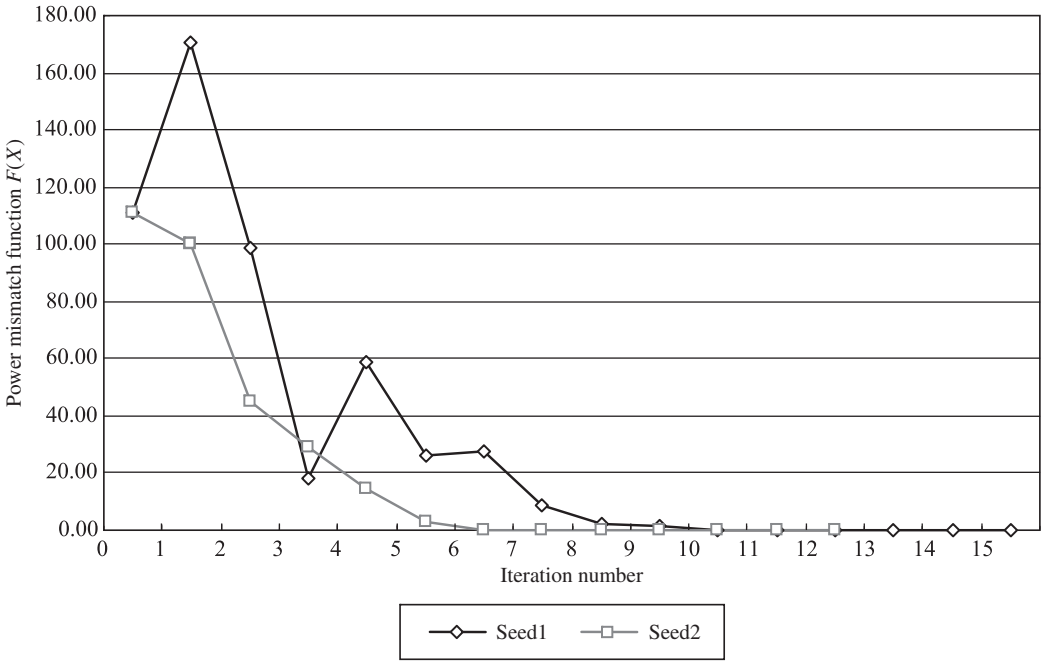

Fig. 4.3
Comparison of convergence processes with different seeds.

4.6 Formulation of Discrete Optimal Power Flow

4.6.1 Similarities and Differences Between LF and OPF

As explained in Section 4.1.1, the traditional power flow problems of N buses can be expressed by $2N$ equations and $4N$ variables (U, θ, P_G, Q_G), and there have to be three types of buses: (1) PQ bus, P and Q are known (U and θ unknown); (2) PV bus, P and U known (Q and θ unknown, Q may be Q_G or Q_L); and (3) $V\theta$ bus, U and θ are known (P_G and Q_G unknown). Thus, the number of variables is equal to the number of equations. However, because variables P and Q have analytic formulas, U and θ are actually the only variables of power flow, and solving the power flow finds the distribution situation of voltage and phase angle of the network buses. Branch power flows P_{ij} and Q_{ij} are functions of U and θ, as well as R and X; thus, P and Q can be easily calculated by determining U and θ.

If N buses (total $2N$ variables of U and θ) have $2N$ added variables (P and Q), the power flow problems of N buses have $2N$ equations and $4N$ variables, so that the number of variables is greater than the number of equations. Thus, the square power flow equation becomes a rectangular optimization equation. Such an equation set theoretically has an infinite number of solutions, among which there are optimized ones depending upon different objectives and how the variables of the buses are optimized. For the optimization calculation, all buses are generally treated as PQ buses, so that each bus maintains two equations (P balance equation and Q balance equation), and the number of equations is $2N$. If the $2N$ equations and $4N$ variables are used to solve the traditional power flow, just set the upper and lower limits of P and Q of the PQ bus as the known P and Q values, the upper and lower limits of P and U of the PV bus as the known P and U values, and the upper and lower limits of U and θ of the $V\theta$ bus (balance bus) as the known U and θ values. P and Q may be deemed as P_G and Q_G or P_L and Q_L. The load optimization and reactive power optimization are discussed in Chapters 5 and 6, respectively.

Therefore, traditional power flow calculation is equivalent so that two of the four variables for each bus are fixed in the optimization calculation. The similarities and differences between LF and OPF are listed in Table 4.8.

Table 4.8 Similarities and differences between LF and OPF

Algorithm	Power Flow Calculation	Optimization Calculation
Content	Each bus can have only two variables $\begin{cases} P, Q \\ P, U \\ U, \theta \end{cases}$ Tap ratio T and capacitor banks C are fixed Number of variables = number of equations Solve nonlinear equations Without objective function	Each bus can have six variables: P, Q, U, θ, T, C Tap ratio T and number of capacity banks C are variables Number of variables > number of equations Solve nonlinear equations With objective function

After the optimization calculation, it is usually necessary to conduct the power flow calculation to verify the nonlinear solution. This power flow calculation uses the integer solution of reactive power output and tap ratio, as well as bus voltages and angles of optimized solution to calculate the new bus voltages and angles, and generator reactive outputs. In this case, the recalculated power flow can theoretically result in a solution identical to the optimized solution. Therefore, it is unnecessary to calculate the power flow again after nonlinear optimization, because the optimized solution has already provided the integer solution of reactive power and tap ratio, bus voltages and angles, and generator reactive outputs.

In fact, the feasible solution obtained from the optimization algorithm is not necessarily feasible in the power flow calculation. For example, the Q and U values of a generator bus may have reached their limit values in an optimized solution, but due to reasons such as computer word length, Q violations may be caused if the bus is treated as a PV bus or a U violation may be caused if the bus is treated as a PQ bus. Therefore, the optimized power flow calculation may cause the optimized solution to deviate from the optimal value to a certain extent or even lead to an infeasible solution.

Hence, if the reactive power of the generator at a bus has reached its upper limit in an optimized result, the reactive power is very likely to go beyond the upper limit at this bus in the power flow calculation. There are two ways to address this problem: the first is to change the bus to a PQ bus before the power flow calculation, and the second is to lower the upper and lower limits of the reactive power. Generally, to obtain a satisfactory power flow solution, it is necessary to make certain adjustments in the power flow calculation using the optimized configuration.

Besides, under the same conditions of power flow calculations, such as the integer fixed, voltage of PV bus is known, and other constraints are removed; the same result as the power flow calculation can also be obtained using the optimization program. This means that the optimized solution process is even more widely applicable. Therefore, under the same conditions, the optimization algorithm can produce a feasible solution, whereas the power flow solution process may not.

In conclusion, the results of the power flow calculation after the optimization of initial value of power flow show that the system operation condition is considerably improved. Any process reliant on the power flow calculation alone will require much more effort and will not necessarily produce a feasible solution. The greatest advantage of the optimization calculation is that it helps the system planner quickly find a feasible solution and reduces the time spent on adjustment of the input parameters, such as transformer tap T and capacitor bank number C.

4.6.2 Description of the Problem

The OPF problem becomes important as electric power system operations become increasingly complex. Its objective is usually taken as the minimization of the sum of fuel cost of generators under the conditions of operating constraints.

Many excellent algorithms have been developed for OPF calculation. In these algorithms, the OPF problem is formulated as a continuous nonlinear problem in which the number of transformer taps and the numbers of capacitor and reactor units are all treated as continuous variables. However, some of the variables in the OPF problem can be adjusted only by discrete steps: transformer ratios are changed tap by tap, and capacitors and reactors are adjusted by unit operations.

If the OPF problem is solved by the existing algorithms, the number of transformer taps and the number of capacitor and reactor units are determined by the discrete values closest to optimum continuous values, and the supplied reactive power is settled according to these discrete values. Therefore, the operating points obtained by such algorithms might be nonoptimum and/or unfeasible.

From the foregoing viewpoint, transformer tap ratios and the number of capacitor units, as well as the number of reactor units, should be treated as discrete variables in the OPF problem.

When taking into account the discrete nature of the number of transformer taps and the number of capacitor and reactor units, the OPF problem becomes a nonlinear MIP problem with numerous integer variables. Hence, in this chapter, such a discrete problem is referred to as a "discrete OPF problem." Until now, the existing general mathematical programming techniques could not solve such a large-scale nonlinear MIP problem accurately from the viewpoint of memory size and computing time.

To solve the practical discrete OPF problem, this section presents a new algorithm that can obtain a good near-optimal discrete solution. This algorithm is based on an optimization procedure in which the nonlinear discrete OPF problem is linearized iteratively and solved by an approximation method (see Appendix C).

To obtain a nonlinear load flow solution, the algorithm exploits the concept of the SLP method. Because LP is carried out repeatedly in the approximation method, the computer code of this algorithm can easily be developed by making use of existing LP software options.

In the proposed algorithm, an initial solution is generated by rounding off the discrete variables of the solution of a continuous OPF. When the solution of the continuous OPF is infeasible after the discrete variables are rounded off, the proposed algorithm becomes very effective.

4.6.3 Features of the Problem

The discrete OPF studied in this section is an operation planning problem whose objective is to minimize the generator operation cost under the operational constraints of the power system. For convenience of description, both capacitor and reactor are referred to as reactive devices. The number of capacitor banks and reactor banks installed at each bus is deemed as an integer variable, whereas the transformer tap is considered a discrete variable. The objective functions and constraints of the discrete OPF are explained here.

(1) Objective function is to minimize the system loss, which is equal to the total generator output minus the total load. Because the load is fixed, to minimize the generator output means to minimize loss. The objective function is a nonlinear expression.

(2) Constraints: The constraint functions include nonlinear functions.
   1. Constraint of reactive devices: constrained by upper limit of number of reactive device banks.
   2. Operational constraints of the power system.
      a. Constrained by balance between generation and load under given load condition, that is, power flow balance constraint.
      b. Constrained by the upper and lower voltage limits at generator buses and load buses.
      c. Constrained by the upper and lower limits of reactive output of generator. Here, the reactive output of generator is a continuously adjustable variable.
      d. Constrained by variation range of transformer tap. Here, the tap is a discrete adjustable variable.
      e. Constrained by variation range of number of capacitor banks. This number is a discrete adjustable variable.

(3) Number of continuous variables.
   Unlike reactive power optimization, OPF needs to consider not only reactive power optimization but also active power optimization. In active power optimization, the active output of the generator is treated as a continuous variable.

$$\text{Number of continuous variables} = 2 \times \text{number of system buses} +$$

number of reactive output variables of generator + number of active output variables of generator.

(4) Number of discrete variables.

$$\text{Number of discrete variables} = \text{number of variables of reactive devices} + \text{number of variables of tap ratio}$$

   1. Number of problem constraint functions = number of system buses $N \times 2$.
   2. There are two types of variables: continuous variable and discrete variable; each variable has its upper and lower limits, and the number of integer variables is very large.

An actual power system usually has more than 100 buses, so both the number of constraints and number of variables are more than a few hundred. The experimental system studied in this chapter has 135 buses, 36 generators, 17 transformers, 10 capacitors, and 4 reactors. Therefore, the number of continuous variables is $2 \times 135 + 36 \times 2 = 342$, the number of discrete variables is $17 + 10 + 4 = 31$, and the number of constraint functions is $2 \times 135 = 270$.

The previous analysis indicates that the discrete power flow optimization problem is a large-scale MIP problem. The process for solving this complex problem is explained here.

4.6.4 Mathematical Model

In the discrete OPF problem addressed in this section, the objective function is to minimize operation cost of generator and the constraint function is the operation conditions of the power system. The formulated model is shown here.

OPF Problem:

Objective function:

To minimize operation cost of generator (equivalent to minimize loss).

$$\min \sum_{i \in NG} f_i(P_{Gi}) \tag{4.10}$$

Constraints:

Constraint of power flow balance (add variables such as transformer tap T, number of the capacitor banks "C," and number of the reactor banks "R"):

$$P_i(U, \theta, T) - P_{Gi} - P_{Li} = 0, \quad i \in N \tag{4.11}$$

$$Q_i(U, \theta, T, C, R) - Q_{Gi} - Q_{Li} = 0, \quad i \in N \tag{4.12}$$

Constraint of active and reactive outputs of generators:

$$\underline{P}_{Gi} \le P_{Gi} \le \overline{P}_{Gi}, \quad i \in N \tag{4.13}$$

$$\underline{Q}_{Gi} \le Q_{Gi} \le \overline{Q}_{Gi}, \quad i \in N \tag{4.14}$$

Constraint of bus voltage magnitude and phase angle:

$$\underline{U}_i \le U_i \le \overline{U}_i, \quad i \in N \tag{4.15}$$

$$\underline{\theta}_i \le \theta_i \le \overline{\theta}_i, \quad i \in N \tag{4.16}$$

Constraint of transformer tap:

$$\underline{T}_i \le T_i \le \overline{T}_i, \quad i \in N_T \tag{4.17}$$

Constraint of capacitor:

$$\underline{C}_i \le C_i \le \overline{C}_i, \quad i \in N_C \cup E_C \tag{4.18}$$

Constraint of reactor:

$$\underline{R}_i \le R_i \le \overline{R}_i, \quad i \in N_R \tag{4.19}$$

In which:

$$f_i(P_{Gi}) = a_{0i} + a_{1i} P_{Gi} + a_{2i} P_{Gi}^2 \tag{4.20}$$

$$P_i(U,\theta,T)=\sum_{j\in i}P_{ij}(U,\theta,T) \tag{4.21}$$

$$Q_i(U,\theta,T,C,R)=\sum_{j\in i}Q_{ij}(U,\theta,T)-V_i^2(C_i-R_i) \tag{4.22}$$

where N_T—number of transformers; N_C—number of newly installed capacitors; E_C—number of existing capacitors; N_R—number of reactors.

The previous OPF problem is a mixed-integer nonlinear problem; the objective function of Eq. (4.10) is to minimize the sum of fuel costs of the generator. Constraint Eqs. (4.11)–(4.19) are nonlinear power flow equations. In Eqs. (4.21) and (4.22), the power flow function expressions with the added variables T, C, and R are different from the traditional power flow. The variable X in the equations can be U, θ, T, C, R, $P(=P_G-P_L)$, and $Q(=Q_G-Q_L)$.

To address the discrete characteristics of transformer tap T, number of capacitor banks "C," and number of reactor banks "R," the power flow equations for the transformer branch having tap T and the capacitor branch C are given first. Then, the differential equations for T and C are given in the following, respectively.

(1) Power flow equation for transformer branch:

$$\begin{cases}P_{ij}=U_iU_ig_\iota-U_iU_j(g_\iota\cos\theta+b_\iota\sin\theta)/T\\ Q_{ij}=-U_iU_ib_\iota-U_iU_j(-g_\iota\sin\theta+b_\iota\cos\theta)/T\end{cases}$$
$$\begin{cases}P_{ij}=U_jU_jg_\iota/T^2-U_iU_j(g_\iota\cos\theta-b_\iota\sin\theta)/T\\ Q_{ji}=-U_jU_jb_\iota/T^2+U_iU_j(g_\iota\sin\theta+b_\iota\cos\theta)/T\end{cases}$$

(2) Equation for differentiation of T in the power flow of transformer branch:

$$\partial P_{ij}/\partial T=U_iU_j(g_\iota\cos\theta+b_\iota\sin\theta)/T^2$$

$$\partial Q_{ij}/\partial T=U_iU_j(g_\iota\sin\theta-b_\iota\cos\theta)/T^2$$
$$\partial P_{ji}/\partial T=-2U_jU_ib_\iota/T^3+U_iU_j(g_\iota\cos\theta-b_\iota\sin\theta)/T^2$$
$$\partial Q_{ji}/\partial T=2U_jU_jb_\iota/T^3-U_iU_j(g_\iota\sin\theta+b_\iota\cos\theta)/T^2$$

(3) Equation for the power flow of capacitor branch:

$$b_c=\omega\Delta C$$
$$q_c=U^2b_c$$
$$Q_c=Cq_c=CV^2b_c$$

where ΔC—capacity of single capacitor bank; ω—angular frequency of system; b_c—admittance of single capacitor bank; U—rated voltage at access point of capacitor; q_c—reactive power compensated by single capacitor bank; C—number of capacitor banks (integer variable); Q_c—reactive power compensated by capacitor bank.

Differentiation of number of capacitor banks "C":

$$\partial Q_c / \partial C = U^2 b_c$$

To address the discrete attribute of tap ratio T_i, number of capacitor banks "C_i," and number of reactor banks "R_i," the integer variables y_{Ti}, y_{Ci}, and y_{Ri} are defined as follows:

$$T_i = T_i^0 + y_{Ti}\Delta T_i \quad , \quad i \in N_T \tag{4.23}$$

$$C_i = C_i^0 + y_{Ci}\Delta C_i, \quad i \in N_C \cup E_C \tag{4.24}$$

$$R_i = R_i^0 + y_{Ri}\Delta R_i, \quad i \in N_R \tag{4.25}$$

where T_t^0, C_i^0, R_i^0—T_i, C_i, R_i initial value; Δ_{Ti}—tap ratio of each tap position; Δ_{Ci}—unit capacitance; N_R—set of reactor buses; Δ_{Ri}—unit reactance; y_{Ti}—integer variable of tap ratio; y_{Ci}—integer variable of number of capacitor banks; y_{Ri}—integer variable of number of reactor banks.

If Eqs. (4.23)–(4.25) are substituted into Eq. (4.22), the equation can be changed to:

$$Q_i(U, \theta, T, C, R) = \sum_{j \in Ni} Q_{ij}\left[U, \theta, \left(T_i^0 + y_{Ti}\Delta T_i\right)\right] - U_i^2\left[\left(C_i^0 + y_{Ci}\Delta C_i\right) - \left(R_i^0 + y_{Ri}\Delta R_i\right)\right] \tag{4.26}$$

Based on Eqs. (4.10)–(4.26), the equation can be simplified as:

$$\min f(\boldsymbol{X}, \boldsymbol{Y}) \tag{4.27}$$

$$\text{s.t.} \quad G(\boldsymbol{X}, \boldsymbol{Y}) = 0 \tag{4.28}$$

$$\underline{\boldsymbol{X}} \le \boldsymbol{X} \le \overline{\boldsymbol{X}} \tag{4.29}$$

$$\underline{\boldsymbol{Y}} \le \boldsymbol{Y} \le \overline{\boldsymbol{Y}} \tag{4.30}$$

where f—objective function of nonlinear scalar; G—$G = [g_i]$, constraint function vector of nonlinear equation.

$\boldsymbol{X} = [U, \theta, P_G, Q_G]$, continuous variable vector; $\boldsymbol{Y} = [Y_T, Y_C, Y_R]$, integer variable vector; the components are $\boldsymbol{Y}_T = [y_{Ti}]$, $\boldsymbol{Y}_C = [y_{Ci}]$, $\boldsymbol{Y}_R = [y_{Ri}]$.

The expressions for Y_T and Y_C are shown in Appendix B.

4.7 Discrete OPF Algorithm

4.7.1 Main Solution Procedure of Discrete OPF

The solution algorithm is based on an optimization technique such that the discrete OPF problem is linearized iteratively and solved by utilizing an approximation method for linear MIP problems and the SLP method. From the convergence features of both methods, it can be

understood that the proposed algorithm can guarantee convergence. The overall flowchart of the algorithm is shown in Fig. 4.4. The details of the solution algorithm are explained as follows:

Step 1. Set iteration counter $k=0$, and obtain an initial solution $Z^0=(X^0, Y^0)$ by utilizing the power flow algorithm or other OPF algorithms, where "Z" represents the vector of all variables. Note that the final solution depends on Z^0.
Step 2. Formulate the discrete OPF problem as a nonlinear MIP problem as stated in Eqs. (4.10)–(4.22).
Step 3. Construct a linear MIP problem (it is also called mixed-integer linear programming, MILP problem) by linearizing the objective function and constraint functions around point $Z^k=(X^k, Y^k)$ (see Section 4.7.3).
Step 4: Search for a near-optimal integer feasible solution Z^{k+1} of the linear MIP problem by utilizing the approximation method in Appendix A. The calculation procedure will take into account the variation of the limit values of the variable variation range.

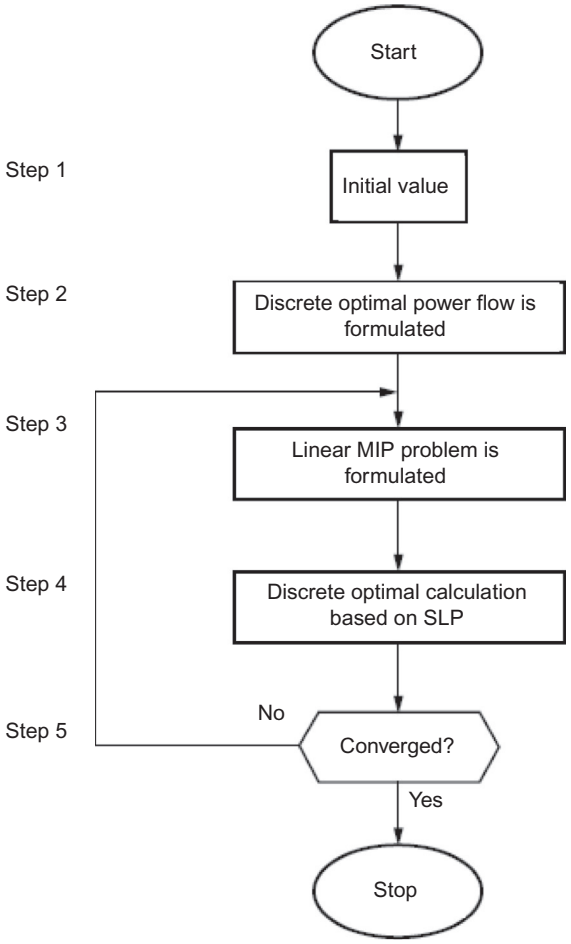

Fig. 4.4
Calculation procedure for discrete optimal power flow.

Step 5: Test for the convergence of the nonlinear OPF problem. If $|Z^k - Z^{k+1}| \leq \varepsilon$ (ε is a small integer), then terminate the calculation procedure, because a near-optimal solution ZR of the nonlinear discrete OPF problem has already been obtained. Otherwise return to Step 3 after setting $k=k+1$.

Note that the final result is relevant to Z^0. The OPF is an operation problem, and the operation bus will not be too far from the optimal solution. Thus, processing the variation of the limit values during the solution process will satisfactorily solve the nonlinear problem. The method is shown in Section 4.7.3 in detail.

4.7.2 Linearization of the Problem

To formulate the mixed-integer LP problem of the discrete OPF, the original problem can be linearized by the Taylor series expansion around Z^k. The Jacobian matrix shown in the next section can be used as a coefficient for the continuous variable vector and integer variable vector of the mixed-integer LP problem shown here. To simplify, the superscript k for the variable in the formula is omitted.

$$\min \quad \boldsymbol{c}^t\boldsymbol{X} + \boldsymbol{d}^t\boldsymbol{Y} \tag{4.31}$$

$$\text{s.t.} \quad \boldsymbol{A}\boldsymbol{X} + \boldsymbol{B}\boldsymbol{Y} = \boldsymbol{b} \tag{4.32}$$

$$\underline{\boldsymbol{X}} \leq \boldsymbol{X} \leq \overline{\boldsymbol{X}} \tag{4.33}$$

$$\underline{\boldsymbol{Y}} \leq \boldsymbol{Y} \leq \overline{\boldsymbol{Y}} \tag{4.34}$$

where $\boldsymbol{X}$—continuous variable; $\boldsymbol{Y}$—integer variable; $\boldsymbol{A}$, $\boldsymbol{B}$—constant coefficient matrix; $\boldsymbol{b}$, $\boldsymbol{c}$, $\boldsymbol{d}$—constant coefficient vector.

Eq. (4.31) can be expressed as $\partial f_i(P_{Gi})/\partial X_i + \partial f_i(P_{Gi})/\partial Y_i$, where coefficients c and d are combinations of coefficients such as a_{1i} and a_{2i}. The method for obtaining the coefficient of the linear equation for the nondifferentiable integer variable Y can be approximated by the difference expression, as shown in Appendix B.

4.7.3 SLP-based Solution Procedure for Linear MIP Problem

The SLP technique is used to calculate the next solution after the linear solution of the LP problem and the limits of variables have been obtained. In this method, the limits of the variable have to be changed to satisfy the given criteria. If such criteria are satisfied, increase the limits; otherwise, decrease the limits. As previously explained, in Step 4 of the general computational procedure for discrete OPF, the approximate mixed-integer LP method in Appendix A can be used to search for the integer feasible solution Z^k of the mixed-integer LP problem. The limits of the variables also need to be determined and adjusted, that is,

during the iterative solving process for the mixed-integer LP problem, the limits of the variables shall be adjusted to solve the nonlinear OPF problem. The calculation process is shown in Fig. 4.5. The reasons for determining and adjusting the limits of variables will be presented at the end of this section. If the solution of the linear MIP problem is acceptable, then this procedure ends. Each step in Fig. 4.5 is a substep of Step 4 in Fig. 4.4. The details of each substep of this procedure, in which the solution Z^{k+1} is calculated from Z^k, are explained as follows:

Substep 1: For the beginning of iteration, initial values of bound S for continuous variable and bound E for discrete variable must be specified (e.g., $S=0.01$ and $E=1$), and the following inequality constraint is given to each continuous variable x_j of the constraints of the linear MIP (also known as MILP) problem:

$$-S \le x_j - x_j^k \le S, \quad S \ge 0 \tag{4.35}$$

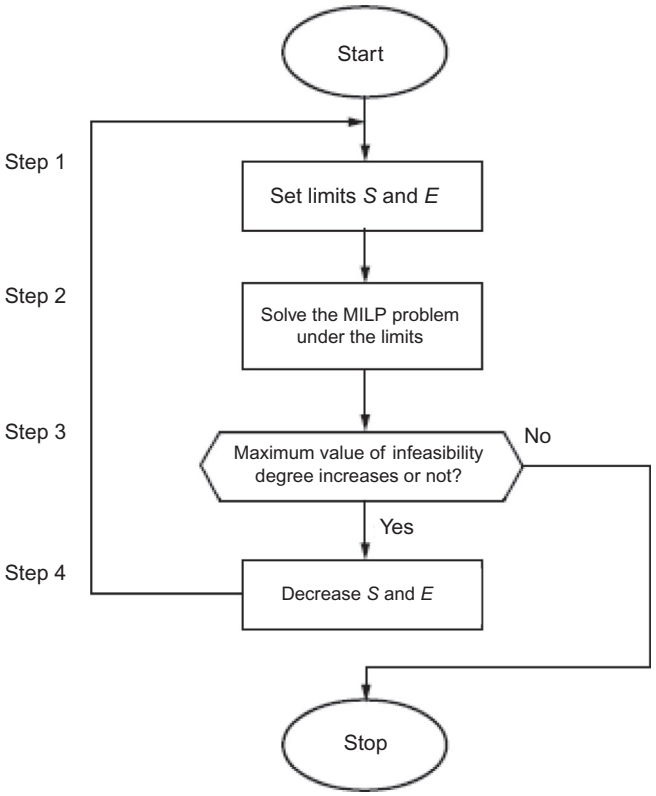

Fig. 4.5
The detailed calculation process for Step 4.

where x_j^k is the continuous variable in the iteration k. The following constraint is given to each integer variable y_j of the constraints in the linear MIP problem:

$$-E \le y_j - y_j^k \le E, \quad E \ge 0, E \quad E \text{ is an integer} \tag{4.36}$$

where y_j^k is the discrete variable of the iteration k.

Substep 2: If the bounds S and E are given, the approximate mixed-integer LP method in Appendix A is used to obtain a near-optimal solution of the linear MIP problem in which the bound constraints, Eqs. (4.35) and (4.36), are added. The obtained near-optimal solution is denoted by Z^{k+1}.

Substep 3: Check whether the maximum infeasibility amount of Z^{k+1} relative to Z^k has been decreased, that is, whether the following condition is satisfied:

$$MAXINF\left(Z^k\right) > MAXINF\left(Z^{k+1}\right) \tag{4.37}$$

where $MAXINF(Z)$ is defined as:

$$MAXINF(Z) = \max\{|\, g_i(X, Y) - u_i|\,\} \tag{4.38}$$

where $g_i\,(X,Y)$ is the power flow constraint function, and u_i is the unbalance amount produced after the solution to the LP problem is substituted into the nonlinear power flow constraint function. That is, Eq. (4.38) means the maximum calculation error of PQ bus or the maximum violation value of the active power and reactive power of generator bus after the linearized solutions X and Y are substituted into the original nonlinear power flow constraint Eqs. (4.11) and (4.12). In the case of $MAXINF(Z^k) = 0$ or $MAXINF(Z^k) = MAXINF(Z^{k+1})$, there is no violation value or the violation values in the two iterations are the same, then $MAXINF(Z^k)$ cannot be used as the criteria. Instead, the change of objective function values between the two iterations is added to the criteria, shown in this formula:

$$MAXINF\left(Z^k\right) + f\left(X^k, Y^k\right) \tag{4.39}$$

where the definition of $f(X^k, Y^k)$ is given in Eq. (4.27). If the conditions for Eq. (4.37) are satisfied, Z^{k+1} is accepted and the iterative procedure for mixed-integer LP problem terminates; otherwise, the next step begins to calculate Z^{k+1}again.

Substep 4: To reduce infeasibility amount, adjust step bounds S and E. If bounds S and E can be further reduced, reduce them. For example, set $S \leftarrow S/2$, $E \leftarrow E - 1$ (if $E > 0$) and return to Substep 1. If the bounds S and E are already small enough, the calculation process terminates. At this time, vector Z cannot be further improved, but it has been forced to converge.

The necessity of the bound constraints in the optimization procedure is discussed here. The SLP technique always converges to a nonlinear solution by controlling the variation range of the

bound for the variables during the iterative process. Therefore, in the initial step of iteration, the variation range of the variables must be determined. In Substep 2 and the subsequent iteration process, the bounds S and E will be changed in Substep 4, and the principle of such change will depend on the nonlinear solutions within the two iterations. If the nonlinear infeasibility amount increases, the values of the bound are reduced by half; otherwise, the values of the bound remain unchanged. The iterative process is to search for the solution under the linear constraint, although the actual constraint is nonlinear. Therefore, in Substep 3 of the iteration, it is necessary to check whether the violation of the nonlinear constraint is improved.

During the entire solution procedure, because the linearized objective function of Eq. (4.31) is optimized under the linearized constraints of Eqs. (4.32)–(4.34), there is no guarantee that the resulting solution Z^{k+1} is better than Z^k, that is, Z^{k+1} may violate the nonlinear constraints of Eq. (4.28) more seriously and with a higher value of objective function. Therefore, after obtaining Z^{k+1} in the optimization procedure of the linear MIP problem, it must be checked whether Z^{k+1} is better than solution Z^k from the previous iteration.

In this algorithm, Z^{k+1} is considered acceptable if it makes the infeasibility of the nonlinear equations smaller. If the foregoing criterion is not satisfied, then the linear MIP problem must be resolved after reducing the bounds S and E (the bounds are within the constraints of the variables X and Y). The reason is that the linearized accuracy is related to the variation of the variable vector Z between two iterations. If the variable range becomes very small, $|Z^k - Z^{k+1}|$ will become smaller, thus, the variable Z converges.

4.8 Implementation of Discrete OPF

4.8.1 Verification by the Concrete Formulation of 5-Bus System

(1) Original data: The 5-bus system is as shown in Fig. 4.6. This system has two adjustable transformer tap ratios and three capacitors. The detailed data are given in Tables 4.9–4.12.

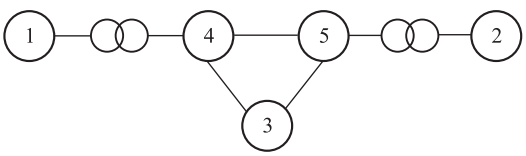

Fig. 4.6
5-Bus system diagram.

Table 4.9 Transformers and branches in 5-bus system

I	Reference Voltage at *I* Side (kV)	*J*	Reference Voltage at *J* Side (kV)	*R* (Per-Unit Value)	*X* (Per-Unit Value)	*T*	Δ	$\underline{N}$	$\overline{N}$	Actual Voltage at *I* Side (kV)	Actual Voltage at *J* Side (kV)
1	10	4	110	0.0	0.015	1.0	2.5%	−4	4	10	121
2	10	5	110	0.0	0.030	1.0	2.5%	−4	4	10	121
3	110	4	110	0.018	0.250						
3	110	5	110	0.012	0.050						
4	110	5	110	0.018	0.060						

Table 4.10 Buses in 5-bus system

Bus	(kV)	Bus Type	P_G (MW)	Q_G (Mvar)	P_L (MW)	Q_L (Mvar)	V_I (kV)	θ (deg)
1	10	*PV*	550				11.0	
2	10	SLACK					10.7	0.0
3	10	*PQ*			250	175		
4	10	*PQ*			250	250		
5	10	*PQ*			250	150		

Table 4.11 Constraints of 5-bus system

Bus	U_B (kV)	Q_{min} (Mvar)	Q_{max} (Mvar)	U_{min} (kV)	U_{max} (kV)	P_{min} (MW)	P_{max} (MW)
1	10	30	275	9.5	10.5		
2	10	0	150	9.5	10.5	0.0	280
3	110			110.0	117.7		
4	110			115.0	121.0		
5	110			110.0	117.7		

Table 4.12 Reactive compensation of 5-bus system

Bus No.	U_{BI} (kV)	Initial Number of Banks	Maximum Number of Banks	*C* (Mvar)/bank	Cost (Per-Unit Value)/Bank
3	110	2	10	10.0	1.00
4	110	2	10	10.0	1.00
5	110	0	10	10.0	1.00

(2) The detailed coefficients of the 5-bus system example in the mathematical model: In the following are the expressions for the 5-bus system examples corresponding to the continuous variable vector $\boldsymbol{X}$, integer variable vector $\boldsymbol{Y}$, continuous variable coefficient matrix $\boldsymbol{A}$, discrete variable coefficient matrix $\boldsymbol{B}$, and right hand side vector $\mathbf{b}$ in Eq. (4.32):

$$\boldsymbol{X} = (U_1, \theta_1, U_2, \theta_2, U_3, \theta_3, U_4, \theta_4, U_5, \theta_5, P_{G1}, Q_{G1}, Q_{G2})$$

$$\boldsymbol{Y} = (Y_{T1}, Y_{T2}, Y_{C1}, Y_{C2}, Y_{C3})$$

$$\boldsymbol{A} = \begin{bmatrix} J_{11} & & J_{14} & & A_{P1} & A_{Q1} & \\ & J_{22} & & J_{25} & & & A_{Q2} \\ & & J_{33} & J_{34} & J_{35} & & \\ J_{41} & & J_{43} & J_{44} & J_{45} & & \\ & J_{52} & J_{53} & J_{54} & J_{55} & & \end{bmatrix}$$

$$\boldsymbol{B} = \begin{bmatrix} A_{T1} & & & & \\ & A_{T2} & & & \\ & & A_{C1} & & \\ A_{T4} & & & A_{C2} & \\ & A_{T5} & & & A_{C3} \end{bmatrix}$$

$$\boldsymbol{b} = [\Delta P_1, \Delta Q_1, \ldots, \Delta P_5, \Delta Q_5]^T$$

where

$$\boldsymbol{J}_{ii} = \begin{bmatrix} \partial P_i/\partial U_i & \partial P_i/\partial \theta_i \\ \partial Q_i/\partial U_i & \partial Q_i/\partial \theta_i \end{bmatrix}, \quad \boldsymbol{J}_{ij} = \begin{bmatrix} \partial P_i/\partial U_j & \partial P_i/\partial \theta_j \\ \partial Q_i/\partial U_j & \partial Q_i/\partial \theta_j \end{bmatrix}$$

$$\boldsymbol{A}_{pi} = \begin{bmatrix} \partial p_i/\partial p_i \\ 0 \end{bmatrix} = \begin{bmatrix} 1 \\ 0 \end{bmatrix}, \quad \boldsymbol{A}_{Qi} = \begin{bmatrix} 0 \\ \partial Q_i/\partial Q_i \end{bmatrix} = \begin{bmatrix} 0 \\ 1 \end{bmatrix}$$

$$\boldsymbol{A}_{Tij} = \begin{bmatrix} \partial P_{ij}/\partial T_i \\ \partial Q_{ij}/\partial T_i \end{bmatrix}, \quad \boldsymbol{A}_{Tji} = \begin{bmatrix} \partial P_{ji}/\partial T_i \\ \partial Q_{ji}/\partial T_i \end{bmatrix}, \quad A_{Ci} = U_i^2 q_{Ci}$$

If $U_0 = 1.0$ and $\theta_0 = 0$, the coefficients of $\boldsymbol{A}$, $\boldsymbol{B}$, and $\mathbf{b}$ are:

$$\boldsymbol{A} = \begin{bmatrix} 66.67 & 0 & 0 & 0 & 0 & 0 & -66.67 & 0 & 0 & 0 & 1 & 0 & 0 \\ 0 & 66.67 & 0 & 0 & 0 & 0 & 0 & -66.67 & 0 & 0 & 0 & 1 & 0 \\ 0 & 0 & 33.33 & 0 & 0 & 0 & 0 & 0 & -33.33 & 0 & 0 & 0 & 0 \\ 0 & 0 & 0 & 33.33 & 0 & 0 & 0 & 0 & 0 & -33.33 & 0 & 0 & 1 \\ 0 & 0 & 0 & 0 & 22.8904 & 4.8247 & -3.9794 & -0.2865 & -18.911 & -4.539 & 0 & 0 & 0 \\ 0 & 0 & 0 & 0 & -4.8255 & 22.8898 & 0.2865 & -3.9794 & 4.539 & -18.911 & 0 & 0 & 0 \\ -66.67 & 0 & 0 & 0 & -3.9794 & -0.2865 & 85.9404 & 4.8737 & -15.291 & -4.5872 & 0 & 0 & 0 \\ 0 & -66.67 & 0 & 0 & 0.2865 & -3.9794 & -4.8737 & 85.9328 & 4.5872 & -15.291 & 0 & 0 & 0 \\ 0 & 0 & -33.33 & 0 & -18.911 & -4.539 & -15.291 & -4.5872 & -67.532 & 9.1252 & 0 & 0 & 0 \\ 0 & 0 & 0 & -33.33 & 4.539 & -18.911 & 4.5872 & -15.291 & -9.1262 & 67.5372 & 0 & 0 & 0 \end{bmatrix}$$

$$\boldsymbol{B} = \begin{bmatrix} 0 & 0 & 0 & 0 & 0 \\ 1.66675 & 0 & 0 & 0 & 0 \\ 0 & 0 & 0 & 0 & 0 \\ 0 & 0.833325 & 0 & 0 & 0 \\ 0 & 0 & 0 & 0 & 0 \\ 0 & 0 & 10.0 & 0 & 0 \\ 3.3335 & 0 & 0 & 0 & 0 \\ -1.66675 & 0 & 0 & 10.0 & 0 \\ 0 & 1.66675 & 0 & 0 & 0 \\ 0 & -0.833325 & 0 & 0 & 10.0 \end{bmatrix}$$

$$\boldsymbol{b} = \begin{bmatrix} 5.5 \\ 0 \\ 0 \\ 0 \\ -2.4996 \\ -1.7494 \\ -2.5 \\ -2.4962 \\ -2.4995 \\ -1.5026 \end{bmatrix}$$

(3) The optimization calculation results for 5-bus system are given in Tables 4.13–4.15.

Table 4.13 Bus voltage solutions in 5-bus system (kV)

Bus No.	1	2	3	4	5
Bus voltage solution	10.5	10.5	110.42	119.50	115.95

Table 4.14 Transformer tap solutions in 5-bus system

Bus *I*–Bus *J*	Tap Position *T*	Gear Position Y_T
1–4	0.95	4
2–5	0.925	5

Table 4.15 Reactive compensation solution in 5-bus system (number of banks)

Bus No.	3	4	5
Number of reactive capacitor banks "Y_c"	10	6	8

4.8.2 Conditions and Results of Four Cases for 135-Bus Large-scale System

This case study uses a real-scale 135-node test system that consists of 36 generators, 98 loads, and 17 transformers. The mathematical programming system (MPS) is used for solving LP problems. Calculation results for the four cases shown in Tables 4.16–4.18 are given to demonstrate the performance of the algorithm. The initial points of cases 1 and 3 are the results of continuous OPF solutions obtained by the nonlinear method MINOS/AUGMENTED Ver. 4.0 [22].

Because the discrete OPF is a nonconvex problem, the optimal solution obtained by the SLP technique is related to the initial value. To demonstrate the effectiveness of the algorithm proposed in this chapter, four cases are studied. The initial values in case 1 and case 3 utilize the optimal solutions of continuous OPF obtained by the nonlinear method of MINOS/AUGMENTED Ver. 4.0. The algorithm proposed requires an initial integer solution, thus, the integer variables of the optimal solution to the continuous OPF is rounded off to form the initial integer solution. In comparison, the initial values of case 2 and case 4 utilize the conventional power flow solutions under the normal operation condition. In addition, the initial values of cases 1–4 are continuously feasible, whereas the rounded values are infeasible, which validates the effectiveness of the algorithm.

In these numerical cases, to distinguish the local optimal solutions, a big difference for the generation cost is assigned according to the characteristics of the generators. The resulting difference value of the objective function between the optimal operation state and the general one is about 10%. The voltage magnitude is allowed a variation of ranges with 0.94–1.06 for case 1 and case 2, and 0.97–1.03 for case 3 and case 4.

The calculation results for the four cases are listed in Tables 4.16–4.18. Table 4.16 summarizes the calculation results of the four cases. All the values in the table are relative values calculated based on the initial values of case 1. The initial condition of objective functions of case 1 and case 3 are 10% less than that of case 2 and case 4. Such a big difference is intended to examine the effect of initial values on the optimization results. The results in the tables indicate that better initial values will produce better results, because the optimization procedure of the algorithm is based on the SLP technique, and the algorithm tends to converge to the local optimal point near the initial solution.

Table 4.16 Comparisons of objective function values corresponding to different initial values

Case Name	Case 1	Case 2	Case 3	Case 4
Initial value	1.0000	1.1142	1.0002	1.1141
Result	1.0044	1.0599	1.0008	1.0712
CPU(s)	54.0	49.04	41.81	37.98

Tables 4.17 and 4.18 give detailed changes of the objective functions and integer variables in the calculation process of case 1. In this case, the optimal solution to continuous OPF is used as the initial value, and then the linearized MIP problem is solved after setting the rounded-off continuous power flow solution as the initial solution. The values in the objective function value column in Table 4.17 are the relative values calculated by using the OPF solutions as the initial values. Similarly, the value of maximum infeasibility is the relative value calculated by using the initial maximum infeasibility as the reference. The infeasibility is defined in Eq. (4.38). In these tables, "Variation of Bound S" represents the maximum changeable amount of continuous variables. "Max. Infeasibility" represents the maximum amount of the violations of constraints of Eqs. (4.11)–(4.19). "Initial Value" means an initial solution Z. That is, this value means a rounded-off solution of the result of continuous OPF. As shown in Table 4.18, not all integer variables change in each iteration.

Table 4.17 Iteration process in case 1 (CPU = 54s)

Content		Number of LP Problem Solved	Variation of Bound S	Objective Function	Max. Infeasibility
Initial value				1.0000	1.0000
Iteration counter	1	3	0.04	1.0013	1.5320
	2	3	0.01	1.0012	1.4030
	3	4	0.01	1.0139	0.0820
	4	3	0.01	1.0045	0.0060
	5	2	0.0025	1.0044	0.0010
	6	1	0.00125	1.0044	0.0000

In Table 4.17, the objective value and infeasibility amount are normalized by those of case 1 in which the initial rounded-off values are set as 1.0. Table 4.18 shows the changes of integer variables, such as transformer taps. Variation of bound S in Table 4.17 is described as follows:

At the first iteration: Setting the initial bound as $S = 0.01$, the linearized MIP problem is solved by the LP method, and the problem is infeasible. Then setting the bound as $S = 0.02$, the MIP problem is solved and is still infeasible. And again setting the bound as $S = 0.04$, the MIP problem is solved and feasible; transformer tap 16 is decreased by 1 relative to the reference value, the objective function value is 1.0013, and the maximum infeasibility (nonlinear) is 1.5320.

At the second iteration: Setting the bound as $S = 0.04$ to solve the MIP problem by LP, the maximum infeasibility (nonlinear) is not smaller than that in the first iteration; then setting the bound as $S = 0.02$, the MIP problem is solved, and transformer tap 16 is reduced by 1. Again, setting the bound as $S = 0.01$, the MIP problem is solved, and transformer tap 2 is reduced by 1; last, to solve the problem by LP, the objective function is improved; the maximum infeasibility (nonlinear) is reduced to 1.4030.

Table 4.18 Variation of integer in case 1

Equipment		**Change in Transformer Taps**																
S/N		1	2	3	4	5	6	7	8	9	10	11	12	13	14	15	16	17
Initial deviation		0	0	0	0	0	0	0	0	0	0	0	0	0	0	0	0	0
Iteration counter	1																−1	
	2								−1								−1	
	3								−1								−1	−1
	4				1							−1						
	5																	
	6																	
Final deviation		0	0	0	1	0	0	0	−2	0	0	−1	0	0	0	0	−3	−1

At the fifth and sixth iterations: To reduce the maximum infeasibility (nonlinear), the bound S is reduced to 0.025 and 0.00125. The objective function is no longer reduced, and the maximum infeasibility is within the allowable range, so the calculation terminates.

From case 1 to case 4, the same bound adjustment method is used at Step 4. That is, bound S for continuous variables is decreased by setting $S = S/2$, and bound E is always set as 1. Although there are a variety of methods to adjust the bounds S and E, the convergence properties are almost the same according to our experience.

Table 4.19 indicates the variation of bound S during iteration in case 2. This case uses the conventional power flow as the initial value. Table 4.20 indicates the variation of transformer tap position in case 2. Table 4.21 shows the variation of capacitor and reactor in case 2.

Table 4.19 Iteration process in case 2 (CPU = 49.04 s)

Content		Number of LP Problem Solved	Variation of Bound *S*	Objective Function	Max. Infeasibility
Initial value				1.1142	2.0400
Iteration counter	1	3	0.01	1.0889	0.917
	2	6	0.01	1.0889	0.9180
	3	4	0.01	1.0806	0.1580
	4	6	0.01	1.0729	0.1150
	5	5	0.01	1.0674	0.0330
	6	4	0.005	1.0625	0.0170
	7	3	0.005	1.0599	0.0030

Table 4.20 Variation of transformer tap position in case 2

Equipment		Transformer																
S/N		1	2	3	4	5	6	7	8	9	10	11	12	13	14	15	16	17
Initial deviation		0	0	0	0	0	0	0	0	0	0	0	0	0	0	0	0	0
Iteration counter	1					−1		−1										
	2												1	−1				
	3													−1				
	4			1		1	1	1										
	5														1			
	6														1			
	7																	
Final deviation		0	0	1	0	0	1	0	0	0	0	0	1	−2	2	0	0	0

Table 4.21 Variation of capacitor and reactor in case 2

Equipment		Capacitor										Reactor			
S/N		1	2	3	4	5	6	7	8	9	10	1	2	3	4
Initial deviation		0	0	0	0	0	0	0	0	0	0	0	0	0	0
Iteration counter	1	−1													
	2				1		1								
	3	1			1										−1
	4														
	5				1	1	1								
	6					1	1								
	7														
Final deviation		0	0	0	3	2	3	0	0	0	0	0	0	0	−1

The bound adjustment method described in Step 4 (shown in Fig. 4.5), that is, reducing bounds S and E to reduce the infeasibility, is used for the calculation in cases 1–4. Every time the bound is changed, set $S \leftarrow S/2$ and keep $E = 1$ unchanged. There are many different methods for adjusting S, but their convergence characteristics are almost the same according to the experience in this chapter.

The results in Tables 4.16–4.21 show that the algorithm proposed in this chapter can be used to solve the discrete OPF problem for real scale systems and meet actual engineering needs in terms of calculation time and space.

4.9 Conclusion

The existing power flow algorithm is a nonlinear power flow algorithm without objective and constraints. This chapter has changed the traditional power flow problem solution method. The new method provides a basic reference system for the two power flow calculation methods: (1) unconstrained power flow algorithm with objective, and (2) constrained power flow algorithm with objective. To address the problems of convergence in the traditional power flow, the power flow model is reformulated in this chapter. Based on the introduction of the objective function, the SA algorithm is used to solve the ill-conditioned power flow problem that is difficult to converge. Based on the introduction of the constraint function, the approximate mixed-integer linear programming method is used to solve the OPF problem.

(1) This chapter first studies the application of the SA technique in solving ill-conditioned power flow in power system. A combined mathematics model based on the N-R technique and the SA technique is proposed. It has no significant differences with the pure N-R technique when used for solving the system power flow under normal conditions. However, the model may result in converged solutions when used for solving an ill-conditioned system. The numerical examples of ill-conditioned power flow in actual

systems indicate that the algorithm proposed in this chapter can effectively improve the convergence of the ill-conditioned power flow calculation in a large-scale system. It provides an alternative algorithm for power flow calculation in the power system.

(2) This chapter proposes a new algorithm for solving the discrete OPF problem. This algorithm can systematically process discrete variables such as transformer tap ratio, and number of capacitor and reactor banks in the actual-scale discrete OPF problem. The results of calculation used for an actual system show that the algorithm proposed is effective. The characteristics of this algorithm include:

1. The algorithm can treat the tap ratio, and number of capacitor and reactor banks as discrete variables.
2. The approximate mixed-integer LP algorithm (see Appendix A) can be used to solve the actual-scale discrete OPF problem.
3. The SLP calculation technique is used to obtain the power flow solution that satisfies the power flow equation.
4. The bounds of variable variation are adjusted to improve the linear approximation accuracy of the power flow equation.

The discrete feasible near-optimal solution can be obtained by the proposed algorithm. When the initial values are rounded off from the integer variable of the traditional OPF algorithm, the solution is infeasible. In this case, the algorithm is particularly effective.

CHAPTER 5

Load Optimization for Power Network

Chapter Outline

Mathematical Models and Algorithms for Power System Optimization. https://doi.org/10.1016/B978-0-12-813231-9.00005-4

5.1 Introduction

The bus loads P and Q are derived variables in the traditional power flow algorithm, so the bus load cannot be optimized. The total load of the urban power grid is the sum of the load of each bus, because most of the buses are PQ bus, that is, the loads of these buses have generally specified values in the power flow calculation. Under normal or faulty operating conditions, to meet certain requirements, the bus loads need to be adjusted manually. However, if P, Q, U, and θ are all set as independent variables, then P_G, Q_G, P_L, and Q_L can be optimized, respectively. The optimization model based on the AC power flow (OPF) discussed in Chapter 3 sets P_G and Q_G as independent variables under the condition of taking P_L and Q_L as specified values.

To optimize the bus loads P_L and Q_L, this chapter considers setting P_L and Q_L as independent variables under the given value of P_G and Q_G conditions. Because an accurately mathematical description of P_L is not required at the planning stage, some simplified power flow methods can be applied, for example, DC power flow, on which a load optimization model is proposed to optimize load P_L. The optimization calculation of load P_L in this chapter includes two aspects: (1) minimization of load curtailment (LC) under $N-1$ conditions, and (2) maximization of load supply capacity (LSC) under a given network structure and power generation conditions.

5.1.1 Description of Minimizing Load Curtailment

The ability to operate with any one major equipment unit out of service is called an $N-1$ capability, and this requirement is a criterion for the planning and design in the power system. However, during high-risk periods (summer or winter peak, some components are maintained), some events of multiple forced outages, $N-k$, may happen. Then the load will have to be curtailed to ensure system safety. To reduce the loss of power as much as possible when the system is in a state of $N-k$, it is necessary to choose the best one from all feasible options, namely, the minimum load reduction option. Rescheduling generation outputs and ensuring load transfer may avoid the LC as much as possible or minimize the total LC when unavoidable.

LC minimization is a problem of operation planning. It is to minimize total load reduction when unavoidable, which can give an optimal option for LC, improve the rationality of LC at each substation, and provide an auxiliary decision option for the dispatcher in the actual restriction of power.

5.1.2 Description of Maximizing Load Supply Capability

The rational planning of a power system always requires determination of its LSC. The maximum LSC refers to the maximum load that can be supplied on any branch (line or transformer) in a power grid without overload. LSC can be used as a key index for assessing the

LSC of a power grid. The LSC index is initially used as a reliability index to determine the event of load supply shortage. LSC can be used to determine system load level. When the system load exceeds this level, a failure occurs somewhere in the system. LSC helps to indicate the load that cannot be supplied by a system.

The power grid is a complex structure involving multiple aspects, such as power generation, transmission, transformation, distribution, and consumption, all of which should be considered in determining the grid's LSC. In the past, the LSC of a power grid was often assessed by using the simple capacity-load ratio method or a trial-and-error method. The capacity-load ratio is a single macroindex used to assess the grid's LSC. This index is applied to examine the grid's LSC from the grid's transformation aspect but not applied to the mutual relationship between the grid's power generation, transmission, distribution, and consumption. The trial-and-error method continues to increase system load, distribute load to each load point by a certain load distribution coefficient, and execute the power flow calculation until a very small increase in load would cause power over branch. In this method, the load distribution coefficient is the key issue to the accuracy of the final assessment result.

The LSC model based on linear programming can be applied to scientifically and accurately assess the maximum LSC of the urban power grid.

5.1.3 Overview of This Chapter

This chapter discusses the bus load optimization problem under fault and normal conditions. It also introduces bus load as a variable to formulate a simple linear programming model based on a DC power flow model. The model is used to determine the basic expressions of objective function and constraints. The different weights, assigned to each load bus based on different load properties, are considered in the cost coefficient, so the total curtailed load is minimized under fault condition, whereas the load is maximized under normal condition, which meets the reliability requirements for different loads. The bus load variable is added to the power balance constraint (grid power balance, bus power balance, and branch power balance) in equality constraints. The bus load constraint is added to inequality constraints (grid branch power constraint and generation bus output constraint).

Section 5.2 specifically gives basic ideas of formulating an optimization model; Section 5.3 provides a load optimization mathematical model; Section 5.4 introduces the algorithm and calculation process of LC optimization (LCO); Section 5.5 first uses a small-scale case study to verify the proposed LCO model and algorithm, and then gives detailed results of an actual case study for analysis to confirm the effectiveness of the proposed LCO model and algorithm; Section 5.6 gives the calculation process of maximizing LSC; and Section 5.7 uses a case study to verify the proposed optimization model and algorithm for maximizing LSC.

5.2 Basic Ideas of Load Optimization Modeling

5.2.1 Way of Processing the Objective Function

(1) The objective function is to minimize ($\min \sum_{i \in N_D} C_i P_{Ci}$) after $N-1$, in which different weight C_i is assigned to each bus load P_{Ci} due to different load properties. Based on load reliability requirements, cost coefficient is set as -1 (precutting), 0, or +1 (postcutting), by which the bus LC P_{Ci} will be minimized during the optimization calculation, and the reliability requirements are automatically met.

(2) The objective function is maximized ($\max \sum_{i \in N_D} C_i P_{Li}$) under the given network structure conditions where load is supplied. The different weight C_i is assigned to each bus load P_{Li} due to different load properties. Based on load reliability requirements, cost coefficient is set as +1 (preoperating), 0, or -1 (postoperating), by which the bus load will be maximized during the optimization calculation with the reliability requirements automatically satisfied.

5.2.2 Way of Processing the Variable Settings and Constraints

The load optimization model is an optimal model based on the DC power flow method. The optimization model of minimizing total curtailed load and the model of maximizing LSC are the supplement and improvement to the static security analysis. On the basis of existing network structure, bus load is optimized by way of setting variables described as follows:

(1) Idea of setting variables for minimizing total curtailed load: set bus output as P_G; set variable of bus LC as P_C whose upper limit is bus load P_L; P_L in the bus power balance expression is divided into two parts, $P_L - P_{C,}$ of which P_C is taken as the variable of objective function minimization.

(2) Idea of setting variables for maximizing LSC: set bus load variable as P_L; P_L in the bus power balance expression is directly taken as the variable of objective function maximization.

Although the variables in the two models are different, the forms of constraints in the two models are basically the same: equality constraints are power balance constraints of the DC power flow (grid power balance, bus power balance, and branch power balance); inequality constraints include network branch power constraint, generation bus output constraint, and load bus capacity constraint.

(3) Except for different variables, equality constraints in the two models have basically the same forms, including:

1. Power balance constraint (DC power flow): grid power balance, bus power balance, and branch power balance.
2. Inequality constraint: network branch power constraint.
3. Variable constraint: generation bus output constraint, load bus capacity (or LC) constraint, and voltage power angle variable constraint.

5.3 Formulation of Load Optimization Problem

The problem of minimizing LC can be described as follows: the objective function is to minimize the total curtailed load at load points; the optimal solution is the curtailed load and generation output at each bus.

The problem of maximizing LSC can be described as follows: the objective function is to maximize the load that network can supply; the optimal solution is the load and generation output at each bus.

The LCO can be explained by a LP mathematics optimization problem: minimize the total values of LCs; the optimal solution is the curtailment quantities at all load buses. So, based on the standard form of mathematics optimization, the variables, objective function, and constraint conditions are given as follows.

This chapter gives the expressions of variables, objective function, and constraints, respectively, in the standard form of mathematical programming.

5.3.1 Notations

Table 5.1 shows mathematical notations.

Table 5.1 Mathematical notations

Notations	Descriptions
N	The set of nodes in the grid, and the number of nodes is N. N': the set of nodes except slack node; N_D: the set of load nodes; N_G: the set of generation nodes except slack node; there may be some intersections between N_D and N_G.
N_B	The set of branches in grid, and the number of nodes is b.
W	The weighted column vector of load nodes (specified); W_i: the weight of load node i.
P_C	The column vector of curtailed load nodes; P_{Ci}: the LC of node i; P_{Cs}: the LC of slack node s; $P_C{}'$: the column vector of curtailed load nodes except slack node, $P_C = \begin{bmatrix} P_C{}' \\ P_{Cs} \end{bmatrix}$.
P_L	The column vector of nodes (specified current active power), P_{Li}; P_{Ls}: the current active power of node i or slack node s; $P_L{}'$: the column vector of nodes for current active power but the slack node, and $P_L = \begin{bmatrix} P_L{}' \\ P_{Ls} \end{bmatrix}$.
P_G	The column vector of nodes for active power output; P_{Gi}: active output of bus i; P_{Gs}: active output at slack bus s; $P_G{}'$: the active power output of node for active power output except the slack node, and $P_G = \begin{bmatrix} P_G{}' \\ P_{Gs} \end{bmatrix}$.
$\overline{P_G}$ $\underline{P_G}$	The upper or lower limit column vector of generation nodes (specified active power output), $\overline{P_{Gi}}$ $\underline{P_{Gi}}$: the upper or lower limit of node i for active power.

Continued

Table 5.1 Mathematical notations—Cont'd

Notations	Descriptions
P_b	The column vector of branch active power; P_{bj}: the active power of the branch j.
$\overline{P_b}$	The upper limit column vector of branch active power (specified); $\overline{P_{bj}}$: the upper limit of the branch j for active power.
θ	The column vector of nodes for phase angle; θ': the column vector of nodes for phase angle but slack node, after ordered, $\theta = \begin{bmatrix} \theta' \\ 0 \end{bmatrix}$.
R	The connection matrix of node and branch.
B'	The node susceptance transport matrix (the slack node is eliminated); $B_{ij}(=1/x_{ij})$: the mutual susceptance of node i and j; $B_{ii}\left(=-\sum_{\substack{j\in i \\ j\neq i}} B_{ij}\right)$: the self-susceptance of node i.
B_b	The diagonal matrix of branch susceptance.

5.3.2 Model of Load Curtailment Optimization (LCO)

(1) Objective function:

$$\min \sum_{i\in N_D} C_i P_{Ci}$$

(2) Constraints of LCO model:

1. Equality constraints. Power balance constraints (DC power flow): Power balance in the whole grid (no loss).
   (a) Grid power balance: $\sum_{i=1}^{N} P_{Gi} - \sum_{i=1}^{N} P_{Li} + \sum_{i=1}^{N} P_{Ci} = 0$.
   (b) Bus power balance: $P_G - P_L + P_C = B\theta$.
   (c) Branch power balance: $P_0 = B_b R\theta$.
2. Inequality constraints.
   (a) Network branch power constraints: $|P_{bj}| \le \overline{P}_{bj}, \quad j \in N_B$.
   (b) Variable constraints.
      a. Generation bus output constraint: $\underline{P}_{Gi} \le P_{Gi} \le \overline{P}_{Gi}, \quad i \in N_G$.
      b. Load bus capacity constraint: $0 \le P_{Ci} \le P_{Li}, \quad i \in N_D$.

5.3.3 Model of Load Supply Capability (LSC)

(1) Objective function:

$$\max \sum_{i\in N_D} C_i P_{Li}$$

(2) Constraints of LSC optimization model:

1. Equality constraints. Power balance constraints (DC power flow).
   (a) Grid power balance: $\sum_{i=1}^{N} P_{Gi} - \sum_{i=1}^{N} P_{Li} = 0$.
   (b) Bus power balance: $P_G - P_L = B\theta$.
   (c) Branch power balance: $P_b = B_b R\theta$.

2. Inequality constraints.
   (a) Network branch power constraint: $|P_{bj}| \le \overline{P_{bj}}$, $j \in N_B$.
   (b) Variable constraints.
      a. Generation bus output constraint: $\underline{P_{Gi}} \le P_{Gi} \le \overline{P_{Gi}}$, $i \in N_G$.
      b. Load bus capacity constraint: $\underline{P_{Li}} \le P_{Li} \le \overline{P_{Li}}$, $i \in N_D$.

5.3.4 The Derivation Process of LP Model for LCO

Select the LC and generation output of buses as state variables. The linear programming model of LCO is derived from the following procedures:

(1) Variables. State variable $\boldsymbol{x} = \begin{bmatrix} P_C \\ P_G \end{bmatrix}$, cost coefficient vector $c = [C \;\; 0]$.
(2) Objective function.

$$\min [C \;\; 0] \begin{bmatrix} P_C \\ P_G \end{bmatrix} \tag{5.1}$$

(3) Equality constraints.

$$\sum_{i=1}^{N} P_{Gi} - \sum_{i=1}^{N} P_{Li} + \sum_{i=1}^{N} P_{Ci} = 0 \tag{5.2}$$

is expressed as linear programming equality constraints:

$$[1_{1\times n} \;\; 1_{1\times n}] \begin{bmatrix} P_C \\ P_G \end{bmatrix} = 1_{1\times n} \times P_L \tag{5.3}$$

(4) Range constraints.
   1. Based on the DC power flow model, bus phase angle variables can be eliminated to obtain the relationship matrix between branch power and bus power.

$$P_b = A\left(P'_G - P'_L + P'_C\right) \tag{5.4}$$

   where

$$A = B_b R \begin{bmatrix} B'^{-1} \\ 0 \end{bmatrix}$$

   2. The branch power constraint $-\overline{P_{bj}} \le P_{bj} \le \overline{P_{bj}}$ $(j \in N_B)$ can be expressed as the following matrix formation:

$$-\overline{P_b} \le P_b \le \overline{P_b} \tag{5.5}$$

   3. Eq. (5.2) is substituted into Eq. (5.3) to obtain:

$$-\overline{P_b} \le A\left(P'_G - P'_L + P'_C\right) \le \overline{P_b} \tag{5.6}$$

After expanding and transposing, then it becomes:

$$A \times P'_{\mathrm{L}} - \overline{P_{\mathrm{b}}} \le A \times P'_{\mathrm{C}} + A \times P'_{\mathrm{G}} \le A \times P'_{\mathrm{L}} + \overline{P_{\mathrm{b}}} \tag{5.7}$$

Thus, it can be expressed as linear programming range constraints:

$$B_{\mathrm{b}}R\begin{bmatrix} B'^{-1} \\ 0 \end{bmatrix} \times P'_{\mathrm{L}} - \overline{P_{\mathrm{b}}} \le \left[B_{\mathrm{b}}R\begin{bmatrix} B'^{-1} \\ 0 \end{bmatrix} B_{\mathrm{b}}R\begin{bmatrix} B'^{-1} \\ 0 \end{bmatrix}\right]\begin{bmatrix} P'_{\mathrm{C}} \\ P'_{\mathrm{G}} \end{bmatrix} \le B_{\mathrm{b}}R\begin{bmatrix} B'^{-1} \\ 0 \end{bmatrix} \times P'_{\mathrm{L}} + \overline{P_{\mathrm{b}}} \tag{5.8}$$

(5) Bound constraints. Output constraints of generation bus and curtailment constraints of load bus can be processed as bound constraints.

$$\begin{bmatrix} 0 \\ \underline{P}_{\mathrm{G}} \end{bmatrix} \le \begin{bmatrix} P_{\mathrm{C}} \\ P_{\mathrm{G}} \end{bmatrix} \le \begin{bmatrix} P_{\mathrm{L}} \\ \overline{P}_{\mathrm{G}} \end{bmatrix} \tag{5.9}$$

(6) Specific expressions. Based on the previous processing results of the LCO model, combine Eqs. (5.1), (5.3), (5.8), and (5.9) to derive the following linear programming model:

$$\min \quad [C \;\; 0]\begin{bmatrix} P_{\mathrm{C}} \\ P_{\mathrm{G}} \end{bmatrix} \tag{5.10}$$

Equality constraints:

$$[1 \;\; 1]\begin{bmatrix} P_{\mathrm{C}} \\ P_{\mathrm{G}} \end{bmatrix} = 1 \times P_{\mathrm{L}} \tag{5.11}$$

Range constraints:

$$B_{\mathrm{b}}R\begin{bmatrix} B'^{-1} \\ 0 \end{bmatrix} \times P'_{\mathrm{L}} - \overline{P_{\mathrm{b}}} \le \left[B_{\mathrm{b}}R\begin{bmatrix} B'^{-1} \\ 0 \end{bmatrix} B_{\mathrm{b}}R\begin{bmatrix} B'^{-1} \\ 0 \end{bmatrix}\right]\begin{bmatrix} P'_{\mathrm{C}} \\ P'_{\mathrm{G}} \end{bmatrix} \le B_{\mathrm{b}}R\begin{bmatrix} B'^{-1} \\ 0 \end{bmatrix} \times P'_{\mathrm{L}} + \overline{P_{\mathrm{b}}} \tag{5.12}$$

Bound constraints:

$$\begin{bmatrix} 0 \\ \underline{P}_{\mathrm{G}} \end{bmatrix} \le \begin{bmatrix} P_{\mathrm{C}} \\ P_{\mathrm{G}} \end{bmatrix} \le \begin{bmatrix} P_{\mathrm{L}} \\ \overline{P}_{\mathrm{G}} \end{bmatrix} \tag{5.13}$$

5.3.5 The Derivation Process of LP Model for LSC

(1) Developing process of model. The linear programming model of maximizing LSC is similar to the linear programming model of minimizing LC, but only their variables are different. Therefore, the linear programming model of maximizing LSC can be derived similarly to that of processing the linear programming model of minimizing LC, according to the principles given in Table 5.2.

Table 5.2 Variable processing principles for linear programming model of maximizing LSC

Variables	Replace LC variable P_C with load variable P_L; set the original P_L as the upper limit of P_C.
Objective function	Replace LC variable P_C with load variable P_L.
Equality constraints	Delete LC variable P_C.
Range constraints	Delete LC variable P_C.
Bound constraints	Replace LC variable P_C with load variable P_L; replace load variable P_L with its upper limit.

(2) Specific expressions:

Objective function:

$$\min \begin{bmatrix} C & 0 \end{bmatrix} \begin{bmatrix} P_L \\ P_G \end{bmatrix} \tag{5.14}$$

Equality constraints:

$$\begin{bmatrix} 1 & 1 \end{bmatrix} \begin{bmatrix} P_L \\ P_G \end{bmatrix} = 1 \times \overline{P_L} \tag{5.15}$$

Range constraints:

$$B_b R \begin{bmatrix} B'^{-1} \\ 0 \end{bmatrix} \times \underline{P'_L} - \overline{P_b} \le \left[B_b R \begin{bmatrix} B'^{-1} \\ 0 \end{bmatrix} B_b R \begin{bmatrix} B'^{-1} \\ 0 \end{bmatrix} \right] \begin{bmatrix} P'_L \\ P'_G \end{bmatrix} \le B_b R \begin{bmatrix} B'^{-1} \\ 0 \end{bmatrix} \times \overline{P'_L} + \overline{P_b} \tag{5.16}$$

Bound constraints:

$$\begin{bmatrix} 0 \\ \underline{P}_G \end{bmatrix} \le \begin{bmatrix} P_L \\ P_G \end{bmatrix} \le \begin{bmatrix} \overline{P}_L \\ \overline{P}_G \end{bmatrix} \tag{5.17}$$

5.4 Calculation Procedure of Minimizing LCO

For a real urban power grid structure with several hundred buses, the data size is large and the format is stringent. To avoid tedious manual data input and possible errors, this chapter directly uses the Bonneville Power Administration's (BPA's) data format, adding two undefined fields in the BPA procedures for generator output lower limit in columns 81–85 and load bus weight in columns 86–90 of bus data card (B card). The calculation result is in form of text output that gives the optimal LC results in a specific system state. The basic calculation procedure is shown in the following section.

Therefore, the LCO is defined as a process of avoiding LCs, if possible, or minimizing the total LCs, if unavoidable, by rescheduling generation outputs and load transfer when the system is in a state of $N-k$.

Step 1: Input data, including the grid structure and the load level of all the nodes.

Step 2: Preprocess data to formulate the cost coefficient, coefficient matrix, right hand side items, range constraints, and variable constraints. Select system state (based on methods of state enumerating or Monte Carlo simulation), including the grid structure and the load level of all the nodes after $N-k$.
Step 3: Carry out optimization calculation by using LP mathematical programming system.
Step 4: Output optimization calculation results.

Details of these four steps are described in the following:

5.4.1 Step One: Input Data

Basic data of the network shall reflect the power grid topology, current load (or output) at each bus, and the upper and lower limits of generation bus power output. Based on the given grid structure and load level information, input calculation files (DAT files) are generated by directly using the BPA data format and field location to define the bus data card (B card), the line data card (L card), and the transformer data card (T card). Data formats of the three types of card are shown in Tables 5.3–5.5.

Table 5.3 Bus data card (B card)

Field	Format	Column	Description
B	A1	1	B indicating bus
SUBTYPE	A1	2	S indicating balance bus
BUSNAME	A8	7–14	Name of bus
KV	F4.0	15–18	Reference voltage at bus
PMW	F5.0	21–25	Current load at bus (also indicating the bus as load bus)
PGMAX	F4.0	39–42	Maximum active output at bus (also indicating the bus as generation bus)
PG	F5.0	43–47	Current output at bus
PGMIN	F5.0	81–85	Lower limit of active output at bus (added on the basis of BPA; default value of 0)
W	F5.5	86–90	Weight of load bus (added on the basis of BPA; default value of 1.0)

Table 5.4 Line data card (L card)

Field	Format	Column	Description
L	A1	1	L indicating line
BUSNAME1	A8	7–14	Bus name1
KV1	F4.0	15–18	Reference voltage at bus1 (kV)
BUSNAME2	A8	20–27	Bus name2
KV2	F4.0	28–31	Reference voltage at bus2 (kV)
LINEID	A1	32	Identification of parallel circuit, that is, circuit No.
CURRENTAMP	F4.0	34–37	Rated current of line, used as upper limit of branch capacity after being converted into capacity
XPU	F6.5	45–50	Per-unit reactance

Table 5.5 Transformer card (T card)

Field	Format	Column	Description
T	A1	1	T indicating transformer
BUSNAME1	A8	7–14	Bus name1
KV1	F4.0	15–18	Reference voltage at bus1 (kV)
BUSNAME2	A8	20–27	Bus name2
KV2	F4.0	28–31	Reference voltage at bus2 (kV)
TRANID	A1	32	Identification of parallel sets, that is, transformer No.
MVARATE	F4.0	34–37	Rated capacity of transformer (MVA)
XPU	F6.5	45–50	Per-unit reactance

5.4.2 Step Two: Data Preprocessing

Assign values respectively by editing subprograms to formulate the cost coefficient, coefficient matrix, and various constraints.

5.4.3 Step Three: Optimization Calculation

The LCO model can be formed as the following standardized linear programming model:

$$\begin{gathered}\min\ CX \\ \text{s.t. } \boldsymbol{AX} = \boldsymbol{b} \\ \underline{\boldsymbol{X}} \le \boldsymbol{X} \le \overline{\boldsymbol{X}}\end{gathered}$$

Therefore, the LCO calculation can be executed by the standardized linear programming procedure.

5.4.4 Step Four: Result Output

Calculation results consist of four parts: (1) basic data of network, (2) LCO result, (3) line load output results, and (4) transformer load output results. Their formats are presented in Tables 5.6–5.9.

Table 5.6 Basic data of network

Format	Description	Format	Description
A12	Network bus name	I4	Number of network branches
I4	Number of network buses	A26	Multiple of branch safety load
A12	Network branch name	F4.2	Branch overload coefficient

Table 5.7 Bus load curtailment output results

Format	Description	Format	Description
A8	Bus name	F10.3	Current power
A4	Bus type	F10.3	Corrected power
F10.5	Bus radian	F10.3	Bus curtailment amount
F10.5	Bus angle		

Table 5.8 Line load output results

Format	Description	Format	Description
A8	Bus name	F10.0	Safe current (A)
A8	Bus name	F10.0	Carrying capacity (A)
A5	Circuit No.	F10.0	Load rate (%)
F10.4	Reactance (per-unit value)		

Table 5.9 Transformer load output results

Format	Description	Format	Description
A8	Bus name	F10.0	Main transformer capacity (MVA)
A8	Bus name	F10.0	Load (MW)
A5	Transformer set No.	F10.0	Load rate (%)
F10.4	Reactance (per-unit value)		

5.5 Implementation of LCO

5.5.1 Verification of the Proposed Models and Calculation Methods

To verify the proposed mathematical model and algorithm based on the linear programming model of the LCO proposed under Section 5.3, this chapter first uses the 5-bus system to specifically implement the model, then uses a real urban power grid of several hundred buses for calculation.

5.5.1.1 Example of 5-bus system

Fig. 5.1 shows the 5-bus system, its bus No., and branch No. The branch direction is also defined due to the need of forming the bus branch incidence matrix. This section verifies and analyzes the LC in the three states of the test system.

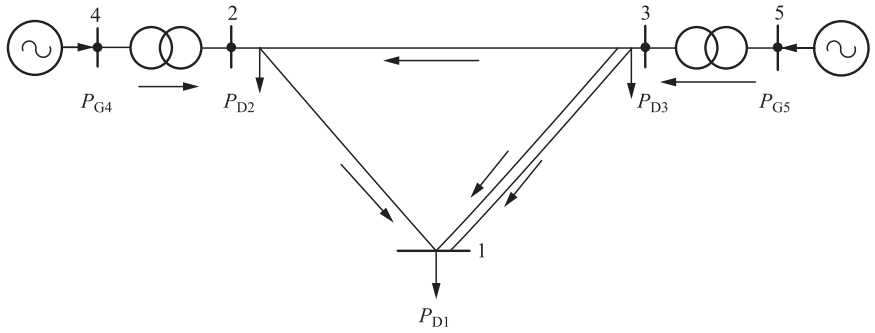

Fig. 5.1
5-Bus test system.

Tables 5.10–5.12 provide the basic data of the bus, line, and transformer in the 5-bus system and conducts per-unit calculation using SB = 100 MVA as the system reference values.

Table 5.10 Bus data

Bus	Voltage Class (kV)	Bus Type	Current Load or Output (MW) [lower limit, upper limit]	Per-Unit Value
1	110	Load bus	120	1.2
2	110	Load bus	60	0.6
3	110	Load bus	150	1.5
4	10	Output bus	100 [30, 140]	1.0 [0.3, 1.4]
5	10	Output bus (balance bus)	230 [200, 300]	2.3 [2.0, 3.0]

5.5.1.2 Concrete expression of the LP model

A certain "state 1" in the previous 5-bus test system is given: one circuit of the double-circuit line at bus 1 and bus 3 exits operation, as shown in Fig. 5.2.

To simplify, the weight coefficient of all loads is taken as 1; the upper limit of the line power is converted according to the safe current; the upper limit of transformer load is considered based on the transformation capacity.

Basic calculation procedure:

(1) Renumber the buses and branches of the 5-bus system, and balance bus (bus 5) is listed at the end.

Table 5.11 Line data

Name of Line	From	To	Conductor Model	Positive Sequence Reactance Per Unit Length (Ω/km)	Length of Line (km)	Safe Current (A)	Upper Limit of Power (MW)	Per-Unit Value of Upper Limit of Power	Reactance (Ω)	Per-Unit Value of Reactance
Line 1	1	2	LGJ-185	0.395	10	515	98.12	0.98	3.95	0.0326
Line 2	2	3	LGJ-240	0.388	10	610	116.2	1.16	3.88	0.0321
Line 3	1	3	LGJ-185	0.395	10	515	98.12	0.98	3.95	0.0326
Line 4	1	3	LGJ-185	0.395	10	515	98.12	0.98	3.95	0.0326

Table 5.12 Transformer data

Name of Transformer	From	To	Transformer Model	Transformer Capacity (MVA)	Per-Unit Value of Transformation Capacity Constraint	Impedance Voltage (%)	Per-Unit Value of Reactance
Transformer 5	4	2	SFZ8-150000/110	150	1.50	11.03	0.0735
Transformer 6	5	3	SFZ8-300000/110	300	3.00	14	0.0467

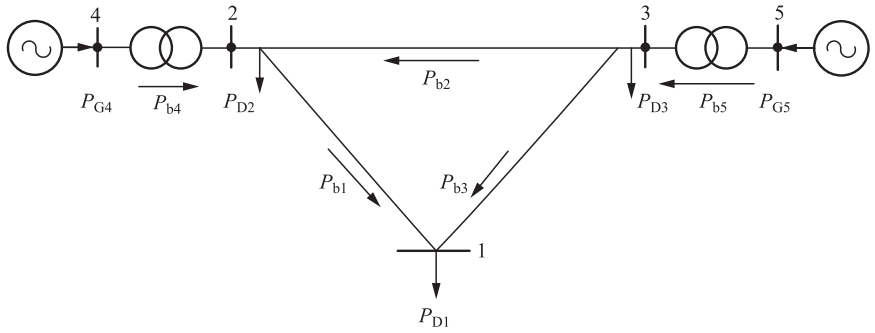

Fig. 5.2
5-Bus test system for state 1.

(2) Based on basic data and topology of the network, find the bus branch incidence matrix $\boldsymbol{R}$, branch admittance diagonal matrix $\boldsymbol{B}_{\mathrm{b}}$, bus admittance matrix $\boldsymbol{B}$, and bus admittance dimension reduction matrix $\mathbf{B}'$, respectively.

$$\boldsymbol{R}=\begin{bmatrix}-1 & 1 & 0 & 0 & 0\\ 0 & -1 & 1 & 0 & 0\\ -1 & 0 & 1 & 0 & 0\\ 0 & -1 & 0 & 1 & 0\\ 0 & 0 & -1 & 0 & 1\end{bmatrix}$$

$$\boldsymbol{B}_b=\begin{bmatrix}1/x_{12} & 0 & 0 & 0 & 0\\ 0 & 1/x_{23} & 0 & 0 & 0\\ 0 & 0 & 1/x_{13} & 0 & 0\\ 0 & 0 & 0 & 1/x_{24} & 0\\ 0 & 0 & 0 & 0 & 1/x_{35}\end{bmatrix}=\begin{bmatrix}30.675 & 0 & 0 & 0 & 0\\ 0 & 31.153 & 0 & 0 & 0\\ 0 & 0 & 30.675 & 0 & 0\\ 0 & 0 & 0 & 13.605 & 0\\ 0 & 0 & 0 & 0 & 21.413\end{bmatrix}$$

$$\boldsymbol{B}=\begin{bmatrix}61.350 & -30.675 & -30.675 & 0 & 0\\ -30.675 & 75.433 & -31.153 & -13.605 & 0\\ -30.675 & -31.153 & 83.241 & 0 & -21.413\\ 0 & -13.605 & 0 & 13.605 & 0\\ 0 & 0 & 0 & -21.413 & 21.413\end{bmatrix}$$

$$\boldsymbol{B}'=\begin{bmatrix}61.350 & -30.675 & -30.675 & 0\\ -30.675 & 75.433 & -31.153 & -13.605\\ -30.675 & -31.153 & 83.241 & 0\\ 0 & -13.605 & 0 & 13.605\end{bmatrix}$$

(3) Derive respectively $\boldsymbol{B}_{\mathrm{b}}\boldsymbol{R}, \boldsymbol{B}_{\mathrm{b}}\boldsymbol{R}\begin{bmatrix}\boldsymbol{B}'^{-1}\\ 0\end{bmatrix}$.

$$\boldsymbol{B}_{\mathrm{b}}\boldsymbol{R}=\begin{bmatrix}-30.675 & 30.675 & 0 & 0 & 0\\ 0 & -31.153 & 31.153 & 0 & 0\\ -30.675 & 0 & 30.675 & 0 & 0\\ 0 & -13.605 & 0 & 13.605 & 0\\ 0 & 0 & -21.413 & 0 & 21.413\end{bmatrix}$$

$$\boldsymbol{B}_{\mathrm{b}}\boldsymbol{R}\begin{bmatrix}\boldsymbol{B}'^{-1}\\ 0\end{bmatrix}=\begin{bmatrix}-0.3344 & 0.3282 & 0 & 0.3282\\ -0.3365 & -0.6698 & 0 & -0.6698\\ -0.6656 & -0.3313 & 0 & -0.3313\\ 0 & 0 & 0 & 1\\ -1 & -1 & -1 & -1\end{bmatrix}$$

(4) Based on the general expression of the LCO model from this section, combined with the specific form of the case, and note the fact that $P_{\mathrm{D4}}=P_{\mathrm{D5}}=P_{\mathrm{C4}}=P_{\mathrm{C5}}=0$, $P_{\mathrm{G1}}=P_{\mathrm{G2}}=P_{\mathrm{G3}}=0$ and balance bus $\theta 5=0$, the specific expression of linear programming can be found.

(5) Formulate the specific expression of linear programming for the LCO model, where there are five variables, one equality constraint, five range constraints, and five bound constraints.

$$\min \quad (C_1P_{\mathrm{C1}}+C_2P_{\mathrm{C2}}+C_3P_{\mathrm{C3}})$$

s.t. Equality constraint:

$$\begin{bmatrix}1 & 1 & 1 & 1 & 1\end{bmatrix}\begin{bmatrix}P_{\mathrm{C1}}\\ P_{\mathrm{C2}}\\ P_{\mathrm{C3}}\\ P_{\mathrm{G4}}\\ P_{\mathrm{G5}}\end{bmatrix}=3.3$$

Range constraints:

$$\begin{bmatrix}-1.1843\\ -1.9656\\ -1.9776\\ -1.5000\\ -6.3000\end{bmatrix}\leq\begin{bmatrix}-0.3344 & 0.3282 & 0 & 0.3282\\ -0.3365 & -0.6698 & 0 & -0.6698\\ -0.6656 & -0.3313 & 0 & -0.3313\\ 0 & 0 & 0 & 1\\ -1 & -1 & -1 & -1\end{bmatrix}\begin{bmatrix}P_{\mathrm{C1}}\\ P_{\mathrm{C2}}\\ P_{\mathrm{C3}}\\ P_{\mathrm{G4}}\end{bmatrix}\leq\begin{bmatrix}0.7757\\ 0.3544\\ -0.0176\\ 1.5000\\ -0.3000\end{bmatrix}$$

Bound constraints:

$$\begin{bmatrix}0\\ 0\\ 0\\ 0.3\\ 2.0\end{bmatrix}\leq\begin{bmatrix}P_{\mathrm{C1}}\\ P_{\mathrm{C2}}\\ P_{\mathrm{C3}}\\ P_{\mathrm{G4}}\\ P_{\mathrm{G5}}\end{bmatrix}\leq\begin{bmatrix}1.2\\ 0.6\\ 1.5\\ 1.4\\ 3.0\end{bmatrix}$$

5.5.1.3 Result of 5-bus system for state 1

According to the linear programming model of optimizing 5-bus system LC, use the linear programming STYRP1.10 software package developed in China to calculate LCO for Status 1.

STYRP1.10 solves the linear programming problem by using a modified simplex method. It only requires a general form of linear programming, and the program will automatically process range and bound constraints. The specific input data requirements and formats are described in the following section:

(1) The objective function, equality constraints, and inequality constraints are written into the coefficient *A* matrix (as variable *C* in the program), which designates the location of objective function by IOB = 1; the right hand side constraint variable is *D*; set the right hand side constraint of the objective function to 0.
(2) The type of equation is represented with *ITYPE* (−1 indicates less than or equal to, or maximizing; 1 indicates more than or equal to, or minimizing; 0 indicates equal to).
(3) The bound constraints of linear programming are represented with variable IBD (boundary index) and BD (boundary value): if the *n*th variable has bound constraints, then *n* indicates upper bound constraint and *–n* indicates lower bound constraint; BD is the specific upper and lower boundary values of each variable.
Thus, according to the expressions for two linear programming models of state 1 of 5-bus system discussed previously, the input variables *A*, *D*, *ITYPE*, *IBD*, and *BD* from the STYRP1.10 solution are expressed as follows:
(4) Input variable coefficient for the linear programming software package:

$$A = \begin{bmatrix} 1 & 1 & 1 & 0 & 0 \\ 1 & 1 & 1 & 1 & 1 \\ -0.3344 & 0.3282 & 0 & 0.3282 & 0 \\ -0.3365 & -0.6698 & 0 & 0.6698 & 0 \\ -0.6656 & -0.3313 & 0 & -0.3313 & 0 \\ 0 & 0 & 0 & 1 & 0 \\ -1 & -1 & -1 & -1 & 0 \end{bmatrix},$$

$$ITYPE = \begin{bmatrix} 1 \\ 0 \\ -1 \\ -1 \\ -1 \\ -1 \\ -1 \\ 1 \\ 1 \\ 1 \\ 1 \\ 1 \end{bmatrix}, \quad D = \begin{bmatrix} 0 \\ 3.3 \\ -1.1843 \\ -1.9656 \\ -1.9776 \\ -1.5000 \\ -6.3000 \\ 0.7757 \\ 0.3544 \\ -0.0176 \\ 1.5000 \\ -0.3000 \end{bmatrix}, \quad IBD = \begin{bmatrix} 1 \\ 2 \\ 3 \\ -4 \\ 4 \\ -5 \\ 5 \end{bmatrix}, \quad BD = \begin{bmatrix} 1.2 \\ 0.6 \\ 1.5 \\ 0.3 \\ 1.4 \\ 2.0 \\ 3.0 \end{bmatrix}$$

5.5.1.4 Results of 5-bus system for three states

The results of LCO are identical to that of state 1 of the 5-bus system, which are solved by a software package for the linear programming calculation.

(1) LCO results for state 1. One of the two circuit lines between bus 1 and bus 3 exits operation. The LCO results for state 1 are shown in Table 5.13.

Table 5.13 Result of LCO for State 1

Result of load curtailment optimization				
Bus	**Type**	**Current power flow distribution (MW)**	***N*-1 state power flow distribution (MW)**	**Curtailment (MW)**
1	Load	120	120	0
2	Load	60	60	0
3	Load	150	150	0
4	Output	100	100	0
5	Balance	230	230	0
Result of line and transformer load rate in load curtailment optimization				
Bus	**Bus**	**Safety current (A)**	**Carrying current (A)**	**Load rate (%)**
3	1	515	350	68
3	2	610	70	12
2	1	515	280	54
Bus	**Bus**	**Main transformer capacity (MVA)**	**Power (MW)**	**Load rate (%)**
5	3	300	230	77
4	2	150	100	67

(2) LCO results for state 2: the one-circuit line between bus 1 and bus 3, and the line between bus 2 and bus 3 exit operation. The result of LCO for state 2 is shown in Table 5.14; the diagram of status 2 and 3 of 5-bus test system is shown in Fig. 5.3.

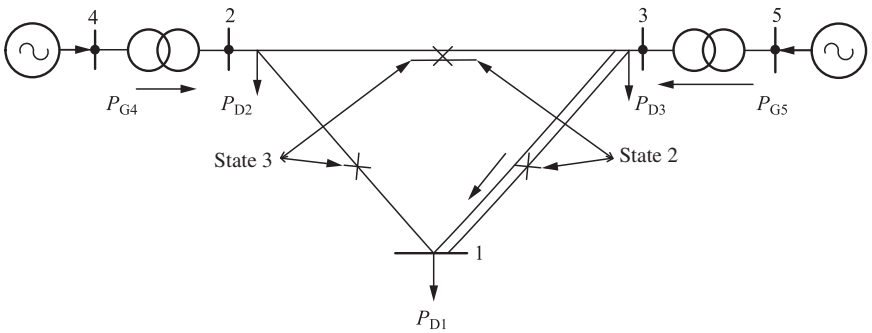

Fig. 5.3
5-Bus test system for state 2 and 3.

Table 5.14 Results of LCO for State 2

Result of load curtailment optimization				
Bus	**Type**	**Current power flow distribution (MW)**	***N*-2 state power flow distribution (MW)**	**Curtailment (MW)**
1	Load	120	120	0
2	Load	60	60	0
3	Load	150	150	0
4	Output	100	100	0
5	Balance	230	230	0
Result of line and transformer load rate in load curtailment optimization				
Bus	**Bus**	**Safety current (A)**	**Carrying current (A)**	**Load rate (%)**
3	1	515	420	82
2	1	515	210	34
Bus	**Bus**	**Main transformer capacity (MVA)**	**Power (MW)**	**Load rate (%)**
5	3	300	230	77
4	2	150	100	67

(3) LCO results for state 3: the one-circuit line between bus 1 and bus 3, and the line between bus 1 and bus 2 exit operation. The result of LCO for state 3 is shown in Table 5.15.

Table 5.15 results of LCO for State 3

Result of load curtailment optimization				
Bus	**Type**	**Current power flow distribution (MW)**	***N*-2 state power flow distribution (MW)**	**Curtailment (MW)**
1	Load	120	98.121	21.879
2	Load	60	60	0
3	Load	150	150	0
4	Output	100	100	0
5	Balance	230	208.121	−21.879
Result of line and transformer load rate in load curtailment optimization				
Bus	**Bus**	**Safety current (A)**	**Carrying current (A)**	**Load rate (%)**
3	1	515	515	100
3	2	610	−210	34
Bus	**Bus**	**Main transformer capacity (MVA)**	**Power (MW)**	**Load rate (%)**
5	3	300	208	69
4	2	150	100	67

The analysis and calculation of the three states of the 5-bus system reveals: the result of LCO for system states 1 and 2 is 0, that is, there is no need for LC; for state 3, curtailment of 21.879 MW at bus 1 and 21.879 MW at balance bus 5 are needed, in which the line load rate between buses 1 and 3 is up to 100%, that is, the LC is minimized when the load at bus 1 is curtailed until the line between buses 1 and 3 is at full rate without violation.

Meanwhile, the static security analysis of the three states show only that state 3 cannot pass and the line load rate between buses 1 and 3 reaches 122%. This also verifies the conclusion that the LCO model supplements improve the static security analysis.

5.5.2 Basic Conditions of a Real-Scale System

In an actual case, there are 74 buses and 91 branches, and 0.90 is selected as the branch safety load ratio.

Fig. 5.4 shows the geographical single line diagram of 110 kV or above grid in an actual case. The main grid power supply consists of a 500 kV XIJIANG substation and two unified dispatched power plants, FUNENG and XINTIAN, with a total capacity of 2760 MVA; local power plants include HENGYI, JIANGNAN, CHANGHAI, SHAKOU, HUANBAO, FOSHAND, and FOSHANE with a total installed capacity of 656 MW, but in summer's heavy load mode, the total output is 484 MW. The main network is constructed by interconnecting six 220 kV substations, such as ZHUYUAN, ZIDONG, NANHAI, HONGXING, FENGJIANG, and FOSHAN, and power supply points (FOSHAN and HONGXING substations originally formed a ring through TENGSHA and JI-AN) with a total capacity of 2580 MVA. Each 220 kV substation radially supplies power to 110 kV HV distribution network substations. The network data are given in Tables 5.16–5.18.

5.5.3 Results of the Real-Scale System

Different postfault operating states and different load levels at each substation in a zone are given. The grid risk index data by circular call of the optimization calculation procedure are given. The input/output data for a certain state are presented in Section 5.7.

According to project requirements, the weights at each load point are equal (default value of 1.0 used for column 86–90), the upper limit of branch capacity is 0.9, the upper limit of local plant output is given a conservative value, and its lower limit is taken as default value of 0. Therefore, this model directly uses the BPA data from FOSHAN Power Supply Bureau for its calculation. First, simulate a certain system state through Monte Carlo, then conduct static safety analysis by scanning calculation; for states that cannot pass, modify the current load of BPA by adding "." before each data row. The output result for each state are written out using the field in the result of LCO.

For this particular state, the data output consists of four components:

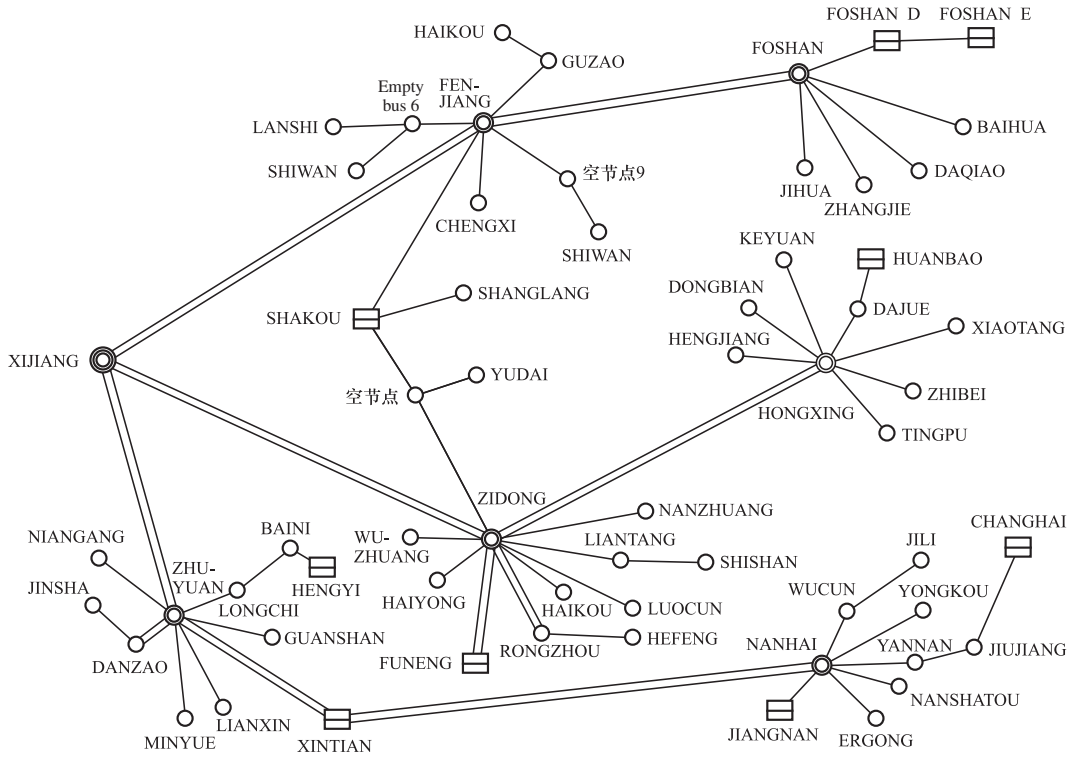

Fig. 5.4
Geographical single line diagram of a practical grid with 110 kV and above.

Table 5.16 Power supply for main grid in XIJIANG zone

Power Supply for Main Grid	Description	Capacity (MVA)
Substation	XIJIANG Substation	1000 × 2
Unified dispatching power plant	FUNENG Power Plant	(120 + 60) × 2
	XINTIAN Power Plant	200 × 2

(1) Basic data of the network: including 74 buses, 91 branches, and a branch safety load ratio of 0.9. Thus, the linear programming calculation scale for this state can also be derived: 59 variables (number of load buses + number of generation buses, excluding 15 link buses); 1 equality constraint, that is, grid power balance equation; 91 (the number of branches) range constraints as upper and lower limit constraints of the branch power; and 59 bound constraints.

(2) LCO output result: including rated voltage, radian value, current power, corrected power, and LC at each bus; LC is needed at 4 load buses with a total curtailment amount of 62.242 MW, detail of which is 15.403 MW at XIAOTANG-1, 27.747 MW at DALAN-1, 13.592 MW at WUCUN-1, and 5.5 MW at ZHUYUAN-1. At the same time, generators SHAKOU-1, SHAKOU-2, and SHAKOU-3 reduces output by 65, 54.645, and 80 MW, respectively, as shown in Table 5.19.

Table 5.17 Local power plant for grid in XIJIANG zone

Power Plant	Installed Capacity (MW)	Type	Summer Heavy Load Mode	Summer Light Load Mode
FOSHAN-D Plant	50	Coal-fired	0	0
FOSHAN-E Plant	50	Coal-fired	0	0
SHAKOU Power Plant	280(=95 × 2+90)	Gas-steam combined cycle	230	200
JIANGNAN Power Plant	100(=25 × 4)	Coal-fired	90	70
CHANGHAI Power Plant	50	Coal-fired	48	40
HUANBAO Power Plant	6	Waste burning	6	6
HENGYI Power Plant	120(=60 × 2)	Coal-fired	110	90

Note: Under the influence of factors such as constant rise in the primary energy price, the motivation of local plants to start operating has been declining and the situation of peak power generation of local plants is not optimistic. Therefore, the typical start-up mode of local plants shall be determined in a conservative way. The overall output of local plants on the FOSHAN grid in summer heavy load in 2008 is significantly less than the maximum output of local plants in 2007.

Table 5.18 220 kV Main network substations in XIJIANG zone

Name of Substation	Voltage Level (kV)	Total Capacity (MVA)
ZIDONG Substation	220	540(=3 × 180)
HONGXING Substation	220	300(=2 × 150)
ZHUYUAN Substation	220	480(=2 × 240)
NANHAI Substation	220	300(=2 × 150)
FENGJIANG Substation	220	480(=2 × 240)
FOSHAN Substation	220	480(=2 × 240)

Table 5.19 List of real case LC and generator adjustment for a certain state

Bus	Type	Rated Voltage (kV)	Angle	Current Power (MW)	Corrected Power (MW)	Curtailment Amount (MW)
XIAOTANG-1	Load	110	−15.27	114	98.597	15.403
DALAN-1	Load	110	−14.54	56.8	29.053	27.747
WUCUN-1	Load	110	−12.07	30.3	16.708	13.592
ZHUYUAN-1	Load	110	−12.01	42	36.5	5.5
SHAKOU-1	Output	110	−10.03	85	20	65
SHAKOU-2	Output	110	−12.5	85	30.355	54.645
SHAKOU-3	Output	110	−13.82	85	5	80

(3) Line load output result: including name of bus at both ends, number of circuits, reactance (per-unit value), safety current, carrying current, and load capacity; thus, the line of HONGXING-1 to XIAOTANG-1 and NANHAI-1 to WUCUN-1 has reached 90% of its upper limit, as shown in Table 5.20.

Table 5.20 List of lines whose carrying current is up to upper limit after LCO for a certain state of the real case

Bus		Circuit No.	Reactance (Per-Unit Value)	Safe Current (A)	Carrying Current (A)	Load Rate (%)
HONGXING-1	XIAOTANG-1		0.0211	575	517	90
NANHAI-1	WUCUN-1		0.0387	494	445	90

(4) Transformer load output result: including name of bus at both ends, parallel No., reactance (per-unit value), main transformer capacity, and power and load capacity; thus, 2# transformer at ZIDONG Substation, 1# and 2# transformers at ZHUYUAN Substation, and 1# transformer at HONGXING Substation have reached 90% of the upper limit, as shown in Table 5.21.

Table 5.21 List of transformers whose load is up to upper limit after LCO for a certain state of the real case

Bus		Parallel No.	Reactance (per-unit value)	Main Transformer Capacity (MVA)	Power (MW)	Load rate (%)
ZIDONG-2	ZIDONG-1	2	0.0727	180	162	90
ZHUYUAN-2	ZHUYUAN-1	1	0.0583	240	216	90
ZHUYUAN-2	ZHUYUAN-1	2	0.0583	240	216	90
HONGXING-2	HONGXING-1	1	0.0947	150	135	90
HONGXING-2	HONGXING-1	2	0.0953	150	134	89

This chapter sets load weights as equal values in both the 5-bus test system and the real 74 bus system. However, in actual operation of an urban grid, the "weight" of some important users is indeed high, and even the load cannot be curtailed in any system state. In such a case, the weight

of the load can be taken as a higher value, or the LC at this point is directly set as zero ($P_{Ci}=0$); the corresponding safety load multiple of the power supply line and transformer shall be increased accordingly.

5.6 Calculation Procedure of Maximizing LSC

(1) Input data: Data input is the basis of the LSC calculation, including the network connection relationship, type and output of bus, load constraints, line and transformer capacity constraints, and impedance parameters.
(2) Formulate the linear programming model: Generate coefficient matrix $\boldsymbol{A}$ and $\boldsymbol{C}^{\mathrm{T}}$ of the linear programming model to formulate the linear programming model, where $\boldsymbol{A}=\boldsymbol{B}_{\mathrm{L}}\times \boldsymbol{R}\times\begin{bmatrix}\boldsymbol{B}^{-1}\\0\end{bmatrix},\boldsymbol{C}^{\mathrm{T}}$, where $\boldsymbol{C}^{\mathrm{T}}$ is a [0, 1] vector; $c_i=1$ for load-type buses; and $c_i=0$ for other buses.
(3) Execute the linear programming calculation. Solve the linear programming problem using the simplex method.
(4) Output maximum LSC index of the network: output the solution to the linear programming problem, including the LSC indicator, active power at buses in the network, active power flow at branches (line and transformer), and load rate.
(5) Verify the method using the traditional power flow algorithm (LF). Specifically, substitute each bus load obtained from Step (4) as known conditions into the traditional AC power flow calculation model, then calculate power flow.

5.7 Implementation for Maximizing LSC

This section uses actual network data for a certain region in China as an example to demonstrate the rationality and accuracy of assessing the maximum LSC of an urban grid with a linear programming model.

5.7.1 Description of the Test System

This test system has a total of 35 buses, including 3 output buses, 16 load buses, and 16 link buses (including buses without output or load and neutral points of a three-circuit transformer); 36 branches, including 8 110 kV lines, 8 three-circuit transformers, and 4 two-circuit transformers. In the network, the total 330 kV transformation capacity is 300 MVA, and total 110 kV transformation capacity is 349 MVA. Set the limit of power at each branch to 95% of its

rated capacity. The system has $35-1=34$ variables and 36 range constraints. Network relations are shown in Fig. 5.5.

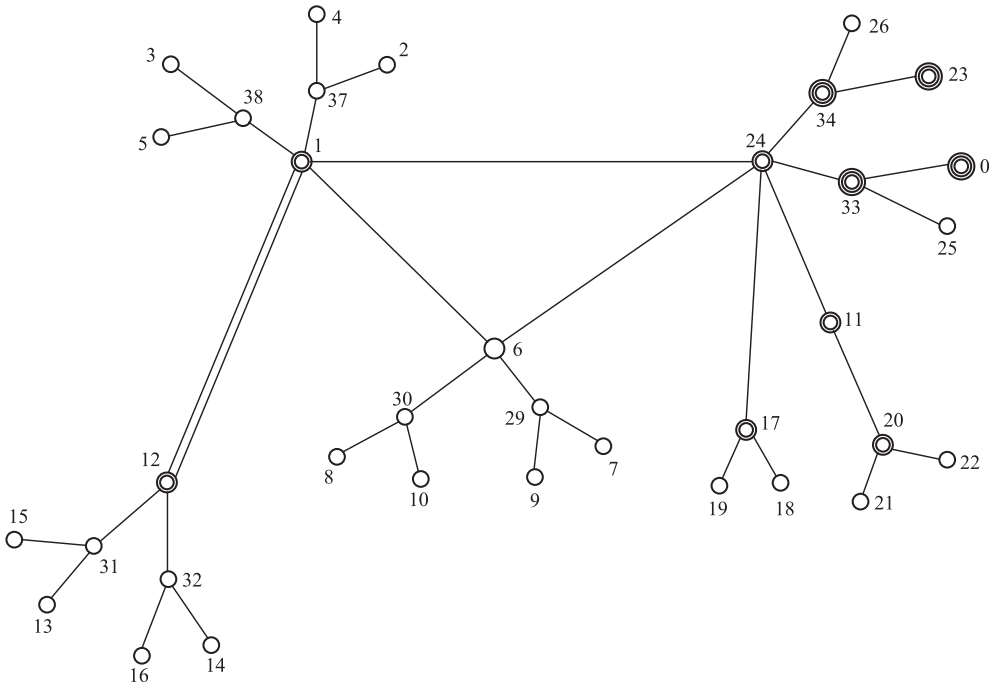

Fig. 5.5
Network relations.

5.7.2 Results Analysis

The linear programming model is used to obtain maximum LSC of 315.55 MW for this network, 200 MW of which is from 330 kV power substations and 115.55 MW from 110 kV network power supply sources. The average load rate of 110 kV transformers is 90.4%. The distribution of system power flow is shown in Fig. 5.6.

Substitute the active load and output at each bus from the linear programming calculation into a traditional power flow calculation model, and calculate the power flow to obtain such results as shown in Fig. 5.7. No power violation occurs at any of the branches; the load rate of 75% transformers has reached more than 95%, and a very small load added to any load bus will lead to power violation at some branches. Thus, the system's maximum LSC is deemed as the system's total load in this operating mode, which is 315.55 MW.

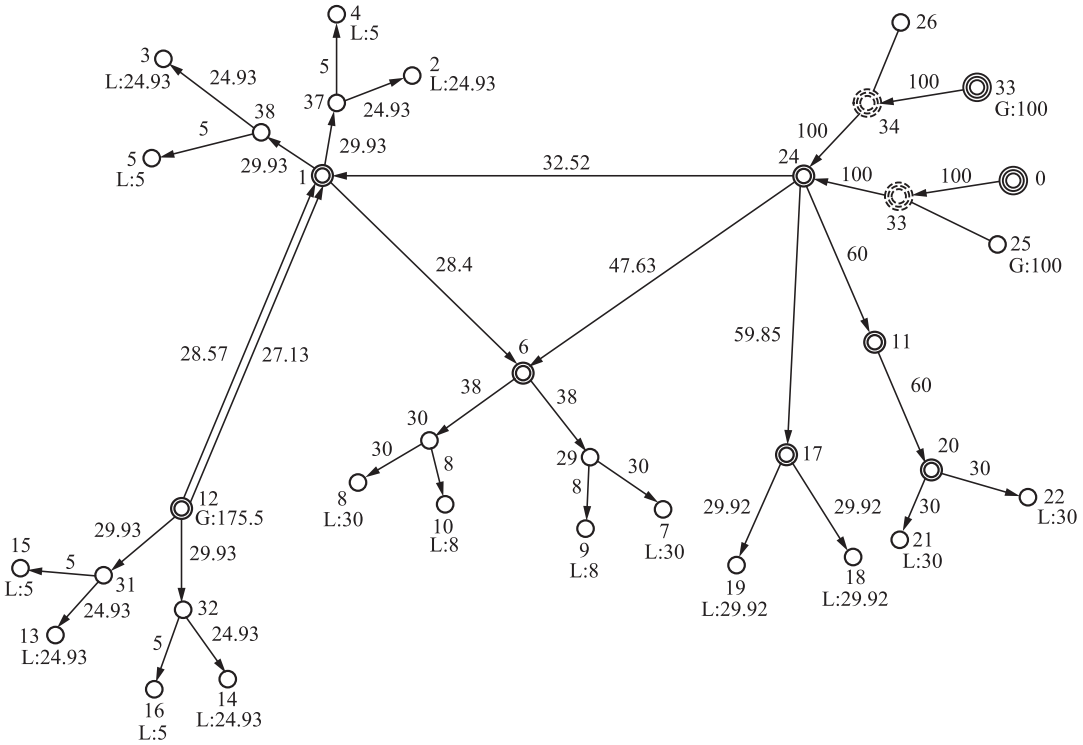

Fig. 5.6
Power flow distribution result obtained from linear programming model.

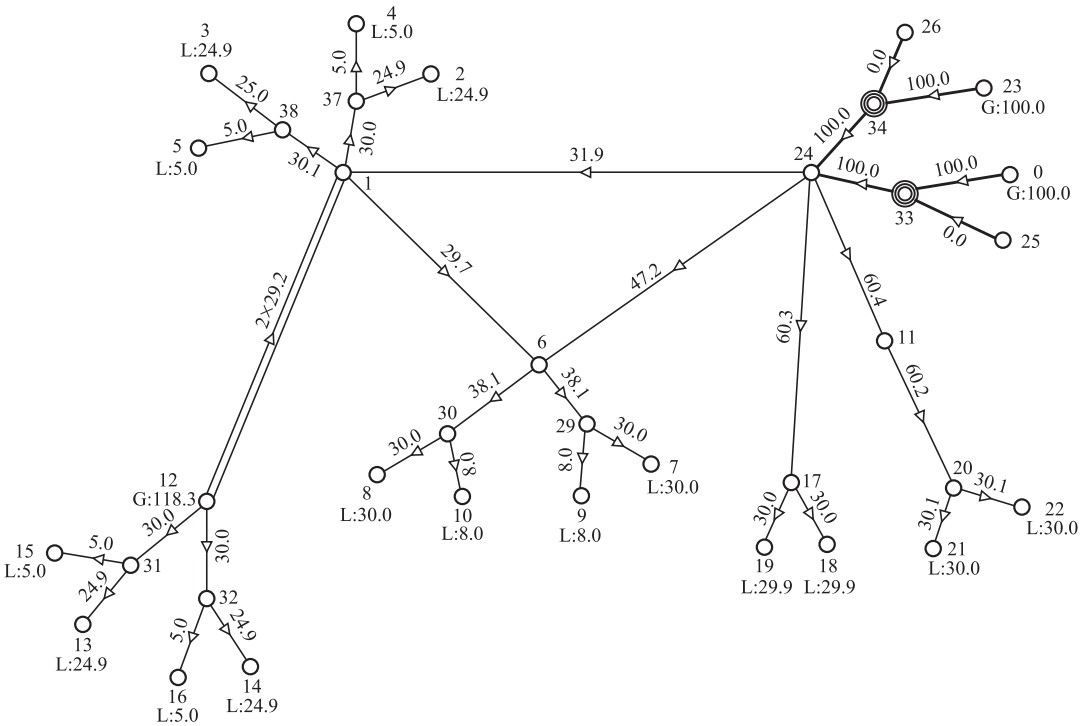

Fig. 5.7
BPA power flow calculation result.

From the previous optimization calculation with the linear programming model and the traditional power flow calculation, the bus power is obtained, as shown in Table 5.22. Active power flow in line and its load rate are shown in Table 5.23. Active power flow in transformer and its load rate are shown in Table 5.24.

Table 5.22 Bus power (MW)

Bus	Bus Type	Lower Limit of Bus Power	Upper Limit of Bus Power	LP Bus Power	LF Bus Power
23	Output bus	100	150	100	100
0	Output bus	100	150	100	100
12	Output bus	0	200	115.55	118.3
2	Load bus	10	30	24.925	24.925
3	Load bus	5	30	24.925	24.925
4	Load bus	5	30	5	5
5	Load bus	5	30	5	5
7	Load bus	5	30	30	30
8	Load bus	5	30	30	30
9	Load bus	5	30	8	8
10	Load bus	5	30	8	8
13	Load bus	5	30	24.925	24.925
14	Load bus	5	30	24.925	24.925
15	Load bus	5	30	5	5
16	Load bus	5	30	5	5
18	Load bus	5	31.5	29.925	29.925
19	Load bus	5	31.5	29.925	29.925
21	Load bus	5	30	30	30
22	Load bus	5	30	30	30

Table 5.23 Active power flow and load rate on lines

From	To	Parallel No.	LP Power Flow (MW)	LP Load Rate (%)	LF Power Flow (MW)	LF Load Rate (%)
11	20	0	60	49.383	60.2	49.55
11	24	0	−60	47.815	−60.4	48.13
24	17	0	59.85	47.696	60.3	48.05
6	24	0	−47.63	37.953	−47.2	37.61
12	1	1	28.572	27.854	29.2	28.47
12	1	2	28.572	27.854	29.2	28.47
1	6	0	28.375	27.662	29.7	28.95
24	1	0	32.525	25.92	31.9	25.42

Table 5.24 Active power flow and load rate of transformer

Bus at HV Side	Bus at MV Side	Bus at LV Side	LP Power Flow (MW)	LP Load Rate (%)	LF Power Flow (MW)	LF Load Rate (%)
1	2	4	29.92	95	30	95.25
1	3	5	29.92	95	30.1	95.57
12	14	16	29.92	95	30	95.25
12	13	15	29.92	95	30	95.25
6	7	9	38	95	38.1	95.25
6	8	10	38	95	38.1	95.25
23	24	26	100	66.67	100	66.67
0	24	25	100	66.67	100	66.67
Note: The previous data apply to three-phase transformers and the following data apply to two-phase transformers.						
17		18	29.92	95	30	95.25
17		19	29.92	95	30	95.25
20		21	30	75	30.1	75.25
20		22	30	75	30.1	75.25

5.8 Conclusion

In this chapter, based on the DC power flow, the load optimization models are developed, including the minimization of LC under the $N-k$ condition and the maximization of the LSC under a given network. The two models are the supplement and improvement to traditional static security analysis.

(1) LCO model: by setting the objective function of minimizing bus LC, this model can give an optimal program for LCO. The model proposed uses several variables (vector of bus load and power generation) for linear programming model and gives constraints of equality, range, and bound respectively in the form of block matrix. The equality constraints can be considered as a special form of range constraints. The linear programming calculation can give the adjusted value of generation output and optimal value of load at each bus.

(2) LSC model: by setting the objective function of maximizing bus load, the maximum LSC (maximum load level) of the power grid can be analyzed. The model can accurately give the network's maximum LSC indicator without repeating power flow calculations. To evaluate the power supply level of the network, compared with the capacity-load ratio that reflects the macro LSC of urban grid, it is more rational, accurate, and effective to use this model to calculate the maximum LSC index of the network. Based on the calculation model of the maximum LSC index of urban grid, the $N-1$ check of the network can also be conducted. The extent of the network's LSC decline caused by disconnection fault of a single line can also be estimated with a quantitative index.

CHAPTER 6

Discrete Optimization for Reactive Power Planning

Chapter Outline

Mathematical Models and Algorithms for Power System Optimization. https://doi.org/10.1016/B978-0-12-813231-9.00006-6

6.1 Introduction

Reactive power optimization in power system operation is an important issue that directly affects both the voltage quality of the system and the economic operation of the power grid. Because system voltage is related to both the reactive and active power distribution of the power grid, under the condition of meeting the normal operation of the power system, the objective function of reactive power optimization can be the minimum investment of the new reactive power equipment or it can be the minimum active power losses of the system.

Generally, reactive compensation equipment, such as capacitors and other volt-ampere reactive (VAR) sources, have been installed in substations of power systems. To meet the need of present load and future system development, new capacitors should perhaps be installed. Therefore, configuration planning of the new VAR devices is required. When planning a new capacitor, it is necessary not only to consider the existing capacitors but also to consider the discrete characteristics of the capacitor bank. With the expansion of the system, VAR optimization issues involve not only massive integer variables but also nonlinear constraints of a large-scale power system.

VAR optimization can be attributed to a nonlinear mathematical programming problem. Considering the discrete characteristics of the number of transformer taps and capacitor banks, it becomes a more complicated mixed-integer nonlinear programming (MINLP) problem. Therefore, with regard to VAR optimization for a practical-scale power system, dealing with dozens or even hundreds of integer variables is required.

This chapter studies the discrete VAR optimization of the power system and power distribution system in detail, and proposes various models and algorithms for discrete reactive power optimization.

This chapter deals with the problem of reactive power optimization as a mixed-integer, nonlinear problem. The current algorithms for exact-integer programming optimization have

not yet been able to solve large-scale mixed-integer nonlinear problems for power systems. When the number of adjustable tap ratios and adjustable capacitor banks in the power system are large, the method of processing the tap position and number of capacitor banks as continuous variables and then rounding the transformer does not always provide a discrete feasible solution. It is very difficult to directly apply the discrete optimization method to the VAR optimization of the power system. Therefore, the approximate algorithm is one of the approaches to solve the discrete VAR optimization problem.

The algorithm here employs an excellent approximation method for solving linear mixed-integer programming (MIP) problems, because an exact optimal solution of MIP problems can hardly be obtained. Furthermore, to solve a nonlinear MIP problem, the algorithm exploits the concept of recursive LP so that it is capable of obtaining an AC load flow solution to the VAR planning problem. The program can easily be developed based on this algorithm, by incorporating the options of existing LP software.

This chapter combines the expert rules, fuzzy mathematical concepts, and genetic algorithms (GA) with traditional optimization methods to improve the possibility of obtaining discrete solutions. To verify the validity and reliability of the algorithm, the corresponding verification procedures were developed, and the numerical calculations were performed using the actual-scale power system. The results of a practical test system show that the proposed algorithm can effectively solve the discrete optimization VAR problems of power systems and power distribution systems in practical scale.

6.1.1 Practical Method for Discrete VAR Optimization

The difference of constraints are the key issues of various VAR optimization models, which are identified as being with and without constraint functions, and with or without integer variables. The main practical methods currently used for VAR optimization of a power system could be described as follows:

(1) Power flow method: The number of capacitor banks and transformer tap positions are taken as constant values that are manually adjusted by one's experience, then repeatedly executed until the feasible solution is obtained. Due to the large number of capacitors and transformers, the wide adjustable range, and rapid increase in the number of adjustment solutions, along with the increase in the number of devices, it is impossible to consider all feasible solutions, which can only be adjusted according to engineering experience. It is difficult to guarantee that the schemes made in this way are optimal or superior by using the so-called current adjustment method to select the system's reactive operation or planning scheme. Normally, such a method can provide a feasible solution at best at the cost of a great deal of labor power and time.
For example, in a real power supply system with 40 nodes, 2 generators, and 2 sets of adjustable transformers, experienced system engineers must design more than 10 cases of

adjustments, then calculate power flow more than 10 times, which will map the grid loss curve to obtain the tap ratio number of adjustable transformers. For a real system containing hundreds of nodes, the design of a calculation case itself is hard work.

(2) Continuous VAR optimization method: This method uses the continuous reactive power optimization method to obtain a continuous optimal solution, then truncates the nearest solution to the integer solution. The method is applicable when there are fewer discrete variables, and the upper and lower limit values of the discrete variables are close. For a real system with several hundred nodes, when there are many discrete variables and the upper and lower limit values of the discrete variables are distant, the solution obtained by simply truncating may not be feasible. It is even more difficult to obtain a suboptimal solution. For radiator-like distribution networks, the tap position of the transformer must be used as a discrete variable. When the number of discrete variables (>50) is high, the truncated solution after continuous optimization generally does not guarantee a discrete feasible solution. Truncation solutions can sometimes lead to an increase in the objective function and may also lead to inequality constraints.
Another approach is to use a truncated solution fixed by the continuous optimization method and to use the continuous optimization method to optimize continuous variables. This approach will increase the workload of optimization calculations, which cannot assure that the obtained discrete solution is feasible either.
Whether the optimized truncated solution is used as the final solution, or the optimized truncated solution is fixed and then the continuous variable is reoptimized, neither the discrete feasible solution nor the discrete optimal solution can be obtained.

(3) Discrete VAR optimization method: This method can directly lead to discrete solutions for transformer tap position and capacitor bank number, for example, in a real power supply system with 40 nodes, 2 units of generators, and 2 units of adjustable transformers, as long as the bound of all variables are given. For systems of such small scale, there are already solutions in some international literature. As long as there are solutions, it is always possible to find the discrete optimal solution. However, for the large-scale real systems containing hundreds of nodes, these methods cannot assure that discrete solutions can be obtained. As the existing algorithms cannot assure obtaining a discrete feasible solution or optimal solution, in this chapter, some explorations are made in this respect to find the discrete feasible solution of a large-scale real system.

6.1.2 Overview of This Chapter

(1) Single-state discrete VAR optimization: In Section 6.3 of this chapter, the discrete reactive power optimization algorithm is studied under the single operating mode of the power system, namely, the study of the single-state algorithm in which only the number of capacitor banks is treated as a discrete variable. The algorithm uses an approximate algorithm for solving mixed-integer LP to deal with the reactive-optimized, mixed-integer linear programming (MILP) problem and approximates the nonlinear problem of reactive

power optimization through the loop iteration of LP. To effectively reduce the investment cost of reactive power devices, an improved algorithm that simultaneously changes two integers is also proposed.

(2) Multistate discrete VAR optimization: Because the operating mode of the system is constantly changing, reactive power planning under specific operating modes is generally difficult to meet the needs of multiple operating modes. Therefore, it is necessary to study the reactive power optimization that can comprehensively consider the various operating modes of the system, that is, to study VAR optimization under a multistate condition. Section 6.4 of this chapter proposes a multistate reactive power optimization model and decomposition coordination algorithm with a diagonal block shape. This algorithm decomposes and coordinates each state with the amount of reactive equipment associated with each state as a coupling quantity to achieve overall optimization. This algorithm considers the influence of reactive power equipment quantity on each state comprehensively, without considering optimization of a single state, and pursues overall state optimality, so as to make the minimal total investment.

(3) Expert rule-based discrete VAR optimization: Because the optimization algorithm generally depends on the initial value, to obtain a better initial value, the concept of the expert rule is introduced in Section 6.5 of this chapter to obtain the initial value of the integer, so that the proposed algorithm can effectively find a better discrete solution. The expert rule given in this chapter determines the rounded-off direction of the discrete variable based on the ambiguity of the integer initial value, reducing the possibility of the voltage over limits, after changing the ratio grade and the number of reactive equipment groups, saving calculation time and greatly improving the possibility of getting a better integer-feasible solution.

(4) GA-based discrete reactive power optimization: Because the traditional optimization algorithm cannot ensure the global optimal solution, and the GA has the ability to obtain a global optimal solution, in the discrete feasible solution obtained in Section 6.6 of this chapter, the GA based on a natural biological mechanism is used to stochastically modify the integer-feasible solution so as to arrive at a new solution. The use of GA techniques can generate different stochastic initial values, which may lead to different feasible solutions. Compared with traditional optimization algorithms that can only give a unique feasible solution, GA techniques provide the possibility to filter better feasible solutions.

6.2 Basic Ideas of Forming an Optimization Model

6.2.1 Way of Processing Discreteness

Reactive power compensation equipment in a power system, such as capacitors and reactors, are switched in groups, whereas the tap of a transformer is adjusted by steps. Thus, the number of capacitors and reactors, and taps of a transformer shall be expressed as integer variables rather than continuous variables.

In this chapter, a nonlinear integer programming model is used to represent the discrete reactive power optimization, and discrete variables are used to represent tap position and the number of capacitor banks and reactors. Moreover, a linear integer programming model is used in iteration calculation to represent discrete reactive power optimization. The relationship between objective function values for an MIP problem is as follows: the objective function value upon integer constraint slack is the lower limit of the problem; the objective function value upon integer variable rounded-off is the upper limit of the problem; and the objective function value obtained with an integer programming method falls between the two limits. Thus, an approximation algorithm based on solving a linear integer programming problem is designed to search for a discrete linear optimization solution around a continuous linear optimization solution. The basic idea of the algorithm is to slack integer variable constraint in the linear integer programming problem, which uses LP method to obtain the lower limit of objective function of the problem, so as to form the exploration space of integer solution based on the slack solution, and to obtain a discrete solution within a calculation procedure of limited steps. In other words, the basic idea of the algorithm is to transform complicated discrete optimization into an LP problem, so as to obtain the discrete solution within a short period.

6.2.2 Way of Processing Nonlinearity

The balance condition for power system operation is power balance, which is the condition that the reactive power optimization must meet, whereas in a power balance equation, the voltage has a nonlinear relation with power. If the discrete characteristics of the transformer tap and capacitor bank number are taken into account, the reactive power optimization will be a MINLP problem.

Unlike the LP simplex method, the continuous nonlinear algorithm has no common algorithm. The existing nonlinear algorithms have rigorous rules on the mathematical characteristics of the problem, such as convexity, the objective function is a secondary function, etc. Otherwise, it would be impossible to prove that the obtained solution is the global optimal solution. In this chapter, under the assumption that most constraint functions are linear, nonlinear constraint functions can be adjusted continuously and slightly. The successive linear programming (SLP) algorithm is used to deal with the nonlinearity of discrete reactive power optimization.

6.2.3 Way of Processing Multiple States

A power system has different operating modes, which may change in different seasons, days, or even in a single day. In addition, equipment maintenance of a line, generator, or transformer may also lead to a change of operating mode. Because the system operating mode is changing all the time, certainly reactive power planning made under a specific operating mode can hardly meet the needs of multiple operating modes, so many kinds of system operating modes should be comprehensively taken into consideration. Therefore, to meet the

practical needs of a power system, it is necessary to consider both the requirements of a single-operating mode (single state) and multioperating mode (multistate) for the reactive power compensation equipment.

With the multistate taken into account, discrete reactive power optimization will become even larger in scale and more complicated. As mentioned previously, no mathematical algorithm to perfectly solve discrete reactive power optimizations is available thus far. In this chapter, diagonal block matrix model is used to express a multistate problem, and a reactive variable is used to express a coupling variable, so it is possible to solve multistate discrete reactive power optimizations using a decomposition coordination method.

6.2.4 Way of Selecting of Initial Values

The steady-state operation of a power system is normally expressed as a power flow equation, which is a transcendental equation. Thus, power system operation is a nonconvex problem, that is, there may be multiple solutions. A loop-iteration linear programming (SLP) algorithm proposed in the 1960s may be used to solve large-scale nonlinear problems. However, the convergence of solutions cannot be tested even under a convexity hypothesis. As most constraints for power system operation problems are nonlinear, when a discrete variable is introduced, it would be difficult to meet the continuously adjustable requirement. For this reason, if an SLP algorithm is used to solve MINLP, the obtained discrete feasible solution will be related to the initial value configuration.

The initial value for discrete reactive power optimization is normally configured in two ways. The first way is to take the continuous optimal solution and truncate it as the initial value for a discrete solution. The second way is to take the power flow solution as the initial value, then truncate it as the initial value for a discrete solution. The former way is more desirable. However, the power flow solution is taken as the initial value in this chapter in consideration of the necessity to calculate continuous optimization when calculating discrete optimization and the use of more computing resources by the continuous optimization.

In fact, the power flow solution is also normally taken as an initial value for continuous reactive power optimization, so using the power flow solution as the initial value is acceptable for an operational problem. However, for programming problems, an optimization calculation may be conducted only after obtaining a converged power flow solution with the help of expert rules because it is rather difficult to obtain even a converged power flow solution.

6.2.5 Consideration to Obtain Global Optimization

As there is no way to prove reactive power optimization meets a convexity condition, and when considering its discrete variable, reactive power optimization even becomes a nonconvex problem; thus, its optimal solution is usually related to its initial value. Normally, the nonlinear method can

only provide a local optimal solution, that is, an optimal solution around the initial value. It is also clearly indicated in the MINOS User Manual of Stanford University that the solution obtained is the optimal solution around the initial value. In that way, the author failed to obtain a feasible solution with MINOS when using straight start-up of power flow as the initial value. All optimal solutions mentioned in this chapter refer to local optimal solutions. It is possible to determine the initial values for different discrete solutions using different methods based on the continuous solution. In this chapter, the influence of different initial values on the algorithm is discussed.

6.2.6 Verification of the Correctness of Discrete Solutions

The order of magnitude of nodes number Nin power system is normally 102–103. The number of constraints for optimization calculation is approximately $2N$.

Most of the constraints are nonlinear constraints, and the number of variables is about $3N$, in which about one-third account for integer variables. At present, it is difficult for a precision-integer programming optimization algorithm to deal with problems of such large scale. IBM's MILP package can only solve problems with fewer than 50 integer variables. Common nonlinear algorithms cannot deal with more than 200 nonlinear constraints either.

To validate the procedure developed and the discrete solution obtained, several comparisons are made in this chapter as follows:

(1) Verification of differential value calculation formula: To validate the procedure developed with the algorithm proposed in this chapter, all differential value calculation formulas for the calculation procedure are verified with the original differential value calculation formula.
(2) Verification of the discrete optimal solution: There are not many new algorithms for discrete optimization. Moreover, a precision discrete optimization algorithm cannot be used to deal the real-scale discrete optimizations. Thus, it is necessary to validate the discrete optimization solution obtained with the new algorithm. Generally, for the same problem, the objective function value of a continuous optimization solution obtained by the same procedure should be the smallest, the objective function value of discrete optimization solution should be in the middle, and the objective function value of the truncated solution should be the largest. The results in this chapter support these criteria.
(3) Comparison with results from MILP algorithm programming software package: If the number of integer variables is less than 50, the linear integer programming with calculation procedure based on the algorithm proposed in this chapter can reach the same solution as that of an MILP algorithm programming software package.
(4) Comparison with results from MINOS nonlinear software package: Optimal power flow (OPF) discrete solution obtained with the algorithm proposed in this chapter will be taken

as the initial value, and MINOS nonlinear software package can reach the same continuous optimal solution as the calculation results in this chapter.

(5) Comparison with power flow calculation results: Under the conditions that voltage of the generator terminal, node angle of the balancing machine, and integer variable are fixed, and bound of other variables are infinitely slack, then calculating power flow with the calculation procedure based on the algorithm proposed in this chapter can lead to the same power flow solution as the Newton-Raphson algorithm.

(6) Comparison with manual programming results: The manual programming method normally only makes a few cases. It is obvious that the results of a discrete optimization algorithm are better than the manual programming method. However, results of this chapter are still compared with that of a manual programming method to prove the superiority of the algorithm. Furthermore, when some variables cross the threshold and some variables reach their limits after optimization calculation, if a feasible solution still cannot be obtained, the discrete optimization algorithm therefore may only reach one conclusion: the problem is unsolvable. In contrast, manual programming may adjust the limits for variables to obtain the feasible solution. If the engineer's experience is summarized to form a rule library or reasoning procedure, then combined with the outcomes from optimization mathematics, the obtained results will be much better than any of the solely used methods.

Verification of procedure validity is a complicated problem in itself. As the algorithm in this chapter is newly proposed, it is hereby important to verify its validity in the study.

6.2.7 Special Treatments for Practical Problems

Discrete reactive power optimization procedure developed based on the algorithm in this chapter deals with not only discrete variables but also special problems incurred in practical calculation, such as installing new reactive power compensation equipment at the original reactive power compensation equipment location; setting the upper limit for new reactive power compensation equipment; using the habitual tap position to express the transformer ratio and ensuring the transformer ratio integer solutions of the transformers in series must be equal; verifying data according to infeasible solution information; etc. It is quite often that practical problems may not be expressed with mathematical formulas. As for this, researchers should have a good mathematical foundation and engineering background to abstract mathematical models and common rules, or to adopt flexible methods acceptable to engineering practices in solving problems. In applying the procedure, this chapter has solved some problems. However, there is still a great deal of work to do before solving all practical problems.

6.2.8 Way of Processing Objective Function

If capacitor investment minimization is taken as the objective function, the number of variables of T (transformer tap) and C (capacitor capacity and bank number) may be increased, and the coefficient G_{ij} and B_{ij} of power flow equation may be modified so as to turn the equations of G_{ij} and B_{ij} into the equations of T and C, obtaining the partial derivatives of equations T and C, and to calculate out the investment on capacitor C: $\min \sum_{i \in N_C} (d_i W_i + c_i C_i)$.

6.2.9 Way of Processing Transformer Tap T and Capacitor Bank C

The power flow equation of transformer line and capacitor line should be modified, so as to obtain the partial derivatives for T and C, and to establish the linear equations containing T and C. The detailed modification method is shown in Appendix B.

6.3 Single-State Discrete VAR Optimization

6.3.1 Outline

As for single-state discrete reactive power optimization, its objective is to determine the minimum cost expansion plan of new reactive sources so as to guarantee feasible operations under a single-state operating mode. The basic feature is that, when solving large-scale reactive power compensation equipment planning problems, the number of capacitors may be taken as a discrete variable.

As power system problems have better linearity around a static stable point, the MILP method may hereby be used to solve its linearized integer programming problem and its nonlinear problem through iteratively executing LP.

The algorithm here employs an excellent approximation method for solving linear MIP problems because an exact optimal solution of MIP problems can hardly be obtained. Furthermore, to solve a nonlinear MIP problem, the algorithm exploits the concept of recursive LP so that it is capable of obtaining an AC load flow solution of the VAR planning problem. The program can easily be developed based on this algorithm by incorporating the options of existing LP software.

It should be pointed out that an integer-feasible solution can be quickly obtained by the approximation method, but it is a somewhat impractical solution because there is only one capacitor unit to be installed in each of several adjacent nodes. Hence, an improved procedure is proposed to remedy this impractical solution.

This section treats only normal operations without considering contingency states. The algorithm developed here provides a fundamental mathematical tool for multiple states. The extension of the algorithm from a single-state problem to a multistate problem is described in Section 6.4.

6.3.2 Single-State Model for Discrete VAR Optimization

6.3.2.1 Description of the problem

The reactive power planning problem in this section focuses on capacitor allocation. All VAR sources mentioned in the following text are capacitors. The objective function is to minimize investment on newly installed capacitor banks with constraints, including investment cost and operating constraint. The number of capacitor banks installed at each node is taken as an integer variable. The objective and constraint for single-state reactive power planning problems are stated as follows.

(1) Objective: to minimize total investment on capacitors by deciding the location and capacity of newly installed capacitors. The key to this section is a discrete optimization algorithm. Here, for the objective function, only the investment cost of capacitors is considered, whereas its operating cost will be ignored.
(2) Investment cost constraint: investment cost of capacitor is comprised of two aspects:
    1. Capital cost of investment location is a fixed cost, which has a complicated calculation procedure. The more investment locations, the higher total capital cost. Different investment locations also lead to different construction costs. Thus, the fixed cost will be used to differentiate costs of different locations. This is a relative value, which may lead to significant influence toward selection of location for newly installed reactive power compensation equipment. For existing reactive power compensation equipment locations, the algorithm in this chapter will take their fixed costs as 0, because they may be considered in an optimization calculation formula and so they are differentiated from new locations. As it is a problem related to investment minimization, it is natural that the equipment with a fixed cost of 0 will be installed first if it meets the operation constraint conditions.
    2. Unit capacity cost of a capacitor is a variable cost, which is calculated based on the investment cost needed for capacitors. The more capacitor banks to be installed, the higher the cost, so it shall be expressed as a variable cost. Like the fixed cost, the variable cost of reactive power compensation equipment is assumed as 0.

    This method can easily handle the situation of adding new reactive power compensation equipment to an existing reactive node. The test system in this section is not involved in such a situation, but in Section 6.5, a similar situation is involved.
(3) Power system operation constraint: power system operation constraint consists of several aspects:
    1. The power generation and load balancing constraint under the given load conditions, namely the power flow constraint. In reactive power optimization, except for active power output of the balancing node, the active power outputs of the generators are given.
    2. Generator node and load node bound constraint: location and capacity of capacitors are closely related to local voltage distribution.

3. Transformer tap variation range constraint: operators may adjust the tap to change reactive power distribution in a power system, but this cannot provide reactive power to the power system. In this section, the tap is treated as continuously adjustable.
4. Generator reactive power generation bound constraint: operators may adjust generator reactive power output to change the reactive power supplied to the system. In this section, generator reactive power generation is treated as continuously adjustable.

Table 6.1 shows notations.

Table 6.1 Notations

Notation Name	Description	Notation Name	Description
N	Set of all nodes	G_{ij}, B_{ij}	Real and imaginary parts of the ith and jth elements in node admittance matrix
N_T	Set of transformer nodes	$T=(T_i)$	Vector of transformer ratio
N_G	Set of generator nodes	$C=(C_i)$	Vector of capacitor number, which is an integer vector
N_C	Set of newly planned capacitor nodes	$W=(W_i)$	0, 1 integer variable, indicating whether new reactive nodes are deployed
E_C	Set of original capacitor nodes	$c_i(>0)$	Variable cost coefficient
P_i, Q_i	Active and reactive power injection in node i	$d_i(>0)$	Fixed cost coefficient
P_{Gi}, Q_{Gi}	Generator active and reactive power at node i	$\overline{C_i}$	Maximum number of capacitor banks installed at node i
P_{Li}, Q_{Li}	Active and reactive load of node i	$X=(X_i)$	Vector of continuous variable
$U=(U_i)$	Vector of voltage magnitude	$Y=(Y_i)$	Vector of integer variable
$\theta=(\theta_i)$	Vector of phase angle		

The same notations in the following sections will not be repeatedly defined.

6.3.2.2 Mathematical model

(1) Nonlinear MIP problem
Problem P:

$$\min \sum_{i \in N_C} (d_i W_i + c_i C_i) \tag{6.1}$$

subject to:

1. Investment cost constraint:

$$C_i \le \overline{C}_i W_i, \quad i \in N_{\mathrm{C}} \tag{6.2}$$

where

$$C_i = 0, 1, \ldots, \overline{C}_i, \quad i \in N_{\mathrm{C}} \cup E_{\mathrm{C}} \tag{6.3}$$

$$W_i = 0, 1, \quad i \in N_{\mathrm{C}} \tag{6.4}$$

2. Operation constraint
   Power flow balance equation:

$$F_{1i} = P_i(U, \theta, T) - P_{\mathrm{G}i} - P_{\mathrm{L}i}, \quad i \in N \tag{6.5}$$

$$F_{2i} = Q_i(U, \theta, T, C) - Q_{\mathrm{G}i} - Q_{\mathrm{L}i}, \quad i \in N \tag{6.6}$$

where

$$P_i = \sum_{j \in i} U_i U_j \left(G_{ij} \cos\theta_{ij} + B_{ij} \sin\theta_{ij}\right)$$

$$Q_i = \sum_{j \in i} U_i U_j \left(G_{ij} \sin\theta_{ij} - B_{ij} \cos\theta_{ij}\right)$$

Active power output limits of generator balance node:

$$\underline{P}_{\mathrm{S}i} \le P_{\mathrm{S}i} \le \overline{P}_{\mathrm{S}i} \tag{6.7}$$

Generator reactive power output limits:

$$\underline{Q}_{\mathrm{G}i} \le Q_{\mathrm{G}i} \le \overline{Q}_{\mathrm{G}i}, \quad i \in N_{\mathrm{G}} \tag{6.8}$$

Voltage limits of all nodes:

$$\underline{U}_i \le U_i \le \overline{U}_i, \quad i \in N \tag{6.9}$$

Transformer tap limits:

$$\underline{T}_i \le T_i \le \overline{T}_i, \quad i \in N_{\mathrm{T}} \tag{6.10}$$

Problem P is a minimization problem with integer variables and nonlinear constraints. When $C_i = 0$, the value of W_i shall be 0 as well, so that equation of $d_i W_i$ in objective function shall be:

$$d_i W_i = \begin{cases} 0, C_i = 0 \\ d_i, C_i = 1, 2, \ldots, \overline{C}_i \end{cases} \tag{6.11}$$

(2) Some rules for the mathematical model:

1. Variables are not divided into state variable and control variable. Variables are taken as a whole, so that state variable X and control variable U are not differentiated in the optimization procedure. The algorithm divides variables into continuous variables and discrete variables. When solving LP, a discrete variable is always treated as a nonbasic variable (see Appendix A), whereas a fixed variable is treated as a variable with the same bound. Thus, in the solution procedure, the nonbasic variable always prevails. This measure has no significant influence on problem scale. The key to this chapter is the discrete variable.
2. Reactive power generation constraint of generator is treated as variable constraint. Reactive power generation of Eq. (6.8) is equivalent to control variable in form. However, it is a derived variable of Eq. (6.6), which may be treated as a constraint equation with upper and lower bounds. If it is treated as a constraint equation, Eq. (6.6) may not contain the balance equation for the generator node. Thus, the reactive power generation of a generator is not actually a control variable. In Chapter 4, the reactive power generation of a generator is written as a constraint equation, which is equivalent to the way of writing in this chapter. This chapter does not intend to compare the calculation speed of the two processing methods. However, they are completely equivalent in a mathematical sense.
3. Integer variable in the model is equivalent to the control variable. Shown by Eqs. (6.5) and (6.6), only U, T, and C are changed in the optimization procedure to meet power flow balance. As it takes no cost to adjust voltage U, transformer ratio T, and existing capacity bank number, these variables will be preferentially adjusted when solving LP. Integer variable YC of newly installed capacitors will be adjusted only when it is impossible to keep all variables within their bounds. When solving LP, a discrete variable will always be treated as a nonbasic variable, which is a function of continuous variable voltage U and generator reactive power generation QG. Thus, the integer variable is equivalent to the control variable in this chapter.
4. Phase angle is treated as free variables. Like other variables, phase angle is also treated as a whole. Phase angle of balance node is treated as a fixed variable with equal upper limit and lower limit, yet the phase angle of a common node is treated as a free variable without upper and lower limits.

The previously discussed method runs through the whole chapter. The solving method for such complex problem will be described in the next section.

(3) Model linearization: nodes in a network are divided into three classes of power flow calculation: PQ, PV, and $V\theta$ node. For the convenience of taking into consideration reactive power Q constraint, all nodes, except for $V\theta$, are treated as PQ node in reactive planning model. In other words, every node has P constraint and Q constraint equation. Please refer to the previous section for generator node processing method, as well as bound of Q variable. For the convenience of bound processing, all algorithms proposed adopt a polar coordinate form.

If nonlinear constraint is linearized, the linear expression for the nonlinear Eqs. (6.5) and (6.6) shall be:

$$\begin{bmatrix}\Delta F_1\\ \Delta F_2\end{bmatrix}=\begin{bmatrix}\partial F_1/\partial U & \partial F_1/\partial\theta & \partial F_1/\partial P_G & 0 & \partial F_1/\partial T & 0\\ \partial F_2/\partial U & \partial F_2/\partial\theta & 0 & \partial F_2/\partial Q_G & \partial F_2/\partial T & \partial T_2/\partial C\end{bmatrix}\begin{bmatrix}\Delta U\\ \Delta\theta\\ \Delta P_G\\ \Delta Q_G\\ \Delta T\\ \Delta G\end{bmatrix} \tag{6.12}$$

Let $\Delta X_k = X_{k+1} - X_k$; the kth linear expression of Eq. (6.5) and (6.6) may be written as:

$$\boldsymbol{A}_{k-1}\boldsymbol{X}_k + \boldsymbol{B}_{k-1}\boldsymbol{Y}_k = \boldsymbol{b}_k \tag{6.13}$$

where

$$\boldsymbol{A}_k=\begin{bmatrix}\partial F_1/\partial U & \partial F_1/\partial\theta & \partial F_1/\partial P_G & 0\\ \partial F_2/\partial U & \partial F_2/\partial\theta & 0 & \partial F_2/\partial Q_G\end{bmatrix}$$

$$\boldsymbol{B}_k=\begin{bmatrix}\partial F_1/\partial T & 0\\ \partial F_2/\partial T & \partial F_2/\partial C\end{bmatrix}$$

$$b_k=\Delta\boldsymbol{F}_{k-1}+\boldsymbol{A}_{k-1}\boldsymbol{X}_{k-1}+\boldsymbol{B}_{k-1}\boldsymbol{Y}_{k-1}$$

Jacobi matrix elements in $\mathbf{A}_k$ include:

(1) Elements related to voltage U and angle θ are the same as those in the conventional power flow.

(2) Elements related to active power P and reactive power Q of a generator (P is only related to active power output PS of balance node, and Q is only related to reactive power generation QG of generator node).

$$\partial F_{1i}/\partial P_{Si}=1.0$$
$$\partial F_{2i}/\partial Q_{Gi}=1.0$$

Jacobi matrix elements in the matrix $\boldsymbol{B}_k$ include:

1. Elements related to tap ratio: In this chapter, T is temporarily treated as a continuous variable to reduce the number of integer variables, because only a continuous variable has a partial derivative. If T is taken as a discrete variable, a partial derivative shall not be solved for in a simple manner. Instead, it shall be specially processed, and tap ratio T is treated as an integer via the processing method used in Section 6.5.
2. Elements related to C: as a partial derivative of C is equal to the difference expression of C, a partial derivative of C may hereby be directly taken as a coefficient of a discrete variable.

6.3.2.3 Characteristics of the problem

The mathematical expression of a single-state model has the following six characteristics in the field of mathematics for programming:

(1) High dimensionality of problem variable:
   1. Number of continuous variables:
      The number of voltage variables = The number of system nodes N
      The number of angle variables = The number of system nodes N
      The number of generator reactive power variables = The number of generators N_G
      The number of tap ratio variables = The number of transformers N_T
      The number of active power variables at generator balance node = The number of balance nodes N_S
      The number of continuous variables $= N \times 2 + N_G + N_T + N_S$
   2. Number of discrete variables:
      The number of newly installed capacitor variables $\times 2 = N_c \times 2$
      The number of existing capacitor variables $= N_E$
      The number of discrete variables $= N_c \times 2 + N_E$

      A practical power system normally contains more than 100 nodes. Taking the test system in this chapter as an instance, the number of nodes is 135, the number of generators is 36, the number of transformers is 17, the number of newly installed capacitors is 20, the number of existing capacitors is 29, the number of continuous variables is $135 \times 2 + 36 + 1 + 17 = 324$, and the number of discrete variables is $20 \times 2 + 29 = 69$.

      Note: If the upper limit and lower limit are the same, the variable shall be a fixed variable, such as the phase angle of balancing machine node.

(2) Huge number of constraints.
   The number of constraint conditions is:
   The number of power flow balance constraints = The number of system nodes $N \times 2$
   The number of investment constraints = The number of capacitor nodes $N_c + N_E$

   If the number of nodes is 135, the number of newly installed capacitors is 20, and the number of existing capacitors is 29, then the number of constraints $= 135 \times 2 + 20 + 29 = 319$.

(3) Cost function is a linear expression.

(4) Constraint function is a nonlinear function.

(5) Variables are divided into two types: continuous variables and discrete variables, and there is a large number of integer variables.

(6) Both the number of constraints and variables are more than a few hundred.

6.3.3 Single-State Algorithm for Discrete Optimal VAR Optimization

6.3.3.1 The main computational procedure

The way to solve problem P is to linearize problem P in the iteration procedure to create the linearized problem PL. Meanwhile, the approximation method of mixed-integer linear programming is used to solve the linear problem. The following section discusses the calculation steps:

Step 1: Formulate the VAR planning problem as a nonlinear MIP problem (or MINLP problem) described as problem P in Section 6.3.2.2.
Step 2: Set $k=0$, and assume an initial value Z^0 based on power flow solution of the system, and vector Z defined as:

$$Z=(X,Y,W)=(U,\theta,P_G,Q_G,T,C,W) \tag{6.14}$$

This initial value z^0 can be obtained by relaxing the limits for V, θ and T and setting Y, W to zero when repeatedly solving linearized LF equations by LP. Certainly, the initial value can also be obtained by any load flow solution method, but only the sequence of variables should be V, θ, T, Y.
Step 3: Construct a linear MIP problem (or MILP problem) PL by linearizing load flow Eqs. (6.5)–(6.8) at point z^k, where PL is the problem with the same objective function and constraints as problem P, except that Eqs. (6.5) and (6.6) are linearized.
Step 4: Obtain an integer-feasible solution of the linear MIP problem PL and improve the obtained solution by using the approximation method in Appendix A. In searching for an integer-feasible solution, this method treats integer variables as fixed values, that is, as nonbasic variables, then only one integer variable is increased by +1 or decreased by −1 each time when repeatedly using the simplex method for LP.
Step 5: Obtain a better integer solution than that of Step 4 by changing the values of two integer variables each time to decrease the installation cost further and to install capacitors at fewer nodes. The detailed steps for the improved algorithm in Step 5 are shown in Section 6.3.3.2.
Step 6: Test for convergence if $Z^k \neq Z^{k+1}$, make $k \leftarrow k+1$, then go to Step 3; otherwise, go to next step.
Step 7: Terminate the algorithm because z^k is an optimal solution of problem P.

In fact, this algorithm can be effectively executed and can quickly find an integer-feasible solution by the approximation method in Step 4 even if Step 5 is not executed. However, based on existing experience, the solution from Step 4 was somewhat an impractical solution, that is, it might allocate only one capacitor unit to each of several adjacent nodes. This makes the total cost increase due to fixed costs.

To prevent such an undesirable situation, an innovative improvement procedure is proposed in Step 5 for adjusting two integers at each time to decrease the fixed costs.

The solution flow chart of the discrete VAR planning is shown in Fig. 6.1.

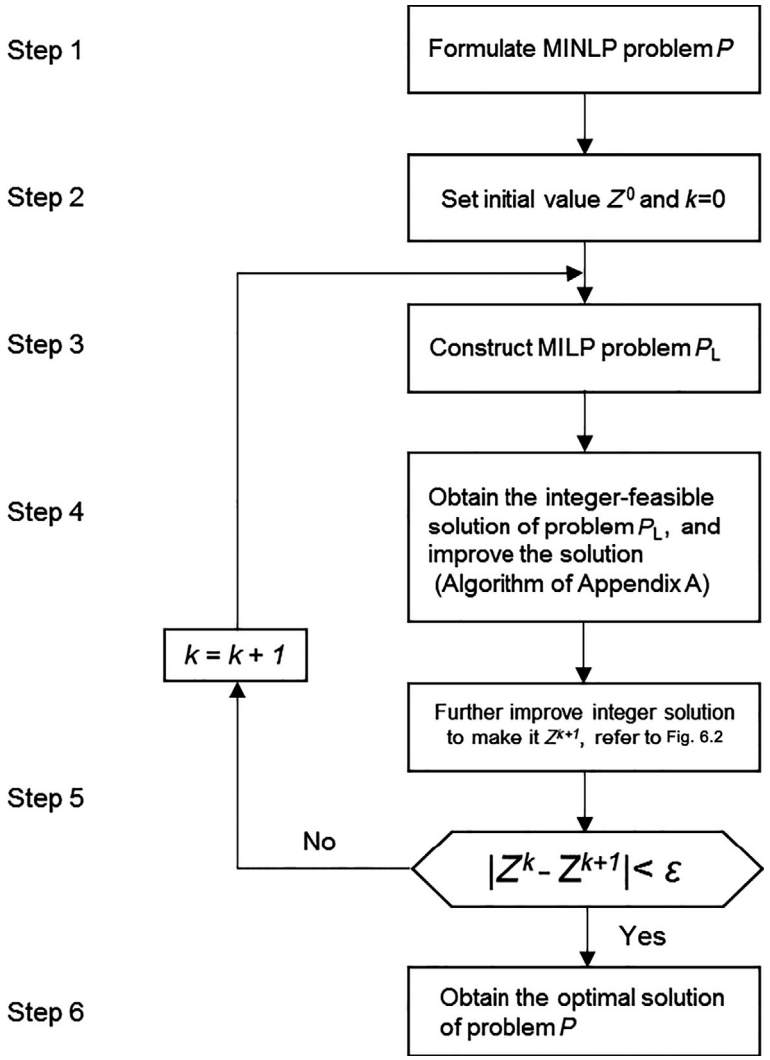

Fig. 6.1
Flow chart of discrete reactive power optimization algorithm.

6.3.3.2 *Improved algorithm for integer solutions*

As previously mentioned, using an integer solution directly with the prototype of an MIP approximation method may not be reasonable for the real power system. To be more specific, the situation in which some adjacent reactive power compensation installation

nodes are installed with reactive power compensation equipment, but each node has a small compensation, is likely to occur. The reason is that only the most promising integer variable can be processed once in the calculation procedure of the original algorithm, adding or deducting the integer by 1, then solving LP to make the problem feasible. Such a calculation procedure may lead to a small amount of reactive power investment on each adjacent node. The need for increasing the fixed cost without connection to the equipment capacity at the location of new installed reactive equipment leads to an increment of total cost.

An improved algorithm is proposed in this section by changing two integers at the same time to overcome the deficiencies of the original algorithm.

One of the integers is added by 1 or 2, whereas another integer is deducted, until the latter becomes zero. In other words, when the integer-feasible solution has been solved with the original algorithm, two nonzero integer variables will be comprehensively considered and selected. If the problem is still feasible based upon the procedure previously mentioned, and the objective function value decreases, this pair of integer variables will be used to replace the original pair of integer solutions. This will continue until a new integer pair cannot be obtained. From the perspective of system operation, it is workable to add reactive power compensation equipment to one of two adjacent nodes, yet reduce reactive power compensation equipment from another node, and this won't lead to problem infeasibility. However, reduction of a new reactive power node will help cut the fixed cost, so as to avoid installing a small number of reactive power compensation equipment at adjacent nodes at the same time.

The principle of the improved integer solution algorithm is to reduce the number of nodes for the newly installed reactive power compensation equipment, replacing a pair of nonzero integers with one nonzero integer and one zero integer. The detailed steps are given as follows:

Substep 1: Express the feasible solution obtained in Step 4 as:

$$Z^* = (X^*, Y^*, W^*) \tag{6.15}$$

Substep 2: Stochastically select a pair of nonzero integer variables y_u^* and y_s^* from node u and s, and adjust the number of capacitor banks installed at the two nodes, then recalculate the new investment cost; if the cost is reduced, they will be taken as a new pair of changeable integers, then go to the next step. Otherwise, it means that present integer solutions cannot be further improved, and the calculation terminates.

Substep 3: Make the new integer variable vector Y_n by increasing one of the integers, y_u^*, by 1 or 2, and decreasing another integer y_s^* by 1, then readjust the fixed cost vector W^* to satisfy Eq. (6.14). For example, if $y_s^* = 1$, then let $y_s^* = 0$, $\quad w_s^* = 0$. Thus, the fixed cost at node s becomes zero.

Substep 4: When LP is not resolved for the new (Y^n, W^n), check whether the cost stated in Eq. (6.1) can be decreased. If the cost decreases, then go to Substep 5. Otherwise, move to Step 7. Simplex tableau is used to check whether the infeasibility of the problem is smaller than 0 (infeasibility calculation formula is shown in Appendix A).
Substep 5: Check whether the new (Y^n, W^n) makes continuous variable vector X violate operating constraints, that is, check whether (Y^n, W^n) results in an insufficient or excessive VAR supply. With integer variable vector (Y, W) fixed to (Y^n, W^n), the checking is finished in two ways. The first way is to calculate the violations without resolving problem LP; if the violations do not happen, then go to Substep 6. Otherwise, readjust continuous variable vector X, that is, resolve the LP problem. If resolving problem LP is feasible, then go to Substep 6, otherwise proceed to Substep 7, that is, abandon (Y^n, W^n).
Substep 6: Accept the new integer solution (Y^n, W^n). It is better than (Y^*, W^*), because the installation cost decreases, and insufficient or excessive VAR supply does not occur. Replace (Y^*, W^*) with (Y^n, W^n) and return to Substep 2 to decrease the cost further.
Substep 7: Readjustment of these two integer variable values makes it impossible to decrease the installation cost or supply appropriate quantity of VAR resources. Abandon this new integer solution (Y^n, W^n), and return to Substep 2 to check another pair of integers in Y^*.

Please refer to Fig. 6.2 for the improved integer algorithm.

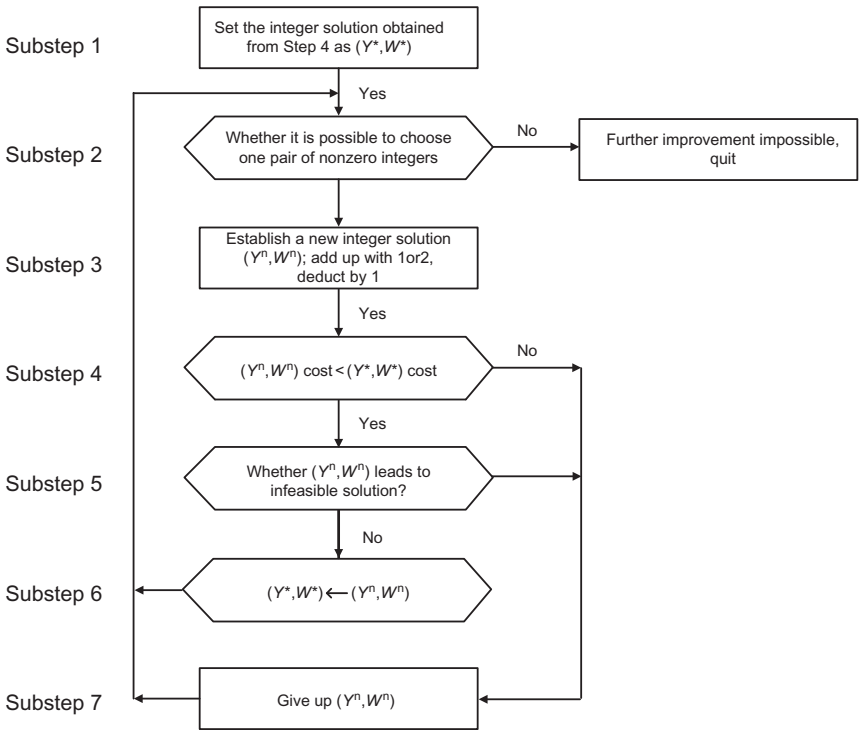

Fig. 6.2
Flow chart of integer improved algorithm of Step 5 in algorithm flow.

6.3.4 Implementation

6.3.4.1 135 node practical system

In this section, a real case is implemented based on the real-scale 135-node system of Chugoku Electric Power, demonstrating that the proposed algorithm can deal with the real-scale discrete reactive power optimization. The system is comprised of 36 generators, 98 loads, and 17 transformers, with a base power of 1000 MVA. The LP section of the algorithm adopts HITACMPS-II mathematical programming software package. The 135-node system is shown in Fig. 6.3.

6.3.4.2 Numerical results of five cases

The numerical performance of the proposed algorithm is examined by five cases of VAR planning problems. Case 1 is solved to explain the flow chart of the algorithm step by step. Cases 2–5 are solved to show the effectiveness of the algorithm. Table 6.2 specifies all items one by one in detail.

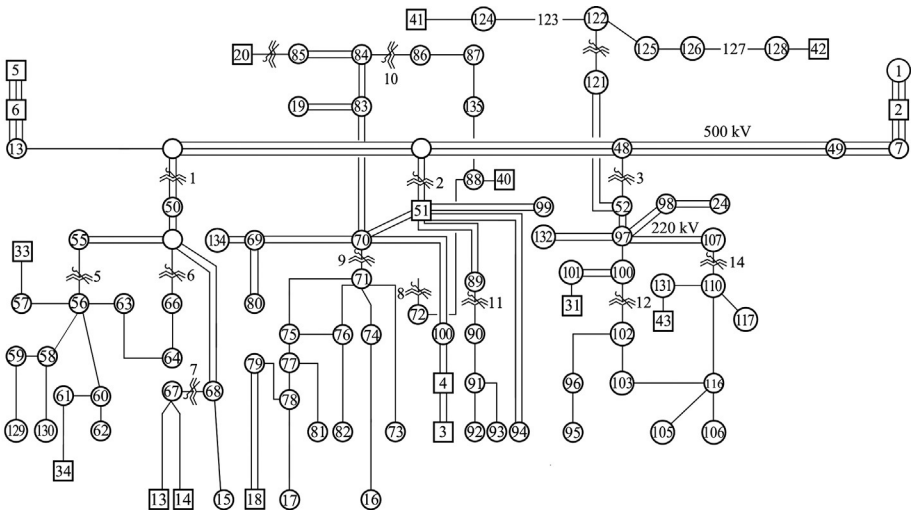

Fig. 6.3
135-Node system.

"Voltage bound" means upper and lower bounds of voltage magnitudes for almost all nodes, not including special nodes. "Initial violations" refers to the number of nodes with violated mean voltage magnitude and generator reactive power violations of a load flow solution.

Because Cases 1–5 adopt an infeasible power flow solution as the initial value, infeasible power flow means voltage or reactive of some nodes may violate the limits.

"Fixed cost" refers to construction cost coefficients of Cases 1–5, which are relative values. The range of fixed cost for Case 1 is 2.6–3.8, and for Cases 2–5 is 0.5–0.9.

"Variable cost" is the single bank cost coefficient of capacitors in Cases 1–5. The variable cost of all single bank capacitors in Cases 1–5 is 1.

"The number of existing capacitor nodes" refers to the number of existing capacitor nodes.

"The number of new capacitor nodes" refers to the number of candidate nodes to be installed with new capacitors.

"The number of new nodes" refers to the number of nodes to be installed with new capacitors based on the algorithm in this section.

The convergence tolerance for continuous variables is 0.0001.

In Table 6.2, Cases 2 and 3 have the same voltage bound and the same candidate nodes installed with capacitors. The difference is that Case 3 increases the upper limit of existing capacitor bank number, yet decreases the upper limit of new capacitor bank number. Except for the difference in voltage bound, Cases 4 and 5 have the same calculation conditions as that of Cases 2 and 3 in Table 6.2.

All over limits of nodes may be eliminated in the first iteration with the algorithm to find the integer-feasible solution. Generally, nonlinear convergence solution can be obtained in eight iterations, and an average over six LPs will be calculated in one iteration, the second and third stage will be calculated in each iteration, and each stage has to calculate more than three LPs. When changing each integer to recalculate LP, the algorithm utilizes the use of the function provided by MPS-II to calculate LP from the original base. Thus, the calculation time is acceptable.

In Cases 1–5 where the number of newly installed reactive compensation equipment is zero, then zero is used as the initial power flow value. The calculation results show that, although the number of newly installed capacitor nodes is decreased from 6 to 5 after the upper limit of existing capacitor bank number is increased, the fixed investment cost can be largely reduced. Cases 2 and 3 have almost the same calculation time. Different voltage bounds lead to more initial voltage values crossing the threshold. Moreover, more violation volume means higher investment in newly installed capacitor nodes and more calculation time. The total sum of existing capacitor node number and newly installed capacitor node number can be up to 49 (see Table 6.2). The capacity of the capacitor provided for each node shall be expressed with an integer variable. Whether it is necessary to provide capacitors for the newly installed capacitor nodes is also expressed with the integer variable. As for this, the number of integer variables to

be processed can be as many as 69. The overall results of Cases 1–5 show that the algorithm can effectively deal with integer variables and solve the reactive power optimizations of real-scale system within 1 min.

Table 6.2 Initial conditions and basic results

Items	Case 1	Case 2	Case 3[a]	Case 4	Case 5[a]
Voltage limits (per-unit value)	0.92–1.08	0.95–1.05	0.95–1.05	0.97–1.03	0.97–1.03
Initial violation number	18	49	49	68	68
Fixed cost (10,000 yuan)	2.6–3.8	0.5–0.9	0.5–0.9	0.5–0.9	0.5–0.9
Per bank variable cost (10,000 yuan)	1.0	1.0	1.0	1.0	1.0
The number of existing capacitor nodes	3	29	29	29	29
The number of newly installed capacitor nodes	7	20	20	20	20
The number of newly installed nodes	2	6	5	8	8
CPU(s)	39	41	39	37	57

[a]The upper limit of existing capacitor bank number increases while the upper limit of newly installed capacitor bank number decreases.

Table 6.3 specifies in detail MIP results of Case 1 in iteration procedures and the results of the improved procedure.

To clarify the specific concept of the proposed algorithm, following text offers explanations to the calculation results of Case 1 in Table 6.3.

First iteration:

(1) First, capacitor units are taken as continuous variables to solve this LP problem. Then the continuous values of capacitor units are rounded off to the nearest integer values shown in the line with brackets in Table 6.3.

(2) Take the obtained rounded-off integer solution as the initial value and capacitor bank number of integer variables, then adopt approximation integer programming method to solve MILP problem. In the second stage, the integer solution was feasible. In the third stage, the integer solution was improved. However, the integer solution decreasing objective function was not obtained. The integer solution of approximation algorithm is shown in the line with method of *A* in Table 6.3. Details of approximation integer

Table 6.3 Iteration results of Case 1

Iteration Times	Method	Total Cost (1 million yuan)	Node No.									
			57	74	102	106	107	111	116	119	123	127
			N_C	N_C	N_C	N_C	N_C	N_C	N_C	E_C	E_C	E_C
			⟨2⟩	⟨0⟩	⟨0⟩	⟨3⟩	⟨0⟩	⟨0⟩	⟨2⟩	⟨0⟩	⟨3⟩	⟨3⟩
1	*A*	20.8	2	0	0	3	1	0	2	3	3	3
	P	20.8	2	0	0	3	1	0	2	3	3	3
2	*A*	18.7	2	0	1	3	1	0	0	3	3	3
	P	13.3	2	0	0	6	0	0	0	3	3	3
3–7	*A*	12.3	2	0	0	5	0	0	0	3	3	3
	P	12.3	2	0	0	5	0	0	0	3	3	3

Note: *A*, adopting approximation integer programming method; E_C, existing capacitor compensation point; N_C, newly installed capacitor node; *P*, adopting integer solution improved algorithm; ⟨⟩, round-off.

programming method are shown in Appendix A, and the method only changes one integer each time.

(3) The improvement procedure is then used to enhance this solution further, but no improvement solution is found in this iteration. Thus, the solution obtained is only by the approximation method, and first iteration ends with an integer solution in the line with method of P and cost as 20.8. The integer solution has not been improved after it becomes feasible.

Second iteration:

(1) With the integer solution from the first iteration as the starting point, approximation integer programming method will be used to solve MILP problem after the solution is linearized. Its integer solution changes in both the second and third stage. The obtained integer solution is shown in line 5 and cost as 13.3.

(2) As the integer solution improved algorithm that can change two integers each time is used, the solution may be further improved. After several substeps of improvement, seven installed nodes have been decreased to five installed nodes, that is, three installed adjacent nodes 102, 106, and 107 are reduced to one installed node, 106. According to the result of the iteration, the cost is 13.3 million yuan.

Third to seventh iteration:

With the integer solution of the second iteration as the starting point, the execution procedure is the same as that of the second iteration. However, from the third to seventh iteration, even continuous variable convergence and integer variables no longer change and improve, except for the number of reactive capacitor compensations at node 106, which was reduced by one bank in Step 3. This means that the integer solution obtained in the second iteration is a nonlinear power flow solution meeting problem P.

The results of Cases 2–5 are briefly explained as follows. Cases 2 and 3 have the same voltage magnitude bounds of 0.95–1.05 and the same capacitor candidate set. The difference between Cases 2 and 3 is that $\overline{Y}_i(i \in E_C)$ is decreased and $\overline{Y}_i(i \in N_C)$ is increased in Case 3 as indicated by mark superscript a in Table 6.2 in which both cases are successfully solved with almost the same CPU time.

Cases 4 and 5 have the same conditions as Cases 2 and 3, respectively, except for voltage magnitude bounds of 0.97–1.03. The change of voltage bounds makes more violations occur, and more violations may cause larger computation time and more capacitor installations. Compared with Case 2, Case 4 is successfully solved with almost the same computation time, although more initial violations exist in Case 4 than in Case2. As for Case 5, the number of existing capacitor units is decreased, and it takes longer computation time to adjust new capacitor units.

Referring to Tables 6.2 and 6.3, various operating conditions and candidate node sets have been tested. The test cases show that the proposed algorithm can solve real-scale VAR planning problems within a reasonable computation time.

6.3.5 Summary

An efficient algorithm for solving single-state discrete variable reactive power optimization was proposed in this section, which could treat capacitors as discretely adjustable devices in real-scale systems. The proposed approach is superior to other algorithms in the following aspects:

(1) Reactive power optimization mathematical model is an MIP model, which takes capacitor bank number as a discrete variable.
(2) Excellent approximation integer programming algorithm is used to solve large-scale integer programming problems.
(3) Iteration method is used to solve LP, and the obtained solution is an AC power flow solution rather than an approximation DC power flow solution.
(4) In accordance with actual situation of a power system, this chapter puts forward an improved algorithm in allusion to integer programming, which can change two integers each time. The algorithm can decrease fixed investment costs of capacitor bank and avoid the unreasonable situation of setting a small amount of reactive power at adjacent nodes.

Calculation results based on an actual system with 135 nodes show that the algorithm is reasonable and valid. The algorithm in this section provides basic mathematical tools and lays a foundation for a discrete reactive power optimization algorithm.

6.4 Multistate Discrete VAR Optimization

6.4.1 Overview

The study in Section 6.3 comprehensively discussed discrete reactive power optimization under single-state conditions. However, reactive power planning may also be implemented under changing network (multistate) conditions. Multistate reactive power planning takes into account normal operation, routine maintenance, and accidental failure, and is able to realize reactive power configuration under multiple operating modes, so as to meet multistate requirements of changing networks. There is some literature considering reactive power planning under multiple power flows. Yet they did not take into account the discreteness of reactive power compensation equipment. Based on the study in Section 6.3, this section proposes a multistate discrete reactive power optimization model that can be applied to more complicated actual situations.

The idea of considering a discrete variable under a multistate situation is to transform reactive power optimization into complicated multistate discrete reactive power optimization. The key to this section is to present a pragmatic algorithm to solve multistate discrete reactive power optimization. Multistate as mentioned in this section includes: normal state, transmission line failure, transformer failure, and generator failure.

To consider multistate problems, Literature [30] proposed a direct energy decomposition method. To apply the algorithm to multistate discrete reactive power optimization, the number of capacitor banks at the location of reactive power compensation equipment is treated as the energy for each state. If the value of the energy is fixed, the whole multistate discrete reactive power optimization may be decomposed into several mutually independent subproblems, because multistate discrete reactive power optimizations have a special structure, that is, diagonal block structure. Thus, these subproblems may be solved separately. By coordinating results from these subproblems, the minimum reactive power investment cost of the entire problem can be found. The coordination process is actually to comprehensively consider the infeasibility of each state, and install the reactive power compensation equipment at nodes where the infeasibility of all states can be minimized.

According to traditional multistate reactive power optimization, reactive power optimization under each single state will be calculated separately. The maximum reactive power compensation equipment number of nodes under a respective single state will be taken as the reactive power configuration of the node. This method only considers optimization of a single state and ignores the mutual effect of reactive power configuration under all states. This might not be economically efficient, because it may deploy newly installed reactive power compensation equipment at adjacent nodes or many nodes. Even if the total reactive power compensation capacity keeps still, the method may also increase fixed capital cost of new reactive power compensation equipment, in turn, increasing total investment.

The proposed algorithm fully takes into consideration the mutual support role of reactive power under multiple states. The proposed integer improvement procedure for multistate conditions can help new reactive power meet the requirements of each state to the largest extent, and comprehensively and optimally balance under single state to achieve the overall optimum of all states. As for this, new reactive power compensation equipment will be centrally allocated to make the total investment less than the conservative investment results obtained by separately calculating each single state. In addition, compared with a single-state calculation procedure, the calculation procedure for multistate reactive power optimization developed with the algorithm will not lead to more workload of calculation.

In the previous chapter, only the normal state in a power system is considered. VAR planning, without considering possible changes in the system configuration, may not be realistic. There might exist a minimum VAR equipment installation that can correct unacceptable voltage profiles during anticipated normal and contingency states in power systems. The contingencies

considered in this program only include the static outages, such as transmission lines, transformers, or generator outages, not including some severe dynamic faults in the power system. This research discusses development of a computer algorithm, a multiple state algorithm, that can select one overall reactive power installation pattern that will satisfy system performance for both base state and contingency states. Most importantly, this algorithm needs only a little more computer storage than that of a single-state algorithm.

As previously mentioned, VAR planning should provide a system with VAR equipment, which can experience the most severe state along with each possible state. The consideration of several contingency states of various load conditions (light, medium, and peak load) creates an enormous nonlinear mixed-integer optimization problem. For example, there are more than 900 continuous variables and 120 integer variables for a 135 node system VAR planning problem under three contingencies.

The goal of the reactive power planning problem is to find the minimum cost installation plan of new reactive power sources so that the system voltage is maintained within an acceptable range. The formulation of the multistate VAR planning problem must take into account the following two aspects:

(1) The number of installed VAR sources takes an integer value.
(2) The installed VAR sources must be sufficient even in contingency states or in anticipated operating states.

A consideration of multiple states, together with the discrete nature of VAR facilities, creates a large-scale nonlinear MIP problem. Because no general mathematical programming technique for solving such a problem exists, a new algorithm should be developed that can handle both the discrete nature of capacitor units and multiple states in power systems.

In previous researches, the consideration of both the multiple states in power systems and the discrete nature of VAR facilities has not been well treated. In this section, based on the previous study, an approximate solution method for MIP problems is employed. Because the method is LP-based, it is efficient for large-scale problems.

To take multiple states into account, a resource directive decomposition approach is used in the proposed algorithm. To apply the approach to the multistate VAR planning problem, the number of installed VAR sources is treated as "resources," which are assigned to each state. If the value of a resource (installed VAR source) is fixed, the overall problem can be decomposed into mutually independent subproblems. This is because the multistate VAR planning problem has a special form of a block diagonal structure. Then subproblems are coordinated to give a minimum cost VAR installation pattern for the overall problem. This method takes into consideration the "cooperative" effect of a VAR source installation for multiple operating states. The states considered in this section include not only normal operating states but also such outages as transmission line outages, transformer outages, and generator outages.

6.4.2 Multistate Model for Discrete VAR Optimization

6.4.2.1 Description of the problem

In this section, the VAR optimization problem aims to study the allocation of capacitors under multistate conditions. The objective function is to minimize cost of the new installed capacitors, and the constraint condition includes the cost constraint and the multistate operation constraint, which are described as follows:

(1) Objective: to decide the location and capacity of newly installed capacitors, so as to meet system operation constraint under all states and minimize total investment in capacitors. The key to this section is discrete optimization algorithm. Thus, for the objective function, only investment cost of capacitors is considered, while capacitor operational cost will be ignored.
(2) Investment cost constraint: investment cost of capacitor includes two aspects: fixed cost and variable cost. Definition of the cost is the same as that specified in Section 6.3.
    1. Power system operation constraint: power system operation constraint consists of several aspects below:
    2. Generation and load balancing constraint under given load conditions, that is, power flow balancing constraint between generation and load; under a multistate condition, one reactive power planning mode has to meet multistate power flow balance.
    3. For multistate power flow solutions, generator node and load node shall be able to meet their respective bound constraints.
    4. For each state, transformer tap shall be able to meet the constraint of variation range. Transformer tap is taken as continuously adjustable, so that transformer tap under different states has different solutions.
    5. For each state, generator reactive power generation shall meet its bound constraint. The reactive power generation of generator is taken as continuously adjustable. Generator reactive power generation under different states may have different solutions.
    6. For each state, the current of outage line should meet its bound constraint.

Please refer to Table 6.4 for notations.

Table 6.4 Notations

Notation	Description	Notations	Description
M	Set of all states	$\overline{\boldsymbol{Y}} = (\overline{Y_i})$	Upper limit of vector of VAR sources newly installed
N	Set of all nodes where VAR source can be installed	$[\overline{\boldsymbol{Y}}]$	Diagonal matrix of diagonal elements

Continued

Table 6.4 Notations—Cont'd

Notation	Description	Notations	Description
N_G, N_S, N_L	Set of generator node, balance node, and load node	$C=(c_j)$	Vector of coefficient of variable cost of VAR equipment
g_i	Power flow equation vector of state i	$D=(d_j)$	Vector of coefficient of fixed cost of VAR equipment
$X_i=(X_{ij})$	Continuous variable vector of state i		
$Y_i=(Y_{ij})$	Integer variable vector of state i, that is, number of VAR units installed		
$Y_C=(Y_{Cj})$	Upper limit of vector of new VAR units		
$W_C=(W_{Cj})$	0–1 variable vector of whether VAR equipment are installed		

6.4.2.2 Formulation of multistate problem

The optimization problem of multistate VAR planning here is of a distinctive form—a block diagonal form because there is only one coordinate variable for each state in the VAR planning optimization procedure, and there is only one solution of VAR equipment installation for each state. Such a special structure of the problem suggests the use of a decomposition method. The method proposed here decomposes the whole problem into different subproblems for different contingencies, then solves and coordinates each subproblem to give a VAR installation for the whole large-scale problem.

The objective of multistate VAR planning is to determine the minimum cost installation pattern of new capacitor units. The constraints for multiple states are to be considered jointly in the formulation.

The overall multistate optimization problem (Master Problem: MP) is expressed as a nonlinear MIP problem in the following form:

Master problem MP:

$$\min \ (C^t Y_c + D^t W_c) \tag{6.16}$$

$$\text{s.t. } g_i(X_i, Y_i) = 0 \tag{6.17}$$

$$\underline{X}_i \le X_i \le \overline{X}_i \tag{6.18}$$

$$0 \le Y_i \le Y_C \le \overline{Y} \tag{6.19}$$

$$Y_C \le \left[\overline{Y}\right] W_C \tag{6.20}$$

In this equation, i is the number of states, and $i=1,2,\ldots, M$, where Eq. (6.16) is minimum investment cost, Eq. (6.17) is power flow equation of state i, Eq. (6.18) is the limits for continuous variable of state i, Eq. (6.19) is the relation between the number of VAR equipment already installed and the number of newly installed VAR equipment, and Eq. (6.20) is the relation expression of the fixed cost for newly installed VAR equipment.

The difference between constraint of single state and that mentioned in Section 6.5.2 is that the limit value of line current I is additionally considered in the continuous variable. Power flow Eq. (6.17) of state i in master problem (MP) and construction Eq. (6.18) of continuous variable are given as follows:

$$\underline{P}_j \le P_j(U,\theta,T) \le \overline{P}_j \tag{6.21}$$

$$P_j(U,\theta,T) = P_{js} \tag{6.22}$$

$$\underline{Q}_j \le Q_j(U,\theta,T,C,R) \le \overline{Q}_j \tag{6.23}$$

$$Q_j(U,\theta,T,C,R) = Q_{js} \tag{6.24}$$

$$\underline{U}_j \le U_j \le \overline{U}_j \tag{6.25}$$

$$\underline{I}_{kj} \le I_{kj} \le \overline{I}_{kj} \tag{6.26}$$

$$\underline{T}_j \le T_j \le \overline{T}_j \tag{6.27}$$

For simplicity, subscript i used to describe state-i is omitted in these expressions, and only node symbols of k and j are used.

Master problem Eqs. (6.16)–(6.20) are linearized, with the main linearized problem shown as follows:

The linearized master problem (LMP):

$$\min\ (C^t Y_C + D^t W_C) \tag{6.28}$$

$$\text{s.t. } \boldsymbol{A}_i X_i + B_i Y_i = b_i \tag{6.29}$$

$$\underline{X}_i \le X_i \le \overline{X}_i \tag{6.30}$$

$$0 \le Y_i \le Y_C \le \overline{Y} \tag{6.31}$$

$$Y_C \le \left[\overline{Y}\right] W_C \tag{6.32}$$

where A_i is Jacobi matrix of continuous variable, and B_i is coefficient of integer variable.

With multiple states considered, Eqs. (6.28)–(6.32) will be optimization of large scale. Eq. (6.33) is matrix expression of Eqs. (6.29), (6.31), and (6.32). For simplicity, continuous variable bound does not appear in Eq. (6.34).

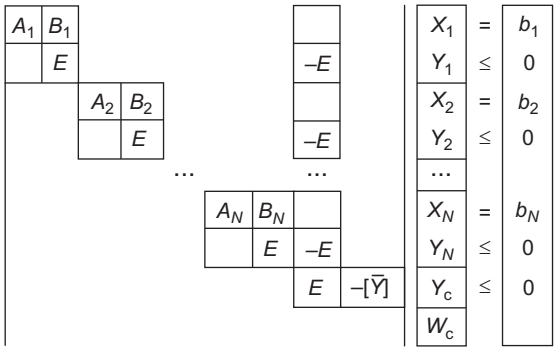

(6.33)

where E is a unit matrix, with blank place as 0. Eq. (6.34) shows that only the upper limit of newly installed reactive power is related to the respective state. If all subproblems are decoupled in feasible region of Eq. (6.31) and Eq. (6.32), they will be considered as coupling variables. Therefore, if coupled variable YC is fixed as Y_C^*, according to Eq. (6.33), it is possible to decompose the problem LMP into several independent subproblems, with the linearized subproblem i described as follows:

Linearized subproblem (LSP)

$$A_i X_i + B_i Y_i = b_i \tag{6.34}$$

$$\underline{X}_i \le X_i \le \overline{X}_i \tag{6.35}$$

$$0 \le Y_i \le Y_C^* \tag{6.36}$$

As Y_C and W_C are fixed on Y_C^* and W_C, and the previous problem has no objective function, so that the previous problem is the feasible solution of Eqs. (6.34)–(6.36). Linearized subproblems are referred to as subproblems in the following subsections.

6.4.2.3 Characteristics of multistate problem

The mathematical expression of multistate model has the following characteristics in programming mathematics:

(1) The number of question variables.
   1. Continuous variable: (system node number $N \times 2$ + generator reactive power generation variable number + tap ratio variable number + generator balancing node active power variable number) × state number.
   2. Discrete variable: the number of capacitor variables $= N_C \times 2 + N_E$.

   A real power system normally contains more than 100 nodes. For instance, if the number of nodes is 135, the number of generators is 36, the number of transformers is 17, the number of newly installed capacitors is 20, the number of existing capacitors

is 29, and the number of states is 7, then the number of continuous variables shall be $(135 \times 2 + 36 + 1 + 17 + 7 = 331) \times 7 = 2317$, and the number of discrete variables shall be $20 \times 2 + 29 = 69$.

(2) The number of problem constraints: (the number of system nodes $N \times 2) \times$ the number of states + the number of capacitor nodes $N_C + N_E$.
If the number of nodes is 135, the number of newly installed capacitors is 20, the number of existing capacitors is 29, and the number of states is 7, then the number of constraints shall be $2 \times 135 \times 7 + 20 + 29 + 7 = 1946$.

(3) Cost function is a linear expression.

(4) Constraint function is a nonlinear function.

(5) Variables are divided into two types: continuous variables and discrete variables, and there is a large number of integer variables.

(6) Both the number of constraints and variables are more than a thousand.

The listed points show that multistate discrete reactive power optimization is an MIP problem of super-large scale.

6.4.3 Overall Solution Procedure of Multistate VAR Optimization

6.4.3.1 Main calculation procedure

Although the algorithm in Section 6.3 can effectively solve a nonlinear MIP problem for a single state, it cannot directly be applied to a multistate problem because of the large numbers of constraint equations and integer variables.

In the solution algorithm of this section, the nonlinearity is resolved by using the successive linearization technique, and the decomposition and coordination techniques are employed to overcome the huge scale of the problem. The approximation algorithm employed in Section 6.3 is also applicable to treat the integral nature of variables.

The generalized overall solution algorithm is shown in the flow chart in Fig. 6.4.

The outline of the solution procedure proposed here is that the multistate VAR planning problem (Master Problem: MP) is decomposed into subproblems (LSP) state by state, and each LSP is solved by using the decomposition and coordination procedure. Further, an improved procedure is employed to enhance the solution. After that, the master problem is linearized again, and this procedure is repeated until a nonlinear solution is obtained. A little more detailed explanation of each procedure is given as follows:

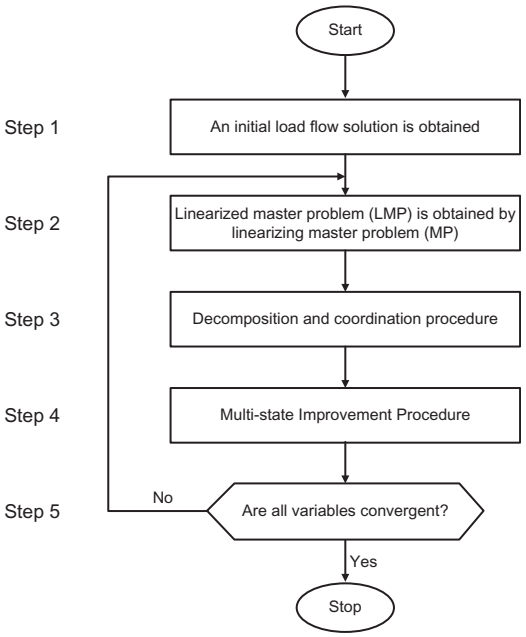

Fig. 6.4
Flow chart of multistate VAR planning algorithm.

Step 1: After formulating the overall nonlinear MIP problem as master problem MP, set iteration count $k \leftarrow 0$; initial solution Z^{k} is calculated according to power flow solution for each state. Here variable Z is defined as follows:

$$Z = (X_1, Y_1, \ldots, X_M, Y_M, Y_C, W_C) \tag{6.37}$$

Step 2: Linearize main problem MP around the point Z^k, and the problem has a diagonal block form, as shown by Eq. (6.34).
Step 3: Fix coordination variable Y_C, and decompose linearized master problem into linearized subproblems. The overall problem (LMP) is decomposed into several linearized subproblems state by state, and each subproblem is solved independently. The results are then coordinated to get solution z^{k+1} for the overall problem (LMP). On this basis, adjust coordination variable Y_C to reduce the infeasibility and objective function of the whole problem, that is, to coordinate solutions of corresponding problems to get the solution of linearized main problem LMP. Detailed explanation will be given in Section 6.4.3.1.
Step 4: Maintain the feasibility of each state, and change the value of coordination variable Y_C, that is, execute multistate integer improvement procedure to further reduce investment cost; two integers are changed simultaneously while maintaining the feasibility of all states. The detailed solution procedure is given in Section 6.4.3.2.

Step 5: The convergence of this procedure is checked, that is, whether $|Z^k - Z^{k+1}|$ meets convergence conditions. If all variables converge, that is, all subproblems converge, then the solution algorithm is terminated. The convergence of all the subproblems means that a solution for nonlinear problem MP has been obtained. Otherwise, $k \leftarrow k+1$ and linearize again, then move to Step 2.

6.4.3.2 Decomposition and coordination within main procedure

This is a key procedure for multistate VAR planning problem. As previously mentioned, linearized subproblem LSP in this section has no objective function, so that it is not applicable to take objective function of ordinary decomposition and coordination procedure as the function of coordination variable. Appendix A shows infeasibility and feasibility of a single state calculated in simplex tableau form.

Table 6.5 illustrates the concept of the decomposition and coordination procedure for a simple example composed of two states. First, here is the basic concept of this procedure.

Under multistate situation, state i has two reactive nodes. Table 6.5 only shows simplex tableau with two basic variables. In Table 6.5, vector x refers to the basic vector of a continuous variable, and vector x_N and y stands for nonbasic vector of a continuous variable and a nonbasic vector of an integer variable, respectively, because the basic concept of the simplex method is that the values of basic variables are expressed as linear functions of nonbasic variables. Therefore, if the nonbasic variables y_j ($j = 1, 2$) are changed, then the basic variables are also changed at the same time, and this sometimes leads to infeasibility of the problem. This nature may be used to define infeasibility and feasibility.

Table 6.5 Simplex tableau of state *i* ($j = 1, 2$)

	Continuous Basic Variable		Continuous Nonbasic Variable		Discrete Nonbasic Variable	
Basic Value	x_1	x_2	x_{N1}	x_{N2}	y_1	y_2
a_1	1	0	c_{11}	c_{21}	d_{11}	d_{21}
a_2	0	1	c_{12}	c_{22}	d_{12}	d_{22}

To simplify the description, assume that:

(1) Table 6.5 is feasible at VAR unit allocation $\boldsymbol{Y}_C^*$.
(2) When y_j ($j = 1, 2$) are independently changed by an amount of ± 1, the following conditions hold:

$$\begin{aligned} &d_{11} < 0, d_{21} < 0, d_{12} > 0, d_{22} < 0 \\ &a_1 - d_{11} > \overline{x}_1 \qquad a_1 - d_{21} > \overline{x}_1 \\ &\underline{x}_2 > a_2 - d_{12} \qquad \underline{x}_2 < a_2 - d_{22} < \overline{x}_2 \end{aligned} \tag{6.38}$$

Based on the situation, one unit of infeasibility degree ($j=1, 2$) is added and defined as follows:

$$\begin{aligned} q_{i1} &= \{[(a_1 - d_{11}) - \overline{x}_1] + [\overline{x}_2 - (a_2 - d_{12})]\} \\ q_{i2} &= \{[(a_1 - d_{21}) - \overline{x}_1] + 0\} \end{aligned} \tag{6.39}$$

Therefore, as shown in Eq. (6.39), the value of q_{i1} is the sum of infeasibilities when the value of y_1 in state-i is increased by one. Assuming the condition in Eq. (6.38) also holds, the feasibility measure h_{ij} is defined as:

$$\begin{aligned} h_{i1} &= \min[(a_1 - \underline{x}_1)/(-d_{11}), (\overline{x}_2 - a_2)d_{12}] \\ h_{i2} &= \min[(a_1 - \underline{x}_1)/(-d_{21}), (a_2 - \underline{x}_2)/(d_{22})] \end{aligned} \tag{6.40}$$

It may be seen from Eq. (6.40) that the value of h_{i1} means that the value of y_1 can be decreased by h_{i1} without making state-i infeasible. Eqs. (6.39)and 6.40) give the simple case with only two integers and two basic variables. This is the foundation for this section to introduce the concepts of multistate infeasibility q_{ij} and feasibility h_{ij}, which will then be used to consider for the coordination procedure.

To illustrate the practical sense of q_{ij} and h_{ij}, as well as decomposition and coordination procedure, in Fig. 6.5, q_{ij} and h_{ij} in each subproblem i represent the infeasibility measure and feasibility measure, respectively. These measures are used to determine the integer variable Y_{cj} to be adjusted in the linearized master problem (LMP). A simple two-state decomposition and coordination procedure is used to illustrate the concept of decomposition and coordination in Fig. 6.6.

Based on this preparation, the decomposition and coordination procedure is shown in Fig. 6.5. Given in the following text is the detailed procedure step by step.

Substep 0: The number of existing and newly installed VAR equipment is determined by the following procedures:

(1) If iteration counter $k=0$, the integer constraints are relaxed, and each subproblem can be solved with LP, then the obtained solution shall be rounded off, and Y_{ij} will be used to determine the upper limit of coordinate variable, assuming that:

$$Y_{Cj} = \max_{i \in M} \left[Y_{ij}\right], \quad j \in N \tag{6.41}$$

(2) If the iteration count $k>0$, the integer solution from the previous iteration may be taken as the initial integer solution for this iteration.

Substep 1: Each subproblem with integer constraints is solved by using the approximation method in Section 6.2, where the value of Y_C is taken as the upper limit of the number of VAR source unit installation. If all of the subproblems ($i=1, 2, \ldots, N$) are feasible, then go to Substep 4. Otherwise, go to Substep 2.

Substep 2: For each of the infeasible states, infeasibility measure q_{ij} is calculated, and infeasibility measure q_j, when Y_{cj} is increased by one, is defined as:

$$q_j = \sum_{i \in N_{\text{inf}}} q_{ij} \tag{6.42}$$

where N_{inf} is the set of infeasible subproblems.

Substep 3: Each of the infeasible states is resolved until they become feasible in the following way: Choose a node with newly installed VAR equipment, and add the number of the VAR equipment by one unit; try to reduce the infeasibility of the problem (as its value is the upper limit of the number of VAR sources, the feasibility of problem may be increased by increasing Y_{C}). To select the most effective node for decreasing infeasibility as much as possible and increasing cost as little as possible, the node u is selected by evaluating the following criterion:

$$q_u = \min_{j \in M} \left[q_j \times r_j \right] \tag{6.43}$$

where r_j refers to change of investment cost, which shall be calculated by this formula:

$$r_j = C_j, \quad \text{if} \quad Y_{\text{C}j} > 0 \tag{6.44}$$

$$r_j = C_j + D_j, \quad \text{if} \quad Y_{\text{C}j} = 0 \tag{6.45}$$

Then, increase the upper limit $Y_{\text{C}u}$ of node u by 1, and its infeasible state shall be resolved with MILP.

Substep 4: Select a node with newly installed VAR equipment, and decrease the number of VAR equipment by one unit to reduce the investment cost of the whole problem. Node u with newly installed VAR equipment shall be selected to reduce the investment cost as much as possible with the feasibility of each subproblem maintained. For each state in which the number of VAR units installed is equal to the upper limit (i.e., $Y_{ij} = Y_{\text{C}j}$), the feasibility h_{ij} ($h_{ij} > 0$, i is symbol of state, j refers to the serial number of reactive power node) shall be calculated. Then, the following equation will be applied to the calculation of h_j:

$$h_j = \sum_{i \in N_{\text{act}}} h_{ij} \tag{6.46}$$

where N_{act} is the set of states in which the number of VAR units installed is equal to the upper limit.

Substep 5: Choose the most promising node u with the following equation to improve the solution:

$$h_u = \max_{j \in M} \left[h_j \right] \tag{6.47}$$

Then, decrease Y_{Cu} by 1, that is, $Y_{Cu} = Y_{Cu} - 1$. On this basis, the MILP algorithm shall be used to resolve each state in which the number of VAR units installed is equal to the upper limit. If there is no infeasible state, accept the new solution. Otherwise, abandon the solution of Y_{Cu}.

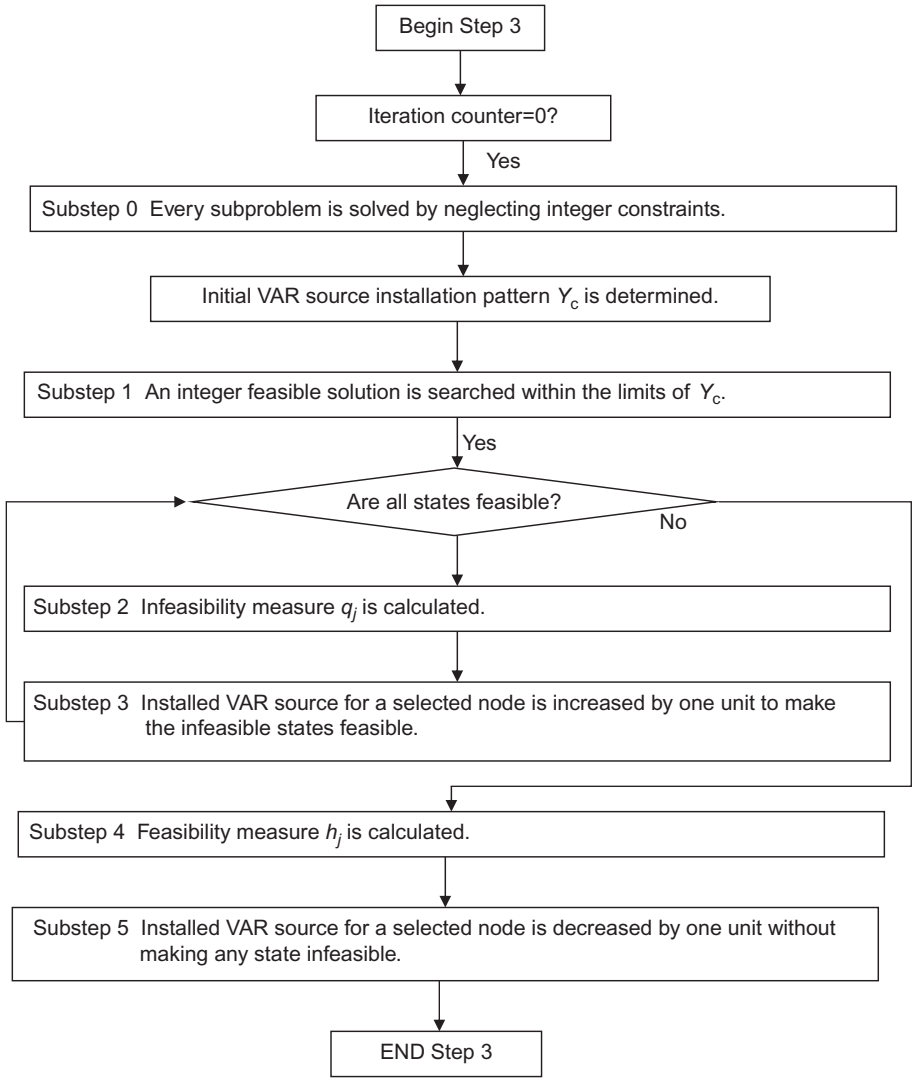

Fig. 6.5
Decomposition and coordination procedure.

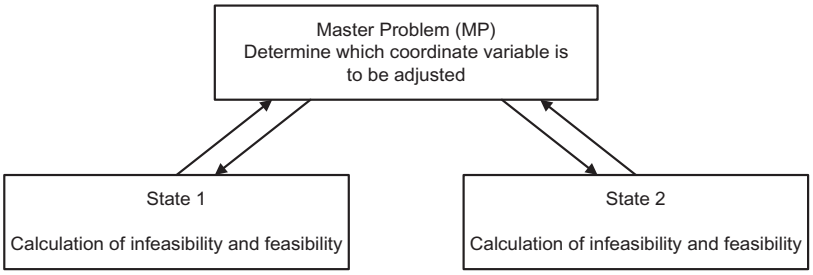

Fig. 6.6
Schematic diagram of decomposition and coordination procedure.

6.4.3.3 *Improvement of integer variables within main calculation procedure*

In the previous section, integer variables are changed one by one, making it not satisfactory in reducing fixed cost and requiring further improvement. This section introduces integer improvement procedure in detail whose principle is similar to the integer improvement procedure introduced in Section 6.2. However, this principle emphasizes selection among states. To obtain a practical solution and to further decrease the installation cost, two integers are changed simultaneously while keeping the feasibility of the overall problem. To accomplish this, the improvement procedure is divided into two stages. In Stage I, for the purpose of computational efficiency, the infeasibility is checked by using the simplex tableau without executing pivot exchange operation. In Stage II, the most promising (but likely infeasible) pair is tried by resolving the MIP problem to find a feasible solution.

Stage I: Select one pair of integers for infeasibility calculation. As the number of LPs is calculated based on the number of states $\times$ the number of reactive power nodes, infeasibility is only expressed as simplex in the calculation without the pivoting operation to improve calculation efficiency. If a pair of integers can be chosen, then plus one to one integer and minus one from another. If a pair of integers cannot be chosen, rank the infeasibility of each pair of integers, and move to Stage II.
Stage II: Choose the most possible pair of integers, that is, the pair of integers with lowest infeasibility, and solve the problem with MILP method. If it is feasible and the integer solution is improved, then accept the integer solution; otherwise, abandon the integer solution.

6.4.4 *Implementation*

The algorithm is implemented with LP package HITACMPS-II. Numerical calculation is carried out on the same 135-node practical system as in Section 6.3. In the test system, all

transmission lines are double-circuit lines. System design normally shall meet $N-1$ condition, however, outage states considered in this section consist of double outages of line and generator, that is, meeting $N-2$ condition.

As a preliminary test, two cases are used in calculation, where the double outages on a single-circuit and a generator are selected as contingency conditions. Table 6.6 shows Case 1 with five double outages, and Table 6.7 shows Case 2 with seven double outages. CPU calculation time of Case 1 is approximately 3 min, and Case 2 is about 5 min. For planning problems, the calculation time is acceptable.

Table 6.6 Outage states of Case 1

State Number	Outage Line	Outage Generator
1	104–110	Node 27
2	95–96	Node 31
3	96–102	Node 22
4	75–76	Node 36
5	71–75	Node 37

Table 6.7 Outage states of Case 2

State Number	Outage Line	Outage Generator
1	104–110	Node 27
2	95–96	Node 31
3	96–102	Node 22
4	75–76	Node 36
5	71–75	Node 37
6	104–110	Node 25
7	102–103	Node 25

For comparison, the two cases are solved independently and coordinately, and the results are shown in Tables 6.8–6.11, respectively. A row labeled "Y_C" in the table indicates the maximum number of VAR units at the node; a column labeled "Sum of units" indicates the total number of units in each state.

Results of Case 1 are listed in Tables 6.8 and 6.9. Table 6.8 shows integer solutions of the decomposition and coordination algorithm. Table 6.9 lists integer solutions obtained with independent solution method. The values in "sum of setting" column of Table 6.8 are larger than that in Table 6.9. However, the values in "Y_C" column are smaller than that in Table 6.9. These tables show that the installation cost obtained by decomposition and coordination algorithm is less than that by independent solution method.

Results of Case 2 are shown in Tables 6.10 and 6.11. Table 6.10 shows integer solutions of the decomposition and coordination algorithm, whereas Table 6.11 shows the integer solutions by independent solution method. Similarly, the values in "sum of setting" column in Table 6.10 are larger than that in Table 6.11. However, the values in "Y_C" column are smaller than that in Table 6.11, that is, installation cost is smaller by decomposition and coordination algorithm.

The results of Case 1 show that results of the algorithm proposed is better than independent solution method in the number of newly installed nodes, as well as the number and cost of newly installed VAR nodes. The results of Case 2 show that the algorithm proposed obtains a better solution in the number and cost of newly installed VAR nodes, even if the same number of newly installed VAR nodes is selected.

To further explain the coordination procedure, Table 6.12 shows the detailed process of total infeasibility reduction in the first iteration of Case 1:

(1) With integer constraint conditions relaxed, each state will be separately solved by LP. On this basis, integer solutions of each state will be rounded off, and the maximum value of integers under each state will be taken as the initial integer solution.
(2) Under initial integer constraint, MILP algorithm in Section 6.3 will be used to solve all states. At the moment, States 2, 4, and 5 are found infeasible, leading to a total infeasibility of 0.336.
(3) Coordinate each state: Calculate the infeasibility q_{ij} of each infeasible state, then calculate total infeasibility q_j. According to q_j, node 75 is the node that can minimize the infeasible q_{ij}; set new VAR unit at the node; repeat the previous procedure, until all states are feasible, that is, total infeasibility is 0.
(4) Improvement of integer solution: Select a pair of nonzero integers, and add one of the integers by 1 and reduce another by 1, so as to reduce the fixed costs (Table 6.13).

Table 6.8 Results of Case 1 by coordinated solution method

State	Node No.										Sum of Setting
	74	75	82	95	97	99	101	102	106	123	
1					1			6	2		9
2		2	1	7	2	1	7	7			27
3				7				2			9
4	1	2	1	2	2	1	7	7	1	1	25
5	1	2	1	1	2	3	1	1	2	2	16
Y_C	1	2	1	7	2	3	1	7	2	2	28

Table 6.9 Results of Case 1 by independent solution method

State	Node No.												Sum of Setting
	74	75	82	95	97	99	101	102	104	106	110	123	
1								3	2	2			7
2		3		7	2		7	7					26
3				7									7
4	1	3						2		3		1	10
5	1		3			2					6	3	15
Y_C	1	3	3	7	2	2	7	7	2	3	6	3	46

Table 6.10 Results of Case 2 by coordinated solution method

State	Node No.												Sum of Setting
	59	74	75	80	82	95	97	101	102	104	106	123	
1			1			1			3	2	1		8
2	2		2	1	1	7	2	7	7				29
3						7			2				9
4	2	1	5	1	2				1	2	1	1	16
5	2	1	2	1	1	2	2	5	7	3	1	2	29
6		1	2		1	1	1	1	7	3	1	2	20
7		1	2		1		2	4	7	3	1	2	23
Y_C	2	1	5	1	2	7	2	7	7	3	1	2	40

Table 6.11 Results of Case 2 by independent solution method

State	Node No.												Sum of Setting
	74	75	82	95	97	99	101	102	104	106	110	123	
1								3	2	2			7
2		3		7	2		7	7					26
3				7									7
4	1	3						2		3	1		10
5	1		3			2					6	3	15
6	1	3						6	6			2	18
7	1	3						5	3	1		2	14
Y_C	1	3	3	7	2	2	7	7	6	3	6	3	50

Table 6.12 Coordination process of Case 1

Infeasible State No.	Sum of Infeasibility	New VAR Node Number
2,4,5	0.336	75
2,4,5	0.136	99
5	0.093	99
5	0.060	110
5	0.046	99
5	0.011	123
5	0.00085	123
—	0.0	—

Table 6.13 Investment costs of VAR sources

Cases	Methods	The Number of New VAR Node	The Number of New VAR Banks	Investment Costs (10,000 yuan)
1	Decomposition and coordination	10	28	50.8
	Independent	12	46	66.6
2	Decomposition and coordination	12	40	60.2
	Independent	12	50	70.6

Because the algorithm is an approximation algorithm and the multistate VAR optimization problem is nonconvex, the optimal solution obtained is related to the initial value. To verify the algorithm, Table 6.14 shows different cases with different initial settings (VAR installation units and tap ratio) and the results by different methods (decomposition coordination and independent solution). Table 6.14 also shows that, under any different initial conditions, all of the investment cost obtained by the decomposition coordination are less than that of the independent solution.

Table 6.14 Comparison of the effects of different initial values on results

Initial Value		Decomposition Coordination		Independent Solution	
VAR Installation	Tap Ratio	The Number of Installation Nodes	Investment Cost (10,000 yuan)	The Number of Nodes	Investment Cost (10,000 yuan)
0.0	1.0	7	40.8	9	48.8
0.0	0.98	7	43.8	8	48.8
0.01	1.0	7	42.8	10	53.9
0.01	1.01	8	44.7	10	55.7
0.02	1.0	8	44.7	10	57.1

Table 6.15 shows the voltage limit and voltage margin of Case 1 before and after optimization. Voltage margin is the difference between voltage solution and voltage limit, where voltage limits of each state is 0.95–1.05. Before optimization, there is an initial voltage over limit for all states. After optimization with decomposition and coordination algorithm, the over limit value of voltage is eliminated, and average voltage margin is increased to 0.03 (per-unit value).

Table 6.15 Improvements of voltage margin

State	Items	Initial Value	Optimal Solution	Improvement of Voltage Margin
1	Over limit value	0.01207	0.0	0.0
	Voltage margin	—	0.03050	0.04257
2	Over limit value	0.02436	0.0	
	Voltage margin	—	0.03110	0.05546
3	Over limit value	0.02268	0.0	
	Voltage margin	—	0.03110	0.05378
4	Over limit value	0.00862	0.0	
	Voltage margin	—	0.03420	0.04282
5	Over limit value	0.01811	0.0	
	Voltage margin		0.03344	0.05155

6.4.5 Summary

In this section, the decomposition coordination algorithm for multistate discrete VAR optimization is proposed. The multistate discrete VAR optimization is a large-scale MIP problem, which can hardly be directly solved. The integer-feasible solution of each state is separately solved by decomposing each state based on a fixed number of VAR units under all power flow states. When the state is not feasible, the VAR units are used as a coordination variable to integrate the maximum VAR units needed for each state, so as to effectively solve the multistate optimization problem.

In the successive linearization, the step limit for the solution should have been initially set, but it is not necessary because of the planning problem. To obtain a nonlinear solution, the introduction of step limit for the successive linearization solution is necessary. However, when the step limit of the solution is added, the number of iterations in successive linearization is increased, thus, the computational effort is increased. This issue is fully considered in this chapter.

6.5 Discrete VAR Optimization based on Expert Rules

6.5.1 Overview

The basic algorithm used in this section is to approximately solve the MINLP through solving the MILP problem with iterations of LP. The algorithms in the first three sections mainly focus on the MINLP algorithm itself. To implement the algorithm, mathematical programming

system with complete functions is used. Calculation results show that the algorithm is able to perfectly deal with the discrete VAR optimization problem.

The algorithm in this section is, in fact, closely related to functions of a programming system. If a mathematical programming system capable of running on a mainframe computer is not available, for the convenience of applying the algorithm, the mathematical system used in this section is a LP programming program package that can be operated under existing PC conditions. At present, such a programming package does not have some functions that a mainframe computer LP programming system possesses, so it is impossible in the LP calculation to return to specified base and change constraints or modify the fixed value of a variable. Thus, each time an integer is changed, it is necessary to recalculate the LP once more, increasing the computational effort, as the algorithm itself is still valid.

Sections 6.3 and 6.4 of this chapter focused on the effectiveness of the algorithm, that is, finding the discrete feasible solution under the condition without limiting the initial value too much, so it is unnecessary to have a discrete feasible initial value. It is well known that the optimization problem, once described as a mathematical problem, is the most pressing problem to find the solution. To satisfy some strict conditions, such as convexity and continuous differentiable, the nonlinear optimization algorithm can only obtain the local optimal solution. Therefore, for the algorithm adopted in this section, the results must be related to the initial value. Generally speaking, a better initial value can simplify and speed up the solution process and increase the possibility of finding discrete feasible solutions. Therefore, it is necessary to further study the initial value selection method.

An expert system can help solve some problems that cannot be solved with analytical mathematics, which is of great importance in recent years. Study of the application of an expert system in power system calculation combines the expert system with a traditional optimization algorithm, which is able to solve some problems that are difficult to solved with a traditional optimization algorithm; it can also reach better solutions than those obtained with traditional optimization algorithms. However, so far, there are no researchers who noticed that expert rules may be used to seek initial values. Based on real physical background on power systems, it may sometimes find better initial values that cannot be given by analytical mathematics.

To achieve better initial value, the concept of expert rules is introduced in this section to solve the rounded-off problems of the integer initial value of transformer ratio and reactive power compensation equipment. This section determines what kind of rounded-off method to use depending on the degree of fuzziness of integer initial value, that is, a simple rounded-off method or an expert rule based on a rounded-off method. The rounded-off method based on expert rules judges the transformer type according to the direction of active power flow, then determines whether the tap ratio shall be geared up or geared down according to node voltage. This method reduces the possibility of voltage violation after the gearing of tap ratio, shortens calculation time, and lays a solid foundation for further finding of discrete solution.

Basic procedure of the algorithm in this section: First set the power flow initial value, then determine discrete solution with continuous operation and expert rules; eventually calculate optimized power flow. If there is still violation variable with optimized power flow, then the algorithm in Chapter 4 will be used to carry out the calculation. Shown by calculation results with the help of expert rules, there is no violation variable in optimized power flow calculation results. The algorithm in this section is very pragmatic, which improves the possibility of finding a feasible solution.

6.5.2 Necessity of Introducing Expert Rules

In reactive power optimization calculation, setting of transformer ratio is very important. It is held in previous studies that transformer ratio may be taken as a continuous variable, so that the adjustment range of each tap position is small, such as 0.25%, then obtain the discrete solution by truncating it. However, when the number of tap ratios increases, such as 106 adjustable tap ratios in the test system in this chapter, a qualitative change will be elicited by quantitative change. Thus, the truncated solution processed with the method is sometimes infeasible. There are two types of transformers: step-up and step-down transformers. However, this is not differentiated in input data, and their calculation model are not different either, which is always the case in both power flow calculation and optimization calculation. As the reverse transmission of reactive power is likely to occur, then the voltage at the receiving end may be higher than that of the sending end. Thus, it is impractical to judge whether it is a step-up transformer or a step-down transformer simply with the voltage drop method. Active power flow method must be used to identify the type of transformer: the transformer with active power flow flowing from low voltage end to high voltage end is taken as a step-up transformer, whereas a transformer with active power flow flowing from high voltage end to low voltage end is taken as a step-down transformer.

In a power flow calculation, tap ratio position and the number of VAR source installations are given manually. However, in a continuous optimization calculation, the position and number of VAR installations are figured throughout calculation. In the end, there is also the problem of truncation. Generally, in continuous reactive power optimization calculation, transformer ratio and capacitor bank number are truncated following a round-off principle, and the calculation ends there. Such purely truncation method does not take into consideration the relation between tap ratio and voltage, so it is hard to avoid voltage violation at the corresponding node after tap ratio truncation. In this chapter, the approximation MIP method also uses an initial integer solution obtained with truncation method as the initial value, then finds the integer solution close to optimum.

In accordance with fuzzy mathematics, fuzzy numbers close to 0.5 have the highest fuzziness degree. That is, membership function values of 0.49 and 0.51 are quite close, which cannot be

used to judge the gearing direction in case of integer truncation. According to a simple tail-off method, 0.49 is 0, and 0.51 is 1. However, real projects are not that simple. Such a simple tail-off method may lead to a result where the number of reactive power compensation equipment installed or the direction of adjustment of transformer tap position may be different from expectation, which may further lead to voltage violation, increasing calculation time, and reducing the possibility of obtaining integer solution. Expert rules may help judge truncation direction, and it is possible to obtain an integer-feasible solution faster.

6.5.3 Algorithm based on Expert Rules for Discrete VAR Optimization

6.5.3.1 Basic procedure of the algorithm

As described in Section 6.6.1, selecting a different objective function does not affect the structure of the algorithm but has different expression and leads to different solutions. However, sometimes two objective functions are contradictory: to minimize the investment cost may increase the operating cost (such as network loss), but minimizing network loss may increase the investment cost. Practical engineering calculations are restricted by many conditions, which have to consider multiple aspects. Thus, practical engineering calculation requires VAR optimization with at least two different objective functions, so that planning engineers may make comparisons. Discrete VAR optimization in this section takes into account two objective functions: investment cost and active power grid loss.

Objective function of discrete VAR optimization:

(1) Minimization of VAR investment costs – investment planning for VAR sources; the objective function expression is the same as that in Section 6.3.
(2) Minimization of network power loss – optimization of VAR unit operation; the objective function expression is:

$$\min\left(\Sigma P_{\mathrm{S}}\right) \tag{6.48}$$

P_{S} is active power variable at balancing node. Because grid loss is calculated based on the sum of active power output minus the sum of active power load, to minimize active power output at the balancing node is equivalent to minimizing total active power grid loss.

In addition, different weight coefficients are taken for the previous objective functions to form discrete VAR optimization objective functions, which can take both the grid loss and investment cost into consideration. One of the objectives can be treated as constraint in optimization calculation, and a multiobjective problem may as well be transformed into a single objective problem. Weight coefficient and transformation method are involved in another research field. This section focuses on discrete optimization with a single objective.

Constraints of discrete VAR optimization are:

(1) Node reactive power and active power flow equations.
(2) Generator voltage limits.
(3) Reactive generation limits.
(4) Transformer tap setting limits for all adjustable tap position.
(5) VAR limits for the new installation nodes.
(6) VAR limits for the existing installation nodes.

Except for the expression of adjustable transformer tap position, the constraint expressions are the same as those in Section 6.3. In this section, the capacitor bank number and transformer ratio number in real-scale distribution system are treated as discrete adjustable equipment.

Taking into consideration a planning engineer's practical demand, the algorithm is divided into five major steps:

Step 1: Perform power flow to provide initial value before optimization.
Step 2: Calculate continuous optimization with relaxed integer constraints.
Step 3: Obtain discrete solution based on expert rules, and fix the discrete solution.
Step 4: Perform power flow after optimization.
Step 5: If some over limits occurred in the power flow solution after optimization, then execute the algorithm in Section 6.2;

To obtain discrete solutions, Steps 1–4 may be executed first; if the results are infeasible, execute Step 5.

Through Steps 1–4, the power flow after optimization has been improved both in grid loss or over limit values compared with that before optimization.

6.5.3.2 Way of processing transformer tap ratio

The mathematical model for the tap ratio in this section is the same as that in previous sections. The only difference is the calculation method of tap position number. In the calculation, the tap ratio number is expressed by the practical expression method corresponding to the real equipment. That is, the upper limit of tap ratio corresponds to the highest tap position number 1, and the lower limit corresponds to the lowest tap position number N. The variation range of integer tap ratio number Y_T is $[1, N]$. The expression of tap ratio T based on tap position number shall be:

$$T = \overline{T} + (1 - Y_T)\Delta T$$

where Y_T—optimal solution of tap position number; $\overline{T}$—upper limit of tap ratio; ΔT—unit step size of tap ratio.

For example, if U_N(kV) in the nameplate of a certain transformer is $110 \pm 2 \times 2.5\%/11$, variation range of its tap ratio number T shall be [0.95,1.05], and variation range of tap ratio

number Y_T shall be [1,5]. In the example, when Y_T is 3, the corresponding T shall be 1.0. Tap position number Y_T will directly be given in the optimization solution. Refer to Table 6.16 for the relations between Y_T and T.

Table 6.16 Relations between Y_T and T

Y_T	T	Tap Position
1	1.05	+2
2	1.025	+1
3	1.0	0
4	0.975	−1
5	0.95	−2

Note: $\Delta T = 0.025$.

6.5.3.3 Detailed calculation steps

The overall calculation procedure of this section consists of five steps, as shown in Fig. 6.7. Detailed procedure is given in the following section.

Step 1: Obtain the initial value by executing power flow before optimization calculation. The power flow solution of the planned system must be convergent, as it is not always feasible since there is an over limit value. The solution with flat start-up point cannot be taken as initial value for optimization calculation.
Step 2: Solve VAR optimization problem with the integer constraint relaxed by the SLP method, which could provide a continuous optimal solution for the problem. If the problem is not feasible, execute the expert rules in Section 6.5.3.5 to make it feasible.
Step 3: Determine the integer-feasible solution by the expert rules in Section 6.5.3.5. Based on the analysis of results, such as the results for the power flow and the results from the SLP, it can help the system engineer determine the discrete solution of capacitor banks and transformer tap ratio. According to the voltage and active power at transformer node, and the voltage at the capacitor node, the most appropriate integer value can be obtained in this step.
Step 4: Calculate the power flow based on optimization results after determining the discrete solution. At this stage, the resulting integer solution may not be feasible; if it is infeasible, perform the next step, or make some adjustments manually, and calculate the power flow again. Obtain a discrete feasible solution by performing the SLP in the second phase.
Step 5: Take the results of Steps 1–4 as an initial value, and execute the MINLP algorithm proposed in Section 6.3.

6.5.3.4 Rules of making LP solution feasible by relaxing integers

For a new planned system, it is difficult to obtain a convergent initial value from its power flow solution. Similarly, it is also difficult to obtain its LP feasible solution. The reason is varied, such as data, inappropriate constraints, and so on. The LP program applied in this

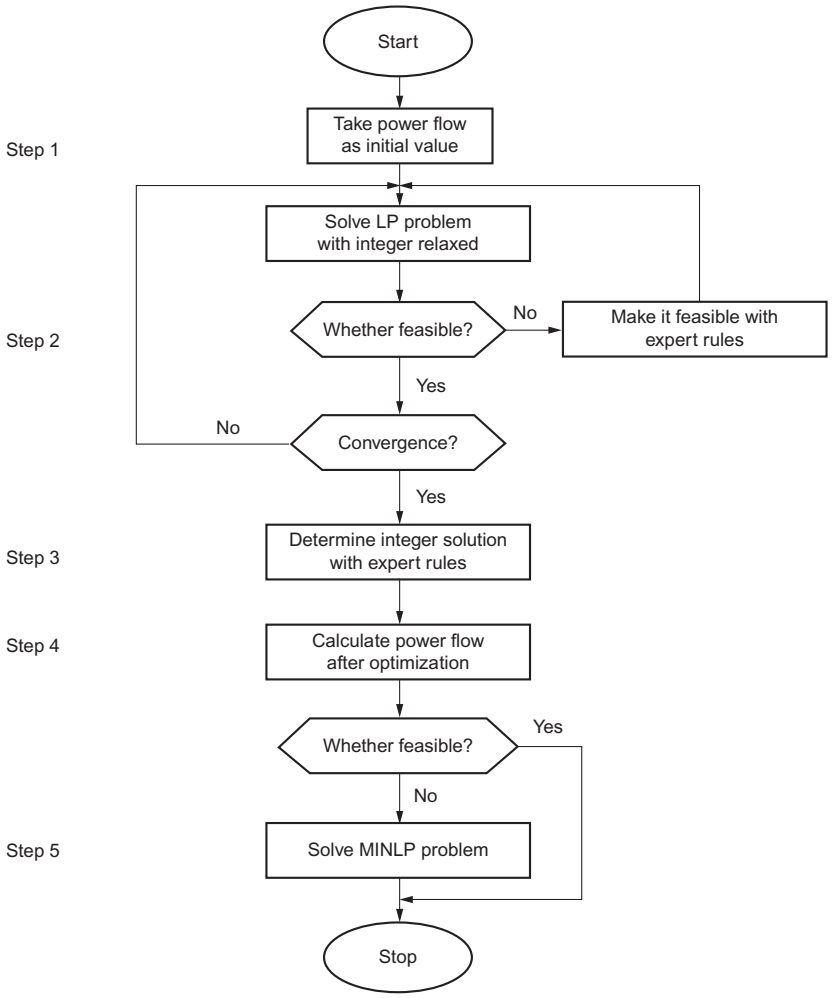

Fig. 6.7
Flow chart of discrete VAR optimization algorithm based on expert rules.

chapter can provide constraints and variables when LP is not feasible. Although the over limit value of the linear solution is different from the one of the nonlinear solution, the algorithm first requires obtaining the linear feasible solution.

The purpose of applying an expert system approach is to make the relaxed solution feasible. The expert system is established and implemented from practical experience and knowledge of system planners and operators. The following rules are used when searching for a feasible relaxed solution, which comes from practical experience.

Rule 1. If the Q constraint of node i is over the upper limit, then (1) change the voltage limits of the node, if possible; (2) change the voltage limits of the adjoining nodes; (3) install new capacitors at this node, if possible; or (4) install new capacitors at adjoining nodes, if possible; otherwise (5) change the tap position limit, if possible, which is equivalent to changing transformer settings.
Rule 2. If the Q constraint of node i is below the lower limit, then (1) change the voltage limits of the node, if possible; (2) change the voltage limits of the adjoining nodes; or (3) check the input data; otherwise (4) change the tap position limits, if possible.
Rule 3. If the linearized P equation of node i is unbalanced, then (1) check the related node data and line data, and (2) change the voltage limits, if possible.
Rule 4. If the linearized Q equation of node i is unbalanced, then (1) check the related node data and line data; (2) change the voltage limits, if possible; and (3) install new capacitors or change the new tap position, if possible.

6.5.3.5 Rules to determine integer variables for tap ratio

The basic idea of expert rules is to consider the relationship between tap ratio and voltage to keep voltage within the limits after the gearing of tap ratio. The rule is not complicated and is helpful in reducing voltage violation. Expert rules introduced in this section are: first, determine whether the transformer is a step-up or a step-down transformer according to the active power flow direction; then, determine transformer tap position according to voltage bound, which reduces the possibility of voltage violation after transformer tap position adjustment and lays a solid foundation for finding subsequent discrete solution.

As previously mentioned, the main basis for the rules given in this section is the relation between the active power flow direction and the tap ratio and voltage, and the rounded-off value is determined based on the position of the integer solution. According to fuzzy mathematics, values around 0.5 are fuzzy, and it is hard to determine the transformer tap gearing direction with integer initial value truncation. Simple round-off truncation leads to the same results as that of expert rules. Thus, the following rules only determine truncation with tap ratio number Y_{T} within the range of fuzzy values.

Suppose that a transformer is located between node i and node j, where i is the fixed side and j is the changeable side for this transformer. When $y_{T_k} = 1$, the tap is located at the highest position; otherwise, the tap is located at the lowest position. The following rules to set taps are formulated after obtaining a relaxed solution:

$$T_k = \overline{T_k} + (1 - y_{T_k})\Delta T_k$$

Rule 1. If the tap is changeable, calculate the tail setting of the continuous solution Y_{T} and its decimal value ΔY_{T}.

Rule 2. If ΔY_T is located outside $[a, b]$, that indicates that it will not be a fuzzy number. Therefore, rounded-off tap position number Y_T would be an integer solution, and it would be unnecessary to apply the expert rules. Normally, $a = 0.3$, $b = 0.7$.

Rule 3. If ΔY_T is located inside $[a, b]$, that indicates that it would be necessary to judge whether the transformer is a step-up or step-down transformer.

Rule 4. If the transformer branch power $P_{ij} > 0$, then it is a step-up transformer. Check whether the voltage on the j side is located above or below the average voltage. If it is above the average value, integer solution of $Y_T = \text{INT}(Y_T) + 1$; if it is below the average, integer solution of $Y_T = \text{INT}(Y_T)$.

Rules 5. If $P_{ij} < 0$, then it is a step-down transformer. Check whether the voltage on the i side is located above or below the average voltage. If it is above the average value, integer solution of $Y_T = \text{INT}(Y_T)$; if it is below the average, integer solution of $Y_T = \text{INT}(Y_T) + 1$.

Note: $[a, b] = [0.3, 0.7]$. INT means a function converting a floating number to an integer. After Y_T is decided, then tap T is calculated by Eq. (6.49).

Capacitor bank number may as well be judged with similar rules.

6.5.4 Implemetation

To validate the expert rules proposed, two test systems are used in this section: one is a 5-node system, and another is a 230-node real system. LP software used is STYR-PC/LP2.1 developed by computing center, Chinese Academy of Sciences. The LP software has passed the assessment of main test systems in LP library, which is stable and reliable.

6.5.4.1 Verification by 5-Node test system

The parameters and structure of the 5-node system are shown in the example of Section 4.8.1. The system consists of two adjustable tap ratios and three capacitors. The comparison of both solutions, one based on rounded-off expert rules and another is only based on rounded-off conditions, in Tables 6.17–6.19 shows that there is only a slight difference between the two solutions, as shown in Table 6.18. However, the final results are quite different. For example, voltage variables under simple rounded-off condition in Table 6.17 have over limits.

Table 6.17 Node voltage solutions (kV) of 5-node test system

Node No.	1	2	3	4	5
Expert rules	10.5	10.5	110.42	119.50	115.95
Simple rounded-off	10.5	10.5	112.69	120.09	118.16

Table 6.18 Transformer tap location solutions (per-unit value) of 5-node test system

Node *I* – Node *J*	Expert Rules	Simple Rounded-Off
1–4	0.95	0.95
2–5	0.925	0.95

Table 6.19 VAR source solutions (group) of 5-node test system

Node No.	3	4	5
Expert rules	10	6	8
rounded-off	10	6	8

6.5.4.2 230-Node practical system

Fig. 6.8 shows a 230-node practical system, with basic calculation conditions given in Table 6.20. All initial values and constraints are given by the planning engineer.

Under the 1995 forecasting load conditions given in Table 6.21, expert rules and a simple rounded-off method are used to obtain tap ratio position and capacitor bank number. $\Sigma\Delta U$ (per-unit value) in the table is the sum of absolute value of voltage violations, and $\max\Delta U$ (per-unit value) is the maximum value of voltage violations. Table 6.21 shows that the effect of expert rules is obvious, because both the amount and quantity of constraint violations are smaller. Results of Case 952D show that integer-feasible solution can be obtained by expert rules alone.

Fig. 6.9 shows comparison of initial tap ratio, optimal tap ratio, and rounded-off tap ratio. From Fig. 6.9A, only 10% of tap ratio solutions obtained by expert rules are different from rounded-off ones. However, the effect of expert rules is quite different, as shown in Table 6.21. Fig. 6.9B and Fig. 6.9C show that the initial tap ratio must be changed to meet the requirement of the voltage level.

Table 6.22 shows that the initial number of nodes and costs for VAR allocation are greatly reduced through discrete VAR optimization calculation. All calculation cases demonstrate that discrete VAR optimization calculation can reduce VAR investment costs and installation capacity.

Table 6.23 shows the number of nodes at which VAR sources are initially installed. However, the node number after optimization is different from the original node. In addition to existing and newly installed VAR sources, VAR optimization calculation also must consider adding new VAR units to existing nodes. This can be easily done with the algorithm proposed in this section. “Original nodes” in the table refers to the nodes at which the original VAR units are installed. “Original+new” refers to adding new VAR unit to the original VAR nodes. “New nodes” refers to new VAR nodes. All calculation cases show that discrete VAR optimization calculation is able to reduce the number of VAR installation nodes.

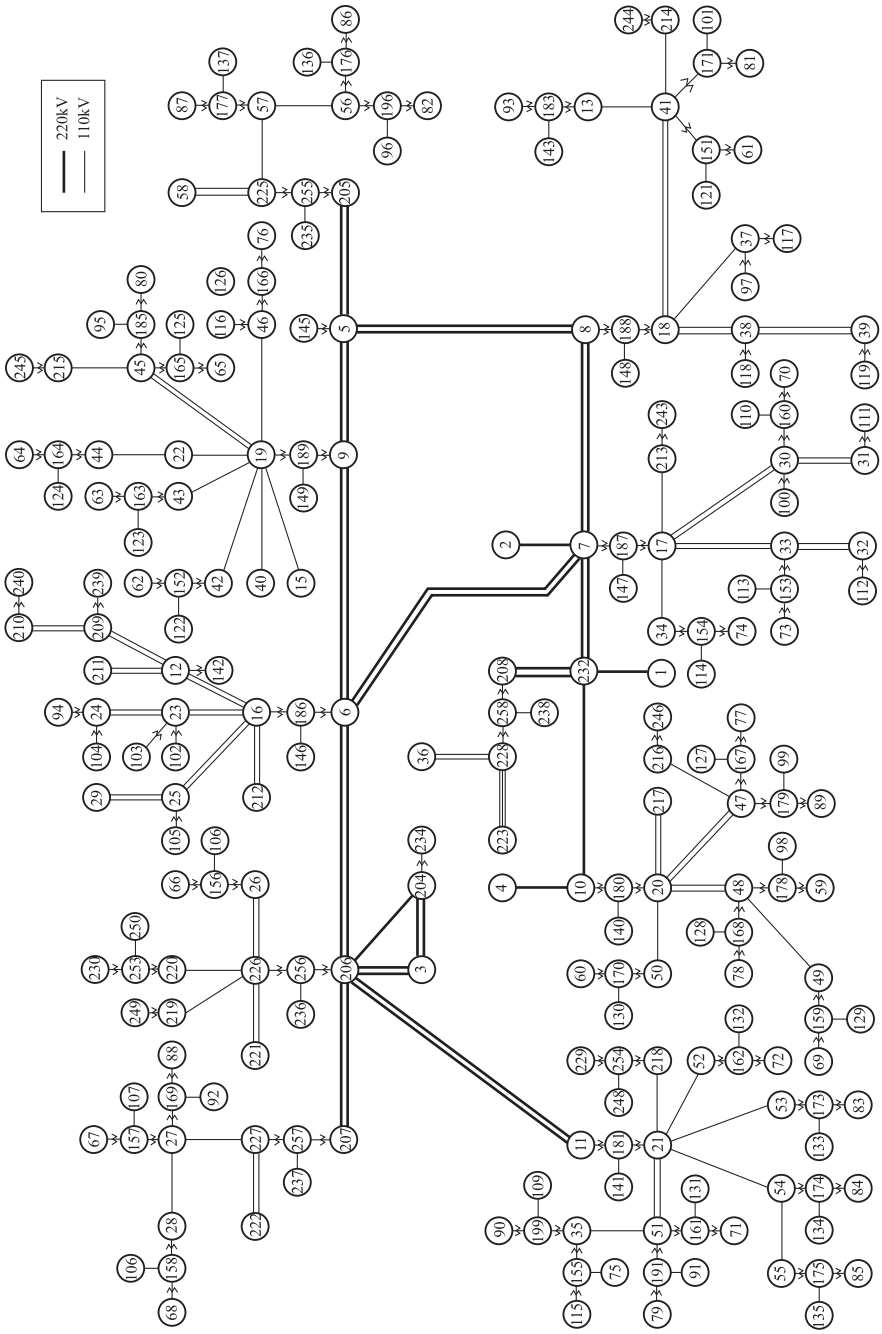

Fig. 6.8
230-Node system.

Table 6.20 Basic calculation conditions for the algorithm based on expert rules

The Number of Nodes	The Number of Branches	The Number of Variable Tap Ratios	The Number of Capacitor Nodes		
230	270	105	59		
			Original nodes 30	Original + new 10	New nodes 19

Table 6.21 Comparison of constraint violations

Case Name	Expert System – Violation Value		Only Rounded-Off – Violation Value	
	$\Sigma\Delta U$ (p.u.)	$\max\Delta U$ (p.u.)	$\Sigma\Delta U$ (p.u.)	$\max\Delta U$ (p.u.)
951D	0.2409	0.0257	0.2954	0.0207
951X	0.2108	0.0172	0.3148	0.0310
952D	0.0464	0.0097	0.3731	0.0279
952X	0.2736	0.0221	0.2826	0.0236

Fig. 6.10 shows the comparison between the original and the new capacitor bank number. To simplify, the system nodes are ranked in such a sequence: nodes 1–31 are existing capacitor nodes, nodes 32–43 are mixed nodes with both old and new capacitors, and nodes 44–64 are new capacitor nodes. According to the optimization calculation results, more existing capacitors shall be installed in nodes 1–31, less new capacitors installed in nodes 32–43, and fewer new capacitor nodes installed in nodes 44–64.

The partial planning results of large mode and small mode in winter-summer in 1995 are listed in Tables 6.24 and 6.25, respectively. In the tables, ΔP_z is total grid loss (MW), ΔP_{110} is 110kV grid loss (MW), and COST is investment (10,000 yuan).

Tables 6.24 and 6.25 show that the results of VAR optimization procedure are much better than manual planning results. With investment minimization as the objective, investment costs are greatly reduced. Moreover, grid loss is also less than that with manual planning. If power loss minimization is taken as the objective, grid loss will be further reduced. However, the cost of investment on VAR units will be increased. The objective of investment minimization can help to reduce initial investment but lead to a higher operating cost in a long-term operation. By contrast, with power loss minimization as the objective, operating conditions will be improved, and long-term operating costs will be reduced. However, initial investment has to be increased. How to make a trade-off between the two factors? Planning personnel can perform further economic and technical analysis according to capital source, operating characteristics, and manpower allocation, etc.

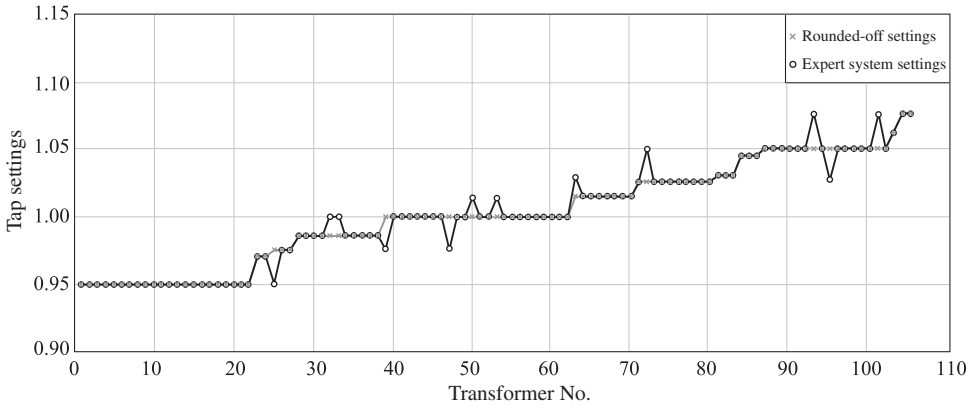

(a)

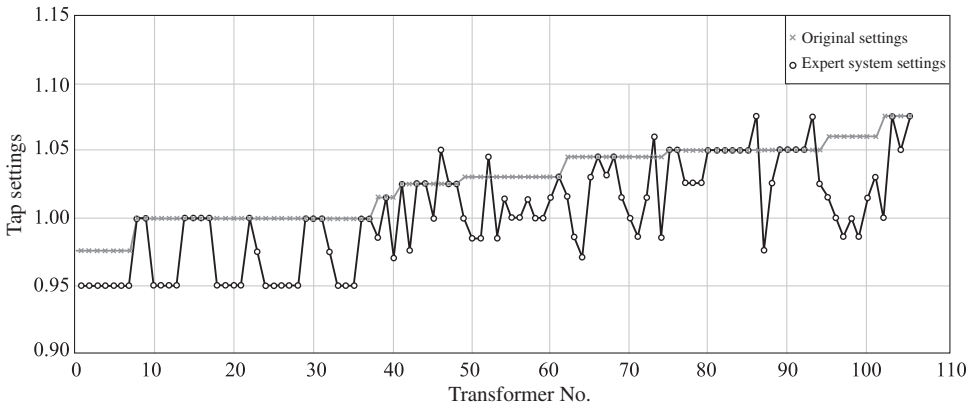

(b)

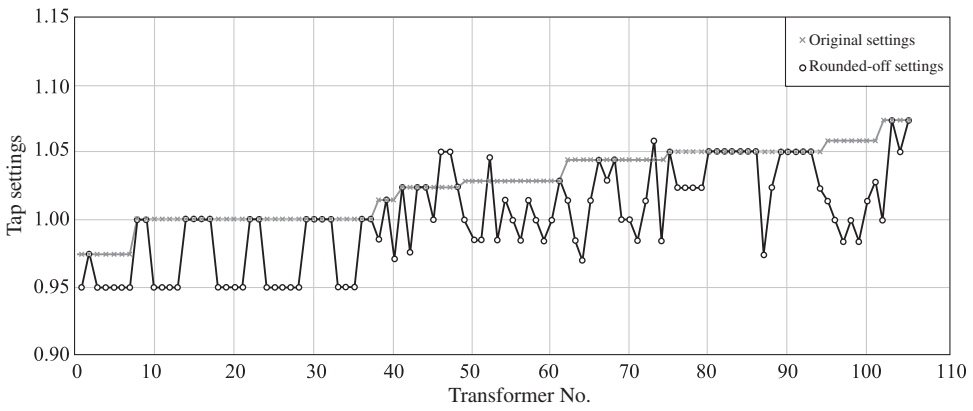

(c)

Fig. 6.9
Comparison of tap ratio settings. (A) Initial tap ratio; (B) optimized tap ratio; (C) rounded-off tap ratio.

Table 6.22 Optimization results of investment costs and reactive compensation

	Investment Costs			VAR Installation		
Case Name	Initial Value (10,000 yuan)	Optimal Value (10,000 yuan)	Descending Rate (%)	Initial Value (Mvar)	Optimal Value (Mvar)	Descending Rate (%)
951D	306.6	0.0	100	233.8	174.8	25.2
951X	226.1	0.0	100	183.0	66.8	63.5
952D	359.1	75.6	78.9	286.4	223.8	21.9
952X	226.1	0.0	100	183.0	98.6	46.1

Table 6.23 Optimization results of VAR installation nodes

	Initial Installation Nodes				Optimized Installation Nodes				Descending Rate After Optimization (%)
Case Name	Original Nodes	Original +New	New Nodes	Total	Original Nodes	Original +New	New Nodes	Total	
951D	30	10	19	59	33	0	0	33	44.1
951X	12	9	12	33	14	0	0	14	57.6
952D	27	10	21	58	33	4	2	39	32.8
952X	14	7	14	35	14	0	0	14	60.0

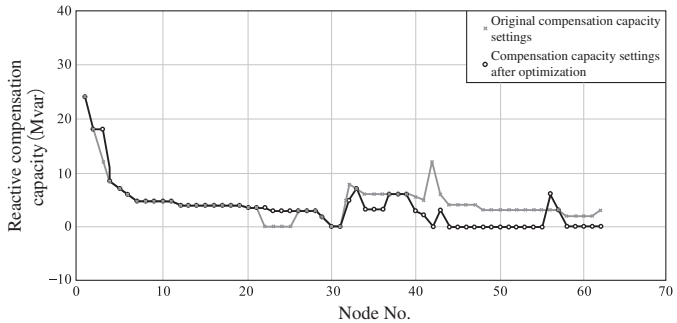

Fig. 6.10
Comparison of initial and new capacitor bank number.

6.5.5 Summary

The expert rule-based algorithm proposed in this section can effectively solve the discrete VAR optimization problem for large-scale distribution systems. Fuzzy numbers are used to determine the rounded-off method for tap ratio, and expert rules are used to calculate the integer value of the capacitor bank number. The proposed algorithm can greatly improve the possibility of obtaining an integer-feasible solution. The calculation results of the two cases have shown that the algorithm can achieve good discrete solutions. Main conclusions of this section are provided as follows:

Table 6.24 Partial results 1 of urban grid planning in 1995

Objective function	Case9501D			Case9501X		
	ΔP_z (MW)	ΔP_{110} (MW)	COST (10,000 yuan)	ΔP_z (MW)	ΔP_{110} (MW)	COST (10,000 yuan)
Manual planning	56.5	53.0	306.6	47.76	45.35	226.1
Minimum grid loss	53.57	50.32	405.1	46.18	43.87	243.6
Minimum investment cost	55.32	51.98	0	46.4	44.07	0

Table 6.25 Part results 2 of urban grid planning in 1995

Objective function	Case9501D			Case9501X		
	ΔP_z (MW)	ΔP_{110} (MW)	COST (10,000 yuan)	ΔP_z (MW)	ΔP_{110} (MW)	COST (10,000 yuan)
Manual planning	43.47	40.16	359.1	33.0	30.57	226.1
power loss Minimization	41.52	38.3	438.6	31.75	29.41	264
investment Minimization	42.75	39.43	76.6	32.10	29.74	0

(1) The algorithm proposed in this section is pragmatic and can be used to solve large-scale integer programming problems that an integer programming system cannot solve.
(2) After obtaining an integer relaxation solution of tap ratio, the proposed expert rules can effectively determine the integer solution of tap ratio, so as to avoid voltage violations caused by simple rounding off.
(3) After obtaining an integer relaxation solution of capacitor allocation, the proposed expert rules can effectively determine the capacitor integer solution, so as to avoid voltage violations caused by simple rounding off.
(4) After optimization calculation, power flow calculation may be used to obtain a nonlinear solution. However, sometimes it is impossible to guarantee that the power flow solution is feasible as the optimal solution.

In summary, the algorithm solves the VAR optimization problem by applying expert rules, which can flexibly adapt to variable system conditions and is good for obtaining feasible solutions under different initial value conditions.

6.6 Discrete VAR Optimization based on GA

6.6.1 Overview

In Sections 6.3 and 6.4, an approximation discrete optimization algorithm was proposed to solve large-scale nonlinear integer programming problems. In Section 6.5, expert rules were introduced to seek better initial values, and the discrete optimization was discussed from the perspective of programming mathematics. Because traditional optimization algorithm is not always able to provide global optimal solutions, to search for a solution close to global optimum, a stochastic searching method is used in this section to solve local optimal solution problems in optimization calculation.

GA and simulated annealing (SA) are typical stochastic optimization algorithms that try to consider optimization from another perspective, that is, biological or physical perspectives rather than an engineering perspective. The process of biological evolution is a process of survival of the fittest, and the process of metal sintering annealing is a process to change crystalline structure; both are capable of developing toward optimization. Scientific researchers make use of mathematical measures to simulate these processes, so as to solve the optimization problem.

The SA method was used in Chapter 4 to solve ill-conditioned power flow problems. The method solves the optimization problem through four main steps. However, there was no common method for selecting parameter and initial value, so it cannot be simply used in the optimization calculation.

GA is a stochastic optimization algorithm based on natural selection of biology and was proposed by University of Michigan, US, in recent years, which is characterized by the use of chromosomes to represent problem variables and the use of multispot searching in the solution space. Thus, the objective function and constraint function of the problem are continuous, so it is applicable to the discrete optimization problem.

The basic approach of the generic algorithm is to test the occasional new parts under random conditions. However, this procedure is not a simple arbitrary search. Instead, it only maintains searching with performance that may be possibly improved. Moreover, it can effectively make use of the system information to suspect new searching spots. The strategy of biological evolution is to change its own structure and function to adapt to the surrounding environment. Such biological evolution strategy can be simulated with mathematical measures to solve the discrete optimization problem.

GA technology also has the problem of how to set an initial searching spot. However, the algorithm itself does not have any requirement for an initial searching spot. To accelerate a solution procedure, expert rules are used in this section during the calculation process to control basic operations of GA.

6.6.2 Necessity of Applying Artificial Intelligence Algorithms

The optimization methods can be divided into two broad categories, that is, an analytic method and a direct method. The former is to employ the first- and second-order derivatives of functions in the solution of n-dimension extremum, and the latter is not to use such derivatives. Because the derivative of the function indicates a change in rules of function values, it is natural to utilize such derivatives of the function when solving the extremum value. The specific approach to the analytic method is to solve a set of nonlinear equations with the derivative of objective function as 0.

However, the analytical expression of objective function in practical problems is rather complicated; it is difficult to find a derivative for some, and some only give the corresponding relation between variables and objective functions. Hence the direct method must be adopted to solve the extremum value of such functions, searching for the optimization solution of function values in the possible descent direction in a maximum gradient. In fact, some direct methods will take advantage of the analytic properties of the function, whereas the analytic method can also be implemented only with the function values. Therefore, the two methods cannot be separated completely.

Regardless of their effectiveness in many cases, the two methods are local optimal ones, or rather the optimal points obtained are only the local ones around the existing points. For the nonconvex optimization problem, different initial values may give different solutions, and further improvement of objective functions must be able to resume stochastically or adopt other means to enable the search process to proceed around another peak value. The prerequisite of a derivative-based analytic method is that the function shall be continuously differentiable, which is a very harsh condition, but still a strict one even allowed to use the difference approximation.

In this section, the coefficients of tap ratio and capacitor bank number are approximately represented by the differential values. Actually, the parameter space is not smooth, and thus, the locally search optimization method is of a certain approximation.

The enumeration method is quite straightforward: in a finite finding space or a discrete finite space, the search algorithm seeks from the objective function of each point at a time. Because the power system optimization is a typical large-scale optimization, this algorithm cannot be applied as its efficiency is too low. The dimensionality of dynamic programming algorithm is too large to be solvable for the power system problems. Those to be handled in the power system are generally large-scale problems, which is difficult to be solved using the existing algorithms. Therefore, it is generally acceptable to find a near-optimal solution with practical values.

To sum up, when fully aware of the shortcomings of the differential method and enumeration method, many researchers are trying to solve the local optimum problem in the optimization

calculation using the stochastic search method. The SA based on simulated metal welding process has even been used for the reactive power optimization and ill-conditioned power flow calculation.

Similar to the SA algorithm, GA is also a stochastic search method, but it is based on the searching algorithm of natural selection and natural biological mechanism. The query algorithm will exchange the most suitable chromosomal structure of the string with the structural but random chromosome to form a new chromosome structure, so as to achieve the goal of evolution. This algorithm uses the chromosome to indicate the variables of the problems and can be combined into many exploration points. The multipoint search in the solution space can avoid the local point optimization and possibly obtain the global optimal point in which the objective function and constraint function are not required to be continuous, and thus can adapt to the discrete reactive power optimization.

The combination of GA with power system expert rules and traditional algorithms can handle the integer variables and improve the solution's efficiency. The calculation results in this section show that GA can give a number of integer-feasible solutions for engineering technicians to make the final decision, whereas the traditional algorithm can generally give only one solution.

6.6.3 GA-based Model for Discrete VAR Optimization

There can be numerous objective functions for VAR optimization, such as active power loss minimization, VAR source investment minimization, voltage deviation minimization, etc. The algorithm in this section applies to a real distribution system, with the following selected objective function:

$$f = \min \left(\text{system active power loss}\right)$$

The following constraints must be satisfied:

(1) Node reactive and active power flow equations.
(2) Upper and lower limits of generator voltage.
(3) Upper and lower limits of generator reactive output.
(4) Upper and lower limits of transformer tap.
(5) VAR limits for all new capacitor installation nodes.
(6) VAR limits for all existing capacitor installation nodes.

Constraints (1)–(3) are the same as those in Section 6.3. Considering that the algorithm is essentially an unconstrained algorithm, the voltage deviations and the reactive power deviations must be considered within the objective function. Therefore, the fitness of GAF is

$$F = f + \lambda \sum (\text{voltage deviation})^2 + \lambda \sum (\text{reactive power deviation})^2 \tag{6.49}$$

6.6.4 GA-based Algorithm for Discrete VAR Optimization

As mentioned earlier, GA is a random search algorithm with the ability to obtain the global optimal solution, thus it may be applied to the discrete VAR optimization problem. However, if the GA search process is applied directly without considering the relations among VAR sources, transformers, and voltages in power system, there will be a lot of blind points, and the search efficiency will be very low. This section attempts to combine the expert rules and GA technology to improve the efficiency of GAs. The main points are as follows.

6.6.4.1 String performance of integer variables

(1) Integer variables are represented by the decimal system, whereas GA handles variables based on the binary system. Thus, in this section, if GA is based upon the decimal system, the solution space in the practical system may be reduced. This section employs the following method to handle integer variables:

$$Y_i = \left[\overline{Y}_i \times \lambda\right] \begin{cases} \text{if} \quad Y_i = 0, \quad \text{then} \quad Y_i = \underline{Y_i} \\ \text{if} \quad Y_i \neq 0, \quad \text{then} \quad Y_i = Y_i \end{cases} \tag{6.50}$$

where $\overline{Y}_i$—upper limit of each integer variable; $\underline{Y_i}$—lower limit of each integer variable; λ—random numbers evenly distributed in [0,1]; Y_i—integer by rounded-off $\overline{Y}_i \times \lambda$; if the rounded-off $Y_i = 0$, then let Y_i equal to the lower limit.

For example, if the upper and lower limits of tap ratio is [1,17], then $\overline{Y}_i = 17$, and if the random number $\lambda = 0.789$, the random tap position of transformer is set as:

$$Y = \left[\overline{Y} \times \lambda\right] = [17 \times 0.789] = [13.413] = 13$$

Considering the fact that multiple-integer-feasible solutions in a system may not be of great difference. For instance, the initial feasible tap ratio of the earlier discussed transformer is 1, and the final feasible tap ratio solution might be 17, and thus, after obtaining the initial feasible solution, it is possible to narrow down the random variation into:

$$\underline{Y}^* = \begin{cases} Y^0 + N, \text{if} \quad Y^0 + N > \underline{Y} \\ \underline{Y}, \text{if} \quad Y^0 + N < \underline{Y} \end{cases} \tag{6.51}$$

$$\overline{Y}^* = \begin{cases} Y^0 + N, \text{if} \quad Y^0 + N < \overline{Y} \\ \overline{Y}, \text{if} \quad Y^0 + N > \overline{Y} \end{cases} \tag{6.52}$$

where N ranges from 1 to 3, $\underline{Y}^*$ is the new lower limit, and $\overline{Y}^*$ is the new upper limit. After changing the new limits, the random integer variables are also changed using Eq. (6.50).

(2) Crossover and mutation principles. Basic GA operations are crossover and mutation, thereby generating new solutions. The essential basis to accept the crossover and mutation depends on whether the fitness function F is improved or not.

In this section, some improvements have been made to the original GA algorithm by crossover and mutation operations within a meaningful range, so as not to induce many meaningless operations. This section follows such a practice; the expert rules give the GA operation scope where the variables are changing. The tap ratio and capacitor bank shall be operated based on the expert rules in this section, and the expert rules of crossover and mutation operations are detailed as follows:

1. Changing range of integer variables to be within ±(1–3) of initial feasible solutions.
2. No need for crossover among different voltage levels for capacitors due to the locality of voltages.
3. In case of no directly interconnected lines, capacitors at two nodes are not required to cross.
4. Crossover is not necessary for the transformer ratios at different voltage levels.
5. In case of no directly interconnected lines, two transformers are not required to cross.
6. If not in the same substation, the transformer ratio and capacitor bank are not required to cross.
7. The integer variables generated randomly from variations shall be within a meaningful range, and only one or finite variables are allowed to mutate at a time.
8. Crossover shall be among integer variables of interconnected nodes, and only one or finite pairs of variables are allowed to cross at a time.

In this section, the VAR units and tap ratios are integer variables, also equivalent to control variables, and changing of integer variables can alter the system's power flow distribution. The method of random number can produce multiple integer solutions. The solutions (if any) of the optimization calculation and power flow generally could converge after several to dozens of iterations, namely equivalent to several to dozens of GA generations, the optimization calculation and power flow calculation may generate the only feasible solution from each iteration, whereas each GA breeding may produce several generations (feasible solutions). The larger the calculation scale, the more the combinations of feasible solutions and vice versa. Therefore, the upper limits of GA breeding generations and maximum generations from each breeding should be identified according to the calculation scale.

6.6.4.2 Calculation procedure

The main procedure of the GA-based discrete VAR optimization is shown in Fig. 6.11. Because the existing mathematic model in the power system can be used to obtain the numerical solutions for GA-based method, the power flow calculation and MILP method in Section 6.3 have been selected. The initial values of MILP method are used at the initial exploration points, so as to significantly reduce the calculation time of GA-based method.

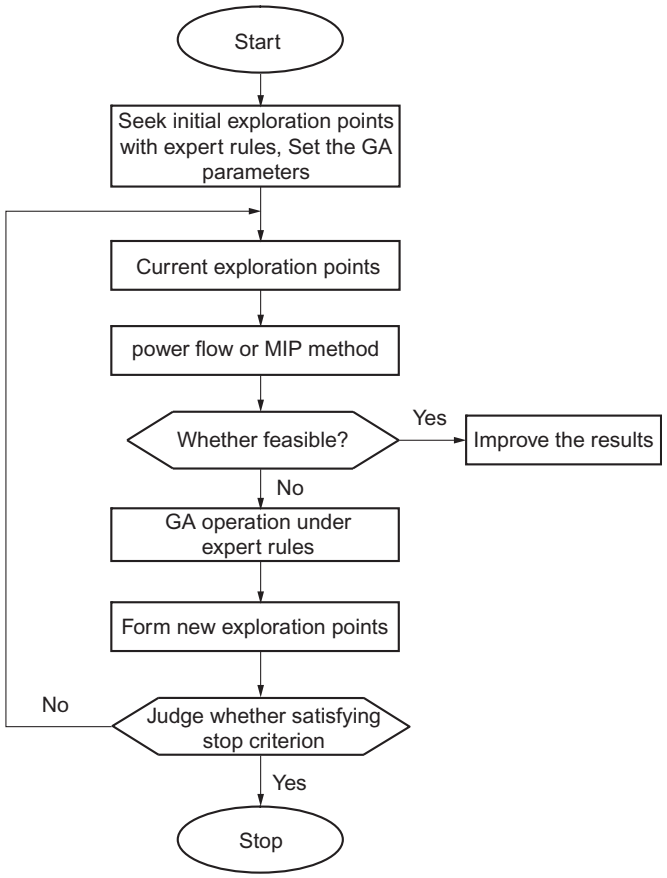

Fig. 6.11
Flow chart of GA-based discrete reactive power optimization algorithm.

Main calculation procedure includes the following three major stages:

1st stage: Formulate nonlinear discrete VAR optimization problem, and take initial values of power flow calculation (or optimization calculation) as one of exploration points. Set the GA parameters and variable bounds to avoid the unnecessary stochastic optimization searching.

2nd stage: Obtain the integer-feasible solutions using the MILP method in Section 6.3 and expert rules in Section 6.5. Take objective function and infeasibility degree as the evaluation function to make the elimination. If only the power flow calculation is used, then take the grid loss and voltage violation values, etc. as the evaluation function to make the elimination. If there is no integer-feasible solution obtained, enter the 3rd stage; if a pair of integer-feasible solutions are obtained, enter the improvement procedure to obtain new integer solutions.

3rd stage: Generate new exploration points with GA, that is, reset the solution and variable bounds to the problem. When the exploration points have been over M (generally 10–50, given based on the calculation scale and experience), it is believed that the problem has no integer-feasible solution stop exploring; otherwise re-enter the 2nd stage.

Improvement procedure for new integer solutions:

Similar to the main process, such procedure is equivalent to the steps to produce the new exploration groups in GA:

(1) Set the new bounds of the problem.
(2) Generate new problems.
(3) Resolve the problem, and if the objective is improvable, enter the next step, otherwise stop.
(4) To generate new solutions using GA and judge whether they satisfy the stopping criterion, that is, when exploration points $>M$ (generally 10–50, given based on the calculation scale and experience), stop exploring, otherwise reenter Step (2). Fig. 6.12 shows the improvement procedure of GA-based integer solutions.

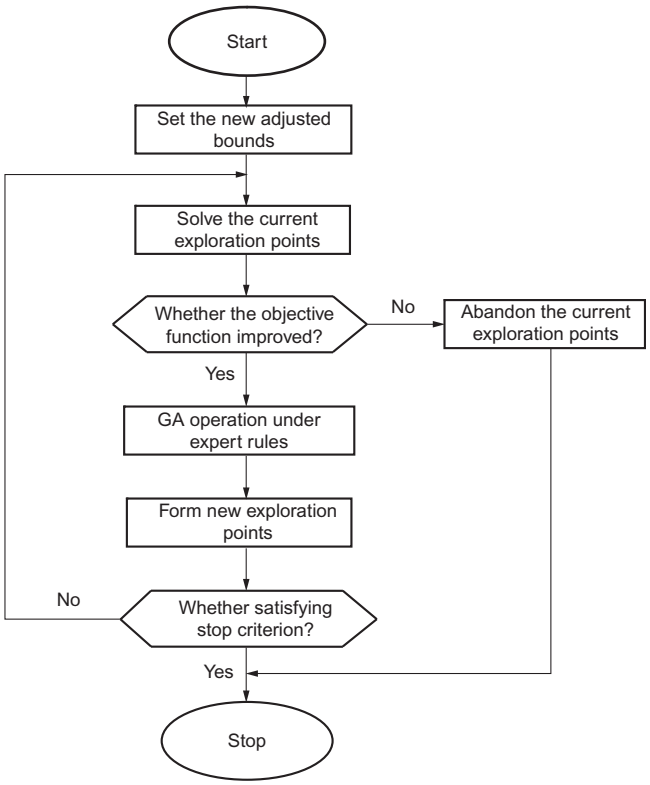

Fig. 6.12
Improvement of GA-based integer solution.

Table 6.26 Basic calculation conditions for the algorithm based on GA

Number of Nodes	Number of Lines	Number of Tap Ratios	Number of Capacitors
38	12	27	7

6.6.5 Implementation

6.6.5.1 38-node Practical System

The test system used is an actual distribution system, and the calculation scale is shown in Table 6.26. The algorithm is verified by two cases with identical network structures where Case 1 is a low-load mode and Case 2 is a high-load mode.

Table 6.27 shows the calculation conditions of integer variables for Cases 1 and 2 based upon the computational experience. For the actual system of the previous scale, the GA breeding can be controlled to about 50 generations, each having about 10 offsprings, and GA operations shall be carried out under the guidance of expert rules as stated in Section 6.6.4.

As shown in Table 6.27, there are 18 tap ratios and 7 capacitor banks with a total of 25 integer variables. INI is the condition given by the actual system operators (or alternatively, take the optimal solutions generated by MILP method as the initial value). For the sake of saving space, only the stochastic initial solutions INI1–INI3 are given here.

In Table 6.27, the same figure in "Interconnection" indicates that there are interconnected or parallel lines between the two integer variables; "UH" means the rated voltage at the high voltage side of transformer and rated voltage at the capacitor node; and "BOUND" means the upper and lower limits of integer variables. If the planning engineer fails to determine the upper limit of newly installed capacitor banks, the power factor at this node may be considered as 1.0.

6.6.5.2 Numerical Results

The objective function values and voltage violation values of Case 1 are given in Table 6.28.

The objective function values and voltage violation values of Case 2 are given in Table 6.29.

Based on Table 6.27, GA operations are executed to make the optimization calculation, and the approximated global optimal solution would be obtained.

To illustrate the multiplicity of integer solutions, Table 6.30 shows the detailed calculation results of integer variables for Case 2. Due to the limited space, this table gives only the final nine solutions for integer variables.

As shown in Table 6.30, SO6–SO9 have obtained the same objective function in spite of different initial values, that is, there are identical objective function values for these four solutions. However, only one solution may be chosen because of the multiplicity of

Table 6.27 Calculation conditions of integer variables for Case 1 and Case 2

Variable	INI	INI1	INI2	INI3	Interconnection	UH (kV)	BOUND
T1	1	1	1	1		35.0	1–5
T2	2	2	2	2		35.0	1–5
T3	1	1	1	1		110.0	1–5
T4	3	3	3	3		35.0	1–5
T5	1	1	1	1	1	110.0	1–3
T6	5	5	5	5	2	35.0	1–5
T7	1	1	1	1	1	110.0	1–5
T8	3	3	3	3	2	110.0	1–5
T9	1	1	1	1	3	110.0	1–3
T10	9	9	9	9	3	35.0	1–17
T11	5	5	5	5		110.0	1–17
T12	3	3	3	3		35.0	1–5
T13	1	1	1	1		110.0	1–5
T14	3	3	3	3		35.0	1–5
T15	9	9	9	9	4	110.0	1–17
T16	9	9	9	9	4	110.0	1–17
T17	1	1	1	1	5	220.0	1–5
T18	1	1	1	1	5	220.0	1–5
C1	2	3	3	3		10.0	0–7
C2	0	0	0	0		10.0	0–7
C3	2	3	3	3		10.0	0–7
C4	2	3	3	3		10.0	0–7
C5	2	3	3	3		10.0	0–7
C6	2	3	3	3		10.0	0–7
C7	2	3	3	4		10.0	0–7
Objective function value	2.86	2.25	2.01	2.00			0–7
Variable violation value	0.18	0.065	0.045	0.043			0–7

Table 6.28 Objective function values and voltage violation values of Case 1

Variable	Active Power Loss (MW)	Max. Voltage Violation Value (p.u.)	Number of Voltage Violation Nodes
INI	2.24	0.0656	10
SO1	1.93	0.0	0
SO2	1.90	0.0	0
SO3	1.89	0.0	0
SO4	1.88	0.0	0
SO5	1.93	0.0	0

Table 6.29 Objective function values and voltage violation values of Case 2

Variable	Active Power Loss (MW)	Max. Voltage Violation Value (p.u.)	Number of Voltage Violation Nodes
INI	2.86	0.1083	20
SO1	2.20	0.0127	6
SO2	2.17	0.0105	4
SO3	2.15	0.0089	2
SO4	1.97	0.0	0
SO5	1.90	0.0	0
SO6	1.83	0.016	5
SO7	1.83	0.0019	3
SO8	1.83	0.0048	3
SO9	1.83	0.0048	3
SO10	1.85	0.0	0
SO11	1.87	0.0	0
SO12	1.88	0.0	0

such GA breeding. The parenthesized figures in this table indicate different integer solutions available for SO1–SO9, of which the objective functions are slightly different accordingly.

The computational experience shows that, if the objective function value of the solution is no longer improved or nearly equal, then the solution can be regarded as an approximate global optimal solution.

The results in Tables 6.30 and 6.31 show that the GA-based discrete VAR optimization techniques can be used to search different objective functions or different integer solutions for the same VAR optimization problem. The results of Case 1 also come to a similar conclusion.

6.6.6 Summary

This section has combined the GA with MILP algorithm and expert rules to resolve the discrete VAR optimization of the distribution system, with conclusions as follows:

Table 6.30 Integer solutions and constraints of tap ratio in Case 2

Variable	SO1	SO2	SO3	SO4	SO5	SO6	SO7	SO7	SO8	SO9	SO9
T1	1	1	1	1	1	1	1	1	1	1	1
T2	3	3	3	3	3	3	3	3	3	3	3
T3	2	2	2	2	(3)	2	(1)	2	2	(1)	(1)
T4	4	4	4	4	4	4	4	(5)	(5)	4	4
T5	1	1	1	1	1	1	1	1	1	1	1
T6	3	3	3	3	3	(4)	(4)	(4)	(4)	(4)	(4)
T7	1	1	1	1	1	1	1	1	1	1	1
T8	3	3	3	3	3	3	3	3	3	3	3
T9	1	1	1	1	1	1	1	1	1	1	1
T10	5	(6)	(6)	(6)	(6)	5	5	5	5	5	5
T11	6	6	(7)	(7)	6	6	6	6	6	6	6
T12	4	4	4	4	4	4	4	4	4	4	4
T13	1	1	2	2	2	1	1	1	1	1	1
T14	4	4	4	4	4	4	4	4	4	4	4
T15	5	5	5	5	5	6↓	6	6	6	6	6
T16	6	6	6	6	6	5↑	5	5	(4)	(4)	(4)
T17	1	1	1	1	1	1	1	1	1	1	1
T18	1	1	1	1	1	1	1	1	1	1	1

Table 6.31 Integer solutions and constraints of capacitor in Case 2

Variable	SO1	SO2	SO3	SO4	SO5	SO6	SO7	SO7	SO8	SO9	SO9
C1	3	3	(2)	3	(4)	3	3	3	3	3	3
C2	0	0	(1)	(1)	(1)	0	0	0	0	0	0
C3	3	3	(2)	3	(4)	3	3	3	3	3	3
C4	3	3	(2)	3	3	3	3	3	3	3	3
C5	1	1	(2)	(3)	(3)	1	1	1	1	1	1
C6	2	2	2	(3)	(3)	2	2	2	2	2	2
C7	(3)	4	(2)	(3)	4	4	4	4	4	4	3
OBJ	2.20	2.17	2.15	1.97	1.90	1.83	1.83	1.83	1.83	1.84	1.85

(1) The algorithm proposed has increased the possibility to obtain the global optimal solution.
(2) The compensation effects of capacitors at different voltage levels in the distribution network can be predicted by the expert rules, because the capacitors work for corresponding voltage levels only.
(3) The calculation results show that, when the capacitor compensates the voltage at the related point node to a power factor of 1.0, the transformer tap ratio and capacitor can be adjusted simultaneously to improve the voltage distribution in the electrical power distribution system.
(4) The algorithm proposed can satisfy the VAR reactive power optimization requirements of the transmission network.

6.7 Conclusion

Discrete VAR optimization is a typical discrete optimization problem in power systems and has been conducted in a detailed and systemic way in this chapter. This chapter treated the reactive power optimization as an MINLP problem, in which the capacitor bank number and transformer taps can be treated as discrete variables. This chapter proposed an algorithm to solve the large-scale discrete reactive power optimization. The efficiency of the algorithm is considered under good sparsity, linearized feature, and other properties in the static calculation of power system. To verify the validity and reliability of the algorithm, a corresponding degree of verification was compiled. The actual scale power system is used in the calculation. In terms of algorithm, this chapter mainly involves the approximate MIP algorithm, expert rules algorithm, and GA-based algorithm. In terms of a model, this chapter mainly involves the single-state model and multistate model of diagonal block matrix.

This study mainly focuses on the offline discrete reactive power optimization. It will also consider its online application in the future. Besides the discrete reactive power optimization, there are some other discrete optimization problems in power systems, such as generator maintenance scheduling problems, generating unit commitment calculation, power equipment

planning in the transmission and distribution system, power equipment operation in the transmission and distribution system, etc., which may be study topics in the future.

In addition to the algorithm in this chapter, the current algorithms that can be used to solve discrete optimization problems to some extent include Bound & Branch method, dynamic programming method, Benders decomposition method, Lagrangian relaxation method, internal path method, etc.

At present, the simplex method can be used to solve the LP problem with thousands or even hundreds of thousands of variables, but the accurate-integer programming algorithm can only solve the optimal solutions of less than 100 variables, because its calculation time varies with integer variables. Therefore, to solve the discrete optimization problem in the power system, it is necessary to fully consider the actual physical background of different problems. This is also of great significance for programming mathematics itself.

Discrete optimization is still a new research area in the power system. There are still many issues that need further exploration and study. In the future, new algorithms will be developed on the basis of this research, which will result in the application on other discrete optimization problems of power systems.

CHAPTER 7

Optimization Method for Load Frequency Feed Forward Control

Chapter Outline

Mathematical Models and Algorithms for Power System Optimization. https://doi.org/10.1016/B978-0-12-813231-9.00007-8

7.1 Introduction

7.1.1 Descriptions of the Problem

The objectives for load frequency control are to provide a mechanism to track the desired generation allocation specified by an economic dispatching program, and to regulate the system frequency and tie line interchanges in specified values. The most widely used load frequency controller in the power system is the integral feedback type. In recent years, many applications of optimal linear quadratic control theory have also been examined to improve power system control performance. However, in the optimal linear load frequency controller, much information between various plants or areas is not accessible due to communication and economic difficulties. Furthermore, optimal linear quadratic control is optimal only for a particular type of load disturbances, whose mathematical model is not clearly known.

This chapter studies the issues of load frequency control in the power system under normal operating conditions. Due to the stochastic characteristics of load, the power system is subject to different types of load disturbances even under normal operating conditions. Therefore, it is necessary to study the model and algorithm, which is applicable to small disturbances (second-level power load changes) and to maintain the system frequency in the given range by controlling the power angular acceleration of the generator. Maintaining stable frequency of the power system is an important part of power system control. The changes of frequency will affect the production targets of industrial enterprises, such as to change the speed of rotation of the machine, to make the power of the working machine insufficient or overloaded, and to damage production in severe cases. Hence, the frequency control of the power system must be fast, stable, and accurate.

The most basic operation requirements of synchronous operation of power systems are to maintain system frequency, voltage distribution, active and reactive powers of generators, and active and reactive powers of transmission lines within specified steady-state values. The stochastic variations of system load and different disturbances make the system deviate from its

steady state. By means of various controls, the effects of such disturbances will be counteracted. The most important types of control include the following four:

(1) The prime mover torque of the system generator.
(2) Excitation current of generator excitation coil.
(3) Adjustment and control of the transformer tap changer.
(4) Various switches or circuit breakers.

This chapter studies Scenario (1) only, that is, active power control.

The active power control of the power system in normal operation is divided into two branches, specifically economic dispatch and load frequency control, both of which are currently closed. Since 1945–1950, particularly the 1950s when the computer came into practical application, both branches have achieved substantial developments. In recent years, there have been new advances, such as the application of optimal controls. These new research results can be applied to existing devices.

Voltage control, related with reactive power distribution, is another branch of normal operation condition, which is not discussed in this chapter based on the following: (1) the unbalance of active power mainly affects the system frequency, with little impact on the voltage and (2) the unbalance of reactive power mainly affects the voltage, with weak impact on the frequency.

In the early days, the integral feedback control method was used to keep the frequency stable. However, the essence of feedback control is that the feedback system plays the role of detecting the correcting the deviation after the disturbance occurs, that is, the feedback system works after the deviation occurs. However, because some objects are of serious inertia or hysteresis, the controlled variable will not vary until a long time after the disturbance and is not easily or rapidly corrected once it varies, with poor adjustment effects.

If the disturbance can be predicted and the change can be preadjusted to the system, then the effects of these disturbances can be suppressed as long as the controlled quantity changes, this control method is called feedforward control. However, feedforward control requires that the disturbance is measurable or predictable. But some of the disturbance is not measurable or difficult to measure, people at that time did not grasp the theory of the estimation and forecasting system, thus such feedforward method was not further studied.

Later, many literatures utilized the modern control theory to study the load frequency control problem, trying to solve load frequency control with the modern linear control theory. Its basic idea is the state feedback, which can be used to improve the system performance by means of linear quadratic optimal control or pole assignment, etc.

The power system is a complex large system; some literatures have considered the multiunit system but only employed a method of centralized state feedback control. Such a method needs an appropriate amount of information, without which it is hard to put into practice application.

In addition, the existing literatures only made the load step disturbance simulation test. As previously mentioned, the power system operation process is a random process, and the load disturbance is a process of continuous change. The system state changing under such a disturbance is also a continuous change process. Therefore, it is not enough to only study the system changes under the step disturbance, because the resulting control law and control method may not be able to meet the requirements for actual control performance.

7.1.2 Overview of this Chapter

Proceeding from the stochastic control theory, based on the applications of the identification, estimation, and control theories, and combines computer technology, this chapter studied the load frequency control problem in the normal operation of the power system. As previously mentioned, the load disturbance of the power system is a complex type of disturbance. First, this chapter studies the power system load disturbance model identification problem. A time series correlation function analysis method was applied to determine the model structure and its parameters of the load disturbance, and a mathematical model of the load disturbance was established.

Second, due to the complexity of the power system, this chapter adopts the idea of decomposition and stratification to construct the state estimators at different levels, so as to estimate the operating status of the system and predict the trend of the load disturbance. Finally, the law of load frequency control is derived by applying the principle of invariance, and a load frequency compensator (i.e., feedforward controller) is designed. Based on the feedforward controller, a digital computing simulation of the load frequency random tracking control is performed to implement system frequency control for an actual power system structure.

The performance of the controller designed by this principle is much better than that of the integral feedback controller. Moreover, this chapter also handles all linear model transformations required for identification, estimation, and control. The transformations include those from difference equation to differential equation, and from differential transfer function to difference transfer function. Some of these problems have not been proposed or yet solved before, and the solution of these problems will bring us great convenience.

In Section 7.3, an identification method is used to build the model of load disturbances of the power system based on time series ananlysis, in which the process to identify the order of model and the method to estimate parameters are given.

In Section 7.4, the power system equivalent model is constructed; blocks (govermor, prime mover, generator) of power plant are taken into consideration except for the excitation because only the small disturbance of the load is considered.

In Section 7.5, hierarchical decomposition principles are utilized to construct all levels of state estimators to estimate or track the disturbances. A hierarchical estimator and a central predictor are constructed according to the decomposition and aggregation principle. In both local and central estimators, the Kalman filters are used to filtrate the random load fluctuations. The central estimator (combined with load prediction model) can provide system relative speed and load prediction based on the on-line measurements of power and frequency.

In Section 7.6, to compensate for the load error prediction, a load frequency controller, called an error predication compensator, is derived via the invariance principle. Both the absolute compensator for the thermal unit and the approximate one for the hydro unit give much better performance than the conventional integral load frequency controller.

Section 7.7 settles the transformation methods among mathematical models required for identification, estimation, and control, including the transformation of difference equation into differential equation, the transformation of differential transfer function into difference transfer function, in which proposes a series of new transformation methods of practical significance.

Section 7.8 illustrates the results of simulation on a simple two-unit system and a more complicated five-unit system by the digital simulation of load frequency control based on stochastic tracking, which proves that the control method proposed in this chapter is feasible. The tracking control simulation test more realistically reflects the whole system control process. The proposed load frequency controller can effectively control different types of disturbances in the power system, with better performance than the widely used integral feedback controllers.

7.2 Basic Ideas of Modeling

It is well known that the various control objects of the power system are widely distributed. It is obviously uneconomical and unreasonable to realize a large amount of information exchange among various control objects. Moreover, the linear optimal controller is only optimal for some special type of load disturbance. Because load disturbance of the power system is a kind of

complex disturbance, and only when an accurate model of such disturbance is determined, the previously discussed controller can show its advantages. When studying the issue of load frequency control, this chapter has noticed many useful ideas in the classical control theory and tried to combine many new achievements in modern control theory, so as to improve control performance, practically apply new methods, and be able to use the existing actual control instruments at that same time. The basic ideas for modeling in this chapter are illustrated in the following text.

7.2.1 Way of Formulating the Load Disturbance Model

The operation process of the power system is a random process, and the load disturbance is present at any time. The law of the change is not easy to grasp. The frequency of the power system can be used as an indicator of the balance of power system operation. The load disturbances inevitably cause frequency changes. Conversely, if the mathematical model of the load disturbance is known, the variation of the load disturbance can be estimated based on the frequency change. Because the power system load disturbance is a complex type of disturbance, the appropriate model problem for establishing the load disturbance has not been properly solved in the previous load frequency controller.

The mathematical model of the discrete state equation of the load disturbance is established in this chapter, in which the time series correlation function analysis method is applied to stabilize the nonstationary time series by using the high-order difference method, and the model structure (moving or moving with autoregressive-moving) and its parameters (autocorrelation function, partial autocorrelation function) of the load disturbance is determined by autoregressive, moving, and autoregressive-moving that describes the stationary random process.

7.2.2 Way of Constructing Estimator at All Levels

The successful control of the power system depends on knowing exactly its state at any time, and some states are determined from the direct observation by distributed measuring instruments. The speed and placement of the measuring device depends largely on the control system's ability on disturbances. The effective control by the application of computer control requires reliable data, which can be provided by the online state estimation based on the future system variables.

Because the power system is a complex large-scale system consisting of various power plants, and each power plant is composed of a speed control, excitation, prime mover, and generator, this chapter only considers the variation of the load frequency under small disturbances.

Therefore, the mathematical model of each block except the excitation is considered, and the equivalent model of the power system is established.

This chapter uses decomposition techniques to decompose a complex system into easily solvable subsystems and to handle the consistency between the solution of the subsystem and the solution of the system.

On the basis of the establishment of the mathematical model and the power system equivalent model of each block of the power plant, according to the situation where the lowest level of the power system is the power station or generator set, and the second level is the dispatching center at all levels, state estimators of all levels are hierarchically constructed by the hierarchically decomposed ideas.

In summary, the state estimation of the hierarchically structured power system should use the hierarchical estimation method. Two-stage estimators have been applied to the power system, that is, local estimator and central estimator. Because variable $\Delta\omega_j$ in the system can be measured only by the cheap frequency meter, $\Delta\omega_j$ is taken as a measured variable. Based upon the power system model, all state variables of the system can be estimated using the Kalman filter, so as to estimate the system operation status (frequency changes) and predict the changing trend of load disturbance.

7.2.3 Way of Setting Up the Load Frequency Controller based on the Invariance Principle

The task of the load frequency controller is to find a control law to compensate for the influence of the load disturbance to maintain the power system frequency within the allowable range of the specified value. The integral feedback controller can attenuate the effect of the disturbance, but it cannot completely cancel it out. However, under certain conditions, the feedforward controller (or compensator) based on the invariance principle does not suffer from the effects of disturbances. That is, a control law can be found to completely compensate for the disturbance and control the frequency change.

The power system load frequency controller has an integral type and a state feedback type. This chapter attempts to apply the invariable principle to establish a new type of discrete compensation controller suitable for digital control to compensate for the load disturbance of the system so as to control the system state.

In the past, the feedback control did not need to resist the system disturbance, that is, without any compensation to the disturbance, and the control was left after the state of the system was changed. In general, the feedforward control is to perform compensation control after disturbance measurement. If the system can be continuously measured, estimated, forecasted, and controlled, the tracking control to the power system can be achieved.

The load frequency compensator (i.e., feedforward controller) is designed based on this principle. The state of the unit is estimated by the local estimator, by which data $\Delta\hat{P}_{Tj}$ and $\Delta\hat{\omega}_j$ are estimated and then to be the input of the center estimator, to estimate the state variable of the equivalent machine and the load forecast value ΔP_L. ΔP_L then is taken as the disturbance value in the next step. This process is repeated with the value ΔP_L as the next disturbance value. In this process, the compensation controller is used to compensate for the disturbance and control the system state, thereby forming an entire tracking control process.

7.2.4 Considerations of Transformation Methods for Linear Models

When addressing the load frequency control problem of the power system, this chapter tries to apply a series of system theories in identification, estimation, and control, however some problems cannot be solved by the existing linear model transformation theory. This chapter has made innovation and improvement to the existing linear model transformation theory to solve some never-encountered problems, which may bring great convenience.

Because the time interval (60 s) for measuring load disturbance is different from the time interval (1 or 4 s) adopted by the controller, which should be taken into consideration for the formulating of mathematical models for discrete state equations of load disturbance, this study employs two methods to solve the new problem: ① transforming the discrete model into an equivalent continuous model, based on which desired discrete model will be derived, and ② directly using the discrete transformation to develop the desired discrete model. This has brought a question of mutually transforming the continuous and difference models. When the model is of a higher order, based on the computer control, the problem of numerical solution of transforming the differential transfer into difference transfer type is solved.

7.3 Identification of Load Disturbance Model ΔP_L

The load disturbance of a power system is a complex disturbance, and when addressing the load frequency control, it is required to first understand the variation of the disturbance, then use a proper mathematical model to fit it.

The operation process of the power system is a stochastic process; users can cut off or put on the loads anywhere and anytime, so the load disturbance is ubiquitous, and its change rules are not easy to grasp. However, the power system frequency can be taken as an indicator whether the power system is in balance operation, that is, a balance indication between the generation and load. The load disturbance is bound to cause frequency changes, and in turn, if the mathematical model of load disturbance has been developed, the changes in load disturbance can be estimated based on frequency changes. Therefore, to carry out effective control on the load and frequency, it is imperative to develop the mathematical model for load disturbance and master its essence.

The load disturbance ΔP_{L} is defined as follows:

$$\Delta P_{\mathrm{L}} = \text{planned generation output} - \text{actual generation output}.$$

ΔP_{L} per minute record can be obtained from the actual operation records of the power system, from which the mathematical model can be developed. Because the order of such mathematical model is unknown, the model identification method must be adopted to determine the order. The current model identification methods are numerous, such as least square method, auxiliary variable method, time series analysis method, etc., among which the time series analysis method is widely applied in the actual engineering problem, in which the order of mathematical model is easily characterized by the correlation function and partial autocorrelation function. This chapter also employs such a method to develop the mathematical model of load disturbance ΔP_{L}. The following shows the main contents of such a method.

7.3.1 Brief Descriptions of Time Series and Stochastic Process

7.3.1.1 Time series analysis

Measuring a variable or a set of variables $X(t)$ in the actual process, at time $t_1 < t_2 <, \ldots, < t_n$, a set of ordinal numbers with time t as a parameter is obtained:

$$X(t_1), X(t_2), \ldots, X(t_n) \tag{7.1}$$

Generally, it is called a time series. Here, parameter t is called time, and in practice, t may refer to different physical meanings, and the time series are one- or multidimensional.

Measuring once a minute in the power system, some sequential number sets with independent variables of t can be obtained, constituting the sample time series of $\Delta P_{\mathrm{L}}(t)$. The time series $X(t)$ is called definite if its value is given by a completely definite mathematical function, for instance:

$$X(t) = a + b\cos\omega t \tag{7.2}$$

where a, b, and ω are the given constant values, and thus the time series are determined. However, in practice, the time series are complicated. Generally speaking, $X(t)$ cannot, like Eq. (7.2), be given by a completely definite mathematical function but may be described by a stochastic function with a certain probability distribution, as does $\Delta P_{\mathrm{L}}(t)$. Such time series are called random, and the stochastic time series can simply be referred to as a time series.

The so-called analysis and forecasting of a time series, mathematically, is regarding measured data Eq. (7.1) as a sample function of stochastic process $X(t)$. Based on an analysis of Eq. (7.1), by estimating the general characteristics of stochastic process $X(t)$, the probability distribution of future values of $X(t)$ is estimated, thereby giving the predicted value of $X(t)$ when $t > t_n$:

$$X^*_{N+1}, X^*_{N+2}, \ldots, X^*_{N+L}$$

Make the square expectation difference between this and future measured values $X(t)$:

$$X_{N+1}, X_{N+2}, \ldots, X_{N+L}$$

$$\delta_l = X_{N+l} - X^*_{N+l} (l = 1, 2, \ldots, L)$$

When squared expectation is minimized:

$$E\left[\delta_l^2\right] = E\left[\left(X_{N+l} - X^*_{N+l}\right)^2\right] \tag{7.3}$$

According to the statistical properties of time series Eq. (7.1), different mathematical probability models can be constructed, and the analysis and prediction of time series $X(t)$ are discussed as follows.

7.3.1.2 Stationary time series analysis

A stochastic process $X(t)$ is called stationary when its statistical property does not vary with the elapse of time from the original point. A stationary stochastic process $X(t)$ has the following two significant features:

(1) Its measured data $X(t)$ revolves around a fixed horizontal line, characterized by evenly stochastic oscillation.
(2) The statistical properties between random data $X(t)$ and $X(t+\tau)$ obtained at any two different moments t and $t+\tau$ are only functions of their time interval τ, independent of the position of origin time t_0.

Mathematically, this means the mathematical expectation and variance of random process $X(t)$ is constant:

$$\mu(t) = E[X(t)] = \mu \tag{7.4}$$

$$\sigma^2(t) = E\left[(X(t) - \mu)^2\right] = \sigma^2 \tag{7.5}$$

And the correlation function:

$$\begin{aligned} \rho(t, t+\tau) &= E\left\{\left[\frac{X(t) - \mu(t)}{\sigma(t)}\right]\left[\frac{X(t+\tau) - \mu(t+\tau)}{\sigma(t+\tau)}\right]\right\} \\ &= E\left\{\left[\frac{X(t) - \mu}{\sigma}\right]\left[\frac{X(t+\tau) - \mu}{\sigma}\right]\right\} \\ &= E\left[\left(\hat{X}(t)\hat{X}(t+\tau)\right)\right] \\ &= \rho(\tau) \end{aligned} \tag{7.6}$$

has no relation with time t but a function of their timer interval τ.

7.3.1.3 Nonstationary time series analysis

The so-called nonstationary time series refer to a very wide range of physical data with their statistical properties varying with time. Most of physical data encountered in the practical problem are generally nonstationary. A group of original measured data are assumed to be stationary only when the primal problems are simplified or roughly approximated. The nonstationary time series are so complicated that there is no generalized method to deal with it. The high-order difference method, namely the difference method, may be used to stabilize it shown as follows:

A stationary stochastic process is still stationary after the linear difference operation.

For example, a $d-1$ order polynomial:

$$f(t) = c_0 + c_1 t + \cdots + c_{d-1} t^{d-1} \tag{7.7}$$

After d order difference, it is changed into:

$$\nabla^d f(t) = 0 \tag{7.8}$$

And a periodic function with integer s as the period:

$$P(t) = P(t+ns) \quad (n = \pm 1, \pm 2, \ldots) \tag{7.9}$$

Through difference

$$\nabla_s P(t) = (1 - B^s) P(t) = P(t) - P(t-s) \tag{7.10}$$

The periodic component can be eliminated.

Therefore, for a general nonstationary stochastic process:

$$X(t) = f(t) + P(t) + \eta(t) \tag{7.11}$$

where $\eta(t)$ is stationary stochastic process, and through difference:

$$\nabla^d \nabla_s X(t) \nabla^d \nabla_s \eta(t) \tag{7.12}$$

A stationary stochastic process can be obtained.

7.3.2 Brief Descriptions of Linear Models for Stochastic Process

7.3.2.1 AR, MA, and ARMA models

In general, the stationary stochastic process can be described by the combination of the multiorder linear autoregressive (AR) model, moving average (MA) model, and autoregressive moving average (ARMA) model. This section first introduces the definition and classification of linear models, then searches for their special autocorrelation function models.

(1) Multiorder linear AR model:

$$\phi(B)Z_t = a_t \tag{7.13}$$

where a_t is white noise, Z_t is output, $\phi(B) = 1 - \sum_{k=1}^{P} \phi_k B^k$, B means the delay of one-step operation, P refers to the order.

Condition: When the module of each root in $\phi(B) = 0$ is greater than 1, the stationary solution Z_t of such model is called stationary autoregressive process, denoted as AR model.

(2) MA model:

$$Z_t = \theta(B)a_t \tag{7.14}$$

where $\theta(B) = 1 - \sum_{k=1}^{g} \theta_k B^k$, k means the order.

Condition: When the module of each root in $\theta(B) = 0$ is greater than 1, the stationary solution of such model is called reversible moving average process, denoted as MA model.

(3) ARMA model:

$$\phi(B)Z_t = \theta(B)a_t \tag{7.15}$$

If satisfying the two previous conditions, the stationary solution Z_t of such model is called an ARMA process. (p,q) means the orders of AR and MA models.

7.3.2.2 Autocorrelation functions and partial autocorrelation functions of AR, MA, ARMA process

(1) AR process. Rewrite the expansion of Eq. (7.13)

$$Z_t = \phi_1 Z_{t-1} + \phi_2 Z_{t-2} + \ldots + \phi_p Z_{t-p} + a_t$$

Multiply Z_{t-k} with two sides of the equation to take the mean and allow for $E(Z_{t-k}a_t) = 0$, $k > 0$ to get the covariance function:

$$\gamma_k = \phi_1 \gamma_{k-1} + \phi_2 \gamma_{k-2} + \cdots + \phi_p \gamma_{k-p} \tag{7.16}$$

Denoted as:

$$B\rho_k = \rho_{k-1}$$

And autocorrelation function:

$$\rho_k = \phi_1 \rho_{k-1} + \phi_2 \rho_{k-2} + \cdots + \phi_p \rho_{k-p} \quad (k > 0) \tag{7.17}$$

Eq. (7.17) can be transformed into:

$$\phi(B)\rho_k = 0 \tag{7.18}$$

This is a difference equation with the coefficient of ϕ_k. Assume that the solution of Eq. (7.18) is:

$$\rho_k = A_1 G_1^k + A_2 G_2^k + \cdots + A_p G_p^k \quad (k > -p) \tag{7.19}$$

where $G_1^{-1}, G_2^{-1}, \ldots, G_p^{-1}$ are different single roots under the stationary condition of $\phi(B) = 0$, and their modules $|G_i^{-1}| > 1$. $A_1, A_2, \ldots, A_p$ in Eq. (7.19) are simultaneous solutions of the following equations:

$$\left.\begin{array}{l} A_1 + A_2 + \cdots + A_p = 1 \\ A_1\left(G_1^k - G_1^{-k}\right) + A_2\left(G_2^k - G_2^{-k}\right) + \cdots + A_p\left(G_p^k - G_p^{-k}\right) = 0 \\ k = -1, \ldots, -p+1 \end{array}\right\} \tag{7.20}$$

Because $|G_j^{-1}| > 1$, namely the roots of $\varphi(B)$ are outside the unit circle, from which $|G_k|$ declines along the exponential curve, approach zero, thus, the absolute value of autocorrelation function determined by Eq. (7.20) follows the same rules, approaching zero. Different from the MA process, ρ_k is not identically equal to zero after a certain k. Such autocorrelation function is called tailing.

Further, based on the first P equations of Eq. (7.17), allowing for $\rho_k = \rho_{-k}$, we have:

$$\left.\begin{array}{c} \rho_1 = \phi_1\rho_0 + \phi_2\rho_1 + \cdots + \phi_p\rho_{p-1} \\ \rho_2 = \phi_1\rho_1 + \phi_2\rho_0 + \cdots + \phi_p\rho_{p-2} \\ \vdots \\ \rho_p = \phi_1\rho_{p-1} + \phi_2\rho_{p-2} + \cdots + \phi_p\rho_0 \end{array}\right\} \tag{7.21}$$

It can be seen clearly that $\phi_1, \phi_2, \phi_3, \ldots, \phi_p$ is the solution of linear equation Set (7.21), the coefficients of which are made up of $\rho_0, \rho_1, \ldots, \rho_p$. Eq. (7.21) is called the Yule-Walker equation.

The truncation of autocorrelation function ρ_k is the basic characteristic of MA process. But the tail of ρ_k is not the unique characteristic of AR process, because the autocorrelation function in ARMA process is also tailing. The partial autocorrelation function of AR process will be discussed in (3).

(2) MA process. Rewrite the expansion of Eq. (7.14):

$$\begin{aligned} Z_t &= a_t - \theta_1 a_{t-1} - \theta_2 a_{t-2} - \cdots - \theta_q a_{t-q} \\ Z_{t-k} &= a_{t-k} - \theta_1 a_{t-k-1} - \theta_2 a_{t-k-2} - \cdots - \theta_q a_{t-k-q} \end{aligned}$$

Multiply these two equations, then take the mathematical expectation to get the variance function:

$$\gamma_k = \begin{cases} \sigma^2\left(1 + \theta_1^2 + \theta_2^2 + \cdots + \theta_q^2\right) & (k = 0) \\ \sigma^2\left(-\theta_k + \theta_1\theta_{k+1} + \cdots + \theta_{q-k}\theta_q\right) & (0 < k \le q) \\ 0 & (k > q) \end{cases} \tag{7.22}$$

The corresponding autocorrelation function is:

$$\rho_k = \begin{cases} 1 & (k=0) \\ \dfrac{-\theta_k + \theta_1\theta_{k+1} + \cdots + \theta_{q-k}\theta_q}{1+\theta_1^2+\cdots+\theta_q^2} & (0<k\le q) \\ 0 & (k>q) \end{cases} \tag{7.23}$$

Eq. (7.23) shows, when the steps between Z_t and Z_t' are greater than q, they are no longer correlated to each other. Seen from $\rho_0, \rho_1, \ldots, \rho_q, \ldots$, the origin part of such sequence is zero as from q, and this autocorrelation function is called truncation.

(3) Partial autocorrelation function. The approximation of Z_k is represented by a linear combination of $Z_{t-1}, \ldots, Z_{t-k}$ and the coefficient ϕ_{kz} is chosen so that:

$$\min S = E\left(Z_t - \sum_{j=1}^{k} \phi_{kj} Z_{t-j}\right)^2 \tag{7.24}$$

To obtain ϕ_{kj}, take partial derivative to be zero:

$$\frac{\partial S}{\partial \phi_{kj}} = 0 \quad (j=1,2,\ldots,k) \tag{7.25}$$

Expand S to get:

$$S = \gamma_0 + \sum_{j=1}^{k} \phi_{kj}^2 \gamma_0 - 2\sum_{j=1}^{k} \phi_{kj}\gamma_i + 2\sum_{j>i}^{k} \phi_{kj}\phi_{ki}\gamma_{j-i} \tag{7.26}$$

Substitute it into Eq. (7.25) and then divide by γ_0 to get:

$$\begin{bmatrix} 1 & \rho_1 & \cdots & \rho_{k-1} \\ \rho_1 & \vdots & & \rho_{k-2} \\ \vdots & \vdots & & \vdots \\ \rho_k & \rho_{k-2} & & \vdots \end{bmatrix} \begin{bmatrix} \phi_{k1} \\ \vdots \\ \vdots \\ \phi_{kk} \end{bmatrix} = \begin{bmatrix} \rho_1 \\ \vdots \\ \vdots \\ \rho_k \end{bmatrix} \tag{7.27}$$

$\phi_{11}, \phi_{22}, \ldots, \phi_{kk}$ is called partial autocorrelation function of Z_k. The following shows how to solve ϕ_{kj}, proceeding directly from the definition of S, substitute Eq. (7.13) into S to get:

$$\begin{aligned} S &= E\left[\phi_1 Z_{t-1} + \phi_2 Z_{t-2} + \cdots + \phi_p Z_{t-p} + a_t - \sum_{j=1}^{k} \phi_{kj} Z_{t-j}\right]^2 \\ &= E\left[a_t + \sum_{j=1}^{p} (\phi_j - \phi_{kj}) Z_{t-j} - \sum_{j=p+1}^{k} \phi_{kj} Z_{t-j}\right]^2 \\ &= \sigma_a^2 + E\left[\sum_{j=1}^{p} (\phi_j - \phi_{kj}) Z_{t-j} - \sum_{j=p+1}^{k} \phi_{kj} Z_{t-j}\right]^2 \\ &\ge \sigma_a^2 \end{aligned} \tag{7.28}$$

To make S minimal, when $k \geq p$, it shall take:

$$\phi_{kj} = \begin{cases} \phi_j & (1 \leq j \leq p) \\ 0 & (p+1 \leq j \leq k, \quad k = p, p+1 \cdots) \end{cases} \tag{7.29}$$

In particular, when $k = p+1$, …:

$$\phi_{kk} = 0$$

It can be seen that the partial autocorrelation function of AR process is truncated; truncation of ϕ_{kk} is the unique characteristic of AR process.

For MA and ARMA processes, the partial autocorrelation function is still defined by Eq. (7.27), however, ϕ_{kk} is not truncated but tailing. The autocorrelation function and partial autocorrelation function of ARMA process are not derived here; only their results as shown in Table 7.1.

Table 7.1 Three types of autocorrelation functions and partial autocorrelation functions

	Model Name		
	AR(p,0)	**MA(0,q)**	**ARMA(p,q)**
Model equation	$\phi(B) = Z_t = a_t$	$Z_t = \theta(B)a_t$	$\phi(B)Z_t = \theta(B)a_t$
Stationary condition	Module of root of $\phi(B) > 1$	Always stationary	Module of root of $\phi(B) > 1$
Invertible condition	Always invertible	Module of root of $\theta(B) > 1$	Module of root of $\theta(B) > 1$
Autocorrelation function	Tailing	Truncated	Tailing
Partial autocorrelation function	Truncated	Tailing	Tailing

Table 7.1 shows the characteristics of the previous three models: stationary conditions, invertible conditions, and properties of autocorrelation and partial autocorrelation functions. In summary, if model parameters are given, the autocorrelation and partial autocorrelation functions can be calculated. On the contrary, if the autocorrelation and partial autocorrelation functions are given, models and parameters can be set. This is of vital importance to the following model identification.

7.3.3 Identification of the Model ΔP_L

Because the load disturbance sequence is known:

$$Z_1, Z_2, \ldots, Z_n \quad (n \text{ is the number of sequence})$$

Its mathematical model can be identified using the following steps:

(1) Basis of identification: As mentioned earlier, if the sample autocorrelation function $\hat{\rho}_k$ is truncated after step q, it is judged to be qth order MA model. Similarly, it is judged to be the pth order stationary AR model from the truncation of partial autocorrelation function $\hat{\phi}_{kk}$ after step p.

(2) Truncation criteria of $\hat{\rho}_k$ and $\hat{\phi}_{kk}$: Theoretically, the truncation of autocorrelation function ρ_k and partial correlation function ϕ_{kk} mean the tails are absolutely zero. However, $\hat{\rho}_k$ and $\hat{\phi}_{kk}$ are only approximate estimates to ρ_k and ϕ_{kk}, including some errors. Therefore, even the $\hat{\rho}_k$ of MA model will not be all zero after step q but fluctuate around zero. It can be assumed that such fluctuation is of normal distribution. Judging from the normal distribution, as $P\left[|\hat{\rho}_k| \leqslant \frac{2}{\sqrt{n}}\right] = 95.5\%$, for $k > q$, if the number of $|\hat{\rho}_k| > \frac{2}{\sqrt{n}}$ is not greater than 4.5%, the $\hat{\rho}_k$ can be truncated. $\hat{\phi}_{kk}$ can be judged following the same method.

(3) Identification of order d of the nonstationarity stochastic model: If the $\hat{\rho}_k$ and $\hat{\phi}_{kk}$ calculated from the sample sequence are neither truncated nor tailing, then its first-order sequence ∇Z_t, second order sequence $\nabla^2 Z_t$,..., are tested until getting desired $\hat{\rho}_k$ and $\hat{\phi}_{kk}$. Generally, satisfactory results can be obtained when the difference d is no more than three times.

(4) Identification of p and q for ARMA: p and q have to be identified by tests from low to high orders, for example, sequential tests (1,1), (1,2), (2,1),..., until appropriate p and q are selected.

The load disturbance model obtained from identification is generally expressed with the following difference equation:

$$\Delta P_{\mathrm{L}}(k) + a_1 \Delta P_{\mathrm{L}}(k-1) + \cdots + a_n \Delta P_{\mathrm{L}}(k-n) = \xi_k + b_1 \xi_{k-1} + b_2 \xi_{k-2} + \cdots + b_n \xi_{k-n} \tag{7.30}$$

where ξ_k is the white noise sequence. Eq. (7.30) can be transformed into the following discrete state equation:

$$\left.\begin{aligned} y(k+1) &= \Phi^* y(k) + B^* \xi(k) \\ \Delta P_L(k) &= H^{*T} y(k) \end{aligned}\right\} \tag{7.31}$$

where

$$\Phi^* = \left[\begin{array}{ccccc} 0 & & & & \\ \vdots & & & & \\ \vdots & & I & & \\ 0 & & & & \\ \hline -a_n & -a_{n-1} & \cdots & -a_1 \end{array}\right], H^{*T} = [1,0,\cdots,0]$$

Eq. (7.31) can be further transformed into the following equivalent continuous state equation:

$$\left.\begin{aligned} \dot{y}(t) &= A^* y(t) + B^* \xi(t) \\ \Delta P_{\mathrm{L}}(t) &= H^{*T} y(t) \end{aligned}\right\} \tag{7.32}$$

Section 7.7 gives the method to calculate A from the given ϕ^*.

7.3.4 *Parameter Estimation of the Model* ΔP_{L}

After identifying the order of models, the parameter estimation can be made. This section only discusses the parameter estimation of AR models.

Substituting the covariance function $\hat{\rho}_k$ of sample for ρ_k into Eq. (7.23), the following equation, that is, the Yule-Walker equation is obtained:

$$\begin{bmatrix} \hat{\rho}_0 & \hat{\rho}_1 & \cdots & \hat{\rho}_{p-1} \\ \vdots & \cdots & \cdots & \cdots \\ \hat{\rho}_{p-1} & \cdots & \cdots & \hat{\rho}_0 \end{bmatrix} \begin{bmatrix} \hat{\phi}_1 \\ \vdots \\ \hat{\phi}_n \end{bmatrix} = \begin{bmatrix} \hat{\rho}_1 \\ \vdots \\ \hat{\rho}_p \end{bmatrix} \tag{7.33}$$

Solve the equation to get autoregressive parameters $\hat{\phi}_1, \ldots, \hat{\phi}_n$.

Estimation of constant $\hat{\theta}_{00}$ by:

$$\hat{\theta}_{00} = \begin{cases} \mu\left(1 - \sum_{i=1}^{p} \hat{\phi}_i\right) & (p > 0) \\ \mu & (p = 0) \end{cases} \tag{7.34}$$

where μ is the mean value of the given time series.

Estimation of white noise variance σ_a^2 by:

$$\sigma_a^2 = \gamma_0 - \sum_{i=1}^{p} \hat{\phi}_i \gamma_i \tag{7.35}$$

These estimation methods are approximated estimations, and there are more exact estimation methods. In the case of AR models, based on Reference [78], the approximated and exact estimation values are of little difference; in this section, the AR model is selected, and the exact estimation is not discussed herein.

7.4 Model for a Typical Power System

The power generation system is a typical large system consisting of all power plants, each of which is made up of a governor block, excitation block, prime mover block, and generator block. As previous discussed, this chapter only considers the changes of load frequency under small disturbances, taking no account of the excitation block of the unit. The mathematical models for various blocks of the units will be discussed respectively as follows.

7.4.1 Generator Model

Under small disturbance, the motion equation of generator rotor is:

$$M\frac{d\Delta\omega}{\mathrm{d}t} + D\Delta\omega = \Delta p_{\mathrm{T}} - \Delta p_{\mathrm{L}} \tag{7.36}$$

This power balance equation is suitable for all units.

All power values in Eq. (7.36) are the per-unit value of rated powers; M is inertia constant, $M = 2\mathrm{H}$, H is generally 2–8 s, and this chapter takes 5 s.

The transfer function of generator model can be obtained by Laplace transform of Eq. (7.36):

$$\Delta\omega = \frac{1}{Mp + D}(\Delta p_{\mathrm{T}} - \Delta p_{\mathrm{L}}) \tag{7.37}$$

where $p = \dfrac{\mathrm{d}}{\mathrm{d}t}$ is the differential operator.

Its block diagram is shown in Fig. 7.1.

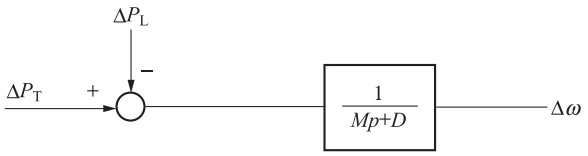

Fig. 7.1
Generator model.

7.4.2 Thermal-generator Model

7.4.2.1 Dynamic characteristics of a steam turbine governor

General transfer function block diagram of a steam turbine governor is shown in Fig. 7.2.

In this block diagram, by omitting the block of adjusting the valve opening and speed restriction, eliminating the negative feedback therein and ignoring the pilot oil valve inertia (T_1 is the time constant for pilot oil regulating valve, K_i is the hard feedback magnification, $K_i = 1$), a simplified block diagram is obtained (see Fig. 7.3).

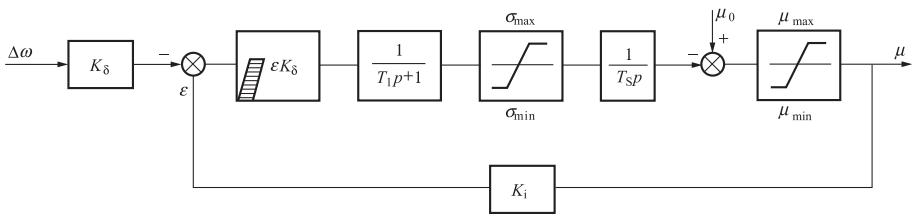

Fig. 7.2
Transfer function block diagram of a steam governor.

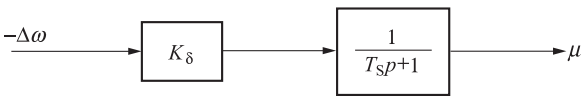

Fig. 7.3
Simplified block diagram of steam turbine governor. T_S—time constant of servomotor; K_δ—amplification factor of speed measuring parts; $\Delta\omega$—frequency deviation.

7.4.2.2 Dynamic characteristics of a steam turbine

The effect of steam volume is reflected in the inertia of steam in the pipelines and reheaters during the transient process of the steam turbine. When the steam turbine adjusts the steam valve opening due to the existence of certain steam volume between the steam valve and nozzle, the steam pressure cannot be changed immediately, so the power input goes into turbine, and there is a time lag. The effects of steam volume can be mathematically simulated by first-order inertial model, with transfer function expressed as follows:

$$\Delta P_{\mathrm{T}} = \frac{1}{T_{\mathrm{CH}}p+1}\mu$$

where T_{CH}—time constant of steam volume; μ—steam valve opening.

For an intermediate reheat steam turbine, the intermediate reheat system has a larger steam volume, and the change in the output power of the medium/low-pressure cylinder will be affected by this portion of the steam inertia, which can also be expressed by a first-order inertia model. For the general turbine, the block diagram of steam volume simulation of reheat turbines is shown in Fig. 7.4.

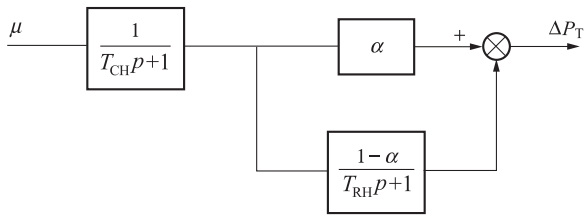

Fig. 7.4
Block diagram of steam volume simulation of reheat turbine.

In Fig. 7.4, α and $1-\alpha$ are the ratio of total power of the high (and medium and low) pressure cylinder to the total turbine power, respectively. T_{CH} and T_{RH} are the time constants of high-pressure cylinder and reheat system steam volume, respectively. In Fig. 7.4, the proportional element α and inertial element $\frac{1-\alpha}{T_{\mathrm{CH}}p+1}$ are put in parallel to get Fig. 7.5.

Fig. 7.5
Block diagram of dynamic characteristics for a steam turbine.

7.4.2.3 Dynamic characteristics of thermal generating unit

Based on the combination of Figs. 7.1, 7.3 and 7.5, with the input control signal Δu, a disturbance model of thermal unit can be obtained, as shown in Fig. 7.6 (where $R = \frac{1}{K_\delta}$ is speed adjusting rate).

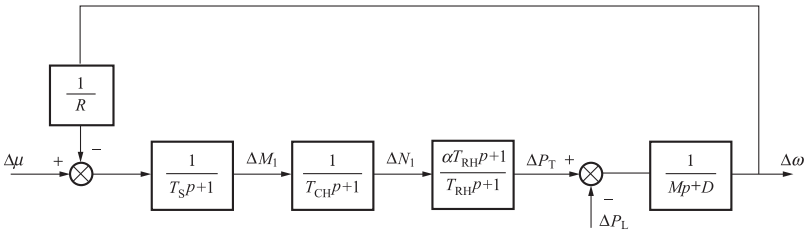

Fig. 7.6
Disturbance model of the thermal unit.

Adding the intermediate variables ΔM_1 and ΔN_1 into previous the block diagram, the corresponding differential equations based on transfer functions of each block can be obtained.

$$
\begin{aligned}
p\Delta M_1 &= -\frac{1}{T_S}\left(\frac{1}{R}\Delta\omega - \Delta\mu\right) - \frac{1}{T_S}\Delta M_1 \\
p\Delta N_1 &= \frac{1}{T_{CH}}\Delta M_1 - \frac{1}{T_{CH}}\Delta N_1 \\
p\Delta P_T - \alpha|\Delta N_1 &= \frac{1}{T_{RH}}\Delta N_1 - \frac{1}{T_{RH}}\Delta P_T \\
p\Delta\omega &= -\frac{D}{M}\Delta\omega + \frac{1}{M}\Delta P_T - \frac{1}{M}\Delta P_L
\end{aligned}
$$

Arrange these equations to get the following equation:

$$
\begin{bmatrix} p\Delta M_1 \\ p\Delta N_1 \\ p\Delta P_T \\ p\Delta\omega \end{bmatrix} = \begin{bmatrix} \frac{1}{T_S} & 0 & 0 & -\frac{1}{RT_S} \\ \frac{1}{T_{CH}} & -\frac{1}{T_{CH}} & 0 & 0 \\ \frac{\alpha}{T_{CH}} & -\frac{1}{T_{CH}} - \frac{1}{T_{CH}} & -\frac{1}{T_{CH}} & 0 \\ 0 & 0 & \frac{1}{M} & -\frac{D}{M} \end{bmatrix} \begin{bmatrix} \Delta M_1 \\ \Delta N_1 \\ \Delta P_T \\ \Delta\omega \end{bmatrix} + \begin{bmatrix} \frac{1}{T_S} \\ 0 \\ 0 \\ 0 \end{bmatrix} \Delta\mu + \begin{bmatrix} 0 \\ 0 \\ 0 \\ -\frac{1}{M} \end{bmatrix} \Delta P_L \quad (7.38)
$$

Eq. (7.38) is the state equation of the thermal unit model, which can be used as the basis for future analysis. Such form of expression is the most basic one, but for simplicity, it is an relatively detailed model we can use. The hydro unit model will be discussed in the following section.

7.4.3 Hydrogenerator Model

7.4.3.1 Dynamic characteristics of hydroturbine speed governing system

Block diagram of transfer function of the hydroturbine governor is shown in Fig. 7.7.

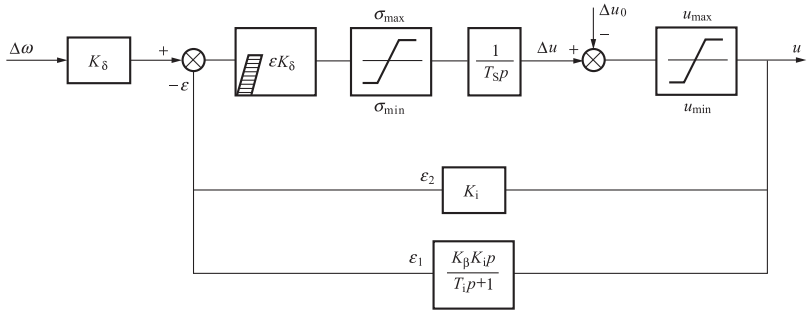

Fig. 7.7
Block diagram of transfer function of a hydroturbine governor.

This block diagram can be simplified through equivalent conversion of transfer function after removing the guide vane opening and speed restriction elements. First, it integrates hard and soft feedback block into an equivalent block; the transfer function is:

$$K_F(p) = \frac{K_\beta K_i p}{T_i p + 1} + K_i$$

Second, it eliminates the feedback and connects in series with the measurement element; the transfer function of the whole hydrogovernor is obtained as follows:

$$K_T(p) = \frac{K_\delta \dfrac{1}{T_S p}}{1 + \dfrac{1}{T_S p} \cdot K_F(p)} = \frac{K_\delta (T_i p) + 1}{T_S T_i p^2 + \left[T_S + \left(K_\beta + K_i\right) T_i\right] p + K_i}$$

Such a transfer function can be rewritten into:

$$K_T(p) = \frac{K}{T_1 p + 1} \cdot \frac{T_i p + 1}{T_2 p + 1}$$

And split into two series-connected blocks, where:

$$K = \frac{K_\delta}{K_i}, \quad T_1, T_2 = \frac{T_B}{2} \mp \sqrt{\left(\frac{T_B}{2}\right)^2 - T_A}$$

$$T_A = \frac{T_S T_i}{K_i}, \quad T_B = \frac{T_S + \left(K_\beta + K_i\right) T_i}{K_i}$$

Assume $K = \frac{1}{R}$ as the static regulation coefficient, and add the control signal to get the simplified block diagram of the hydrogovernor (see Fig. 7.8).

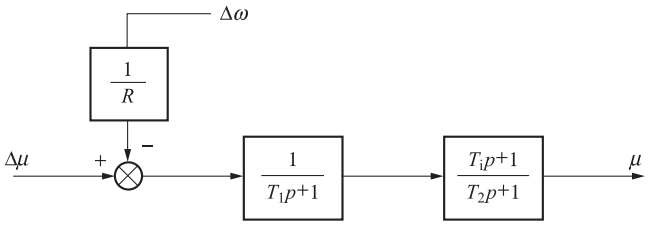

Fig. 7.8
Simplified block diagram of a hydro governor.

7.4.3.2 Dynamic characteristics of hydroturbine

The simulation of dynamic characteristics of the hydroturbine has taken into account the transient process caused by the inertia of water flow in the hydroturbine and diversion pipes. The process is also called the water hammer effect.

With the water hammer effect included, dynamic characteristics of the hydroturbine and water diversion system thereof can be expressed by the following approximately linear model:

$$\Delta P_{\mathrm{T}} = \frac{1 - T_{\mathrm{W}} p}{1 + 0.5 T_{\mathrm{W}} p} \mu$$

where T_{W}—water flowing time constant; μ—opening of guide vane.

Fig. 7.9 shows the block diagram of dynamic characteristics of the hydroturbine.

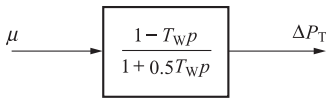

Fig. 7.9
Block diagram of dynamic characteristics of the hydroturbine.

7.4.3.3 Dynamic characteristics of hydrogenerating unit

Based on Figs. 7.1, 7.8, and 7.9, the disturbance model of a hydrogenerating unit can be obtained (shown in Fig. 7.10).

Based on the transfer functions of all blocks, the corresponding differential equation can be obtained by adding the intermediate variables ΔM_2 and ΔN_2 into the prior block diagram

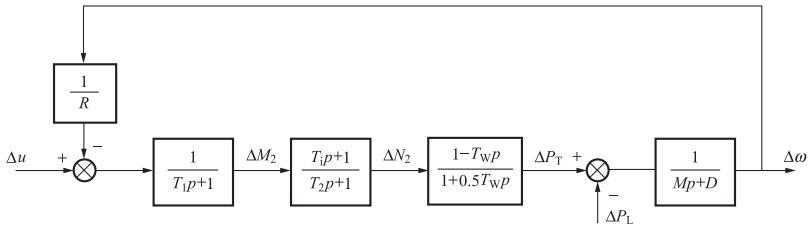

Fig. 7.10
Hydrogenerating unit disturbance model.

$$\left.\begin{aligned}
p\Delta M_2 &= -\frac{1}{T_1}\left(\frac{1}{R}\Delta\omega - \Delta\mu\right) - \frac{1}{T_1}\Delta M_2 \\
p\Delta N_2 - \frac{T_\mathrm{i}}{T_2}p\Delta M_2 &= \frac{1}{T_2}\Delta M_2 - \frac{1}{T_2}\Delta N_2 \\
p\Delta P_\mathrm{T} + 2p\Delta N_2 &= \frac{2}{T_\mathrm{W}}\Delta N_2 - \frac{2}{T_\mathrm{W}}\Delta P_\mathrm{T} \\
p\Delta\omega &= -\frac{D}{M}\Delta\omega + \frac{1}{M}\Delta P_\mathrm{T} - \frac{1}{M}\Delta P_\mathrm{L}
\end{aligned}\right\} \tag{7.39}$$

Rearrange this equation to get:

$$\begin{bmatrix} p\Delta M_2 \\ p\Delta N_2 \\ p\Delta P_\mathrm{T} \\ p\Delta\omega \end{bmatrix} = \begin{bmatrix} -\frac{1}{T_1} & 0 & 0 & -\frac{1}{RT_1} \\ \frac{1}{T_2} - \frac{T_\mathrm{i}}{T_1T_2} & -\frac{1}{T_2} & 0 & -\frac{1}{RT_1T_2} \\ -2\left(\frac{1}{T_2} - \frac{T_\mathrm{i}}{T_1T_2}\right) & 2\left(\frac{1}{T_2} - \frac{1}{T_\mathrm{W}}\right) & -\frac{2}{T_\mathrm{W}} & \frac{2}{RT_2} \\ 0 & 0 & \frac{1}{M} & -\frac{D}{M} \end{bmatrix} \begin{bmatrix} \Delta M_2 \\ \Delta N_2 \\ \Delta P_\mathrm{T} \\ \Delta\omega \end{bmatrix} + \begin{bmatrix} \frac{1}{T_1} \\ \frac{T_\mathrm{i}}{T_1T_2} \\ \frac{-2T_\mathrm{i}}{T_1T_2} \\ 0 \end{bmatrix} \Delta\mu + \begin{bmatrix} 0 \\ 0 \\ 0 \\ -\frac{1}{M} \end{bmatrix} \Delta P_\mathrm{L} \tag{7.40}$$

The state equation obtained here for the hydrogenerator model are the same as those for the thermal generator model and also the basis for future analysis. The physical meaning and data values of all parameters in the thermal generator and hydrogenerator models are detailed in Reference [84].

The combination of the previously mentioned thermal and hydro plants can constitute a multiunit power system. When the number of generators increased, to study the entire system, it is very difficult to directly simulate the system differential equations either by numerical calculation method or by simulated simulator. Thus, the equivalent problem of power system is considered in the following section.

7.4.4 Equivalent Generator Model of the Power System

Suppose there are n generators in the system, and the equation for the K-th generator is:

$$M_K \Delta\dot{\omega}_K + D_K \Delta\omega_K = \Delta P_{TK} - \Delta P_{LK} \tag{7.41}$$

Add the n equations in the system together as the following equation:

$$\sum_{k=1}^{n} M_K \Delta\dot{\omega}_K + \sum_{k=1}^{n} D_K \Delta\omega_K = \sum_{k=1}^{n} \Delta P_{TK} - \sum_{k=1}^{n} \Delta P_{LK} \tag{7.42}$$

Now, it is required to transform Eq. (7.42) into an equivalent generator equation of n generators, which can be completed by different transformation types. The following parameters are defined for the equivalent system:

$$M_e = \sum M_K \ = \text{Inertia constant of equivalent generator}$$

$$\Delta\omega_e = \frac{\sum M_K \Delta\omega_K}{M_e} \ = \text{Relative rotation speed of equivalent generator}$$

$$D_e \ = \frac{\sum D_K \Delta\omega_K}{\Delta\omega_e} \ = \text{Damping coefficient of equivalent generator}$$

and

$$M_e \Delta\dot{\omega}_e + D_e \Delta\omega_e = \Delta P_{Te} - \Delta P_{Le} \tag{7.43}$$

can be obtained,

where

$$\Delta P_{Te} = \sum \Delta P_{TK}, \quad \Delta P_{Le} = \sum \Delta P_{LK}$$

Under small disturbance, some effects can be generally neglected, such as the electromagnetic damping torque caused by the rotor damping winding and the mechanical damping caused by the prime mover and motor rotation loss, due to the small change in the unit rotation speeds. These effects should be considered only in the case of great changes in the rotation speed or under circumstances where accurate calculation results are required. Hence, the damping terms in Eq. (7.43) can be generally neglected, namely assume $D_e = 0$.

Taking into account the static effect of the system load ΔP_{Le} as follows:

$$\Delta P_{Le} = D\Delta\omega_e + \Delta P_L$$

That is, ΔP_{Le} is the sum of static load response $D\Delta\omega_e$ and stochastic load disturbance ΔP_L irrelevant to $\Delta\omega$, where D is static response coefficient of load correlated to $\Delta\omega_e$.

Finally, the equivalent Eq. (7.43) can be simplified as:

$$M_e \Delta\dot{\omega}_e + D\Delta\omega_e = \Delta P_{Te} - \Delta P_L$$

In this chapter, the five-unit system (including four hydro units and one thermal unit) is considered, and the block diagram of equivalent generator model is detailed in Fig. 7.11, where

$$W_{SUM} = \frac{\sum M_K \Delta\omega_K}{\sum M_K}$$

As shown in Fig. 7.11, the task of load frequency control for a power system is to search for the control law Δu_i under any load disturbance ΔP_L to carry out stable frequency control. That is, to maintain the frequency changes in a relatively small range, and to carry out fast, stable, and accurate frequency control.

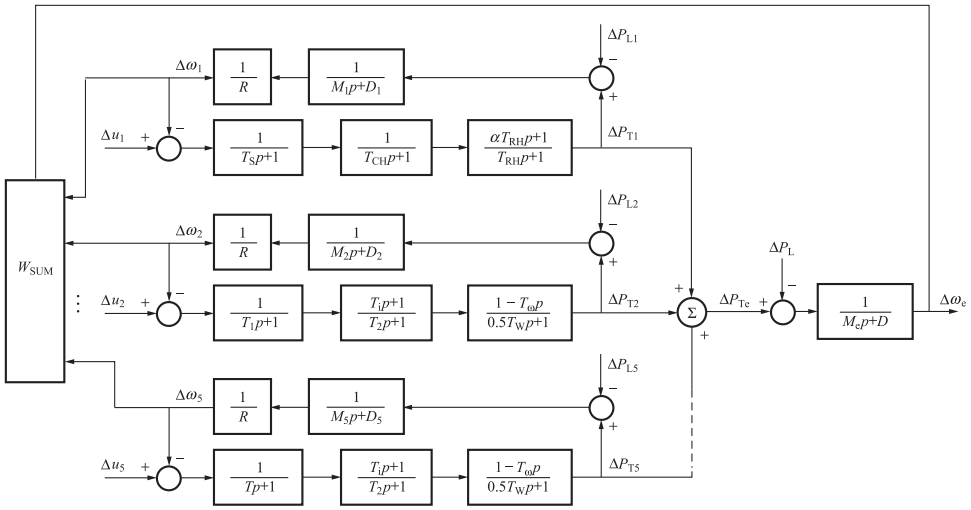

Fig. 7.11
Block diagram of equivalent generator model.

7.5 Hierarchical Estimation for the Power System

After formulating the power system model, the system can be then controlled. To control a system, it is required to understand the system state, that is, to make state estimation to the system. The geographical distribution properties of all power plants in the power system facilitate the application of decomposition method in the system analysis and control. Naturally, the power system divides the system into three levels: the bottom is the power station or generating units, the middle is dispatching centers at all levels, and the highest is a joint

dispatching center. In terms of the current situation, the estimation shall be considered only for the first two levels.

The decomposition, multiorder, and hierarchical system theories can provide a useful foundation for large-scale power system control. With the decomposition technology, a complex system can be decomposed into easily solved subsystems, and the recombination of subsystem solutions can determine the solution for the whole system. In view of the interaction between subsystem solutions, it is often required to repeatedly deal with the relationship consistency between the subsystem solutions and the solution of the whole system.

The reason why this decomposition method is explored in power system control is due to the high costs to deliver messages from remote areas to the control center under any circumstances, and the fact that collected information is used for local operation only.

The successful control of the power system depends on an accurate knowledge of its states at any time, and some states are determined from direct observation of distributed measuring equipment. The speed and placement of measuring equipment depends largely on the function of the control system to the disturbance. The introduction of computer control requires reliable data to achieve effective control. The online state estimation has provided a reliable data foundation to the future system variables.

In conclusion, the hierarchical estimation method is employed to make state estimation to the power system with hierarchical structure, using two-stage estimators applied to the power system, that is, a local estimator and a central estimator. Because variable $\Delta\omega_j$ in the system can be measured using only the cheap frequency meter, $\Delta\omega_j$ is taken as a measured variable. Based upon the power system model, all state variables of the system can be estimated using the Kalman filter. The coordinated operation of local estimator and central estimator is shown in Fig. 7.12.

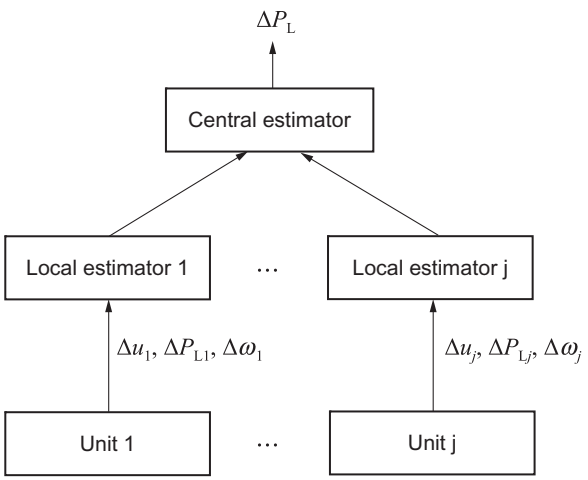

Fig. 7.12
Coordinated operation of hierarchical estimator for the power system.

7.5.1 Local Estimator

From Eqs. (7.39) to (7.41), motion equations of the steam turbine and hydro turbine have the following structures:

$$\dot{X}_{\mathrm{T}j} = A_{\mathrm{T}j}X_{\mathrm{T}j} + B_{\mathrm{T}j}\Delta u_j + C_{\mathrm{T}j}\Delta P_{\mathrm{L}j} \tag{7.44}$$

The difference between the above mentioned equations is that the elements in $A_{\mathrm{T}j}$, $B_{\mathrm{T}j}$, and $C_{\mathrm{T}j}$ are different,

where

$$X_{\mathrm{X}j}^{\mathrm{T}} = \left\{\Delta M_j \quad \Delta N_j \quad \Delta P_{\mathrm{T}j} \quad \Delta\omega_j\right\}$$

Local measurement includes:

$$\Delta\omega_{\mathrm{m}j} = \Delta\omega_j + \eta_j = H_j^{\mathrm{T}}X_{\mathrm{T}j} + \eta_j \tag{7.45}$$

$$\Delta u_{\mathrm{m}j} = \Delta u_j + \eta_{\mathrm{m}j} \tag{7.46}$$

$$\Delta P_{\mathrm{mL}j} = \Delta P_{\mathrm{L}j} + \eta_j \tag{7.47}$$

From Eqs. (7.44)–(7.47), we know

$$\begin{aligned}\dot{X}_{\mathrm{T}j} &= A_{\mathrm{T}j}X_{\mathrm{T}j} + B_{\mathrm{T}j}\Delta u_{\mathrm{m}j} + C_{\mathrm{T}j}\Delta P_{\mathrm{mL}j} + V_{\mathrm{T}j}\\ \Delta\omega_{\mathrm{m}j} &= H_{\mathrm{T}j}^{\mathrm{T}}X_{\mathrm{T}j} + \eta_{\mathrm{T}j}\end{aligned} \tag{7.48}$$

η and V in Eq. (7.45)–(7.48) are white noise. Transform the Eq. (7.44) into equivalent discrete state equation:

$$X_{\mathrm{T}j}(k+1) = \phi_{\mathrm{T}j}X_{\mathrm{T}j}(k) + G_{\mathrm{T}j}\Delta u_{\mathrm{m}j}(k) + T_{\mathrm{T}j}\Delta P_{\mathrm{mL}j}(k) + V_{\mathrm{T}j} \tag{7.49}$$

$$\Delta\omega_{\mathrm{m}j}(k) = H_{\mathrm{T}j}^{\mathrm{T}}X_{\mathrm{T}j} + \eta_{\mathrm{T}j} \tag{7.50}$$

Transformation methods are shown in Section 7.6.

$V_{\mathrm{T}j}$ and $\eta_{\mathrm{T}j}$ are white noise. Kalman filtering equations corresponding to Eqs. (7.49) and (7.50) are:

$$\hat{X}_{\mathrm{T}j}(k+1) = \overline{X}_{\mathrm{T}j}(k+1) + K(k+1)\left[\Delta\omega_{\mathrm{m}j}(k+1) - \overline{X}_{\mathrm{T}j}(k+1)\right] \tag{7.51}$$

$$\overline{X}_{\mathrm{T}j}(k) = \phi_{\mathrm{T}j}\hat{X}_{\mathrm{T}j}(k-1) + G_{\mathrm{T}j}\Delta u_{\mathrm{m}j}(k-1) + T_{\mathrm{T}j}\Delta P_{\mathrm{mL}j}(k-1) \tag{7.52}$$

$$K_{\mathrm{T}j}(k+1) = P_{\mathrm{T}j}(k+1/k)H_{\mathrm{T}j} + \left[H_{\mathrm{T}j}P_{\mathrm{T}j}(k+1/k)H_{\mathrm{T}j}^{\mathrm{T}} + R_{\mathrm{T}j}\right]^{-1} \tag{7.53}$$

$$P_{\mathrm{T}j}(k+1/k) = \phi_{\mathrm{T}j}P_{\mathrm{T}j}(k)\phi_{\mathrm{T}j}^{\mathrm{T}} + Q_{\mathrm{T}j} \tag{7.54}$$

$$P_{\mathrm{T}j}(k+1) = \left[1 - K(k)H_{\mathrm{T}j}\right]P_{\mathrm{T}j}(k+1/k) \tag{7.55}$$

where $R_{\mathrm{T}j}$ and $Q_{\mathrm{T}j}$ mean the covariance matrix of $\eta_{\mathrm{T}j}$ and $V_{\mathrm{T}j}$, respectively.

7.5.2 Central Estimator

From the hierarchical estimator, it is possible to acquire the information of all power plants, and accordingly, the central estimator can be used to estimate the whole system information.

First, discretize the system equivalent generator equation:

$$M_e \Delta\dot{\omega}_e = -D\Delta\omega_e + \Delta P_{Te} - \Delta P_L$$

into difference equation, then combine it with the load model Eq. (7.31) to get:

$$X(k+1) = \phi X(k) + G\Delta\hat{P}_T(k) + V \tag{7.56}$$

The measurement equation is expressed as:

$$\begin{aligned}\Delta\omega_m(k) &= \frac{\sum M_j\left[\Delta\omega_j(k) - \eta\right]}{M} \\ &= \Delta\omega_m(k) + \eta = H^T X(k) + \eta\end{aligned} \tag{7.57}$$

where

$$\boldsymbol{X} = \{y_1 \quad y_2 \ldots y_n \Delta\omega\} \quad \text{(the number of } y \text{ depends on the load model)}$$

In Eq. (7.56), $\Delta\hat{P}_T = \sum\Delta\hat{P}_{Tj}$ is obtained by the local estimator. V and η are assumed to be white noise; Kalman filtering equations corresponding to Eqs. (7.56) and (7.57) are:

$$\hat{X}(k+1) = \overline{X}(k+1) + k(k+1)\left[\Delta\omega_m(k+1) - \overline{X}(k+1)\right] \tag{7.58}$$

$$\overline{X}(k+1) = \phi\hat{X}(k) + G\Delta P_T(k) \tag{7.59}$$

$$K(k+1/k) = P(k+1/k)H^T\left[HP(k+1/k)H^T + R\right]^{-1} \tag{7.60}$$

$$P(k+1/k) = \phi P(k)\phi^T + Q \tag{7.61}$$

$$P(k+1) = [I - K(k)H]P(k+1/k) \tag{7.62}$$

where R and Q mean the covariance matrix of η and V respectively.

7.5.3 Estimation and Forecasting of Load Disturbance ΔP_L

From the second equation of load model Eq. (7.31), the estimation formula of ΔP_L is

$$\Delta\hat{P}_L(k) = H^{*T}\hat{Y}(k) = H^{*T}W\hat{X}(k) \tag{7.63}$$

where $\hat{X}(k)$ is obtained by the local estimator. W means the transformation matrix from X to Y. Based on Eq. (7.56), the load disturbance forecasting formula calculated from kth step is obtained as follows:

$$\Delta\hat{P}_L(k+1) = H^{*T}(\phi^*)^1\hat{y}(k) \tag{7.64}$$

where ϕ^* is given by the load model. The system can be controlled based upon the forecasting values of load disturbance ΔP_L.

7.6 Load Frequency Controller of the Power System

As previously discussed, the power system load frequency controller is of an integral and state feedback type. Here with the invariance principle, a new discrete compensation controller is set up, which is suitable for the digital machine control to compensate the system load disturbance and control the system state.

7.6.1 Invariance Principle

The invariance principle has been applied to the automatic control field since the 1960s, and it is well known that the feedback can reduce the effects of disturbance, but it cannot completely eliminate its influence. Therefore, the system adopts the invariance principle so that it can respond sensitively to disturbances.

In the open loop system of Fig. 7.13A, output C is only required to be the result of reference input, but the pure output is:

$$C = C_R + C_V = GR - V \tag{7.65}$$

where V is the disturbance.

In Fig. 7.13B, the feedback is introduced, and the disturbance in the system output affects the C_V as follows:

$$C_V = \frac{-V}{1+GH} \tag{7.66}$$

In Fig. 7.13C, the disturbance is obviously smaller than that given by Eq. (7.65).

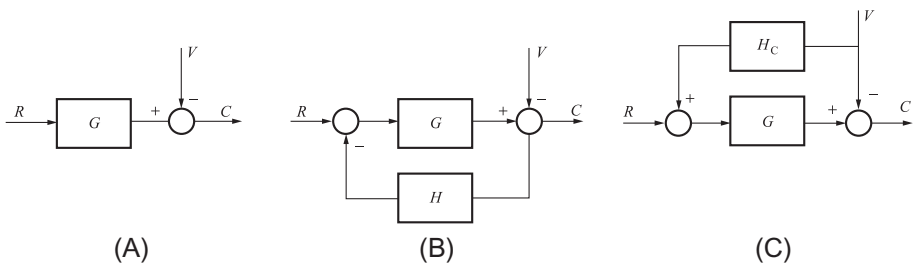

Fig. 7.13
Control modes of different systems.
(A) Open loop system; (B) Feedback system; (C) Invariance system.

Disturbance is given by a compensator:

$$C_V = (GH_C - 1)V$$

If select

$$H_C = \frac{1}{G}$$

Then the output is completely independent of the perturbation. If the compensator cannot be completely equal to $1/G$ for some reason, the disturbance output is approximately independent of the disturbance. When the feedforward loop fails to fully compensate, it can be regulated by the feedback loop, as shown in Fig. 7.14.

The disturbance quantity is

$$C_V = \frac{H_C G - 1}{HG + 1} V \tag{7.67}$$

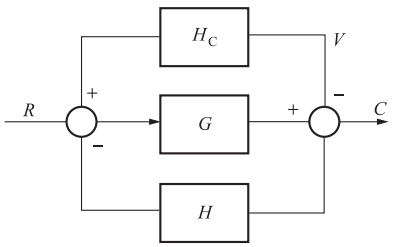

Fig. 7.14
Combined control structure diagram of Fig. 7.13B and C.

It can be seen from Eq. (7.67) that, when the feedforward regulation loop fails to fully compensate the disturbance influence, it is possible to adopt the feedback regulation, that is, the combined feedforward-feedback system. It must be noted that estimation and forecasting with regard to load disturbance ΔP_L makes it possible to constitute the feedforward control loop. Failure to know the disturbance signals means that the feedforward control loop cannot be constituted.

7.6.2 Load Frequency Control based on Invariance Principle

As mentioned earlier, the task of the load frequency controller is to find such a control law to compensate for the effect of the load disturbance and to maintain the power system frequency within the allowable range of the specified value. It is known that the integral load frequency controller (see Fig. 7.15) can curtail the disturbance influence but cannot be completely offset. Nevertheless, the feedforward controller (or compensator) based on the invariance principle, under certain conditions (when the compensated transfer function is invertible and accurate

disturbance is known), does not need to bear any the impact of disturbance, namely, it is possible to find a control law to fully compensate the disturbance quantity and control the frequency changes.

The following shows how to derive the load frequency control law as per the invariance principle.

The estimation or forecasting values of load disturbance ΔP_{L} are distributed to each unit by the following equation:

$$\Delta P_{\mathrm{L}j} = \alpha_j \Delta P_{\mathrm{L}}$$

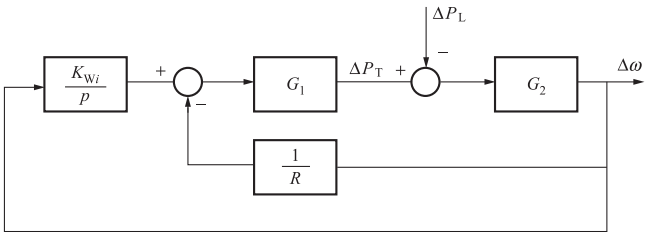

Fig. 7.15
Integral load frequency controller.

The distribution coefficient in Fig. 7.15 can be allocated according to the electrical distance perturbed to the unit and can also be calculated in advance by the optimization calculation. The optimal approach to select αj is beyond the scope of this chapter. The distributed method used in this chapter is based on the electrical distance.

Fig. 7.16 shows the schematic diagram of feedforward control (load frequency compensator) of a thermal-(or hydro-) generating unit, where G_{1j} represents the transfer function of prime mover and regulating system thereof, and G_{2j} represents the transfer function of generator and system.

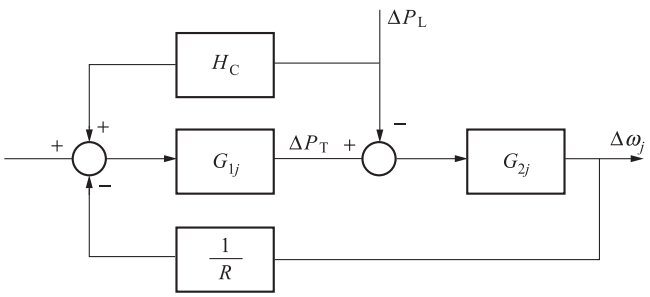

Fig. 7.16
Load frequency compensator.

From the system diagram, for the thermal generating unit:

$$G_1 = \frac{\alpha T_{RM} p + 1}{(T_S p + 1)(T_{CH} p + 1)(T_{RH} p + 1)}$$

$$G_2 = \frac{1}{M_1 p + D_1}$$

For the hydro generating unit:

$$G_1 = \frac{(T_1 p + 1)(1 - T_W p)}{(T_1 p + 1)(T_2 p + 1)(0.5 T_W p + 1)}$$

$$G_2 = \frac{1}{M_2 p + D}$$

In Fig. 7.14, H_{Cj} means the transfer function of the compensator.

$$H_{Cj} = \frac{1}{G_{1j}}$$

Obviously, if the corresponding compensation control law is as follows:

$$\Delta u_j = \frac{1}{G_{1j}} \Delta P_L = H_{Cj} \Delta P_{Lj}$$

It is possible to fully compensate for the effect of the disturbance. However, this complete compensation can only be achieved if the unit transfer function is reversible. Experimental results show that $H_{Cj} = 1$ can achieve good control effect when G_{1j} is irreversible.

When the digital control is achieved, it is required to transform the continuous differential transfer function in Fig. 7.16 into the discrete difference transfer function, using the methods proposed in the next section. After such transformation, it is quite easy to achieve this compensation control with the help of a digital computer.

7.6.3 Simulation Procedure of Tracking Control

In the past, the feedback control was not necessary to understand the system perturbation, that is, no compensation to the disturbance, and the control is only performed after the system state changes. In general, the feedforward control is to perform compensation control after measuring the disturbance. The tracking control of the power system can be achieved by continuously measuring, estimating, forecasting, and controlling. The simulation test of tracking control is shown in Fig. 7.17.

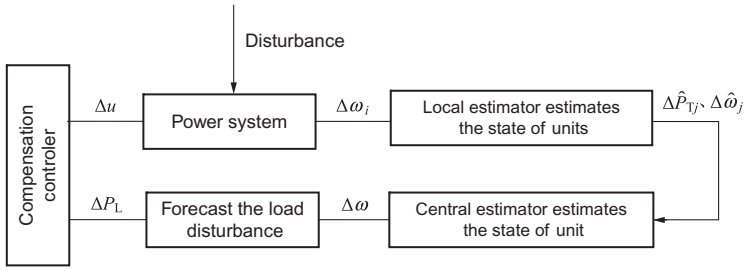

Fig. 7.17
Schematic diagram for simulation test of tracking control.

The concrete simulation process is, (1) the initial disturbance is given by the identified load disturbance model, (2) the actual state of the simulation is calculated according to the principle of electrical distance distribution, (3) $\Delta\omega_j$ is taken as the actual value the measurement errors in Gaussian distribution as a measurement value, (4) the unit state at that time is estimated by the local estimator, (5) the $\Delta\hat{P}_{\mathrm{T}j}$ and $\Delta\hat{\omega}_j$ estimated by the local estimator is taken as the input to the center estimator, (6) the state variables of the equivalent generator is estimated and used to make load forecasting. Take the load forecasting value ΔP_{L} as the next step of disturbance value, and repeat the above process, during which the compensation controller shall be used to compensate disturbance and control the system state, thereby forming the whole process of tracking control.

7.7 Transformation Methods of Linear Models

The accurate mathematical descriptions for many industrial processes are unknown. The task of the modern identification method is to build the suitable or approximate mathematical models for these processes from the measurement data, which are often in discrete forms. Though the performance of a stochastic process can be well represented by discrete models, the continuous models are sometimes convenient for the system analysis and control. It is well known that the time interval of identified discrete models is fixed, which depends on the fixed sampling interval to a large extent in the measuring device. However, in the real time estimation and control of power system, from time to time it is desirable to change such time intervals to achieve the ideal control performance. For example, 1-s and 4-s sampling time intervals are allowed during estimation and control.

When addressing the load frequency control problem of the power system, this chapter applies a series of system theories including identification, estimation, and control, and develop many specified types of models, such as state equation, transfer function, difference equation, and differential equation. Sometimes the model forms need to be transformed to each other for the special purpose. This section proposes some new methods to solve those problems. For the conversion problem between models with different sampling intervals, this section proposes

two solution methods: one is to first transform the discrete model into an equivalent continuous one, which is solved to derive the required discrete model; the other is to determine the desired discrete model by directly using the mutually transformation. Furthermore, this chapter has brought us to the computer solution of discrete transfer function when the model is of higher orders.

For this purpose, three models for discrete-continuous and discrete-discrete model transformations are proposed in this section, including the eigenvalue method, the logarithmic matrix expansion method and the successive approximation method. The condition of equivalence between models is theoretically proved and the mutual conversion of linear models is solved practically. Three methods have different scopes of application. The eigenvalue method can obtain the accurate results, independent of the time interval, but not applicable for the higher order equations. The logarithmic matrix method is affected by the time interval. The successive approximation method, whose calculation results are more accurate for the examples with a smaller sampling time, surely depends on the accuracy required for the practical problems. In addition, this section also proposes a solution method to transform a differential transfer function into a difference transfer function, which is suitable for various complicated situations even for higher-order equations, and only requires inverse, and is superior to the conventional method. These theoretical innovations and improvements to the existing linear model transformations have shown that they are applicable to engineering practice needs by the practical results in section 7.8.

7.7.1 Transformation of Difference Equation into Differential Equation

Formulation of the known difference equation, a discrete linear time-invariant model is of the form:

$$X(k+1) = \phi(\tau)X(k)$$

Formulate the corresponding equivalent steady continuous equation:

$$\dot{X} = \boldsymbol{A}X$$

where $\boldsymbol{A}$ is an unknown constant coefficient matrix. The problem is to determine the constant matrix $\boldsymbol{A}$ by the transition matrix $\phi(\tau)$. Two methods, that is, eigenvalue method and logarithmic matrix method are proposed.

7.7.1.1 Eigenvalue method

Consider the constant linear discrete model:

$$X(k+1) = \phi(\tau)X(k) \tag{7.68}$$

where $\phi(\tau)$ is known, and τ is the sampling time interval.

Theorem 1 *If matrix $\phi(\tau)$ has n different eigenvalues $\phi_i(i=1, 2, \ldots, n)$ with modulo less than 1 and n eigenvectors $e_i(i=1, 2, \ldots, n)$ corresponding to ϕ_i and mutually independent, then a constant matrix $\boldsymbol{A}$ can be found, which satisfies the equivalent condition to make the continuous model Eq. (7.69) equal to the discrete model Eq. (7.68):*

$$\dot{X}(t) = \boldsymbol{A}X(t) \tag{7.69}$$

Proof
Let

$$\boldsymbol{T} = (e_1, e_2, \cdots, e_n) \tag{7.70}$$

because $(e_1, e_2, \ldots, e_n)$ are independent of each other, so the inverse of matrix $\boldsymbol{T}$ exists. From linear algebra, we have:

$$\boldsymbol{\phi}(\phi_t) = \boldsymbol{T}\begin{bmatrix} \varphi_1 & & & \\ & \varphi_2 & & \\ & & \ddots & \\ & & & \varphi_n \end{bmatrix}\boldsymbol{T}^{-1} \tag{7.71}$$

Let

$$\varphi_i = e^{\lambda_i \tau} = x_i + \mathrm{j}y_i \tag{7.72}$$

where

$$\lambda_i = \frac{1}{\tau}\ln\varphi_i, \quad \ln\varphi_i = \ln|\varphi_i| + \mathrm{j}\arg\varphi_i, \quad \arg\varphi_i = \tan^{-1}\frac{y_i}{x_i} \tag{7.73}$$

Hence

$$\boldsymbol{\varphi}(\tau) = \boldsymbol{T}\begin{bmatrix} e^{\lambda_1\tau} & & & \\ & e^{\lambda_2\tau} & & \\ & & \ddots & \\ & & & e^{\lambda_n\tau} \end{bmatrix}\boldsymbol{T}^{-1} \tag{7.74}$$

Expand the above expression to get

$$\boldsymbol{\phi}(\tau) = \boldsymbol{T}\left(I + \Lambda\tau + \frac{2}{2!}\Lambda^2\tau^2 + \cdots + \frac{1}{K!}\Lambda^K\tau^K + \cdots\right)\boldsymbol{T}^{-1} \tag{7.75}$$

where

$$\Lambda = \begin{bmatrix} \lambda_1 & & & \\ & \lambda_2 & & \\ & & \ddots & \\ & & & \lambda_n \end{bmatrix} \tag{7.76}$$

Let

$$\boldsymbol{A} = \boldsymbol{T}\boldsymbol{\Lambda}\boldsymbol{T}^{-1} \tag{7.77}$$

Eq. (7.69) has a steady-state solution because λ_i and φ_i corresponds one by one, that is, $\lambda_i (i = 1, 2, \ldots, n)$ are different from each other, and their real parts are located at the left half plane. Substituting Eq. (7.77) into Eq. (7.75) results in:

$$\phi(\tau) = I + \boldsymbol{A}\tau + \frac{1}{2!}(\boldsymbol{A}\tau)^2 + \cdots + \frac{1}{K!}(\boldsymbol{A}\tau)^K + \cdots \tag{7.78}$$

□

This equation shows that the continuous model Eq. (7.69) determined by matrix $\boldsymbol{A}$ is equivalent to the previous discrete model Eq. (7.68), so the Theorem is proven. The above discussion is the case where the eigenvectors of $\boldsymbol{\phi}(\tau)$ have no multiple eigenvectors.

As for the case of multi-eigenvalues of $\boldsymbol{\phi}(\tau)$, the following two conditions shall be considered respectively.

(1) $\boldsymbol{\phi}(\tau)$ has a complete set of eigenvectors.

Theorem 2 *For the necessary and sufficient condition of the $n \times n$ matrix φ to be similar to a diagonal matrix is that φ must have a complete set of eigenvectors. Thus, $\boldsymbol{A}$ can be solved using the foregoing method.*

(2) $\boldsymbol{\phi}(\tau)$ has no complete set of eigenvectors.
In this case, $\boldsymbol{\phi}(\tau)$ cannot be transformed into a diagonal form but a jordan form. Then $\ln\boldsymbol{\phi}(\tau)$ can be solved directly following the definition of matrix function, that is:

$$\boldsymbol{A} = \frac{1}{\tau}\boldsymbol{T}\ \ln J\boldsymbol{T}^{-1} = \frac{1}{\tau}T\begin{bmatrix} \ln(\lambda_i) & \ln^1(\lambda_i) & \frac{1}{2!}\ln^2(\lambda_i) & \cdots & \frac{1}{(n-1)!}\ln^{n-1}(\lambda_i) \\ 0 & \ln(\lambda_i) & \ln^1(\lambda_i) & \cdots & \vdots \\ \vdots & \vdots & & \ddots & \vdots \\ \vdots & \vdots & & \cdots & \ln^1(\lambda_i) \\ 0 & 0 & & \cdots & \ln(\lambda_i) \end{bmatrix}\boldsymbol{T}^{-1} \tag{7.79}$$

If eigenvalues have complex roots, the conjugate complex roots shall be treated as a single root, and multiple conjugate complex roots are taken as multiple roots. All arguments are taken according to the principal value region to avoid the multivalued solution of logarithmic function $\ln\boldsymbol{\phi}(\tau)$, such as $\ln 1 = 0$ instead of $\ln 1 = 0 + 2\pi i$.

The above problem can also be solved by the minimum polynomial method, since it not only needs to do the above main work, but also needs to solve a group of linear equations, the details will not be elaborated here.

7.7.1.2 Logarithmic matrix expansion method

To find a numerical solution of $\ln\boldsymbol{\phi}(\tau)$, avoiding the multivalued solution of eigenvectors and logarithms, thereby use the derivation of the logarithm matrix method as follows.

Definition 1 Let

$$\boldsymbol{\phi}(\tau) = e^{\boldsymbol{A}\tau} \tag{7.80}$$

By contrast with the logarithmic definition of real field, the logarithm matrix is defined as:

$$\ln\boldsymbol{\phi}(\tau) = \boldsymbol{A}\,\tau \tag{7.81}$$

Definition 2 Define the series expansion of logarithmic matrix as:

$$\begin{aligned}\ln\boldsymbol{\phi}(\tau) = 2\Bigg\{&[\boldsymbol{\phi}(\tau)-\boldsymbol{I}][\boldsymbol{\phi}(\tau)+\boldsymbol{I}]^{-1} + \frac{1}{3}\left[(\boldsymbol{\phi}(\tau)-\boldsymbol{I})(\boldsymbol{\phi}(\tau)+\boldsymbol{I})^{-1}\right]^3 + \cdots \\ &+ \frac{1}{2k-1}\left[(\boldsymbol{\phi}(\tau)-\boldsymbol{I})(\boldsymbol{\phi}(\tau)+\boldsymbol{I})^{-1}\right]^{2k-1} + \cdots\Bigg\} \quad (k=1,2,\cdots)\end{aligned} \tag{7.82}$$

where the real part of eigenvalue of matrix $\boldsymbol{\phi}(\tau)$ is greater than 0.

Theorem 3 *If the real parts of all eigenvalues of matrix $\boldsymbol{\phi}(\tau)$ are positive, according to Eqs. (7.81) and (7.82), then matrix $\boldsymbol{A}$ can be expressed as:*

$$\begin{aligned}\boldsymbol{A} = \frac{2}{\boldsymbol{\tau}}\Bigg\{&[\boldsymbol{\phi}(\tau)-\boldsymbol{I}][\boldsymbol{\phi}(\tau)+\boldsymbol{I}]^{-1} + \frac{1}{3}\left[(\boldsymbol{\phi}(\tau)-\boldsymbol{I})(\boldsymbol{\phi}(\tau)+\boldsymbol{I})^{-1}\right]^3 + \cdots \\ &+ \frac{1}{2k-1}\left[(\boldsymbol{\phi}(\tau)-\boldsymbol{I})(\boldsymbol{\phi}(\tau)+\boldsymbol{I})^{-1}\right]^{2k-1} + \cdots\Bigg\} \quad (k=1,2,\cdots)\end{aligned} \tag{7.83}$$

Proof Using the proof by contradiction, that is, assuming Eq. (7.83) is satisfied, then the real parts of all eigenvalues of $\boldsymbol{\phi}(\tau)$ are positive.

Let

$$\boldsymbol{B} = [\boldsymbol{\phi}(\tau)-\boldsymbol{I}][\boldsymbol{\phi}(\tau)+\boldsymbol{I}]^{-1} \tag{7.84}$$

Judging from Eq. (7.81), the necessary and sufficient condition for matrix $\boldsymbol{A}$ to exist is:

$$\lim_{k\to\infty}\boldsymbol{B}^k = 0 \tag{7.85}$$

It means that the modulo of eigenvalue of matrix $\boldsymbol{B}$ must be less than 1. Let λ' represent the eigenvalues of matrix $\boldsymbol{B}$, then:

$$|\lambda'| < 1 \tag{7.86}$$

Based on Eq. (7.84), the characteristic equation of matrix $\boldsymbol{B}$ is

$$\left|\lambda'\boldsymbol{I} - [\boldsymbol{\phi}(\tau)-\boldsymbol{I}][\boldsymbol{\phi}(\tau)+\boldsymbol{I}]^{-1}\right| = 0 \tag{7.87}$$

or

$$\left|(\lambda'+1)\boldsymbol{I} - (1-\lambda')\boldsymbol{\phi}(\tau)\right|\left|[\boldsymbol{\phi}(\tau)+\boldsymbol{I}]^{-1}\right| = 0 \tag{7.88}$$

or

$$\left|\left(\frac{\lambda'+1}{(1-\lambda')}\right)\boldsymbol{I}-\boldsymbol{\phi}(\tau)\right||(1-\lambda')||[\boldsymbol{\phi}(\tau)+\boldsymbol{I}]^{-1}|=0 \tag{7.89}$$

Consequently, we have:

$$|\lambda\boldsymbol{I}-\boldsymbol{\phi}(\tau)|=0 \tag{7.90}$$

where

$$\lambda=\frac{\lambda'+1}{1-\lambda'} \tag{7.91}$$

Apparently, λ is the eigenvalue of matrix $\boldsymbol{\phi}(\boldsymbol{\tau})$. From Eq. (7.89), we know

$$\lambda'=\frac{\lambda-1}{\lambda+1} \tag{7.92}$$

From Eq. (7.91), we obtain:

$$|\lambda+1|>|\lambda-1| \tag{7.93}$$

Let

$$\lambda=\alpha+\mathrm{j}\beta \tag{7.94}$$

Substituting it into Eq. (7.93), we have:

$$\alpha>0 \tag{7.95}$$

That is, the real parts of eigenvalues λ of matrix $\boldsymbol{\phi}(\tau)$ are positive. Hence the theorem is proven. □

The difference between the eigenvalue method and logarithmic matrix method is that the former is of computational complexity, whereas the latter requires real parts of all eigenvalues are positive. Because the eigenvalues of most systems are dominated by real parts, and real roots are normally meeting the condition, the simple method of logarithmic matrix can normally be used to solve. In case of failure to satisfy the previous condition, the following successive approximation method can be used to solve.

7.7.2 Mutual Transformation Method Between Difference Equations (Successive Approximation Method)

Formulation of the known difference equation is:

$$X(k+1)=\boldsymbol{\phi}(\tau)X(k)$$

its corresponding difference equation is:

$$X(k+1)=\boldsymbol{\phi}(\tau_1)X(k)$$

where $\tau\neq\tau_1$, that is, with different sampling intervals.

The following two cases are to be considered, respectively:

(1) $\tau_1>\tau$, τ_1 is the integral multiple of τ, that is, $\tau_1=n\tau$
From the definition of transition matrix, we know:

$$\boldsymbol{\phi}(\tau_1)=\boldsymbol{\phi}^n(\tau)$$

$\boldsymbol{\phi}(\tau_1)$ can be solved using the above equation.

(2) $\tau_1<\tau,\quad \tau=n\tau_1$
Take the first two terms of polynomial expansion of $e^{\boldsymbol{A}\tau}$

$$e^{\boldsymbol{A}\tau}=\boldsymbol{I}+\boldsymbol{A}\tau+\frac{1}{2!}\boldsymbol{A}^2\tau^2+\cdots \tag{7.96}$$

to get the approximate equation of matrix $\phi(\tau)$

$$\phi(\tau)\approx\boldsymbol{I}+\boldsymbol{A}\tau \tag{7.97}$$

Hence,

$$\boldsymbol{A}\approx\frac{1}{\tau}[\phi(\tau)-\boldsymbol{I}] \tag{7.98}$$

Because $\tau_1=\tau/n$, correspond to Eq. (7.98), the approximate expression of $\boldsymbol{A}$ and the transition matrix $\boldsymbol{\phi}(\tau_1)$ of τ_1 is:

$$\boldsymbol{A}\approx\frac{1}{\tau_1}[\boldsymbol{\phi}(\tau_1)-\boldsymbol{I}] \tag{7.99}$$

Combining Eqs. (7.98) and (7.99), we know:

$$\boldsymbol{\phi}(\tau_1)=\frac{\tau_1}{\tau}[\boldsymbol{\phi}(\tau)-I]+\boldsymbol{I} \tag{7.100}$$

Apparently, $\boldsymbol{\phi}(\tau_1)$ obtained from Eq. (7.100) is very rough and needs to be further refined generally by iteration. Let the k-th iterative values $\boldsymbol{\phi}(\boldsymbol{\tau}_1)$ and $\boldsymbol{\phi}(\boldsymbol{\tau})$ be $\boldsymbol{\phi}_k(\tau_1)$ and $\boldsymbol{\phi}_k(\tau)$. Let $\boldsymbol{\phi}(\tau_1)$ solved from Eq. (7.100) be $\boldsymbol{\phi}_1(\tau_1)$. Judging from the properties of transition matrix, we have

$$\boldsymbol{\phi}_k^n(\boldsymbol{\tau}_1)=\boldsymbol{\phi}_k(\boldsymbol{\tau}) \tag{7.101}$$

In the k-th iteration, if the error lies between $\phi_k(\tau)$ and $\boldsymbol{\phi}(\tau)$, where the former is solved by Eq. (7.101) and the latter is the given one, is not satisfactory.

$\phi_{k+1}(\tau_1)$ can be rectified using the following:

$$\boldsymbol{\phi}_{k+1}(\tau_1)=\boldsymbol{\phi}_k(\tau_1)+\alpha[\boldsymbol{\phi}(\tau)-\boldsymbol{\phi}_k(\tau)] \tag{7.102}$$

where α is the step factor. Generally, take $\alpha = \tau_1/\tau$, or adjust based on test results. The iterative process shall continue until the norm of residual matrix $\Delta\boldsymbol{\phi}(\tau)$:

$$\|\Delta\boldsymbol{\phi}_k(\tau)\| = \|\boldsymbol{\phi}_k(\tau) - \boldsymbol{\phi}(\tau)\| \tag{7.103}$$

is less than a given error.

Apparently, based upon the finalized $\boldsymbol{\phi}(\tau_1)$, it is easy to solve the transition matrix of any time interval $t = m\tau_1 = \dfrac{m}{n}\tau$:

$$\boldsymbol{\phi}(t) = \boldsymbol{\phi}^m(\tau_1) \tag{7.104}$$

If n is large enough, based on the transition matrix equation:

$$\dot{\boldsymbol{\phi}}(t) = \boldsymbol{A}\boldsymbol{\phi}(t) \tag{7.105}$$

the equation of $\boldsymbol{A}$ can be approximately determined as

$$\boldsymbol{A} \approx \frac{1}{\tau_1}[\boldsymbol{\phi}(\tau_1) - \boldsymbol{I}] \tag{7.106}$$

7.7.3 Transformation Method From Differential Into Difference Transfer Function

Subject to the control by digital computer, the computer can conveniently access the sampling signals in the past moment, and also easily perform the arithmetic operations of addition, subtraction, multiplication, and division. Thus, in the sampling adjustment, differential equations can be replaced by difference ones to describe the objects. For an engineering system, what we often encounter is the Laplace transform of transfer function, by which a method is proposed to obtain the Z transform of transfer function, that is, difference transfer type is proposed.

7.7.3.1 Method of direct Z transform

Traditionally, the differential transfer function $G(S)$ of any system is directly transformed into $G(Z)$ by direct Z transform, that is:

$$G(Z) = Z\{G(S)\} \tag{7.107}$$

In fact, obtaining of the difference equation has taken into account the retainer, without which the system output is in a pulse form, and the coefficients of difference transfer equations are somewhat different; therefore, the relationship between the continuous differential and difference transfer functions is:

Differential transfer function × Sampling switch × Retainer = Difference transfer function

To transform the differential equation into difference equation, it is equal to require a retainer set after the sampling switch, and the following direct Z transform is utilized:

$$G(Z) = Z\left\{G(S)\frac{1-\mathrm{e}^{-TS}}{S}\right\} \tag{7.108}$$

where

$$G(S) = \frac{P(S)}{Q(S)}$$

When the characteristic equation $Q(S) = 0$, it does not include the n-order singularity, the following equation or Z transform can be used:

$$G(Z) = \sum \frac{P(S_{\mathrm{K}})}{Q_1'(S_{\mathrm{K}})} \times \frac{1-Z^{-T}}{1-\mathrm{e}^{S_{\mathrm{K}}T}Z^{-1}} \tag{7.109}$$

where S_{K} is the root of characteristic equation $Q(S)$, $Q_1(S) = Q(S)\cdot S$, and T is the sampling time.

When the characteristic equation $Q_1(S) = 0$ and it has the n-order singularity, for instance, the transfer function including the factor $\frac{1}{S^n}$ or $\frac{1}{(S+a)^n}$, $\frac{P(S)}{a(S)}$ can be expanded into partial fraction equations by the partial fraction expansion method

After $G(S)$ has been expanded into partial fraction equation, the single root part can be transformed directly into Z transform based upon Eq. (7.109). As for the transfer function including $\frac{1}{(S+a)^n}$ factor can be transformed using the following equation, that is, when

$$G'(S) = \frac{1}{(S+a)^{n+1}}$$

the Z transform is

$$\begin{aligned} G'(Z) &= Z\left[(-1)^n\frac{1}{n!}\times\frac{\partial^n}{\partial a^n}\left(\frac{1}{S+a}\right)\left(1-\mathrm{e}^{-TS}\right)\right] \\ &= (-1)^n\frac{1}{n!}Z\left[\frac{\partial^n}{\partial a^n}\left(\frac{1}{S+a}\right)\left(1-\mathrm{e}^{-TS}\right)\right] \\ &= (-1)^n\frac{1}{n!}\frac{\partial^n}{\partial a^n}\left(\frac{1}{1-\mathrm{e}^{-aT}Z^{-1}}\right)\left(1-Z^{-T}\right) \end{aligned} \tag{7.110}$$

When $G'(S)=\dfrac{1}{S^{n+1}}$, a function can be constructed to be similar with the above equation and equivalent to $\dfrac{1}{S^n}$, to make:

$$\frac{1}{S^{n+1}}=\lim_{a\to 0}\frac{1}{(S+a)^{n+1}}$$

and we have:

$$G'(Z)=(-1)^n\frac{1}{n!}\lim_{a\to 0}\frac{\partial_n}{\partial a_n}\left(1-\frac{1}{1-e^{-aT}Z^{-1}}\right)\left(1-Z^{-T}\right) \tag{7.111}$$

To sum up, it can be seen that such transformation method must obtain the root of the model first, yet the root of the equation with higher order cannot be obtained because there is no available direct algorithm. Therefore, it is necessary to use the computer to make the iteration solving (such as *QR* solution) in addition to a great deal of partial methods and combining the same terms, the following state equation solution is hereby proposed, without needing any iteration solving.

7.7.3.2 Method of state equation solution

The first method can be used to solve the problem, but it is not fit for the high-order models of multiple roots or three orders or above, and even difficult to program. According to the detailed process of the first method, the state equation solution method is conceived in the following three steps:

Step 1: Transform the differential equation into a difference one.

1. The differential transfer function $G(S)$ is available.
   If the transfer function $G(S)$ has been given by the actual engineering system, it must be transformed into differential state equation.
   In case of

$$G(S)=\frac{y(S)}{u(S)}=\frac{b_1S^n+b_2S^{n-1}+\cdots+b_{n-1}S+b_n}{S^n+a_1S^{n-1}+\cdots+a_{n-1}S+a_n} \tag{7.112}$$

   it can be transformed into state equation using the following equation:
   Let:

$$X_1=Y$$

   Then:

$$\begin{aligned}X_2&=\dot{Y}-d_1u=\dot{X}_1-d_1u\\&\vdots\\X_n&=Y^{n-1}-d_1u^{n-2}-d_2u^{n-3}-\cdots-d_{n-1}u=\dot{X}_{n-1}-d_{n-1}u\end{aligned} \tag{7.113}$$

where $d_1, \ldots, d_n$ are:

$$\begin{bmatrix} d_1 \\ \vdots \\ \vdots \\ \vdots \\ d_n \end{bmatrix} = \begin{bmatrix} 1 & & & & \\ a_1 & \ddots & 1 & & \\ a_2 & & a_1 & 1 & \\ \vdots & & & \ddots & \\ a_{n-1} & & a_{n-2} & \cdots & a_1 \quad 1 \end{bmatrix}^{-1} \begin{bmatrix} b_1 \\ \vdots \\ \vdots \\ \vdots \\ b_n \end{bmatrix} \tag{7.114}$$

Rearrange Eq. (7.113) to get the state equation:

$$\begin{bmatrix} \dot{X}_1 \\ \vdots \\ \vdots \\ \vdots \\ \dot{X}_n \end{bmatrix} = \begin{bmatrix} 0 & & & \\ \vdots & & I & \\ \vdots & & & \\ 0 & & & \\ -a_n & -a_{n-1} & \cdots & -a_1 \end{bmatrix} \begin{bmatrix} X_1 \\ \vdots \\ \vdots \\ \vdots \\ X_n \end{bmatrix} + \begin{bmatrix} d_1 \\ \vdots \\ \vdots \\ \vdots \\ d_n \end{bmatrix} u \tag{7.115}$$

$$Y = [1,0,\cdots,0] \begin{bmatrix} X_1 \\ \vdots \\ X_n \end{bmatrix}$$

or alternatively, the transfer function is represented the factorization form, or rewrite Eq. (7.112) into the factorization form:

$$\begin{aligned} D(S) &= \frac{K(S+b_1)\cdots(S+b_m)}{(S+a_1)(S+a_2)\cdots(S+a_n)} \\ &= \frac{S+b_1}{S+a_1} \times \frac{S+b_2}{S+a_2} \times \cdots \times \frac{S+b_m}{S+a_m} \times \frac{1}{S+a_{m+1}} \times \cdots \times \frac{K}{S+a_n} \\ &= D_1(S) \cdot D_2(S) \cdots D_n(S) \end{aligned} \tag{7.116}$$

$D(S)$ can be depicted into the following block diagram:

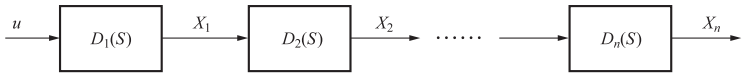

where

$$D_1(S) = \frac{S+b_1}{S+a_1}, \quad D_2(S) = \frac{S+b_2}{S+a_2}, \ldots, D_n(S) = \frac{K}{S+a_n}$$

List the first-order differential equations of each block, and make them in a simultaneous way to get the state equation of the whole system.

$$\dot{\boldsymbol{X}} = \boldsymbol{A}\boldsymbol{X} + \boldsymbol{B}u$$

$$\dot{\boldsymbol{Y}} = \boldsymbol{C}\boldsymbol{X} + \boldsymbol{D}u$$

The coefficients $\boldsymbol{A}$ and $\boldsymbol{B}$ are finalized by simultaneously uniting all first-order differential equations, the coefficient of equations $\boldsymbol{C}$ and $\boldsymbol{D}$ are:

$$\boldsymbol{C} = [0, 0, \ldots, 1], \quad \boldsymbol{D} = 0$$

provided the system output is X_n.

2. If the system's differential equation is known, its difference equation can be solved using the following equation:

$$\begin{aligned} \phi(\tau) &= \mathrm{e}^{\boldsymbol{A}\tau} \\ \phi(\tau) &= \int_0^{\tau} \mathrm{e}^{AT}\mathrm{d}T \cdot \boldsymbol{B} \end{aligned} \tag{7.117}$$

Consequently:

$$X(k+1) = \phi(\tau)X(k) + G(\tau)u(k)$$

Step 2: Normalizing the difference equation. The state equation and transfer function of a system are correlated by the normalization of state equation. The coefficients of the normalized equation reflect those of the transfer function. Therefore, the state equation must be normalized to obtain the system's transfer function.
The dynamic system has been given as follows:

$$\begin{aligned} X(k+1) &= \phi X(k) + Gu(k) \\ Z(k) &= h^T X(k), h^T = [h_1, h_2, \ldots, h_n]_{1\times n} \end{aligned} \tag{7.118}$$

which can be transformed into:

$$\begin{aligned} Y(k+1) &= \phi^* Y(k) + G^* u(k) \\ Z(k) &= h^{*T} Y(k) \end{aligned} \tag{7.119}$$

where

$$\Phi^* = \begin{bmatrix} 0 & & \\ \vdots & & \\ \vdots & I & \\ 0 & & \\ \hline -a_n & -a_{n-1} \quad \cdots & -a_1 \end{bmatrix}, G^* = \begin{bmatrix} d_1 \\ \vdots \\ \vdots \\ \vdots \\ d_n \end{bmatrix}, h^{*T} = [1,0,\cdots,0]$$

The transform process is shown as follows

Let:

$$Y(k) = FX(k)$$

As:

$$X(k) = F^{-1}Y(k) \tag{7.120}$$

Substitute Eq. (7.120) into Eq. (7.118), then we have:

$$\begin{aligned} Y(k+1) &= F\phi F^{-1}Y(k) + FGu(k) \\ &= \phi^* Y(k) + G^* u(k) \\ Z(k) &= h^T F^{-1}Y(k) = h*^T Y(k) \end{aligned}$$

where

$$F = \begin{bmatrix} h^T \\ h^T\phi \\ \vdots \\ h^T\phi^{n-1} \end{bmatrix}$$

Now, the coefficients $a_1, \ldots, a_n$ of transfer function have been determined, which are used together with $G^* = [d_1, \ldots, d_n]T$ to obtain the coefficients $b_1, \ldots, b_n$ of the transfer function.

Step 3: Obtain the system's transfer function based on the normalized equation.

According to Eq. (7.119), the calculation formula is as follows:

$$\begin{bmatrix} b_1 \\ \vdots \\ \vdots \\ \vdots \\ b_n \end{bmatrix} = \begin{bmatrix} 1 & & & & \\ a_1 & 1 & & & \\ a_2 & a_1 & 1 & & \\ \vdots & \vdots & \ddots & \ddots & \\ a_{n-1} & a_{n-2} & \cdots & a_1 & 1 \end{bmatrix} \begin{bmatrix} d_1 \\ \vdots \\ \vdots \\ \vdots \\ d_n \end{bmatrix} \tag{7.121}$$

From this, the coefficients $a_1, \ldots, a_n, b_1, \ldots, b_n$ of transfer function have been determined; in other words, the state equations of difference transfer function from differential transfer function have been solved, which is an advisable method suitable for all complex conditions. In particular to high-order models, such a method only needs to obtain the inverse of transformation matrix without having to iteratively solve the root of the model, which greatly speeds up the calculation and facilitates the programming, thereby demonstrating great superiority. As for low-order models, it can be solved by the direct solution and thus can be solved in any of the two solutions.

7.8 Implementation

7.8.1 Parameters From Figs. 7.4 and 7.7

The model of Figs. 7.6 and 7.10 is chosen in the simulation test of which the parameters are as follows:

Parameters of thermal Generating Unit	Parameters of Turbine Generating Unit
$T_S = 0.3$s	$T_1 = 0.53$s
$T_{CH} = 0.5$s	$T_2 = 45$s
$T_{RH} = 5$s	$T_i = 5$s
$\alpha = 0.3$	$T_W = 1$s
$M_1 = 10$s	$M_2 = 10$s
$D_1 = 2$ (per-unit value)	$D_2 = 2$ (per-unit value)
$R_1 = 0.05$	$R_2 = 0.05$

$D = 2$ (per-unit value) in system parameter. The load sample sequence is included in Table 7.2.

Table 7.2 Load data

0.0	0.4	0.47	0.27	1.87	1.97	−3.63	0.47	0.27	0.5
2.27	3.27	2.07	2.27	1.67	3.07	2.27	2.07	2.17	2.2
2.77	2.17	2.77	4.07	3.07	2.87	2.97	3.37	4.17	3.0
4.77	4.37	2.67	3.17	2.97	2.87	2.97	2.4	1.0	2.0
1.8	2.4	2.0	1.2	2.4	1.98	2.98	3.08	2.8	2.0
2.0	1.8	2.8	2.4	3.0	2.7	3.0	2.3	2.2	1.7
0.0	1.7	0.1	2.4	0.8	0.0	−0.4	1.1	2.0	0.4
0.0	−0.1	0.2	0.4	−0.1	0.0	−0.2	−0.1	0.1	0.6
0.0	0.0	3.9	4.5	−0.3	5.0	5.8	4.5	−0.9	5.8
5.0	0.0	3.9	4.5	−0.3	5.0	5.8	4.5	−0.9	5.8
5.0	4.1	−1.1	4.3	4.4	3.1	4.3	1.4	0.4	−0.1
0.0	−0.1	−0.4	0.1	−0.8	−1	−1	−1.5	−0.2	−2.1
−2	−0.8	−1.6	−1.4	−0.8	−1.4	−1.7	−1.5	−1.7	−2.4
−2	1	1.7	0.9	0.6	0.5	0.3	0.5	1.4	1.9
1	0.2	0.2	0.5	0.5	1.4	0.1	0.0	0.6	−0.2
0.0	0.0	0.2	−0.9	−0.8	−0.6	−1.4	−0.2	−0.5	−1
−1.4	−1.6	−1.5	−1.2	−1.6	−2.3	−2.6	−2	−1.4	−2
−1.6	1.2	−2.6	−2.9	−3	−2.6	−2.9	−2.5	−2.7	−3
−3.9	−4.7	−4.2	−5.8	−6.4	−7.2	−6.6	−7.7	−7.5	−7
−7	−8.8	−9.4	−8.6						

7.8.2 Simulation Results of Identification for Load Disturbance Model ΔP_L

Values of autocorrelation function and partial correlation function for ΔP_L sequence are shown in Table 7.3.

According to the tailing and truncation properties of autocorrelation and partial correlation function, the third-order AR model is selected, of which the parameters are estimated. Finally, the model of load disturbance is obtained:

$$\Delta P_L(k) - 0.623\Delta P_L(k-1) - 0.0698\Delta P_L(k-2) - 0.218\Delta P_L(k-3) = \xi(k) + 0.02 \quad (7.122)$$

Table 7.3 Values of autocorrelation function and partial correlation function for ΔP_L sequence

$\hat{\rho}_1$	0.8541	$\hat{\phi}_{11}$	0.854148
$\hat{\rho}_2$	0.788	$\hat{\phi}_{22}$	0.215901
$\hat{\rho}_3$	0.7684	$\hat{\phi}_{33}$	0.218149
$\hat{\rho}_4$	0.7571	$\hat{\phi}_{44}$	0.152241
$\hat{\rho}_5$	0.68	$\hat{\phi}_{55}$	−0.162649
$\hat{\rho}_6$	0.6391	$\hat{\phi}_{66}$	0.011698
$\hat{\rho}_7$	0.6174	$\hat{\phi}_{77}$	0.026242
$\hat{\rho}_8$	0.5749	$\hat{\phi}_{88}$	−0.057051
$\hat{\rho}_9$	0.5004	$\hat{\phi}_{99}$	−0.120347
$\hat{\rho}_{10}$	0.4663	$\hat{\phi}_{1010}$	0.009277
$\hat{\rho}_{11}$	0.4416	$\hat{\phi}_{1111}$	0.010564
$\hat{\rho}_{12}$	0.3976	$\hat{\phi}_{1212}$	−0.021949
$\hat{\rho}_{13}$	0.3661	$\hat{\phi}_{1313}$	0.065523
$\hat{\rho}_{14}$	0.3389	$\hat{\phi}_{1414}$	−0.020765
$\hat{\rho}_{15}$	0.3081	$\hat{\phi}_{1515}$	−0.023581
$\hat{\rho}_{16}$	0.2801	$\hat{\phi}_{1616}$	0.029347
$\hat{\rho}_{17}$	0.2727	$\hat{\phi}_{1717}$	0.063110
$\hat{\rho}_{18}$	0.2683	$\hat{\phi}_{1818}$	0.048860
$\hat{\rho}_{19}$	0.2499	$\hat{\phi}_{1919}$	−0.000147
$\hat{\rho}_{20}$	0.2204	$\hat{\phi}_{2020}$	−0.064544

The corresponding transition matrix of discrete state equation [see Eq. (7.31)] is:

$$\phi^*(\tau) = \begin{bmatrix} 0.0 & 1.0 & 0.0 \\ 0.0 & 0.0 & 1.0 \\ 0.218 & 0.0698 & 0.623 \end{bmatrix} \tag{7.123}$$

$$H^{*T} = [1, 0, 0]$$

where time interval is $\tau = 60\,\text{s}$ in the sample time series. Because the time interval $\tau_1 = 1\,\text{s}$ and $\tau_1 = 4\,\text{s}$ are adopted in the estimator controller, the transition matrix $\phi^*(\tau)$ must be transformed into $\boldsymbol{\phi}^*(\tau_1)$, which is calculated with the method proposed in Section 7.7:

$$\boldsymbol{\phi}^*(1) = \begin{bmatrix} 0.663 & 1.333 & -1.036 \\ -0.226 & 0.591 & 0.687 \\ 0.149 & -0.179 & 1.019 \end{bmatrix}$$

$$\boldsymbol{\phi}^*(4) = \begin{bmatrix} 0.582 & 1.4 & -1.0196 \\ -0.222 & 0.511 & 0.765 \\ 0.167 & 0.167 & 0.988 \end{bmatrix}$$

7.8.3 Simulation Results of Local Estimator and Central Estimator

To facilitate the test, assuming that the power system contains only a thermal generator and a hydro generator, Fig. 7.18 shows the block diagram for the two-unit system.

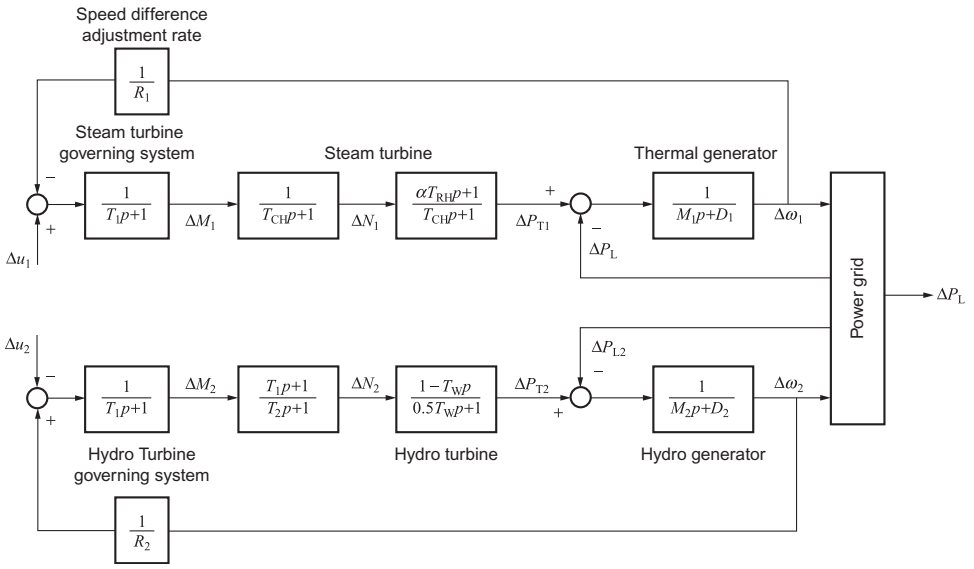

Fig. 7.18
Block diagram for the two-unit system.

Using Eq. (7.120), the normal random number generator is utilized to generate the load disturbance step function $\Delta P_L(k)$, as shown in Fig. 7.19. ΔP_{L1} and ΔP_{L2} shall be calculated based on the power grid condition. To simplify the experiment, in the model testing, let:

$$\Delta P_{L1} = \Delta P_{L2} = 0.5\Delta P_L$$

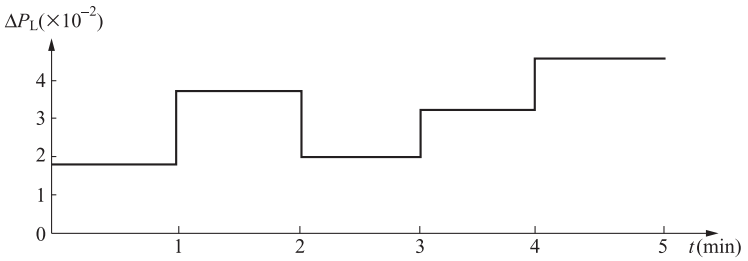

Fig. 7.19
The given load disturbance step function.

Substitute step functions ΔP_{L1} and ΔP_{L2} into Eqs. (7.38) and (7.40), solve the foregoing differential equations using the Runge-Kutta method, and obtain the motion traces of all state variables. These traces are treated as the real state of the system, of which part of traces are showed in Fig. 7.20. Take $\Delta\omega_j$ as the measurement variable, which is equal to the true value of $\Delta\omega_j$ plus the error in measurement of Gaussian distribution, with the curves shown in Fig. 7.20. Then use the Kalman filter Eqs. (7.51)–(7.55) to calculate the estimated curves of

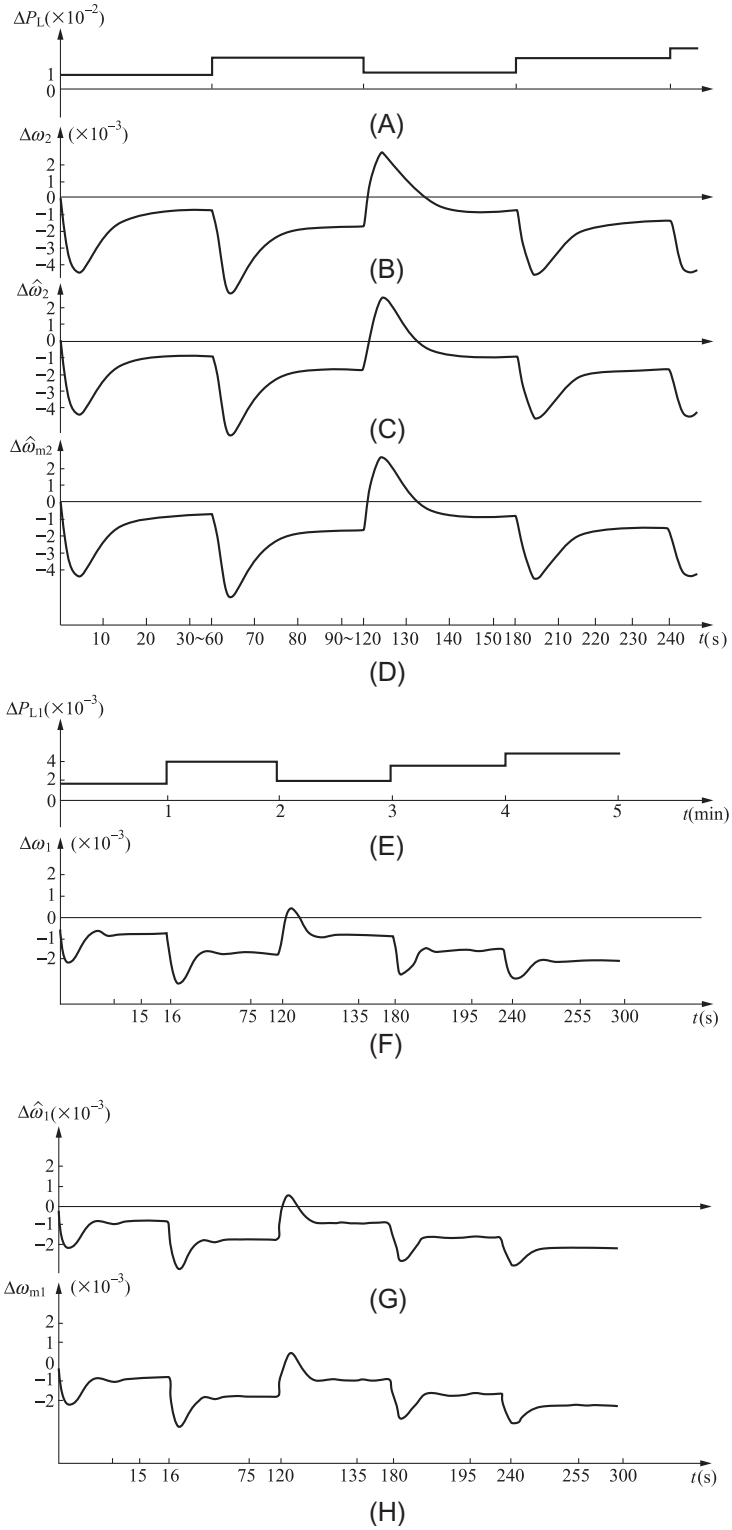

Fig. 7.20

Test results of local estimator. (A) Load disturbance function of the given hydro unit; (B) actual curve trace of $\Delta\omega_2$; (C) estimates of $\Delta\omega_2$; (D) measurements of $\Delta\omega_2$; (E) load disturbance function of the given thermal unit; (F) actual curve trace of $\Delta\omega_1$; (G) estimates of $\Delta\omega_1$; (H) measurements of $\Delta\omega_1$.

state variable, detailed in Fig. 7.20. Fig. 7.21 shows the actual values, measurements, and estimates of $\Delta\omega_j$.

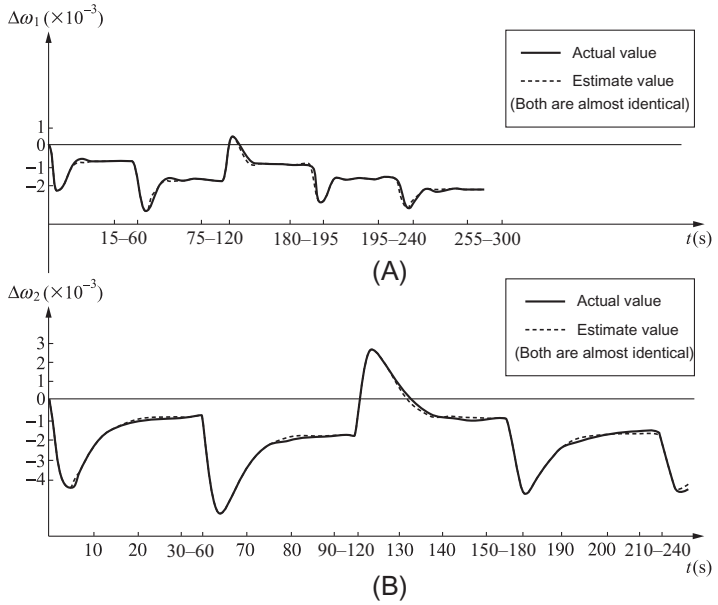

Fig. 7.21

Comparison of actual curve trace, estimated curve and measured curve of $\Delta\omega$. (A) comparison of $\Delta\omega$ of thermal units; (B) comparison of $\Delta\omega$ of hydro units.

The ΔP_{Tj} of the local estimator is regarded as the input of the central estimator, and the evaluation curves of the state variables of the equivalent machine and the estimation curve of the load disturbance are calculated from Eqs. (7.58) to (7.62) (see Figs. 7.22 and 7.23). From Figs. 7.20 to 7.22, the results show that the local estimator and the center estimator perform well.

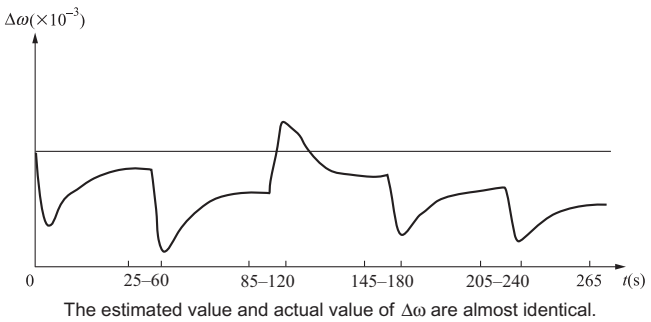

Fig. 7.22

Comparison of actual trace and estimated curve ($\Delta\omega$) of central estimator.

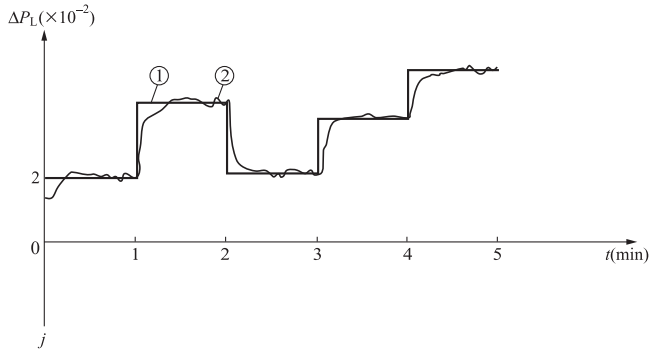

Fig. 7.23
Test results of central estimator. (Comparison of step functions ①, ② for given system load disturbance ΔP_L)

7.8.4 Simulation Results of Compensation Controller

7.8.4.1 Difference $T = 1$ s

The transfer function of the compensator of thermal generating unit is:

$$H_C = \frac{1 - 1.0999B + 0.203B^2 - 0.0099B^3}{0.24B - 0.107B^3 - 0.04B^3} \tag{7.124}$$

Corresponding control law for the compensator:

$$\Delta u_1(k) = \frac{1 - 1.0999B + 0.203B^2 - 0.0099B^3}{0.24B - 0.107B^2 - 0.04B^3} \Delta P_{L1}(k) \tag{7.125}$$

where B means one step shift operator, or:

$$\begin{aligned} \Delta u_1(k) &= 0.449\Delta u_1(k-1) + 0.16\Delta u_1(k-2) + 4.17\Delta P_L(k+1) \\ &-4.59\Delta P_{L1}(k) + 0.84\Delta P_{L1}(k-1) - 0.041\Delta P_{L1}(k-2) \end{aligned} \tag{7.126}$$

For the hydro generating unit:

$$G_1 = \frac{-0.00204B + 0.08954B^2 - 0.07149B^3}{1 - 1.265B + 0.3B^2 - 0.02B^3}$$

Because the numerator of G_1 has a root of no less than 1 and is irreversible, it is thus unable to solve H_C. Test shows that, letting $H_C = 1$ can achieve good results. Similarly, let:

$$\Delta u_2(k) = \Delta P_{L2}(k) \tag{7.127}$$

Test results are shown in Fig. 7.24.

The results of the controller in Fig. 7.14 with the conventional integrated feedback control are also shown for comparison. It can be seen from the curves that the compensator shown in

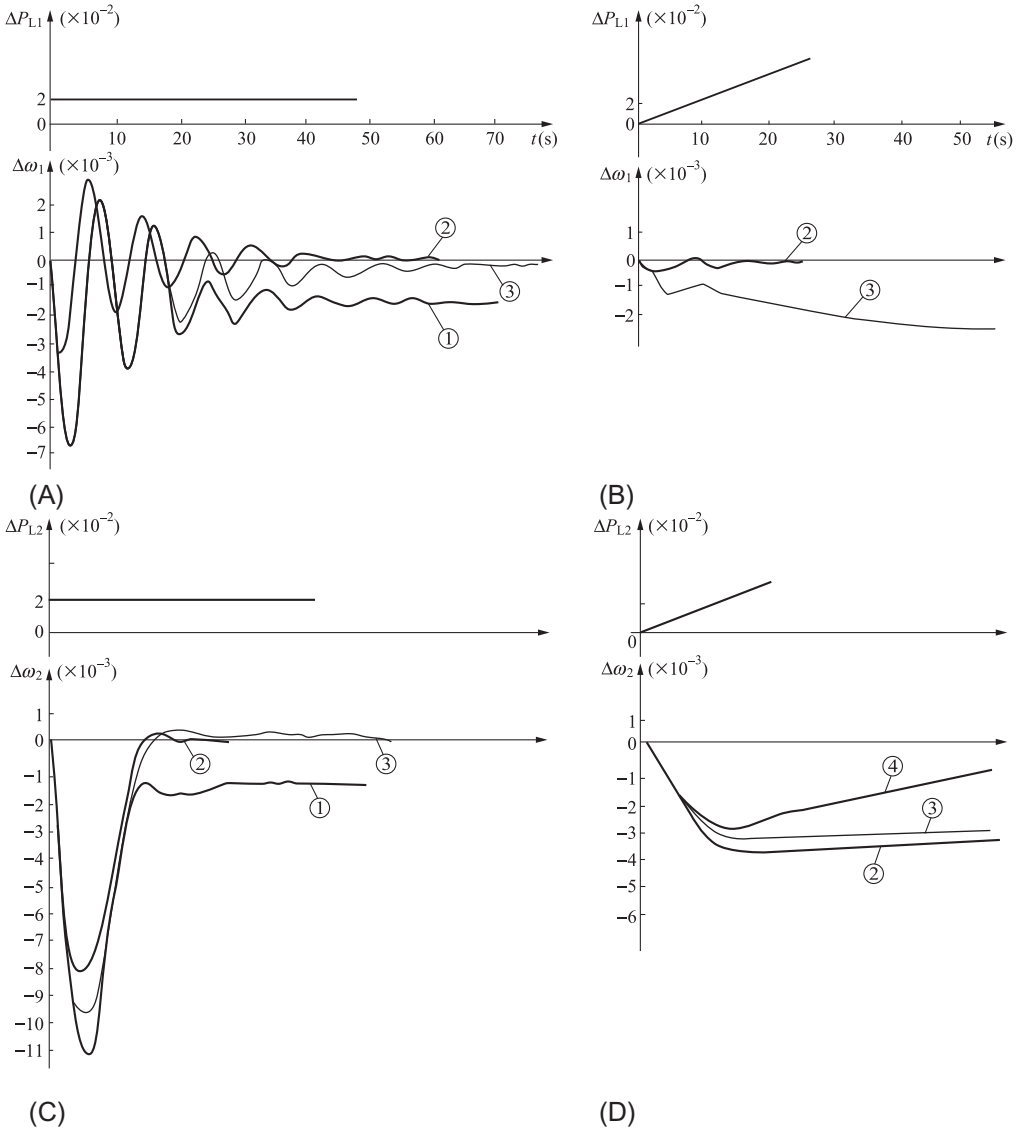

Fig. 7.24

Response comparison of test results for load frequency controller. (A) Response to (step disturbance) of thermal unit; (B) (incremental DC disturbance) of thermal unit; (C) response to (step disturbance) of hydro unit (D) (incremental DC disturbance) of hydropower unit. ①—uncontrolled; ②—feedforward control; ③—integral control; ④—feedforward + integral control.

Fig. 7.15 is of good performance. Although the hydro unit fails to achieve absolute compensation, the test results show that two types of controllers are interacting, which significantly improve the performances of each controller. The performance of the controller with difference $T = 1$ s is illustrated in Fig. 7.25.

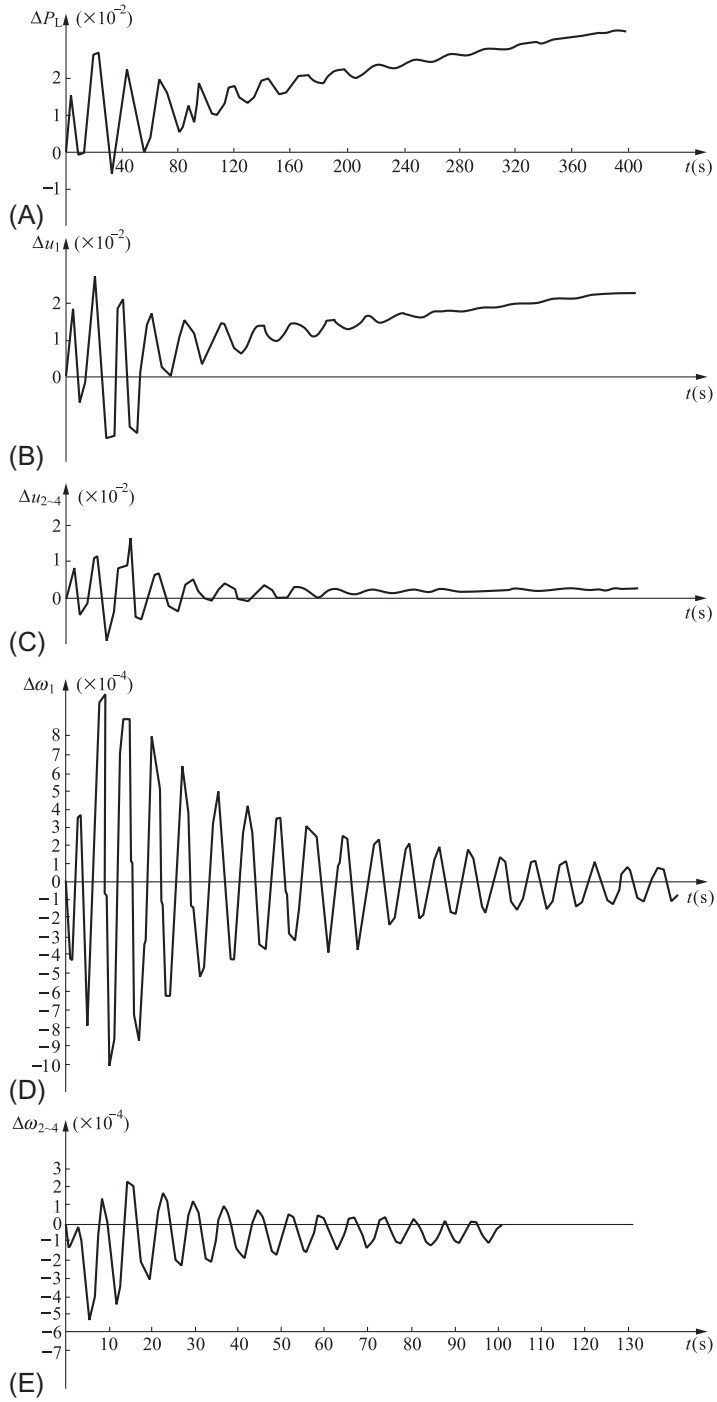

Fig 7.25

System tracking control test results of five-unit system.

(A) Forecasting curve of load disturbance ΔP_L; (B) Control law of thermal unit; (C) Control law of hydro unit; (D) Frequency curve of thermal unit; (E) Frequency curve of hydro unit.

7.8.4.2 Difference $T=4$ s

The transfer function of the compensator of thermal generating unit is:

$$H_C=\frac{1-0.6069B+0.00023B^2-9\times10^{-9}B^3}{0.5433B-0.14977B^2-0.000202B^2} \tag{7.128}$$

Corresponding control law for the compensator:

$$\Delta u_1(k)=\frac{1-0.6069B+0.0023B^2-9\times10^{-9}B^3}{0.5433B-0.14977B^2-0.000202B^3}\Delta P_{L1}(k) \tag{7.129}$$

or

$$\begin{aligned}\Delta u_1(k)=&0.27567\Delta u_1(k-1)+0.000376\Delta u_1(k-2)+1.8406\Delta P_{L1}(k+1)\\&-1.1708\Delta P_{L1}(k)+0.0004233\Delta P_{L1}(k-1)\end{aligned} \tag{7.130}$$

The transfer function of the compensator of hydro generating unit is:

$$H_C=\frac{1-0.9163B+0.00079B^2-1.67\times10^{-7}B^3}{0.14742B-0.06204B^2-0.0008607B^2} \tag{7.131}$$

Corresponding control law for the compensator:

$$\Delta u_2(k)=\frac{1-0.9163B+0.00079B^2-1.67\times10^{-7}B^3}{0.14742B-0.06204B^2-0.0008607B^3}\Delta P_{L2}(k) \tag{7.132}$$

or

$$\begin{aligned}\Delta u_2(k)=&0.42085\Delta u_2(k-1)+0.005838\Delta u_2(k-2)+6.7833\Delta P_{L2}(k+1)\\&-6.2155\Delta P_{L2}(k)+0.00536\Delta P_{L2}(k-1)-0.0000011\Delta P_{L2}(k-2)\end{aligned}$$

The performance of tracking control using the controller of difference $T=4\,s$ is illustrated in Fig. 7.26.

7.8.5 Simulation Results of Tracking Control for Five-Unit Test System

The hypothetic test results of two-unit test system suggest that the local estimator, central estimator, load disturbance model, and compensation controller proposed in this chapter have good effects and can effectively estimate and control the system state. On this basis, the simulation test for tracking control to a practical five-unit test system structure has been performed, in which the disturbance ΔP_{Li} is distributed to the five units following the electric distance distribution principle. The simplified diagram of a five-unit test system is shown in Fig. 7.27.

So

$$\begin{aligned}&\Delta P_{L1}=0.6\Delta P_L\\&\Delta P_{L2}\sim\Delta P_{L5}=0.4/4\Delta P_L=0.1\Delta P_L\end{aligned}$$

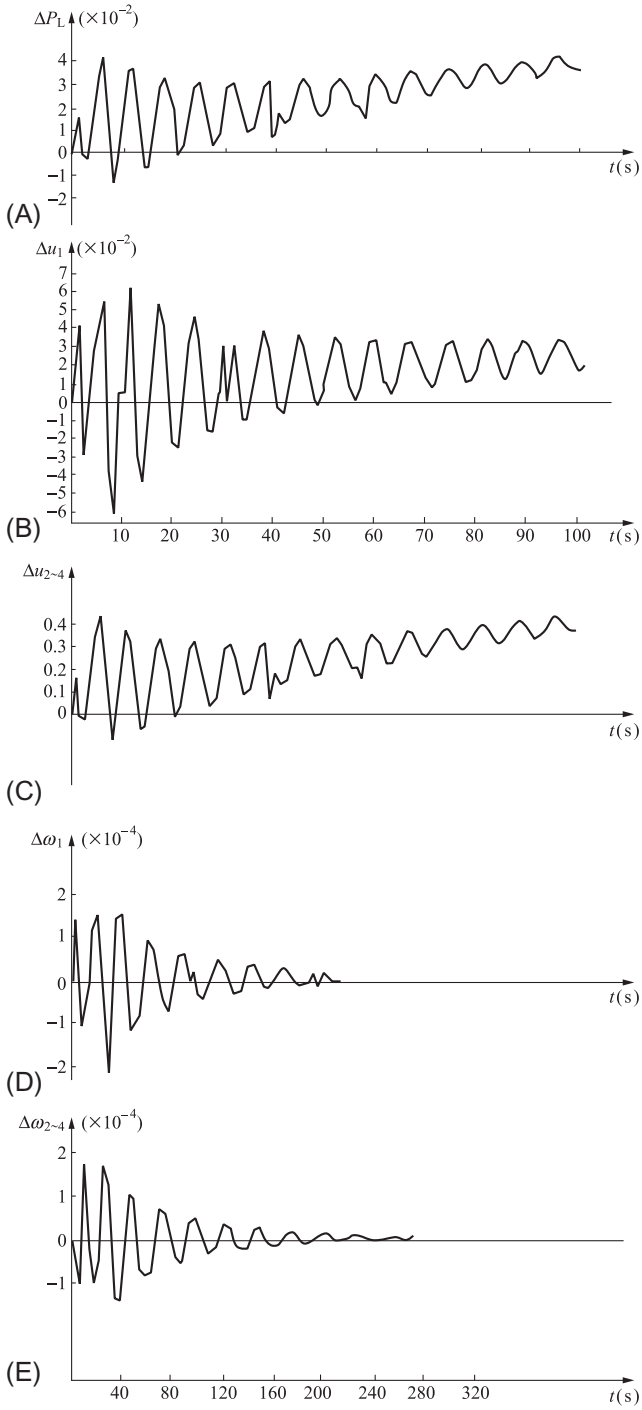

Fig. 7.26

Test results ($T=4$s) (I) of tracking control to five-unit system.
(A) Forecasting curve of load disturbance ΔP_L; (B) Control law of thermal unit; (C) Control law of hydro unit. (D) Frequency curve of thermal unit; (E) Frequency curve of hydro unit.

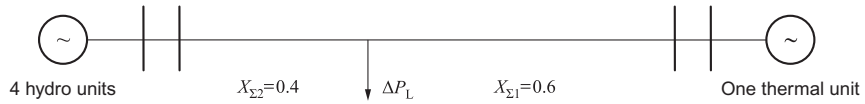

Fig. 7.27
Simplified diagram of five-unit test system.

The simulation process is shown in Fig. 7.17. The simulation test for tracking control takes $T=1$ s and $T=4$ s, as shown in Figs. 7.25 and 7.26, respectively. It includes the $\Delta\omega_j$ estimate curve, central estimate $\Delta\omega$ curve, load disturbance forecasting curve, and compensation control curve of the units. It can be seen from the figures that the control performance of $T=4$ s is better than that of $T=1$ s. This is because $T=4$ s is the full compensation control for the hydro plant, whereas $T=1$ s is not.

7.8.6 Verifications of Transformation Methods among Mathematical Models

7.8.6.1 Results of Example 1

The parameters A and $\boldsymbol{\phi}$ for continuous and discrete models of a hydro unit and its governing system are:

$$\boldsymbol{A}=\begin{bmatrix}-1.88624 & 0 & 0 & -37.725\\ -0.18624 & -0.02209 & 0 & -4.1667\\ 0.37049 & 2.04418 & -2 & 8.333\\ 0 & 0 & 0.1 & -0.2\end{bmatrix}$$

$$\boldsymbol{\phi}(1)=\begin{bmatrix}0.11382 & -0.51236 & -0.54953 & -15.77041\\ -0.08704 & 0.91856 & -0.06562 & -1.94727\\ -0.001908 & 0.91868 & 0.16088 & -0.04293\\ 0.002896 & 0.05509 & 0.04015 & 0.88352\end{bmatrix}$$

of which the eigenvalue of matrix $\boldsymbol{\phi}$ is:

$$\lambda_{1,2}=0.604916\pm \mathrm{j}0.197911$$
$$\lambda_{3,4}=0.818749$$

and the eigenvectors are:

$$\boldsymbol{T}_{1,2}=\begin{bmatrix}1\\ 0.08083\mp \mathrm{j}0.02176\\ 0.12265\mp \mathrm{j}0.9905\\ -0.03098\mp \mathrm{j}0.00839\end{bmatrix}\quad \boldsymbol{T}_3=\begin{bmatrix}1\\ 0.09526\\ 0.14018\\ -0.05886\end{bmatrix}\quad \boldsymbol{T}_4=\begin{bmatrix}1\\ 0.05949\\ 0.08754\\ -0.04967\end{bmatrix}$$

(1) Using the eigenvector method to obtain $\boldsymbol{A}$.
By Eq. (7.77)

$$\boldsymbol{A}=\boldsymbol{T}\boldsymbol{\Lambda}\boldsymbol{T}^{-1}$$

Substitute the eigenvalue and eigenvector into the previous equation to get:

$$\boldsymbol{A} = \begin{bmatrix} 1.88626 & 0 & 0 & -37.725 \\ -0.18624 & -0.02209 & 0 & -4.1667 \\ 0.37249 & 2.04418 & -2 & 8.333 \\ 0 & 0 & 0.1 & 0.2 \end{bmatrix}$$

(2) Using the logarithmic matrix method to obtain $\boldsymbol{A}$.
The real parts of all eigenvalues are greater than 0, satisfying Eq. (7.95), and by Eq. (7.83), we obtain:

$$\boldsymbol{A} = \begin{bmatrix} 1.88616 & 10^{-3} & -0.00018 & -37.7232 \\ -0.18623 & -0.02208 & -0.000018 & -4.1665 \\ 0.37242 & 2.04408 & -1.99985 & 8.3315 \\ 2\times 10^{-6} & 3\times 10^{-6} & 0.099995 & -0.19995 \end{bmatrix}$$

(3) Using the successive approximation method to obtain $\boldsymbol{A}$.
First, obtain $\varphi(0.001)$ [or alternatively, determine $\boldsymbol{\phi}(\tau_1)$, $\tau_1 < 0.001$ with a smaller difference interval], then use Eq. (7.106) to obtain $\boldsymbol{A}$:

$$\boldsymbol{A} \approx \begin{bmatrix} 1.8846 & 0.00004 & -0.00195 & -37.685 \\ -0.18606 & 0.022085 & -0.000215 & -4.16266 \\ 0.371552 & 2.042078 & -1.9975 & 8.31203 \\ 0.000019 & 0.000103 & 0.09988 & -1.996 \end{bmatrix}$$

From this example, the calculation accuracy of matrix $\boldsymbol{A}$ varies with different methods, which affects the choice of any kind of algorithm as required. The eigenvector method is not affected by the sampling time interval, the latter two methods are affected, however. The second method is logarithmic matrix; if $\tau = 0.1$, then a completely accurate solution A for the hydro plant model can be obtained. Namely, logarithmic matrix method is affected by difference r, and to what extent it is affected will be discussed in the future. The third method is successive approximation, whose calculation results are more accurate for examples with a smaller sampling time, that surely depends on the accuracy required for the practical problems.

7.8.6.2 Results of Example 2

The $\boldsymbol{A}$ and $\boldsymbol{\phi}$ matrix $\boldsymbol{A}$ of a system is given in the following:

$$\boldsymbol{A} = \begin{bmatrix} 1 & -1 & 0 \\ 4 & 3 & 0 \\ -1 & 0 & -3 \end{bmatrix}$$

$$\boldsymbol{\phi}(1) = \begin{bmatrix} 1.10364 & -0.36788 & 0 \\ 1.47152 & -0.36788 & 0 \\ -0.50321 & 0.13534 & 0.13534 \end{bmatrix}$$

where the eigenvalue of matrix $\boldsymbol{\phi}$ is

$$\lambda_1 = 0.1353353, \quad \lambda_{2,3} = 0.367879$$

(1) Using the eigenvector method to solve $\boldsymbol{A}$.
Because $\boldsymbol{\phi}$ has multiple roots, it cannot obtain $\boldsymbol{A}$ by Eq. (7.77), but by using Eq. (7.78). It is required to first obtain the transformation matrix $\boldsymbol{T}$.
For the eigenvalue λ_1, the basic solution of its characteristic equation is:

$$|\lambda_1 \boldsymbol{I} - \boldsymbol{\phi}| = 0$$

of which the basic solution is (0,0,1).

For the eigenvalue λ_2, the basic solution of its eigenvalue equation:

$$|\lambda_2 \boldsymbol{I} - \boldsymbol{\phi}| = 0$$

is (1, 2, −1), and the rank of characteristic equation is 2, that is the degree of eigenvalue λ_1 is $n - \gamma = 1$, which is less than the multiple number, and hence it is unable to find another linearly independent eigenvector. Instead, the following method shall be used to seek the high-order root vector, making the rank of augmented matrix:

$$[\boldsymbol{\phi} - \lambda_3 \boldsymbol{I} | \eta_2]$$

also to be 2, that is, solving:

$$|\boldsymbol{\phi} - \lambda_3 \boldsymbol{I}| X_3 = X_2$$

where $X_2 = (1, 2, -1)$, X_3 means the vector to be solved. With this equation, we have:

$$X_3 = (0, \quad -0.367879, \quad 2.7182816)$$

Now, we have solved the transformation matrix:

$$\boldsymbol{T} = \begin{bmatrix} 0 & 1 & 0 \\ 0 & 2 & -0.367879 \\ 1 & -1 & 2.7182816 \end{bmatrix}$$

Substitute it into Eq. (7.77):

$$\boldsymbol{A}=\boldsymbol{T}\begin{bmatrix}\ln\lambda_1 & & \\ & \ln\lambda_2 & \ln'(\lambda_1)\\ & & \ln\lambda_2\end{bmatrix}\boldsymbol{T}^{-1}$$
$$=\begin{bmatrix}1 & -1 & 0\\ 4 & -3 & 0\\ -1 & 0 & -2\end{bmatrix}$$

(2) Using the logarithmic matrix method to obtain $\boldsymbol{A}$:

$$\boldsymbol{A}=\begin{bmatrix}1 & -1 & 0\\ 4 & 3 & 0\\ -1 & 3\times10^{-8} & -2+3\times10^{-9}\end{bmatrix}$$

(3) Using the successive approximation method to obtain $\boldsymbol{A}$.
After obtaining $\phi(0.01)$, use the Eq. (7.106) to solve $\boldsymbol{A}$:

$$\boldsymbol{A}=\begin{bmatrix}0.995 & -1 & 0\\ 4 & -3.005 & 0\\ -1 & 0.006 & -2.001\end{bmatrix}$$

7.8.6.3 Results of Example 3

If the transfer function for hydro turbine governor and prime mover is known:

$$G(S)=\frac{(5S+1)(1-S)}{(0.53S-1)(45.2698S+1)(0.5S+1)}$$

To be solved is the difference transfer function with difference time of $T=1\,\mathrm{s}$.

(1) Solve the transfer function by the Direct Z transform method.
With Eq. (7.108):

$$G(Z)=Z\left[G(S)\frac{(1-\mathrm{e}^{-TS})}{S}\right]$$

First, expand $G(Z)=\dfrac{1}{S}$ into the form of partial fractions

$$G(Z)=\frac{1}{S}=\frac{A}{0.53S+1}+\frac{B}{45.27S+1}+\frac{C}{0.5S+1}+\frac{D}{S}$$

$$A=G(S)\frac{1}{S}(0.53S+1)\Big|_{S=-\frac{1}{0.53}}=-2.68775$$

$$B=G(S)\frac{1}{S}(45.27S+1)\Big|_{S=-\frac{1}{45.27}}=-42.1123$$

$$C=G(S)\frac{1}{S}(0.5S+1)\Big|_{S=-\frac{1}{0.5}}=2.5$$

$$D=G(S)\frac{1}{S}\cdot S\Big|_{S=0}=1$$

Substitute them into Eq. (7.98) to get:

$$G(Z)=\left(\frac{-5.0679}{1-e^{1/0.53}Z^{-1}}+\frac{-0.93025}{1-e^{1/45.27}Z^{-1}}+\frac{4.999999}{1-e^{1/0.53}Z^{-1}}+\frac{1}{1-Z^{-1}}\right)(1-Z^{-1})$$
$$=\frac{E}{(1-0.15156Z^{-1})(1-0.97815Z^{-1})(1-0.1353353Z^{-1})}$$

where

$$E=-5.0697\left(1-e^{\frac{-1}{0.5}}Z^{-1}\right)\left(1-e^{\frac{-1}{0.527}}Z^{-1}\right)(1-Z^{-1})$$
$$-0.93024\left(1-e^{\frac{-1}{0.53}}Z^{-1}\right)\left(1-e^{\frac{-1}{0.5}}Z^{-1}\right)(1-Z^{-1})$$
$$+4.99997\left(1-e^{\frac{-1}{0.53}}Z^{-1}\right)\left(1-e^{\frac{-1}{45.27}}Z^{-1}\right)(1-Z^{-1})$$
$$+\left(1-e^{\frac{-1}{0.53}}Z^{-1}\right)\left(1-e^{\frac{-1}{45.27}}Z^{-1}\right)\left(1-e^{\frac{-1}{0.5}}Z^{-1}\right)$$
$$=-0.0020285Z^{-1}+0.0895481Z^{-2}-0.0714933Z^{-3}$$

Finally

$$G(Z)=\frac{-0.0020285Z^{-1}+0.0895481Z^{-2}-0.714933Z^{-3}}{1-1.265Z^{-1}+0.3Z^{-2}-0.02Z^{-3}}$$

(2) Solve the transfer function by the State equation method.
First, transform $G(S)$ into a state equation (and in reference to the hydro unit model)

$$\begin{bmatrix} p\Delta M_2 \\ p\Delta N_2 \\ p\Delta P_{\mathrm{T}} \end{bmatrix} = \begin{bmatrix} -1.88624 & 0 & 0 \\ -0.18624 & -0.02209 & 0 \\ 0.3729 & 2.04418 & -2 \end{bmatrix} \begin{bmatrix} \Delta M_2 \\ \Delta N_2 \\ \Delta P_{\mathrm{T}} \end{bmatrix} + \begin{bmatrix} 1.88625 \\ 0.208335 \\ -0.4167 \end{bmatrix} \Delta u$$

$$Z = [0, 0, 1] \begin{bmatrix} \Delta M_2 \\ \Delta N_2 \\ \Delta P_{\mathrm{T}} \end{bmatrix}$$

1. Calculate the coefficient of difference equation ($T = 1$):

$$X(k+1) = \phi(\tau)X(k) + G(\tau)u(k), \quad Z(k) = [0, 0, 1]X(k)$$

$$\phi(\tau) = \begin{bmatrix} 0.15164 & 0 & 0 \\ -0.08257 & 0.97815 & 0 \\ -0.00436 & 0.87106 & 0.13534 \end{bmatrix}, \quad G(\tau) = \begin{bmatrix} 0.84836 \\ 0.10443 \\ -0.00204 \end{bmatrix}$$

2. Normalize the difference equation:

$$Y(k+1) = \phi^*(\tau)X(k) + G^*(\tau)u(k)$$
$$Z(k) = h^{*T}Y(k)$$

$$\phi^*(\tau) = \begin{bmatrix} 0 & 1 & 0 \\ 0 & 0 & 1 \\ 0.02 & -0.3 & 1.265 \end{bmatrix}, \quad G^*(\tau) = \begin{bmatrix} -0.00204 \\ 0.08698 \\ 0.03916 \end{bmatrix}$$

3. $$h^{*T} = [1, 0, 0]_{\circ}$$

(3) Solve the transfer function by the normalized equation method.
$\phi^*(\tau)$ has been solved, that is, the coefficients $a_1,\ldots,a_n$ of difference transfer function have been obtained:

$$a_1 = -1.265, \quad a_2 = 0.3, \quad a_3 = -0.02$$

and the coefficient b can, by Eq. (7.119), be determined

$$\begin{bmatrix} b_1 \\ b_2 \\ b_3 \end{bmatrix} = \begin{bmatrix} 1 & 0 & 0 \\ -1.265 & 1 & 0 \\ 0.3 & -1.265 & 1 \end{bmatrix} \begin{bmatrix} -0.00204 \\ 0.08698 \\ 0.03919 \end{bmatrix} = \begin{bmatrix} -0.00204 \\ 0.08956 \\ -0.07148 \end{bmatrix}$$

Thus, finally we have

$$G(Z) = \frac{-0.00204Z^{-1} + 0.08956Z^{-2} - 0.07148Z^{-3}}{1 - 1.265Z^{-1} + 0.3Z^{-2} - 0.02Z^{-3}}$$

Seen from this example, the latter method is much simpler than the former one. When determining coefficient b, it is not required to do a lot of work to combine the similar terms, only applying Eq. (7.121). As a result, the latter method is adopted as worthy.

7.9 Conclusion

The study in this chapter establishes an accurate model of the load disturbance, improves the estimation and forecast accuracy of the load disturbance, and provides a reliable basis for designing the new load frequency controller. The hierarchical estimators are utilized not only to minimize the estimated amount of calculations but also to create conditions for centralized and decentralized coordinated control of large-scale power systems. The compensation controller can effectively control the load disturbance. The combination of the compensation controller and the integral feedback controller can make up for their own defects and improve the control performance, in which the follow-up control reflects the actual control process. The three model transformation methods (including the eigenvalue method, the logarithmic matrix expansion method and the successive approximation method) proposed in this chapter prove to be the effective methods by the practical results and have shown that they are applicable to set up the hierarchical estimator and compensation controller.

The following is calculation formulation ($N=194$, $m=20$):

$$M=\frac{1}{N}\sum_{k=1}^{N}Z_k$$

$$S^2=\frac{1}{N}\sum_{k=1}^{N}(Z_k-\mu)^2$$

$$\hat{\rho}_\tau=\frac{1}{N}\sum_{k=1}^{N-\tau}\left(\frac{Z_k-\mu}{S}\right)\left(\frac{Z_{k+\tau}-\mu}{S}\right),\tau=0,1,\cdots,m$$

$$\hat{\phi}_{ll}=\begin{cases}\hat{\rho}_1, l=1\\ \dfrac{\hat{\rho}_l-\sum_{j=1}^{l-1}\hat{\phi}_{l-1,j}\hat{\rho}_{l-j}}{1-\sum_{j=1}^{l-1}\hat{\phi}_{l-1,j}\hat{\rho}_j}, l=2,3,\cdots,m\end{cases}$$

where

$$\hat{\phi}_{lj}=\hat{\phi}_{l-1,j}-\hat{\phi}_{ll}\hat{\phi}_{l-1,l-j}, j=1,2,\cdots,l-1$$

CHAPTER 8

Local Decoupling Control Method for Transient Stability of a Power System

Chapter Outline

Mathematical Models and Algorithms for Power System Optimization. https://doi.org/10.1016/B978-0-12-813231-9.00008-X

8.1 Introduction

8.1.1 Description of the Problem

Power system stability is an important issue to ensure the power supply security of the system, which has always been of concern and of value.

To ensure the stable operation of the system, people constantly strive to make the grid structure reasonable and improve the generator to enhance the antidisturbance capability of the system. At the same time, to cope with serious emergencies that damage normal operation, such as lightning strikes, maloperation, short circuits, and other unpredictable disasters, urgent measures are also required to minimize the impact of major interruptions on the stability of the system's operation in terms of both time and space.

In the case of emergencies, the following measures ensure the system's stability in general: excitation forcing, synthetic reclosing, generator tripping, fast regulation of generator output, electric braking, automatic switching on-off, intensified compensation of the series compensation capacitor, and fault load shedding. Obviously, stability measures are taken and carried out locally in the system.

In case of any power system failure emergency, it is necessary to take one or several of the previously mentioned control measures at the right time to maintain and restore stability. However, it is fairly complex to ensure the stable operation of the power system, as it is determined by system structure, operation mode, fault nature, load distribution, power supply reliability standard, etc. In other words, in case of any emergency, the selection and implementation of stability measures will not be arbitrary but subject to certain rules and requirements. Otherwise, it will go against the will of keeping the power system stable.

In theory, given the previous premise, it is possible to use the computer to perform stability control calculations on the power system, but in reality, it is far from being so simple. On the issue of how to make decisions and implement control, we will encounter more than just theory; it is also a practical difficulty.

First, to analyze a specific system, it is often necessary to carry out a great number of calculations, simply in the hope of getting some answers in the more typical cases in emergency operation situations. For the moment, if a computer is used for centralized online control, even if we make the calculations in advance and just save the calculated control schemes in the computer for retrieval, it is often the case that its scale and speed cannot keep pace with the changing operation requirements.

Second, the information required for collection from the control center for direct control will be extensive across the system, including not only direct information but also skip-level information. Collecting skip-level information is not only of low reliability but also costly. Moreover, the information gathered in this way is often used only for local operations.

Therefore, there will be two practical barriers when pursuing online centralized control. One is the difficulty of real-time data collection, and the investment in data collection systems is huge; the other is that the speed and reliability of computer systems are not enough to accommodate the demand for real-time closed-loop control of a power system.

This shows that centralized stability control is not appropriate and difficult to achieve for such a large interconnected power system in current reality conditions.

In addition, according to the large system theory in modern control theory, from the perspective of reliability, it can be proven that, for complex large systems, the centralized control structure scheme is not the optimal one, whereas decentralized control is suitable in accordance with the interconnection of the controlled objects.

In so-called "decentralized control," that is, the respective stability control of each part of the system, usually only limited information is obtained because it is generally difficult to obtain all information of the system from a certain part of the system (even if it is available, the reliability is very low). What kind of impact can a group of local emergency measures based on this limited information have on systemwide stability?

From a certain point in the system, it is difficult to give a clear answer in advance, because the power system is a complex interconnected system with strong interactions. When the system has a stability problem in an emergency, local stability control is performed based on limited information obtained only in each part of the system. Some are feasible in the local view, but they are not necessarily feasible from a global perspective and may even lead to a systemwide collapse. That means, for complex power systems, there is no simple causal relationship between local stability requirements and global stability requirements.

8.1.2 Investigating the Feasibility of System Stability Control based on Local Information

Therefore, under these conditions, what kind of control method is adopted so that the emergency measures taken locally are not contradictory to the overall stability requirements? This is the problem of local stability control in emergency situations studied in this chapter.

In other words, although the measures for local stability control have long been adopted for stabilizing the system, the concept of reclosing and electric braking was proposed as early as the 1930s to maintain the synchronous operation of the generator in the event of a fault. However, their application has begun to be constrained by various conditions. Our purpose is to find out what these conditions are, and adopt corresponding control methods to determine the ways and conditions they switch in.

Studying this problem has great practical significance, because the current power system is increasingly growing, the internal interconnection is increasingly complicated, and there are more and more constraints between them, which makes local failure cause local power interruption as before, but it also endangers the overall system. Many domestic and international accident cases have confirmed this. For example, in a major blackout in New York in the 1970s, one of the reasons for the accident was that the localized loss of magnetic protection was not coordinated with the requirements of global stability. In the 1970s, in an oscillation accident on the Danhan line in China, the accidental power protection action destroyed the possibility of pull-in synchronization, thus expanding the accident. These examples highlight the importance of studying local stability control with new ideas and methods.

This chapter proposes control criteria and models for local stability control in accordance with the previously mentioned requirements from an overall power system stability point of view, and discusses the feasibility of control law through examples of simulation calculation.

8.1.3 Overview of This Chapter

This chapter introduces a new observation decoupling state space from the perspective of ensuring the stability of the power system. The new state vector is called the local equilibrium state vector, and its elements are decentralized local reference values or local equilibrium reference state vectors. In this state space, the state of the system can be obtained by conventional calculation methods based on traditional local measurements. According to the dynamic characteristics of the power system, the local online stability control of the system is divided into two stages from the time domain. The corresponding methods and models for local online stability control are given in each stage. Finally, the practical feasibility of the proposed method is discussed through an example of simulation calculation.

In theoretical analysis and simulation calculations, the mathematical models selected are the most simplified, and the control measures taken are also single, whereas some technical details are ignored. In addition, the network used for calculation is also given after the equivalent simplification of the actual system. But these simplifications and approximations do not affect the conclusions and can make the issues discussed clearer and certain, which will be more conducive to understanding and explaining the problem.

In this chapter, Section 8.2 provides the ideas of two stage local control via constructing a new state space (local equilibrium state); Section 8.3 describes the concept for system stability control via two stage local controls; Section 8.4 gives mathematical formulation and proof for the first stage control criterion; Section 8.5 proves that the new constructed state space for the second stage control criterion, which is observable and decoupled by a mathematical theory, from which the new state space is topologically equivalent to the original system state space; Section 8.6 expounds on the general simulation calculation process for two stage control; Section 8.7 provides a numerical calculation model in simulation calculation for two stage control; and Section 8.8 makes a simulating calculation for a small-scale example, by which the correctness and effectiveness of the proposed mathematical theory and relevant criteria has been verified.

8.2 Basic Ideas of Solving the Problem

8.2.1 Analysis of Two Scenarios in Power System Instability

There are two scenarios of stability loss in the power system:

(1) The local generator loses its synchronism with the system within the first swing period.
(2) The local generator does not lose its synchronism with the system within the first swing period, but it loses synchronism in the following swing period as a result of the severe oscillation of the system.

In the first scenario, the main reason is that a serious short circuit fault happened near the generator without timely and effective control measures. Because of the short circuit, the local generator only provides limited power (three-phase short circuit is zero power) for the system, and at the beginning of the moment, due to the inertia, the input shaft power is almost the same as that before the failure. Therefore, the power balance of the local generators is destroyed, and the generator rotor will be quickly accelerated by the input shaft power from the prime mover, thus increasing the relative angle between the local generator and the rest of the system.

It is worth noting, however, that at the beginning of the first swing cycle of the system, the rest of the system has not yet had a serious swing.

In the second scenario, the main reason is that the power system is a large interconnected system with strong interaction; the impact of local disturbance will gradually spread to the rest of the system after the first swing cycle, making the entire system oscillate. This type of oscillation sometimes will be aggravated due to the absence of the system damping for various reasons, resulting in some local generators' loss of synchronism with the system. For instance, if the stabilization measures taken at the point of failure are not reasonable (their strength or switching time), these measures are used in the first swing cycle; in the later system oscillation, the requirements for local stability will become unmatched with the one for overall stability; thus, it is likely to aggravate the oscillation, resulting in system breakdown.

In view of the first scenario, to keep the system stable (once the fault is removed as quickly as possible in the initial stage), the only feasible remedial measure to prevent the synchronous generator from desynchronizing with the rest of the system within the first swing period is to brake the synchronous generator as soon as possible, so as to absorb the excess energy obtained during the fault and to avoid loss of synchronism in the first swing period, thus minimizing its impact on the rest of the system.

In view of the second scenario, the local generator after the first swing period, as a result of intense interaction among the parts of the system, the impact of local fault will spread to the overall system, putting the system in danger of disconnection at any time due to its severe oscillation, then it is still necessary to continue taking effective control measures in due time at each part of the system. However, these stability measures should not only be favorable for local stability but also promote overall stability.

Nevertheless, it is difficult to obtain all information of the system because the local parts in the system provide only limited local information. Normally, it is very difficult to make a decision and control in such a way as to realize the consistency between a local and overall stability goal based only on local information.

8.2.2 Purposes of Introducing an Observation Decoupled State Space

To overcome the previously mentioned difficulties (the difficulty to obtain all information of the system based on limited local information, and the difficulty to make decisions and controls that harmonize local stability with global stability based on local information) and to make the local stability control in line with the limited local information favorable to overall system stability, it is required to decouple local information of the whole system and eliminate the impact of the rest of the system on local information, so as to reach accordance between goals of local and overall stability during local stability control in line with local decoupled observation information.

This chapter attempts to achieve this purpose of decoupling by introducing a new state space, that is, observation decoupled state space. The system state can be estimated by local

calculation only based on local measurements, by which norm reduction control criterion is derived for local stability control. The control criterion consists of local observable decoupled state variables, so it requires local feedback only. Theoretically, if the operation mode exists after the fault happened, and the system could make each local stability control always meet the norm reduction control criterion in an online manner, the overall system is asymptotically stable in the sense of Lyapunov.

8.2.3 Two Stage Countermeasures in Local Stability Controls

In summary, the countermeasures in local stability control in emergency situations can be divided into two stages:

In the first stage: Implement emergency control over the instability of local single generator in the first swing period, so as to brake the synchronous generator, which is required to estimate or determine the excess energy obtained during the fault as soon as possible, so as to withdrawal or absorb the excess energy.

To achieve this, the switching of the braking resistor is desirable because it has a certain degree of fastness and the required flexibility for the operation. In addition, fast valve can also be considered if it can be opened and closed quickly enough.

It is known from the equal area criterion that when the sum of the energy absorbed during the braking period and the excess energy obtained during the fault period is zero, then the impact of switching off the brake on the subsequent oscillation is minimal. Therefore, this criterion can be carried out for the first stage control. Because this criterion is based on the energy equilibrium, it can be called the first stage control criterion (energy equilibrium).

In the second stage: Control multiple swings of multiple generators in each part of the system by following the norm reduction control criterion, based on no loss of synchronism of the local single generator in the first swing at the first stage. Because this criterion is based on the value of critical power, it can be called the second stage critical power control criterion.

However, it should be pointed out that, in the actual local stability control of the system, it is difficult to rigidly meet the norm reduction control criterion because the value of critical power needs to be calculated online and is thus time-varying. Furthermore, the actual control measures based on the critical power value could be only switched on and off in a step-wise form in general.

In addition, the norm reduction control criterion requires that each part of the system must be controlled in line with the derived respective criterion value. To this end, even if it is not difficult, it will be costly, so only a limited number of stability control devices are set at several critical local parts for the actual system.

Therefore, in the course of actual control, it is necessary to rely on the norm reduction control criterion as much as possible. As a matter of fact, it is sufficient to achieve this as far as possible because strict conformance with the norm reduction control criterion is a sufficient condition for overall system stability rather than a necessary condition. The simulation calculation for the analog system indicates that, as long as the criterion is met as much as possible, system stability will be satisfied.

In addition, it should be pointed out that, to simplify the calculation and better describe the problem, the simplest models are used in both theoretical analysis and system simulation calculation, the problems are idealized, and less technical details involved in realization are considered. Theoretically, it will not affect the effectiveness of the conclusion, and it could liberate us from numerous minor details. This is more favorable to the problem to be clarified.

8.3 Basic Concepts of Control Criteria based on Local Control

To describe the physical background and requirements of transient stability control, a simplified mathematical model and typical network of power system is given in Section 8.3.1; the control countermeasure adopted for the power system is divided into two stages (emergency and norm reduction), which are described in Sections 8.3.2–8.3.3.

8.3.1 Simplified Model and Typical Network of the Power System

To describe the idea how to solve the problem mentioned in Section 8.2, a power system network model with N buses is provided, as shown in Fig. 8.1.

In Fig. 8.1, $\{U_i, \alpha_i\}$ is the voltage and phase angle of bus i, $\{Z_{ij}, \varphi_{ij}\}$ is the impedance value and phase angle of line i-j, X_C is one-half the capacitive reactance of line i-j, and $\{P_{Li}, Q_{Li}\}$ is the load. In addition, within the dotted line are generator bus parameters, $\{E_i', \delta_i\}$ is the internal electromotive force and phase angle of the generator, P_{mi} is the generator input power, P_{Di} is the generator damping coefficient, J_i is the rotary inertia of generator rotor, X_{di}' is the transient reactance of the generator, and u_i is the controlled quantity imposed on the generator bus i. Obviously, there is no parameter for the passive bus within the dotted line.

The electromechanical equation of the power system for the network in Fig. 8.1 is as follows:

(1) Rotor motion equation:

$$J_i\ddot{\delta}_i + P_{Di}\dot{\delta}_i - P_{mi} + \frac{E_i'U_i}{X_{di}'}\sin(\delta_i - \alpha_i) + u_i = 0 \quad (i \in [1, N]) \tag{8.1}$$

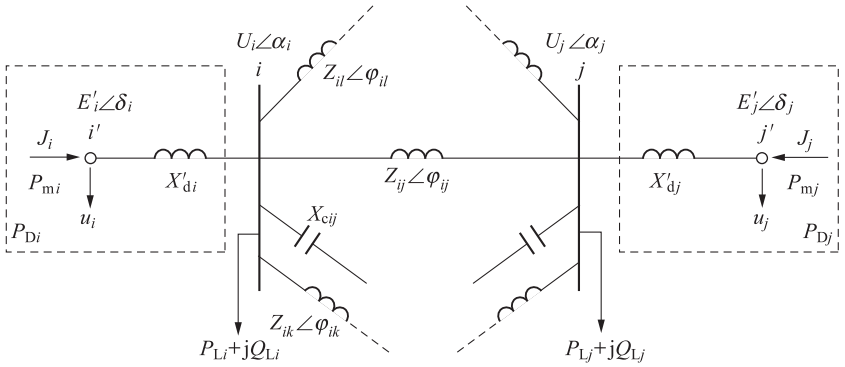

Fig. 8.1
Circuit connecting two buses of *i*-*j* in the power system network.

(2) Power balance equation:

$$\begin{aligned}\frac{E'_iU_i}{X'_{di}}\sin(\delta_i-\alpha_i)=&\sum_{\substack{j=1\\j\neq 1}}^{N}C_{ij}\frac{U_iU_j}{Z_{ij}}\sin(\alpha_i-\alpha_j+\varphi_{ij}-90^\circ)\\&+U_i^2\sum_{\substack{j=1\\j\neq i}}^{N}C_{ij}\frac{\cos\varphi_{ij}}{Z_{ij}}+P_{Li}\quad(i\in[1,N])\end{aligned}\tag{8.2}$$

$$\begin{aligned}\frac{E'_iU_i}{X'_{di}}\cos(\delta_i-\alpha_i)-\frac{U_i^2}{X'_{di}}=&-\sum_{\substack{j=1\\j\neq 1}}^{N}C_{ij}\frac{U_iU_j}{Z_{ij}}\cos(\alpha_i-\alpha_j+\varphi_{ij}-90^\circ)\\&+U_i^2\sum_{\substack{j=1\\j\neq i}}^{N}C_{ij}\left(\frac{\sin\varphi_{ij}}{Z_{ij}}-\frac{1}{x_{cij}}\right)+Q_{Li}\quad(i\in[1,N])\end{aligned}\tag{8.3}$$

where $C_{ij}=\begin{cases}1 & (i \text{ and } j \text{ are directly connected})\\ 0 & (i \text{ and } j \text{ are not directly connected})\end{cases}$; the definition of other parameters is as previously mentioned. In the case of passive bus, Eq. (8.1) does not exist, and the left side item of Eqs. (8.2) and (8.3) is 0.

In Eq. (8.1), the rotor motion equation, described by second-order differential equation, can also be written in the form of a state equation of two simultaneous first-order differential equations:

$$\begin{cases}\dfrac{\mathrm{d}\delta_i}{\mathrm{d}t}=\omega_i-\omega_0 & (i\in[1,N])\\[2ex] \dfrac{\mathrm{d}\omega_i}{\mathrm{d}t}=\dfrac{1}{J_i}\left[P_{mi}-\dfrac{E'_iU_i}{X'_{di}}\sin(\delta_i-\alpha_i)-P_{Di}(\omega_i-\omega_0)-u_i\right]\end{cases}$$

where ω_i is the generator speed, and ω_0 is the synchronous speed in steady-state.

8.3.2 Basic Concept of the First Stage Control Criterion (Energy Equilibrium)

The major theoretical foundation for the first stage (energy equilibrium) control is an equal area criterion.

The equal area criterion generally applies to the analysis of a simple single-machine infinite-bus system only; however, in the initial stage of fault at part i of the system, the rest of the system has not had severe swing yet, and the inertia constant T_{Ji} of part i of the system is far less than the sum $\sum_{j\neq i} T_{Jj}$ of the inertia constants of other parts, that is, $T_{Ji} \ll \sum_{j\neq i} T_{Jj}$. So in the initial stage of the fault, that is, the first stage energy equilibrium control stage, the relation of the faulty part of system to the rest of the system could be temporarily taken as a simple relation with a single-machine infinite-bus system. Therefore, as for the energy equilibrium control in the first stage, the equal area criterion can be used for dynamic analysis for the faulty part i of the system.

It is known from the equal area criterion that, when the maximum possible deceleration area is less than the acceleration area, the system is in transient stability state, and the purpose of the electric braking in the initial period of the fault is to heighten the power angle characteristic curve and enlarge the deceleration area, so as to decrease the power angle swing and avoid loss of synchronism in the first swing period. The optimal switch-off time for the electric braking is discussed via Fig. 8.2. Simply stated, assume the postfault system will restore to the prefault operation state, the brake is always switched on when removing the fault, and the resistance is the same.

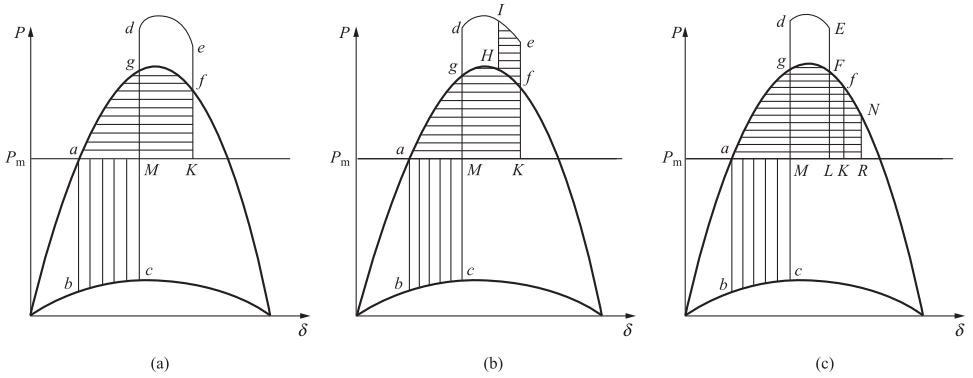

Fig. 8.2
Contrast of backswing potential energy zones for different brake switch-off time.

In Fig. 8.2A–C, the acceleration area S_{abcM} is equal, that is, the fault scenarios are the same, whereas the difference lies in the brake switch-off time.

In Fig. 8.2A, the brake is switched off when $S_{\mathrm{deKM}} = S_{\mathrm{abcM}}$, the electromagnetic power drops to the value corresponding to Point f from the value corresponding to Point e, then ω is equal to the synchronous speed; the power angle δ swings back along fga, and area S_{fgaMK} refers to the potential energy in the course of the power angle backswing.

In Fig. 8.2B, the brake still cannot be switched off when $S_{\mathrm{deKM}} = S_{\mathrm{abcM}}$. However, because ω has reached the synchronous speed, the power angle starts to swing back along el, and the brake is switched off when it swings back to I, the electromagnetic power drops to the value corresponding to Point I from the value corresponding to Point H; hereafter, the power angle swings further back along Hga, and the area S_{eIHgaMKf} refers to the potential energy in the course of the power angle backswing.

In Fig. 8.2C, the brake is switched off at Point E when $S_{\mathrm{dELM}} < S_{\mathrm{abcM}}$, and the electromagnetic power drops to the value corresponding to Point E from the value corresponding to Point F. Because the deceleration area is less than the acceleration area, the power angle will further swing back along FfN. When it reaches N, the deceleration area $S_{\mathrm{dEFfNRKLMg}}$ is equal to acceleration area S_{abcM}, ω is equal to the synchronous speed, and the power angle starts to swing back along NfFga. The area $\mathrm{S}_{\mathrm{NfFgaMLKR}}$ refers to the potential energy in the course of the power angle backswing.

In Fig. 8.2, the shaded area with vertical bars refers to the acceleration area during the fault, whereas the shaded area with horizontal bars refers to the backswing potential energy zone when ω returns to synchronous speed.

In the comparison of the switch-off time for the described three different brakes, if the brake is switched off when the deceleration area is equal to the acceleration area as shown in Fig. 8.2A, the backswing potential energy of the power angle is minimal; if the brake is switched off after the time shown in Fig. 8.2B or before the time shown in Fig. 8.2C, the backswing potential energy of the power angle will become larger, aggregating the subsequent oscillation of the system. Therefore, it could be concluded that it is the optimal brake switch-off time when the deceleration area is equal to the acceleration area, which is deemed as the basis for the first stage energy equilibrium control criterion.

In Fig. 8.2, the acceleration area is equivalent to the excess energy obtained by the local generator rotor during the fault, and the deceleration area is equivalent to the energy absorbed during the braking. The mathematical expression for the first stage energy equilibrium control criterion could be derived by determining the described energy, respectively.

During the fault, the excess kinetic energy ΔW_i accumulated on rotor i of the local unit could be expressed as the online time integral of power difference:

$$\Delta W_i = \int_{t_0}^{t_p} [P_{\mathrm{m}i} - P_{\mathrm{E}i}(t)]\,\mathrm{d}t \tag{8.4}$$

where:

t_0 refers to the initial time of fault, and t_p refers to fault switch-off time.
P_{mi} refers to the net power of the generator prior to the fault, without change during the fault.
$P_{Ei}(t)$ refers to the electromagnetic power of generator in the dynamic course.

The absorbed energy ΔW_{bi} during the braking could be described as the online time integral of power difference:

$$\Delta W_{bi} = \int_{t_p}^{t_1} [P_{mi} - P_{Ei}(t)]\mathrm{d}t \tag{8.5}$$

where t_1 refers to the switch-off time of the brake.

The definitions of other parameters are as previously discussed.

The braking resistor is online when $t_p \le t \le t_1$, because $P_{Ei}(t) > P_{mi}$, the signs for ΔW_{bi} and ΔW_i are opposite. Obviously, if at t_1:

$$\begin{aligned} \Delta W_i + \Delta W_{bi} &= \int_{t_0}^{t_p} [P_{mi} - P_{Ei}(t)]\mathrm{d}t + \int_{t_p}^{t_1} [P_{mi} - P_{Ei}(t)]\mathrm{d}t \\ &= \int_{t_0}^{t_1} [P_{mi} - P_{Ei}(t)]\,\mathrm{d}t = 0 \end{aligned} \tag{8.6}$$

The energy absorbed during the braking will be balanced with the excess energy obtained during the fault, and switch-off of the brake at this moment will have minimum impact on subsequent oscillation of the system. Therefore, Eq. (8.6) is the most logical mathematical expression for the first stage energy equilibrium control criterion.

8.3.3 Basic Concept of the Second Stage Control Criterion (Norm Reduction)

The derivation of critical power control based on the norm reduction control criterion relies on the introduction of the observation decoupled state space, which is based on decoupling the original system state space. To decouple the original system state space, it is required to find the effective decoupling criterion. This section discusses the simplified model of the power system and its typical network given in Section 8.3.1, which is partly shown in Fig. 8.1, and finally gives the mathematical analytical form of norm reduction control criterion for such a typical network.

Section 8.3.3.1 mathematically defines the decoupled reference vector applied in the second stage control; Section 8.3.3.2 describes the feature of a state space composed of the decoupling vector; Section 8.3.3.3 gives the specific mathematical formulation of observable decoupled

state space applied in the power system; Section 8.3.3.4 describes the dynamic relation in observation decoupled state space; Section 8.3.3.5 gives the formulation of norm reduction control criterion and its expression for a typical network structure; and Section 8.3.3.6 gives the formulation of norm reduction control criterion in other observation decoupled state space.

8.3.3.1 The concept of observation decoupled reference state vector

It is known that the power angle δ_{0i} in an equilibrium state for the generator sets of the power system, which is determined by its operation mode that depends on three factors: the unit power output of system, network structure, and load. That is, a change in any factor will change the operation mode, and δ_{0i} will also change accordingly. Thus, a different operation mode will correspond to a different power angle δ_{0i} in the equilibrium state.

When the power system is operated in a steady-state, the input mechanical power of the generator is in balance with the output electromagnetic power, and each generator rotor operates at synchronous speed ω_0. In case of fault, the power balance will be disrupted, so generator speed ω_i will increase or decrease, thus deviating from synchronous speed ω_0. Meanwhile, the power angle δ_i will deviate from the power angle δ_{0i} in a prefault stable equilibrium state as well.

As the operation mode of the system often changes prior to and after the fault, prefault δ_{0i} cannot be used as the stability criterion for the parts of the system. As a matter of fact, even if the system is in a steady-state prior to the fault, its operation does not remain unchanged, so the prefault δ_{0i} is not constant. The operation mode after the fault is often unknown. Even if the change of the network structure is known after the fault, it is impossible to accurately determine the postfault operation mode and the corresponding power angle in a postfault equilibrium state in advance due to the correlation and interaction of generator sets among systems, as well as the stochastic fluctuation of the load. Moreover, the power angle δ_i of each generator bus is a relative quantity with one point in the system as the coordinate reference point 0, and because the power system is an interconnected system with complex coupling relations, the local disturbance of the system will even shift the coordinate of the reference point. Therefore, it becomes impossible to determine the final stability goal for the change of δ_i in advance.

To sum up, the power angles in a steady-state at each part of the system after the fault cannot be determined; thus, it is impossible to determine the final stability goal for each part of the system in advance. So, for δ_i, which keeps changing because of the power unbalance, what criterion will be followed to reach stability? This is the most urgent problem to face and the key to solving the problem lies in whether stability criterion for δ_i can be found.

As mentioned earlier, the power equilibrium is disrupted after a system fault. Assume that at least one generator (set to the Nth unit) maintains power balance; the rest of the power system forms up to $N-1$ local systems. In addition, if δ_{ei} is further defined as the rotational

speed of the assumed power angle in a local equilibrium state, when each local part of the system meets these relations:

$$\begin{cases} \delta_i(t) = \delta_{ei}(t) \\ \dot{\delta}_i(t) = \dot{\delta}_{ei}(t) \end{cases} \quad [1,\ N-1] \tag{8.7}$$

the overall system will be in a steady operation state again.

It must be pointed out that δ_{ei} is assumed as the local power equilibrium state, and in fact is of no actual physical meaning but rather just an abstract virtual variable.

The concept of the power angle δ_{ei} for the assumed local equilibrium state is introduced here, which can be used as the respective stability reference for the local dynamic power angles of the power system. Because its time-varying characteristic, δ_{ei} could serve as the stability reference for δ_i only in a transient dynamic sense, and the criterion is valid only in a local sense.

In line with the assumption when introducing δ_{ei} concept, δ_{ei} could be obviously obtained from the time-varying data set $\{E_i', P_{mi}, P_{Li}, Q_{Li}, U_j, \alpha_j, u_j\}$ for local system i, where the control variable u_i is with non-zero value only when imposing local stability control, and it is of zero value in other time. If the initial value of the time-varying data set is known and can be replaced in a real-time manner, δ_{ei} will be uniquely determined. The equivalent circuit for obtaining the power angle δ_{ei} for the assumed local equilibrium state is shown in Fig. 8.3.

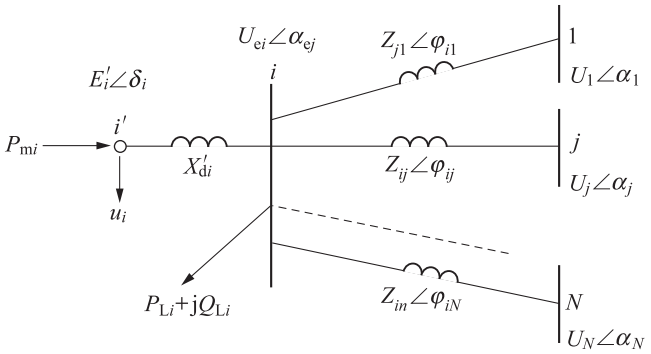

Fig. 8.3
Circuit for defining assumed local equilibrium state.

As is known from common sense in the power system, the process of calculating δ_{ei} is to derive the instant power flow solution of the local network as shown in Fig. 8.3. The virtual instant quantity of U_{ei} and α_{ei} could be derived as well while calculating δ_{ei}. $U_{ei}\angle\alpha_{ei}$ can be deemed as the instant local equilibrium reference for the generator terminal voltage $U_i\angle\alpha_i$. U_{ei}, α_{ei} and δ_{ei} together constitute the time-varying data set $\{\delta_{ei}, U_{ei}, \alpha_{ei}\}$ belonging to the assumed local power equilibrium state, so the time-varying data set is regarded as the instant stability balance reference vector $[\delta_{ei}, U_{ei}, \alpha_{ei}]^T$ for the actual local operation parameter vector $[\delta_i, U_i, \alpha_i]^T$ of the power system. If their

derivatives are further defined as $\left[\dot{\delta}_i, \dot{U}_i, \dot{\alpha}_i\right]^{\mathrm{T}}$ and $\left[\dot{\delta}_{ei}, \dot{U}_{ei}, \dot{\alpha}_{ei}\right]^{\mathrm{T}}$, when each part of the power system could persistently meet this equation at the same time:

$$\begin{cases} \begin{bmatrix} \delta_i \\ U_i \\ \alpha_i \end{bmatrix} = \begin{bmatrix} \delta_{ei} \\ U_{ei} \\ \alpha_{ei} \end{bmatrix} \\ \begin{bmatrix} \dot{\delta}_i \\ \dot{U}_i \\ \dot{\alpha}_i \end{bmatrix} = \begin{bmatrix} \dot{\delta}_{ei} \\ \dot{U}_{ei} \\ \dot{\alpha}_{ei} \end{bmatrix} \end{cases} \quad [i \in [1, N-1]] \tag{8.8}$$

then the overall system will be in a steady equilibrium state. In the dynamic stability analysis of a practical power system, the related variables are normally not explicitly including $\left[\dot{U}_i, \dot{\alpha}_i\right]$ and $\left[\dot{U}_{ei}, \dot{\alpha}_{ei}\right]$. Therefore, Eqs. (8.7), (8.8) are deemed as equivalent.

In addition, the conception of "local/part" previously mentioned doesn't refer to the abstract conception of some point or any small neighborhood in a mathematical sense but rather a subset of the generator nodes and its associated nodes.

It can be seen from Fig. 8.3 that δ_{ei} is derived in the "local/part" sense, and the time-varying data set for deriving δ_{ei} falls into two parts: one part consists of the parameters of bus i itself $\{E_i', P_{mi}, P_{Li}, Q_{Li}, u_i\}$, and another part consists of U_j and α_j of bus $j(C_{ij}=1)$ in direct connection with bus i. Although the voltage $U_j \angle \alpha_j$ at bus j is also derived locally, what is noteworthy is that it will certainly bring the impact from the rest of the system for bus i via respective neighboring bus k ($C_{ik}=0$, $C_{jk}=1$), because $U_j \angle \alpha_j$ is derived in the dynamic process of the system. Therefore, δ_{ei} which is derived from the time-varying data set $\{E_i', P_{mi}, P_{Li}, Q_{Li}, U_j, \alpha_j, u_i\}$, including $\{U_j, \alpha_j\}$, reflects the impact of the rest of the system on bus i.

In fact, as the coupling relationship among bus states is always mutual in such an interconnected power system, the impact of the dynamic behavior of bus i state on the rest of the system will be transferred via $\{U_j, \alpha_j\}$ in the dynamic process.

In the dynamic process of the power system, the local dynamic power angle δ_i is a state variable that is always in close connection with the rest of the system, and δ_{ei} reflects the impact of the rest of the system on bus i. When using δ_i minus δ_{ei}, and the purpose of eliminating the coupling impact of the rest of system on bus i could be achieved. Therefore, δ_{ei} is not only the local equilibrium reference for δ_i but also the observation decoupled variable for δ_i.

However, it is necessary to make clear that the decoupling does not truly eliminate the actual effect of the rest of the system on bus i, but it is only a form of the formulation. For instance, if difference variable $\overline{\delta}_i = \delta_i - \delta_{ei}$ is constructed, obviously $\overline{\delta}_i$ will be a local decoupled variable. As $\overline{\delta}_i$ is constructed, δ_i is a true variable in the actual system, but it will also be regretfully of no actual physical meaning due to the virtual characteristic of δ_{ei}. Therefore, the decoupling characteristic of $\overline{\delta}_i$ is only valid in an observational sense, that is, $\overline{\delta}_i$ is a local decoupled variable only from the perspective of observing system dynamic behavior.

8.3.3.2 Composition and characteristics of observation decoupled state space

As stated in the previous section, the difference of δ_i minus δ_{ei} can be defined as a new state variable:

$$\overline{\delta}_i = \delta_i - \delta_{ei} \ (i \in [1, N]) \tag{8.9}$$

where $\overline{\delta}_i$ is a local decoupled variable from the observation perspective.

Obviously, when $\overline{\delta}_i = 0$, the power of the local system is balanced, that is, the point 0 of state variable δ_i is the local power equilibrium point of the system.

In a mathematical sense, the meaning of $\overline{\delta}_i$ is equivalent to a translation transformation of δ_i. Each δ_i translates the original point by δ_{ei} from the uniform coordinate center and is set up in their respective local position. Due to the dynamic time-varying characteristics of δ_{ei}, the coordinate system where each $\overline{\delta}_i$ located is dynamic as well, but it does not matter. What is important is that the respective origins of $\overline{\delta}_i$ will be the constant power equilibrium points for each part of the system after such a translation transformation.

Likewise, a new state variable could be redefined:

$$\dot{\overline{\delta}}_i = \dot{\delta}_i - \dot{\delta}_{ei} \quad (i \in [1, N]) \tag{8.10}$$

A new state space $\left\{\overline{\delta}, \dot{\overline{\delta}}\right\}$ could also be constructed, which is similar to the state space $\{\delta, \omega\}$ in the study of the dynamic behavior of the system. In line with the nature of the state variable in the state space, the new state space could be defined as observation decoupled state space, and its origin is the steady equilibrium point of system, which is a fairly important characteristic of observation decoupled state space. Because the steady-state position in the original state space is not at the coordinate origin of the system but in $\{\delta_{0i}, \omega_0 \,|\, i \in [1, N]\}$, and δ_{0i} is related to the operation mode of the system, it could be any value within the given scope; thus, it is not easy to determine the stability goal of the system. However, by observation decoupled state space, if the system fails, the state of the deviation from the origin can be restored to the origin $\{0,0\}$ of the decoupled state space. Regardless of the way the system fails, the system will operate in a steady-state. In the original state space, the state variable ω_i is a local variable. Therefore, the form of the second state variable can be flexible when observation decoupled state space is constructed by the original state space structure. For example, when the system capacity is large relative to each local part, the variable can also be defined:

$$\dot{\delta}_i(50) = \omega_i - \omega_0 \quad (i \in [1, N]) \tag{8.11}$$

as the second state variable, where $\omega_0 = 2\pi f_0 = 2\pi \times 50 = 100\pi$ (rad/s), and the rated frequency of system is 50 Hz, that is, $\left\{\overline{\delta}, \overline{\delta}(50)\right\}$ could be used to constitute an observation decoupled state space. In addition, if ω_i of each bus in the system can be derived:

$$\dot{\delta}_{si} = \omega_i - \omega_s \quad (i \in [1, N]) \tag{8.12}$$

also can be defined the second state variable, where ω_s could be determined by the equation:

$$\omega_s = \frac{\sum_{j=1}^{N} J_j \omega_j}{\sum_{j=1}^{N} J_j} \tag{8.13}$$

Then observation decoupled state space could be constructed with $\{\overline{\delta}, \dot{\delta}_s\}$.

This shows that the observation decoupled state space is not unique in the form, and it could be formulated according to different requirements and conditions. But it is important to emphasize that, the form of $\overline{\delta}_i$ is the most fundamental and also unique, because of the local observation decoupled characteristic, $\overline{\delta}_i$ is the only specific expression of the new state space, which is called as observation decoupled state space.

8.3.3.3 Formulation of observation decoupled state space in the power system

The observation decoupled state space is constituted in the existence of a decoupling reference. Follow the power system simplified model and the equations to derive the δ_{ei} from Eqs. (8.1)–(8.3) in line with the local power balance assumption, which are listed here:

$$G_{ei} = P_{mi} - \frac{E'_i U_{ei}}{X'_{di}} \sin(\delta_{ei} - \alpha_{ei}) - u_i = 0 \quad (i \in [1, N]) \tag{8.14}$$

$$\begin{aligned} G_{ePi} = \frac{E'_i U_{ei}}{X'_{di}} \sin(\delta_{ei} - \alpha_{ei}) - \sum_{\substack{j=1 \\ j \neq i}}^{N} C_{ij} \frac{U_{ei} U_j}{Z_{ij}} \sin\left(\alpha_{ei} - \alpha_j + \varphi_{ij} - 90^\circ\right) \\ - U_{ei}^2 \sum_{\substack{j=1 \\ j \neq i}}^{N} C_{ij} \frac{\cos\varphi_{ij}}{Z_{ij}} - P_{Li} = 0 \end{aligned} \tag{8.15}$$

$$\begin{aligned} G_{eQi} = \frac{E'_i U_{ei}}{X'_{di}} \cos(\delta_{ei} - \alpha_{ei}) - \frac{U_{ei}^2}{X'_{di}} + \sum_{\substack{j=1 \\ j \neq i}}^{N} C_{ij} \frac{U_{ei} U_j}{Z_{ij}} \cos\left(\alpha_{ei} - \alpha_j + \varphi_{ij} - 90^\circ\right) \\ - U_{ei}^2 \sum_{\substack{j=1 \\ j \neq i}}^{N} C_{ij} \left(\frac{\sin\varphi_{ij}}{Z_{ij}} - \frac{1}{X_{cij}} \right) - Q_{Li} = 0 \quad (i \in [1, N]) \end{aligned} \tag{8.16}$$

$$\left|\alpha_{ei} - \alpha_j + \varphi_{ij} - 90^\circ\right| < \frac{\pi}{2} - \varepsilon, \quad |\delta_{ei} - \alpha_{ei}| < \frac{\pi}{2} - \varepsilon, \quad \forall \varepsilon > 0 \tag{8.17}$$

Eqs. (8.14)–(8.17) are only valid for active bus, and $u_i=0$ when there is no control action, so that the decoupled reference $\{\delta_{ei}, U_{ei}, \alpha_{ei}\}$ could be solved. If Eqs. (8.14)–(8.16) derive differentiation against the time, then the following equations could be derived:

$$\frac{\partial G_{ei}}{\partial t}=\frac{\partial G_{ei}}{\partial \delta_{ei}}\dot{\delta}_{ei}+\frac{\partial G_{ei}}{\partial U_{ei}}\dot{U}_{ei}+\frac{\partial G_{ei}}{\partial \alpha_{ei}}\dot{\alpha}_{ei}=0 \tag{8.18}$$

$$\frac{\partial G_{ePi}}{\partial t}=\frac{\partial G_{ePi}}{\partial \delta_{ei}}\dot{\delta}_{ei}+\frac{\partial G_{ePi}}{\partial U_{ei}}\dot{U}_{ei}+\frac{\partial G_{ePi}}{\partial \alpha_{ei}}\dot{\alpha}_{ei}=0 \tag{8.19}$$

$$\frac{\partial G_{eQi}}{\partial t}=\frac{\partial G_{eQi}}{\partial \delta_{ei}}\dot{\delta}_{ei}+\frac{\partial G_{eQi}}{\partial U_{ei}}\dot{U}_{ei}+\frac{\partial G_{eQi}}{\partial \alpha_{ei}}\dot{\alpha}_{ei}=0 \tag{8.20}$$

$\left\{\dot{\delta}_{ei}, \ddot{U}_{ei}, \dot{\alpha}_{ei}\right\}$could be solved from Eqs. (8.18)–(8.20).

Based on the definition for the observation decoupled state space and the existing observation decoupled reference, the following equations can be written:

$$\overline{\delta}_i=\delta_i-\delta_{ei},\quad \dot{\overline{\delta}}_i=\dot{\delta}_i-\dot{\delta}_{ei},\quad \overline{U}_i=U_i-U_{ei},\quad \overline{\alpha}_i=\alpha_i-\alpha_{ei} \tag{8.21}$$

Then the observation decoupled state coordinate $\left\{\overline{\delta}_i, \dot{\overline{\delta}}_i\right\}$ could be solved, and Eqs. (8.14)–(8.17) could be rewritten into the following forms by means of Eq. (8.21):

$$G_i=P_{mi}-\frac{E'_i}{X'_{di}}\left(U_i-\overline{U}_i\right)\sin\left[\delta_i-\overline{\delta}_i-\left(\alpha_i-\overline{\alpha}_i\right)\right]-u_i=0\quad (i\in[1,N]) \tag{8.22}$$

$$\begin{aligned}G_{Pi}=&\frac{E'_i}{X'_{di}}\left(U_i-\overline{U}_i\right)\sin\left[\delta_i-\overline{\delta}_i-\left(\alpha_i-\overline{\alpha}_i\right)\right]\\&-\sum_{\substack{j=1\\ j\neq 1}}^{N}C_{ij}\frac{U_j}{Z_{ij}}\left(U_i-\overline{U}_i\right)\sin\left(\alpha_i-\overline{\alpha}_i-\alpha_j+\varphi_{ij}-90^{\circ}\right)\\&-\left(U_i-\overline{U}_i\right)^2\sum_{\substack{j=1\\ j\neq i}}^{N}C_{ij}\frac{\cos\varphi_{ij}}{Z_{ij}}-P_{Li}=0\quad (i\in[1,N])\end{aligned} \tag{8.23}$$

$$\begin{aligned}G_{Qi}=&\frac{E'_i}{X'_{di}}\left(U_i-\overline{U}_i\right)\cos\left[\delta_i-\overline{\delta}_i-\left(\alpha_i-\overline{\alpha}_i\right)\right]-\frac{\left(U_i-\overline{U}_i\right)^2}{X'_{di}}\\&+\sum_{\substack{j=1\\ j\neq 1}}^{N}C_{ij}\frac{U_j}{Z_{ij}}\left(U_i-\overline{U}_i\right)\cos\left(\alpha_i-\overline{\alpha}_i-\alpha_j+\varphi_{ij}-90^{\circ}\right)\\&-\left(U_i-\overline{U}_i\right)^2\sum_{\substack{j=1\\ j\neq 1}}^{N}C_{ij}\left(\frac{\sin\varphi_{ij}}{Z_{ij}}-\frac{1}{X_{cij}}\right)-Q_{Li}=0\quad (i\in[1,N])\end{aligned} \tag{8.24}$$

$$\left|\alpha_i-\overline{\alpha}_i-\alpha_j+\varphi_{ij}-90^{\circ}\right|<\frac{\pi}{2}-\varepsilon,\quad \left|\delta_i-\overline{\delta}_i-(\alpha_i-\overline{\alpha}_i)\right|<\frac{\pi}{2}-\varepsilon,\quad \forall\varepsilon>0 \tag{8.25}$$

When $\overline{\delta}_i$ exists, Eq. (8.25) ensures the uniqueness of $\overline{\delta}_i$.

Eqs. (8.22)–(8.25) are defined by the observation decoupled state space of the power system, by which the state coordinate $\left\{\overline{\delta}_i,\dot{\overline{\delta}}_i\right\}$ or the observation decoupled for the local part i of the power system could be solved.

8.3.3.4 The dynamic relationship in observation decoupled state space

The state space consisting of $\left\{\overline{\delta}_i,\dot{\overline{\delta}}_i\right\}$ is observation decoupled. However, as the power system is a nonlinear dynamic system, it is actually impossible to realize the full decoupling in the dynamic process. In the dynamic case, it is only expected to achieve quasidecoupling. The following is the equation for the observation decoupled space in the power system dynamic process. Let

$$W_{1i}=\overline{\delta}_i=\delta_i-\delta_{ei},\quad W_{2i}=\dot{\overline{\delta}}_i=\dot{\delta}_i-\dot{\delta}_{ei},\quad \overline{U}_i=U_i-U_{ei},\quad \overline{\alpha}_i=\alpha_i-\alpha_{ei} \tag{8.26}$$

then the dynamic equation has the following form:

$$\begin{cases}\dot{W}_{1i}=\dot{\overline{\delta}}_i=W_{2i}\\ \dot{W}_{2i}=\ddot{\overline{\delta}}_i=\dfrac{1}{J}\left\{P_{\mathrm{m}i}-\dfrac{E_i'}{X_{\mathrm{d}i}'}\left(\overline{U}_i+U_{ei}\right)\sin\left[W_{\mathrm{L}i}+\delta_{ei}-(\overline{\alpha}_i+\alpha_{ei})\right]-P_{\mathrm{D}i}\left(W_{2i}+\dot{\delta}_{ei}\right)-u_i\right\}-\ddot{\delta}_{ei}\end{cases}\quad (i\in[1,N]) \tag{8.27}$$

In Eq. (8.27), the variables $\left\{\overline{\delta}_i,\dot{\overline{\delta}},\overline{U}_i,\overline{\alpha}_i,u_i\right\}$ are all fully localized, however, there are still items inclusive of variables $\left\{\delta_{ei},\dot{\delta}_{ei},\ddot{\delta}_{ei},U_{ei},\alpha_{ei}\right\}$. These variables are not local ones, but they are the function of state variables of all other buses in the system, which reflects the cumulative effective of other subsystems in local part i and the impact of the rest of system on the bus i in input mode formally. The existence of $\left\{\delta_{ei},\dot{\delta}_{ei},\ddot{\delta}_{ei},U_{ei},\alpha_{ei}\right\}$ makes the dynamic equation not fully decoupled but quasidecoupled.

It is generally difficult to determine the analytical form of $\left\{\delta_{ei},\dot{\delta}_{ei},\ddot{\delta}_{ei},U_{ei},\alpha_{ei}\right\}$. However, they could act as the function of time t in the power system, and they are instantly identified locally. As a matter of fact, they could serve as the intermediate result to work with $\overline{\delta}_i$. Therefore, control variable u_i together with these variables can be considered as a time-varying input, that is, let

$$\overline{g}_i\left(\delta_{ei},\dot{\delta}_{ei},\ddot{\delta}_{ei},U_{ei},\alpha_{ei},U_i\right)=\overline{g}_i(t)\quad (i\in[1,N]) \tag{8.28}$$

where $\overline{g}_i$ is called a disturbing function. Although it is difficult to determine the analytical form of $\overline{g}_i$, the dynamic decoupled differential equation, after defining $\overline{g}_i(t)$, is just locally feasible in time domain (the time domain local in a mathematical sense, that is, an infinitely small time period at certain moment following closely). It means that $\overline{g}_i(t)$ should be continuous in the time domain if the dynamic decoupled differential equation could meet the local feasibility in the time domain sense.

8.3.3.5 Formulation of norm reduction control criterion

The origin of observation decoupled state space is the steady equilibrium point of the system. If the maximum deviation of the observation decoupled state variable $\left\{\overline{\delta}_i, \dot{\overline{\delta}}_i\right\}$ of the system after the fault is monotonously decreasing with the time t against the origin $\{0, 0\}$, then the system will finally return to the steady equilibrium state.

Based on this consideration, a norm $\overline{V}$ similar to Lyapunov function (such as a Euclidean norm) is introduced to measure the deviation of the observation decoupled state starting from the steady equilibrium point. Let

$$\begin{cases} \overline{V} = \overline{V}\left(\overline{\delta}, \dot{\overline{\delta}}\right) = \sum \overline{V}_i = \sum \frac{1}{2}\left(\overline{\delta}_i^2 + \dot{\overline{\delta}}_i^2\right) > 0 \\ \overline{V}(0,0) = 0 \end{cases} \tag{8.29}$$

Because $\overline{V}$ is positive definite, the condition for $\overline{V}$ monotonous decreasing is the first-order derivative against the time t is less than 0, that is, it is required that:

$$\dot{\overline{V}} = \sum \dot{\overline{V}}_i = \sum \left(\overline{\delta}_i \dot{\overline{\delta}}_i + \dot{\overline{\delta}}_i \ddot{\overline{\delta}}_i\right) \le 0 \tag{8.30}$$

When $t \in [0, +\infty)$, it is always true.

In Eq. (8.30), if $\dot{\overline{V}}_i$ in each local part is smaller than 0, then Eq. (8.30) is self-evidently true, which is also the sufficient condition for $\overline{V}$ monotonous decrease:

$$\dot{\overline{V}}_i = \overline{\delta}_i \dot{\overline{\delta}}_i + \dot{\overline{\delta}}_i \ddot{\overline{\delta}}_i \le 0 \quad (i \in [1, N]) \tag{8.31}$$

To ensure $\dot{\overline{V}}$ is monotonous decreasing, it is obvious to seek help from control variable u_i, by which the condition to be satisfied by u_i must be found.

When substituting Eq. (8.27) into Eq. (8.31), then:

$$\overline{\delta}_i \dot{\overline{\delta}}_i + \dot{\overline{\delta}}_i \frac{1}{J_i}\left\{P_{\mathrm{m}i} - \frac{E_i'}{X_{\mathrm{d}i}'}\left(\overline{U}_i + U_{ei}\right)\sin\left[\overline{\delta}_i + \delta_{\mathrm{e}i} - \left(\overline{\alpha}_i + \alpha_{\mathrm{e}i}\right)\right] - P_{\mathrm{D}i}\left(\dot{\overline{\delta}}_i + \delta_{\mathrm{e}i}\right) - u_i\right\} - \dot{\overline{\delta}}_i \ddot{\delta}_{\mathrm{e}i} \le 0 \tag{8.32}$$

Multiply the two sides of Eq. (8.32) by J_i, after sorting and moving items, and obtain:

$$\dot{\overline{\delta}}_i u_i \ge J_i \overline{\delta}_i \dot{\overline{\delta}}_i + \dot{\overline{\delta}}_i \left\{P_{\mathrm{m}i} - \frac{E_i'}{X_{\mathrm{d}i}'}\left(\overline{U}_i + U_{ei}\right)\sin\left[\overline{\delta}_i + \delta_{\mathrm{e}i} - \left(\overline{\alpha}_i + \alpha_{\mathrm{e}i}\right)\right] - P_{\mathrm{D}i}\left(\dot{\overline{\delta}}_i + \delta_{\mathrm{e}i}\right) - J_i \ddot{\delta}_{\mathrm{e}i}\right\} \tag{8.33}$$

Three scenarios are discussed here:

(1) When $\dot{\overline{\delta}}_i = 0$, u_i does not exist in a mathematical sense. That is, $u_i = 0$, no control, which is consistent with the actual situation of the power system.
(2) When $\dot{\overline{\delta}}_i > 0$, divide both sides of Eq. (8.33) by $\dot{\overline{\delta}}_i$, and derive:

$$u_i \geq J_i\overline{\delta}_i + P_{\mathrm{m}i} - \frac{E'_i}{X'_{\mathrm{d}i}}\left(\overline{U}_i + U_{\mathrm{e}i}\right)\sin\left[\overline{\delta}_i + \delta_{\mathrm{e}i} - \left(\overline{\alpha}_i + \alpha_{\mathrm{e}i}\right)\right] - P_{\mathrm{D}i}\left(\dot{\overline{\delta}}_i + \dot{\delta}_{\mathrm{e}i}\right) - J_i\ddot{\delta}_{\mathrm{e}i} \tag{8.34}$$

(3) When $\dot{\overline{\delta}}_i < 0$, divide both sides of Eq. (8.33) with $\dot{\overline{\delta}}_i$, and derive:

$$u_i \leq J_i\overline{\delta}_i + P_{\mathrm{m}i} - \frac{E'_i}{X'_{\mathrm{d}i}}\left(\overline{U}_i + U_{\mathrm{e}i}\right)\sin\left[\overline{\delta}_i + \delta_{\mathrm{e}i} - \left(\overline{\alpha}_i + \alpha_{\mathrm{e}i}\right)\right] - P_{\mathrm{D}i}\left(\dot{\overline{\delta}}_i + \dot{\delta}_{\mathrm{e}i}\right) - J_i\ddot{\delta}_{\mathrm{e}i} \tag{8.35}$$

For the sake of convenience, rewrite Eqs. (8.34), (8.35) into the following equivalents:

$$\begin{cases} u_i \geq J_i\overline{\delta}_i + P_{\mathrm{m}i} - \dfrac{E'_i U_i}{X'_{\mathrm{d}i}}\sin\left(\delta_i - \alpha_i\right) - P_{\mathrm{D}i}(\omega_i - \omega_0) - J_i\ddot{\delta}_{\mathrm{e}i}, & \dot{\overline{\delta}}_i > 0 \\ u_i \leq J_i\overline{\delta}_i + P_{\mathrm{m}i} - \dfrac{E'_i U_i}{X'_{\mathrm{d}i}}\sin\left(\delta_i - \alpha_i\right) - P_{\mathrm{D}i}(\omega_i - \omega_0) - J_i\ddot{\delta}_{\mathrm{e}i}, & \dot{\overline{\delta}}_i \end{cases} < 0 \tag{8.36}$$

When the control power u_i satisfies Eq. (8.36), it is obvious that the norm $\dot{\overline{V}}_i$ will monotonously decrease. Therefore, the system stability could be restored through satisfying Eq. (8.36) showing control power u_i. Eq. (8.36) shows that u_i is time-varying. However, u_i in the actual system normally joins in a discrete stage-wise manner, which is caused by the specific device itself for the stability measures. In addition, in line with the difference of symbols for $\dot{\overline{\delta}}_i$, the control mode of u_i should proceed from increasing or decreasing the electromagnetic power (such as imposing brake and shedding load).

Eq. (8.36) is the norm reduction control criterion to be followed by the local control power u_i during the second control period.

8.3.3.6 Formulation of norm reduction control criterion in other observation decoupled state space

(1) The form of the norm reduction control criterion in the space $\left\{\overline{\delta}, \dot{\overline{\delta}}(50)\right\}$. Let

$$W_{1i} = \overline{\delta}_i = \delta_i - \delta_{\mathrm{e}i}, \quad W_{2i} = \dot{\delta}(50)_i = \omega_i - \omega_0, \quad \overline{U}_i = U_i - U_{\mathrm{e}i}, \quad \overline{\alpha}_i = \alpha_i - \alpha_{\mathrm{e}i} \tag{8.37}$$

Then the dynamic equation follows the following form in the space $\left\{\overline{\delta}, \dot{\overline{\delta}}(50)\right\}$:

$$\begin{cases} \dot{W}_{1i} = \dot{\overline{\delta}}_i = W_{2i} - \dot{\delta}_{\mathrm{e}i} \\ \dot{W}_{2i} = \ddot{\delta}(50)_i = \dfrac{1}{J_i}\left\{P_{\mathrm{m}i} - \dfrac{E'_i}{X'_{\mathrm{d}i}}\left(\overline{U}_i + U_{\mathrm{e}i}\right)\sin\left[W_{\mathrm{L}i} + \delta_{\mathrm{e}i} - \left(\overline{\alpha}_i + \alpha_{\mathrm{e}i}\right)\right] - P_{\mathrm{D}i}W_{2i} - u_i\right\} \end{cases} \quad (i \in [1, N]) \tag{8.38}$$

Define the norm as:

$$\begin{cases} \overline{V} = \overline{V}\left[\overline{\delta}, \dot{\delta}(50)\right] = \sum \overline{V}_i = \sum \dfrac{1}{2}\left(\overline{\delta}_i^2 + \dot{\delta}_{(50)_i}^2\right) > 0 \\ \overline{V}(0, 0) = 0 \end{cases} \tag{8.39}$$

The first derivative of time t for $\overline{V}$ is required to be less than zero:

$$\dot{\overline{V}}=\sum\dot{\overline{V}}_i=\sum\left[\overline{\delta}_i\dot{\overline{\delta}}_i+\dot{\delta}(50)_i\ddot{\delta}(50)_i\right]\le 0 \tag{8.40}$$

The sufficient condition for $\overline{V}$ monotonous decreasing is that each component $\dot{\overline{V}}_i$ of $\dot{\overline{V}}$ should be less than 0, that is:

$$\dot{\overline{V}}_i=\left[\overline{\delta}_i\dot{\overline{\delta}}_i+\dot{\delta}(50)_i\ddot{\delta}(50)_i\right]\le 0 \tag{8.41}$$

Substitute Eq. (8.38) into Eq. (8.41); the forms of the norm reduction control criterion in the space $\left\{\overline{\delta},\overline{\delta}(50)\right\}$ could be derived as follows after sorting and moving, etc.:

$$\begin{cases} u_i\ge\dfrac{J_i\overline{\delta}_i\dot{\overline{\delta}}_i}{\dot{\delta}(50)_i}+P_{\mathrm{m}i}-\dfrac{E_i'U_i}{X_{\mathrm{d}i}'}\sin(\delta_i-\alpha_i)-P_{\mathrm{D}i}\dot{\delta}(50)_i & \left(\dot{\delta}(50)_i>0\right) \\ u_i\le\dfrac{J_i\overline{\delta}_i\dot{\overline{\delta}}_i}{\dot{\delta}(50)_i}+P_{\mathrm{m}i}-\dfrac{E_i'U_i}{X_{\mathrm{d}i}'}\sin(\delta_i-\alpha_i)-P_{\mathrm{D}i}\dot{\delta}(50)_i & \left(\dot{\delta}(50)_i>0\right) \end{cases} \tag{8.42}$$

(2) The form of the norm reduction control criterion in the space $\left\{\overline{\delta},\overline{\delta}_{\mathrm{s}}\right\}$. Let

$$W_{1i}=\overline{\delta}=\delta_i-\delta_{\mathrm{e}i},\quad W_{2i}=\dot{\delta}_{\mathrm{s}i}=\omega_i-\omega_{\mathrm{s}},\quad \overline{U}_i=U_i-U_{\mathrm{e}i},\quad \overline{\alpha}_i=\alpha_i-\alpha_{\mathrm{e}i} \tag{8.43}$$

where

$$\omega_{\mathrm{s}}=\frac{\sum J_j\omega_j}{\sum J_j}$$

Then the dynamic equation in the space $\left\{\overline{\delta},\overline{\delta}_{\mathrm{s}}\right\}$ is of the following form:

$$\begin{cases} \dot{W}_{1i}=\dot{\overline{\delta}}_i=W_{2i}-\dot{\delta}_{\mathrm{e}i}-\omega_0+\omega_{\mathrm{s}} \\ \dot{W}_{2i}=\ddot{\delta}_{\mathrm{s}i}=\dfrac{1}{J_i}\left\{P_{\mathrm{m}i}-\dfrac{E_i'}{X_{\mathrm{d}i}'}\left(\overline{U}_i+U_{\mathrm{e}i}\right)\sin\left[W_{\mathrm{L}i}+\delta_{\mathrm{e}i}-\left(\overline{\alpha}_i+\alpha_{\mathrm{e}i}\right)\right]-P_{\mathrm{D}i}\left(W_{2i}-\omega_0+\omega_{\mathrm{s}}\right)\right\} \\ -\dot{\omega}_{\mathrm{s}}\quad (i\in[1,N]) \end{cases} \tag{8.44}$$

Define the norm as:

$$\overline{V}=\sum\overline{V}_i=\sum\frac{1}{2}\left(\overline{\delta}_i^2+\dot{\delta}_{\mathrm{s}i}^2\right) \tag{8.45}$$

The first derivative of time t for $\overline{V}$ is required to be less than zero:

$$\dot{\overline{V}}=\sum\dot{\overline{V}}=\sum\left(\overline{\delta}_i\dot{\overline{\delta}}_i+\dot{\delta}_{\mathrm{s}i}\ddot{\delta}_{\mathrm{s}i}\right)\le 0 \tag{8.46}$$

The sufficient condition for $\overline{V}$ monotonous decreasing is that each component $\dot{\overline{V}}_i$ of $\dot{\overline{V}}$ should be less than 0, that is:

$$\overline{V}_i = \left(\overline{\delta}_i \dot{\overline{\delta}}_i + \dot{\delta}_{si} \ddot{\delta}_{si}\right) \leq 0 \quad (i \in [1, N]) \tag{8.47}$$

Substitute Eq. (8.44) into Eq. (8.47); the form of the norm reduction control criterion in the space $\left\{\overline{\delta}, \overline{\delta}_s\right\}$ could be derived as follows after sorting and moving:

$$\begin{cases} u_i \geq \dfrac{J_i \overline{\delta}_i \dot{\overline{\delta}}_i}{\dot{\delta}_{si}} + P_{mi} - \dfrac{E_i' U_i}{X_{di}'} \sin(\delta_i - \alpha_i) - P_{Di}\left(\dot{\delta}_{si} - \omega_0 + \omega_s\right) - J_i \dot{\omega}_s & \left(\dot{\delta}_{si} > 0\right) \\ u_i \leq \dfrac{J_i \overline{\delta}_i \dot{\overline{\delta}}_i}{\dot{\delta}_{si}} + P_{mi} - \dfrac{E_i' U_i}{X_{di}'} \sin(\delta_i - \alpha_i) - P_{Di}\left(\dot{\delta}_{si} - \omega_0 + \omega_s\right) - J_i \dot{\omega}_s & \left(\dot{\delta}_{si} < 0\right) \end{cases} \tag{8.48}$$

8.4 Formulation and Proof of the First Stage Control Criterion (Energy Equilibrium)

The first stage control criterion (energy equilibrium) determines the excess kinetic energy accumulated in the unit i during the fault period ($t_0 \leq t \leq t_p$) and the energy absorbed during the brake period ($t_p \leq t \leq t_1$). These two transient energies could be described as the online time integral for the power difference, and its normal form could be written as:

$$\Delta W_i = \int_t^{t+\Delta t} [P_{mi} - P_{Ei}(t)] \mathrm{d}t, \quad \Delta t > 0 \quad (i \in [1, N]) \tag{8.49}$$

where:

Δt refers to the time interval during the fault or brake period.
P_{mi} refers to the generator net input power.
$P_{Ei}(t)$ refers to the generator electromagnetic power.

In addition, as known from the theoretical mechanics, the transient energy during the said time period could be written as the form:

$$\Delta W_i = \frac{1}{2} J_i \omega_i^2(t + \Delta t) - \frac{1}{2} J_i \omega_i^2(t) \quad (i \in [1, N]) \tag{8.50}$$

where J_i refers to the rotational inertia for generator i. ω_i refers to the generator speed.

In the actual power system operation or simulation stability calculation, ω_i for each system local part could be measured or calculated directly. Therefore, it is simpler to calculate the transient energy by Eq. (8.50) than by the online time integral of the

power difference. It is self-evident that Eqs. (8.49), (8.50) are equivalent, though different in form, that is:

$$\int_t^{t+\Delta t}[P_{\mathrm{m}i}-P_{\mathrm{E}i}(t)]\mathrm{d}t=\frac{1}{2}J_i\omega_i^2(t+\Delta t)-\frac{1}{2}J_j\omega_i^2(t) \tag{8.51}$$

A proof of the establishment of Eq. (8.51) is given to further elucidate the relationship between the two different expressions of transient energy.

Proof
As

$$J_i\ddot{\delta}_i=\frac{P_{\mathrm{m}i}-P_{\mathrm{E}i}}{\omega_i}$$
$$\dot{\delta}_i=\omega_i-\omega_0$$

so

$$\begin{aligned}
&\int_t^{t+\Delta t}(P_{\mathrm{m}i}-P_{Ei})\mathrm{d}t\\
&=\int_t^{t+\Delta t}\left(\frac{P_{\mathrm{m}i}-P_{\mathrm{E}i}}{\omega_i}\right)\omega_i\mathrm{d}t\\
&=\int_t^{t+\Delta t}J_i\ddot{\delta}_i\left(\dot{\delta}_i+\omega_0\right)\mathrm{d}t\\
&=\int_t^{t+\Delta t}J_i\left(\dot{\delta}_i+\omega_0\right)\mathrm{d}\dot{\delta}_i\\
&=\left[\frac{1}{2}J_i\dot{\delta}_i^2+J_i\omega_0\dot{\delta}_i\right]_t^{t+\Delta t}\\
&=\left[\frac{1}{2}J_i(\omega_i-\omega_0)^2+J_i(\omega_i-\omega_0)\dot{\delta}_i\right]_t^{t+\Delta t}\\
&=J_i\left[(\omega_i-\omega_0)^2\left(\frac{1}{2}\omega_i-\frac{1}{2}\omega_0+\omega_0\right)\right]_t^{t+\Delta t}\\
&=\frac{1}{2}J_i\left[\omega_i^2-\omega_0^2\right]_t^{t+\Delta t}\\
&=\frac{1}{2}J_i\omega_i^2[t+\Delta t]-\frac{1}{2}J_i\omega_i^2(t)
\end{aligned}$$

□

Using Eq. (8.50), excess kinetic energy of the unit i during the fault period and the absorbed energy during the brake period as well as the energy control criterion at the first stage could be represented as follows:

(1) The excess kinetic energy of unit i during the fault period:

$$\Delta W_i=\frac{1}{2}J_i\omega_i^2\left(t_{\mathrm{p}}\right)-\frac{1}{2}J_i\omega_i^2(t_0) \tag{8.52}$$

As the system is still in a steady-state during t_0, then:

$$\omega_i(t_0) = \omega_0 \tag{8.53}$$

Therefore, Eq. (8.52) could be also written as:

$$\Delta W_i(t_p) = \frac{1}{2}J_i\omega_i^2(t_p) - \frac{1}{2}J_i\omega_0^2 \tag{8.54}$$

(2) Absorbed energy during the brake:

$$\Delta W_{bi}(t_1) = \frac{1}{2}J_i\omega_i^2(t_i) - \frac{1}{2}J_i\omega_i^2(t_p) \tag{8.55}$$

(3) Energy equilibrium control criterion at the first stage:

$$\begin{aligned}\Delta W_i + \Delta W_{bi} &= \frac{1}{2}J_i\omega_i^2(t_p) - \frac{1}{2}J_i\omega_0^2 + \frac{1}{2}J_i\omega_i^2(t_1) - \frac{1}{2}J_i\omega_i^2(t_p) \\ &= \frac{1}{2}J_i\omega_i^2(t_1) - \frac{1}{2}J_i\omega_0^2 = 0\end{aligned} \tag{8.56}$$

8.5 Formulation and Proof of the Second Stage Control Criterion (Norm Reduction)

Section 8.5.1 describes the mathematical model of the critical power control for the second stage control criterion; Section 8.5.2 gives the mathematic proof of the topological properties of the observation decoupled state space; Section 8.5.3 shows the topological equivalence proof of the observation decoupled state space and the original state space; Section 8.5.4 provides that the origin of the observation decoupled state space is the only equilibrium point of the power system; and Section 8.5.5 gives sufficient conditions for the norm reduction criterion.

8.5.1 Mathematical Model of the Observation Decoupled State Space

The second stage norm reduction control criterion followed by the local on-line stability control is derived on the basis of introducing the observation decoupled state space. Whether the derived norm reduction control criterion is reasonable and feasible can be determined only by sufficiently explaining and studying the relations between the observation decoupled state space and original system state space.

Therefore, to facilitate the discussion, it is required to first show the structure of the power system mathematical model, present its general form in the original system state space, and then

derive the general form of the mathematical model in the observation decoupled state space according to the definition.

(1) Structure of mathematical model for the power system.

(a) State variable:

$$Z_i = \begin{bmatrix} \chi_i \\ \xi \end{bmatrix} = \begin{bmatrix} \delta_i \\ \omega_i \end{bmatrix} = \begin{bmatrix} \text{Connected state variable} \\ \text{nonconnected state variable} \end{bmatrix}$$

(b) Coupled variable:

$$\varphi_i = \begin{bmatrix} U_i \\ \alpha_i \end{bmatrix}$$

(c) Input variable:

$$r_i = \begin{bmatrix} P_{\mathrm{m}i} \\ E_i' \\ P_{\mathrm{L}i} \\ Q_{\mathrm{L}i} \\ U_j \\ \alpha_j \end{bmatrix}$$

(d) Control variable:

$$u_i$$

The previous classification is derived based on the power system simplified model. When considering a more detailed model (Park equation and exciter equation, etc.), it will only enlarge the nonconnected state variable ξ_i rather than introducing new theoretical matter.

(2) The generalized formulation of the mathematical model.

The system dynamic equation could be written as:

$$\dot{Z}_i = f_i(\chi_i, \xi_i, \varphi_i, r_i, u_i, t) \quad (i \in [1, N]) \tag{8.57}$$

The system coupled equation could be written as:

$$\sum_{j=1}^{N} C_{ij} f_{ij}\left(\chi_i, \varphi_i, \chi_j, \varphi_j, r_i, u_i, t\right) = 0 \quad (i \in [1, N]) \tag{8.58}$$

where

$$Z_i, f_i \in R^{n_i}, \quad f_{ij}, \varphi_i \in R^{k_i}, \quad r_i \in R^{P_i}, \quad u_i \in R^{m_i} \quad (P_i, m_i \le n_i)$$

And f_{ij} is continuously differentiable.

In normal operation, the system is in equilibrium state, the system static solution (system power flow) $Z_{0i}=\{\chi_{0i}, \xi_{0i}\}$ is implicitly defined in the following equations:

$$f_i(\chi_{0i}, \xi_{0i}, \varphi_{0i}, r_i, 0, t)=0 \quad (i\in[1,N]) \tag{8.59}$$

$$\sum_{i=1}^{N} C_{ij} f_{ij}\left(\chi_{0i}, \varphi_{0i}, \chi_{0j}, \varphi_{0j}, r_i, 0, t\right)=0 \quad (i\in[1,N]) \tag{8.60}$$

Before the system failure, it is assumed that there is a unique steady point $\{Z_{0i}\}\in\Omega_0$, and there is an equation for any time t as follows:

$$\{r_i\}\neq 0, \quad \{Z_{0i}\}\neq 0 \tag{8.61}$$

The previously assumed arguments are self-evident for any actual system in a normal operation state. For instance, if $\{r_i\}=0$, then it indicates that there is no power flow in the system, that is, the system is not in operation.

(3) Existence condition for decoupled criterion (local equilibrium criterion).

In line with the power equilibrium state assumption, if the equilibrium coordinate $\{\chi_{0j}, \varphi_{0j}\}$ for the adjacent bus $j(C_{ij}=1)$ of the generator bus i is known and capable of being arbitrarily replaced with the actual transient value during the online calculation, then Eqs. (8.57), (8.58) become the decoupled equations follows:

$$f_i(\chi_{ei}, \xi_{ei}, \varphi_{ei}, r_i, u_i, t)=0, \quad \forall t>0 \quad (i\in[1,N]) \tag{8.62}$$

$$\sum_{j=1}^{N} C_{ij} f_{ij}\left(\chi_{ei}, \varphi_{ei}, \chi_j, \varphi_j, r_i, u_i, t\right)=0 \quad (i\in[1,N]) \tag{8.63}$$

In Eqs. (8.62), (8.63), the control variable u_i is equal to 0 when there is no control. The decoupled reference $Z_{ei}(t)=\{\chi_{ei}, \xi_{ei}\}$ is implicitly defined as the only stability solution for Eqs. (8.62), (8.63) within the given scope. In addition, although Z_{ei} is formally designed as the equilibrium reference at bus i, as a matter of fact, $\{Z_{ei}\}$ is just the transient virtual variable defined in a mathematical sense without any actual physical significance.

(4) The generalized form of mathematical model in observation decoupled state space.

Based on the existence of the decoupled reference, the observation decoupled state vector $W_i=\{Y_i, \eta_i\}$ is defined as:

$$W_i=Z_i-Z_{ei}, \quad Y_i=X_i-X_{ei}, \quad \eta_i=\xi_i-\xi_{ei}, \quad \psi_i=\varphi_i-\varphi_{ei} \tag{8.64}$$

Substitute Eq. (8.64) into Eqs. (8.62), (8.63), then:

$$G_i=f_i(X_i-Y_i, \ \xi_i-\eta_i, \ \varphi_i-\psi_i, \ r_i, u_i, t)=0 \quad (i\in[1,N]) \tag{8.65}$$

$$G_{PQi} = \sum_{i=1}^{N} C_{ij} f_{ij}\left(X_i - Y_i, \varphi_i - \psi_i, X_j, \varphi_j, r_i, u_i, t\right) = 0 \quad (i \in [1, N]) \tag{8.66}$$

The previous nonlinear algebraic equations implicitly define a mapping from the original state space of the system to the observation decoupled state space.

$$F : Z \to W \tag{8.67}$$

The existence of the mapping F, that is, whether the original state space of the system can enter the decoupled state space, lies in whether or not the χ_i, ξ_i of the local subsystem and the χ_j, φ_j of the neighboring nodes j ($C_{ij} = 1$) can be measured or calculated at node i of the local subsystem. If this condition can be met, then in a given range, W space is indeed observed decoupling, which can always be achieved for the power system under consideration.

The major mathematical theoretical basis for discussing the second stage local online stability control mainly consists of the following aspects:

(1) The observation decoupled state space is topologically equivalent to the original state space of the system on a suitable convex region.
(2) Although the form of the observation decoupled state space is not the unique, the optional observation decoupled state spaces are topologically equivalent to the original state space of the system.
(3) The origin of the observation decoupled state space is the only stability equilibrium point for the power system.
(4) The control based on the norm reduction control criterion will reach the only stability equilibrium point along the given trajectory guidance system, that is, the origin of the observation decoupled state space.

These aspects together constitute an integral mathematical structure, which will be the theoretical foundation for the norm reduction control criterion at the second stage.

8.5.2 Proof of Topology Equivalence Between Observation Decoupled State Space and Original System State Space

8.5.2.1 Simplification of the network

The dynamic operation of the power system mainly relies on the relative angle between the generators to judge whether the system is in stable operation. Therefore, to simplify the discussion, a simplification approximation is introduced, that is, the load is transferred to the generator within the interior points. Such a load transformation makes all generator buses involved into purely passive buses, hence the network itself is purely passive. This kind of passive network could be easily simplified into an equivalent network with all buses acting as the electrodynamic potential $E_i' < \delta_i$ points within the generators through the standard network simplification method (such as star network); its structure is shown in Fig. 8.4.

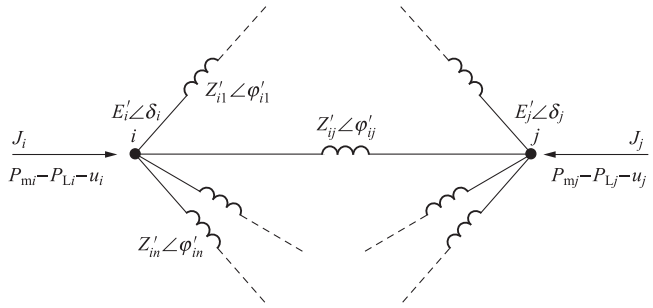

Fig. 8.4
A part of power system equivalent to the simplified network model.

Obviously, such a simplified network will only have a generator bus, and its network association matrix is fairly sparse in contrast with the presimplified matrix. This network model related to the generator angle is referred to as the generator angle model. The basic power equilibrium equation will be in the following form:

$$\left.\begin{aligned}&\frac{\mathrm{d}\delta_i}{\mathrm{d}t}=\omega_i-\omega_0\quad(i\in[1,n])\\&\frac{\mathrm{d}\omega_i}{\mathrm{d}t}=\frac{1}{J_i}\left[P_{\mathrm{m}i}-P_{\mathrm{L}i}-\sum_{j=1}^{N}C_{ij}'\frac{E'^2{}_i}{Z_{ij}'}-\sum_{j=1}^{n}C_{ij}'\frac{E_i'E_j'}{Z_{ij}'}\sin\left(\delta_i-\delta_j+\varphi_{ij}'-90^\circ\right)-P_{\mathrm{D}i}(\omega_i-\omega_0)-u_i\right]\quad(i\in[1,n])\end{aligned}\right\}\tag{8.68}$$

$$C_{ij}'=\begin{cases}0 & (i=j)\\ 1 & (i\neq j)\end{cases}\tag{8.69}$$

where n is the number of generator buses, and $n\leq N$; $Z_{ij}'\angle\varphi_{ij}'$ is the line impedance after the network simplification.

If the line resistance is ignored, then $Z_{ij}'=jX_{ij}$, $\varphi_{ij}=90°$, and Eqs. (8.68), (8.69) can be further simplified as below:

$$\frac{\mathrm{d}\delta_i}{\mathrm{d}t}=\omega_i-\omega_0\quad(i\in[1,n])\tag{8.70}$$

$$\frac{\mathrm{d}\omega_i}{\mathrm{d}t}=\frac{1}{J_i}\left[P_{\mathrm{m}i}-P_{\mathrm{L}i}-\sum_{j=1}^{n}C_{ij}'\frac{E_i'E_j'}{X_{ij}}\sin\left(\delta_i-\delta_j\right)-P_{\mathrm{D}i}(\omega_i-\omega_0)-u_i\right]\quad(i\in[1,n])\tag{8.71}$$

Prior to the network simplification, the system mathematical model could be expressed with simultaneous dynamic equation and decoupled equation. After simplifying the network, the system mathematical model could be uniformly expressed by Eqs. (8.68)–(8.71), which offer great convenience for the discussion. All of the following proofs are based on the network simplification.

8.5.2.2 The unique existence of the decoupled criterion

It is known from the $\overline{\delta}_i$ definition, the observation decoupled state space is derived from the original system state space via the coordinate translation based on the unique existence of the decoupled reference δ_{ei}. Therefore, with reference to the generator angle model, the decoupled reference δ_{ei} and its equivalent $\overline{\delta}_i$ for the observation decoupled state space are defined by the following equations:

$$G_i = P_{mi} - P_{Li} - \sum_{j=1}^{n} C'_{ij} \frac{E'_i E'_j}{X_{ij}} \sin\left(\delta_i - \delta_j - \overline{\delta}_i\right) - u_i = 0 \quad i \in [1, n] \tag{8.72}$$

$$\left|\delta_i - \delta_j - \overline{\delta}_i\right| < \frac{\pi}{2} - \varepsilon, \quad \forall \varepsilon > 0 \tag{8.73}$$

where $\overline{\delta}_i = \delta_i - \delta_{ei}$

Lemma 1 *For a given δ_i and its corresponding E'_j, if the solution δ_{ei} and its equivalent $\overline{\delta}_i$ exist, then such solution is unique for Eq. (8.72) when $\delta_i = \delta_{ei}$, it is locally stable in Lyapunov sense.*

Proof
As

$$\begin{aligned}
&\sum_{j=1}^{n} C'_{ij} \frac{E'_i E'_j}{X_{ij}} \sin\left(\delta_i - \delta_j - \overline{\delta}_i\right) \\
&= \sum_{j=1}^{n} C'_{ij} \frac{E'_i E'_j}{X_{ij}} \sin\left(\delta_{ei} - \delta_j\right) \\
&= \mathrm{Re}\left[\dot{E}'_i \hat{I}_i\right] \\
&= \mathrm{Re}\left(\dot{E}'_i \sum_{j=1}^{n} C'_{ij} \frac{\hat{\dot{E}}'_i \hat{\dot{E}}'_j}{-jX_{ij}}\right) \\
&= \mathrm{Re}\left[\left(E'_{xi} + jE'_{yi}\right) \sum_{j=1}^{n} C'_{ij} \frac{E'_{xi} - jE'_{yi} - E'_{xj} + E'_{yj}}{-jX_{ij}}\right] \\
&= \mathrm{Re}\left[\left(E'_{xi} + jE'_{yi}\right) \sum_{j=1}^{n} C'_{ij} \left(\frac{E'_{yi} - E'_{yj}}{X_{ij}} + j\frac{E'_{xi} - E'_{xj}}{X_{ij}}\right)\right] \\
&= \sum_{j=1}^{n} C'_{ij} \frac{E'_{yi} E'_{xi} - E'_{xi} + E'_{yj}}{X_{ij}} \\
&= E'_{yi} \sum_{j=1}^{n} C'_{ij} \frac{E'_{xj}}{X_{ij}} - E'_{xi} \sum_{j=1}^{n} C'_{ij} \frac{E'_{yj}}{X_{ij}}
\end{aligned}$$

$$= \mathrm{Re}\left[\left(E'_{xi} + jE'_{yi}\right)\sum_{j=1}^{n} C'_{ij}\frac{E'_{xi} - jE'_{yj}}{jX_{ij}}\right]$$

$$= \mathrm{Re}\left[\dot{E}'_i\sum_{j=1}^{n} C'_{ij}\frac{\hat{\dot{E}}}{jX_{ij}}\right] \tag{8.74}$$

Let

$$I_{i0} = \left|\sum_{j=1}^{n} C'_{ij}\frac{\dot{E}'_j}{jX_{ij}}\right|, \quad \delta_{i0} = \angle\sum_{j=1}^{n} C'_{ij}\frac{\dot{E}'}{X_{ij}} \tag{8.75}$$

Then Eq. (8.72) could be written into:

$$G_i = P_{\mathrm{m}i} - P_{\mathrm{L}i} - u_i - E'_i I_{i0}\sin\left(\delta_{\mathrm{e}i} - \delta_{i0}\right) = 0 \tag{8.76}$$

$$\left|\delta_{\mathrm{e}i} - \delta_{i0}\right| < \frac{\pi}{2} - \varepsilon, \quad \forall\varepsilon > 0 \tag{8.77}$$

Take $\frac{\pi}{2} - \varepsilon$ as the upper bound, and substitute it into Eq. (8.76), and then:

$$P_{\mathrm{m}i} - P_{\mathrm{L}i} - E'_i I_{i0}\cos\varepsilon = 0 \tag{8.78}$$

$$\cos\varepsilon = \frac{P_{\mathrm{m}i} - P_{\mathrm{L}i} - u_i}{E'_i I_{io}} \tag{8.79}$$

Obviously, when $E_i{}' I_{i0}\cos\varepsilon > P_{\mathrm{m}i} - P_{\mathrm{L}i} - u_i$, Eq. (8.76) has a unique solution, and then Eq. (8.72) also has a unique solution. In addition, the local stability of Eq. (8.72) could be directly guaranteed by Eq. (8.73). □

Lemma 1 proves the uniqueness of the decoupled reference $\delta_{\mathrm{e}i}$ (or its equivalent $\dot{\bar{\delta}}_i$). Mark the state variable of the original state space and the observation decoupled state space, and define a mapping g based on Lemma 1 to prove the uniqueness of the other coordinate of the observation decoupled state space, that is, the unique existence of $\bar{\delta}_i$.

Let the state variable of the original state space be:

$$Z^{\mathrm{T}} = \left\{\delta^{\mathrm{T}}, \dot{\delta}^{\mathrm{T}}\right\} \tag{8.80}$$

where:

$$\delta = \left\{\delta_i \middle| \delta = \{\delta_i\} \in \Omega_\delta, \quad i \in [1, n]\right\} \in R^{n-1} \tag{8.81}$$

$$\dot{\delta} = \left\{\dot{\delta}_i = \omega_i - \omega_0 \middle| \dot{\delta} = \left\{\dot{\delta}_i\right\} \in R^{n-1}, \quad i \in [1, n]\right\} \tag{8.82}$$

$$\Omega_\delta \doteq \left\{\delta \in R^{n-1} \middle\| \delta_i - \delta_j\right| < \pi, C'_{ij} = 1\right\} \subset R^{n-1} \tag{8.83}$$

Thus:

$$Z \in \Omega_\delta \times R^{n-1} \tag{8.84}$$

Let the state variable of the observation decoupled state space be:

$$W^{\mathrm{T}} = \left\{ \overline{\delta}^{\mathrm{T}}, \dot{\overline{\delta}}^{\mathrm{T}} \right\} \tag{8.85}$$

where:

$$\begin{aligned} \overline{\delta} &= \left\{ \overline{\delta}_i = \delta_i - \delta_{ei} \middle| \, \overline{\delta} = \left\{ \overline{\delta}_i \right\} \in \Omega\overline{\delta}, \quad i \in [1, n] \right\} \in R^{n-1} \\ \dot{\overline{\delta}} &= \left\{ \dot{\overline{\delta}}_i = \dot{\delta}_i - \dot{\delta}_{ei} \middle| \, \dot{\overline{\delta}} = \left\{ \dot{\overline{\delta}}_i \right\} \in R^{n-1}, \quad i \in [1, n] \right\} \end{aligned} \tag{8.86}$$

$$\Omega_{\overline{\delta}} = \left\{ \overline{\delta} \in R^{n-1} \middle| \, \forall \delta \in \Omega_\delta, \exists \overline{\delta} \in R^{n-1}, G\left(\delta, \overline{\delta}\right) = 0 \right\} \subset R^{n-1} \tag{8.87}$$

$$G\left(\delta, \overline{\delta}\right) = [G_1, \ldots, G_{n-1}]^{\mathrm{T}} \tag{8.88}$$

Thus:

$$W \in \Omega_{\overline{\delta}} \times R^{n-1} \tag{8.89}$$

Definition Each $\delta \in \Omega_\delta$ corresponds to a $g(\delta)$, when satisfying $G[\delta, g(\delta)] = 0$, the unique existence of g is guaranteed by Lemma 1, and the mapping g is shown as:

$$g : \Omega_\delta \to \Omega_{\overline{\delta}} \subset R^{n-1} \tag{8.90}$$

Lemma 2 *For all* $\delta \in \Omega_\delta$ *and* $\dot{\delta} \in R^{n-1}\left(\dot{\delta} = \omega - \omega_0\right)$, *that is, there exists a unique solution* $\left\{ \overline{\delta}, \dot{\overline{\delta}} \right\}$ *for all* $Z = \left\{ \delta, \dot{\delta} \right\} \in \Omega_\delta \times R^{n-1}$.

Proof For any $\delta \in \Omega_\delta$, the unique existence of $\overline{\delta}$ has been guaranteed by Lemma 1. Now let's prove the unique existence of $\overline{\delta}$. Find the derivation of Eq. (8.72) to the time t, then:

$$H\left(\delta, \dot{\delta}, \overline{\delta}, \dot{\overline{\delta}}\right) = \frac{\partial G\left(\delta, \overline{\delta}\right)}{\partial t} = \frac{\partial}{\partial \delta} G\left(\delta, \overline{\delta}\right) \dot{\delta} + \frac{\partial}{\partial \overline{\delta}} G\left(\delta, \overline{\delta}\right) \dot{\overline{\delta}} = 0 \tag{8.91}$$

where:

$$\begin{aligned} \frac{\partial G\left(\delta, \overline{\delta}\right)}{\partial \overline{\delta}} &= \left[\frac{\partial G_i}{\partial \overline{\delta}_j} \right] \\ \frac{\partial G_i}{\partial \delta_j} &= \begin{cases} 0 & (i \neq j) \\ \displaystyle\sum_{k=1}^{n} C'_{ik} \frac{E'_i E'_k}{X_{ik}} \cos\left(\delta_i - \delta_k - \overline{\delta}_i\right) & (i = j) \end{cases} \end{aligned} \tag{8.92}$$

It can be seen from Eq. (8.92) that $\frac{\partial G(\delta,\overline{\delta})}{\partial\overline{\delta}}$ is a diagonal matrix, thus $\frac{\partial G(\delta,\overline{\delta})}{\partial\overline{\delta}}$ is nonsingular, and then $\dot{\overline{\delta}}$ can be written as:

$$\dot{\overline{\delta}} = -\left[\frac{\partial}{\partial\overline{\delta}}G(\delta,\overline{\delta})\right]^{-1}\left[\frac{\partial}{\partial\delta}G(\delta,\overline{\delta})\right]\dot{\delta} \tag{8.93}$$

In addition, because $\dot{\overline{\delta}} = \dot{\delta} - \dot{\delta}_{\mathrm{e}}$, thus $\dot{\delta}_{\mathrm{e}} = \dot{\overline{\delta}} - \dot{\delta}$, which proves the unique existence of $\dot{\overline{\delta}}$ or $\dot{\overline{\delta}}_{ei}$ for all $\dot{\delta} \in R^{n-1}$. □

Lemma 1 and Lemma 2 prove the unique existence of decoupling criterion $Z_{\mathrm{e}i} = \{\delta_{\mathrm{e}i}, \dot{\delta}_{ei}\}$ within a given scope, which constitutes the foundation for the existence of observation decoupled state space.

8.5.2.3 The topological property of the observation decoupled state space

As for the system after network simplification, the mathematical model has been written as the general form, so that the generator angle model is:

$$\dot{Z}_i = f_i(\delta_i, \dot{\delta}_i, \delta_j, u_i, t) \quad (i \in [1, n]) \tag{8.94}$$

where $f_i \in R^{n_i}$, and $Z_i \in \Omega_{\delta_i} \subset R^{n_i}$ is satisfied.

In the generator angle model, if the balance coordinate $\{E_{0j}', \delta_{0j}\}$ within the time-varying data set $\{E_i', P_{\mathrm{m}i}, P_{\mathrm{L}i}, Q_{\mathrm{L}i}, E_j', \delta_j\}$ is already known and capable of being replaced at will on an online basis, then the decoupled equation can be rewritten from Eq. (8.94) as follows:

$$f_i(\delta_{ei}, \dot{\delta}_{ei}, \delta_j, u_i, t) = 0 \quad (i \in [1, n]) \tag{8.95}$$

In Eq. (8.95), when there is no control $u_i = 0$, which have been readily proven by Lemma 1 and Lemma 2. Within the scope of $|\delta_{ei} - \delta_j| < \frac{\pi}{2} - \varepsilon$, the unique stability solution $Z_{ei} = \{\delta_{\mathrm{e}i}, \dot{\delta}_{\mathrm{e}i}\}$ can be obtained, where $Z_{\mathrm{e}i}$ is the real time decoupled reference for the observation decoupled state space. Let:

$$\begin{cases} \overline{\delta}_i = \delta_i - \delta_{\mathrm{e}i} \\ \dot{\overline{\delta}}_i = \dot{\delta}_i - \dot{\delta}_{\mathrm{e}i} \end{cases} \tag{8.96}$$

Substitute Eq. (8.96) into Eq. (8.95), then:

$$G_i = f_i(\delta_i - \overline{\delta}_i, \dot{\delta}_i - \overline{\delta}_i, u_i, t) \quad (i \in [1, n]) \tag{8.97}$$

Eq. (8.97) is a nonlinear algebraic equation, which implicitly defines mapping from the original state space to the observation decoupled state space:

$$F : Z \to W \tag{8.98}$$

In the original state space, the time-varying curve set of the state variable $\{\delta, \dot{\delta}\}$ depicts the change law of the system dynamic characteristics. Based on the unique existence of decoupled reference Z_{ei}, it is possible to enter the observation decoupled state space from the original state space via

the coordinate translation. As a result of the time-varying characteristic of the decoupled reference Z_{ei}, such a coordinate translation is nonlinear. The observation decoupled state variable $\left\{\delta, \dot{\overline{\delta}}\right\}$ derived through the nonlinear coordinate translation is almost different everywhere from the original state variable $\{\delta, \dot{\delta}\}$. However, the time-varying curve change law of $\left\{\overline{\delta}, \dot{\overline{\delta}}\right\}$ should retain the system intrinsic dynamic characteristic reflected at the original state space. Thus, when the original state space is in a steady equilibrium state, the observation decoupled state space corresponding to it is also in steady equilibrium state. And conversely, when the coordinate of the original state space deviates from the steady equilibrium position due to disturbance, the coordinate of the observation decoupled state space also deviates from the steady equilibrium position. That is, for both state spaces with different topological structures, it is required that their effectiveness in determining the limit point in their respective region should be absolutely the same. In this way, it makes sense to observe the system dynamic characteristic through the observation decoupled state space.

The previously discussed requirements indicate that the introduced observation decoupled state space should be the same as the original system state space in nature, that is, the observation decoupled state space and the original system state space should be topologically equivalent.

It is seen that the communication between the observation decoupled state space and original state space is realized through mapping F, then what requirements should F satisfy to ensure the observation decoupled state space topologically equivalent to the original system state space, that is, both spaces are the same in nature?

First, it is required that mapping F should be filled single mapping, that is, F should send the different points in Z to different points in W, and all the points in W should have a preimage in Z. The one-to-one mapping is also called filled single mapping in short. Because F is required to be filled single mapping, the relations between the observation decoupled state space and original state space communicated by F could be recorded as $F(Z)=W$.

Second, it is required that mapping F should be continuous. As is known, the trajectories of the original state space coordinates are continuous in the dynamic process, and F is filled single mapping, there exists any basic domain $V_Z \in \Omega_\delta \times R^{n-1}$ for Z, in any point of Z for $\Omega_\delta \times R^{n-1}$, enabling $F(V_Z) \in \Omega_{\overline{\delta}} \times R^{n-1}$. Therefore, it is required that F should be continuous.

In addition, as F should be a filled single mapping, then the inverse mapping F^{-1} for F should exist. And the trajectory for observation decoupled state space coordinate should be continuous in a given area as well. For the image of Z, $F(Z)=W$ for $\Omega_{\overline{\delta}} \times R^{n-1}$, there exists any basic neighborhood $V_W \in \overline{\delta} \times R^{n-1}$ of W, enabling the preimage of V_W $F^{-1}(V_W) \in \Omega_\delta \times R^{n-1}$. Therefore, it is required that the inverse mapping F^{-1} of F should be continuous mapping as well. These requirements on F are summarized as follows:

(1) F is a one-to-one mapping, that is, filled single mapping.
(2) F is a continuous mapping.
(3) The inverse mapping of F F^{-1} exists, and F^{-1} is also a continuous mapping.

It is known from the topologic theory that the mapping satisfied by the previous three requirements is called homeomorphism mapping, whereas homeomorphism relation is just an equivalent relation in the topology, which is of great significance for our discussion as such a problem could be translated into this: as long as F is proven to be a homeomorphic mapping, then the observation decoupled state space can be deemed to be topologically equivalent to the original state space.

Lemma 1 and Lemma 2 are used to prove the unique existence of the real-time decoupled reference. Obviously, the conclusions for Lemma 1 and Lemma 2 are the foundation for the existence of F, and then the mapping F is explicitly defined as follows:

Definition For each $Z \in \Omega_{\delta} \times R^{n-1}$, there is a corresponding $W = F(Z)$, which could satisfy $G\left(\delta, \overline{\delta}\right) = 0$ and $H\left(\delta, \dot{\delta}, \overline{\delta}, \dot{\overline{\delta}}\right) = 0$. The unique existence of F is guaranteed by Lemma 1 and Lemma 2, and mapping F is taken as:

$$F : \Omega_{\delta} \times R^{n-1} \to F\left(\Omega_{\delta} \times R^{n-1}\right) \triangleq \Omega_{\overline{\delta}} \times R^{n-1} \tag{8.99}$$

The following lemmas are also necessary in proving F to be a homeomorphism mapping.

8.5.2.4 Several Necessary Lemmas and Definitions

Lemma 3 *Let $f : \Delta \subset R^n \to R^n$ be continuously differentiable in open convex set Δ, if any point n set $\{x^1\ x^n\} \in \Delta$, then matrix:*

$$\left[f_1'\left(x^1\right), \ldots, f_n'\left(x^n\right)\right]^{\mathrm{T}} \tag{8.100}$$

is invertible, then f is one-to-one mapping, where:

$$f_i'\left(x^i\right) = \left\{\frac{\partial f_i\left(x^i\right)}{\partial x_j^i}\right\}$$

Proof Let $S_1, S_2 \in \Delta$, and $f(S_1) = f(S_2)$, that is, $f_i(S_1^i) = f_i(S_2^i)$ $i \in [1, n]$. Because Δ is an open convex set, it could be derived via differential mean value theorem for each f_i: $\Delta \to R$:

$$f_i\left(S_1^i\right) - f_i\left(S_2^i\right) = f_i'\left(x^i\right)\left(S_1^i - S_2^i\right) \quad \left(x^i \in \Delta, i \in [1, n]\right) \tag{8.101}$$

Substitute the condition of $f(S_1) = f(S_2)$ into Eq. (8.101), then:

$$\begin{bmatrix} 0 \\ \vdots \\ 0 \end{bmatrix} = \left[f_1'\left(x^1\right) \cdots f_n'\left(x^n\right)\right]^{\mathrm{T}} \quad (S_1 - S_2) \tag{8.102}$$

As $[f_1'(x^1) \cdots f_n'(x^n)]^{\mathrm{T}}$ is nonsingular, if Eq. (8.102) is established, then $S_1 = S_2$, such that it is proven that f is one-to-one mapping. □

Lemma 4 *Let $A=[a_{ij}]$ be a $k\times k$ order real matrix, and:*

$$a_{ii}\geq A_i\ (i=1\cdots k) \tag{8.103}$$

Then:

$$0\leq m_1\cdots m_k\leq \det(A)\leq M_1\cdots M_k \tag{8.104}$$

where:

$$A_i=\sum_{\substack{j=1\\ j\neq i}}^{k}\left|a_{ij}\right| \tag{8.105}$$

$$m_i=|a_{ii}|-\sum_{j=i+1}^{k}\left|a_{ij}\right|\geq 0 \tag{8.106}$$

$$M_i=|a_{ii}|+\sum_{j=i+1}^{k}\left|a_{ij}\right| \tag{8.107}$$

Proof Let:

$$\det(A)=\begin{vmatrix} a_{11} & \cdots & a_{1k}\\ \cdots & \cdots & \cdots\\ a_{k1} & \cdots & a_{kk}\end{vmatrix} \tag{8.108}$$

Define:

$$D_t=\begin{vmatrix} a_{tt} & \cdots & a_{tk}\\ \cdots & \cdots & \cdots\\ a_{kt} & \cdots & a_{kk}\end{vmatrix}\ (t=1,\ldots,k) \tag{8.109}$$

And structure $t-1$ sets of equations:

$$a_{it}+\sum_{\substack{j=t+1\\ j\neq i}}^{k}a_{ij}x_j=0,\ \ t=1\cdots k-1,\ i=t+1,\ldots,k \tag{8.110}$$

As

$$a_{ii}\geq A_i,\ i=1\cdots k \tag{8.111}$$

So $\forall a_{ii}>0,\ \ i=1\cdots k$, each set of equations in Eq. (8.110) will have a unique solution.

$$\left\{x_{t+1}^{(t)}\cdots x_k^{(t)}\right\},t=1\cdots k-1 \tag{8.112}$$

It is known from Cramer rule that:

$$x_j^{(t)} = \frac{\begin{vmatrix} a_{t+1,t+1}, \cdots, a_{t+1,j-1}, -a_{t+1,j+1}, \cdots, a_{t+1,k} \\ \cdots\cdots \\ a_{k,t+1}, \cdots, a_{k,j-1}, -a_{k,t}, a_{k,j+1}, \cdots, a_{k,k} \end{vmatrix}}{\begin{vmatrix} a_{t+1,t+1} & \cdots & a_{t+1,k} \\ \cdots & \cdots & \cdots \\ a_{k,t+1} & \cdots & a_{kk} \end{vmatrix}}$$

$$= \frac{(-1)^{j+1}\begin{vmatrix} a_{t+1,t}, a_{t+1,t+1}\cdots, a_{t+1,j-1}, a_{t+1,j+1}, \cdots, a_{t+1,k} \\ \cdots\cdots \\ a_{k,t}, \cdots, a_{k,t+1}, -a_{k,j-1}a_{k,j+1}, \cdots, a_{k,k} \end{vmatrix}}{\begin{vmatrix} a_{t+1,t+1} & \cdots & a_{t+1,k} \\ \cdots & \cdots & \cdots \\ a_{k,t+1} & \cdots & a_{k,k} \end{vmatrix}}$$

$$= \frac{A_{tj}^{(t)}}{A_{tt}^{(t)}} \quad j = t+1 \cdots k,\ t = 1 \cdots k-1 \tag{8.113}$$

where $\{A_{tt}^{(t)}, A_{t,\,t+1}^{(t)}, \ldots, A_{tk}^{(t)}\}$ is the algebraic complement that unfolded for the row of D_t.

Let:

$$\left|x_i^{(t)}\right| = \max\left\{\left|x_{t+1}^{(t)}\right| \ldots \left|x_k^{(t)}\right|\right\} \quad i \in [t+1, k],\ t = 1 \cdots k-1 \tag{8.114}$$

Then from Eq. (8.110), we can obtain:

$$-a_{ii}x_i^{(t)} = a_{it} + \sum_{\substack{j=t+1 \\ j \neq i}}^{k} a_{ij}x_j^{(t)} \quad i \in [t+1, k],\ t = 1 \cdots k-1 \tag{8.115}$$

Take the absolute value for each item on both sides of Eq. (8.115):

$$|a_{ii}| \cdot \left|x_i^{(t)}\right| \leq |a_{it}| + \sum_{\substack{j=i+1 \\ j \neq 1}}^{k} |a_{ij}| \cdot \left|x_j^{(t)}\right| \tag{8.116}$$

When dividing both sides of Eq. (8.116) by $|x_i^{(t)}|$, then:

$$|a_{ii}| \leq |a_{it}| \cdot \frac{1}{\left|x_i^{(t)}\right|} + \sum_{\substack{j=i+1 \\ j \neq 1}}^{k} |a_{ij}| \cdot \frac{\left|x_j^{(t)}\right|}{\left|x_i^{(t)}\right|} \tag{8.117}$$

It is known from Eq. (8.103) that the matrix $A=[a_{ij}]$ is a diagonally dominance matrix and from Eq. (8.114) that $|x_j^{(t)}|/|x_i^{(t)}|\le 1$. Therefore, if Eq. (8.117) is established, then at least $|x_i^{(t)}|<1$, that is, the solution of Eq. set (8.110) must satisfy the following equation:

$$\max\left\{\left|x_{t+1}^{(t)}\right|\cdots\left|x_k^{(t)}\right|\right\}<1,\quad t=1\cdots k-1 \tag{8.118}$$

Unfold det(A) according to the first row, then derive:

$$\begin{aligned}\det(A)=D_1&=a_{11}A_{11}^{(1)}+\cdots+a_{1k}A_{1k}^{(1)}\\&=\left(a_{11}+a_{12}\frac{A_{12}^{(1)}}{A_{11}^{(1)}}+\cdots+a_{1k}\frac{A_{12}^{(1)}}{A_{11}^{(1)}}\right)A_{11}^{(1)}\\&=\left(a_{11}+a_{12}x_2^{(1)}+\cdots+a_{1k}x_k^{(1)}\right)D_2\end{aligned} \tag{8.119}$$

Unfold D_2 according to the first row, and then derive:

$$\begin{aligned}D_2&=a_{22}A_{22}^{(2)}+a_{23}A_{23}^{(2)}+\cdots+a_{2k}A_{2k}^{(2)}\\&=\left(a_{22}+a_{23}\frac{A_{23}^{(2)}}{A_{22}^{(2)}}+\cdots+a_{2k}\frac{A_{2k}^{(2)}}{A_{22}^{(2)}}\right)A_{22}^{(2)}\\&=\left(a_{22}+a_{23}x_3^{(2)}+\cdots+a_{2k}x_k^{(2)}\right)D_3\end{aligned} \tag{8.120}$$

Generally, unfold D_t according to the first row, then derive:

$$\begin{aligned}D_t&=a_{tt}A_{tt}^{(t)}+\cdots+a_{tk}A_{tk}^{(t)}\\&=\left(a_{tt}+a_{t,t+1}\frac{A_{t,t+1}^{(t)}}{A_{tt}^{(t)}}+\cdots+a_{tk}\frac{A_{tk}^{(t)}}{A_{tt}^{(t)}}\right)A_{tt}^{(t)}\\&=\left(a_{tt}+a_{t,t+1}x_{t+1}^{(t)}+\cdots+a_{tk}x_k^{(t)}\right)D_{t+1}\end{aligned} \tag{8.121}$$

Then det(A) can be written as follows:

$$\begin{aligned}\det(A)=&\left(a_{11}+a_{12}x_2^{(1)}+\cdots+a_{1k}x_k^{(1)}\right)\cdots\left(a_{ii}+a_{i,i+1}x_{i+1}^{(i)}+\cdots+a_{ik}x_k^{(i)}\right)\\&\cdots\left(a_{k-1,k-1}+a_{k-1,k}x_k^{(k-1)}\right)a_{kk}\end{aligned} \tag{8.122}$$

that is

$$\det(A)=\prod_{t=1}^{k-1}\left(a_{tt}+\sum_{\substack{j=t+1\\ j\ne i}}^{k}a_{ij}x_j^{(t)}\right)a_{kk} \tag{8.123}$$

because

$$\left|x_j^{(t)}\right| < 1, \quad t = 1 \cdots k-1, \quad j = t+1 \cdots k \tag{8.124}$$

so

$$a_{tt} + \sum_{\substack{j=t+1 \\ j \neq t}}^{k} a_{ij} x_j^{(t)} \leq a_{tt} + \sum_{\substack{j=t+1 \\ j \neq t}}^{k} \left|a_{ij}\right| = M_t, \quad t = 1 \cdots k-1 \tag{8.125}$$

$$\begin{gathered} a_{tt} + \sum_{\substack{j=t+1 \\ j \neq t}}^{k} a_{tj} x_j^{(t)} \geq a_{tt} - \sum_{\substack{j=t+1 \\ j \neq t}}^{k} \left|a_{ij}\right| = mt \geq 0, \quad t = 1 \cdots k-1 \\ 0 \leq m_1 \cdots m_k \leq \det(A) \leq M_1 \cdots M_k \end{gathered} \tag{8.126}$$

□

In the practical power system, δ is nonmutation because the trajectory of δ is sufficiently smooth and continuously differentiable, hence the space where δ is located will be compact. In fact, for any $\delta \in \Omega_\delta$, there exists an infinite subset $S \subset \Omega_\delta$ for Ω_δ, enabling δ to be the accumulation point of S. Therefore, the space where δ is located is not only compact but also countable compact. Because compactness is the topological nature for keeping the continuous mapping constant, the space where the coordinate $\overline{\delta}$ of observation decoupled state is located should be compact as well.

Because coordinate $Z = \left\{\delta, \dot{\delta}\right\}$ of original state space and coordinate $Z = \left\{\overline{\delta}, \dot{\overline{\delta}}\right\}$ of the observation decoupled state space appear in vector form, then their respective inner product could meet the definition for Euclidean space E. Therefore, the space where Z and W are located is the subspace of Euclidean space, that is:

$$\Omega_\delta \times R^{n-1} \subset E^{2(n-1)} \quad \text{and} \quad \Omega_{\overline{\delta}} \times R^{2(n-1)} \subset E^{2(n-1)} \tag{8.127}$$

It is known from Brouwer invariance theorem of domain that the homeomorphy of the interior point in Euclidean space E must still be interior point l. However, it may not be established in non-Euclidean space. Therefore, the observation decoupled state space and original system state space are integrated with the Euclidean space, which is favorable for the discussion.

For each actual power system, the dimension of the state space formed is uniquely identified. For instance, for a system with n generators, the dimension of the state space is $2(n-1)$ (nth generator as the reference point). The conception of topological manifold is further introduced as follows.

Definition: Let M be a topological space; if there is an integer m to enable that each point of M has a basic neighborhood homeomorphic to the open subset of E^m, then M is called m-dimensional topological manifold.

In this definition, integer m is uniquely determined by the topological space M. Because the interior point and the boundary point could be topological invariance, if $m \neq n$, then the open set of E^m and E^n could not be homeomorphic. Therefore, integer m is the topological invariant of M, which is called as the dimension of M.

Obviously, because Z and W are compact, Z and W have a basic neighborhood, which is the homeomorphism of the open subset of $E^{2(n-1)}$. Therefore, both the original system state space where Z is located and the observation decoupled space where W is located are $2(n-1)$-dimensional topological manifold.

Because the topological manifold is the topological space based on the global Euclidean space, many properties of Euclidean space can be used to study topological manifolds in a certain way. For instance, the discussion here could be simplified through studying the continuous mapping differentiability of the topological manifold.

In the original state space of the system, because the mathematical model is of a differential structure, it will still be kept when the homeomorphic mapping enters into the observation decoupled space. Therefore, these two $2(n-1)$-dimensional topological manifolds, namely the original state space of the system and the observation decouple state space, could also be called as $2(n-1)$-dimensional differential manifolds.

Lemma 5 *$g : \Omega_\delta \to g(\Omega_\delta) \triangleq \Omega_{\bar{\delta}}$ is one diffeomorphism for open convex subset Ω_δ' of any Ω_δ.*

Proof As g is the continuous mapping from differential manifold to differential manifold, if the Jacobian matrix of g is of full rank, then g can be considered as a diffeomorphism in the specified region. Obviously, if g meets the invertible condition in Lemma 3, then Lemma 5 is established. The Jacobian matrix in mapping g is:

$$[g'(\delta)]_{ij} = \left[\frac{\partial \bar{\delta}_i}{\partial \delta_j}\right] \tag{8.128}$$

It is known from Eq. (8.93) that:

$$\frac{\partial \bar{\delta}_i}{\partial t} = -\left[\frac{\partial}{\partial \bar{\delta}_i} G_i\right]^{-1} \left[\frac{\partial}{\partial \delta_j} G_i\right] \frac{\partial \delta_j}{\partial t} \tag{8.129}$$

So

$$\frac{\partial \bar{\delta}_i}{\partial t_j} = -\left[\frac{\partial G_i}{\partial \bar{\delta}_i}\right]^{-1} \left[\frac{\partial G_i}{\partial \delta_j}\right] \tag{8.130}$$

where:

$$\frac{\partial G_i}{\partial \bar{\delta}_i} = \sum_{k=1}^{k} C'_{ik} \frac{E'_i E'_k}{X_{ij}} \cos\left(\delta_i - \delta_k - \bar{\delta}_i\right) \ (i \in [1, n]) \tag{8.131}$$

$$\frac{\partial G_i}{\partial \delta_i} = \begin{cases} C'_{ij}\dfrac{E'_i E'_j}{X_{ij}}\cos\left(\delta_i - \delta_j - \overline{\delta}_i\right), & i \neq j \\ -\displaystyle\sum_{k=1}^{n} C'_{ik}\frac{E'_i E'_k}{X_{ij}}\cos\left(\delta_i - \delta_k - \overline{\delta}_i\right), & i = j \end{cases} \quad (i, j \in [1, n]) \tag{8.132}$$

So

$$[g'(\delta)]_{ij} = \left[\frac{\partial \overline{\delta}_i}{\partial \delta_j}\right] = \left[-\left[\frac{\partial G_i}{\partial \overline{\delta}_i}\right]^{-1}\left[\frac{\partial G_i}{\partial \delta_j}\right]\right]_{ij}$$

that is:

$$[g'(\delta)]_{ij} = \begin{cases} 1 & (i = j) \\ -\dfrac{C'_{ij}\dfrac{E'_i E'_j}{X_{ij}}\cos\left(\delta_i - \delta_j - \overline{\delta}_i\right)}{-\displaystyle\sum_{k=1}^{n} C'_{ik}\frac{E'_i E'_k}{X_{ij}}\cos\left(\delta_i - \delta_k - \overline{\delta}_i\right)} & (i, j \in [1, n]) \\ & (i \neq j) \end{cases} \tag{8.133}$$

Let $\{\delta^{(1)}, \delta^{(2)}, \ldots, \delta^{(n-1)}\}$ be any $n-1$ point in Ω_δ and $\left\{\overline{\delta}^{(1)}, \overline{\delta}^{(2)}, \ldots, \overline{\delta}^{(n-1)}\right\}$ be the corresponding point defined by g, and let:

$$A = \{a_{ij}\} = \left\{[g'(\delta)]_{ij}\right\} \tag{8.134}$$

Then matrix A in Eq. (8.134) is obviously the matrix required by Eq. (8.100) in Lemma 3. It is known from Eq. (8.133) that $\det(A)$ will be non-zero, and $\det(A) \neq 0$ is equivalent to the requirement in Lemma 3 that the transpose of the matrix is not equal to zero, that is, $\det(A^{\mathrm{T}}) \neq 0$ will be established as well. It is further found in Eq. (8.133) that the matrix A will meet the condition of Eq. (8.103) in Lemma 4, and from Eq. (8.133), we could derive the expression in Lemma 4 for m_i as follows:

$$m_i = 1 - \sum_{j=i+1}^{n}\left|\frac{C'_{ij}\dfrac{E'_i E'_j}{X_{ij}}\cos\left(\delta_i^{(i)} - \delta_j^{(i)} - \overline{\delta}_i^{(i)}\right)}{\displaystyle\sum_{k=1}^{n} C'_{ik}\frac{E'_i E'_k}{X_{ik}}\cos\left(\delta_i^{(i)} - \delta_k^{(i)} - \overline{\delta}_i^{(i)}\right)}\right| \quad (i \in [1, n]) \tag{8.135}$$

In Eq. (8.135):

$$C'_{ij} = \begin{cases} 0 & (i = j) \\ 1 & (i \neq j) \end{cases}$$
$$\frac{E'_i E'_j}{X_{ij}} > 0 \tag{8.136}$$

It is known from Eq. (8.73) that:

$$|\delta_i^{(i)} - \delta_j^{(i)} - \overline{\delta}_i^{(i)}| < \frac{\pi}{2} - \varepsilon, \quad \forall \varepsilon > 0 \tag{8.137}$$

Therefore, Eq. (8.135) could be rewritten into:

$$\begin{aligned} m_i &= 1 - \sum_{j=i+1}^{n-1} \frac{C'_{ij} \dfrac{E'_i E'_j}{X_{ij}} \cos\left(\delta_i^{(i)} - \delta_j^{(i)} - \overline{\delta}_i^{(i)}\right)}{\displaystyle\sum_{k=1}^{n} C'_{ik} \frac{E'_i E'_k}{X_{ik}} \cos\left(\delta_i^{(i)} - \delta_k^{(i)} - \delta_i^{(i)}\right)} \\ &= \frac{\displaystyle\sum_{j=1}^{i-1} C'_{ij} \frac{E'_i E'_j}{X_{ij}} \cos\left(\delta_i^{(i)} - \delta_j^{(i)} - \overline{\delta}_i^{(i)}\right) + C'_{in} \frac{E'_i E'_k}{X_{ik}} \cos\left(\delta_i^{(i)} - \delta_k^{(i)} - \overline{\delta}_i^{(i)}\right)}{\displaystyle\sum_{k=1}^{n} C'_{ik} \frac{E'_i E'_k}{X_{ik}} \cos\left(\delta_i^{(i)} - \delta_k^{(i)} - \overline{\delta}_i^{(i)}\right)} \end{aligned} \tag{8.138}$$

Let:

$$\varepsilon_{ij} = C'_{ij} \frac{E'_i E'_j}{X_{ij}} \cos\left(\frac{\pi}{2} - \varepsilon\right) \quad (i, j \in [1, n]) \tag{8.139}$$

$$F_i = \sum_{k=1}^{n} C'_{ik} \frac{E'_i E'_k}{X_{ik}} \cos 0 \quad (i, j \in [1, n]) \tag{8.140}$$

$$\varepsilon_0 = \min\left\{\varepsilon_{ij}\right\} \quad (i, j \in [1, n]) \tag{8.141}$$

Then m_i will meet the following inequality:

$$m_i \geq \frac{\varepsilon_0}{F_i} = \alpha^{(i)} > 0 \tag{8.142}$$

In line with Lemma 4, it is known from Eq. (8.142) that det(A) will meet the following inequality:

$$0 < \alpha^{(i)} \cdots \alpha^{(n)} = \alpha \leq \det(A) = \det\lfloor g'(\delta) \rfloor \tag{8.143}$$

As $\det\lfloor g'(\delta) \rfloor > 0$, the inverse of $[g'(\delta)]$ exists, and it is known from Lemma 3 that g is one-to-one mapping. Therefore, g is a differential homeomorphism in the specified region. □

8.5.2.5 Mapping is a homeomorphism within the specified region

In the previous sections, several necessary lemmas are demonstrated, based on which the main results discussed can be proven, that is, F in a given region is a homeomorphism.

It is known from the proof of Lemma 2 that $\dot{\overline{\delta}}$ could be derived from Eq. (8.91). Therefore, Eq. (8.91) also implicitly defines a mapping:

$$h:\left(\delta,\dot{\delta},\overline{\delta}\right)=\left[\delta,\dot{\delta},g(\delta)\right]\rightarrow\dot{\overline{\delta}} \tag{8.144}$$

As h is derived via the differential on the basis of g, h will also be a differential homeomorphism. In fact, the mapping F under our discussion consists of g and h, that is:

$$F:Z\rightarrow W\leftrightarrow\begin{cases}g:\delta\rightarrow\overline{\delta}\\ h:\left(\delta,\dot{\delta},\overline{\delta}\right)\rightarrow\dot{\overline{\delta}}\end{cases} \tag{8.145}$$

Therefore, F should be not only a homeomorphism but also a differential homeomorphism. Therefore, the said three requirements could be rewritten into the below forms to be more in favor of the proof:

(1) $F:\Omega_{\delta}\times R^{n-1}\rightarrow F(\Omega_{\delta}\times R^{n-1})\triangleq\Omega_{\overline{\delta}}\times R^{n-1}$ are one-to-one mapping.
(2) F is continuous differentiable in $\Omega_{\overline{\delta}}\times R^{n-1}$.
(3) The Jacobian matrix F' of F is nonsingular everywhere in $\Omega_{\overline{\delta}}\times R^{n-1}$.

Prove F to be a homeomorphism within the specified scope, and (1)–(3) are equivalent to the three requirements of the previously discussed F mapping.

Theorem 1 *Mapping F is a homeomorphism* (*diffeomorphism*) *from* $\Omega_{\overline{\delta}}\times R^{n-1}$ *to* $\Omega_{\overline{\delta}}\times R^{n-1}$.

Proof The proof falls into three parts in line with (1)–(3) conditions to be met by F:

(1) $F:\Omega_{\delta}\times R^{n-1}\rightarrow F(\Omega_{\delta}\times R^{n-1})\triangleq\Omega_{\overline{\delta}}\times R^{n-1}$ are one-to-one mapping.

If Ω_Z is an open convex subset in $\Omega_{\overline{\delta}}\times R^{n-1}$, and point $\left\{\delta_1,\dot{\delta}_1\right\}$ and point $\left\{\delta_2,\dot{\delta}_2\right\}$ are in Ω_Z, and then:

$$F\left\{\delta_1,\dot{\delta}_1\right\}=F\left\{\delta_2,\dot{\delta}_2\right\}=\left(\overline{\delta},\dot{\overline{\delta}}\right) \tag{8.146}$$

Because the mapping g is a differential homeomorphism, there is:

$$\overline{\delta}=g(\delta_1)=g(\delta_2) \tag{8.147}$$

The projection $p(\Omega_Z)$ of Ω_Z in Ω_{δ} is an open convex subset of Ω_{δ}, and in line with Lemma 5:

$$\delta_1=\delta_2=\delta \tag{8.148}$$

could be derived. Then from Eq. (8.93):

$$\begin{aligned}\dot{\delta}&=-\left[\frac{\partial}{\partial\delta}G\left(\delta,\overline{\delta}\right)\right]^{-1}\left[\frac{\partial}{\partial\delta}G\left(\delta,\overline{\delta}\right)\right]\dot{\delta}_1\\&=-\left[\frac{\partial}{\partial\delta}G\left(\delta,\overline{\delta}\right)\right]^{-1}\left[\frac{\partial}{\partial\delta}G\left(\delta,\overline{\delta}\right)\right]\dot{\delta}_2\end{aligned} \tag{8.149}$$

It is known from Eq. (8.92) that $\left[\frac{\partial}{\partial\delta}G\left(\delta,\overline{\delta}\right)\right]$ is nonsingular, and then:

$$\dot{\delta}_1 = \dot{\delta}_2 \tag{8.150}$$

Therefore, F is one-to-one mapping. □

(2) F is continuously differentiable in $\Omega_\delta \times R^{n-1}$.

Write mapping F into the following form:

$$W = \left\{\overline{\delta}, \dot{\overline{\delta}}\right\} = F(Z) = F\left(\left\{\overline{\delta}, \dot{\overline{\delta}}\right\}\right) = \left\{g(\delta), \frac{\partial g(\delta)}{\partial \delta}\dot{\delta}\right\} \tag{8.151}$$

In Eq. (8.151), the continuous differentiability of $g(\delta)$ is guaranteed by Lemma 5. Likewise, as g is a differential homeomorphism, $\frac{\partial g(\delta)}{\partial \delta}\dot{\delta}$ is also continuously differentiable in $\Omega_\delta \times R^{n-1}$. Therefore, F is continuously differentiable in $\Omega_\delta \times R^{n-1}$.

(3) The Jacobian matrix F' of F is nonsingular in $\Omega_\delta \times R^{n-1}$.

It is known from Eq. (8.151) that:

$$F(Z) = F\left(\left\{\overline{\delta}, \dot{\overline{\delta}}\right\}\right) = \left\{g(\delta), \frac{\partial g(\delta)}{\partial \delta}\dot{\delta}\right\} \tag{8.152}$$

Therefore, the Jacobian matrix F' of F has the following form:

$$\begin{aligned} F' &= \begin{bmatrix} \dfrac{\partial g(\delta)}{\partial \delta} & , & \dfrac{\partial g(\delta)}{\partial \dot{\delta}} \\ \dfrac{\partial}{\partial \delta}\left(\dfrac{\partial g(\delta)}{\partial \delta}\dot{\delta}\right) & , & \dfrac{\partial}{\partial \dot{\delta}}\left(\dfrac{\partial g(\delta)}{\partial \delta}\dot{\delta}\right) \end{bmatrix} \\ &= \begin{bmatrix} \dfrac{\partial g(\delta)}{\partial \delta} & , & 0 \\ \dfrac{\partial}{\partial \delta}\left(\dfrac{\partial g(\delta)}{\partial \delta}\dot{\delta}\right) & , & \dfrac{\partial g(\delta)}{\partial \delta} \end{bmatrix} \end{aligned} \tag{8.153}$$

It is known from Lemma 5 that $\left[\frac{\partial g(\delta)}{\partial \delta}\right] = \left[\frac{\partial \overline{\delta}}{\partial \delta}\right]$ is nonsingular, hence F' is also nonsingular. As F could meet the previous three points, the mapping F is a homeomorphism (diffeomorphism) from $\Omega_\delta \times R^{n-1}$ to $\Omega_{\overline{\delta}} \times R^{n-1}$. □

Based on discussions on the generator angle model by the network transformation simplification, the mapping F is proven to be a homeomorphic mapping from the original system state space to the observation decoupled state space. Therefore, it could be concluded that the observation decoupled state space introduced is topologically equivalent to the original state space.

It is necessary to further highlight one point that, when proving F to be a homeomorphism from $\Omega_\delta \times R^{n-1}$ to $\Omega_{\overline{\delta}} \times R^{n-1}$, assume the space R^{n-1} where Ω_δ and $\Omega_{\overline{\delta}}$ are located to be convex. In fact, if bus i has more than two transmission lines connecting with the rest buses in the system, it is possible that region Ω_δ is not convex. However, in such a case, a maximum open convex subset of Ω can be used, and its existence could be guaranteed by the Zorn lemma in topology.

8.5.3 Proof of Topology Equivalence Between Different Forms of Observation Decoupled State Space and Original System State Space

The difference of various forms of observation decoupled state space mainly lies in the formal difference of the second state variable. It has been proven that $\left\{\overline{\delta}, \dot{\overline{\delta}}\right\}$ is topologically equivalent to $\left\{\delta, \dot{\delta}\right\}$. For other forms of observation decoupled state space $\left\{\overline{\delta}, \dot{\overline{\delta}}(50)\right\}$ and $\left\{\overline{\delta}, \dot{\delta}_s\right\}$, their first state variable is the same as the first state variable of $\left\{\overline{\delta}, \dot{\overline{\delta}}\right\}$, and they embrace a structural difference in the second state variable. Therefore, to prove that the observation decoupled state space $\left\{\overline{\delta}, \dot{\overline{\delta}}(50)\right\}$ and $\left\{\overline{\delta}, \dot{\overline{\delta}}\right\}$ are topologically equivalent to the original system state space, we need to prove that the mapping from $\dot{\delta}$ (w equivalent to it) to $\dot{\delta}(50)$ or $\dot{\delta}_s$ are a homeomorphism in their respective region. The following proofs are also made on the generator angle model.

In space $\left\{\overline{\delta}, \dot{\overline{\delta}}(50)\right\}$, $\dot{\overline{\delta}}(50)$ is defined as:

$$\dot{\delta}\ (50)_i = \omega_i - \omega_0 \left(= \dot{\delta}_i\right) \tag{8.154}$$

where:

$$\omega_0 = 2\pi f_0 = 100\pi\ (\mathrm{rad/s}) \tag{8.155}$$

In space $\left\{\overline{\delta}, \dot{\overline{\delta}}\right\}$, the definition of $\dot{\delta}_s$ is:

$$\dot{\delta}_{si} = \omega_i - \omega_s\ (i \in [1, n]) \tag{8.156}$$

where:

$$\omega_s = \frac{\sum J_i \omega_j}{\sum J_i} \tag{8.157}$$

Their respective proof is as follows:

(1) The observation decoupled state space $\left\{\overline{\delta}, \dot{\overline{\delta}}(50)\right\}$ is topologically equivalent to the original system state space.

Proof If f_2 is a mapping from ω to $\dot{\delta}(50)$:

$$f_2 : \omega \to \dot{\delta}(50) \tag{8.158}$$

Then:

$$\dot{\delta}\ (50) = f_2(\omega) = I\omega - L\omega_0 = \omega - L\omega_0 \tag{8.159}$$

where:

$$I = \begin{bmatrix} 1 & 0 \\ \ddots & \\ 0 & 1 \end{bmatrix}_{n\times n},\ L = [1\ \cdots\ 1]^{\mathrm{T}},\ \omega = [\omega_1\ \ \cdots\ \ \omega_n]^{\mathrm{T}} \tag{8.160}$$

As I is an invertible identification matrix of $n \times n$, f_2 will meet the homeomorphism conditions for bicontinuous and filled single mapping. Therefore, f_2 is a homeomorphism between R^n and R^n. □

(2) The observation decoupled state space $\left\{\overline{\delta}, \dot{\delta}_{\mathrm{s}}\right\}$ is topologically equivalent to the original system state space.

Proof If f_3 is a mapping from ω to $\dot{\delta}_{\mathrm{s}}$:

$$f_3 : \omega \to \dot{\delta}_{\mathrm{s}} \tag{8.161}$$

and then:

$$\dot{\delta}_{\mathrm{s}} = f_3(\omega) = I\omega - L\omega_{\mathrm{s}}$$

where:

$$I = \begin{bmatrix} 1 & 0 \\ \ddots & \\ 0 & 1 \end{bmatrix}_{n\times n},\ L = [1\ \ \cdots\ \ 1]^{\mathrm{T}},\ \omega = [\omega_1\ \ \cdots\ \ \omega_n]^{\mathrm{T}} \tag{8.162}$$

As

$$\begin{aligned} L\omega_{\mathrm{s}} &= \sum_{j=1}^{n} J_j\omega_j \\ \sum_{j=1}^{n} J_j &= \frac{1}{\sum_{j=1}^{n} J_j} \begin{bmatrix} 1 \\ \vdots \\ 1 \end{bmatrix} [J_1\ \ \cdots\ \ J_n] \begin{bmatrix} \omega_1 \\ \vdots \\ \omega_n \end{bmatrix} \\ &= \frac{1}{\sum_{j=1}^{n} J_j} \begin{bmatrix} J_1 & J_2 & \cdots & J_n \\ \vdots & \vdots & & \vdots \\ J_1 & J_2 & \cdots & J_n \end{bmatrix} \begin{bmatrix} \omega_1 \\ \vdots \\ \omega_n \end{bmatrix} \end{aligned} \tag{8.163}$$

So

$$\begin{aligned}\delta_{\mathrm{s}} &= f_3(\omega) = I\omega - L\omega_{\mathrm{s}} \\ &= \begin{bmatrix} 1 & & 0 \\ & \ddots & \\ 0 & & 1 \end{bmatrix}\omega - \frac{1}{\sum_{j=1}^{n} J_j}\begin{bmatrix} J_1 & J_2 & \cdots & J_n \\ \vdots & \vdots & & \vdots \\ J_1 & J_2 & \cdots & J_n \end{bmatrix}\omega \\ &= \frac{1}{\sum_{j=1}^{n} J_j}\begin{bmatrix} \sum J_j - J_1 & \cdots & -J_n \\ -J_1 & & \vdots \\ \vdots & & -J_1 \\ -J_1 & \cdots & \sum J_j - J_1 \end{bmatrix}\omega \\ &= \frac{1}{\sum_{j=1}^{n} J_j}\cdot K\omega\end{aligned} \tag{8.164}$$

K is obviously an invertible matrix, thus f_3 is a homeomorphism between R^n and R^n. □
It could be found from the previous proof that the different forms of observation decoupled state space are topologically equivalent to the original system state space, thereby the system dynamic behavior could be monitored with proper observation decoupled state space in line with different conditions of the power system itself.

8.5.4 Origin of Observation Decoupled State Space

When the observation decoupled state variable $\overline{\delta}$ is at the origin (the Only Equilibrium Point in the Power System), assume the local equilibrium power angle δ_{e} is constantly consistent with the steady-state power angle δ_0 of the system, and for all the generator buses, there should be:

$$\delta_{0i} = \delta_{ci} \quad (i \in [1, n]) \tag{8.165}$$

In addition, for the system global stability, the local equilibrium criterion $\delta_{\mathrm{e}i}$ of the power system should be unique and stable in contrast with the local equilibrium criterion $\delta_{\mathrm{e}j}$ of all the connected buses.

Theorem 2 *If the system is in equilibrium state δ_0, then all the generator buses could have:*

$$\delta_{0i} = \delta_{\mathrm{e}i} \quad (i \in [1, n]) \tag{8.166}$$

If δ_{ei} always exists for all the generator buses, then δ_0 is stable. When $\overline{\delta} = \delta_{0i} - \delta_{\mathrm{e}i} = 0$, then the origin of observation decoupled state space will be the only stable equilibrium point.

Proof For the generator angle model after the network simplification, its basic power equilibrium equation is:

$$J_i\ddot{\delta}_i + P_{Di}\dot{\delta}_i = P_{\mathrm{m}i} - P_{\mathrm{L}i} - \sum_{i=1}^{n} C'_{ij}\frac{E'_i E'_j}{X_{ij}}\sin\left(\delta_i - \delta_j\right) - u_i, i \in [1, n] \tag{8.167}$$

Its state equation could be written into the following form:

$$\left.\begin{aligned}\dot{\delta} &= \omega - \omega_0 \\ \dot{\omega} &= f(\delta, \omega) - Lu\end{aligned}\right\} \tag{8.168}$$

where:

$$f_i(\delta, \omega) = \frac{1}{J_i}\left[P_{\mathrm{m}i} - P_{\mathrm{L}i} - \sum_{j=1}^{n} C'_{ij}\frac{E'_i E'_j}{X_{ij}}\sin\left(\delta_i - \delta_j\right) - P_{\mathrm{D}i}(\omega_i - \omega_0)\right] \tag{8.169}$$

$$L = \begin{bmatrix}\frac{1}{J_i} & & \\ & \ddots & \\ & & \frac{1}{J_n}\end{bmatrix} \tag{8.170}$$

At the local equilibrium point of the system, in line with the local equilibrium criterion:

$$|\delta_{ei} - \dot{\delta}_j| < \frac{\pi}{2} - \varepsilon \quad (\forall \varepsilon > 0, i, j \in [1, n]) \tag{8.171}$$

Could be derived. When the system reaches equilibrium within global scope, then $\delta_j = \delta_{\mathrm{e}j}$ in all cases, and Eq. (8.171) evolves into:

$$|\delta_{ei} - \dot{\delta}_{ej}| < \frac{\pi}{2} - \varepsilon \quad (\forall \varepsilon > 0, i, j \in [1, n]) \tag{8.172}$$

With consideration to the equilibrium point and the system linear approximation, the linearized system has the following form:

$$\dot{\gamma} = A\gamma + \omega_0 + \widetilde{L}u \tag{8.173}$$

where:

$$A = \begin{bmatrix}0 & 1 \\ \left.\frac{\partial f}{\partial \delta}\right|_{\delta_{\mathrm{e}}} & 0\end{bmatrix}, \quad \gamma = \lfloor \delta, \omega \rfloor^{\mathrm{T}}$$

$$B = \begin{bmatrix}-1 \\ \vdots \\ -1 \\ 0 \\ \vdots \\ 0\end{bmatrix}, \quad \widetilde{L} = \begin{bmatrix}0 & & & & & 0 \\ & \ddots & & & & \\ & & 0 & & & \\ & & & -\frac{1}{J_1} & & \\ & & & & \ddots & \\ 0 & & & & & -\frac{1}{J_n}\end{bmatrix}$$

It is known from Lyapunov's first method that the solution of Eq. (8.173) will have the form of e^{At}. Therefore, to prove $\{\delta_e, \omega_0\}$ to be a stability operation point, it should sufficiently prove A to be a negative semidefinite matrix, and sufficiently specify $\left.\frac{\partial f}{\partial \delta}\right|_{\delta_e}$ to be a positive semidefinite matrix.

As

$$\left.\frac{\partial f_i}{\partial \delta_j}\right|_{\delta_e} = \begin{cases} -\dfrac{1}{J_i}\displaystyle\sum_{j=1}^{n} C'_{ij}\frac{E'_i E'_j}{X_{ij}}\cos\left(\delta_{ei}-\delta_{ej}\right) & (j=i) \\ \dfrac{1}{J_i}C'_{ij}\dfrac{E'_i E'_j}{X_{ij}}\cos\left(\delta_{ei}-\delta_{ej}\right) & (j\neq i) \end{cases} \tag{8.174}$$

So

$$-\left.\frac{\partial f_i}{\partial \delta_j}\right|_{\delta e} = \begin{cases} \dfrac{1}{J_i}\displaystyle\sum_{j=1}^{n} C'_{ij}\frac{E'_i E'_j}{X_{ij}}\cos\left(\delta_{ei}-\delta_{ej}\right) & (j=i) \\ -\dfrac{1}{J_i}C'_{ij}\dfrac{E'_i E'_j}{X_{ij}}\cos\left(\delta_{ei}-\delta_{ej}\right) & (j\neq i) \end{cases} \tag{8.175}$$

Let:

$$F_e \triangleq \left\{ -\left.\frac{\partial f_i}{\partial \delta_j}\right|_{\delta_e} \right\} = \left\{F_{eij}\right\} \tag{8.176}$$

If F_e is a symmetric matrix with positive diagonal element, and F_e enjoys a dominant diagonal advantage, then F_e will be positive semidefinite. The positive semidefiniteness of F_e is examined in the following text.

All the generator buses should meet $|\delta_{ei}-\delta_{ej}| < \frac{\pi}{2}-\varepsilon$:

So

$$\sum_{j=1}^{n} C_{ij}\frac{E'_i E'_j}{X_{ij}}\cos\left(\delta_{ei}-\delta_{ej}\right) > 0 \quad (i,j\in[1,n]) \tag{8.177}$$

That is, all diagonal elements of F_e are positive, and the symmetry of F_e is obvious. In addition, as F_e enjoys a main diagonal advantage, it could be found:

$$|F_{eii}| \geq \sum_{j=1}^{n} |F_{eij}| \tag{8.178}$$

Therefore, F_e is a symmetric matrix with positive diagonal elements and diagonal dominance, which indicates that the origin of the observation decoupled state space is the unique steady equilibrium point of the power system. □

8.5.5 Sufficient Condition for Convergence of the Second Stage Control (Norm Reduction)

In the observation decoupled state space, $\overline{V}$ is the norm of the observation decoupled state vector.

$$V = \sum V_i \tag{8.179}$$

where $\overline{V}_i$ is the norm of the observation decoupled state vector of local i. As for all the generator buses at any time t, $\overline{V}_i > 0, \overline{V}_i(0) = 0$ could be derived. Therefore, the control amount $u_i(t)$ is selected in real time at each generator node i so that:

$$\dot{\overline{V}}_i(t) < 0 \quad (0 < t < \infty,\ i \in [1, n]) \tag{8.180}$$

Then the power system will reach the steady equilibrium state along the given track.

If the conditions are satisfied at each point of the trajectory, the norm $\overline{V}_i$ is present, and the norm reduction control criterion could be derived in this way. Select the control variable u_i according to the criterion enabling the power system to reach the only stability equilibrium state within a limited time. The conditions are as follows:

(1) The only steady equilibrium state of the system exists (in the given operating mode).
(2) The observation decoupled state vector exists.
(3) For each generator bus, the control mode may be in such a way that the electromagnetic power is increased or decreased.
(4) The value of the required control should meet the constraints for the control device itself. The above four points are sufficient conditions for convergence of norm reduction control.

8.6 General Simulation Calculation Procedure in Two-Stage Control

In the actual power system, according to the energy equilibrium control criterion at the first stage and the norm reduction control criterion at the second stage for the observation decoupled state space, strict local online stability control can be carried out for the system based on the measurement and calculation on the local variables. Of course, this is ideal for realizing online control.

Prior to realizing this point, there is still a lot of work to be done even if there is no technical problem that involves the specific implementation of local stability measures.

First, with the understanding of the dynamic stability of the system after large-scale interference, the dynamic conditions of the system after imposing local stability measures on local parts of the system should also be deeply understood in line with the two previously mentioned control criteria. Second, to determine the rationality of the control criterion, it is still necessary to understand the dynamic stability of the system when it is undercontrolled or overcontrolled based on the control criterion.

These works are related to the dynamic stability calculation of the power system. In practice, these calculations are the dynamic stability calculations that take into account the local stability control measures (based on the criteria). In other words, the offline calculation of local online stability control should be based on the conventional dynamic stability calculation of the power system.

Because the local online stability control is mainly concerned with the dynamic stability problem of the power system after suffering from large-scale interference, the offline calculation of the local online stability control should be combined with the conventional dynamic stability calculation, which not only is beneficial to effective calculation work but also facilitates the understanding of the concept of observation decoupled state space and the application of the derived control criteria in the power system; it could be welcomed by the majority of engineering and technical personnel.

In essence, the difference between the conventional dynamic stability calculation and the dynamic stability calculation considering local stability control is that the observation decoupled state vector has to be calculated in the latter. As for the former, the operation of the control measures is manmade and prearranged. As for the latter, the calculation of the control measures for the switch is based on the control criteria, and then the online calculation is used to determine the switching time.

To simplify the calculation, the simplified mathematical model and network structure are used, and only control measures, such as the electric braking, are considered, which will undoubtedly bring some errors. This chapter mainly aims to illustrate the initial feasibility of the local online stability control made according to the criterion, but the technical details for the actual implementation will not be considered for the time being.

8.6.1 Simplified Assumptions and Network Diagram

Simplified assumptions

(1) Generator: Ignore saliency effect, and deem the electromotive force E' to maintain constant after x_d'.
(2) Load: Constant impedance.
(3) Power network: Described by admittance matrix.
(4) Control measures: Braking resistor.

Network diagram

Network structure in Fig. 8.8 is typical: Much of the actual power system can be equivalent to a part of the three-machine system. Through the appropriate selection of parameters for network, generator, and load, the network can also be converted into two-generator systems or an infinite-bus system to accommodate the calculation of various schemes.

8.6.2 Variables of Measurement and Calculation in Online Control

To realize online local stability control, during the system overall operation period (including two control stages for the stability state and fault state), it is required to calculate the real-time $\left\{\overline{\delta}_i, \dot{\overline{\delta}}_i\right\}$ value in each local part of the system, so as to monitor the system operation condition. Transiently derive Eqs. (8.22), (8.25) with microprocessor, and $\left\{\overline{\delta}_i, \dot{\overline{\delta}}_i\right\}$ could be derived. Therefore, it is necessary to determine the following real-time data set through measurement and calculation.

$$A_i = \left\{E'_i, \delta_i, \omega_i, P_{\mathrm{m}i}, P_{\mathrm{L}i}, Q_{\mathrm{L}i}, U_i, \alpha_i, I_{ij}, \beta_{ij}, U_j, \alpha_j\right\} \tag{8.181}$$

During the fault, it is possible to make use of the set A_i to calculate the energy equilibrium control criterion and norm reduction control criterion, so as to determine whether the local stability measures should be taken.

In the set A_i, ω_i can be measured in real time, $U_i\angle\alpha_i$ and $I_{ij}\angle\beta_{ij}$ (or more precisely they are three-phase transient instantaneous values $e_i\,(t)$ and $i_{ij}\,(t)$) can be obtained by pulse sampling (from the secondary side of the voltage and current transformers connected to the node i) via the AC/DC converter of the microprocessor. The other amounts in the set A_i can be measured for $U_i\angle\alpha_i$, $I_{ij}\angle\beta_{ij}$ and ω_i, and then calculated by the microprocessor.

(1) The parameter at bus i is:

$$\dot{E}'_i = \dot{I}_i \cdot jX'_{\mathrm{d}i} + \dot{U}_i \tag{8.182}$$

where $\dot{E}'_i = \dot{E}'\angle\delta_i, \dot{I}_i - \dot{I}_i\angle\beta_i = \sum I_{ij}\angle\beta_{ij}, \dot{U}_i = U_i\angle\alpha_i$.

$$P_{\mathrm{m}i} = \mathrm{Re}\left[\dot{U}_{0i}\hat{\dot{I}}_{0i}\right] \tag{8.183}$$

where $\dot{U}_{0i} = U_{0i}\angle\alpha_{0i}$ and $\dot{I}_{0i} = U_{0i}\angle\beta_{0i}$ are the voltage and current during the prefault stable state:

$$P_{\mathrm{L}i} + jQ_{\mathrm{L}i} = U_i^2/(R_{\mathrm{L}i} + jX_{\mathrm{L}i}) = \dot{U}_i\hat{\dot{I}}_{\mathrm{L}i} \tag{8.184}$$

where $Z_{\mathrm{L}i} = R_{\mathrm{L}i} + jX_{\mathrm{L}i}$ is the load equivalent impedance, and $\dot{I}_{\mathrm{L}i} = \dot{I}_{\mathrm{L}i}\angle\beta_{\mathrm{L}i}$ is the load current (measured at real time).

(2) $U_j\angle\alpha_j$ at bus j could be analyzed by the π equivalent circuit of specified i-j line.

In line with Fig. 8.5, $U_j\angle\alpha_j$ and $I_{ji}\angle\beta_{ji}$ of bus j could be derived through the following two equations:

$$\dot{U}_j = \frac{Z'_{ij} - Z_{ij}}{Z'_{ij}}\dot{U}_i - Z_{ij}\dot{I}_{ij} \tag{8.185}$$

$$\dot{I}_{ji} = \frac{Z'_{ij} - Z_{ij} - Z'_{ji}}{Z'_{ij}Z'_{ji}} \cdot \dot{U}_i - \frac{Z_{ij} - Z'_{ji}}{Z'_{ji}} \dot{I}_{ij} \tag{8.186}$$

where $\dot{U}_j = U_j \angle \alpha_j, \dot{I}_{ji} = \dot{I}_{ji} \angle \beta_{ji}$).

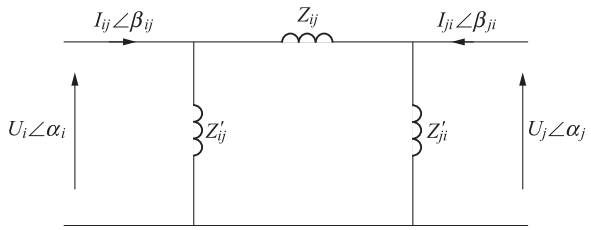

Fig. 8.5
π equivalent circuit of *i-j* line.

After deriving the real-time data set A_i, the value can be solved in real time, and when the fault is calculated, the calculation of the energy balance control criterion and the norm reduction control criterion determines when to start and switch on the stability control measures in the local i to restore the system stability.

8.6.3 Preprocessing of Calculations

The general form of the mathematical equation in the dynamic stability calculation is as follows:

$$\frac{\mathrm{d}x_i}{\mathrm{d}t} = \Phi_i(x_1, \ldots, x_m; y_i, \ldots, y_n) \quad (i = 1, \ldots, m) \tag{8.187}$$

$$0 = F_j(x_1, \ldots, x_m; y_i, \ldots, y_n) \quad (i = 1, \ldots, n) \tag{8.188}$$

Where Eq. (8.187) is the differential equation for describing the dynamic characteristics of the elements in connection with the power system, and Eq. (8.188) is the network algebraic equation for describing the power system nondynamic characteristics. $x_1, \ldots, x_m$ are the power system state parameters, and $y_1, \ldots, y_n$ are the network operation parameters. Generally speaking, $y_1, \ldots, y_n$ are the mutational variables in the calculation. The form and content of Φ_i and F_j are not invariables but will change with the occurrence of the disturbance and implementation of the control measures.

Prior to the power system dynamic stability calculation, it is necessary to first derive the system stable operation state via the power flow calculation, that is, derive the network operation parameters $y_1(0), \ldots, y_n(0)$ and the initial value $x_1(0), \ldots, x_m(0)$ of the state parameters for the related elements of the power system.

In the general power flow calculation, there is no need to calculate the internal situation of the generator and the load, so the network diagram and its parameters generally only determine the

description of the system network admittance matrix. However, in the dynamic calculation, it is necessary to consider the influence of the generator and the load equivalent circuit in the admittance matrix when describing the system network because of consideration needs of the electromechanical transient process inside the generator and the load. Simplified models for analysis and processing are given in the following section.

Prior to this, it is assumed that the results of the power flow calculation and the equivalent impedance of the various faults are known, and in the calculation, the quantities are taken per unitary values.

8.6.3.1 Way of processing generation bus (to provide internal potential and power angle)

Ignore the synchrodyne saliency effect and armature resistance R_a, and keep constant $\dot{E}'$ electromotive force after X_d' to simulate the synchrodyne, equivalent to converting the synchrodyne into the simple voltage source with internal impedance jX_d', whose equivalent circuit is shown in Fig. 8.6. The internal electromotive force could be calculated through the following equation in Fig. 8.6.

$$\begin{aligned}
\dot{E}' &= \dot{I}_{F_0} \cdot jX'_d + \dot{U}_{F_0} \\
&= \frac{P_0 - jQ_0}{\hat{\dot{U}}} \cdot jX'_d + \dot{U}_{F_0} \\
&= \frac{P_0 - jQ_0}{U_{FX0} - jU_{FY0}} \cdot jX'_d + U_{FX0} - jU_{FY0} \\
&= \left[U_{FX0} - \frac{(P_0 U_{FY0} - Q_0 U_{FX0})X'_d}{U_{FX0}^2 + U_{FY0}^2}\right] + j\left[U_{FY0} - \frac{(P_0 U_{FX0} - Q_0 U_{FY0})X'_d}{U_{FX0}^2 + U_{FY0}^2}\right] \\
&= \dot{E}'_{X0} + j\dot{E}'_{Y0} \\
&= E'\angle\delta_0
\end{aligned} \tag{8.189}$$

where:

$$E' = \sqrt{\dot{E}'^2_{X0} + \dot{E}'^2_{Y0}} \cdot \delta_0 = \arctan\frac{\dot{E}'_{y0}}{\dot{E}'_{x0}} \tag{8.190}$$

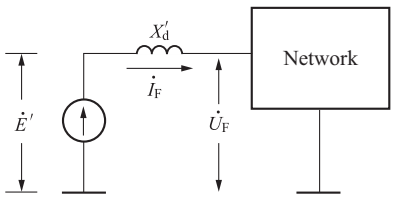

Fig. 8.6

Generator equivalent circuit. $\dot{E}'$—synchrodyne internal electromotive force; X'_d—transient reactance; $\dot{U}_F$—generator terminal voltage; $\dot{I}_F$—synchrodyne stator current $\left(\dot{I}_F = \frac{P-jQ}{\dot{U}_F}\right)$.

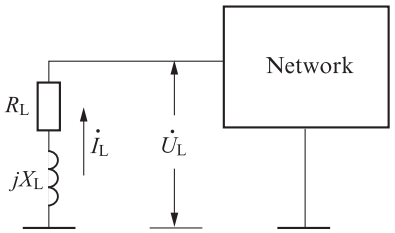

Fig. 8.7

Load equivalent circuit. Z_L—load equivalent impedance; $\dot{U}_L$—voltage of load bus; $\dot{I}_L$—load current $\left(\dot{I}_L = \frac{P_L - jQ_L}{\hat{U}_L}\right)$.

8.6.3.2 Way of processing load bus

Use constant impedance to simulate the load, directly incorporate the load equivalent impedance into the network, and its equivalent circuit is shown in Fig. 8.7.

It is known from Fig. 8.7 that the load equivalent impedance could be calculated from the following equation:

$$\begin{aligned}\dot{Z}_L &= R_L + jX_L \\ &= -\frac{\dot{U}_{L0}}{\dot{I}_{L0}} \\ &= -\frac{\dot{U}_{L0}\hat{\dot{U}}_{L0}}{P_{L0} - Q_{L0}} \\ &= -\frac{U_{LX0}^2 + U_{LY0}^2}{P_{L0} - jQ_{L0}} \\ &= \left[-\left(U_{LX0}^2 + U_{LY0}^2\right)\frac{P_{L0}}{P_{L0}^2 + Q_{L0}^2}\right] + j\left[-\left(U_{LX0}^2 + U_{LY0}^2\right)\frac{P_{L0}}{P_{L0}^2 + Q_{L0}^2}\right]\end{aligned} \tag{8.191}$$

Viz.:

$$R_L = -\left(U_{LX0}^2 + U_{LY0}^2\right)\frac{P_{L0}}{P_{L0}^2 + Q_{L0}^2} \tag{8.192}$$

$$X_L = -\left(U_{LX0}^2 + U_{LY0}^2\right)\frac{Q_{L0}}{P_{L0}^2 + Q_{L0}^2} \tag{8.193}$$

8.6.4 Main Steps of Simulation Calculation Procedure

Step 0: Preparations of generator and load node data.
Step 1: Formulations of dynamic equations and network equations.
Step 2: Calculation of equivalent impedance in case of fault.
Step 3: Calculation of braking power after braking resistor switched on.

Step 4: Calculation of the first stage energy equilibrium control criterion based on given time.
Substep 4.1: Calculation of excess kinetic energy ΔW_i.
Substep 4.2: Calculation of absorbed energy ΔW_{bi} during the brake.
Substep 4.3: Calculation of optimal brake clearing time t_1.
Step 5: Calculation of the second stage critical power control criterion based on given time.
Substep 5.1: Calculation of decoupled reference δ_{ei} by *N-R* method with generator X_d.
Substep 5.2: Calculation of critical control power (equivalence braking resistance).

The given time should cover more than three to five system swing periods.

8.7 Numerical Model in Simulation Calculation

8.7.1 Concrete Formulations of Dynamic Equations and Network Equations

8.7.1.1 Generator rotor motion equation

$$\frac{d\delta_i}{dt} = 2\pi f_0(\omega_i - 1) \quad (i = 1, 2, 3) \tag{8.194}$$

$$\frac{d\omega_i}{dt} = \frac{1}{T_{Ji}}[P_{mi} - P_{Ei} - P_{Di}(\omega_i - 1)] \tag{8.195}$$

where:

P_{mi}—output power for generator steady-state, $P_{mi} = P_{i0}$.
P_{Ei}—generator electromagnetic power.
P_{Di}—generator damping coefficient, the electromagnetic power P_{Ei} could be derived from the following equation:

$$\begin{aligned} P_{Ei} &= \mathrm{Re}\left[\dot{U}_i \hat{\dot{I}}\right] \\ &= \mathrm{Re}\left[\frac{\dot{U}_i \cdot \hat{\dot{E}}'_i - \hat{\dot{U}}_i}{-jX'_{di}}\right] \\ &= \mathrm{Re}\left[\frac{\left(U_{xi} + jU_{yi}\right)\left(E'_{xi} + jE'_{yi}\right) - \left(U_{xi} + jU_{yi}\right)\left(U_{xi} + jU_{yi}\right)}{-jX'_{di}}\right] \\ &= \mathrm{Re}\left[\left(U_{xi}E'_{yi} - U_{yi}E'_{xi}\right)/X'_{di} + j\left(U_{xi}E'_{xi} + U_{yi}E'_{yi} - U_{xi}^2 - U_{yi}^2\right)/X'_{di}\right] \\ &= \left(U_{xi}E'_{yi} - U_{yi}E'_{xi}\right)/X'_{di} = \frac{E'_i U_i}{X'_{di}}\sin(\delta_i - \alpha_i) \end{aligned} \tag{8.196}$$

The initial value of the differential equation is:

$$\begin{cases} \delta_i(0) = \delta_{i0} \\ \omega_i(0) = \omega_0 = 1 \end{cases} \tag{8.197}$$

8.7.1.2 Bus voltage equation of power network

The general form of the bus voltage equation described by the admittance matrix is:

$$\dot{Y}\dot{U} = \dot{I} \tag{8.198}$$

where:

$\dot{I}$—column vector of bus injection current.
$\dot{U}$—column vector of bus voltage.
$\dot{Y}$—bus admittance matrix.

If Eq. (8.198) written in real form is:

$$YU = I \tag{8.199}$$

(1) Dynamic stability calculation matrix $\dot{Y}$. The dynamic calculation matrix $\dot{Y}$ is based on the network connection matrix $\dot{\overline{Y}}$ (i.e., the load flow calculation matrix $\dot{\overline{Y}}$), considering the generator and the load equivalent circuit, through the correction of the corresponding node of the diagonal elements of the matrix $\dot{\overline{Y}}$, so the formation of the matrix can be divided into two steps.

(a) $\dot{\overline{Y}}$ matrix for power flow calculation. In line with the network structure specified in Fig. 8.8, the elements in $\dot{\overline{Y}}$ matrix could be formulated as:

$$\dot{\overline{Y}}_{ii} = \sum_{j \in i} \frac{1}{\dot{Z}_{ij}} \tag{8.200}$$

$$\dot{\overline{Y}}_{ij} = -\frac{1}{\dot{Z}_{ij}} \tag{8.201}$$

where $\dot{Z}_{ij}$ ——— $i-j$ line impedance.

(b) $\dot{Y}$ matrix for dynamic stability calculation. Add in the impact of the generator transient reactance and load equivalent impedance on the $\dot{\overline{Y}}$ matrix for power flow calculation, then $\dot{Y}$ matrix for dynamic stability calculation could be formed, as the generator transient reactance and load equivalent impedance are equivalent to the earth elements. Therefore, when formulating the $\dot{Y}$ matrix, it just needs to change the main diagonal elements of the corresponding bus in the $\dot{\overline{Y}}$ matrix.

$$\dot{Y}_{ii} = \dot{\overline{Y}}_{ii} + \frac{1}{jX'_{\mathrm{d}i}} + \frac{1}{R_{\mathrm{L}i} + jX_{\mathrm{L}i}} \tag{8.202}$$

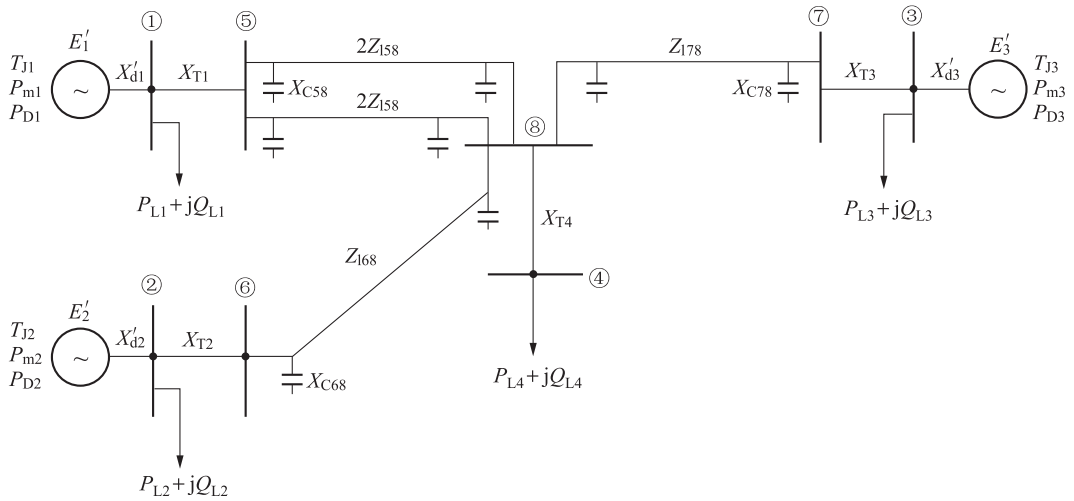

Fig. 8.8
Network diagram for simulation calculation.

$$\dot{Y}_{ij} = \dot{\overline{Y}}_{ij} \tag{8.203}$$

In Eq. (8.202), the second item on the right side is the reciprocal of the added generator transient reactance, and the third item is the reciprocal of the load equivalent impedance; whether to add in them or not shall be determined according to the current situation of the actual bus.

Let:

$$\dot{Y}_{ij} = G_{ij} + jB_{ij}, \quad i, j, = 1, \ldots, 8 \tag{8.204}$$

Then substitute each element $\dot{Y}$ matrix in Eqs. (8.202), (8.203) with second order submatrix as follows:

$$Y_{ij} = \begin{bmatrix} G_{ij} & -B_{ij} \\ B_{ij} & G_{ij} \end{bmatrix} \tag{8.205}$$

So as to write $\dot{Y}$ matrix into the real form consisted of the second order submatrix:

$$Y = \left[\left[Y_{ij} \right]_{2\times 2} \right]_{16\times 16} = \left[\left[\begin{matrix} G_{ij} & -B_{ij} \\ B_{ij} & G_{ij} \end{matrix} \right] \right]_{16\times 16} \tag{8.206}$$

(2) Formulation of column vector I for bus injection current.

When the generator bus is an active bus, its injection current is:

$$\dot{I}_i = \frac{\dot{E}'_i}{jX'_{di}} = \frac{E'_{yi}}{X'_{di}} - j\frac{E'_{xi}}{X'_{di}} \quad (i = 1, 2, 3) \tag{8.207}$$

For passive bus, its injection current is 0, that is

$$\dot{I}_k = 0, k = 4, \cdots, 8 \tag{8.208}$$

(correspond to buses ④–⑧ in Fig. 8.8).

Eqs. (8.207), (8.208) could constitute the column vector of the bus injection current:

$$\dot{I} = \left[\dot{I}_1, \dot{I}_2, \dot{I}_3, 0, 0, 0, 0, 0\right]^{\mathrm{T}} \tag{8.209}$$

Write Eq. (8.209) into real form in correspondence with real Y matrix:

$$I = \left[I_{x1}, I_{y1}, I_{x2}, I_{y2}, I_{x3}, I_{y3}, \underbrace{0, \ldots,}_{10\ \text{pcs}}\right]^{\mathrm{T}} \tag{8.210}$$

where:

$$I_{xi} = \frac{E'_{yi}}{X'_{\mathrm{d}i}}, \quad I_{yi} = -\frac{E'_{xi}}{X'_{\mathrm{d}i}} \quad (i = 1, 2, 3) \tag{8.211}$$

(3) Formulation of column vector for bus voltage.

$$U = \left\lfloor \dot{U}_1 \cdots \dot{U}_8 \right\rfloor^{\mathrm{T}} \tag{8.212}$$

Write it into real form in correspondence with real Y matrix:

$$U = \left\lfloor U_{x1}, Y_{y1} \ldots U_{x8}, U_{y8} \right\rfloor^{\mathrm{T}} \tag{8.213}$$

where:

$$\dot{U} = U_{xi} + jU_{yi} = U_i \angle \alpha_i \quad (i = 1, \cdots, 8) \tag{8.214}$$

8.7.2 Calculation of Fault Equivalent Impedance

In the calculation, it is assumed that the equivalent impedance of each type of fault has been known; what follows is how to use the known fault equivalent impedance to modify the $\dot{Y}$ matrix for dynamic stability calculation.

(1) The short circuit equivalent impedance: To simplify the modification of Y matrix, it is assumed that all the short circuit faults happen on the bus. In this way, just modify the corresponding diagonal element of the original $\dot{Y}$ matrix when a short circuit fault occurs in the system.

Let the equivalent impedance of the short circuit fault $\dot{Z}_{\mathrm{FS}}$ be:

$$\dot{Z}_{\mathrm{FS}i} = R_{\mathrm{FS}i} + jX_{\mathrm{FS}i} \quad (i \in [1, 8]) \tag{8.215}$$

The diagonal element of $\dot{Y}$ matrix for the corresponding bus during the fault could be modified as:

$$\dot{Y}_{sii} = \left(C_{ii} + \frac{R_{\mathrm{FS}i}}{R_{\mathrm{FS}i}^2 + X_{\mathrm{FS}i}^2}\right) + j\left(B_{ii} - \frac{X_{\mathrm{FS}i}}{R_{\mathrm{FS}i}^2 + X_{\mathrm{FS}i}^2}\right) \tag{8.216}$$

In Y matrix in real form, it is needed to modify the corresponding element of the main diagonal second-order submatrix:

$$Y_{\mathrm{S}ii} = \begin{bmatrix} G_{ii} + \dfrac{R_{\mathrm{FS}i}}{R_{\mathrm{FS}i}^2 + X_{\mathrm{FS}i}^2}, & -\left(B_{ii} - \dfrac{X_{\mathrm{FS}i}}{R_{\mathrm{FS}i}^2 + X_{\mathrm{FS}i}^2}\right) \\ B_{ii} - \dfrac{X_{\mathrm{FS}i}}{R_{\mathrm{FS}i}^2 + X_{\mathrm{FS}i}^2}, & G_{ii} + \dfrac{R_{\mathrm{FS}i}}{R_{\mathrm{FS}i}^2 + X_{\mathrm{FS}i}^2} \end{bmatrix} \tag{8.217}$$

(2) Disconnect the equivalent impedance. Assume after the system fault and before the reclosing, the disconnection equivalent impedance of open phase operation or single-circuit line has been known, let the disconnection equivalent impedance $\dot{Z}_{\mathrm{FD}}$ be

$$\dot{Z}_{\mathrm{FD}ij} = R_{\mathrm{FD}ij} + jX_{\mathrm{FD}ij} \tag{8.218}$$

where i is the fault bus number, and i and j are the two terminal bus number of the fault line.

As the disconnection equivalent impedance is in series connection with the fault line i-j, not only the diagonal elements $\dot{Y}_{ii}$and $\dot{Y}_{ij}$ of $\dot{Y}$ matrix for dynamic stability calculation, but also the non-diagonal elements $\dot{Y}_{ii}$and $\dot{Y}_{jj}$ of $\dot{Y}$ matrix need to be modified.

$$\begin{aligned} \dot{Y}_{\mathrm{D}ij} = &\left[G_{ii} - \frac{R_{1ij}}{R_{1ij}^2 + X_{1ij}^2} + \frac{R_{1ij} + R_{\mathrm{FD}ij}}{\left(R_{1ij} + R_{\mathrm{FD}ij}\right)^2 + \left(X_{1ij} + X_{\mathrm{FD}ij}\right)^2}\right] \\ &+ j\left[B_{ii} + \frac{X_{1ij}}{R_{1ij}^2 + X_{1ij}^2} - \frac{X_{1ij} + X_{\mathrm{FD}ij}}{\left(R_{1ij} + R_{\mathrm{FD}ij}\right)^2 + \left(X_{1ij} + X_{\mathrm{FD}ij}\right)^2}\right] \end{aligned} \tag{8.219}$$

$$\begin{aligned} \dot{Y}_{\mathrm{D}jj} = &\left[G_{jj} - \frac{R_{1ij}}{R_{1ij}^2 + X_{1ij}^2} + \frac{R_{1ij} + R_{\mathrm{FD}ij}}{\left(R_{1ij} + R_{\mathrm{FD}ij}\right)^2 + \left(X_{1ij} + X_{\mathrm{FD}ij}\right)^2}\right] \\ &+ j\left[B_{jj} + \frac{X_{1ij}}{R_{1ij}^2 + X_{1ij}^2} - \frac{X_{1ij} + X_{\mathrm{FD}ij}}{\left(R_{1ij} + R_{\mathrm{FD}ij}\right)^2 + \left(X_{1ij} + X_{\mathrm{FD}ij}\right)^2}\right] \end{aligned} \tag{8.220}$$

$$\begin{aligned} \dot{Y}_{\mathrm{D}ij} = \dot{Y}_{\mathrm{D}ji} = &\left[\frac{R_{1ij} + R_{\mathrm{FD}ij}}{\left(R_{1ij} + R_{\mathrm{FD}ij}\right)^2 + \left(X_{1ij} + X_{\mathrm{FD}ij}\right)^2}\right] \\ &+ j\left[\frac{X_{1ij} + X_{\mathrm{FD}ij}}{\left(R_{1ij} + R_{\mathrm{FD}ij}\right)^2 + \left(X_{1ij} + X_{\mathrm{FD}ij}\right)^2}\right] \end{aligned} \tag{8.221}$$

In the above three equations, $\dot{Z}_{1ij} = R_{1ij} + jX_{eij}$ is the impedance of *i-j* line. In addition, follow the method for modifying the short circuit admittance matrix, write the above three equations into the corresponding second-order submatrix form separately, so as to formulate the real form admittance matrix for open-phase operation or single-circuit line operation.

8.7.3 Braking Power Calculation After Braking Resistor Switched on

Electric brake uses excessive energy consumption method to improve the unit power imbalance situation, thereby improving the dynamic stability of the system.

R_{ZD} is used to express the brake resistance value. When switching on the brake resistor, the main diagonal element of the corresponding bus $\dot{Y}$ matrix is modified as:

$$\dot{Y}_{ZD_{ii}} = \left(G_{ii} + \frac{1}{R_{ZD_{ii}}}\right) + jB_{ii} \quad (i \in [1,3]) \tag{8.222}$$

The braking power absorbed by the brake resistance R_{ZD} during the brake is:

$$P_{ZD_i} = \left|\dot{U}_i\right|^2 / R_{ZD_i} = \left(U_{xi}^2 + U_{yi}^2\right) / R_{ZD_i} \tag{8.223}$$

8.7.4 Calculation of the First Stage Control Criterion (Energy Equilibrium)

8.7.4.1 Calculation of excess kinetic energy ΔW_i

To meet the demand of per-unit calculation, it is required to transform the equation for calculating excess kinetic energy as follows:

As:

$$\begin{aligned} \Delta W_i(t_p) &= \frac{1}{2} J_i \left[\omega_i^2(t_p) - \omega_i^2(t_0)\right] \\ &= \frac{1}{2} J_i \left[\omega_i^2(t_p) - \omega_i^2\right] \end{aligned} \tag{8.224}$$

where:

$$\omega_0 = 2\pi f_0$$
$$J_i = \frac{T_{Ji}}{2\pi f_0}$$

So

$$\begin{aligned} \Delta W_i(t_p) &= \frac{1}{2} J_i \left[\omega_i^2(t_p) - \omega_0^2\right] \\ &= \frac{1}{2} \frac{T_{Ji}}{2\pi f_0} \left[\omega_i^2(t_p) - (2\pi f_0)^2\right] \end{aligned}$$

$$
\begin{aligned}
&= \frac{1}{2}\frac{T_{\mathrm{J}i}}{2\pi f_0}\cdot(2\pi f_0)^2\left[\left(\frac{\omega_i^2(t_\mathrm{p})}{2\pi f_0}\right)^2-1\right]\\
&= \pi f_0 T_{\mathrm{J}i}\left[\omega_{*i}^2(t_\mathrm{p})-1\right]
\end{aligned}
\tag{8.225}
$$

where ω_{*i} is the per-unit value of the rotational speed with $2\pi f_0$ as the benchmark. In the case of triggering no confusion, still write ω_{*i} also into ω_i, and Eq. (8.225) could become:

$$
\Delta W_i(t_\mathrm{p}) = \pi f_0 T_{\mathrm{J}i}\left[\omega_i^2(t_\mathrm{p})-1\right] \tag{8.226}
$$

where t_p is the time for clearing the fault.

8.7.4.2 Calculation of absorbed energy ΔW_{bi} during the braking

$$
\begin{aligned}
\Delta W_{\mathrm{b}i}(t_1) &= \frac{1}{2}J_i\left[\omega_i^2(t_1)-\omega_i^2(t_\mathrm{p})\right]\\
&= \frac{1}{2}\frac{T_{\mathrm{J}i}}{2\pi f_0}(2\pi f_0)^2\left[\left(\frac{\omega_i(t_1)}{2\pi f_0}\right)^2-\left(\frac{\omega_i(t_\mathrm{p})}{2\pi f_0}\right)^2\right]\\
&= \pi f_0 T_{\mathrm{J}i}\left[\omega_{*i}^2(t_1)-\omega_{*i}^2(t_\mathrm{p})\right]
\end{aligned}
\tag{8.227}
$$

where $t_1 > t_\mathrm{p}$ is the final value for braking. Likewise, in the case of triggering no confusion, still write ω_{*i} into ω_i, and Eq. (8.227) could written into:

$$
\Delta W_{\mathrm{b}i}(t_1) = \pi f_0 T_{\mathrm{J}i}\left[\omega_i^2(t_1)-\omega_i^2(t_\mathrm{p})\right] \tag{8.228}
$$

8.7.4.3 Calculation of the first stage control criterion and optimal clearing time

As

$$
\begin{cases}
\Delta W_i(t_\mathrm{p}) = \pi f_0 T_{\mathrm{J}i}\left[\omega_i^2(t_\mathrm{p})-1\right]\\
\Delta W_{\mathrm{b}i}(t_1) = \pi f_0 T_{\mathrm{J}i}\left[\omega_i^2(t_1)-\omega_i^2(t_\mathrm{p})\right]
\end{cases}
\tag{8.229}
$$

So

$$
\begin{aligned}
&\Delta W_i(t_\mathrm{p}) + \Delta W_{\mathrm{b}i}(t_1)\\
&\quad= \pi f_0 T_{\mathrm{J}i}\left(\omega_i^2(t_\mathrm{p})-1\right)+\pi f_0 T_{\mathrm{J}i}\left(\omega_i^2(t_1)-\omega_i^2(t_\mathrm{p})\right)\\
&\quad= \pi f_0 T_{\mathrm{J}i}\left(\omega_i^2(t_1)-1\right)
\end{aligned}
\tag{8.230}
$$

Therefore, the first stage control criterion (energy equilibrium) could be summarized as:

$$
\pi f_0 T_{\mathrm{J}i}\left[\omega_i^2(t_\mathrm{p})-1\right] = 0 \tag{8.231}
$$

When this equation is established, the electric braker should be cleared, then t_1 is the optimal clearing time for the electric braking (the optimal backswing potential in minimum sense).

As the digital computer follows discrete calculation, it is fairly difficult for Eq. (8.231) to be equal to 0 in rigid sense. Therefore, in the actual calculation, judge by the following inequality to determine the brake clearing time t_1:

$$\pi f_0 T_{\mathrm{J}i}\left[\omega_i^2(t_1)-1\right]\le 0 \tag{8.232}$$

8.7.5 Calculation of Observation Decoupled State Vector and the Second Stage Control Criterion

8.7.5.1 Calculation of decoupling reference δ_{ei}

As a time-varying transient variable, the decoupled reference δ_{ei} is uniquely determined by the time-varying data set $\{E_i', P_{mi}, P_{Li}, Q_{Li}, U_j, \alpha_j, u_i\}$. In line with the network shown in Fig. 8.8, the equivalent network for calculating δ_{ei} is shown in Fig. 8.9.

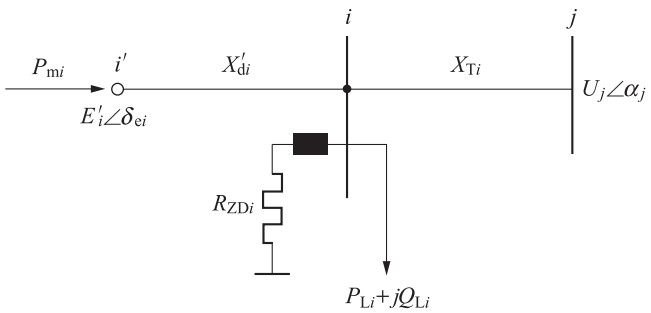

Fig. 8.9
Equivalent network for calculating δ_{ei}.

The process of calculating δ_{ei} refers to the power flow for deriving the previous network structure, where bus j is a $V\theta$ bus, bus i is a PQ bus, and bus i' is a PV bus. Derive the load power of bus i from the following equation:

$$\begin{aligned} P_{Li}+jQ_{Li} &= -\frac{\dot{U}_i\hat{\dot{U}}_i}{\hat{\dot{Z}}_{mi}} \\ &= -\frac{\left(U_{xi}+jU_{yi}\right)\left(U_{xi}-\mathrm{J}U_{yi}\right)}{R_{Li}-jX_{Li}} \\ &= \left(-\frac{U_{xi}^2+U_{yi}^2}{R_{Li}^2+X_{Li}^2}R_{Li}\right)+j\left(-\frac{U_{xi}^2+U_{yi}^2}{R_{Li}^2+X_{Li}^2}X_{Li}\right) \end{aligned} \tag{8.233}$$

It is assumed that the direction of the load current is the direction of the incoming network (opposite of the arrow in Fig. 8.9).

Because solving δ_{ei} involves a nonlinear algebraic equation, it can only be solved by iterative method, and the fast convergence Newton iterative method can be used.

The general form of the Newton iterative method for solving nonlinear algebraic equations is as follows.

It is known that:

$$F(X)=0 \tag{8.234}$$

is a nonlinear algebraic equation.

If:

$$J(X)=\frac{\partial F}{\partial X} \tag{8.235}$$

Then the following iterative formula could be derived:

$$F\left(X^{(k)}\right)=J\left(X^{(k)}\right)\cdot\Delta X^{(k)} \tag{8.236}$$

$$X^{(k+1)}=X^{(k)}-\Delta X^{(k)} \tag{8.237}$$

Solve Eqs. (8.236), (8.237) iteratively until one of the following inequalities is satisfied, then the iteration reaches convergence:

$$\|\Delta X^{(k)}\|<\varepsilon_1 \tag{8.238}$$

$$\|FX^{(k)}\|<\varepsilon_2 \tag{8.239}$$

where ε_1 and ε_2 are very small positive numbers, and $\|\Delta X^{(k)}\|$ and $\|F^{(k)}\|$ are the maximum absolute value in $\|\Delta X^{(k)}\|$ and $\|F^{(k)}\|$, respectively.

In the network shown in Fig. 8.8, the same structural equivalent network is used for all generator nodes to solve the decoupled reference δ_{ei}, so only a unified iterative formula needs to be given, and the parameters of different nodes can be substituted respectively in the calculation.

For the convenience of calculation, the networks shown in Fig. 8.9 are renumbered, and it is shown in Fig. 8.10.

In line with the network shown in Fig. 8.10, calculate the angle α_{E3} of voltage U_{E3} in bus (3), that is, the decoupled reference δ_{ei} of the original generator bus. The Newton iteration formula for solving δ_e is listed in following steps.

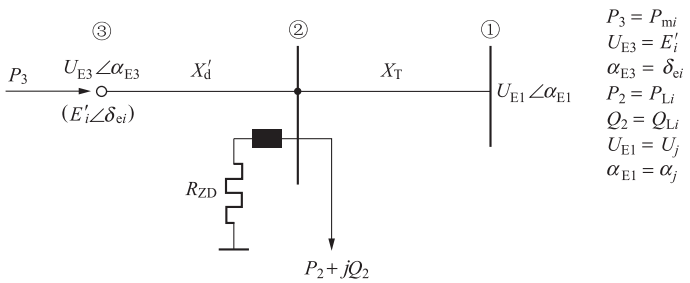

Fig. 8.10
Uniform network for the calculation of δ_e.

(1) Constitute a network admittance matrix$\dot{Y}_E$, where:

$$\left.\begin{aligned}
\dot{Y}_{E11} &= -j\frac{1}{X_T} \\
\dot{Y}_{E12} &= \dot{Y}_{E21} = j\frac{1}{X_T} \\
\dot{Y}_{E13} &= \dot{Y}_{E31} = 0 \\
\dot{Y}_{E22} &= -j\left(\frac{1}{X_T}+\frac{1}{X'_d}\right) \\
\dot{Y}_{E23} &= \dot{Y}_{E32} = j\frac{1}{X'_d} \\
\dot{Y}_{E33} &= -j\frac{1}{X'_d}
\end{aligned}\right\} \tag{8.240}$$

This is the admittance matrix for solving δ_{ei} without control. When switching on the brake resistor, $\dot{Y}_{E22}$ element of $\dot{Y}_E$ matrix should be modified as follows:

$$\dot{Y}_{FZD22} = \frac{1}{R_{ZD}} - j\left(\frac{1}{X_T}+\frac{1}{X'_d}\right) \tag{8.241}$$

Let the element in $\dot{Y}_E$ matrix be:

$$\dot{Y}_{Eij} = G_{eij} + jB_{eij} \quad (i,j=1,2,3) \tag{8.242}$$

Then write the $\dot{Y}_E$ matrix into the admittance matrix in real form consisted of the second-order submatrix:

$$Y_{Eij} = \begin{bmatrix} G_{eij} & -B_{eij} \\ B_{eij} & G_{eij} \end{bmatrix} \tag{8.243}$$

(2) The power equation of PQ bus and PV bus: The basic equation for solving the power flow via Newton method is:

$$\dot{Y}_{\mathrm{E}}\dot{U}_{\mathrm{E}} = \hat{\dot{S}}/\hat{\dot{U}}_{\mathrm{E}} \tag{8.244}$$

where the definition of $\dot{Y}_{\mathrm{E}}$ is the same as the previous one, $\dot{U}_{\mathrm{E}}$ is the bus voltage vector, S is the bus injection vector, and their component forms are as follows:

$$\dot{U}_{\mathrm{E}} = \left[\dot{U}_{\mathrm{E1}}, \dot{U}_{\mathrm{E2}}, \dot{U}_{\mathrm{E3}}\right]^{\mathrm{T}} \tag{8.245}$$

$$\dot{S} = \left[P_1, jQ_1, P_2 + jQ_2, P_3 + jQ_3\right]^{\mathrm{T}} \tag{8.246}$$

Written in real form respectively as:

$$U_{\mathrm{E}} = \left[U_{\mathrm{EX1}}, U_{\mathrm{EY1}}, U_{\mathrm{EX2}}, U_{\mathrm{EY2}}, U_{\mathrm{EX3}}, U_{\mathrm{EY3}}\right] \tag{8.247}$$

$$S = \left[P_1, Q_1, P_2, Q_2, P_3, Q_3\right]^{\mathrm{T}} \tag{8.248}$$

Eq. (8.244) is expanded to separate the real and imaginary parts, and the items are written in the form of a modified equation:

$$\Delta P_i = P_i - \sum_{j=1}^{3}\left[U_{\mathrm{E}xi}\left(G_{eij}U_{\mathrm{E}xj} - B_{eij}U_{\mathrm{E}yi}\right) + U_{\mathrm{E}yi}\left(G_{eii}U_{\mathrm{E}yj} + B_{eij}U_{\mathrm{E}xj}\right)\right] = 0 \quad (i = 2, 3) \tag{8.249}$$

$$\Delta Q_i = Q_i - \sum_{j=1}^{3}\left[U_{\mathrm{E}yi}\left(G_{eij}U_{\mathrm{E}xj} - B_{eij}U_{\mathrm{E}yi}\right) + U_{\mathrm{E}xi}\left(G_{eij}U_{\mathrm{E}yj} + B_{eij}U_{\mathrm{E}xj}\right)\right] = 0 \quad (i = 2) \tag{8.250}$$

(3) The voltage equation of PV bus: Its modified equation follows the form:

$$\Delta U_{\mathrm{E}i}^2 = U_{\mathrm{E}i}^2 - \left(U_{\mathrm{E}xi}^2 + U_{\mathrm{E}yi}^2\right) = 0 \quad (i = 3) \tag{8.251}$$

(4) The formulation of Newton iteration equation: The matrix from of the Newton iteration formula for the network shown in Fig. 8.10 as follows:

$$\begin{bmatrix} \Delta P_2^{(k)} \\ \Delta Q_2^{(k)} \\ \Delta P_3^{(k)} \\ \Delta U_{\mathrm{E3}}^{(k)2} \end{bmatrix} = \begin{bmatrix} H_{22}^{(k)} & N_{22}^{(k)} & H_{23}^{(k)} & N_{23}^{(k)} \\ J_{22}^{(k)} & L_{22}^{(k)} & J_{23}^{(k)} & L_{23}^{(k)} \\ H_{32}^{(k)} & N_{32}^{(k)} & H_{33}^{(k)} & N_{33}^{(k)} \\ R_{32}^{(k)} & S_{32}^{(k)} & R_{33}^{(k)} & S_{33}^{(k)} \end{bmatrix} \begin{bmatrix} \Delta U_{\mathrm{E}x2}^{(k)} \\ \Delta U_{\mathrm{E}y2}^{(k)} \\ \Delta U_{\mathrm{E}x3}^{(k)} \\ \Delta U_{\mathrm{E}y3}^{(k)} \end{bmatrix} \tag{8.252}$$

$$\begin{bmatrix} \Delta U_{\mathrm{Ex2}}^{(k+1)} \\ \Delta U_{\mathrm{Ey2}}^{(k+1)} \\ \Delta U_{\mathrm{Ex3}}^{(k+1)} \\ \Delta U_{\mathrm{Ey3}}^{(k+1)} \end{bmatrix} = \begin{bmatrix} U_{\mathrm{Ex2}}^{(k)} \\ U_{\mathrm{Ey2}}^{(k)} \\ U_{\mathrm{Ex3}}^{(k)} \\ U_{\mathrm{Ey3}}^{(k)} \end{bmatrix} - \begin{bmatrix} \Delta U_{\mathrm{Ex2}}^{(k)} \\ \Delta U_{\mathrm{Ey2}}^{(k)} \\ \Delta U_{\mathrm{Ex3}}^{(k)} \\ \Delta U_{\mathrm{Ey3}}^{(k)} \end{bmatrix} \tag{8.253}$$

Repeatedly solve Eqs. (8.252), (8.253), and the iteration converges until the correction vector $\{\Delta U_{\mathrm{E}}\}$ satisfies the following inequality:

$$\left\| \left[\Delta U_{\mathrm{Ex2}}^{(k)}, \Delta U_{\mathrm{Ey2}}^{(k)}, \Delta U_{\mathrm{Ex3}}^{(k)}, \Delta U_{\mathrm{Ey3}}^{(k)} \right]^{\mathrm{T}} \right\| < \varepsilon \tag{8.254}$$

The details for the iteration Eq. (8.251) are as follows:

$$\Delta P_2^{(k)} = P_2 - \sum_{j=1}^{3} \left[U_{\mathrm{Ex2}}^{(k)} \left(C_{\mathrm{e}2j} U_{\mathrm{Ex}j}^{(k)} - B_{\mathrm{e}3j} U_{\mathrm{Ey}j}^{(k)} + U_{\mathrm{Ey2}}^{(k)} \left(G_{\mathrm{e}2j} U_{\mathrm{Ey}j}^{(k)} + B_{\mathrm{e}2j} U_{\mathrm{Ex}j}^{(k)} \right) \right) \right] \tag{8.255}$$

$$\Delta Q_2^{(k)} = Q_2 - \sum_{j=1}^{3} \left[U_{\mathrm{Ey2}}^{(k)} \left(C_{\mathrm{e}2j} U_{\mathrm{Ex}j}^{(k)} - B_{\mathrm{e}3j} U_{\mathrm{Ey}j}^{(k)} + U_{\mathrm{Ey2}}^{(k)} \left(G_{\mathrm{e}2j} U_{\mathrm{Ey}j}^{(k)} + B_{\mathrm{e}2j} U_{\mathrm{Ex}j}^{(k)} \right) \right) \right] \tag{8.256}$$

$$\Delta P_3^{(k)} = P_3 - \sum_{j=1}^{3} \left[U_{\mathrm{Ex3}}^{(k)} \left(C_{\mathrm{e}3j} U_{\mathrm{Ex}j}^{(k)} - B_{\mathrm{e}3j} U_{\mathrm{Ey}j}^{(k)} + U_{\mathrm{Ey3}}^{(k)} \left(G_{\mathrm{e}3j} U_{\mathrm{Ey}j}^{(k)} + B_{\mathrm{e}3j} U_{\mathrm{Ex}j}^{(k)} \right) \right) \right] \tag{8.257}$$

$$\Delta U_{\mathrm{E3}}^{(k)2} = U_{\mathrm{E3}}^2 - \left(U_{\mathrm{Ex2}}^{(k)2} + U_{\mathrm{Ey3}}^{(k)2} \right) \tag{8.258}$$

$$H_{22}^{(k)} = -2G_{e22} U_{\mathrm{Ex2}}^{(k)} - \sum_{\substack{j=1 \\ j \neq 2}}^{3} \left(G_{e2j} U_{\mathrm{Ex}j}^{(k)} - B_{e2j} U_{\mathrm{Ey}j}^{(k)} \right) \tag{8.259}$$

$$N_{22}^{(k)} = -2G_{e22} U_{\mathrm{Ey2}}^{(k)} - \sum_{\substack{j=1 \\ j \neq 2}}^{3} \left(G_{e2j} U_{\mathrm{Ey}j}^{(k)} + B_{e2j} U_{\mathrm{Ex}j}^{(k)} \right) \tag{8.260}$$

$$J_{22}^{(k)} = 2B_{e22} U_{\mathrm{Ex2}}^{(k)} + \sum_{\substack{j=1 \\ j \neq 2}}^{3} \left(G_{e2j} U_{\mathrm{Ex}j}^{(k)} + B_{e2j} U_{\mathrm{Ey}j}^{(k)} \right) \tag{8.261}$$

$$L_{22}^{(k)} = 2B_{e22} U_{\mathrm{Ey2}}^{(k)} - \sum_{\substack{j=1 \\ j \neq 2}}^{3} \left(G_{e2j} U_{\mathrm{Ex}j}^{(k)} - B_{e2j} U_{\mathrm{Ey}j}^{(k)} \right) \tag{8.262}$$

$$H_{33}^{(k)} = -2B_{e33}U_{Ey3}^{(k)} - \sum_{j=1}^{2}\left(G_{e3j}U_{Exj}^{(k)} - B_{e3j}U_{Eyj}^{(k)}\right) \tag{8.263}$$

$$N_{33}^{(k)} = -2B_{e33}U_{Ey3}^{(k)} - \sum_{j=1}^{2}\left(G_{e3j}U_{Eyj}^{(k)} - B_{e3j}U_{Exj}^{(k)}\right) \tag{8.264}$$

$$R_{33}^{(k)} = -2U_{Ey3}^{(k)} \tag{8.265}$$

$$S_{33}^{(k)} = -2U_{Ey3}^{(k)} \tag{8.266}$$

$$H_{23}^{(k)} = -G_{e23}U_{Ey2}^{(k)} - B_{e23}U_{Ey2}^{(k)} \tag{8.267}$$

$$N_{23}^{(k)} = -G_{e23}U_{Ey2}^{(k)} - B_{e23}U_{Ex2}^{(k)} \tag{8.268}$$

$$J_{23}^{(k)} = -G_{e23}U_{Ey2}^{(k)} - B_{e23}U_{Ex2}^{(k)} \tag{8.269}$$

$$L_{23}^{(k)} = G_{e23}U_{Ex2}^{(k)} - B_{e23}U_{Ey2}^{(k)} \tag{8.270}$$

$$H_{32}^{(k)} = -G_{e32}U_{Ex3}^{(k)} - B_{e32}U_{Ey3}^{(k)} \tag{8.271}$$

$$N_{32}^{(k)} = -G_{e32}U_{Ey3}^{(k)} + B_{e32}U_{Ex3}^{(k)} \tag{8.272}$$

$$R_{32}^{(k)} = 0 \tag{8.273}$$

$$S_{32}^{(k)} = 0 \tag{8.274}$$

(5) The selection of initial value of iteration: The selection of the initial value in Newton iteration method is more stringent. For the general current power flow program of the Newton method, the average value of the initial voltage is normally selected as the initial value, that is:

$$U_{xi}^{(0)} = 1, \quad U_{yi}^{(0)} = 0 \tag{8.275}$$

However, in the observation decoupled state space, the system steady equilibrium point is in the origin $\{0, 0\}$ of the space as follows:

$$\overline{\delta} = \delta_0 - \delta_e = 0 \tag{8.276}$$

Viz.:

$$\delta_e = \delta_0 \tag{8.277}$$

That is, the decoupled reference δ_e is equal to the steady power angle δ_0 of the generator during the steady operation. Likewise, the angle of other buses in Fig. 8.9 network is also equal to the voltage angle of the corresponding bus in the original system during steady operation. During the system swing, the operating point in the observation decoupled state space will deviate from the original one, and such deviation differs depending on the degree of disturbance. Generally

speaking, if the system could ensure no loss of synchronism within the first swing period, then the state deviation will oscillate near to the origin of the observation decoupled state space. Based on this, it is proper to deem the modulus value and angle of the voltage as the iteration initial value for solving δ_{ei} at t moment. Therefore, when making iteration calculation in line with the renumbered network in Fig. 8.10, the initial value and constant in the iteration could be as follows:

$$U_{\mathrm{E}x1} = U_{xj}(t) \tag{8.278}$$

$$U_{\mathrm{E}y1} = U_{yj}(t) \tag{8.279}$$

$$U_{\mathrm{E}x2}^{(0)} = U_{xi}(t) \tag{8.280}$$

$$U_{\mathrm{E}y2}^{(0)} = U_{yi}(t) \tag{8.281}$$

$$U_{\mathrm{E}x3}^{(0)} = E_i' \cos\delta_i(t) \tag{8.282}$$

$$U_{\mathrm{E}y3}^{(0)} = E_i' \sin\delta_i(t) \tag{8.283}$$

$$P_2 = -R_{\mathrm{L}i}\left[U_{xi}^2(t) + U_{yi}^2(t)/\left(R_{\mathrm{L}i}^2 + X_{\mathrm{L}i}^2\right)\right. \tag{8.284}$$

$$Q_2 = -X_{\mathrm{L}i}\left[U_{xi}^2(t) + U_{yi}^2(t)/\left(R_{\mathrm{L}i}^2 + X_{\mathrm{L}i}^2\right)\right. \tag{8.285}$$

$$P_3 = P_{\mathrm{m}i} \tag{8.286}$$

$$U_{\mathrm{E}3} = E'_{\ i} \tag{8.287}$$

The initial value is involved in the iteration. The actual calculation shows that the iteration is convergent after one to two times for the steady-state, and after three to seven times for the dynamic disturbance, which means that the previous initial value selection is reasonable.

After the iteration convergence, the decoupled reference δ_{ei} can be solved by the following equation:

$$\delta_{ei} = \arctan\frac{U_{\mathrm{E}y3}^{(k)}}{U_{\mathrm{E}x3}^{(k)}} \tag{8.288}$$

When the system suffers from strong disturbance, neither the convergence nor computation speed can be guaranteed if δ_{ei} is calculated by the iterative method. Therefore, the calculation of δ_{ei} by the iterative method will significantly bring down the reliability of online control.

To raise the calculation speed of δ_{ei} and reliability of online control, we introduce DC power flow calculation equation to approximately derive δ_{ei}. Because DC power flow calculation is a direct solution method requiring no iteration, its calculation could be significantly accelerated and the results are predictable. The DC load flow method for the calculation of generation angle δ_{ei} is given in Appendix C.

8.7.5.2 Calculation of critical control power for norm reduction control criterion

In the simulation calculation, the form $\{\overline{\delta}, \dot{\delta}(50)\}$ of the observation decoupled state space can be used. In this space, the control power based on the norm reduction control criterion could be shown in the following two inequalities:

$$\left.\begin{aligned} u_i &\geq \frac{J_i\overline{\delta}_i\left(\dot{\delta}(50)_i - \dot{\delta}_{ei}\right)}{\dot{\delta}(50)_i} + P_{mi} - P_{Ei} - P_{Di}\dot{\delta}(50)_i \quad \left(\dot{\delta}(50)_i > 0\right) \\ u_i &\leq \frac{J_i\overline{\delta}_i[(\dot{\delta}(50)_i - \dot{\delta}_{ei}]}{\dot{\delta}(50)_i} + P_{mi} - P_{Ei} - P_{Di}\dot{\delta}(50)_i \quad \left(\dot{\delta}(50)_i < 0\right) \end{aligned}\right\} \tag{8.289}$$

Take the per-unit value for the variables in Eq. (8.289), further as $J_i = \dfrac{T_{Ji}}{2\pi f_0}$, then:

$$\left.\begin{aligned} u_i &\geq \frac{T_i\delta_i\left(\dot{\delta}(50)_i - \dot{\delta}_{ei}\right)}{2\pi f_0\dot{\delta}(50)_i} + P_{mi} - P_{Ei} - P_{Di}\dot{\delta}(50)_i \quad \left(\dot{\delta}(50)_i > 0\right) \\ u_i &\leq \frac{T_{Ji}\overline{\delta}_i[(\dot{\delta}(50)_i - \dot{\delta}_{ei}]}{2\pi f_0\dot{\delta}(50)_i} + P_{mi} - P_{Ei} - P_{Di}\dot{\delta}(50)_i \quad \left(\dot{\delta}(50)_i < 0\right) \end{aligned}\right\} \tag{8.290}$$

When the equality sign in Eq. (8.290) is established, the value of u_i is the critical control power.

$$u_i = T_{Ji}\overline{\delta}_i\left[\frac{\left(\dot{\delta}(50)_i - \dot{\delta}_{ei}\right]}{2\pi f_0\dot{\delta}(50)_i} + P_{mi} - P_{Ei} - P_{Di}\dot{\delta}(50)_i \quad (i = 1, 2, 3)\right. \tag{8.291}$$

The invariables in the dynamic stability calculation in Eq. (8.291) are:

T_{Ji}—the inertia constant of generator i.
P_{Di}—the damping coefficient of generator i.
P_{mi}—net power switch on by generator i during steady-state, no change after fault.
f_0—system steady frequency, $f_0 = 50\,\text{Hz}$.

The time-varying variables in the dynamic stability calculation are as follows:

$P_{Ei} = P_{Ei}(t)$—the electromagnetic power of generator i.
$\overline{\delta}_i = \delta_i(t) - \delta_{ei}(t)$—observation decoupled state variable.
$\dot{\delta}(50)_i = \omega_i(t) - 1$—observation decoupled state variable.
$\dot{\delta}_{ei} = \dfrac{\delta_{ei}(t) - \delta_{ei}(t - \Delta t)}{\Delta t}$ the first-order derivative of decoupled reference δ_{ei} (approximated by the first-order backward difference).

Because only electrical brake is considered as the local stability measures in the simulation calculation, which can only step into or cut control power, it is necessary to

convert the critical value u_i expressed by the power into the corresponding equivalent resistance. When the resistance value meets a certain condition, switch on the electric brake. The equivalent resistance of critical value u_i could be derived from the following equation:

$$R_{ui}(t) = \left[U_{xi}^2(t) + U_{yi}^2(t)\right] / u_i(t) \quad (i = 1, 2, 3) \tag{8.292}$$

When $\dot{\delta}(50)_i > 0$, and $R_{ui}(t)$ is less than some definite value, switch on the brake resistor to improve the system dynamic stability, and clear the brake generally when $\dot{\delta}(50)_i$ reverses.

8.8 Implementation

8.8.1 Network Structure and Parameters

The network structure of testing system is shown in Fig. 8.8 (power flow results are shown in Fig. 8.11), which is constructed based on the component parameters of an actual system. There are two generators for detailed study and a system equivalent generator in the testing system, and the network and generator parameters are presented via the per-unit value; its power and voltage references are as follows:

$$S_B = 100\text{MVA} \tag{8.293}$$

$$U_B = 220\text{kV} \tag{8.294}$$

The impedance reference could be derived from:

$$Z_B = U_B^2 / S_B = 484\Omega \tag{8.295}$$

(1) Network parameters

$$\begin{aligned}
&X_{T1} = j0.018140495\\
&X_{T2} = j0.04644628\\
&X_{T3} = j0.037045454\\
&X_{T4} = j0.026549568\\
&Z_{158} = R_{158} + jX_{158} = 0.0076385743 + j0.050457814\\
&Z_{168} = R_{168} + jX_{168} = 0.017355371 + j0.088636363\\
&Z_{178} = R_{178} + jX_{178} = 0.023304508 + j0.076906206\\
&X_{C58} = -j6.794060537\\
&X_{C68} = -j13.23269726\\
&X_{C78} = -j3.390026033
\end{aligned}$$

(2) Generator parameters

$$T_{J1} = 66.56463$$
$$T_{J2} = 17.1665$$
$$T_{J3} = 1{,}000{,}000$$
$$X'_{dl} = j0.048825468$$
$$X'_{d2} = j0.143955782$$
$$X'_{d3} = j0.001$$
$$P_{D1} = 10$$
$$P_{D2} = 10$$
$$P_{D3} = 10$$

(3) Braking resistance: $R_{ZD1} = 0.78943$; $R_{ZD2} = 0.87295$ (related to node 1 and 2).

8.8.2 Operation Mode ⟨I⟩

8.8.2.1 Fault type

The two-phase to the ground fault happens near to line 5–8 bus (5), the fault is cleared at 0.15 s, and the line is successfully reclosed after clearing the fault at 0.7 s. The braking resistance value and the braking switching on-off time in the control scheme are the actual setting values of the original system.

8.8.2.2 Prefault power flow

The prefault power flow is shown in Fig. 8.11.

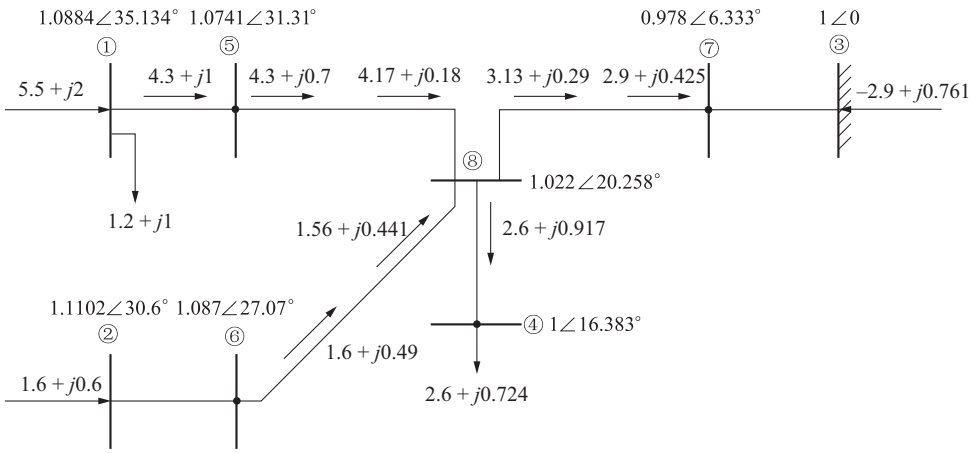

Fig. 8.11
Operation mode ⟨I⟩ of prefault power flow.

8.8.2.3 Results under different control cases

Results of five cases have been given to show the effectiveness of the proposed two-stage control approach. Control schemes of C1–C4 are shown in Table 8.1. As for braking resistance, one braking resistance is switched on node ① in the first stage, and two braking resistances are switched on node ① and node ② in the second stage. To make comparisons, Case 0 is without control; Cases 1 and 2 is with time control in the first stage but with and without control in the second stage; and Cases 3 and 4 are with control in the first stage but with and without control in the second stage.

For the operation time of all cases, fault initial time t_0 is 0.15 s, fault clearing time t_p is 0.3 s, and reclosing time t_z is 1 s. The control results for Cases 1–4 are given in Table 8.2.

The detailed results of each case are explained in the following:

Case 0: No control (loss of synchronism).

Table 8.1 Simulation results of operation mode ⟨I⟩

Case	Control Schemes	I—R_{ZD} (p.u.)	II—R_{ZD} (p.u.)
C0	No control		
C1	I—Time control, II—no control	0.789743	
C2	I—Time control, II-CR2 control	0.789743	1.5, 2.5
C3	I—CR1 control; II—no control	0.35	
C4	I—CR1 control; II—CR2 control	0.35	1.5, 2.5

R_{ZD} (p.u.): Braking resistor (braker). I: first stage; II: second stage; C: case. Time control: braking resistor switching based on presetting time. Energy control: braking resistor switching based on the time by energy equilibrium criterion. Norm control: braking resistor switching based on norm reduction criterion.

Table 8.2 Switching times and actions of cases

Case	First Stage	Second Stage		Results
	t_{E1}-t_{EC1}	t_{N1}-t_{NC1} (s)	t_{N2}-t_{NC2} (s)	
C0				Loss of synchronism
C1	0.3–1.0			Large oscillation
C2	0.3–1.0	1.5–2.225	1.45–2.3	I—oscillation, II—little improved
C3	0.3–0.525			I—large improved, II—oscillation
C4	0.3–0.525	1.575–2.1525	1.825–2.25	Two stage smooth

I—oscillation: power angle curve oscillation in the first stage. II—improved: power angle curve oscillation improved in the second stage. Two stage smooth: power angle curve smooth in both first and second stage. t_{E1}-t_{EC1}: The time for switching on and off braker R_{ZD} in Node 1 in the first stage. t_{N1}-t_{NC1}: The time for switching on and off braker R_{ZD} in Node 1 in the first stage. t_{N2}-t_{NC2}: The time for switching on and off braker R_{ZD} in Node 2 in the second stage.

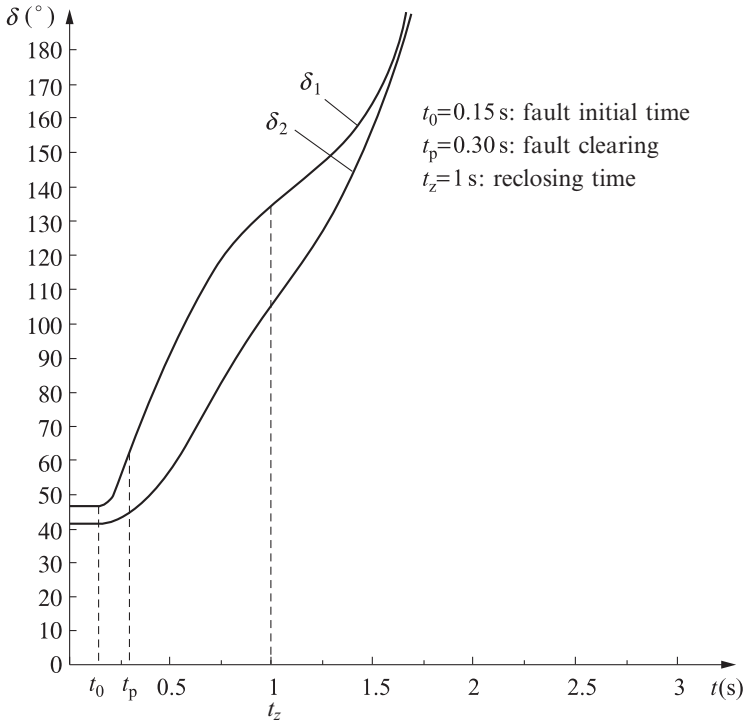

Fig. 8.12
Power angle curve of the generator (C0: no control, loss of synchronism).

The power angle curve of the generator in the system is shown in Fig. 8.12.

Case 1: Timed control at the first stage but no control at the second stage.

Switch on braking resistor at bus ① after clearing the fault.

Switch off braking resistor after the given braking time 0.7s.

Refer to Fig. 8.13 for the dynamic power angle time domain curve of the generator in the system.

Case 2: Timed control at the first stage but norm control at the second stage.

(1) The first stage control: The control process is same as Case 1.
(2) The second stage control: Norm control.

Refer to Fig. 8.14 for the generator dynamic power angle time domain curve and the assumed average power angle time domain curve.

Case 3: Equilibrium control at the first stage but no control at the second stage.

Switch on the braking resistor at bus ① after clearing the fault.

Switch off braking resistor by the time of energy equilibrium criterion.

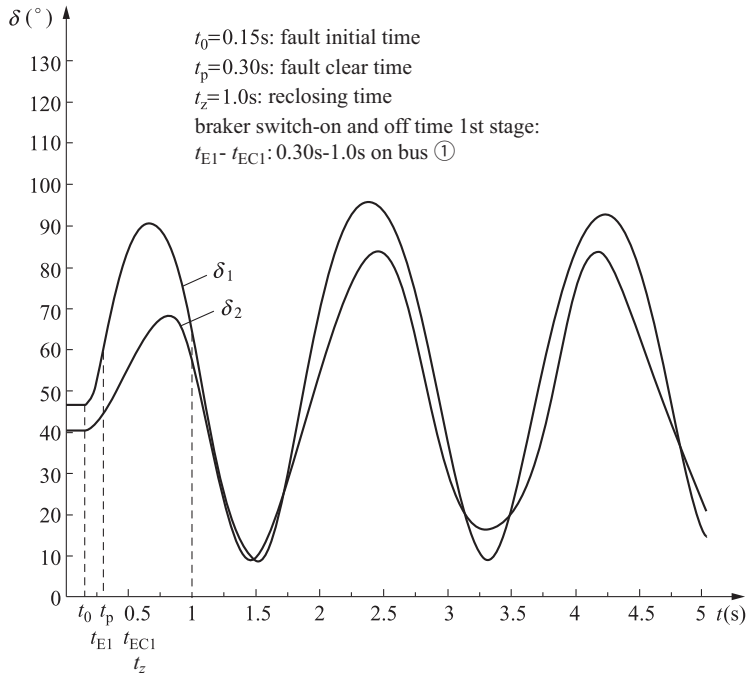

Fig. 8.13
(1) Power angle curve of the generator (C1: I—timed control, II—no control).

Refer to Fig. 8.15 for the generator dynamic power angle time domain.

Case 4: Energy equilibrium control at the first stage and norm reduction control at the second stage.

(1) The first stage control: The control process is same as Case 3.

(2) The second stage control:

Switch on–off of the braking resistor at bus ① and ② according to the norm reduction control criterion (start once respectively).

See Fig. 8.16 for the generator dynamic power angle time domain curve and assumed power equilibrium power angle time domain curve.

8.8.3 Operation Mode ⟨II⟩

8.8.3.1 Fault type

A permanent fault of three-phase short circuit happens near to bus ⑧ of line ⑤–⑧, and the fault is cleared after 0.15 s. After clearing the fault, the line will not be reclosed, and the line ⑤–⑧ operation shifts from double-circuit to single-circuit.

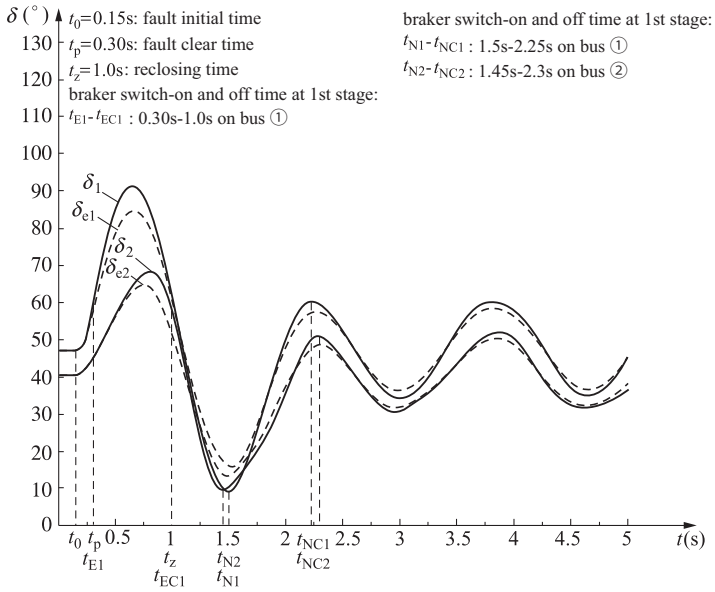

Fig. 8.14
Generator power angle curve (C2: I—timed control, II—norm control).

8.8.3.2 *Prefault steady load flow*

The prefault steady load flow is shown in Fig. 8.17.

8.8.3.3 *Results under different control cases*

Results of five cases have been given to show the effectiveness of the proposed two-stage control approach. Control schemes of C1–C4 are shown in Table 8.3. As for braking resistance, one braking resistance is switched on node ① in the first stage, and two braking resistances are switched on node ① and node ② in the second stage. To make comparisons, Case 0 is without control; Cases 1 and 2 is with time control in the first stage but with and without control in the second stage; and Cases 3 and 4 are with control in the first stage but with and without control in the second stage.

For the operation time of each case, initial fault happens at 0.15 s and clearing fault at 0.3 s. The control results for Cases 1–4 are given in Table 8.4.

The detailed results of each case are explained in the following:

Case 0: No control (loss of synchronism).

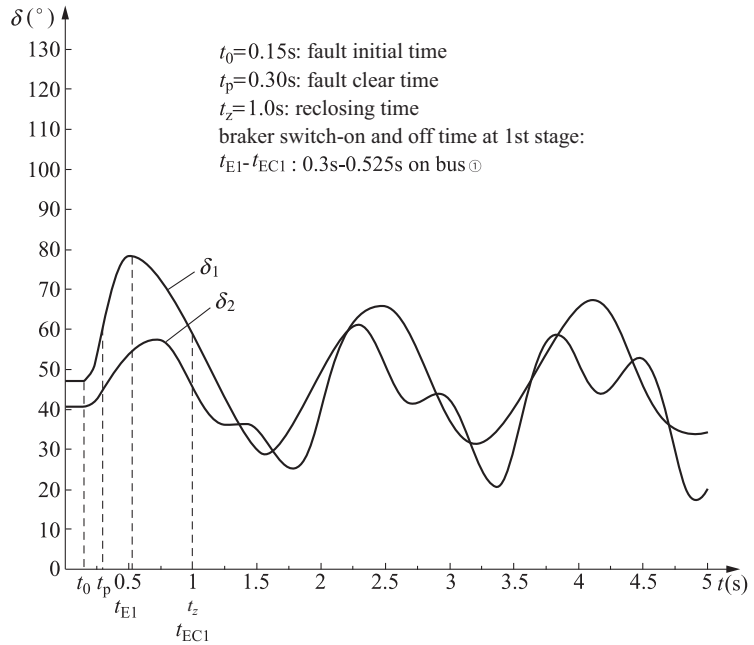

Fig. 8.15
Generator power angle curve (C3: I—energy control, II—no control).

The dynamic power angle time domain curve of the generator in the system is shown in Fig. 8.18.

Case 1: Timed control at the first stage but no control at the second stage (loss of synchronism).
Switch on the electric braking at buses ① and ② respectively after clearing the fault.
Switch off braking resistor after the given braking time 0.7s.
Refer to Fig. 8.19 for generator power angle curve.

Case 2: Timed control at the first stage but norm reduction control at the second stage.

(1) The first stage control: Its control process is same as Case 1.
(2) The second stage control:

Automatically switch on–off of the braking resistor at bus ① and ② according to the norm reduction control criterion (start once respectively).

See Fig. 8.20 for the generator dynamic power time domain curve and assumed power equilibrium power angle time domain curve.

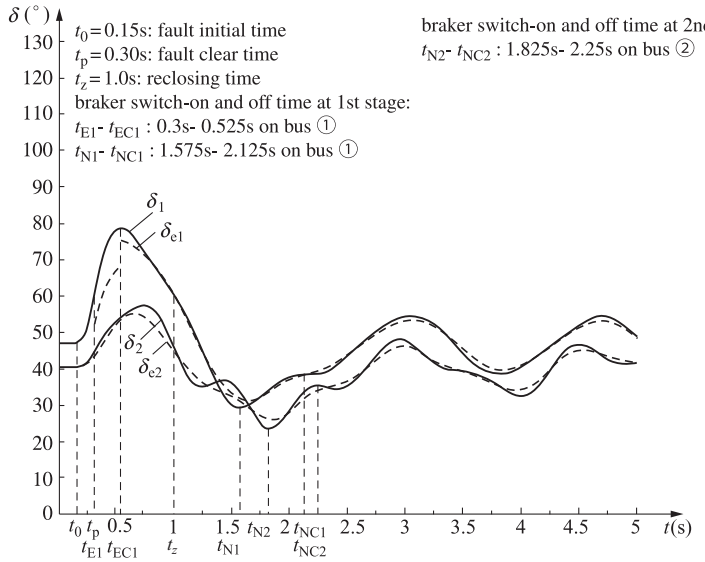

Fig. 8.16
Generator power angle curve (C4: I—energy control, II—norm control).

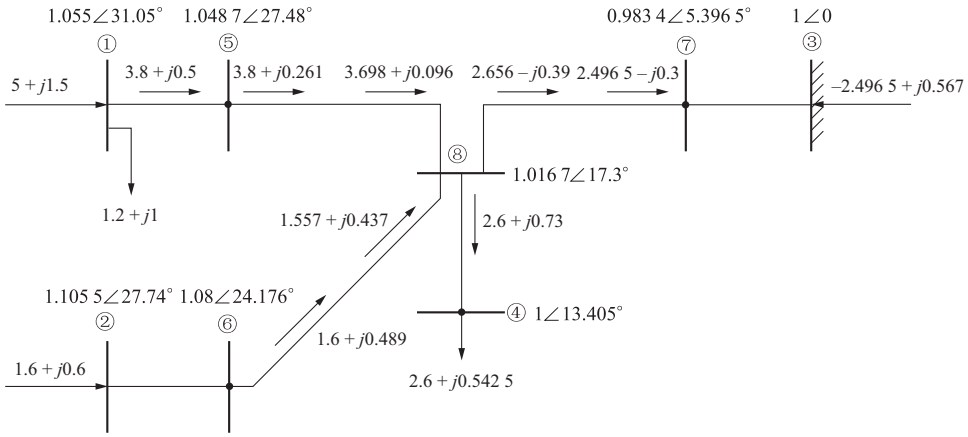

Fig. 8.17
Operation mode ⟨II⟩ prefault steady load flow.

Table 8.3 Simulation results of operation mode ⟨II⟩

Case	Control Schemes	I—R_{ZD} (p.u.)	II—R_{ZD} (p.u.)
C0	No control		
C1	I—Time control, II-no control	0.789743, 0.87295	
C2	I—Time control, II—criterion 2 control	0.789743, 0.87295	1.5, 2.5
C3	I—Criterion 1 control; II—no control	0.35, 0.8	
C4	I—Criterion 1 control; II—criterion 2 control	0.35.0.8	1.5, 2.5

Table 8.4 Switching time and actions of cases

Case	First Stage		Second Stage		
	t_{E1}-t_{EC1} (s)	t_{E2}-t_{EC2} (s)	t_{N1}-t_{NC1} (s)	t_{N2}-t_{NC2} (s)	Results
C0					Loss of synchronism
C1	0.3–0.8	0.3–1.0			Large oscillation
C2	0.3–0.8	0.3–1.0	1.3–2.4	1.6–2.05	I—Oscillation, II—little improved
C3	0.3–0.525	0.3–0.4			I—Large improved, II—oscillation
C4	0.3–0.525	0.3–0.4	1.375–2.3	0.825–1.05	Two stage smooth

I—oscillation: Power angle curve oscillation in the first stage. II—improved: Power angle curve oscillation improved in the second stage. Two stage smooth: power angle curve smooth in both first and second stage. Node 1 (s): the time for switching on and off resistance in node 1. Node 2 (s): the time for switching on and off resistance in node 2.

Case 3: Energy equilibrium control at the first stage but no control at the second stage.

Switch on the electric braking at buses ① and ② after clearing the fault.

Refer to Fig. 8.21 for generator dynamic power angle time domain curve.

Case 4: Energy equilibrium control at the first stage but norm reduction control at the second stage.

(1) The first stage control: Its control process is same as Case 3.
(2) The second stage control:

Automatically switch on-off the braking resistor at buses ① and ② according to the norm reduction control criterion (start once respectively).

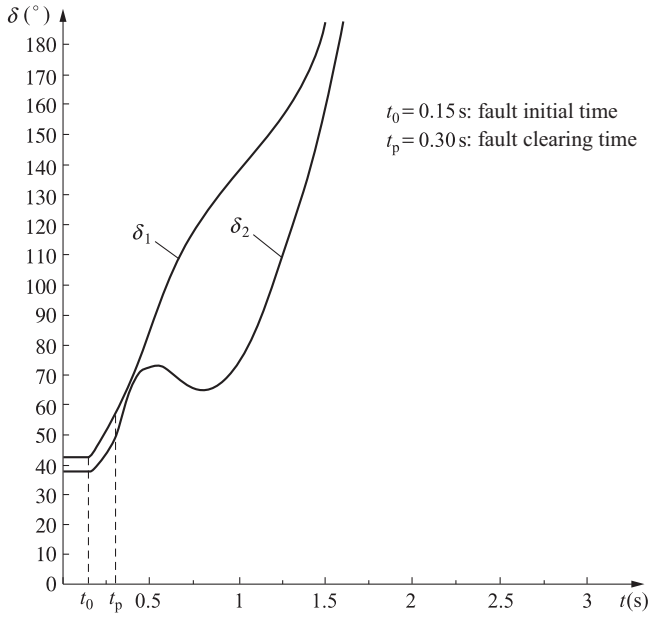

Fig. 8.18

Generator power angle curve (no control, loss of synchronism).

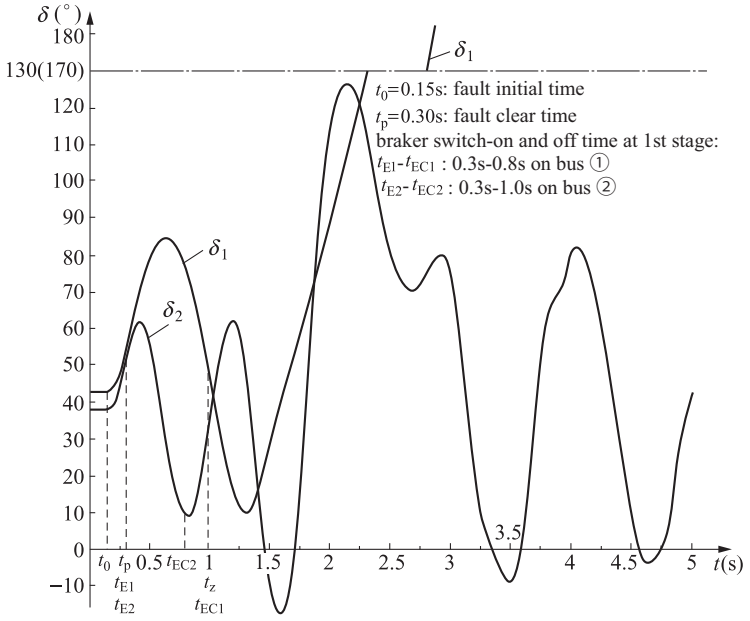

Fig. 8.19

Generator power angle curve (C0: I—timed control. II—no control, loss of synchronism).

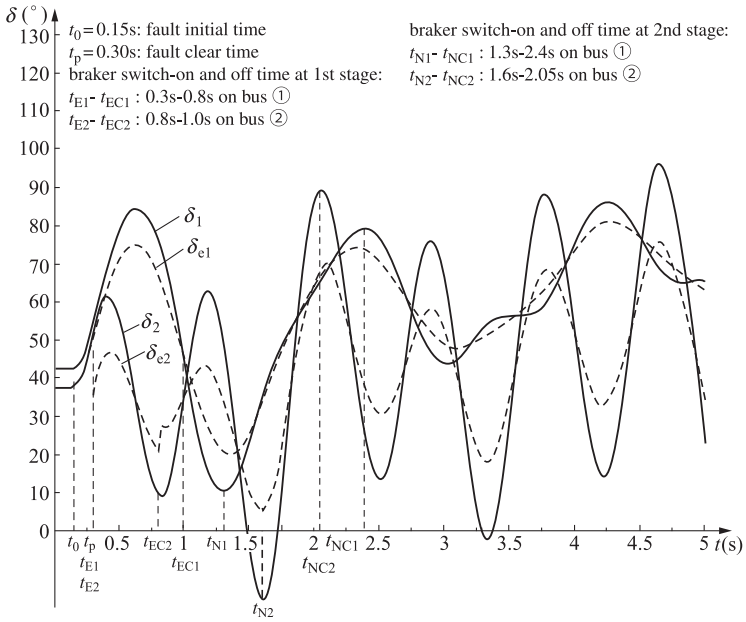

Fig. 8.20

Generator (1) power angle curve (C2: I—timed control, II—norm control).

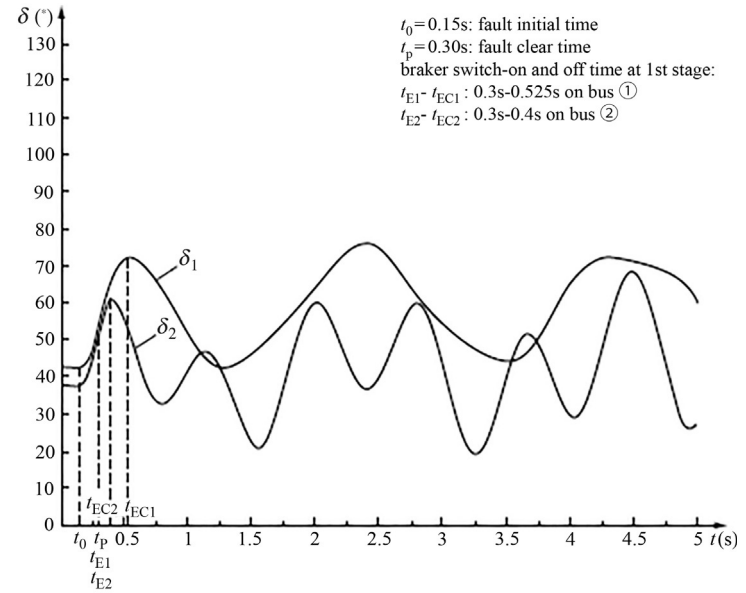

Fig. 8.21

Generator power angle curve (C3: I—energy control, II—no control).

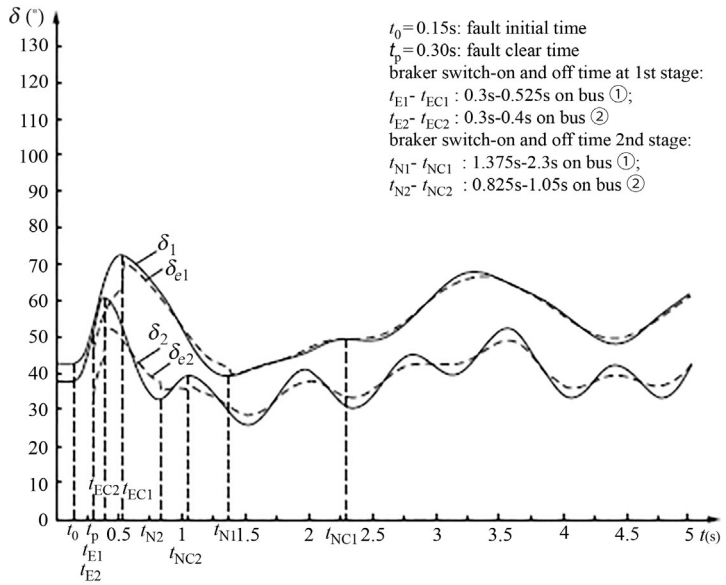

Fig. 8.22
Generator power angle curve (C4: I—energy control, II—norm control).

See Fig. 8.22 for the generator dynamic power time domain curve and assumed power equilibrium power angle time domain curve.

8.8.4 Analysis of Calculation Results

The calculation of different control cases under the previous two operation modes indicates the braking power based on the actual braking resistance in the original system is smaller and braking time is longer, which could ensure no loss of synchronism in the first swing period, but it is difficult to contain the following drastic oscillation if no further control measures are taken. As a result, the unit is still in the danger of losing synchronism.

The swing amplitude of the system will be decreased by increasing the braking power (that is, reducing the braking resistance) and controlling in the first stage according to the energy equilibrium control criterion. The second stage control is then implemented according to the norm reduction control criterion after the first stage control, which could effectively control the subsequent oscillation of system, enabling the system to stabilize as soon as possible.

8.9 Conclusion

This chapter proposes the criteria and models for local stability control from the perspective of ensuring the stability of the whole system. The practical feasibility of the proposed criteria and methods is discussed via the simulation calculation examples. The analysis and proof as well as simulation calculations for the testing system indicate:

(1) Through the qualitative analysis of the physical process of the power system dynamic stability, the reasonability of the local online stability control of the power system, which is divided into two stages in the time domain, have been proven.
(2) The analysis using the area criterion and the results of the simulation calculations show that the local emergency control following the first stage energy balance control criterion not only effectively prevents the local generator from losing synchronization with the system during the first swing period, but also shows the minimum impact on the subsequent oscillation of the system by comparing the calculation results.
(3) The second stage control performed on the basis of no loss of synchronize within first swing period, that is, the local online stability control performed according to the given norm reduction control criterion, although it is started in accordance with the limited information obtained by each part in the system, has played a good role in calming the subsequent oscillations of the system and promoting the wide-scale stability of the whole system.
(4) Because the two control criteria are only required to be composed of local measurement information, the local online stability control based on these control criteria can be started only by local feedback from the limited information, which provides a good prospect for the real-time stability control of the power system.
(5) Because the simulation stability calculation in compliance with the control criteria is based on the conventional dynamic stability calculation of the power system, which will not only be accepted by the broad engineering and technical personnel, but also may offer certain basis for the parameter setting of the actually set stabilizer of the power system.
(6) Because the main purpose of this chapter is to conduct a preliminary theoretical discussion on the feasibility of local online stability control of power systems, the mathematical models selected in theoretical analysis and simulation calculation are the most simplified ones; the control measures adopted are also fairly simple, and some technical details are ignored as well. In addition, the network used for calculation is also given after the equivalent simplification of the actual system. These all make our description of the dynamic characteristics of the power system quite approximate to a large extent. Therefore, the research work needs to be deepened further so as to achieve greater progress not only in theory but also in practice.
(7) In fact, the ultimate goal of this chapter is to make the research results meet the requirements of real-time online local stability control of power systems during large disturbances. For this reason, future research work should be deepened in the following two aspects:

First, study the feasibility of comprehensive online control by multiple local stability countermeasures based on the control criteria for the more complex network structure and the more complex forms of failure.

Second, adopt more accurate models in the selection of mathematical models, such as considering the influence of excitation regulation and prime motor regulation on the dynamic

characteristics of the system, not ignoring the salient pole effect of the generator, considering the load dynamic characteristics, etc. The local stabilization measures themselves consider as much as possible some technical details related to the specific implementation.

Obviously, further research work in the previous two aspects is closely related and not independent of each other. Combining these two aspects can complement each other to lay a solid foundation for the real-time online local stability control of the power system.

To summarize, the theoretical analysis and simulation calculation results in this chapter indicate that it is feasible to achieve large-scale system stability via local online stability control for the system in two stages in compliance with the two specified control criteria. Meanwhile, a lot of work needs to be done to ultimately realize the real-time local stability control for the power system.

Real-time data set that can be determined by measurement and calculation include system variables (voltage and phase angle of bus, generator terminal voltage and rotor phase angle, deviation from previous vector; as well as state of prime mover and boiler, state of speed governor, exciting state of generator, load dynamics). Those variables before the semicolon are the minimum part of information. In the event of failure, the real-time data set can be used to calculate the given energy equilibrium control criterion and critical power criterion, to decide whether to switch on and off local stability measures or not.

CHAPTER 9

Optimization of Electricity Market Transaction Decisions based on Market General Equilibrium

Chapter Outline

9.1 Introduction

9.1.1 Problem Description

In the 1990s, the market-oriented reforms of the electric power industry were set up around the world. Under the traditional model of a vertical integrated monopoly, the pricing mechanism is not transparent, economic efficiency is low, and optimization of resource

Mathematical Models and Algorithms for Power System Optimization. https://doi.org/10.1016/B978-0-12-813231-9.00009-1

allocation is unachievable. Therefore, the introduction of competitive market mechanism became the inevitable trend of the development of power industry. The purpose of marketization reform is to break the monopoly, fully play a role of the market in resource allocation, enable the allocation of resources in a fair and reasonable way, and achieve the maximization of the overall social welfare. The power market is an industry market, which integrates the market principle in microeconomics into the practical operation of power systems. The best state of the electricity market is the equilibrium state, where there is balance of supply and demand, balance of payments is attained, no social surplus is left, and resource allocation is optimal.

However, the power market is an imperfect competitive market; the equilibrium cannot be achieved automatically. Due to the characteristics of the power system, there are losses on the lines during power transmission and congestion when the transmitted power exceeds line capacity, which leads to the market surplus. Therefore, how to construct the decision-making model of electric power market transaction to achieve the market equilibrium is a problem worth studying. Based on the power pool transaction model, this chapter presents an optimal decision model used to determine the transaction prices in both the long-term contract market and the real-time market.

9.1.2 Microeconomics Equilibrium Principle

9.1.2.1 Nash equilibrium

With Nash equilibrium, there exists at least one optimal strategy combination for all participants in a limited behavioral strategy with a limited number of individuals. Under Nash equilibrium, no one can change the strategy to get more profits, so no one has the motivation to change the status quo [94].

9.1.2.2 Competitive equilibrium

Equilibrium is an important theory in the market theory of microeconomics [95]. The competitive equilibrium or general equilibrium (other than Nash equilibrium) of a single commodity is manifested in the form of a well-known intersection of supply and demand curves, as shown in Fig. 9.1.

In the ordinary commodity market, the equilibrium state is achieved automatically through the "invisible hand." The mathematical model can be described as follows:

$$P(C) = S(C) - D(C) = 0 \tag{9.1}$$

$$CP(C) = 0 \tag{9.2}$$

where P represents the excess supply function; $S(C)$, $D(C)$ are the supply and demand functions, respectively; C is the market price. Eq. (9.1) represents the supply and demand balance.

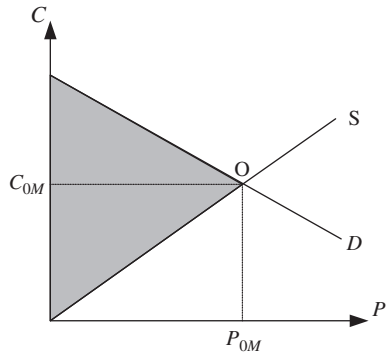

Fig. 9.1
The intersection of supply and demand curves.

Eq. (9.2) represents the revenue and expenditure balance, which means the result of market trading is clear without market surplus.

The characteristics of the market equilibrium include: ① the price of the participants is the unified market marginal price; ② supply and demand are balanced; and ③ revenue and expenditure are balanced. Its superiority lies in: ① the market benefits can be maximized and ② market benefits are allocated fairly.

9.1.2.3 The difference between Nash equilibrium and competitive equilibrium

Nash equilibrium considers the problem from the local perspective, aiming to maximize the benefits of market participants, whereas competitive equilibrium considers the problem from the overall situation, aiming to allocate resources efficiently. There is surplus left when Nash equilibrium is achieved. Because the power companies have a monopoly position in the power market and should not aim at profit, the resulting surplus must be reallocated among market participants. There is an issue of the distribution fairness when the surplus is large, which is the problem with Nash equilibrium. Auctioneers of a power market prefer that competitive equilibrium is achieved, monopoly behavior is restrained, and the competition is more orderly.

9.1.3 The Overview of a Power Market

9.1.3.1 The definition of a power market

The market is the place where buyers and sellers trade goods. If there are many participants in the market, any one participant has no ability to affect the market price and is just a passive price taker. At this time, the market is called a perfect competitive market. The perfect competitive market price is the result of interaction between supply and demand. The characteristics of perfect competitive market include: (1) There are many buyers and sellers on

the market, (2) the various sellers provide roughly the same goods, and (3) enterprises are free to enter the market. General commodity markets are perfect competitive markets, where competitive equilibrium can be achieved automatically. If the number of participants is limited in the market, and a certain monopoly behavior may affect the market price, the market is not perfectly competitive.

The power market provides buyers and sellers with a place for trade of power and related services [96]. These related services include transmission services, operation scheduling services, and a range of other ancillary services. The power market follows the basic characteristics of the general market: The power market is competitive, resource allocation is efficient, there is externality, and the aim of participants is to maximize the profits. The power generation companies, users, organization and management institutions, and power grid companies are the main market players. This chapter assumes that the organization and management institutions are integrated with the power grid companies.

However, a power market is not a perfect competitive market, which is a combination of regulation and competition. The reason is that power production has a certain economy scale, which limits the number of investors. Besides, the number of buyers and sellers of a power market is not necessarily large because of the requirements of security, stability, reliability, and economy. Furthermore, power cannot be easily stored, and power production must be highly coordinated, with network loss and congestion. As a result, the goods offered by the various sellers are not necessarily the same.

In the imperfect competitive market, the lack of effective regulation may lead to higher prices than the marginal cost of generators, and generation companies may use the market power to obtain high profits, harming the interests of consumers. Therefore, to ensure the fair market and achieve the market equilibrium, some regulation measures must be taken.

9.1.3.2 Power market transaction mode

There are mainly two kinds of transaction modes in a power market: one is the power pool transaction, and the other is the bilateral transaction. The basic operation mode of the power pool transaction is that the generation companies submit bids to Power Exchange, and Power Exchange purchases the power from the generation companies according to their bids, clearing the market according certain trading algorithms and determining the electricity generation schedule and price. In the power pool, the equilibrium cannot be achieved automatically but through a systematic method. Bilateral transaction is the mode that a power contract directly signed by the generation companies and the users; the price is determined through bilateral negotiation without the participation of the third party [97]–[99].

Bilateral transaction mode is more in line with the characteristics of the general commodity market, whereas power pool transaction is more convenient for coordinating and scheduling.

In a sense, there is essentially no difference between the power pool transaction and the bilateral transaction. The power pool transaction can be regarded as a special multilateral transaction. Because the result of the bidding in the power pool is to form a series of generation contracts between the Power Exchange and the generation companies, only the electricity generation schedule and price are determined in a special trading mechanism—market transaction algorithm. These two models are complementary and usually coexist in the major power markets in the world. This chapter mainly deals with power pool transaction.

9.1.3.3 Pricing mechanism of a power market

Electricity price is the core and lever of a power market. It is the most sensitive information about the change of supply and demand relationship in the power market and also an important tool to reflect the thoughts of management. Microeconomics believes that prices are determined by the supply and demand of goods in the market. The price of the power market is not formed naturally, but it needs to be priced. Pricing principle is to facilitate the market to optimize the allocation of resources. There are two main pricing methods: accounting cost pricing and marginal cost pricing.

The accounting cost pricing calculates the cost of power generation according to the accounting records of power generation or power supply enterprises and the cost items in the financial statements, and then divides it into fixed cost and variable cost, including taxes and profits. Finally, the costs are allocated to various users according to different methods. For marginal cost pricing, according to microeconomics, if the price of a product is equal to its marginal cost, or the marginal profit equals zero, the price is the optimal price, and the enterprise can obtain the maximum profit. In the power market, different pricing methods will lead to different equilibrium states. The competitive equilibrium model can be derived from the optimal decision model by using accounting cost pricing.

9.1.3.4 Power market simulation

Cournot simulation

When using Cournot simulation, the market participants simply choose the output to maximize their own profits, which are the price takers. There is no difference between general market participants and power market auctioneers. The transaction price is determined through competition in the market. In Cournot simulation, the competitive equilibrium model can be derived from the optimal decision model [100].

When the market price is equal to the marginal cost of production, the benefit of the market participants is maximized, which is consistent with the perfect competitive market. In this case,

the settlement according to marginal price is the same as that settled by the actual bid price of the market participants.

Supply or demand function simulation

When market participants use the supply function to simulate, market participants can maximize their own profits when they choose both output and price. That is, electricity market participants are not only the recipients of prices, but their decisions will have an impact on market prices, which is inconsistent with the conditions of a perfect competitive market.

When using the supply or demand function simulation, the result of a power market decision has no uniform marginal price, and revenue and expenditure are unbalanced. That is, the competitive equilibrium model cannot be derived from the optimal decision model. The supply or demand function simulation is feasible in the imperfect competitive market, where the market participants take certain bidding strategies to maximize their profits by choosing their price and output. At this time, the market participants have a certain ability to manipulate the market, and the power market settlement can only be based on the actual bid price of market participants.

9.1.4 Overview of This Chapter

The power market is an imperfect competitive market, where the equilibrium state cannot be achieved automatically. It is necessary for market operators to make scientific decisions, arrange the transaction plan reasonably, and allocate resources optimally. Therefore, how to establish the optimal decision model for the market transaction and to determine the quantity and price of electricity transaction to achieve equilibrium is the problem to be studied in this chapter. This chapter uses the power pool mode to study the single commodity market with only the active transaction and the multicommodity market with both active and reactive transaction, respectively. Construction and analysis of the optimal decision model demonstrate that the optimal decision model is consistent with the competitive equilibrium model. The result can achieve competitive equilibrium. Based on the characteristics of the power system, the problems of network loss and congestion of power transmission are discussed by using the accounting pricing method, which makes a rational distribution among the market participants, eliminates the market surplus, and avoids the problem of unfair distribution in posttransaction.

Section 9.2 gives the basic idea of optimization modeling for reference. Section 9.3 presents the equivalent optimization model of general equilibrium in a power market. In Section 9.4, the detailed results of an example are given and analyzed.

9.2 Ideas of Establishing the Model

9.2.1 Consideration of the Type of Goods

According to the types of goods involved in a power market, it can be divided into single commodity power market and multicommodity power market. The single commodity electricity market only conducts active trading, whereas a multicommodity electricity market also carries out a variety of ancillary services transactions including ancillary services to meet daily needs, services to avoid power shortages, and recovery after system failure.

9.2.2 Consideration of Power System Characteristics

Network loss and congestion are the two main characteristics of a power network. The existence of network loss causes the power market transactions to generate a surplus, which needs a secondary allocation and may lead to unfair distribution of market interests. The cost accounting pricing method of network loss has already begun to avoid these problems in the process of power market decision-making. Due to the limited transmission power of transmission lines, congestion occurs when the transmission power exceeds the limit. The power market equilibrium in the case of congestion eliminates it by restricting the output of the market participants.

9.2.3 Objective Function

This chapter assumes that the market auctioneer is integrated with the power grid company. As a natural monopoly enterprise, a power grid company cannot pursue maximization of the company interests but should pursue maximization of the benefits of the entire power system. That is, the market auctioneers consider problems from the perspective of social welfare. The benefits of the entire power system are reflected by the interests of the market participants. If the users do not participate in the bidding, the benefits of the entire power system are reflected by the interests of generation companies.

9.2.4 Constraint Conditions

First, the balance between supply and demand must be ensured, that is, the output of generators is equal to the sum of users' demand and network loss. Second, it must satisfy the power network equation, that is, the power flow equation constraint, which is the equality constraint. Finally, the maximum current limit and the upper and lower limits of the bus voltage must be taken into consideration, which are the inequality constraints.

9.3 Equivalent Optimization Model of General Equilibrium in a Power Market

Notations

Symbol name	Description
c_k	The bid price of the generation company located at bus k
p_k	The bid power output of the generation company located at bus k, or the active power injection of generators at bus k, when the users do not participate in the bidding; active power injection of generators or loads at bus k, when the users participate in the bidding
$C_k(p_k)$	The production cost function of generation company at bus k or the utility function of user at bus k
Q_k	Reactive power injection of the generators at bus k when only considering active power transaction
P_{Lk}	Active power load at bus k
Q_{Lk}	Reactive power load at bus k
e_k	Real part of voltage at bus k
f_k	Imaginary part of voltage at bus k
$G_{kj}B_{kj}$	Corresponding elements of node admittance matrix
l	The set of lines
P_D	The total load of the system
P_{Loss}	The total network loss of the system
$F_{pk}(p_k)$	Active power flow equations
α_{pk}	The corresponding Lagrange multiplier of nodal active power balance equation
β_p	The corresponding Lagrange multiplier of total active power balance equation
λ_l	The corresponding Lagrange multiplier of current limit inequality constraint equation of line l
M_l	The set of inequality constraints which plays a role
C_{0M}	The price of network loss, active power, market clearing
η_{pk}	Network loss coefficient
ς_{lk}	Congestion dispatch coefficient
$C_{0M}^{'}$	The marginal price of market in the case of congestion
d_k	The declared reactive power price of generation company of bus k
q_k	Considering reactive power transaction, the reactive power of the generation company located at bus k, when the users do not participate in the bidding; the reactive power of generation company or loads at bus k, when the users participate in the bidding
$C_k(p_k, q_k)$	The production cost function of generation company of bus k
Q_D	The total reactive power load of the system
Q_{Loss}	The total reactive power loss of the system
η_{qk}	Network loss coefficient
φ_{kj}^{l}	The impact factor of reactive power injection to node voltage

9.3.1 Model of Active Power Transaction

In the single commodity power market, the trading is a transaction of the active power or electricity, where the optimal allocation of resources is achieved through market competition. The competitive equilibrium of the single commodity power market is a local equilibrium, also called a local competitive equilibrium or partial equilibrium. Network loss and congestion

are the two main characteristics of a power network. This section discusses the local equilibrium of a power market considering network loss and congestion, respectively. Competitive equilibrium is an issue from a global perspective, which should be considered by the market auctioneer. For convenience, the local equilibrium under the condition of network loss is discussed first. Then, on this basis, the local equilibrium considering congestion is discussed. To pursue profit maximization or utility maximization is the ultimate goal of the generation companies or users involved in the market competition. So, the decision can be represented by the following model:

$$\max \quad c_k p_k - C_k(p_k) \tag{9.3}$$

where $k = 1, 2, \ldots, N$ is the set of buses and c_k, p_k are the bid price and power of the generation company located at bus k. For generation companies, p_k is positive, whereas for users, p_k is negative. $C_k(p_k)$ represented the production cost function of generation company at bus k or the utility function of user at bus k, which is generally a quadratic function.

$$C_k = \frac{1}{2} a_k^0 p_k^2 + b_k^0 p_k + c_k^0 \tag{9.4}$$

where a_k^0, b_k^0, c_k^0 are constant coefficients. For utility function, a_k^0 is a negative constant.

Power grid companies and market auctioneers are considered special market participants. A power grid company is a monopoly enterprise, so it cannot pursue the maximization of its own benefits but rather the maximization of the benefits of the entire power market system. That is, the market auctioneer considers the problem from the perspective of social welfare. When the users do not participate in the bidding, the benefits of the entire power market system are reflected by the benefits of power generators.

$$\max \quad \sum_{k=1}^{N} [c_k p_k - C_k(p_k)] \tag{9.5}$$

Eqs. (9.3)–(9.5) are the same as the description of the simplest power market. Power grid is the carrier of power transaction, so the power network equation must be considered:

$$\begin{aligned} &p_k - P_{LK} - e_k \sum_{j \in k} \left(G_{kj} e_j - B_{kj} f_j\right) - f_k \sum_{j \in k} \left(G_{kj} f_j + B_{kj} e_j\right) = 0 \\ &q_k - Q_{LK} - f_k \sum_{j \in k} \left(G_{kj} e_j - B_{kj} f_j\right) + e_k \sum_{j \in k} \left(G_{kj} f_j + B_{kj} e_j\right) = 0 \quad k = 1, 2, \ldots, N \end{aligned} \tag{9.6}$$

To ensure the security and reliability of the system operation, the following constraints must be met:

$$I_l - I_l^{\max} \leq 0 \quad l = 1, 2, \ldots, M \tag{9.7}$$

where Eq. (9.6) is the power flow equation, which is represented by the bus voltage equation here. p_k, Q_k are the active and reactive power injections of the generators at bus k respectively. P_{Lk}, Q_{Lk} are the active and reactive power of loads at bus k respectively. e_k, f_k are the real and imaginary

parts of voltage at bus k respectively. G_{kj}, B_{kj} are the corresponding elements of the bus admittance matrix. Eq. (9.7) represents the power flow constraint of transmission line. $l = 1, 2, \ldots, M$ is the set of lines. The lower case p_k is variable, and the upper case Q_k, P_{Lk}, Q_{Lk} are constants.

Because the power flow equation does not reflect the power balance of the whole system, the active power flow in Eqs. (9.6) is accumulated and Eq. (9.8) is obtained.

$$\sum_{k=1}^{N} p_k - P_L = P_D \tag{9.8}$$

where P_D, P_L represents load and network loss, $\sum_{k=1}^{N} P_{Lk} = P_D$. So the decision-making model (Problem A) consisting of Eqs. (9.5)–(9.7) is equivalent to the decision-making model (Problem B) consisting of Eqs. (9.5)–(9.8). The solution to Problem A must be the solution to the Problem B, and vice versa.

In the actual process of power market competition, the costs of power generation companies are not disclosed, and it is impossible for power grid companies to know the costs, so the objective function in Eq. (9.5) is usually replaced by the following equation:

$$\max \quad \sum_{k=1}^{N} c_k p_k \tag{9.9}$$

The previous formulas constitute the complete expression of a decision-making model of power market system for generation-side. When the users participate in bidding, power flow Eq. (9.6) changes into:

$$\begin{aligned} &p_k - e_k \sum_{j \in k} \left(G_{kj} e_j - B_{kj} f_j\right) - f_k \sum_{j \in k} \left(G_{kj} f_j + B_{kj} e_j\right) = 0 \\ &q_k - Q_{LK} - f_k \sum_{j \in k} \left(G_{kj} e_j - B_{kj} f_j\right) + e_k \sum_{j \in k} \left(G_{kj} f_j + B_{kj} e_j\right) = 0 \quad k = 1, 2, \ldots, N \end{aligned} \tag{9.10}$$

where p_k represents the active power injection of generator or load at bus k. The active power flow equations are accumulated, and the total power balance Eq. (9.8) changes into:

$$\sum_{k=1}^{N} p_k - P_L = 0 \tag{9.11}$$

Eqs. (9.10) and (9.11) replace Eqs. (9.6) and (9.8), respectively, to form the decision-making model of power markets with users bidding.

In the competition of a power market, generation companies make decisions first, submitting price and amount of electricity curve, and then a market auctioneer makes a decision, determining the price and amount of electricity transaction.

Eqs. (9.6)–(9.9) are formed into expanded Lagrange function:

$$L=\sum_{k=1}^{N}c_k p_k+\sum_{k=1}^{N}\alpha_{pk}F_{pk}(p_k)+\beta_p\left(\sum_{k=1}^{N}p_k-P_L-P_D\right)+\sum_{l=1}^{M_I}\lambda_l\left(I_l-I_l^{\max}\right) \tag{9.12}$$

where $F_{pk}(p_k)$ represents active power flow function in Eq. (9.6). Because only active power is considered as a variable, the reactive power flow equation is not considered in the expanded Lagrange function. α_{pk} is the Lagrange multiplier corresponding to the nodal active power balance equation. β_p is the Lagrange multiplier corresponding to the total active power balance equation. λ_l is the Lagrange multiplier corresponding to the current limit inequality constraint equation of line l. M_I is the set of inequality constraints which play the role of making the equality sign in Eq. (9.7) set up. According to complementary slackness conditions, when the inequality of Eq. (9.7) holds up, the corresponding Lagrange multiplier $\lambda_l=0$; and when the equality holds up, the corresponding Lagrange multiplier $\lambda_l>0$. So is possible to consider only the inequality constraints that play a role in the expanded Lagrange function.

When using Cournot simulation, market participants are the price takers and can choose the output to maximize their benefits. Let p_k be a variable; the Kuhn-Tucker conditions can be obtained as follows:

$$c_k+\alpha_{pk}+\beta_p\left(1-\frac{\partial P_L}{\partial p_k}\right)+\sum_{l=1}^{M_I}\lambda_l\frac{\partial I_l}{\partial p_k}=0\quad k=1,2,\ldots,\ N \tag{9.13}$$

That is

$$c_k=-\alpha_{pk}-\beta_p\left(1-\frac{\partial P_L}{\partial p_k}\right)-\sum_{l=1}^{M_I}\lambda_l\frac{\partial I_l}{\partial p_k}\quad k=1,2,\ldots,N \tag{9.14}$$

c_k *is* the market price that the market participant k faces. When using the supply or demand function simulation, market participants can also choose both price and output at the same time to maximize their benefits. Suppose the supply or demand function is expressed as a linear function, as shown in the following form:

$$c_k=a_k^p p_k+c_k^p \tag{9.15}$$

Because c_k is a function of p_k, let p_k be a variable; the Kuhn-Tucker conditions can be obtained as follows:

$$c_k+\frac{\partial c_k}{\partial p_k}p_k+\alpha_{pk}+\beta_p\left(1-\frac{\partial P_L}{\partial p_k}\right)+\sum_{l=1}^{M_I}\lambda_l\frac{\partial I_l}{\partial p_k}=0\quad k=1,2,\ldots,N \tag{9.16}$$

Substituting Eq. (9.15), the condition of Nash equilibrium at bus k is:

$$c_k = -\frac{\partial c_k}{\partial p_k} p_k - \alpha_{pk} - \beta_p \left(1 - \frac{\partial P_L}{\partial p_k}\right) - \sum_{l=1}^{M_l} \lambda_l \frac{\partial I_l}{\partial p_k} \quad k = 1,2,\ldots,N \tag{9.17}$$

Compared with the Cournot model, one more term $a_{pk}\, p_k$ is added to the price that the market participant k faces.

9.3.1.1 Network loss allocation

When considering network loss and assuming using the cost accounting pricing, the decision-making model of a power market becomes:

$$z = \max \quad \sum_{k=1}^{N} c'_k p_k \tag{9.18}$$

$$\sum_{k=1}^{N} p_k - P_L = 0 \tag{9.19}$$

When users are not considered to participate in bidding, the previous formulas become:

$$\sum_{k=1}^{N} p_k - P_L = P_D \tag{9.20}$$

Compared with the decision-making model of the simplest power market, decision-making model consisting of Eqs. (9.18) and (9.19) [or (9.20)] adds one more term of network loss P_{L} in the power balance Eq. (9.19) [or (9.20)].

When considering the user's bid, Eqs. (9.18) and (9.19) form the augmented Lagrange function as follows:

$$\max \quad \sum_{k=1}^{N} c'_k p_k + \beta_p \left(\sum_{k=1}^{N} p_k - P_{\mathrm{L}} \right) \tag{9.21}$$

By derivation of p_k, the optimal condition is obtained as follows:

$$c'_k + \beta_p \left(1 - \frac{\partial P_{\mathrm{L}}}{\partial p_k}\right) = 0 \tag{9.22}$$

Let $-\beta_p = C_{0M}$ and then:

$$c'_k = C_{0M} \left(1 - \frac{\partial P_{\mathrm{L}}}{\partial p_k}\right) \tag{9.23}$$

Substituting into Eq. (9.18), the objective function becomes:

$$z = C_{0M}\sum_{k=1}^{N}\left(1-\frac{\partial P_L}{\partial p_k}\right)p_k \Rightarrow z = C_{0M}\left(\sum_{k=1}^{N}p_k - \sum_{k=1}^{N}\frac{\partial P_L}{\partial p_k}p_k\right) \tag{9.24}$$

Because $\sum_{k=1}^{N}\frac{\partial P_L}{\partial p_k}p_k \neq P_L$, so $C_{0M}\left(\sum_{k=1}^{N}p_k - \sum_{k=1}^{N}\frac{\partial P_L}{\partial p_k}p_k\right) \neq 0$. Thus, due to the existence of network loss, competitive equilibrium can no longer be achieved in a power market. Network loss is also a kind of active power, so the price of loss is consistent with the price of active power and can be represented as $C_{0M.}$ Actually, $\frac{\partial P_L}{\partial p_k}$ represents network loss allocation coefficient of bus k. If $C_{0M}P_{\mathrm{L}}$ is regarded as the network loss cost, $C_{0M}\frac{\partial P_{\mathrm{L}}}{\partial p_k} = \frac{\partial C_{0M}P_{\mathrm{L}}}{\partial p_k}$ can also represent the network loss price of bus k, meaning the change of network loss cost caused by the change of unit power of bus k, which is a part of real time electricity price, belonging to marginal cost pricing method. Therefore, the marginal cost pricing of network loss is the main reason why the competitive equilibrium cannot be achieved in the above power market. Eq. (9.24) can be rewritten as:

$$z = C_{0M}\left(\sum_{k=1}^{N}p_k - \sum_{k=1}^{N}\frac{\partial P_L}{\partial p_k}p_k\right) = C_{0M}\Delta_{pk}^{\mathrm{loss}}(p_k) \tag{9.25}$$

It is shown that the network loss leads to a surplus of power market transaction. Because power grid companies and market auctioneers do not pursue their own profits, the surplus should take a secondary allocation, which may lead to unfair allocation of market benefits. The marginal cost pricing method of network loss causes the power market to generate surplus, which is the main shortcoming of marginal cost pricing, although the accounting cost pricing method does not exist this problem.

Using accounting cost pricing method can allocate the network loss among the market participants completely, thus Eq. (9.19) becomes:

$$\sum_{k=1}^{N}p_k\left(1-\eta_{pk}\right) = 0 \tag{9.26}$$

Eq. (9.20) becomes:

$$\sum_{k=1}^{N}p_k\left(1-\eta_{pk}\right) = P_{\mathrm{D}} \tag{9.27}$$

When the network loss is allocated according to certain rules of allocation, Eqs. (9.26) and (9.18) are formed into the augmented Lagrange function, thus:

$$L=\sum_{k=1}^{N}c_k'p_k+\beta_p\sum_{k=1}^{N}p_k\left(1-\eta_{pk}\right) \tag{9.28}$$

Whether using Cournot simulation or supply function simulation, the following can be obtained by derivation of p_k:

$$c_k'+\beta_p\left(1-\eta_{pk}\right)=0 \quad k=1,2,\ldots,N \tag{9.29}$$

Let $-\beta_p=C_{0M}$, and then above formula changes into:

$$c_k'=C_{0M}\left(1-\eta_{pk}\right) \quad k=1,2,\ldots,N \tag{9.30}$$

Substituting into the objective function in Equation (9.18), we obtain:

$$\max \quad C_{0M}\sum_{k=1}^{N}\left(1-\eta_{pk}\right)p_k \tag{9.31}$$

Let $(1-\eta_{pk})p_k=p_k'$, and then previous formula changes into:

$$\max \quad C_{0M}\sum_{k=1}^{N}p_k' \tag{9.32}$$

Eq. (9.27) changes into:

$$\sum_{k=1}^{N}p_k'=0 \tag{9.33}$$

Substituting into Eq. (9.34), thus:

$$C_{0M}\sum_{k=1}^{N}p_k'=0 \tag{9.34}$$

The equilibrium of a power market is represented by Eqs. (9.33) and (9.34), which is equivalent to correcting slope of the bid curve of market participants; the correcting coefficient is $1-\eta_{pk}$. Because market participants cannot know the network loss accurately when binding, this amendment is essential.

When the network loss is assumed to be allocated among all the participants in the power market, the final bid curve of a generator is shown as $1'$ in Fig. 9.2, and the bid curve of a user is shown as $2'$. Thus, the power market achieves a new equilibrium, as the point O' shown Fig. 9.2.

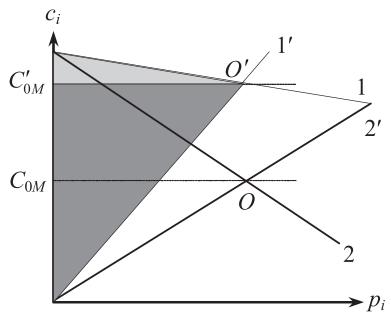

Fig. 9.2
Diagram of power market equilibrium of network loss allocation among all market participants.

When the network loss is just allocated among generator-side, the power market equilibrium is shown in Fig. 9.3, which means that only the bid curve of generator-side is to be amended. And when the network loss is allocated only on the load side, the power market equilibrium is shown in Fig. 9.4, which means only the bid curve of load-side is to be amended.

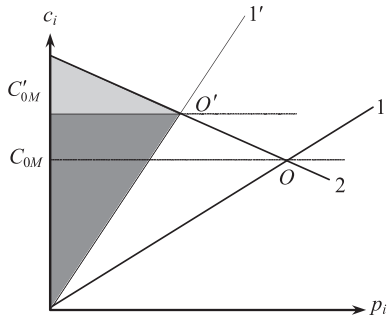

Fig. 9.3
Diagram of power market equilibrium of network loss allocation among generator-side.

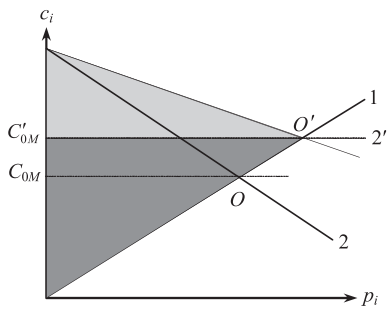

Fig. 9.4
Diagram of power market equilibrium of network loss allocation among load-side.

When the users do not participate in bidding, Eqs. (9.27) and (9.35) are formed into the augmented Lagrange function. Repeat the previous derivation process, and the competitive equilibrium of a power market can be described as follows:

$$\sum_{k=1}^{N} p'_k - P_D = 0 \tag{9.35}$$

$$C_{0M}\left(\sum_{k=1}^{N} p'_k - P_{\mathrm{D}}\right) = 0 \tag{9.36}$$

Expand Eq. (9.34) and obtain:

$$\begin{aligned} C_{0M}\sum_{k=1}^{N}(1-\eta_{pk})p_k = 0 \Rightarrow C_{0M}\left(\sum_{k=1}^{N} p_k - \sum_{k=1}^{N}\eta_{pk}p_k\right) = 0 \\ \Rightarrow C_{0M}\left(\sum_{k=1}^{N} p_k - P_{\mathrm{L}}\right) = 0 \end{aligned} \tag{9.37}$$

In this derivation process, assuming that the network loss coefficient η_{pk} is independent of the bus injection power p_k, that is, if $C_{0M}P_{\mathrm{L}} = C_{0M}\sum_{k=1}^{N}\eta_{pk}p_k$ is regarded as network loss cost, the loss price at bus k is $C_{0M}\eta_{pk}$, regardless of using accounting cost pricing or marginal cost pricing. However, in the allocation process, network loss cost is allocated among market participants according to accounting cost idea, so the pricing has already started in network loss allocation, which belongs to the accounting cost pricing model. Compared with network loss coefficient η_{pk}, $\frac{\partial P_{\mathrm{L}}}{\partial p_k}$ is just the first-order term of Taylor expansion of network loss.

Thus, the accounting cost pricing method of network loss is actually the accounting allocation method of network loss. Compared with the marginal cost pricing method, loss allocation has already started in the process of power market decision-making, instead of making the profit allocation of network loss after the decision is formed, so accounting pricing method can better reflect the fairness of market interest allocation.

9.3.1.2 Congestion dispatch

When considering congestion, the decision-making model is shown as Eqs. (9.7)–(9.9) or Eqs. (9.7), (9.9), and (9.11). Compared with decision-making model with network loss only, one more constraint in Eq. (9.7) is added.

In the case of congestion, the local equilibrium of a power market can be analyzed based on the equilibrium model in Eqs. (9.32) and (9.33), that is, Eq. (9.7) is added to the previous equilibrium model, which can be redescribed as follows:

$$\begin{aligned} &\max \quad C_{0M}\sum_{k=1}^{N}p'_k \\ &\sum_{k=1}^{N}p'_k=0 \\ &I_l-I_l^{\max}\le 0 \quad l=1,2,\ldots,M \end{aligned} \tag{9.38}$$

Eq. (9.38) is written in the form of slackness as follows:

$$\begin{aligned} &\max \quad C_{0M}\sum_{k=1}^{N}p'_k+\sum_{l=1}^{M_I}\lambda_l\left(I_l-I_l^{\max}\right) \\ &\sum_{k=1}^{N}p'_k=0 \end{aligned} \tag{9.39}$$

where $l=1,2,\ldots,M_I$ represents the line with congestion. If λ_l is properly selected, the model in Eq. (9.39) is equivalent to the model in Eq. (9.38).

Similar to the accounting cost allocation method of network loss, congestion will also be allocated among market participants according to the accounting cost allocation method. For the line with congestion, there is the following equation:

$$I_l-I_l^{\max}=\sum_{k=1}^{N}\varsigma_{lk}p_k \tag{9.40}$$

where ς_{lk} is the congestion dispatch coefficient. Substitute into Eq. (9.39), the objective function changes into:

$$\begin{aligned} &\max \quad C_{0M}\sum_{k=1}^{N}p'_k+\sum_{l=1}^{M_I}\lambda_l\sum_{k=1}^{N}\varsigma_{lk}p_k\rightarrow \\ &\max \quad C_{0M}\sum_{k=1}^{N}p'_k+\sum_{k=1}^{N}\left(\sum_{l=1}^{M_I}\lambda_l\varsigma_{lk}\right)p_k \end{aligned} \tag{9.41}$$

Substitute $p_k = \frac{p'_k}{1-\eta_{pk}}$ into this formula, and take the derivation of p'_k, to obtain:

$$C_{0M} + \frac{\sum_{l=1}^{M_l} \lambda_l \varsigma_{lk}}{1-\eta_{pk}} = C'_{0M} \tag{9.42}$$

Substitute the previous formula into the objective function, the local equilibrium model of a power market in the case of congestion can be obtained:

$$\begin{aligned} C'_{0M} \sum_{k=1}^{N} p'_k = 0 \\ \sum_{k=1}^{N} p'_k = 0 \end{aligned} \tag{9.43}$$

where C'_{0M} is the marginal price of a power market considering congestion. In the case of congestion, the equilibrium is achieved by restrict the output of market participants to eliminate congestion. When just considering adjusting output of generators, the market equilibrium is shown as in Fig. 9.5. When considering adjusting power of all market participants, the market equilibrium is shown as in Fig. 9.6.

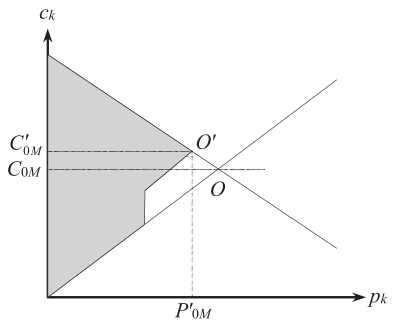

Fig. 9.5

Diagram of power market equilibrium for eliminating congestion by adjusting power output of generators.

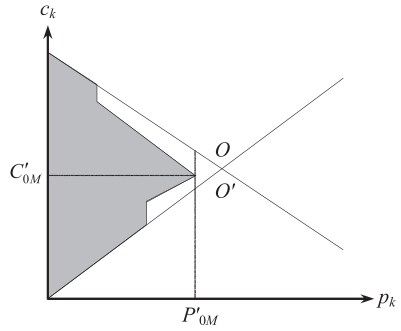

Fig. 9.6
Diagram of power market equilibrium for eliminating congestion by adjusting power of all market participants'.

To achieve the competitive equilibrium of a power market in the case of congestion, the bid curve must be amended, because market participants do not know the congestion status of the line when bidding. Unlike network loss allocation where the amendatory of the bid curve is implemented by changing slope, for the congestion dispatch the bid curve amendatory is implemented by translation. The amplitude of translation is $\frac{\sum_{l=1}^{M_I}\lambda_l\varsigma_{lk}}{1-\eta_{pk}}$

In the previous equilibrium model, $\sum_{l=1}^{M_I}\lambda_l\varsigma_{lk}$ represents the congestion price of bus k, where λ_l is the Lagrange multiplier, ς_{lk} is the congestion dispatch coefficient. Similar to network loss allocation, congestion dispatch should be determined by using the accounting cost allocation method. In this way, the competitive equilibrium can be achieved in the power market.

9.3.1.3 Power market local equilibrium

The following is a complete description of local equilibrium in a power market. Using the account pricing method, the active network loss can be expressed as:

$$P_{\mathrm{L}} = \sum_{k=1}^{N}\left[\frac{\partial P_{\mathrm{L}}}{\partial p_k}p_k + \Delta_{pk}^{\mathrm{loss}}(p_k)\right] = \sum_{k=1}^{N}\eta_{pk}p_k \tag{9.44}$$

where η_{pk} is the loss allocation coefficient.

Similarly, congestion can be expressed as [101]:

$$I_l - I_l^{max} = \sum_{k=1}^{N}\left[\frac{\partial I_l}{\partial p_k}p_k + \Delta_l^{current}(p_k)\right] = \sum_{k=1}^{N}\varsigma_{lk}p_k \quad l = 1,2,\ldots,M_I \tag{9.45}$$

where ς_{lk} is the congestion dispatch coefficient, when using the average allocation pricing method, let $\varsigma_{lk} = \frac{\partial I_l}{\partial p_k} + \frac{\sum_{k=1}^{M_I}\Delta_l^{\mathrm{curret}}(p_k)}{p_k}$, then

$$\sum_{l=1}^{M_I}\lambda_l\left(I_l - I_l^{\max}\right) = \sum_{k=1}^{N}\sum_{l=1}^{M_I}\lambda_l\varsigma_{lk}p_k = \sum_{k=1}^{N}\gamma_k p_k \tag{9.46}$$

Where:

$$\gamma_k = \sum_{l=1}^{M_I}\lambda_l\varsigma_{lk}$$

While using the accounting cost pricing method, the active power flow can be expressed as:

$$F_{pk}(p_k) = \rho_{pk}p_k \tag{9.47}$$

Using the average allocation pricing method, $\rho_{pk} = 1 - \frac{\Delta_{pk}^{flow}(p_k)}{p_k}$

The decision-making model in Eqs. (9.6)–(9.9) can be written in the form of slackness as follows:

$$\max \sum_{k=1}^{N} c_k p_k + \sum_{k=1}^{N}\alpha_{pk}F_{pk}(p_k) + \sum_{l=1}^{M_I}\lambda_l\left(I_l - I_l^{\max}\right) \tag{9.48}$$

Subject to the equality constraint:

$$\sum_{k=1}^{N}\left(1-\eta_{pk}\right)p_k = P_{\mathrm{D}} \tag{9.49}$$

If the Lagrange multipliers α_{pk} and λ_l are properly selected, the decision-making model in Eqs. (9.48) and (9.49) is equivalent to the decision-making model in Eqs. (9.6)–(9.9). And using the accounting cost method Eq. (9.49) is written in the form of augmented Lagrange function as follows.

$$L = \sum_{k=1}^{N} c_k p_k + \sum_{k=1}^{N}\alpha_{pk}\rho_{pk}p_k + \beta_p\left[\sum_{k=1}^{N}\left(1-\eta_{pk}\right)p_k - P_{\mathrm{D}}\right] - \sum_{k=1}^{N}\gamma_k p_k \tag{9.50}$$

Take derivation of p_k, the optimal condition is obtained as follows:

$$c_k + \alpha_{pk}\rho_{pk} + \beta_p\left(1-\eta_{pk}\right) + \gamma_k = 0 \quad k = 1,2,\ldots,N \tag{9.51}$$

That is,

$$c_k = -\alpha_{pk}\rho_{pk} - \beta_p\left(1-\eta_{pk}\right) - \gamma_k \tag{9.52}$$

Substitute Eq. (9.52) into Eq. (9.37), the objective function changes into:

$$\max -\beta_p\sum_{k=1}^{N}\left(1-\eta_{pk}\right)p_k \tag{9.53}$$

That is,

$$\min \beta_p \sum_{k=1}^{N} (1-\eta_{pk}) p_k \tag{9.54}$$

If C_{0M} is defined as the market clearing price, considering Eq. (9.49), there is:

$$C_{0M} \sum_{k=1}^{N} (1-\eta_{pk}) p_k = C_{0M} P_{\mathrm{D}} \Rightarrow C_{0M} \left[\sum_{k=1}^{N} (1-\eta_{pk}) p_k - P_{\mathrm{D}} \right] = 0 \tag{9.55}$$

This is the minimum purchase cost of power generation-side market. Because P_{D} is constant, Eqs. (9.55) and (9.49) constitute the competitive equilibrium model of a power market. If users participate in bidding, Eq. (9.49) changes into:

$$\sum_{k=1}^{N} (1-\eta_{pk}) p_k = 0 \tag{9.56}$$

The competitive equilibrium is achieved in a power market as well.

9.3.2 Model Considering Both Active and Reactive Transactions

There are two ways for reactive power pricing. One is that the reactive power is to participate in market bidding and the price is determined in the competition process; the other is pricing according demand in market [102]–[104]. This chapter analyzes the situation of reactive power participating in market bidding.

When considering the power market with two kinds of commodity including reactive power, it is assumed that the generators are producers of both active and reactive power, and users are consumers of also both active and reactive power.

In the general commodity market, it is always assumed that, in the market, the producers are aiming at maximizing profits, whereas the consumers are pursuing the maximization of utility, that is the greatest commodity satisfaction. This assumption is reasonable in the micromarket, because this is the premise for market to play a regulatory role. This regulatory role appears to be messy on the surface but is actually very orderly.

The producers of power mainly refer to various types of generating units. Although reactive power supply also includes a large number of capacitor banks, SVC, and compensators, SVC and compensators can be used as special generating units, yet most of the capacitor banks are usually installed on user-side can be regarded as power demand.

For power producers-generation companies, the aim of participating in market competition is to maximize profit. When there are both active and reactive transactions in the market, the decision-making model is:

$$\max \quad c_k p_k + d_k q_k - C_k(p_k, q_k) \tag{9.57}$$

where c_k, d_k are the bid prices of active and reactive power of generation company of bus k, respectively. p_k, q_k are the active and reactive power outputs of generation company of bus k, respectively. $C_k(p_k, q_k)$ is the generation cost of generation company of bus k. Usually, it is difficult to distinguish between active and reactive power generation costs for generation companies. In general, most of power generation cost is active power generation cost, usually expressed in the form of a coal consumption curve. Therefore, generation cost can also be expressed as $C_k(p_k)$, which is the same as in the single commodity power market.

Due to the capacity constraints of generating units, the following inequality constraints must be satisfied:

$$p_k^2 + q_k^2 \le \left(S_k^{\max}\right)^2 \tag{9.58}$$

Eqs. (9.57) and (9.58) constitute the decision-making model of market participants-generation companies. For the convenience of analysis, it is assumed that the decision-making model of users is the same as that of the generation companies, just that p_k, q_k are negative.

Because the power grid company is a monopoly enterprise, it cannot pursue its own benefit maximization but rather pursues the benefit maximization of the whole power market system. That is, the market auctioneer considers the problem from the perspective of a social welfare person. The benefits of the whole power market system are reflected through the benefits of market participants. When the users do not participate in the bidding, there is:

$$\max \quad \sum_{k=1}^{N} [c_k p_k + d_k q_k - C_k(p_k)] \tag{9.59}$$

The power network equation, that is, the power flow equation must be satisfied:

$$\begin{aligned} &p_k - P_{LK} - e_k \sum_{j\in k} \left(G_{kj} e_j - B_{kj} f_j\right) - f_k \sum_{j\in k} \left(G_{kj} f_j + B_{kj} e_j\right) = 0 \\ &q_k - Q_{LK} - f_k \sum_{j\in k} \left(G_{kj} e_j - B_{kj} f_j\right) + e_k \sum_{j\in k} \left(G_{kj} f_j + B_{kj} e_j\right) = 0 \quad k = 1,2,\ldots,N \end{aligned} \tag{9.60}$$

where $k = 1, 2, \ldots, N$ represents the number of buses. p_k, $P_{\mathrm{L}k}$ represent the active generation and load of bus k. q_k, $Q_{\mathrm{L}k}$ represent the reactive generation and load of bus k. The active and reactive power balance equations are accumulated respectively, and the total active and reactive power balance equations are obtained:

$$\sum_{k=1}^{N} (p_k - P_{\mathrm{L}k}) - P_{\mathrm{D}} = \sum_{k=1}^{N} p_k - P_{\mathrm{L}} - P_{\mathrm{D}} = 0 \tag{9.61}$$

$$\sum_{k=1}^{N}(q_k - Q_{Lk}) - Q_D = \sum_{k=1}^{N} q_k - Q_L - Q_D = 0 \quad k = 1,2,\ldots, N \tag{9.62}$$

where P_L, Q_L are the active and reactive load of the system respectively. P_D, Q_D are the active and reactive network loss respectively. Besides, the inequality constraints of system security need to be satisfied:

$$I_l - I_l^{\max} \le 0 \quad l = 1,2,\ldots, M \tag{9.63}$$

$$V_k^{\min} \le V_k \le V_k^{\max} \quad k = 1,2,\ldots, N \tag{9.64}$$

In the bidding process, the generation cost of generating company is usually unknown, therefore, the objective function of power market decision-making changes into:

$$\max \quad \sum_{k=1}^{N}(c_k p_k + d_k q_k) \tag{9.65}$$

Eqs. (9.59)–(9.65) constitute the decision-making model of an auctioneer in the generation-side market. In the case of users participate in bidding, power flow Eq. (9.60) changes into:

$$\begin{aligned} &p_k - e_k \sum_{j\in k}\left(G_{kj}e_j - B_{kj}f_j\right) - f_k \sum_{j\in k}\left(G_{kj}f_j + B_{kj}e_j\right) = 0 \\ &q_k - f_k \sum_{j\in k}\left(G_{kj}e_j - B_{kj}f_j\right) + e_k \sum_{j\in k}\left(G_{kj}f_j + B_{kj}e_j\right) = 0 \quad k = 1,2,\ldots,N \end{aligned} \tag{9.66}$$

where p_k, q_k represent the active and reactive power of generation or load injected at bus k respectively. Similarly, the total active and reactive power balance of Eqs. (9.61) and (9.62) change into:

$$\sum_{k=1}^{N} p_k - P_L = 0 \tag{9.67}$$

$$\sum_{k=1}^{N} q_k - Q_L = 0 \tag{9.68}$$

When the reactive power participates in the market bidding, the decision-making model of market auctioneer is shown as Eqs. (9.59)–(9.64). Written in the form of slackness, the objective function becomes:

$$\begin{aligned} &\max \sum_{k=1}^{N}(c_k p_k + d_k q_k) + \sum_{k=1}^{N}\left[\alpha_{pk}F_{pk}(p_k) + \alpha_{qk}F_{qk}(q_k)\right] \\ &+ \sum_{l=1}^{M_l}\lambda_l\left(I_l - I_l^{\max}\right) + \sum_{k=1}^{N_l}\left[\varphi_k^l\left(V_k^{\min} - V_k\right) + \varphi_k^u\left(V_k - V_k^{\max}\right)\right] \end{aligned} \tag{9.69}$$

Satisfy constraints:

$$\sum_{k=1}^{N} p_k - P_L - P_D = D0 \tag{9.70}$$

$$\sum_{k=1}^{N} q_k - Q_L - Q_D = D0 \tag{9.71}$$

When using accounting cost pricing, the network reactive power loss is:

$$Q_{\mathrm{L}} = \sum_{k=1}^{N} \eta_{qk} q_k \tag{9.72}$$

where η_{qk} is the network loss allocation coefficient.

Similarly, assume that reactive power is strongly related to bus voltage, using accounting cost pricing, the upper and lower limit constraints of bus voltage can be expressed as follows:

$$\begin{cases} V_k^{min} - V_k = \sum_{j=1}^{N_I} \varphi_{kj}^{l} q_j \\ V_k - V_k^{max} = \sum_{j=1}^{N_I} \varphi_{kj}^{u} q_j \end{cases} \tag{9.73}$$

Define $\varphi_{kj}^{l} = (V_k^{min} - V_k)/q_j$ as the impact factor of reactive power injection to bus voltage of each bus.

Besides:

$$F_{qk}(q_k) = \rho_{qk} q_k \tag{9.74}$$

Define:

$$\rho_{qk} = 1 - \frac{\Delta_{qk}^{flow}(q_k)}{q_k} \tag{9.75}$$

Where:

$$\Delta_{qk}^{flow}(qk) = -Q_{Lk} - f_k \sum_{j \in k} \left(G_{kj} e_j - B_{kj} f_j \right) + e_k \sum_{j \in k} \left(G_{kj} f_j + B_{kj} e_j \right) \tag{9.76}$$

When using Cournot model, it is assumed that the active power is related to the line power flow, whereas the reactive power is related to the bus voltage.

$$\omega_k = \varphi_{kj}^{l} \sum_{j=1}^{N_I} \varphi_{kj}^{l} + \varphi_{kj}^{u} \sum_{j=1}^{N_I} \varphi_{kj}^{u} \tag{9.77}$$

Write into the form of augmented Lagrange function

$$\begin{aligned}\max &\sum_{k=1}^{N}(c_k p_k + d_k q_k) + \beta_p \sum_{k=1}^{N}(1-\eta_{pk})p_k + \beta_q \sum_{k=1}^{N}(1-\eta_{qk})q_k \\ &+\sum_{k=1}^{N}\left(\alpha_{pk}\rho_{pk}p_k + \alpha_{qk}\rho_{qk}q_k\right) + \sum_{k=1}^{M_I}\gamma_k p_k + \sum_{k=1}^{N_I}\omega_k q_k\end{aligned} \tag{9.78}$$

Take the derivation of p_k, q_k, respectively and the optimal conditions are obtained as follows:

$$c_k = -\alpha_{pk}\rho_{pk} - \beta_p(1-\eta_{pk}) + \gamma_k = 0 \tag{9.79}$$

$$d_k = -\alpha_{qk}\rho_{qk} - \beta_q(1-\eta_{qk}) + \omega_k = 0 \tag{9.80}$$

The objective function can be rewritten as:

$$\max \sum_{k=1}^{N}\left[-\beta_p(1-\eta_{pk})p_k - \beta_q(1-\eta_{qk})q_k\right] \tag{9.81}$$

Eqs. (9.70) and (9.71) change into:

$$\sum_{k=1}^{N}(1-\eta_{pk})p_k = P_{\mathrm{D}} \tag{9.82}$$

$$\sum_{k=1}^{N}(1-\eta_{qk})q_k = Q_{\mathrm{D}} \tag{9.83}$$

Let $C_{0M} = -\beta_p$, $D_{0M} = -\beta_q$, the objective function changes into:

$$C_{0M}P_{\mathrm{D}} + D_{0M}Q_{\mathrm{D}} \tag{9.84}$$

Eqs. (9.82)–(9.84) constitute the general equilibrium model of generation-side power market.

9.3.3 Solution Algorithm

9.3.3.1 A modified equal bidding method considering active power transaction

Eq. (9.81) can be written in the form as follows:

$$\frac{c_k + \alpha_{pk}\rho_{pk} + \gamma_k}{1-\eta_{pk}} = -\beta_p = C_{0M} \tag{9.85}$$

For bus k, the bid price is not equal to c_k, but becomes equal to each other after taking three modifications, such as bus modification $\alpha_{pk}\rho_{pk}$, congestion modification γ_k, and network loss modification $(1-\eta_{pk})$. So the market equilibrium point can be achieved by using modified equal bidding method, whose basic idea is to determine the power p_k of each bus according to

the feature that the modified bid price of bus k is equal to c_k, so that the supply and demand balance of the whole system is met and the competitive equilibrium is achieved [105].

Eq. (9.51) is just one of the optimal conditions of the power market decision-making problem in Eqs. (9.48) and (9.49), and is the differential equation for control variable p_k. If the variables that represent the power network state, such as the real and imaginary parts of the bus voltage, are taken as the state variable, expressed as x_k, then the differential equation of Eq. (9.50) for state variables x_k can be described as follows:

$$\alpha_{pk} p_k \frac{\partial \rho_{pk}}{\partial x_k} - \beta_p p_k \frac{\partial \eta_{pk}}{\partial x_k} + p_k \frac{\partial \gamma_k}{\partial x_k} = 0 \quad k = 1,2,\ldots,N \tag{9.86}$$

That is

$$\alpha_{pk} \frac{\partial \rho_{pk}}{\partial x_k} - \beta_p \frac{\partial \eta_{pk}}{\partial x_k} + \frac{\partial \gamma_k}{\partial x_k} = 0 \tag{9.87}$$

The power market decision-making model in Eqs. (9.48) and (9.49) is a nonlinear programming problem, where Eqs. (9.87), (9.52), (9.49), (9.6), and (9.7) are the Tucker Kuhn conditions of this optimal problem, that is, the optimal conditions. Similar to steps of the gradient method, the modified equal bidding method is to solve these optimal conditions, respectively. The calculation process of modified equal bidding method can be described as follows:

(1) Let $m = 0$, the initial value of marginal price $C_{0M}^{(m)}$ and step size ΔC_{0M} are given, and let ${c_k}^{(m)} = C_{0M}^{(m)}$.
(2) Determine the value of control variable $p_k^{(m)}$ according to ${c_k}^{(m)}$ and the bid curves of each generation company.
(3) Calculate power flow according to Eq. (9.6), and determine the value of state variables x_k, that is the real and imaginary parts of bus voltage.
(4) Determine the value of network loss modification coefficients η_{pk} and ρ_{pk}, according to certain principle of network loss allocation, based on the result of power flow calculation.
(5) Judge whether Eq. (9.49) is satisfied. If satisfied, turn to Step (8), else turn to the next step
(6) Judge the inequality constraints that play a role and calculate the Lagrange multipliers γ_k, α_{pk} corresponding equality and inequality constraints according to Eq. (9.88).
(7) Let $m = m+1$, $C_{0M}^{(m)} = C_{0M}^{(m-1)} + \Delta C_{0M}$, modify the bidding price ${c_k}^{(m)}$ according to Eq. (9.85), and return to Step 2).
(8) The calculation ends.

9.3.3.2 A modified equal quotation method considering active and reactive power transaction

When reactive power participates in bidding, the output of active and reactive power submitted by the generation company is the function of price of active and reactive power. As an example of Cournot simulation, Eqs. (9.79) and (9.80) are written in the following forms:

$$\frac{c_k + \alpha_{pk}\rho_{pk} + \gamma_k}{1 - \eta_{pk}} = -\beta_p = C_{0M} \tag{9.88}$$

$$\frac{d_k + \alpha_{qk}\rho_{qk} + \omega_k}{1 - \eta_{qk}} = -\beta_q = D_{0M} \tag{9.89}$$

where $k = 1, 2, \ldots, N$. For bus k, both the active power price and reactive power price become equal respectively after several times modification, which is also the principle of modified equal bidding method.

Eqs. (9.79) and (9.80) are just one of the optimal conditions, which are the differential equations for control variables p_k, q_k. Besides, the optimal condition also includes the differential equation of expanded Lagrange function to the state variables x_k.

$$\begin{aligned} &p_k\left(\alpha_{pk}p_k\frac{\partial\rho_{pk}}{\partial x_k} + \frac{\partial\gamma_k}{\partial x_k} + C_{0M}\frac{\partial\eta_{pk}}{\partial x_k}\right) \\ &+q_k\left(\alpha_{qk}p_k\frac{\partial\rho_{qk}}{\partial x_k} + \frac{\partial\omega_k}{\partial x_k} + D_{0M}\frac{\partial\eta_{qk}}{\partial x_k}\right) = 0 \end{aligned} \tag{9.90}$$

Subject to the equality constraints:

$$\begin{aligned} &p_k - P_{LK} - e_k\sum_{j\in k}\left(G_{kj}e_j - B_{kj}f_j\right) - f_k\sum_{j\in k}\left(G_{kj}f_j + B_{kj}e_j\right) = 0 \\ &q_k - Q_{LK} - f_k\sum_{j\in k}\left(G_{kj}e_j - B_{kj}f_j\right) + e_k\sum_{j\in k}\left(G_{kj}f_j + B_{kj}e_j\right) = 0 \quad k = 1,2,\ldots,N \end{aligned} \tag{9.91}$$

$$\sum_{k=1}^{N}\left(1 - \eta_{pk}\right)p_k = P_{\mathrm{D}} \tag{9.92}$$

$$\sum_{k=1}^{N}\left(1 - \eta_{qk}\right)q_k = Q_{\mathrm{D}} \tag{9.93}$$

And the working inequality constraints:

$$I_l - I_l^{\max} = 0 \quad l = 1,2,\ldots,M_I \tag{9.94}$$

$$V_k^{\min} - V_k = 0 \quad \text{or} \quad V_k - V_k^{\max} = 0 \quad k = 1,2,\ldots,N_{\mathrm{G}} \tag{9.95}$$

Eqs. (9.88)–(9.95) constitute the complete expression of the optimal conditions.

As mentioned previously, the modified equal bidding method is similar to the gradient method. First, determine state variables based on the equality constraints, and then calculate Lagrange multipliers according to the differential equation of the corresponding state variables. Finally, determine the amount of modification according to the differential equations of the corresponding controls variables. What the modified equal bidding method modifies is not the

control variables but the variable price of the system, and control variables are determined according to the bidding curves. The calculation steps of the modified equal bidding method are as follows:

(1) Let $m=0$, the initial value of marginal price $C_{0M}^{(m)}$, $D_{0M}^{(m)}$and step size are given, and let ${c_k}^{(m)}=C_{0M}^{(m)}$, ${d_k}^{(m)}=D_{0M}^{(m)}$.
(2) Determine the active power $p_k^{(m)}$ and reactive power $q_k^{(m)}$ of each generation company and user according to the bid curves.
(3) Calculate power flow according to Eq. (9.91) and determine the network loss allocation coefficients η_{pk} and η_{qk}based on the established principle of network loss allocation.
(4) Judge whether Eqs. (9.92) are (9.93) are satisfied. If not satisfied, then determine the price deviation ΔC_{0M} and ΔC_{0M} according to the deviation of supply and demand, else turn to Step 7).
(5) Judge whether the inequality in Equations constraints (9.94) and (9.95) work. If not, turn to next step; else determine $\gamma_k$and ω_k, and calculate Lagrange multipliers α_{pk} and α_{qk} according to Eq. (9.90).
(6) Modify the marginal price $C_{0M}^{(m+1)}=C_{0M}^{(m)}+\Delta C_{0M}$, $D_{0M}^{(m+1)}=D_{0M}^{(m)}+\Delta D_{0M}$
(7) Let $m=m+1$, modify the bidding price ${c_k}^{(m)}$ and ${d_k}^{(m)}$ according to Eqs. (9.88) and (9.89), and return to step 2).
(8) The calculation ends

9.4 Implementation

9.4.1 Example Analysis Considering Active Power Transaction

Active power transaction is simulated based on power pool model on the IEEE-30 bus test system, given an initial price of 280 yuan/MW. The results of active power transaction are given in Table 9.1. It is shown that the bus price is basically consistent, which can be considered to achieve a unified market marginal price. Considering network loss, the supply is equal to the sum of demand and loss, so as to achieve the balance between supply and demand. The revenue and expenditure of generation companies and users are balanced, and there is no market surplus. Network loss and congestion are fairly allocated among market participants. The results of power transaction meet the features of market competitive equilibrium, or reach the intersection point of supply and demand functions. In conclusion, the economy optimality is achieved.

Table 9.1 The result of active power transaction

Node No.	1	2	3	4	5	6	7	8
Injected active power	0.857267	0.512408	−0.134565	−0.140648	−0.140857	0	−0.131707	0.413697
Injected reactive power	0.122187	0.219612	0.026162	0.072395	−0.164064	0	−0.110505	−0.027858
Nodal electricity price	2780730	279.920	289.807	289.967	289.949	276.458	289.825	276.097
Node No.	9	10	11	12	13	14	15	16
Injected active power	0	−0.142388	0.435485	−0.219536	0.501308	−0.139873	−0.114740	−0.135191
Injected reactive power	0	−0.111837	0.201830	−0.212755	0.263293	0.019811	0.010285	0.029288
Nodal electricity price	276.458	289.488	279.920	285.476	279.742	289.594	292.221	289.985
Node No.	17	18	19	20	21	22	23	
Injected active power	−0.140305	−0.133879	−0.138020	−0.136305	−0.138922	0	−0.134857	
Injected reactive power	−0.038821	0.042815	−0.011346	0.0484001	−0.140703	0	0.0364030	
Nodal electricity price	289.772	289.985	289.967	289.772	290.002	276.458	290.505	
Node No.	24	25	26	27	28	29	30	
Injected active power	−0.108276	0	−0.136305	0	0	−0.134139	−0.140269	
Injected reactive power	−0.053624	0	0.039915	0	0	0.036745	−0.008992	
Nodal electricity price	292.310	276.458	289.72	276.458	276.458	289.988	289.813	

9.4.2 Example Analysis Considering Active and Reactive Power Transaction

The transaction with bidding for reactive power is simulated to verify the effect of the equilibrium theory used in reactive power pricing. The initial active power price is 300 yuan/MW, and the initial reactive power price is 60 yuan/MW. The modified equal bidding method is used for the iterative calculation with a step size of 0.0011. The final prices of active and reactive power are 298.77 yuan/MW and 57.919 yuan/MW, respectively.

Node	Voltage	Phase Angle	Active Power Generation	Reactive Power Generation	Active Load	Reactive Load
1	1.00775	−11.8108	0	0	0.1060	0.019
2	1.03508	−2.65845	0.491978	0..491978	0.2170	0.127
3	1.03402	−4.31006	0	0	0.0240	0.012
4	1.0296	−5.15664	0	0	0.0760	0.016
5	1.00833	−8.65425	0	0	0.6964	−0.0325
6	1.02527	−5.90234	0	0	0	0
7	1.01064	−7.55517	0	0	0.2280	0.109
8	1.02593	−6.10403	0.246259	0.326635	0.3000	0.3
9	1.05697	−5.69575	0	0	0	0
10	1.05503	−8.20003	0	0	0.0580	0.02
11	1.0822	−0.876312	0.462029	0.150682	0	0.0075
12	1.06426	−8.38509	0	0	0.1120	0
13	1.09602	−7.45593	0.135108	0.249746	0	0.016
14	1.04969	−9.17984	0	0	0.0620	0.025
15	1.04589	−9.18936	0	0	0.0820	0.018
16	1.05346	−8.58068	0	0	0.0350	0.058
17	1.04935	−8.51922	0	0	0.0900	0.009
18	1.03712	−9.52438	0	0	0.0320	0.034
19	1.03501	−9.53384	0	0	0.0950	0.007
20	1.03926	−9.25602	0	0	0.0220	0.112
21	1.04288	−8.73498	0	0	0.1750	0
22	1.04345	−8.75347	0	0	0	0.016
23	1.03619	−9.49111	0	0	0.0320	0.025
24	1.03157	−9.55268	0	0	0.0870	0.018
25	1.03052	−9.84062	0	0	0	0.058
26	1.01305	−10.2482	0	0	0.0350	0.009
27	1.03856	−9.7619	0	0	0	0.034
28	1.02143	−6.30648	0	0	0	0.007
29	1.01904	−10.9551	0	0	0.0240	0.112
30	1.05	0	1.28864	−0.0224092	0	0

9.5 Conclusion

The equilibrium is the optimal state of the power market, which can realize the optimal allocation of resources, and balance the fairness and benefit. The method to achieve the equilibrium in a power market is analyzed by establishing the competitive equilibrium model. The objective of market transaction optimization model is to maximize the social benefits, considering the constraints including the balance of supply, demand, and system security. Using the modified equal bidding method solves the model. The final results show that the equilibrium can be achieved by the market transaction optimization model. The transaction results are consistent with the features of competitive equilibrium: There is a unified market marginal price, achieving the balance of supply and demand, and the balance of revenue and expenditure.

APPENDIX A

An Approximation Method for Mixed Integer Programming

Because successful integer programming methods that guarantee optimal solutions are limited, various approximation methods have been investigated. An approximation method aims at obtaining a good feasible solution relatively quickly. The quality of the obtained solution seems to be quite high. Judging from the computational experience for test problems with known optimal solutions, the obtained integer feasible solutions are usually very close to (and frequently even equal to) the exact optimal solutions. It is concluded that the approximation approach of this type can be considered as one of the most promising practical methods for mixed-integer programs. Therefore, the approximation method for solving the linear mixed-integer programming (MIP) problem (see Chapters 4 and 6) is employed.

The flow chart of the approximation method used is shown in Fig. A.1. The basic idea of the approximation method is to search for a good feasible solution near an optimal solution of the linear programming (LP) problem in which the integer constraints are relaxed.

A.1 Basic Algorithm

To accommodate the requirements on the discrete reactive power optimization calculation of the power system, this Appendix uses an approximate mixed-integer linear programming (MILP) algorithm with some modifications. The algorithm aims at finding the integer-feasible solution at a fast speed, enabling the derived integer-feasible solution to get close to the optimal solution. The approximation algorithm is realized on the LP programming package in the commercial mathematical programming package (MPS). The derived result is compared with the calculation result derived via the integer programming package. The calculation result indicates the derived integer-feasible solution is close and even equal to the optimal solution.

The basic idea of the method is to search for one integer-feasible solution around the optimal solution of LP and keep improving it after deriving the integer solution.
The method falls into three stages.

The outline of each phase in the approximation method is given in the following section.

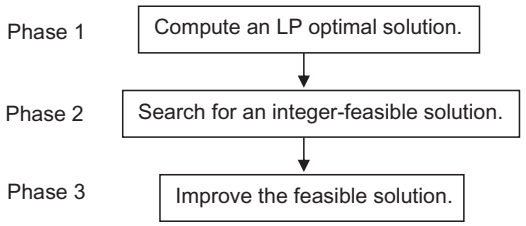

Fig. A.1
Approximation mixed-integer programming method.

A.1.1 Phase 1

Consider the linear MIP problem PLR where the condition that Y and W are integer vectors is relaxed. This relaxed LP problem PLR is described as follows:

$$\text{Problem PLR}: \quad \min \quad V = C^t Y + D^t W \tag{A.1}$$

$$\text{s.t.} \quad AX + BY = b \tag{A.2}$$

$$Y \le \lfloor \overline{Y} \rfloor W \tag{A.3}$$

$$\underline{X} \le X \le \overline{X} \tag{A.4}$$

$$0 \le Y \le \overline{Y} \tag{A.5}$$

$$0 \le W \le I \tag{A.6}$$

$$X, Y, W : \text{continuous variable vectors} \tag{A.7}$$

where "t": Transposition of a vector; v: variable corresponding to the objective function; A,B: Coefficient matrices with respect to X and Y; b: Right-hand side coefficient vector; $C = (c_i)$: vector of fixed costs; $D = (d_i)$: vector of variable costs; $\lfloor \overline{Y} \rfloor$: diagonal matrix with the i–i elements $\overline{y}_i$; $\overline{Y} = (\overline{Y}_i)$: vector of maximum numbers of y_i; I: $(1, 1, \ldots, 1)$.^{t}

The optimal solution (X^S, Y^S, W^S) of the LP problem PLR is obtained by the simplex method. Of the solution (X^S, Y^S, W^S), if Y^S and W^S are integer vectors, then problem PLR gets an optimal solution of the linear MIP problem PL, and the algorithm terminates. Otherwise Phase 2 is performed.

A.1.2 Phase 2

Each of the continuous values in (Y^S, W^S) is rounded off to the nearest integer value and fixed at this value. Then search for an integer-feasible solution. Here, the detail of this search is described. For fixed-integer vectors Y and W, the following LP problem PLRF is constructed and solved:

$$\text{Problem PLRF}: \quad \min \quad V = C^t Y + D^t W \tag{A.8}$$

$$\text{s.t.} \quad AX + BY = b \tag{A.9}$$

$$\underline{X} \le X \le \overline{X} \tag{A.10}$$

$$X: \text{ continuous variable vectors} \tag{A.11}$$

$$Y, W: \text{fixed integer variable vectors} \tag{A.12}$$

Let Eqs. (A.13) and (A.14) denote the simplex tableau of LP problem PLRF.

$$v = e_{oo} + \sum_{i=1}^{m} e_{oj}(-r_j) + \sum_{i=1}^{n2} f_{oj}(-y_j) + \sum_{i=1}^{n3} g_{oj}(-w_j) \tag{A.13}$$

$$u_i = e_{io} + \sum_{j=1}^{m} e_{ij}(-r_j) + \sum_{j=1}^{n2} f_{ij}(-y_j) + \sum_{\substack{i=1,2,\ldots m \\ j=1}}^{n3} g_{ij}(-w_j) \tag{A.14}$$

where $(U,R) = X$; $U = (u_i)$: m-dimensional vector of basic continuous variables; $R = (r_j)$: n_1-dimensional vector of nonbasic continuous variables; e_{ij}, f_{ij}, g_{ij}: Constant coefficients.

If the LP problem PLRF is feasible, then go to Phase 3. Otherwise, only one integer variable is changed by an amount of -1 or $+1$ each time. For simplicity, only how to change integer variable y_j is described hereinafter. Let define q_j and q_j as follows:

$$q_j^- = \begin{cases} -\infty & , \quad y_j = \underline{y}_j \\ \sum_{i=1}^{m} \min\left(0, \overline{u}_j - \left(u_i^s + f_{ij}\right), \left(u_i^s + f_{ij}\right) - \underline{u}_i\right), & y_j > \underline{y}_j \end{cases} \tag{A.15}$$

$$q_j^+ = \begin{cases} -\infty & , \quad y_j = \overline{y}_j \\ \sum_{i=1}^{m} \min\left(0, \overline{u}_j - \left(u_i^s - f_{ij}\right), \left(u_i^s - f_{ij}\right) - \underline{u}_i\right), & y_j < \overline{y}_j \end{cases} \tag{A.16}$$

where $X^S = (U^S, \ R^S)$. Note that $u_i^S + f_{ij}$ and $u_i^s - f_{ij}$ denote the values of basic variables, and that q_j^- and $q_{j,}^+$ respectively, denote infeasibility measures when y_j is changed by -1 and $+1$. Let

$$q_k^* = \max\left\{q_j^+, \ q_j^- : \ j = 1, 2, \ldots, n_2\right\} \tag{A.17}$$

Then y_k is changed by *1 (* denotes + or $-$) because this is the most promising change according to the previous measure. After changing y_k, the problem PLRF is solved again. The previous procedure is repeatedly carried out until problem PLRF becomes feasible.

A.1.3 Phase 3

First, one of integer variables is selected and changed by +1 or −1 so that the objective function value may decrease. If the resulting solution is still feasible, the old solution is replaced and an attempt for improvement is executed again from the new solution. On the other hand, if the resulting solution is not feasible, the search for a feasible solution with a better objective function value takes place in a manner similar to Phase 2.

The selection of the integer variable y_j to decrease the objective function value is done according to parameters h_{ij} $i = 1,2, \ldots, n_2$, $j = 1,2, \ldots, m$, derived from the simplex tableau of LP problem PLRF. The parameters are defined as follows:

$$h_{ij} = 0 \text{ if } f_{0j} = 0 \text{ or } \left(f_{0j} > 0 \text{ and } y_j^s = \overline{y}_j\right) \text{ or } \left(f_{0j} < 0 \text{ and } y_j^s = \underline{y}_j\right) \tag{A.18}$$

Otherwise:

$$h_{ij} = \begin{cases} 0 & \text{if } f_{ij} = 0 \\ \min\left\{\left(u_i^s - \underline{u}_i\right)/\left|f_{ij}\right|, a\right\} & \text{if } f_{oj} \bullet f_{ij} > 0 \\ \min\left\{\left(\overline{u}_i - u_i^s\right)/\left|f_{ij}\right|, a\right\} & \text{if } f_{oj} \bullet f_{ij} < 0 \end{cases} \tag{A.19}$$

where

$$\begin{cases} a = y_j^s - \underline{y}_j & \text{if } f_{oj} < 0 \quad \text{and } y_j^s > \underline{y}_j \\ a = \overline{y}_j - y_j^s & \text{if } f_{oj} > 0 \quad \text{and } y_j^s < \overline{y}_j \end{cases} \tag{A.20}$$

Each $h_{ij}(\geq 0)$ gives the amount of y_j to be changed from y_j^s in the direction of decreasing the objective function value without violating the upper and lower limits of basic variable u_i. It is desirable to determine an integer variable and its direction of the change so that the decrease in the objective function value may be as large as possible while keeping the displacement from the feasibility condition.

$$\underline{u_i} \leq u_i^s \pm f_{ij} \leq \overline{u_i} \tag{A.21}$$

A.2 Comparisons Between the Algorithm and Branch-and-Bound Algorithm

The coefficients of two small-scale integer programming problems are generated with a randomizer, and the scale of the two examples are as follows:

(Case 1) constraint = 40, continuous variable = 30, and discrete variable = 30
(Case 2) constraint = 70, continuous variable = 40, and discrete variable = 60

Table A.1 Results of Case 1

Items	Branch and Bound		Approximation Algorithm	
	Objective Function	Calculation Time (s)	Objective Function	Calculation Time (s)
Continuous optimal solution	1351.14	0.29	1351.14	0.39
Integer feasible solution	1350.95	5.13	1350.55	0.90
Search end		5.41		1.43

Table A.2 Results for Case 2

Items	Branch and Bound		Approximation Algorithm	
	Objective Function	Calculation Time (s)	Objective Function	Calculation Time (s)
Continuous optimal	2610.0454	0.74	2610.0454	1.32
1st integer solution	2608.6760	2.64	2603.5500	2.05
2nd integer solution	2609.3160	8.73	2608.7750	4.00
…	…	…	…	…
*N*th integer solution	Space insufficient	Space insufficient	Continuous	Continuous
Search end		25.94		4.86

The algorithm realized on MPS-II and MPS-II MIP package are used to calculate two cases, Case 1 and Case 2, and results are as shown in Tables A.1 and A.2.

As shown in Table A.1, the calculation results of Case 1 via two methods are fairly close with a difference less than 0.03%. Therefore, the algorithm could be considered the reliable one.

Because the time for deriving an exact solution via the branch-and-bound method is an exponential function of the numbers of integer variables, the calculation time via the branch-and-bound algorithm will sharply rise, and the upper limit of the MIP package to calculate the integer variable is 50. The integer solution of Case 2 in Table A.2 is the solution interrupted by setting the parameters as its branch has reached the upper limit of MIP package. However, the calculation time for the proposed algorithm increases linearly only with the increase of the integer variable, therefore, it could effectively solve large scale integer programming problem. Because the algorithm could derive multiple integer feasible solutions via setting the parameters in the second stage, Table A.2 presents the second integer solution, which is another integer solution and is not necessarily better than the first integer solution.

APPENDIX B

The Differential Expressions for Transformer Tap and Shunt Capacitor Unit

This appendix presents the specific expressions for transformer ratio T (inclusive of tap position Y_T) and shunt capacitor bank Y_c. In the conventional power flow calculation, the transformer ratio T and reactive compensation capacity Q_c (equal to the number of banks $Y_c \times$ single bank capacity q_c) of the reactive compensation capacitor are given as a constant value, and its optimal solution can only be obtained via manual adjustment method. To optimize the transformer ratio T (inclusive of tap position Y_T) and the number of shunt capacitor banks Y_c in the optimal power flow (OPF) and the reactive power optimization model, it is required to expand the expression of the transformer ratio T and number of shunt capacitor banks Y_c in the power flow equation, and differentiate the transformer ratio T, tap position Y_T, and number of shunt capacitor banks Y_c, to optimize the transformer ratio T and tap location Y_T. See Chapters 4 and 6 for the specific models.

The concrete differentiation derivation process for transformer ratio T (tap position Y_T) is that you must first specify the transformer equivalent circuit (transformer π equivalent circuit) of the transformer impedance conversion to the LV side (i side) before deriving the branch power flow expression of transformer, and then take the differentiation expression for T and Y_T. When differentiating the number of capacitor banks Y_c, the ground branch expression of capacitor is given first, and then the differentiation expression for the number of capacitor banks Y_c is given.

(1) Transformer branch power flow equation.

1. The transformer equivalent circuit of the transformer impedance conversion to LV side (i side) is shown in Fig. B.1.

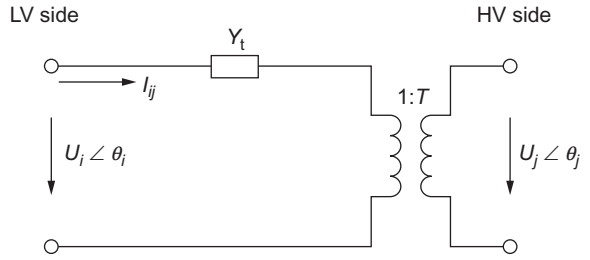

Fig. B.1

Transformer equivalent circuit converted to LV side. Where Y_t is the reciprocal of the transformer impedance, that is, the transformer admittance, and Y_t could be derived from the short circuit percentage U_k% and load loss P_t of the transformer.

T is the per-unit transformer ratio of transformer, $T = (T_i)/(T_j) = (U_i/U_{Bi})/(U_j/U_{Bj})$.

2. The corresponding transformer π equivalent circuit (voltage, current, impedance, and transformer ratio are per-unit values) is shown in Fig. B.2.

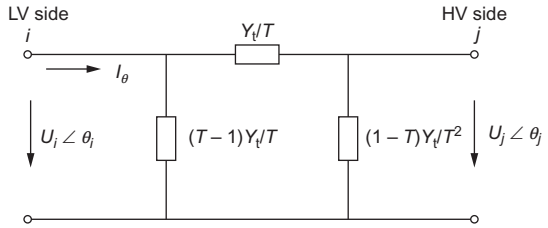

Fig. B.2

Transformer π equivalent circuit.

Let

$$Y_t = g_t + jb_t,\ Y_{ij} = Y_t/T = g_{ij} + jb_{ij}$$

then

$$Y_{i0} = (T-1)Y_t/T = g_{i0} + jb_{i0} = (1-T)Y_t/T^2 = g_{j0} + jb_{j0}$$

3. Derivation process from i to j end for transformer complex power.

$$\begin{aligned}
S_{ij} &= \dot{U}_i I_{ij}^* = \dot{U}_i \left[U_i^* Y_{i0}^* + \left(U_i^* - U_j^* \right) Y_{ij}^* \right] \\
&= U_i^2 Y_{i0}^* + \left(U_i^2 - \dot{U}_i U_j^* \right) Y_{ij}^* \\
&= U_i^2 Y_{i0}^* + \left[U_i^2 - U_i U_j e^{j(\theta_i - \theta_j)} \right] Y_{ij}^* \\
&= U_i^2 (g_{i0} - jb_{i0}) + \left[U_i^2 - U_i U_j (\cos\theta_{ij} + j\sin\theta_{ij}) \right] (g_{ij} - jb_{ij}) \\
&= U_i^2 g_{i0} - jU_i^2 b_{i0} + U_i^2 g_{ij} - jU_i^2 b_{ij} - U_i U_j g_{ij} \cos\theta_{ij} - jU_i U_j g_{ij} \sin\theta_{ij} + jU_i U_j b_{ij} \cos\theta_{ij} - U_i U_j b_{ij} \sin\theta_{ij} \\
&= U_i^2 (g_{i0} + g_{ij}) - U_i U_j (g_{ij} \cos\theta_{ij} + \sin\theta_{ij}) + j\left[U_i U_j (b_{ij} \cos\theta_{ij} - g_{ij} \sin\theta_{ij}) - U_i^2 (b_{i0} + b_{ij}) \right]
\end{aligned}$$

Then:

$$\begin{aligned}P_{ij} &= U_i^2\left(g_{i0}+g_{ij}\right)-U_iU_j\left(g_{ij}\cos\theta_{ij}+b_{ij}\sin\theta_{ij}\right)\\ &= U_i^2\left[\frac{(T-1)g_{\mathrm{t}}}{T}+\frac{g_{\mathrm{t}}}{T}\right]-U_iU_j\left(\frac{g_{\mathrm{t}}}{t}\cos\theta_{ij}+\frac{b_{\mathrm{t}}}{T}\sin\theta_{ij}\right)\\ &= U_i^2g_t-\frac{U_iU_j}{T}\left(g_t\cos\theta_{ij}+b_t\sin\theta_{ij}\right)\end{aligned}$$

$$\begin{aligned}Q_{ij} &= U_iU_j\left(b_{ij}\cos\theta_{ij}-g_{ij}\sin\theta_{ij}\right)-U_i^2\left(b_{i0}+b_{ij}\right)\\ &= U_iU_j\left(\frac{b_{\mathrm{t}}}{T}\cos\theta_{ij}-\frac{g_{\mathrm{t}}}{T}\sin\theta_{ij}\right)-U_i^2\left[\frac{(T-1)}{T}b_{\mathrm{t}}+\frac{b_{\mathrm{t}}}{T}\right]\\ &= -U_i^2b_{\mathrm{t}}-\frac{U_iU_j}{T}\left(g_t\sin\theta_{ij}-b_t\cos\theta_{ij}\right)\end{aligned}$$

Then it could derive:

$$\begin{cases}P_{ij}=U_i^2g_{\mathrm{t}}-\dfrac{U_iU_j}{T}\left(g_{\mathrm{t}}\cos\theta_{ij}+b_{\mathrm{t}}\sin\theta_{ij}\right)\\ Q_{ij}=-U_i^2b_{\mathrm{t}}-\dfrac{U_iU_j}{T}\left(g_{\mathrm{t}}\sin\theta_{ij}-b_{\mathrm{t}}\cos\theta_{ij}\right)\end{cases}$$

Likewise, it could derive:

$$\begin{cases}P_{ji}=\dfrac{U_j^2}{T^2}g_{\mathrm{t}}-\dfrac{U_iU_j}{T}\left(g_{\mathrm{t}}\cos\theta_{ij}-b_{\mathrm{t}}\sin\theta_{ij}\right)\\ Q_{ji}=-\dfrac{U_j^2}{T^2}b_{\mathrm{t}}-\dfrac{U_iU_j}{T}\left(g_{\mathrm{t}}\sin\theta_{ij}+b_{\mathrm{t}}\cos\theta_{ij}\right)\end{cases}$$

Therefore, the transformer branch power flow expression is:

$$\begin{aligned}P_{ij} &= U_iU_ig_i-U_iU_j\left(g_{\mathrm{t}}\cos\theta_{ij}+b_{\mathrm{t}}\sin\theta_{ij}\right)/T\\ Q_{ij} &= -U_iU_ib_{\mathrm{t}}-U_iU_j\left(g_{\mathrm{t}}\sin\theta_{ij}-b_{\mathrm{t}}\cos\theta_{ij}\right)/T\\ P_{ji} &= U_jU_jg_{\mathrm{t}}/T^2-U_iU_j\left(g_{\mathrm{t}}\cos\theta_{ij}-b_{\mathrm{t}}\sin\theta_{ij}\right)/T\\ Q_{ji} &= -U_iU_jb_{\mathrm{t}}/T^2+U_iU_j\left(g_{\mathrm{t}}\sin\theta_{ij}+b_{\mathrm{t}}\cos\theta_{ij}\right)/T\end{aligned}$$

(2) Differentiation equation of transformer branch power flow over transformer T.
The following differential expression could be derived via differentiating the transformer branch power flow.

$$\begin{aligned}\partial P_{ij}/\partial T &= U_iU_j\left(g_{\mathrm{t}}\cos\theta_{ij}+b_{\mathrm{t}}\sin\theta_{ij}\right)/T^2\\ \partial Q_{ij}/\partial T &= U_iU_j\left(g_{\mathrm{t}}\sin\theta_{ij}-b_{\mathrm{t}}\cos\theta_{ij}\right)/T^2\\ \partial P_{ji}/\partial T &= -2U_jU_jb_{\mathrm{t}}/T^3+U_iU_j\left(g_{\mathrm{t}}\cos\theta_{ij}-b_{\mathrm{t}}\sin\theta_{ij}\right)/T^2\\ \partial Q_{ji}/\partial T &= 2U_iU_jb_{\mathrm{t}}/T^3-U_iU_j\left(g_{\mathrm{t}}\sin\theta_{ij}+b_{\mathrm{t}}\cos\theta_{ij}\right)/T^2\end{aligned}$$

(3) Differential expression of transformer branch power flow over transformer tap position.

1. Relation of per unit transformer ratio to tap position and tap location.
   In the power system scheduling, generally the transformer tap position is given to adjust the tap location (see Table B.1).

Table B.1 Basic parameters for two-winding transformer ratio

T_0	ΔT (%)	Tap Location M		U_i (kV)	U_j (kV)
Rated Per Unit Transformer Ratio	Unit Step Length	M_{min}	M_{max}	LV side voltage	HV side voltage
1.0	2.5	−2	2	10	121

In addition, in the optimization calculation, the transformer tap position is easy to be deal as integer variable, so as to derive the optimized tap location of transformer.

$$T = T_{\max} + (1 - Y_T)\Delta T/100$$

where T: per unit transformer ratio; Y_T: tap position, $1 \le Y_T \le 5$; $T_{\max}$: $T_{\max} = T_0 + M_{\max}\Delta T/100$。

See Table B.2 for the relation of transformer tap position Y_T (integer variable) to tap location M and per-unit transformer ratio T.

Table B.2 Relation of transformer tap position Y_T (integer variable) to tap location M and per-unit transformer ratio T

Transformer Tap Position Y_T	Tap Location M	Per Unit Transformer Ratio T
1	2	1.05
2	1	1.025
3	0	1.0
4	−1	0.975
5	−2	0.95

2. Differentiation expression of transformer branch power flow over transformer tap position.
   As $T = T_{\max} + (1 - Y_T)\Delta T/100$, if Y_T is deemed as variable, then:

$$\partial T/\partial Y_T = -\Delta T/100$$

Substitute the previous equation into the differentiation expression of transformer over T:

$$\partial P_{ij}/\partial T = U_i U_j\left(g_t \cos\theta_{ij} + b_t \sin\theta_{ij}\right)/T^2 \quad \partial P_{ji}/\partial T = -2U_j U_j b_t/T^3 + U_i U_j\left(g_t \cos\theta_{ij} - b_t \sin\theta_{ij}\right)/T^2$$

$$\partial Q_{ij}/\partial T = U_i U_j\left(g_t \sin\theta_{ij} - b_t \cos\theta_{ij}\right)/T^2 \quad \partial Q_{ji}/\partial T = 2U_i U_j b_t/T^3 - U_i U_j\left(g_t \sin\theta_{ij} + b_t \cos\theta_{ij}\right)/T^2$$

Then it could derive:

$$\partial P/\partial Y_{\mathrm{T}} = (\partial P/\partial T)(\partial T/\partial Y_{\mathrm{T}})$$

It is the expression for transformer tap position in the optimization model.

(4) Reactive power compensated by shunt capacitor banks and its differentiation expression:

$$b_{\mathrm{c}} = \omega \Delta C$$
$$q_{\mathrm{c}} = U^2 b_{\mathrm{c}}$$
$$Q_{\mathrm{c}} = Y_{\mathrm{c}} q_{\mathrm{c}} = Y_{\mathrm{c}} U^2 b_{\mathrm{c}}$$

where ΔC is the single capacitor bank capacity; ω is the system angular frequency; b_{c} is the admittance of single capacitor bank; U is the rated voltage at capacitor access point; q_{c} is the reactive power compensated by single capacitor bank; Y_{c} is the number of capacitor banks (integer variable); and Q_{c} is the reactive power compensated by capacitor bank.

Differentiate the number of capacitor banks Y_{c} as follows:

$$\partial Q_{\mathrm{c}}/\partial Y_{\mathrm{c}} = U^2 b_{\mathrm{c}}$$

APPENDIX C

A DC Load Flow Method for Calculating Generation Angle

When online control is adopted for the power system via the method defined in Chapter 8, it is necessary to calculate the value of the decoupling reference value δ_{ei} locally in the system. To obtain δ_{ei}, the transient power flow must be calculated. Because the power flow calculation relates to the nonlinear equation, it can only be solved by the iterative method in general. Therefore, during the online calculation, we have to use the microprocessor and corresponding software to achieve it.

Using the method mentioned in Chapter 8 to implement the online control of the power system, it is necessary to calculate the decoupled reference δ_{ei} value locally in the system. The solution of δ_{ei} must calculate the instantaneous power flow of the local network. Because the power flow calculation involves a nonlinear equation, it can only be solved by iterative solution. Therefore, when calculating online, it will have to use the microprocessor and its corresponding software to achieve.

When the system suffers from strong disturbance, neither the convergence nor the computation speed can be guaranteed if δ_{ei} is calculated by the iterative method. Therefore, the calculation of δ_{ei} via the iterative method will significantly decrease the reliability of online control.

To raise the calculation speed of δ_{ei} and reliability of online control, DC power flow calculation equation is introduced to approximately derive δ_{ei}. Because DC power flow calculation is a direct solution method requiring no iteration, its calculation speed could be significantly accelerated, and the results are predictable. In addition, because there is no computational convergence problem, the reliability of online control can be greatly enhanced on the premise of meeting certain precision.

To meet the precision requirement, when the DC method is used to calculate the power flow, it is required that the angle difference between adjacent buses should be smaller. Otherwise, the calculation error will increase along with the increase of the actual angle between the adjacent buses.

The following equation is derived from the general equation of the power flow, and the unified equation for calculating the δ_{ei} of each node of the system is given shown in Fig. C.1.

In Fig. C.1, the angle of bus ③ is the required δ_{ei}.

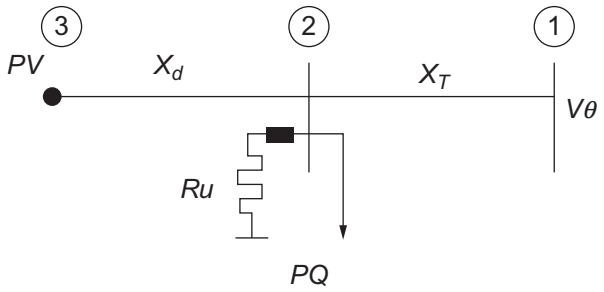

Fig. C.1
The uniform network for calculating $\delta_{ei.}$

The admittance matrix of network shown in Fig. C.1 is as follows:

$$H=\begin{bmatrix} -\mathrm{j}\dfrac{1}{X_\mathrm{T}} & \mathrm{j}\dfrac{1}{X_\mathrm{T}} & 0 \\ \mathrm{j}\dfrac{1}{X_\mathrm{T}} & \dfrac{1}{Ru}-\mathrm{j}\left(\dfrac{1}{X_\mathrm{d}}+\dfrac{1}{X_\mathrm{d}}\right) & \mathrm{j}\dfrac{1}{X_\mathrm{d}} \\ 0 & \mathrm{j}\dfrac{1}{X_\mathrm{d}} & -\mathrm{j}\dfrac{1}{X_\mathrm{d}} \end{bmatrix} \tag{C.1}$$

where each element is:

$$Y_{11}=G_{11}+\mathrm{j}B_{11}=0+\mathrm{j}\left(-\frac{1}{X_\mathrm{T}}\right)$$
$$Y_{12}=G_{12}+\mathrm{j}B_{12}=0+\mathrm{j}\left(-\frac{1}{X_\mathrm{T}}\right)$$
$$Y_{13}=G_{13}+\mathrm{j}B_{13}=0+\mathrm{j}0$$
$$Y_{21}=G_{21}+\mathrm{j}B_{21}=0+\mathrm{j}\left(-\frac{1}{X_\mathrm{T}}\right)$$
$$Y_{22}=G_{22}+\mathrm{j}B_{22}=\frac{1}{Ru}+\mathrm{j}\left(-\frac{1}{X_\mathrm{d}}-\frac{1}{X_\mathrm{T}}\right)$$
$$Y_{23}=G_{23}+\mathrm{j}B_{23}=0+\mathrm{j}\frac{1}{X_\mathrm{d}}$$
$$Y_{31}=G_{31}+\mathrm{j}B_{23}=0+\mathrm{j}0$$
$$Y_{32}=G_{32}+\mathrm{j}B_{32}=0+\mathrm{j}\frac{1}{X_\mathrm{d}}$$
$$Y_{33}=G_{33}+\mathrm{j}B_{33}=0+\mathrm{j}\left(-\frac{1}{X_\mathrm{d}}\right)$$

The expression of P_i for each bus is:

$$\begin{cases} P_1 = U_1U_2B_{12}(\delta_1 - \delta_2) \\ P_2 = U_1U_2B_{21}(\delta_2 - \delta_1) + U_2U_3B_{23}(\delta_2 - \delta_3) + U_2^2G_{22} \\ P_3 = U_2U_3B_{32}(\delta_3 - \delta_2) \end{cases} \tag{C.2}$$

The matrix form of Eq. (C.2) is:

$$\begin{bmatrix} P_1 \\ P_2 \\ P_3 \end{bmatrix} = \begin{bmatrix} U_1U_2B_{12} & -U_1U_2B_{12} & 0 \\ -U_1U_2B_{21} & U_1U_2B_{21} + -U_2U_3B_{23} & -U_2U_3B_{23} \\ 0 & U_2U_3B_{32} & U_2U_3B_{32} \end{bmatrix} \begin{bmatrix} \delta_1 \\ \delta_2 \\ \delta_3 \end{bmatrix} + \begin{bmatrix} 0 \\ U_2^2G_{22} \\ 0 \end{bmatrix} \tag{C.3}$$

This could be derived from Eq. (C.3) (it is known $B_{12} = B_{21}$, $B_{23} = B_{32}$):

$$\begin{cases} \delta_2 = \left(P_2 + P_3 + U_1U_2B_{12}\delta_1 - U_2^2C_{22}\right)/(U_1U_2B_{12}) \\ \delta_3 = \delta_2 + \dfrac{P_3}{U_2U_3B_{23}} \\ P_1 = U_1U_2B_{12}(\delta_1 - \delta_2) \end{cases} \tag{C.4}$$

The expression of Q_i for each bus is:

$$\begin{cases} Q_1 = -(1 + 2\Delta U_1)B_{11} - (1 + \Delta U_1 + \Delta U_2)B_{12} \\ Q_2 = -(1 + \Delta U_1 + \Delta U_2)B_{21} - (1 + 2\Delta U_2)B_{22} - (1 + \Delta U_2 + \Delta U_3)B_{23} \\ Q_3 = -(1 + \Delta U_2 + \Delta U_3)B_{32} - (1 + 2\Delta U_3)B_{33} \end{cases} \tag{C.5}$$

The matrix form of Eq. (C.5) is:

$$\begin{bmatrix} Q_1 + (B_{11} + B_{12}) \\ Q_2 + (B_{21} + B_{22} + B_{23}) \\ Q_3 + (B_{32} + B_{33}) \end{bmatrix} = \begin{bmatrix} -(2B_{11} + B_{12}) & -B_{12} & 0 \\ -B_{21} & -(2B_{22} + B_{23}) & -B_{23} \\ 0 & -B_{32} & -(B_{32} + 2B_{33}) \end{bmatrix} \begin{bmatrix} \Delta U_1 \\ \Delta U_2 \\ \Delta U_3 \end{bmatrix} \tag{C.6}$$

We could derive the following from Eq. (C.6):

$$\Delta U_2 = -(Q_2 + B_{21} + B_{22} + B_{23} + B_{21}\Delta U_1 + B_{23}\Delta U_3)/(2B_{22} + B_{23}) \tag{C.7}$$

Viz:

$$U_2 = 1 + \Delta U_2 = 1 - (Q_2 + B_{22} + B_{21}U_1 + B_{23}U_3)/(2B_{22} + B_{23}) \tag{C.8}$$

In the process of deriving δ_3 (that is, δ_{ei}), U_1, δ_1, P_2, Q_2, P_3, and U_3 are known as transient values, and because:

$$\begin{cases} B_{12} = B_{21} = \dfrac{1}{X_T} \\ B_{23} = B_{32} = \dfrac{1}{X_d} \\ G_{22} = \dfrac{1}{R_u} \\ B_{22} = -\dfrac{1}{X_d} - \dfrac{1}{X_T} \end{cases}$$

Substitute these known values into Eq. (C.9) and Eq. (C.4), and get:

$$\begin{cases} U_2 = (Q_2 X_\mathrm{T} X_\mathrm{d} + X_\mathrm{d} U_1 + X_\mathrm{T} U_3 - X_\mathrm{d})/(2X_\mathrm{d} + X_\mathrm{T}) \\ \delta_2 = \left(\dfrac{P_2 + P_3}{U_1 U_2} - \dfrac{U_2}{U_1 R_u}\right) X_\mathrm{T} + \delta_1 \\ \delta_3 = \delta_2 + \dfrac{P_3 X_\mathrm{d}}{U_2 U_3} \end{cases} \tag{C.9}$$

Derive δ_3 from Eq. (C.9), and obtain the required δ_e. The item with braking resistance R_u in Eq. (C.9), that is, $\frac{U_2}{U_1 R_u}$ existed only when the brake is switched on. And the expression of δ_2 is shown in the following during the steady-state and when no brake is switched on:

$$\delta_2 = \frac{P_2 + P_3}{U_1 U_2} X_\mathrm{T} + \delta_1 \tag{C.10}$$

The network structure and parameters given in the example mentioned in Chapter 8 are used to calculate for the fault type shown in operation mode $\langle I \rangle$ by the mentioned control scheme, and the curve of its power angle δ and decoupling criterion δ_e (δ_e curves are calculated by two methods: iterative method and DC method are given at the same time) are shown in Fig. C.2. It can be seen from the figure that the δ_e curve calculated by DC method is generally 1 degree less than the same curve calculated via iterative method, which is permitted in engineering practices.

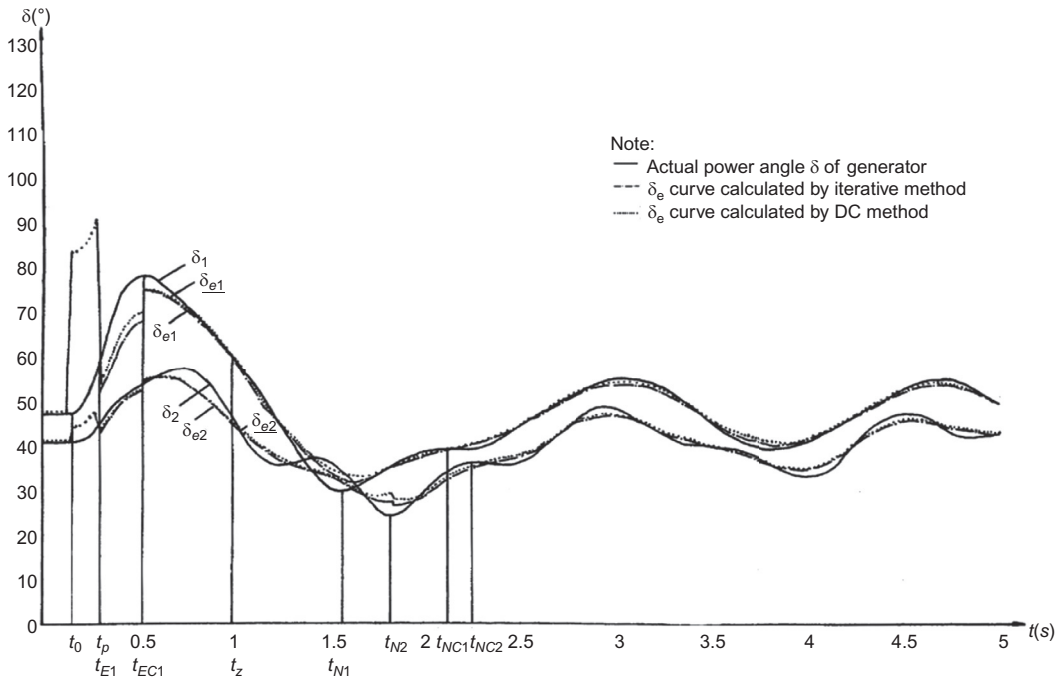

Fig. C.2

Comparison of the results by iterative method and DC method for solving decoupling criterion δ_e.

References

[1] D. Moitre, et al., Economic Dispatch of a Electric Energy System: An Evolutionary Approach, ISAP' 99, Rio de Janeiro (Brazil), 1999.

[2] J.R. Won, et al., Economic Dispatch Solution Using an Improved Genetic Algorithm, ISAP' 99, Riode Janeiro (Brazil), 1999.

[3] X. Guan, P.B. Luh, H. Yan, Optimization-based scheduling of hydrothermal power systems with pumped-storage units, IEEE Trans. Power Syst. 9 (2) (1994) 1023–1031. 93 SM 474–7 PWRS.

[4] L.A.F.M. Ferreira, Short-term scheduling of a pumped storage plant, IEE Proc. C—Gener. Transm. Distrib. 139 (6) (1992) 521–528.

[5] Z. Yamayee, Maintenance scheduling: description, literature survey and interface with overall operations scheduling, IEEE Trans. Apparatus and systems PAS-101 (8) (1982) 2770–2779.

[6] L. Chen, J. Toyota, Optimal generating unit maintenance scheduling for multi-area system with network constraints, IEEE Trans. Power Syst. 6 (3) (1991) 1168–1174.

[7] C.J. Huang, C.E. Lin, C.L. Huang, Fuzzy approach for generator maintenance scheduling, Electr. Power Syst. Res. 24 (1992) 31–38.

[8] C.E. Lin, C.J. Huang, C.L. Huang, C.C. Liang, S.Y. Lee, in: An Expert System for Generator Maintenance Scheduling Using operation Index, IEEE PES Winter Meeting, 1991. Paper No. 91,WM190 - 9 - PWRS.

[9] S. Iwamoto, Y. Tamura, A load flow calculation method for S-conditioned power systems, IEEE Trans. Power Syst. PAS-100 (4) (1981) 1736–1743.

[10] S.C. Tripathy, G. Durga Prasad, O.P. Malik, G.S. Hope, Load-flow solutions for H-conditioned power systems by a Newton - like method, IEEE Trans. Power Syst. PAS-101 (10) (1982) 3648–3657.

[11] D. Rajici, A. Bose, A modification to the fast decoupled power flow for Networks with high R/X ratios, IEEE Trans. Power Syst. 3 (2) (1988) 734–746.

[12] G.X. Luo, A. Semiyen, Efficient load flow for large weakly meshed networks, IEEE Trans. Power Syst. 5 (4) (1990) 1309–1316.

[13] R.C. Burchett, H.H. Happ, K.A. Wirgau, Large scale optimal power flow, IEEE Trans. Power Syst. PAS-101 (10) (1982) 3722–3732.

[14] K. Aoki, M. Kanezashi, A modified newton method for optimal power flow using quadratic approximated power flow, IEEE Trans. Apparatus and systems PAS-104 (8) (1985) 2119–2125.

[15] R.C. Burchett, H.H. Happ, D.R. Vierath, Quadratically convergent optimal power flow, IEEE Transactions on Power Apparatus and Systems PAS-103 (11) (1984) 3267–3275.

[16] D.I. Sun, B. Ashley, B. Brewer, A. Hughes, W.F. Tinney, Optimal power flow by newton approach, IEEE Trans. Apparatus and systems PAS-103 (10) (1984) 2684–2880.

[17] R.C. Burchett, H.H. Happ, K.A. Wirgau, Large scale optimal power flow, IEEE Transactions on Power Apparatus and Systems PAS-101 (10) (1982) 3722–3732.

[18] W.F. Tinney, J.M. Bright, K.D. Demaree, B.A. Hughes, Some deficiencies in optimal power flow, IEEE Trans. Power Syst. 3 (2) (1988) 676–683.

[19] O. Alsac, J. Bright, M. Praise, B. Stott, Further developments in LP-based optimal flow, IEEE Trans. Power Syst. 5 (3) (1990) 697–711.

[20] W.-H.E. Liu, A.D. Papalexopoulos, W.F. Tinney, Discrete Shunt Controls in a Newton Optimal Power Flow, IEEE Trans. Power Syst. 7 (4) (1992) 1509–1516.
[21] M. Fan, K. Aoki, A. Nishikori, K. Nara, An algorithm for discrete optimal power flow: (in Japanese), J. Inst. Electr. Eng. Jpn 110-B (4) (1991) 468–474.
[22] B.A. Murtagh, M.A. Saunders, MINOS/AUGMENTED User's Manual. Report SOL 80 - 14, Department of Operations Research, Stanford University, California, 1980.
[23] R. Billinton, R.N. Allan, Reliability Evaluation of Power Systems, Plenum Press, New York and London, 1996.
[24] W. Li, Incorporating aging failures in power system reliability evaluation, IEEE Power Engineering Review 22 (7) (July 2002) 59.
[25] W. Li, R. Billinton, Common cause outage models in power system reliability evaluation, IEEE Trans. Power Syst. 18 (2) (2003) 966–968.
[26] W. Li, J. Lu, Risk evaluation of combinative transmission network and substation configurations and its application in substation planning, IEEE Trans. Power Syst. 20 (2) (2005) 1144–1150.
[27] H. Lee Willis, Power Distribution Plannmg Reference Book Marcel Dekker, INC, New York, 1997.
[28] I. Kurihara, K. Takahashi, B. Kermanshahi, A new method of evaluating system margin under various system constrains, IEEE Trans. Power Syst. 10 (4) (1995) 1904–1911.
[29] P.N. Vovos, J.W. Bialek, Direct incorporation of fault level constraints in optimal power flow as a tool for network capacity analysis, IEEE Trans. Power Syst. 20 (4) (2005) 2125–2134.
[30] S. Rama Iyer, K. Ramachandran, S. Hariharan, Optimal reactive power allocation for improved system performance, IEEE Trans. Power Syst. PAS-103 (6) (1984) 1509–1515.
[31] W.M. Lebow, R. Rouhani, R. Nadira, P.B. Usoro, R.K. Mehra, D.W. Sobieski, M.K. Pal, M.P. Bhavaraju, A hierarchical approach to reactive volt ampere (VAR) optimization in system planning, IEEE Transactions on Power Apparatus and Systems PAS-104 (8) (1985) 2051–2057.
[32] K. Iba, H. Suzuki, K. Suzuki, K. Suzuki, Practical reactive power allocation/operation planning using successive linear programming, IEEE Trans. Power Syst. PWRS-3 (2) (1988) 558–566.
[33] M.O. Mansour, T.M. Abdel-Rahman, Non-linear VAR optimization using decomposition and coordination, IEEE Transactions on Power Apparatus and Systems PAS-103 (2) (1984) 246–255.
[34] K. Aoki, M. Fan, A. Nishikori, Optimal VAR planning by approximation method for recursive mixed- integer linear programming, IEEE Trans. Power Syst. PWRS-3 (4) (1988) 1741–1747.
[35] K.H. Abdul-Rahman, S.M. Shahidehpour, A fuzzy-based optimal reactive power control, IEEE Trans. Power Syst. 8 (2) (1993) 662–670.
[36] S. Granville, Optimal reactive dispatch through interior point methods, IEEE Trans. Power Syst. 9 (1) (1994) 136–146.
[37] A. Hughes, G. Jee, P. Hsiang, R.R. Shoults, M.S. Chen, Optimal reactive power planning, IEEE Trans. Power Syst. PAS-103 (2) (1984) 246–255.
[38] R.A. Fernandes, F. Lange, R.C. Burchett, H.H. Happ, K.A. Wirgau, Large scale reactive power planning, IEEE Transactions on Power Apparatus and Systems PAS-102 (5) (1983) 183–1088.
[39] S. Granville, M.V.F. Pereira, A. Monticelli, An integrated methodology for Var sources planning, IEEE Trans. Power Syst. PWRS-3 (2) (1988) 549–557.
[40] K. Aoki, M. Fan, T. Satoh, A. Nishikori, K. Nara, A VAR planning method with multiple power flow conditions (in Japanese), J. Inst. Electr. Eng. Jpn 110-B (10) (1990) 797–804.
[41] Y.T. Hsiao, C.C. Liu, H.D. Chiang, Y.L. Chen, A new approach for optimal VAR sources planning in large scale electric power systems, IEEE Trans. Power Syst. 8 (3) (1993) 988–996.
[42] C.C. Liu, K. Tomsovic, An expert system assisting decision-making of reactive power/voltage control, IEEE Trans. Power Syst. PWRS-1 (3) (1986) 195–201.
[43] C.E. Lin, T.C. Chen, C.L. Huang, A real time calculation method for optimal reactive power compensator, IEEE Trans. Power Syst. PWRS-4 (1989) 643–652.
[44] Y.Y. Hong, C.C. Liu, A heuristic and algorithm approach to VAR planning, IEEE Trans. Power Syst. PWRS-7 (1992) 505–512.

[45] C.J. Bridenbaugh, D.A. Dimascio, R.D. Aquila, Voltage control improvement through capacitor and transformer tap optimization, IEEE Trans. Power Syst. PWRS-7 (1992) 222–227.
[46] Y.Y. Hus, K.L. Ho, C.C. Liang, T.S. Lai, Voltage control using a combined integer linear programming and rule-based approach, IEEE Trans. Power Syst. PWRS-7 (1992) 744–752.
[47] M.E. Baran, F.W. Felix, Optimal capacitor placement on radial distribution systems, IEEE Trans. Power Delivery 4 (1) (1989) 725–742.
[48] R. Baldick, F.F. Wu, Approximation formulation for the distribution system: the loss function and voltage dependence, IEEE Trans. Power Delivery 6 (1) (1989) 252–259.
[49] H.-D. Chiang, J.-C. Wang, O. Cockings, Optimal capacitor placements in distribution system: part 1: a new formulation and the overall problem, IEEE Trans. Power Delivery 5 (2) (1990) 634–649.
[50] Y. Baghzouz, S. Ertem, Shunt capacitor sizing for radial distribution feeds with distorted substation voltages, IEEE Trans. Power Delivery 5 (2) (1990) 650–657.
[51] M. Fan, Z. Zhang, C. Lin, Discrete VAR optimizationin in a distribution system using mixed-integer programming with an expert system, Electr. Power Syst. Res. 0378-7796, 27 (3) (1993) 191–201.
[52] K. Nara, A. Shiose, M. Kitagawa, T. Tshihara, Implementation of genetic algorithm for distribution system loss minimum re-configuration, IEEE Trans. Power Syst. 7 (1992) 1044–1051.
[53] M. Fan, Z. Zhang, A power flow algorithm based on modified simulated annealing technique, in: ICPST91 Proceeding, Beijing, Aug., 1993.
[54] M. Fan, Z. Zhang, B. Huang, Discrete VAR optmization near to global optimum by genetic algorithm, in: ICPST94 Proceeding, Beijing, 1994.
[55] F.P. Gomez, L. Lasdon, M. Engquist, Nonlinear optimization by successive linear programming, Manag. Sci. 28 (10) (1982) 1106–1120.
[56] J.Z. Zhang, N.H. Kim, L. Lason, An improved successive linear programming algorithm, Manag. Sci. 31 (10) (1985) 1312–1331.
[57] R. Gary Parker, R.L. Rardin, Discrete Optimization, Academic Press, Inc, 1988.
[58] M. Zhongfan, New Progress on Linear Programming, Science Press, Beijing, 1994 (马仲蕃.线性规划最新进展.北京:科学出版社).
[59] Operations Research Teaching Materials Writing Group, Operations Research, Tsinghua University Press, Beijing, 2004 (运筹学》教材编写组.运筹学.北京:清华大学出版社).
[60] L. Baoding, Z. Ruiqing, W. Gang, Uncertain Programming and Application, Tsinghua University Press, Beijing, 2004 (刘宝碇, 赵瑞清, 王纲.不确定规划及应用.北京:清华大学出版社).
[61] L. Baoding, Z. Ruiqing, Stochastic Programming and Fuzzy Programming, Tsinghua University Press, Beijing, 1998 (刘宝碇, 赵瑞清.随机规划与模糊规划.北京:清华大学出版社).
[62] C. Baolin, Theory and Algorithms of Optimization, Tsinghua University Press, Beijing, 2005 (陈宝林.最优化理论与算法.北京:清华大学出版社).
[63] Z. Detong, Model and Experiment of Optimization, Tongji University Press, Shanghai, 2003 (朱德通.最优化模型与实验.上海:同济大学出版社).
[64] W. Ling, Intelligent Optimization Algorithm and Application, Tsinghua University Press, Beijing, 2001 (王凌.智能优化算法及其应用.北京:清华大学出版社).
[65] L. Wenyuan, Power System Risk Assessment: Model, Method and Application, Translated by Zhou Jiaqi and Lu Jiping, etc, Science Press, 2006 (李文沅著.电力系统风险评估:模型, 方法和应用.周家启, 卢继平等译.北京:科学出版社).
[66] X. Shaolin, Z. Fengzhi, Optimization Computing Method, Shanghai Science and Technology Press, Shanghai, 1983 (席少霖, 赵凤治.最优化计算方法.上海:上海科学技术出版社).
[67] Q. Wenqian, Grid Power Supply Capacity Assessment with Maximum and Minimum Load Multiple, East China Electric Power, tenth ed., 1994, pp. 29–30 (丘文千.用最大最小负荷倍数评估电网供电能力.华东电力).
[68] Q. Fuchang, Load Distribution and Line Power Supply Capacity, Rural Electrician, first ed., (1995) pp. 9–11 (秦富昌.负载分布与线路供电能力.农村电工).

[69] Qiu Li-ping, Fan Ming-tian, A New Algorithm to Evaluate Maximum Power Supply Capability of Urban Distribution Netwrok,Power System Technology, 30 (9) (2006) 68–71.
[70] O.I. Elgerd, C.E. Fosha Jr., Optimum megawatt-frequency control of multi-area electric energy system, IEEE PAS-89 (1970) 556–563.
[71] R.K. Cavin, M.C. Eudge Jr., P. Rasmussen, An optimal linear systems approach to load-frequency control, IEEE PAS-90 (1971) 2472–2482.
[72] J.D. Glover, F.C. Schweppe, Advanced load and frequency control, IEEE PAS-91 (1972) 2095–2103.
[73] M. Calovic, Linear regulation design for a load and frequency control, IEEE PAS-91 (1972) 2271–2285.
[74] J. Zaborszky, A. K. Subramanian, K. M. Lu, Modeling and estimation of the load demand of an area, IEEE Conf. (1975) Paper. TA 3–3. 283–302.
[75] L.K. Kirchmayer, Economic Control of Interconnected Systems, Wiley, New York, 1959.
[76] D.G. Ramry and J.W. Skooglund, Detailed hydro governor representation for system stability studies, IEEE Trans PAS N1, 1970.
[77] R.T. Byerly, Dynamic models for steam and hydro turbines in power system studies, IEEE Trans on PAS N6, 1973.
[78] G.E.P. Box, G.M. Jenkins, Time Series Analysis, Forecasting and Control, Holdenday Inc., San Francisco, 1976.
[79] N. Premakumaran, K.L.P. Mishra, Design of load frequency controller via invariance principle, IFAC Symposium on Automatic Control and Protection of Electric Power Systems, pp. 393–396.
[80] Pullman, J. Morman, Matrix theory and its Applications: selected topics, Marcel Dekker, Inc. 1976.
[81] 自动控制中的矩阵理论, 须田信英等著, 科学出版社, 1979 (Matrix Theory in Automatic Control, Nobuhide Suda etc., Science Press in China, 1979.)
[82] Linear Algebra, Jiang Erxiong etc., People's Publishing House in China, 1978. (线性代数, 蒋尔雄等著, 人民出版社, 1978).
[83] Mathematical Methods for Discrete-Time System Filtering, Institute of Mathematics, Chinese Academy of Sciences, 1975. (离散时间系统滤波的数学方法, 中国科学院数学研究所, 1975.)
[84] Power System Computing, Xi'an Jiaotong University in China, Water Conservancy and Hydro-Power Press in China, 1978. (电力系统计算, 西安交通大学, 水利水电出版社, 1978.)
[85] Foreign System Engineering Album, Chongqing Branch of Science Literature Publishing House in China, 1980. (国外系统工程专辑, 科学文献出版社重庆分社, 1980.)
[86] Basic Design of Optimal Control System, Wang Yongchu Science Press in China, 1980. (最佳控制系统设计基础, 王永初 科学出版社, 1980.)
[87] J. Zaborszky "Operation of the Large Interconnected Power System by Decision and Control in Emergencies" Report No. SSM 7907 Washington University ST. Louis, Missouri 63130. 1983.
[88] J. Zaborszky "On Line Stabilization of the Large Interconnected Power System in Emergency by Local Feedback Control" Report No. SSM 8002 Washington University ST. Louis, Missouri 63130. 1983.
[89] J. Zaborszky, A new state space for emergency control in the interconnected power system, IEEE Trans. Autom. Control AC-22 (4) (1977) 505–517.
[90] M.L. Shelton, Bonneville power administration 1400 MW braking resistor, IEEE Transactions on Power Apparatus and Systems 94 (2) (1975) 602–611.
[91] M. Araki, Stability and transient behaviour of composite nonlinear system, IEEE Trans. Autom. Control 17 (4) (1972) 537–541 On AC.
[92] M. Morse, Critical Point Theory in Global Analysis and Differential Topology, Academic Press, New York, 1969.
[93] G. Price, Bounds for determinants with dominant principal diagonal, Proc. Am. Math. Soc. 2 (1951) 497–502.
[94] J. Nash, Non-cooperative games, Ann. Math. 54 (2) (1951) 286–295.
[95] N.G. Mankiw, Principles of Economics, Cengage Learning, 2014.
[96] A. Kumar, S.C. Srivastava, S.N. Singh, Congestion management in competitive power market: a bibliographical survey, Electr. Power Syst. Res. 76 (1–3) (2005) 153–164.
[97] D.M. Newbery, Power markets and market power, Energy J. (1995) 39–66.

[98] S. Hao, G.A. Angelidis, H. Singh, A.D. Papalexopoulos, Consumer payment minimization in power pool auctions, IEEE Trans. Power Syst. 13 (3) (1998) 986–991.
[99] A.K. David, F.S. Wen, Bilateral transaction bargaining between independent utilities under incomplete information, IEE Proc.-Gener. Transm. Distrib. 148 (5) (2001) 448–454.
[100] J. Barr, F. Saraceno, Cournot competition, organization and learning, J. Econ. Dyn. Control 29 (1–2) (2005) 277–295.
[101] X. Wang, Y.H. Song, Q. Lu, Lagrangian decomposition approach to active power congestion management across interconnected regions, IEE Proc.-Gener. Transm. Distrib. 148 (5) (2001) 497–503.
[102] S. Hao, A. Papalexopoulos, Reactive power pricing and management, IEEE Trans. Power Syst. 12 (1) (1997) 95–104.
[103] J.B. Gil, T.G. San Román, J.A. Rios, P.S. Martin, Reactive power pricing: a conceptual framework for remuneration and charging procedures, IEEE Trans. Power Syst. 15 (2) (2000) 483–489.
[104] Y. Dai, Y.X. Ni, F.S. Wen, Z.X. Han, Analysis of reactive power pricing under deregulation, 2000 Power Engineering Society Summer Meeting (Cat. No. 00CH37134), vol. 4, IEEE, 2000, pp. 2162–2167.
[105] Y. Erkeng, Z. Jingyang, Z. Xuesong, Bidding model and bidding principle for power markets, Autom. Electr. Power Syst. 25 (1) (2001) 24–27.

Index

Note: Page numbers followed by *f* indicate figures, and *t* indicate tables.

M

N

O

P

R

S

T

U

V

Y

Mingtian Fan, Zuping Zhang and Chengmin Wang

Mathematical Models and Algorithms for Power System Optimization

Modeling Technology for Practical Engineering Problems

Mathematical Models and Algorithms for Power System Optimization helps readers build a thorough technical understanding of power system optimization modeling focused on the main aspects of how optimization models are constructed and solved. A number of mathematical models and algorithms are presented in this book for practical problems which are mainly related to four areas of power systems: planning, operation, control, and marketing, such as economic dispatching, generator maintenance scheduling, load flow, optimal load flow, load optimization, reactive optimization, load frequency control, transient stability, and electricity marketing. Many elements relevant to optimization are covered such as algebraic equations, differential equations, difference equations, numerical and non-numerical optimization algorithms. The optimization models discussed include linear (0-1, integer, mixed-integer), nonlinear, mixed integer, and nonlinear mixed integer models. The book delivers important insights into how to transform practical problems into optimization models; how to develop standard optimal mathematical models and utilize commercial programming software; how to deal with various issues that affect the performance of models; and how to evaluate the effectiveness of the models. The ideas and practices of the modeling techniques in this book will be a useful reference for those in universities and research institutes who are actively engaged in power system optimization.

Key Features

- Provides insights on formulating new optimization models for power systems in terms of both theoretical analysis and practical operation
- Illustrates the essential elements of modeling techniques: formulations (e.g., variables, objective functions, constraints), proof, verification, mutual transformation of models, calculation procedures, and implementation
- Demonstrates solution procedures by some practical large-scale examples in power systems

Authors

Mingtian Fan is a Professor at the China Electric Power Research Institute in Beijing, China. Her research focuses on mathematical modeling and algorithms for power system planning and operation, including economic dispatching, optimal load flow, reactive power planning, load frequency control, distribution system planning, and energy storage planning.

Zuping Zhang is a Professor at the China Electric Power Research Institute in Beijing, China. His research includes power system planning and operation analysis, mathematical models and calculation methods of power system analysis, UHV large power grids, and distribution planning methods.

Chengmin Wang is a Professor at Shanghai Jiao Tong University, Shanghai, China. His research includes the planning, operation, and stability of power systems as well as renewable energy integration.

Electrical Power Engineering

ISBN 978-0-12-813231-9

9 780128 132319

ELSEVIER

ACADEMIC PRESS

An imprint of Elsevier

elsevier.com/books-and-journals